

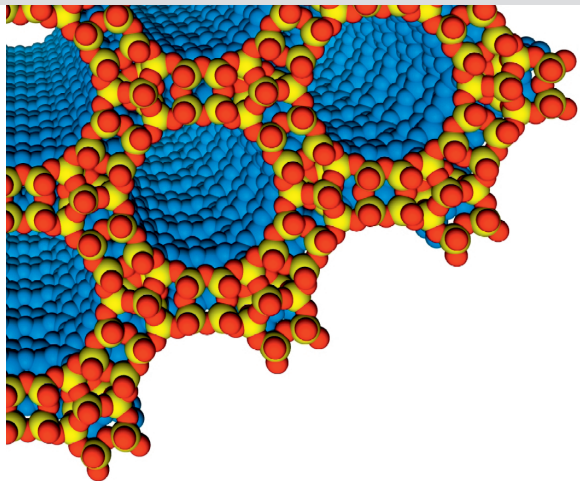
5th INTERNATIONAL
FEZA
conference
Valencia Spain July 3-7 2011



3RD FEZA SCHOOL ON ZEOLITES

JULY 8-9, 2011 | VALENCIA | SPAIN

Cristina Martínez
Joaquín Pérez-Pariente
(Editors)



ZEOLITES AND ORDERED POROUS SOLIDS: FUNDAMENTALS AND APPLICATIONS

EDITORIAL
UNIVERSITAT POLITÈCNICA DE VALÈNCIA

Editors:
Cristina Martínez
Joaquín Pérez-Pariente

**ZEOLITES AND ORDERED POROUS SOLIDS:
FUNDAMENTALS AND APPLICATIONS**

**EDITORIAL
UNIVERSITAT POLITÈCNICA DE VALÈNCIA**

First edition, 2011 (printed)
First Edition, 2011 (electronic)



This editorial is member of the UNE, which guarantees the diffusion and commercialization of its publications at national and international level.

- © of the present edition:
Editorial Universitat Politècnica de València
www.editorial.upv.es
- © All commercial names, brands, or distinctive marks of any kind included in this piece of work are protected by law.
- © Edited by:
Cristina Martínez
Instituto de Tecnología Química, UPV-CSIC
Valencia, Spain

Joaquín Pérez-Pariente
Instituto de Catálisis y Petroleoquímica (CSIC)
Cantoblanco, Madrid, Spain

ISBN: 978-84-8363-707-4 (printed)
ISBN: 978-84-8363-719-7 (electronic)
Ref. editorial: 6026

Any unauthorized copying, distribution, marketing, editing, and in general any other exploitation, for whatever reason, of this piece of work or any part thereof, is strictly prohibited without the authors' expressed and written permission.

Preface

In July 2011 the city of Valencia will host the 5th FEZA Congress and the 3rd FEZA zeolite school. It has been 6 years since the first Edition of the School in 2005, and research in the field of Zeolites remains highly active, not only when related to well established catalytic applications such as those within the refining and petrochemical industry, but also in relatively newer areas such as chemicals, fine chemicals, or upgrading of alternatives raw materials (natural gas, biomass) to fuels and chemicals, and in other uses, such as adsorption and/or separation. Thus, there is still much to tell and more to learn about these amazing materials.

The broad scope covered by the program of this School, and the undisputable expertise of the lecturers, whom kindly accepted to participate in this event, were two major reasons for the edition of a book where the speakers were proposed to contribute with one chapter. This book would be a comprehensive introduction for researchers and students that approach the zeolite field for the first time, and would be distributed to the attendants to the School, but also, hopefully, to all those joining the 5th FEZA Conference. The commitment and effort of the authors which have contributed with their manuscripts have made this possible.

The aim of this third edition of the FEZA School, and thus also of this book, is to cover most of the fields related with zeolites and their applications: structure, synthesis, characterization, applications as adsorbents and catalysts and new applications. Chapters 1 to 4 describe the large variety of zeolite structure types and chemical compositions, their synthesis, their most important properties and how they can be characterized. Chapter 5 shows the application of theoretical methods that can play an important role in understanding and/or complementing experimental data related to zeolite structures, synthesis or applications. Chapter 6 gives a very complete overview of the application of zeolites as commercial adsorbents and chapter 7 introduces the fundamentals of zeolites as heterogeneous catalysts. Chapters 8 to 10 describe various catalytic applications, ranging from refining and petrochemistry to chemicals, fine chemicals and emerging processes. Finally, chapter 11 gives new perspectives on zeolite chemistry and applications.

We would like to greatly acknowledge the participation of lecturers and authors, which submitted their manuscripts despite the short deadlines in order to accomplish with the editions steps. We would also like to thank the 5th FEZA Congress Organizing Committee for supporting the edition of this volume, the Publication Service of the Polytechnic University of Valencia (UPV) for having the book ready on time and the Life-Long Learning Centre (Centro de

Preface

Formación Permanente, CFP) for organization and additional help. Finally, we want to thank financial support of sponsors and Institutions, and the Spanish Ministry of Science and Innovation (MICINN) for Consolider-Ingenio 2010 (proyecto MULTICAT, 2009 CDS 00050).

Madrid/Valencia, June 2011

Joaquín Pérez-Pariente and Cristina Martínez

3rd FEZA SCHOOL ORGANIZING COMMITTEE

Francesco Di Renzo, ICGM, Montpellier (France)

Girolamo Giordano, Universidad de Calabria, Calabria (Italy)

Cristina Martínez, ITQ, Valencia (Spain)

Joaquín Pérez-Pariente, ICP, Madrid (Spain)

Javier Pérez-Ramírez, ETH, Zürich (Switzerland)

SUPPORT AND SPONSORING

Organizing Committee of the 5th FEZA Conference

Universidad Politécnica de Valencia (UPV)

COST Action CM0903: BIOCHEM

Italian Zeolite Association (AIZ)

BRUKER

List of contributors

Philip A. BARRETT

Praxair Inc., 175 East Park Drive, Tonawanda, New York 14150, USA

Dirk E. DE VOS

Centre for Surface Chemistry and Catalysis, Kasteelpark Arenberg 23, 3001 Leuven, Belgium

Jan DIJKMANS

Centre for Surface Chemistry and Catalysis, Kasteelpark Arenberg 23, 3001 Leuven, Belgium

Michiel DUSSELIER

Centre for Surface Chemistry and Catalysis, Kasteelpark Arenberg 23, 3001 Leuven, Belgium

Jan GEBOERS

Centre for Surface Chemistry and Catalysis, Kasteelpark Arenberg 23, 3001 Leuven, Belgium

Hermann GIES

Ruhr-Universität Bochum, 44780 Bochum, Germany

Jean-Pierre GILSON

Laboratoire Catalyse & Spectrochimie, ENSICAEN, Université de Caen, CNRS, 6 bd Maréchal Juin, 14050, Caen, France

Luis GÓMEZ-HORTIGÜELA

Instituto de Catálisis y Petroleoquímica-CSIC. c/ Marie Curie 2. 28049. Madrid. Spain.

Andreas JENTYS

Technische Universität München, Department of Chemistry and Catalysis Research Center, Garching, 85748, Germany

Johannes A. LERCHER

Technische Universität München, Department of Chemistry and Catalysis Research Center, Garching, 85748, Germany

Magdalena LOZINSKA

*EASTCHEM School of Chemistry, University of St Andrews, Purdie Building,
North Haugh, St Andrews, Fife, KY16 9ST, UK*

Gerardo MAJANO

*Centre for Surface Chemistry and Catalysis, Kasteelpark Arenberg 23, 3001
Leuven, Belgium*

Olivier MARIE

*Laboratoire Catalyse & Spectrochimie, ENSICAEN, Université de Caen, CNRS,
6 bd Maréchal Juin, 14050, Caen, France*

Bernd MARLER

Ruhr-Universität Bochum, 44780 Bochum, Germany

Martin MARTIS

*Department of Chemistry, University College London, 20 Gordon Street,
London WC1H 0AJ, United Kingdom*

Roberto MILLINI

*eni s.p.a. – refining & marketing division, San Donato Milanese Research
Center, Via F. Maritano 26, I-20097 San Donato Milanese (Milano – Italy)*

Svetlana MINTOVA

*Laboratoire Catalyse & Spectrochimie, ENSICAEN, Université de Caen, CNRS,
6 bd Maréchal Juin, 14050, Caen, France*

Manuel MOLINER

*Instituto de Tecnología Química, Universidad Politécnica de Valencia-Centro
Superior de Investigaciones Científicas (UPV-CSIC), Valencia, E-46022, Spain*

Annelies PEETERS

*Centre for Surface Chemistry and Catalysis, Kasteelpark Arenberg 23, 3001
Leuven, Belgium*

An PHILIPPAERTS

*Centre for Surface Chemistry and Catalysis, Kasteelpark Arenberg 23, 3001
Leuven, Belgium*

Gopinathan SANKAR

*Department of Chemistry, University College London, 20 Gordon Street,
London WC1H 0AJ, United Kingdom*

Bert F. SELS

*Centre for Surface Chemistry and Catalysis, Kasteelpark Arenberg 23, 3001
Leuven, Belgium*

Kerry SIMMANCE

*Department of Chemistry, University College London, 20 Gordon Street,
London WC1H 0AJ, United Kingdom*

Andrew J. SMITH

*Department of Chemistry, University College London, 20 Gordon Street,
London WC1H 0AJ, United Kingdom*

Bart STEENACKERS

*Centre for Surface Chemistry and Catalysis, Kasteelpark Arenberg 23, 3001
Leuven, Belgium*

Neil A. STEPHENSON

Praxair Inc., 175 East Park Drive, Tonawanda, New York 14150, USA

Takashi TATSUMI

Tokyo Institute of Technology, Yokohama 226-8503, Japan

Valentin VALTCHEV

*Laboratoire Catalyse & Spectrochimie, ENSICAEN, Université de Caen, CNRS,
6 bd Maréchal Juin, 14050, Caen, France*

Stijn VAN DE VYVER

*Centre for Surface Chemistry and Catalysis, Kasteelpark Arenberg 23, 3001
Leuven, Belgium*

Paul A. WRIGHT

*EASTCHEM School of Chemistry, University of St Andrews, Purdie Building,
North Haugh, St Andrews, Fife, KY16 9ST, UK*

CONTENTS

Preface	V
3rd FEZA School Organizing Committee	VII
Support and Sponsoring	VII
List of contributors	IX
Chapter 1 Structural Chemistry and Properties of Zeolites <i>Paul A. Wright and Magdalena Lozinska</i>	1
Chapter 2 Basic principles of zeolite synthesis <i>Manuel Moliner</i>	37
Chapter 3 Crystal Structure Analysis in Zeolite Science <i>Hermann Gies and Bernd Marler</i>	67
Chapter 4 Synchrotron based in situ X-ray techniques for the characterisation of nanoporous solids <i>Gopinathan Sankar, Kerry Simmance, Andrew J. Smith and Martin Martis</i>	91
Chapter 5 Theoretical Methods in Zeolite Chemistry <i>Luis Gómez-Hortigüela</i>	117
Chapter 6 Adsorption Properties of Zeolites <i>Philip A. Barret and Neil A. Stephenson</i>	149

Chapter 7	
Basic concepts in zeolite acid-base catalysis	181
<i>Johannes A. Lercher and Andreas Jentys</i>	
Chapter 8	
Zeolites in refining and petrochemistry	211
<i>Roberto Millini</i>	
Chapter 9	
Emerging Applications of Zeolites	245
<i>Jean-Pierre Gilson, Olivier Marie, Svetlana Mintova and Valentin Valtchev</i>	
Chapter 10	
Zeolites as catalysts for fine chemicals synthesis and renewables conversion	301
<i>Annelies Peeters, Gerardo Majano, Bart Steenackers, An Philippaerts, Michiel Dusselier, Jan Geboers, Jan Dijkmans, Stijn Van de Vyver, Bert F. Sels and Dirk E. De Vos</i>	
Chapter 11	
Perspectives for zeolite chemistry and catalysis	339
<i>Takashi Tatsumi</i>	

Structural Chemistry and Properties of Zeolites

Paul A. WRIGHT and Magdalena LOZINSKA

EASTCHEM School of Chemistry, University of St Andrews, Purdie Building, North Haugh, St Andrews, Fife, KY16 9ST, UK

Abstract

Zeolites in the strict sense are highly porous crystalline aluminosilicates that comprise tetrahedrally-connected three dimensional frameworks and extra-framework charge balancing cations. The frameworks contain pores that are able to take in molecules of up to 1 nm in size (depending on the structure type) and the pore geometry can include cages and/or channels, and be one-, two-, or three-dimensionally connected. The chemical composition of both framework and extra-framework components can extend very widely whilst retaining 'zeolitic' character. This chemical variation can arise directly during synthesis, or post-synthetically: changes include exchange of both charge-balancing and framework cations, inclusion of organic groups into the framework and replacement of framework oxygen. This chapter introduces the current diversity of framework structure types and also describes some of the structural chemistry that zeolite structures undergo, emphasising that the properties of zeolites, which make them so widely applicable, are directly related to both periodic and defect structures.

1. Introduction

Zeolites are crystalline, porous solids based on silica, the framework structures of which are built up of corner-sharing tetrahedra and possess channels and cages large enough to contain exchangeable extra-framework cations and to allow the reversible uptake of molecules up to *ca.* 1 nm in size. As a result of these structural characteristics, zeolites find widespread application as ion exchangers, adsorbents and catalysts. Furthermore, because there is a direct link between their crystal structure and physical properties there is intense interest in their structural chemistry from both academics and technologists.

Originally discovered as natural aluminosilicate minerals, it was not until the pioneering work of Barrer in academia and Breck, Milton, Kerr and Flanigen in industry that the potential of their large scale synthesis and commercial application could start to be realised. Details of the current concepts and strategies of synthesis and an up-to-date account of applications will be given elsewhere in this book, but Figure 1 illustrates the history of the first synthesis of different zeolitic silicate

structure types including structures first observed as minerals, but synthesised later. This demonstrates the continuing and accelerating research effort in this area and also the increased use of organic 'template' molecules to prepare new structures.

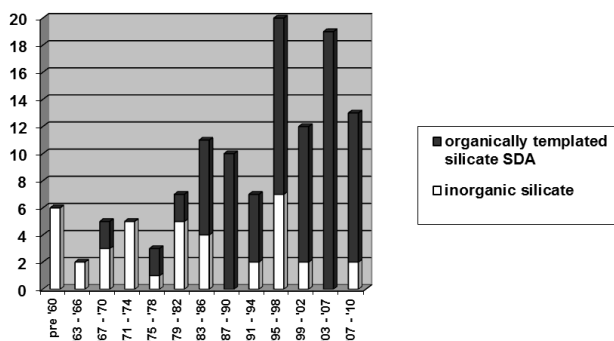


Figure 1. Chronological discovery of novel synthetic zeolitic silicates

We will discuss the structural chemistry of zeolites and the physical and chemical properties that stem directly from it. The term structural chemistry covers not only a description of the different frameworks that zeolites and related materials can exhibit, and the manner in which extra framework cations and guest molecules are arranged in the pore spaces, but also important details of possible chemical substitutions or variants and the nature of structural defects, which may be crystallographic or unrelated to the periodic structure. Furthermore, zeolitic structures should not be considered rigid and inert, but rather responsive, for example to changes in temperature and pressure; open to modification without destruction, for example by ion exchange, hydrothermal treatment or nitridation; and interactive, especially in the processes of adsorption and catalysis. Indeed, application of these materials requires an in-depth understanding of the ways they may be tailored for use pre-application and respond to conditions upon activation and use (regeneration and re-use).

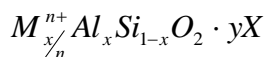
In this chapter, the structural chemistry of zeolites will be described and the underlying crystallo- and physical-chemistry explained. The range of structure types has been produced over decades of innovative synthesis and associated structural details have emerged over the same period via careful structural analysis, using techniques of X-ray and neutron diffraction, electron microscopy and a range of spectroscopic methods that have seen continual improvements in accuracy, resolution and applicability: these, as well as details of applications of these fascinating materials, are described elsewhere in this text and others.¹⁻⁶

2. Fundamentals of zeolite structure

2.1 Basic structural chemistry

Strictly defined, zeolites are aluminosilicates with tetrahedrally-connected framework structures based on corner-sharing aluminate (AlO_4) and silicate (SiO_4) tetrahedra. Conceptually, they may be considered as pure silica frameworks with Si substituted by Al. This $\text{Al}^{3+} \leftrightarrow \text{Si}^{4+}$ substitution gives an overall negative charge to the framework. This is balanced by the presence of extra-framework charge-balancing cations located within the pore space, coordinated to framework O atoms, which is also able to take in neutral atoms and molecules small enough to enter via the pore windows.

A simplified empirical formula for an aluminosilicate zeolite is



where x can vary from 0 - 0.5 and M^{n+} represents inorganic or organic cations. In the as-prepared zeolites they are typically alkali or alkali earth metal cations or alkylammonium cations, but after post-synthetic modifications they can be ion exchanged to almost any inorganic cation or replaced by protons. X represents neutral guest molecules or included species. Figure 2 shows different representations, typical of those used in the literature, of the framework of zeolite Rho, without charge balancing cations.

The primary building blocks of the framework are the tetrahedra. Typically, Al-O and Si-O bond distances are 1.73 and 1.61 Å, respectively, with OTO angles (T is the tetrahedral cation) close to the tetrahedral angle, 109.4°. There is more variation in the Si-O-Si bond angles between tetrahedra, where the average angle is 154° with a range of 135-180° and a mode of 148°. Variation in T-O-T angles enables a wide diversity of frameworks to exist.

Ab initio electronic structure calculations of zeolitic materials indicate a formal charge of +2 is associated with Si, and -1 with framework oxygen.⁹ Al-O-Al linkages are not observed in hydrothermally-synthesised zeolites, because the negative charge associated with the aluminate tetrahedra interact unfavorably, an observation expressed as Löwenstein's rule. At high Al contents, with Si/Al approaching 1, this requires short range ordering; at Si/Al = 1 (as is the case in zeolite A, for example), strict Si-O-Al-O-Si alternation in adjacent tetrahedra is observed.

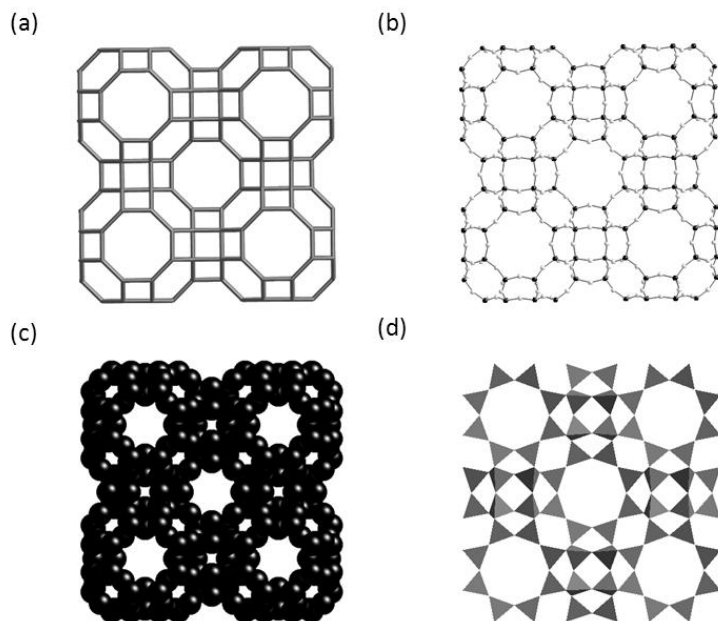


Figure 2. Representations of the projection of the framework structure of zeolite Rho (framework topology type RHO); (a) T-site connectivity only, (b) ball-and-stick, (c) space filling and (d) (Si,Al)O₄ tetrahedra

2.2 Zeolite frameworks : secondary building units and pore geometry

Topological analysis of the possible ways of arranging tetrahedra to give hypothetical zeolite structures indicates that the number is practically limitless, even if the constraint of structural stability is taken into account.¹⁰ Considering silicates, 143 framework topologies have so far been reported: this number rises to 197 for tetrahedral frameworks of all compositions.

A detailed, up-to-date and carefully-refereed listing of all reported tetrahedrally-connected open framework structures (of all compositions, and with framework T-site densities of below 20 T/1000 Å³) is available on the web, courtesy of the Structure Commission of the International Zeolite Association.¹¹ Each observed framework topology is given a three letter code (e.g. LTA for Linde zeolite A, MFI for ZSM-5, etc.) and for the initial type structure, complete details of unit cell dimensions and symmetry, fractional atomic coordinates, building units found in the frameworks (see below), coordination sequences of tetrahedral nodes and pore

connectivity and dimensions are given. A record is also kept of the chemical compositions of all reported structures with each topology type, fully referenced. This 'Atlas of Zeolite Structures' is therefore the essential source of information for zeolite structures, including those referred to below.

Silicate and aluminate tetrahedra are the primary building units of zeolites, but the frameworks can also be considered in terms of secondary building units (SBUs) which are arrangements of linked tetrahedra, often observed in several structures. These, on their own or in combination with other building units, give the frameworks. Which if any of these are actually added intact from solution is currently being determined by careful studies of crystal growth mechanisms. Examples of SBUs are given in Figure 3, where only the topology of the tetrahedral cations is given - these will be linked by oxygen atoms in the structures.

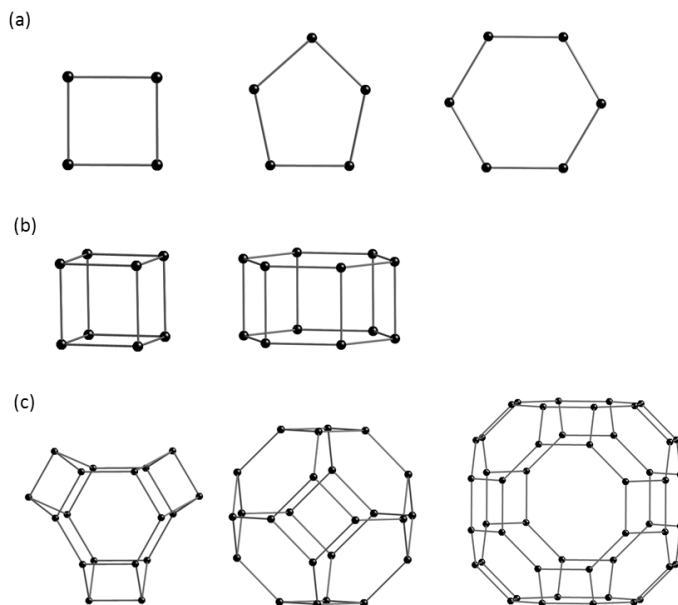


Figure 3. SBUs including rings with different numbers of tetrahedral cations (4MR, 5MR, 6MR), double 4-membered ring, D4R, (two rings of 4 tetrahedral cations), D6R, and polyhedra: cancrinite cage, sodalite or β -cage and the α -cage. Cages can also be described in terms of their faces (or rather the number of edges on each face). In this way a D4R is represented as $[4^6]$, a D6R as $[4^6 6^2]$ and a sodalite cage as $[6^8 4^6]$.

Among all these SBUs, the sodalite cage, or β -cage, is of most importance, because it is a key SBU in two of the most important zeolites types, A and zeolite X, as well as sodalite itself. We use the class of zeolites containing sodalite cages to illustrate some of the key features of zeolite structural chemistry in section 2.3 below.

As well as polyhedral SBUs, characteristic chains are observed in zeolite structures (Figure 4). The ‘crankshaft’ chain, for example, is a key building unit in zeolites, in both single and double chains. Adjacent crankshaft chains can be related either by a mirror plane (4c) or by a centre of inversion (4d). The important natural and synthetic zeolites of the natrolite family contain the 4-1 chain (4d) and so called ‘pentasil’ zeolites ZSM-5 and ZSM-11 contain the chain shown in (4f), built from 5MRs.

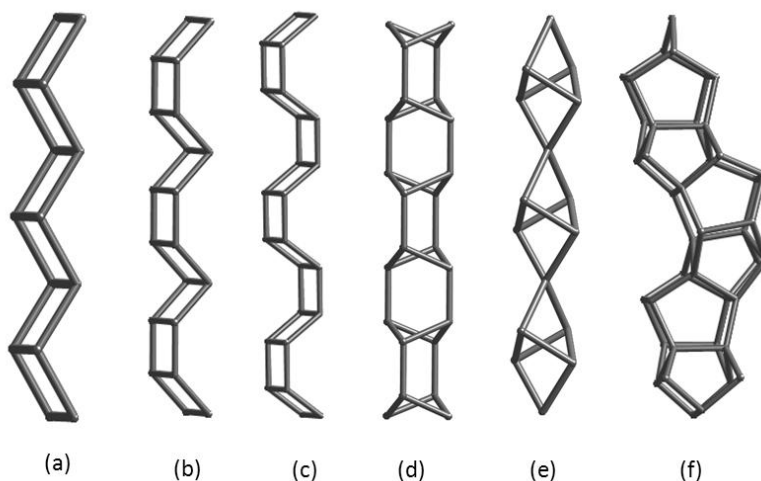


Figure 4. Important chains of linked tetrahedral cations found in zeolite structures.

Zeolite structures are also commonly described in terms of the size, geometry and connectivity of the pore space defined by their frameworks. The size of the channels or pore openings (windows) that control molecular access into the pores is given in terms of the limiting ring size. Zeolites with channels or windows described by planar 8MRs have pore sizes around 4 Å and are known as ‘small pore’, those with planar 10MR windows or channels as ‘medium pore (5.5 Å)’ and those with 12MR windows or channels as large pore (7.5 Å). These are approximate dimensions, and can vary with the planarity and ellipticity of the rings. In addition, zeolites with 7MR, 9MR and 11MR openings are known. Some structures contain openings limited by 14MRs or even 18MRs or more – these are referred to as extra-

large pore solids. The pore space geometry may be described in terms of channels, which may be uniform or non-uniform in cross section and may intersect with other channels or for other structures in terms of cages, linked via windows. Finally, the connectivity of pore space can be one dimensional, 1D, (unconnected channels), 2D (where any point in a plane in the pore system can be accessed from any other point in that plane) or 3D, where any part of the pore space is accessible from any other point within the crystal.

In addition to the framework structure, it is also important to know the location of extra-framework cations. Many such cation site determinations have been performed from diffraction data, in both hydrated and dehydrated solids, and cation site location is found to depend on cation size and charge, temperature and the presence or absence of adsorbed molecules. In general cations minimize their energy by maximising their coordination with framework oxygen atoms (and adsorbates) and minimising their repulsive interactions with other cations.

2.3 Zeolite structures based on the sodalite cage: an illustrative example

The structure of the mineral sodalite consists of β -cages face-sharing through 6MRs (Figure 5a). If they are linked instead through their 4MRs via D4R units, the zeolite A framework results (topology type LTA, Figure 5b). As well as D4Rs and β -cages, the structure contains α -cages, which share 8MR openings that can allow the uptake of small molecules with molecular sizes up to 4 Å. In zeolite A (Si/Al=1) many extra framework cations are required for charge balance, and these are distributed between the α - and β -cages (Figure 6a). Those in the α -cage can influence the pore size if they are close to the window. For Na-A the pore size is around 4 Å ('zeolite 4A'), whereas for the potassium form, K-A, the larger cations restrict the window size ('zeolite 3A'). If Na⁺ is exchanged by half the number of Ca²⁺ cations, the effective pore size is increased ('zeolite 5A').

Sodalite cages can also be linked through D6Rs on their 6MR faces (Figures 5 c, d). Whereas there is only one way of arranging the cages for sodalite and zeolite A, there are different ways of linking layers of sodalite cages through D6Rs. The two end member variants are cubic zeolites with the faujasite (FAU) structure type,¹² where FAU refers to the mineral form of this material, faujasite, and its hexagonal polytype EMC-2 (structure type EMT).¹³ In the FAU topology there is a centre of inversion relating layers of cages, whereas in the EMT topology layers are related by mirror planes. In faujasitic materials the Si/Al ratio can vary from 1.1 to infinity (for X, Si/Al=1.1-1.8, for Y, Si/Al=1.8-infinity). Disordered stacking sequences are also observed.¹⁴ The type of structure that crystallises is determined by the inorganic and organic SDAs that are used in the synthesis. As well as the D6R and β -cages, larger cavities, or supercages, are formed. There is one type of supercage in cubic FAU structures, and two in the EMT structure.

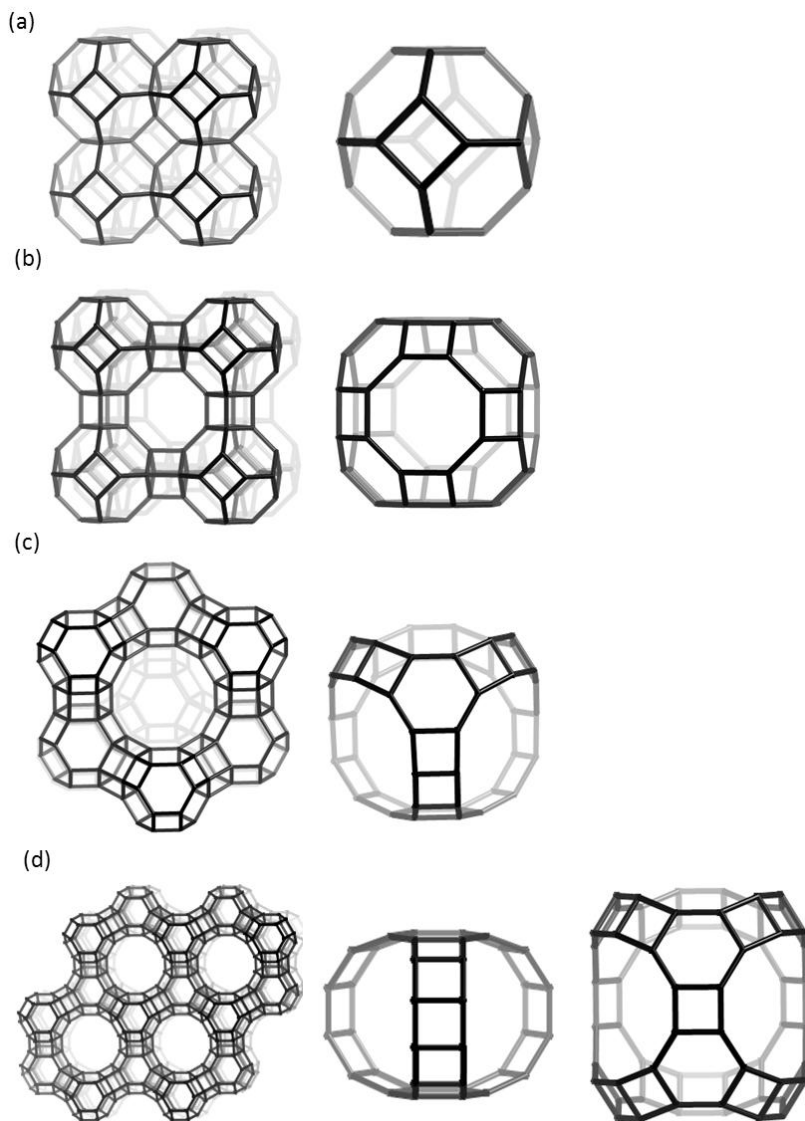


Figure 5. Topology of zeolite structures that contain the sodalite cage SBU, together with other cages found in the structures (a) sodalite, (b) zeolite A, (c) faujasite and (d) EMC-2.

The siting of extra framework cations has been extensively studied because of its importance in determining adsorbent and catalytic properties. Some of the sites observed for faujasite X and Y in these studies are shown in Figure 6b. These include sites in the D6Rs (sites I and I'), in the sodalite cages (II and II'), and in the supercages (III).

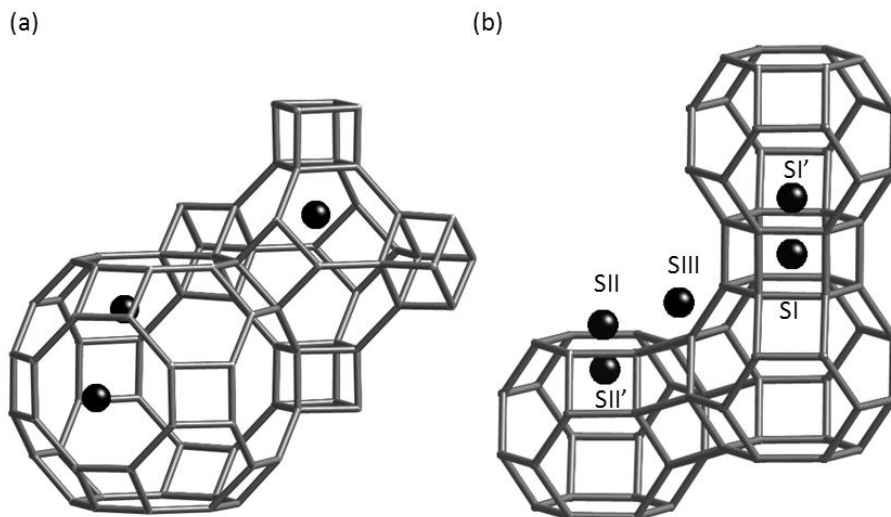


Figure 6. Typical extra framework cation sites in (a) zeolite A and (b) faujasite.

It has been possible to locate the position of protons in the H^+ -form of zeolite Y, which is prepared by heating the ammonium-exchanged form at around 400 °C. In H-Y, protons are mainly on two of the O atoms, in the form of bridging hydroxyl groups, Si-OH-Al, giving strong Bronsted acid sites.¹⁵

3. Historical development and structural examples pre-1990

3.1 Zeolites crystallised with inorganic metal cation templates

As well as zeolites A and the faujasites X and Y, many other zeolite types have been discovered using inorganic cations as structure directing agents, particularly prior to 1980, as seen in Figure 1. Among these, mordenite (1D 12MR with 8MR side channels), ferrierite (1D 10MR \times 8MR), zeolites L (1D 12MR \times 8MR) and P (gismondine), chabazite, and Rho (all 3D 8MR) are important examples and find

industrial applications. These zeolites, prepared using inorganic cations, tend then to have relatively high Al contents, because their pore space contains many exchangeable cations. As a result, low silica (maximum aluminium) P shows important properties as an ion exchanger,¹⁶ as does zeolite A, and chabazite is widely used as an adsorbent and catalyst. Figure 7 illustrates the frameworks and cation sites observed in zeolites P, chabazite and L.

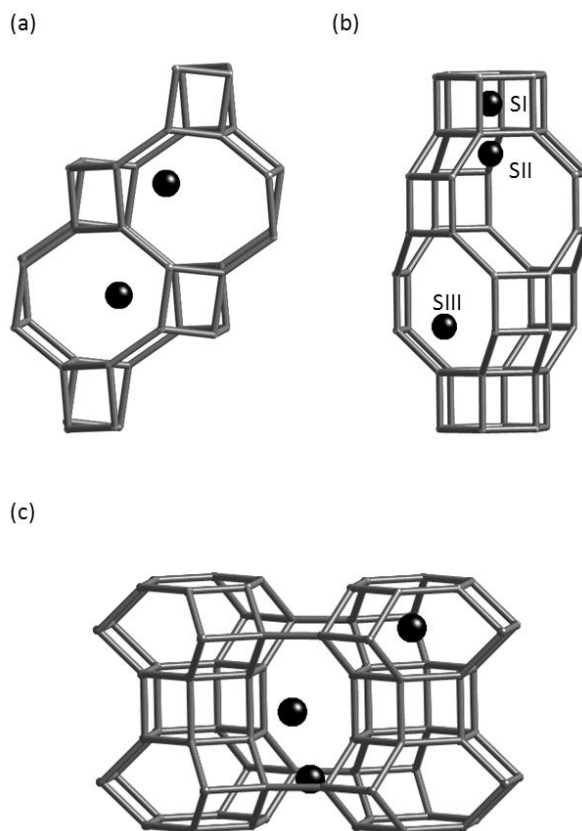


Figure 7. Typical extra framework cation sites in zeolites (a) P, (b) chabazite and (c) L.

The potassium form of chabazite is readily prepared, and in the lithium form this zeolite has important properties in the separation of oxygen and nitrogen in air.¹⁷ Chabazite (topology type CHA) belongs to a large family of synthetic and natural

zeolites that can be considered as being made up from 6MRs, stacked in periodic sequences according to their position (A, B or C) at (0,0), ($\frac{2}{3}, \frac{1}{3}$) or ($\frac{1}{3}, \frac{2}{3}$) in the xy plane of a hexagonal cell. In chabazite all 6MRs are part of D6Rs: the stacking sequence being AABBC. All D6Rs have the same orientation, and link to other D6Rs to give a structure that contains the chabazite cage (Figure 7). Each chabazite cage is connected to 6 others via 8MR windows giving a highly porous, three dimensionally connected small pore structure. Variation in the 6MR stacking sequence gives structures with cages and channels of different sizes, but all bounded at their widest point by 12MRs.

3.2 Synthesis of zeolites with organic templates

Figure 1 also emphasises the increasing importance of using organic cations to obtain new structure types, following pioneering work by Barrer.¹⁸ These are referred to as organic structure directing agents (SDAs) or more loosely, organic templates. They can be bulky, so fewer can be included in the zeolite pores than would be the case for inorganic cations. This necessitates a lower density of framework negative charge and consequently a lower Al content. Zeolites templated by larger organic SDAs therefore have high framework Si/Al ratios. Prior to 1980 most novel zeolites prepared using organic SDAs included commercially available alkylammonium ions, such as tetramethyl-, tetraethyl- and tetrapropylammonium species, or even linear diquats (diquaternary cations). Using TMA⁺ gives cage-like SBUs and, among other structures, gives the LTA topology with Si/Al > 1 (ZK-4) where it templates the sodalite cage, and the 12MR 1D channel structures gmelinite and ZSM-4, each of which contains 'gmelinite' cages templated by the cation.¹⁰

Among the most important new structure types prepared with tetraethylammonium ions were zeolite Beta¹⁹ and ZSM-12. The structure of Beta is built up from layers with tetragonal symmetry connected via stacking. In zeolite Beta, these offsets occur with a high degree of disorder, but this does not block the two sets of perpendicular straight 12MR channels parallel to the layers (shown in Figure 8), or the undulating interconnected 12MR channels perpendicular to these. The high silica content of Beta results in high hydrothermal stability, and because of its 3D connectivity and ease of synthesis it is one of the most important zeolites used in catalysis. ZSM-12 (MTW), a 1D 12MR structure, also crystallises in the presence of TEA⁺.

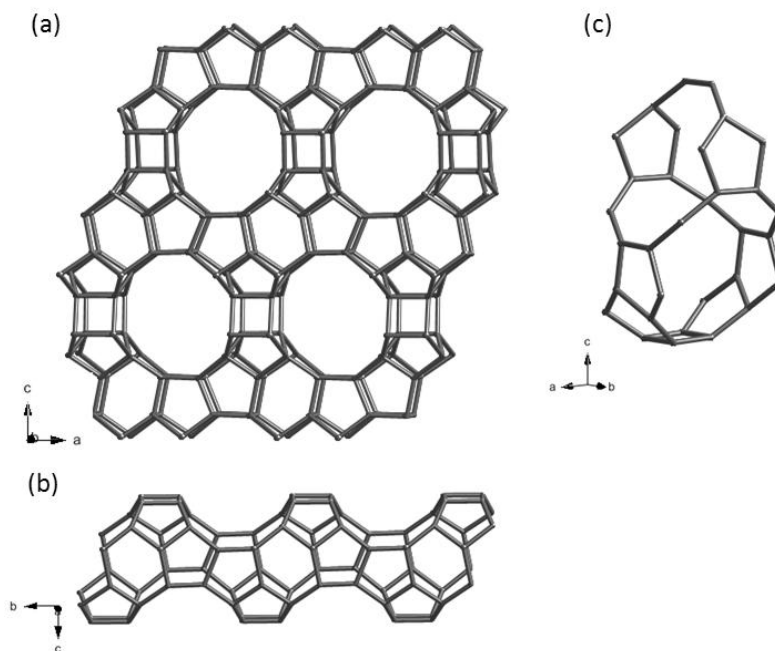


Figure 8. The zeolite Beta structure (a) is built from layers (b) stacked along the c axis. The 12MR channels shown in projection along b in (a) intersect with a set along a to give a 3D 12MR channel system, with channel intersections as shown in (c).

The synthesis of ZSM-5 using tetrapropylammonium (TPA^+) cations as SDAs was a major advance in zeolite chemistry. The structure of ZSM-5 (MFI) is built up from 5-5-1 SBUs as shown in Figure 9. These join to form chains, which in turn link to form sheets. The ZSM-5 structure results when these sheets are linked across a centre of inversion, with TPA^+ cations at channel intersections. ZSM-5 has a pore system consisting of intersecting straight and undulating medium pore channels of pore diameters of 5-5.5 Å.²⁰ The two sets of channels are connected so that the pore space shows 3D connectivity. This pore structure, together with the high stability and high acid strength that derive from its high Si/Al ratio, makes ZSM-5 a highly active and shape selective catalyst.

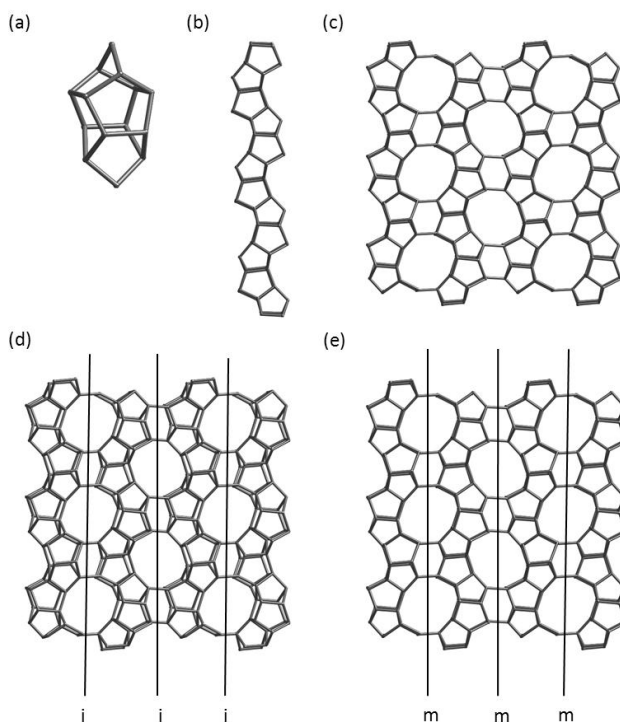


Figure 9. The framework structure of ZSM-5 is based on 5-5-1 SBUs (a) that link to form pentasil chains (b). These connect to give sheets (c) which can link to other adjacent sheets either by centres to give (d) the final MFI topology or (e) via mirrors to give ZSM-11 (MEL).

Straight 10MR channels run parallel to the sheets, and are connected by undulating channels that lie in the plane perpendicular to them. Although there are only two sets of channels, they are connected so that any part of the pore space in a crystal is accessible to any other. Stacking the sheets to give mirror planes between them gives a different structure, ZSM-11 (MEL),¹⁰ also with a 3D 10MR channel system.

Casci *et al.* used the more complex diquatery cations $[(\text{H}_3\text{C})_3\text{N}(\text{CH}_2)_n\text{N}(\text{CH}_3)_3]^{2+}$ and discovered the structures EU-1,²¹ a high silica 1D 10MR zeolite where the channels had 'side-pockets' alternating on either side, and NU-87,²² with a 2D 10MR pore system.

3.3 Structure types from the use of designer templates

The recognition that alkylammonium cations (including diquatery species) were excellent structure directing agents for high silica structures triggered great activity post 1980 to prepare ‘customised’ organic cations and investigate them as SDAs. Alkylammonium ions have been prepared via reactions as simple as methylation of amines and the Menshutkin reaction of primary haloalkanes with tertiary amines through to multistep syntheses of polycyclic species. This has involved industrial and academic labs worldwide, and in particular the groups of Davis at Caltech, Corma (Valencia), Patarin (Mulhouse), Hong (Taejon) and at Mobil, UOP, IFP and especially Chevron (Zones). Figure 10 illustrates the role organic SDAs have in templating for the example of TNU-10, which is the high silica variant of stilbite prepared by the group of Hong using bis-*N*-methylpyrrolidinium butane.²³ The non-bonding interactions, the component of the attractive interaction between organic and framework oxygen atoms that does not take into account the long range electrostatic interactions due to localized charges, are important in discriminating between different crystallising structures.

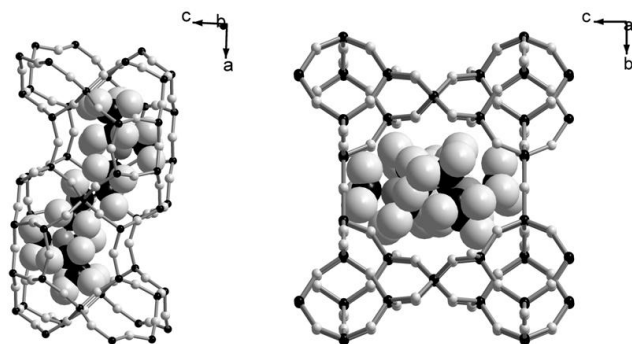


Figure 10. The diquatery bis-*N*-methylpyrrolidinium butane acts as a SDA for high silica stilbite, as shown by these views of the organic within its 10MR channel system.

The rate of discovery of new structures has been maintained by the use of such ‘designer’ templates, together with the widening out of the compositional range of starting gels to include other framework forming elements, combinations of organic and inorganic SDAs, and the development of high throughput methods that have made possible such wide-ranging investigations. The structure solution of these materials is also a crucial step in this story, because zeolites are often formed only as microcrystalline powders, and so require great expertise in powder diffraction and electron microscopy to determine their structures.

Among important novel aluminosilicate zeolites (or borosilicates which can often be modified to give aluminosilicates post-synthetically) that have been discovered are those that possess multidimensional channel systems with intersecting channels of different size (CIT-1,²⁴ MCM-68²⁵ and synthetic boggsite²⁶), those that possess extra-large pore one dimensional channel systems (UTD-1,²⁷ SSZ-53 and SSZ-59²⁸) and those at the limit of structural complexity so far observed; TNU-9²⁹ and IM-5.³⁰

Structures with two or three dimensional intersecting channel systems with different free diameter had long been a target due to the possibilities of ‘molecular transport control’ postulated by Derouane,³¹ where reactants and products in catalytic reactions might find separate diffusion pathways. Two examples of such structures are MCM-68 and synthetic boggsite, the latter recently synthesized using phosphazene-based SDAs (Figure 11).²⁶ In these two structures, 12MR channels are intersected (and connected) by 12MR channels, promising novel catalytic selectivities.

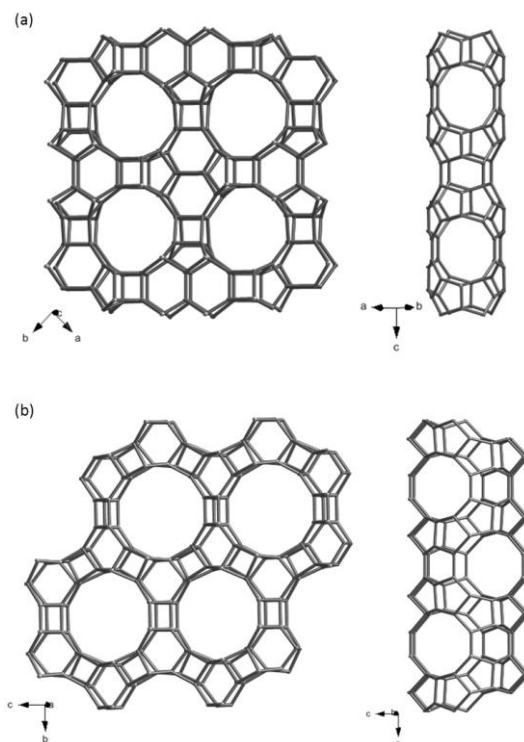


Figure 11. The framework structure of (a) MCM-68 and (b) boggsite both possess 12MR channels (shown in projection on the left) that are intersected by perpendicular 10MR channels (shown on the right).

Zeolites with extra-large pores are sought to extend the size of molecule that can gain access to adsorption or catalytic sites. Of these, UTD-1 was the first 14MR structure (1D, 8.2 Å pores), more recently augmented by SSZ-53 and SSZ-59, both borosilicates with elliptical 1D 14MR channels ca. 8.5 Å × 6.3 Å in size.

The structures of TNU-9 and IM-5, prepared using similar diquateryary bis-N-methylpyrrolidiniumalkane SDAs, are currently the most crystallographically complex zeolite structures known, each possessing 24 crystallographically distinct T-sites. The structure of TNU-9 is described in Figure 12, where it is seen that even for this complex structure, it can be considered as built from one kind of chain. This links to give one kind of sheet, which can join with other similar sheets in only one arrangement to give a 3D connected 10MR zeolite with two different kinds of straight 10MR channel that run parallel to the sheets and to each other.

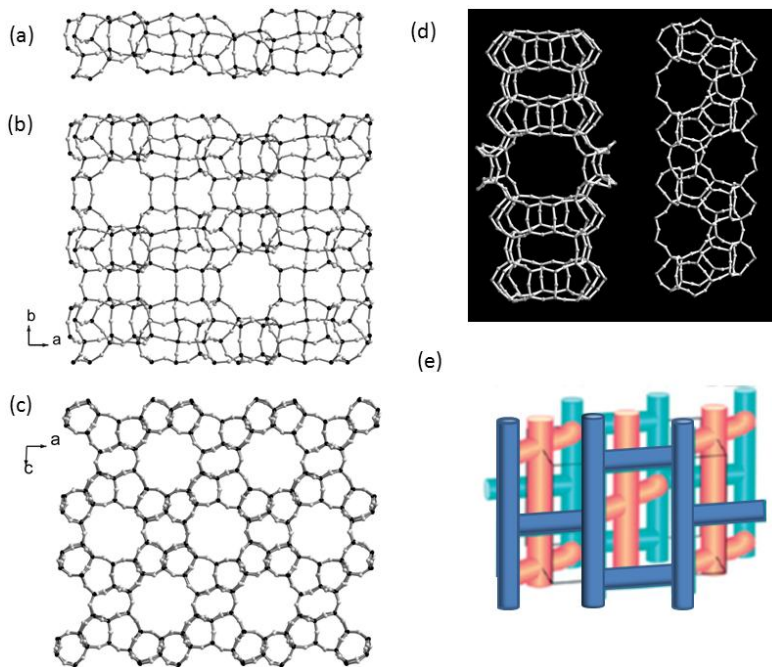


Figure 12. The framework structure of TNU-9, one of the most complex known, is built from chains (a), linked to give sheets (b) that link along the c axis to give a 3D structure with two sets of channels, shown in projection in (c). The channels are shown in plan in figure (d) and complex 3D interconnection of the two kinds of channels (dark, narrow 4.9Å, light, wide 5.4Å) are shown in (e).

4. Expanding the chemical range of zeolitic solids : zeotypes

Although aluminosilicate zeolites are by far the best studied and most widely applied materials that have tetrahedrally-coordinated porous frameworks, many compositional variants (including pure silica forms) have been prepared, and some 20 elements have been reported to be included via substitution into framework cation sites. These can be aliovalent, with a different valency from silicon (3+ or sometimes 2+), or isovalent (with the same valency). The inclusion of some elements has stronger effects on chemical characteristics than on structural features (B^{3+} for Al^{3+} , for example) whereas the inclusion of high levels of elements such as gallium or germanium can result in the crystallization of frameworks with distinctly different structural features. Their ease of substitution, stability in the tetrahedral site and structure directing properties depend on cationic radius³² (e.g. Li^+ , 0.59; Be^{2+} , 0.27 Å; Zn^{2+} , 0.60 Å; B^{3+} , 0.11 Å; Al^{3+} , 0.39 Å; Ga^{3+} , 0.47 Å; Fe^{3+} , 0.49 Å; Ti^{4+} , 0.42 Å; Ge^{4+} , 0.39 Å compared to Si^{4+} , 0.26 Å) and electronegativity. In addition to metallosilicates, extensive families of zeotypic (tetrahedrally-connected) metal phosphates and germanates have been prepared, with their own patterns of cationic substitution. All these different families will be discussed, with emphasis on the silicates, but the discussion of structures that possess framework cations with coordinations greater than fourfold is beyond the scope of this current chapter.

4.1 Pure silica zeolites

Many zeolites prepared using bulky organic cations have very high Si/Al ratios, but it is possible to prepare pure silica zeolites. Many of these have been prepared in fluoride-containing solutions, so that the positive charge on the SDA is balanced by fluoride ions coordinated to framework silicon, which then becomes 5-fold SiO_4F . Consequently, the ability of a pure silica structure to provide Si sites for stable F^- coordination will play a role in determining the products of such a synthesis. Cambor summarises the use of F^- ions in synthesis, describing the many examples where F^- siting, often favored on Si where it can project into small cages, is known.³³ Upon removal of the organic SDA by calcination the fluoride is also removed, leaving a perfect tetrahedrally coordinated silica.

Without fluoride ions in the synthesis, other mechanisms of charge balance are required. For SSZ-74,³⁴ which has a 3D connected 10MR pore system and is prepared using a template similar to that used for TNU-9 and IM-5 (bis-N-methylpyrrolidiniumheptane) the structure has 23 T-sites and an ordered tetrahedral vacancy (effectively an empty 24th T-site) (Figure 13). The vacant T-site is surrounded by four framework oxygen atoms forming a distorted tetrahedron. Two of these make closer contacts with the charge on the template and are thought to be siloxy groups (Si-O) leaving the other two as silanol groups, hydrogen atoms of which are involved in H-bonds with the siloxy oxygen atoms. Although ordering of

such defects is rare, it is likely that interactions of this type are a widespread mechanism of charge balancing of pure silica polymorphs templated by organocations when fluoride not available, so that SSZ-74 can be used as a model system. Upon calcination and removal of the organic SDA, it is likely that vacancies remain, leaving possible sites for further heteroatom inclusion.

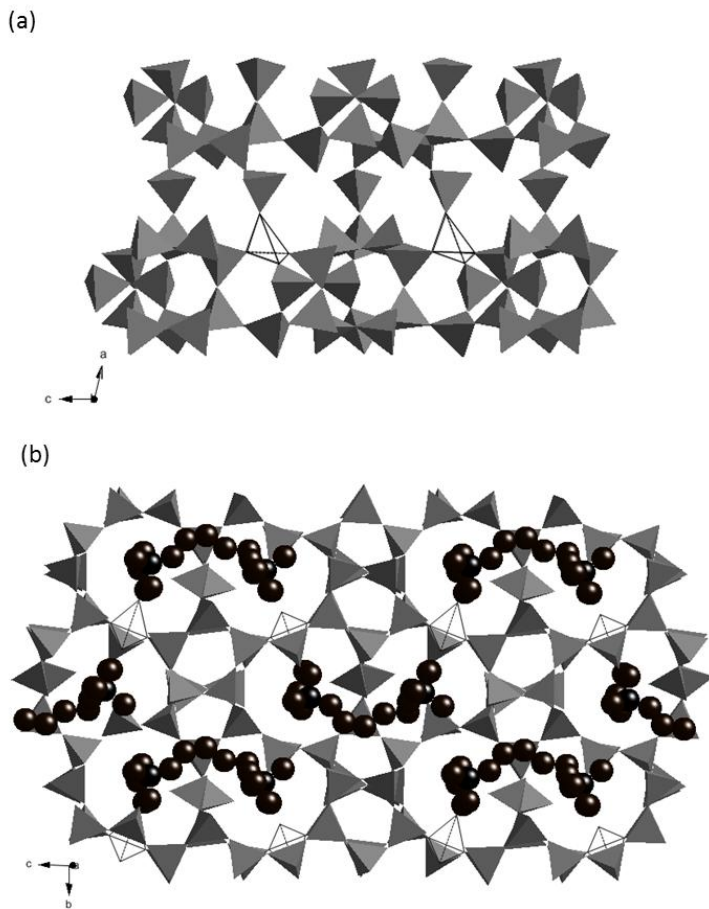


Figure 13. The zeolite SSZ-74 possesses ordered T site vacancies (shown as empty tetrahedra). These are close to the positively charged-N atoms of its diquatery SDA (shown in (b)).

Many pure silica zeolites have been prepared by direct synthesis, with silicalite-1 and -2, all-silica variants of the 10MR medium pore structures ZSM-5 and ZSM-11 the best known. Other examples include the small pore ITQ-29 (LTA)³⁵ and the large pore zeolite Beta (*BEA).³⁶ In other important cases the pure silica forms have only been prepared post-synthetically, as described in section 5.3.

4.2 *Metallosilicates: Aliovalent substitutions*

There is strong experimental evidence that B^{3+} , Fe^{3+} and Ga^{3+} can be included within tetrahedral silicate frameworks, indicating that a wide range of cation sizes can be tolerated. It is likely that all can influence crystallization differently from Al^{3+} , but the tendency for Ga^{3+} in particular to direct framework formation is strong. ECR-34, for example, which possesses 18MR channels, has only been prepared as a gallosilicate.³⁷ Although like aluminosilicates they show ion exchange behavior and permanent porosity, they show lower hydrothermal stability.

The substitution of divalent metal cations such as Be^{2+} and Zn^{2+} has also been observed, often giving unique structures, such as the zincosilicate VPI-9³⁸ and the berylliosilicate OSB-2.¹⁰ Finally, it is also possible to include Li^+ in framework positions.³⁹ Although of considerable structural interest, these materials do not usually exhibit stability desirable for applications.

4.3 *Metallosilicates: Isovalent substitutions*

Three isovalent substitutions are of importance in zeotypic silicates, of Ti^{4+} , Sn^{4+} and Ge^{4+} . The titanosilicates and to a lesser extent stannosilicates are primarily of significance for their catalytic properties whereas germanosilicates are remarkable for the novel topologies they exhibit. Titanium-containing high silica zeotypes such as TS-1 (Ti-equivalent of silicalite-1)⁴⁰ contain a few mole percent of Ti in framework cation sites. Although the Ti is tetrahedral in the template-free, dehydrated form, it readily acts as a Lewis acid to expand its coordination sphere in the presence of water or, with important applications in selective oxidation, peroxide species. Other zeotypic titanosilicates have been reported (including the large pore Ti- β ⁴¹) but these should not be confused with titanosilicates such as ETS-10,⁴² in which the framework contains octahedrally-coordinated Ti in chains or clusters. There is also strong evidence for the inclusion of Sn^{4+} in zeolitic structures, where again selective oxidation via Lewis acidity of the active metal site is the principal interest.⁴³

There is much current interest in the synthesis and structure of germanosilicates, arising in part from the observation that pure germanate FOS-5 possessed the Beta C (BEC) structure topology (Beta C is the name given to a hypothetical polytype of zeolite Beta formed by ordered stacking of similar structural layers).⁴⁴ Subsequently, the inclusion of germanium in silicates has resulted in the

crystallization of remarkable zeotypic structures (channel systems given in brackets), including Beta C, ITQ-17 (12 MR \times 12 MR \times 12MR),⁴⁵ IM-12 (14MR \times 12MR \times 12MR),⁴⁶ ITQ-33 (18MR \times 10MR \times 10MR),⁴⁷ IM-20 (12MR \times 10MR \times 10MR) and ITQ-44 (18MR \times 12MR \times 12MR).⁴⁸ The fully tetrahedral frameworks of these structures are characterized by D4R units, 3MRs and even D3Rs, giving rise to frameworks with low tetrahedral site densities and large pores (as predicted by Meier for frameworks containing high densities of 3Rs and 4Rs)⁴⁹ The structures of the germanosilicates ITQ-17 (BEC) and ITQ-44, shown in Figure 14, display some of these structural features.

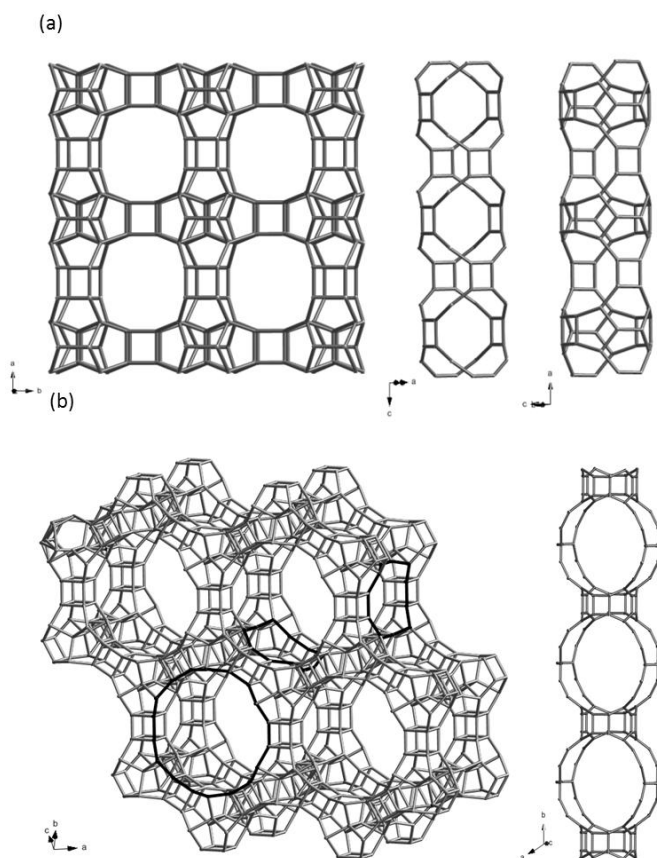


Figure 14. Germanosilicate zeotypes such as (a) ITQ-17 and (b) ITQ-44 show typical D4R SBUs, as well as low framework densities and, for ITQ-44, 18MR channels.

The tendency for the inclusion of germanium in tetrahedral sites to favour the formation of small ring SBUs is attributed to the larger non-bonding radius of Ge vs. Si, and consequently the ability to form smaller OTO angles that stabilize 3MRs and 4MRs.⁵⁰ The recently reported germanosilicate ITQ-37⁵¹ possesses Ge and Si in tetrahedral coordination, and also a high density of D4Rs, but in this case one of the apices of the 4MRs is made up be a O₃GeOH group, with a dangling hydroxyl group projecting into the pore space and giving a so-called interrupted structure (represented in the 3 letter code by a dash, -ITV). The chiral crystal structure is mesoporous, with the lowest framework density observed for a zeolite (10.2 T /1000 Å³) and cavities in the mesoporous regime (3D connected via 30MR openings, each 20 Å × 5 Å).

Although such high Ge structures possess potentially attractive features for catalysis, the relatively high cost of GeO₂ and the low hydrothermal stability of germanosilicates are obstacles to their application. Nevertheless, they do offer inspiration to those searching for extra-large pore zeolitic solids.

4.4 Aluminophosphates and substituted aluminophosphates

The discovery of aluminophosphate (AlPO) zeotypes by UOP in 1982⁵² heralded a major expansion of the compositional range of this type of microporous solid. They can be thought of as derived from pure silica zeolites by the ordered substitution Al + P ↔ 2Si, so that their framework composition is AlPO₄ and Al and P show strict alternation in tetrahedral framework sites. There are strong similarities between AlPO zeotypes and zeolites in their structure and synthesis (like high silica zeolites, AlPOs crystallise hydrothermally via the use of organic SDAs) but there are also important differences in structure and more importantly, in chemistry. The most obvious structure difference is that the strict alternation of Al and P in framework sites rules out the presence of odd numbered rings in AlPO structures. Also, although many framework types are observed as both silicates and AlPOs (LTA, FAU, CHA, AFI, etc) there are examples where this is not the case, most notably for VPI-5, an 18MR AlPO.⁵³ In this structure the reason is probably because the VPI-5 structure (Figure 15) is originally prepared with Al in octahedral coordination with four framework oxygen atoms and two from water molecules. Only after dehydration is a fully tetrahedrally-coordinated framework produced. This additional coordination to Al (to make it 5- or 6-fold) is also significant to enable the positive charge of alkylammonium SDAs to be balanced by framework-coordinated F⁻ or OH⁻ ions in as-synthesised AlPOs.

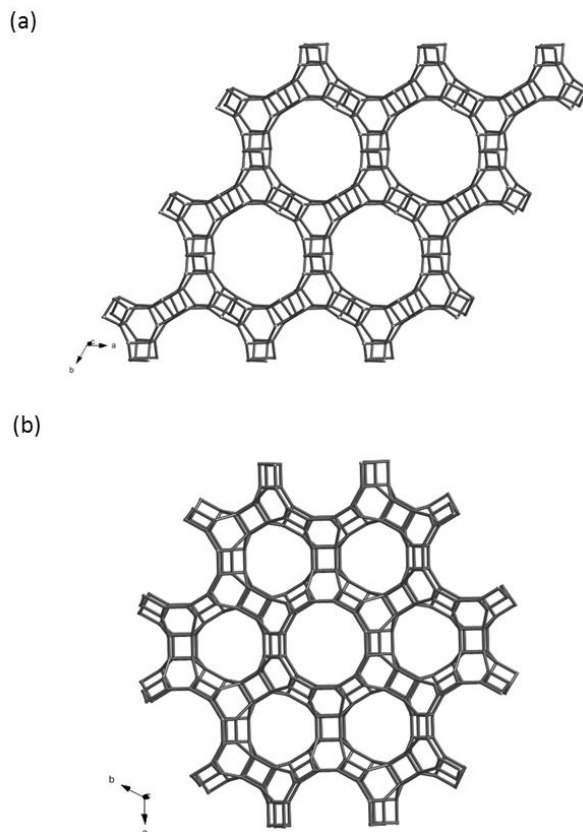


Figure 15. The aluminophosphate VPI-5 (a) and the magnesium aluminophosphate DAF-1 (b) show interesting tetrahedral frameworks not yet observed as silicates.

Chemically, zeotypic AIPO frameworks have a higher degree of ionic character than that of zeolites,⁵⁴ and can be considered in terms of phosphate ions linked by metal cations. As well as influencing the ability of Al to increase its coordination, this greater ionicity affects patterns of framework substitution. The most important are of divalent metal cations for Al and of Si for P (or for P and Al).

The substitution of M^{2+} for Al^{3+} has a strong effect on the synthesis. For crystallisations involving positively charged SDAs, a negative charge results on the framework that balances that on the SDA. No coordination of anions is required and the synthesis is commonly accelerated. In many cases, MAPOs as yet without AIPO

analogues have been prepared in this way (such as the large pore DAF-1 (Figure 15)⁵⁵). As is the case in the aliovalent substitution of Si^{4+} by Al^{3+} in zeolites, that of Al^{3+} by M^{2+} , followed by removal of the charged SDA, can give rise to anionic protonated frameworks that permit ion exchange. When M can undergo oxidation to the trivalent state (Mn, Fe, Co) the additional possibility of framework oxidation arises, which is of catalytic significance. This type of redox chemistry is not observed for zeolites.

Silicoaluminophosphates (SAPOs) are derived from AIPOs by two mechanisms.⁵⁶ In the first, P is replaced by Si, leaving a net negative charge on the framework that is charge-balanced by a proton after template removal ($\text{H}_x\text{AlP}_{1-x}\text{Si}_x\text{O}_4$). This bridging hydroxyl Si-OH-Al is usually less strongly acidic than those found in the H^+ form of aluminosilicate zeolites. The second mechanism of substitution involves the coupled replacement of Al and P by two Si atoms. This cannot happen in isolation, due to the unfavorability of Si surrounded by (next) nearest neighbor P atoms, but can be considered to occur when direct Si P substitution has resulted in enough Al sites fully surrounded by Si, and therefore able to be substituted without the formation of Si-O-P linkages. This second type of substitution results in the formation of aluminosilicate islands. When prepared in the protonated form, $\text{H}_x\text{Al}_y\text{Si}_y(\text{P}_{1-x}\text{Si}_x)\text{O}_4$, some of the protons associated with these islands will have acidities similar to those of zeolites. Among the SAPOs that have been prepared (not all AIPOs are amenable to this substitution) the SAPO-34 (CHA) structure is worthy of particular mention, because its acidity, stability and catalytic selectivities (a consequence of its structure) makes it of interest as a commercial catalyst, for example for the methanol-to-olefins synthesis.⁵⁷

4.5 Organozeolites

Considerable synthetic efforts have been made to include organic groups in place of oxygen atoms in the zeolite framework, with the goal of modifying the zeolite properties to make it more hydrophobic. Results are summarized in the review of Tatsumi.⁵⁸ It is clear that for some zeolites, such as zeolite Beta, high levels of substitution are possible by direct synthesis using methylene-bridged siloxanes $\text{O}_3\text{Si-CH}_2\text{-SiO}_3$. This has research been overwhelmed in the last decade by the large number of hybrid metal organic frameworks that are built exclusively using organic linkers, so it is likely that the initial idea will ultimately find expression in a much wider range of materials.

5. Post synthetic modification of structure

Once prepared, zeolites exhibit a wide range of chemical behavior. Extra-framework cations, usually hydrated, are readily ion exchanged, giving zeolites their important applications as, for example, detergent builders for water softening or in the removal of radioactive Cs^+ cations from low level radioactive waste. Water

molecules can be removed and re-adsorbed, as can other adsorbate molecules, giving rise to zeolites' important applications as sorbents and catalysts. Furthermore, zeolites can act as hosts for many different forms of intra-zeolitic solid state chemistry, where their main function is as stable and well-ordered hosts. In this section we consider the effects on zeolite structure of heating and applying pressure, and also of modification of the framework composition by reactions at high temperature in the presence of steam and ammonia.

5.1 A word on cation exchange

The cation exchange properties of zeolites are of great importance, and vary strongly from one structure to the next, in terms of both selectivities and extent of ion exchange due to strong effects of structure on cation exchange, and vice versa. For many low silica zeolites, complete ion exchange is possible (for example with zeolites A, X, chabazite, Rho), whereas for some, such as zeolite L, it is possible to exchange extra-framework cations in the main channels but not those held within the cancrinite cages. For flexible zeolites, the ion exchange can cause structural effects. Upon ion exchange with K^+ , Rb^+ and Cs^+ , for example, the zeolite Natrolite is found to exhibit volume expansion of 10, 16 and 18 %, the largest observed for zeolites. This arises through the flexibility of the link between natrolite chains, so that the linking TÔT angle changes from 176° to 130° and the channel cross-section changes from strongly elliptical to nearly circular as hydrated sodium cations are replaced by larger hydrated cesium cations.⁵⁹ In maximum Al zeolite P, it is found that replacement of sodium with calcium causes a structural change that is so thermodynamically important that there is a miscibility gap in the Na-Ca MAP solid solution, so that for most of the compositional range two different phases exist.⁶⁰

5.2 The structural response to increased temperature, pressure and adsorption

The response of as-prepared zeolites to increased temperature depends on whether they contain inorganic or organic cations. For those that contain only inorganic cations (including natural zeolites) heating results in loss of zeolitic water with resultant effects on the location of cations and the position of framework atoms, whereas for those containing organic molecules heating (usually in air or O_2) results in decomposition and combustion of the organic. If the organic is a cation, and fulfils a charge balancing role, calcination results in preparation of the H-form of the zeolite. Ion-exchanged forms of zeolites also show reversible dehydration upon heating, except for the ammonium forms, which liberate ammonia upon heating at around 300 – 400 °C to leave the H-form, along with framework dealumination, the mechanism and structural consequences of which are described in the following section. In addition to bringing about dehydration, deammoniation and template

removal, thermal treatment can also bring about intrazeolitic cation migration in dehydrated zeolites as they move to more favorable sites.

As well as these thermally activated transformations that occur with increasing temperature, thermal motion of framework and extra framework atoms increases. This leads to the generally observed phenomenon of negative thermal expansivity, for example as transverse vibrations of oxygen atoms leads to shorter time-averaged T-O-T bond lengths.⁶¹ Some zeolitic structures undergo displacive (and therefore reversible) phase transitions upon temperature increase, as the symmetry increases as a result of these framework vibrations: silicalite-1 changes from monoclinic (24 T-sites) to orthorhombic (12 T-sites), for example.⁶² Finally, at elevated temperatures that vary with framework type and overall composition, crystallinity is lost.⁶³

The structural role of dehydration is to reduce the coordination of cations, which then move to achieve better coordination by framework oxygen atoms and so lower the overall energy. In rigid frameworks, this results in cation migration either closer to framework oxygen atoms or to different cation sites. The latter was observed upon heating Ni-Y, where Ni²⁺ cations migrate from SII sites in the sodalite cage to SI D6R sites to achieve better coordination.⁶⁴ There are many such examples of this type of behaviour. In zeolite potassium L partially exchanged with lanthanide cations, for example, we have observed the migration of lanthanide ions from the main channel to sides in side pockets upon dehydration, followed by their high temperature migration (700 °C) to cancrinite cages, where they replace K⁺ cations.⁶⁵ This requires motion of both La³⁺ (radius *ca.* 1.2 Å) and K⁺ (1.5 Å) through strongly non-planar 6MRs of the cancrinite cage suggesting strong framework vibrations or bond breaking occur under these conditions.

The flexibility of zeolite frameworks is further illustrated by structures that show marked changes in framework geometry and symmetry in order to achieve better coordination of cations when they lose their waters of hydration. In the potassium form of natrolite, for example (represented here for the potassium gallosilicate PST-1), removal of water of hydration results in the same type of rotation and twisting of the 4-1 chains observed upon ion exchange of hydrated alkali metal cations of different sizes into natrolite referred to earlier, in this case reducing the size of the 8MR openings and improving cation coordination (Figure 16a).⁶⁶

The effect of temperature and dehydration of cationic forms of the flexible zeolite Rho are also well studied. The framework of as-prepared, hydrated Cs,Na-Rho has Im-3m symmetry at room temperature, as shown in figure 2, as does the H-form of Rho at this temperature. Upon cooling, the framework distorts to I-43m symmetry, indicating this is the lowest energy form.⁶⁷ Another type of framework behavior is exhibited by the hydrated Cd²⁺-form of zeolite Rho on dehydration. In the hydrated state the hydrated Cd²⁺ ions occupy distorted 8MR sites in the acentric I43m

structure, where they also achieve coordination with water molecules in the α -cage, but upon dehydration at high temperature these cations move into the α -cage, where they find better coordination at 6MR sites⁶⁸ (Figure 16b).

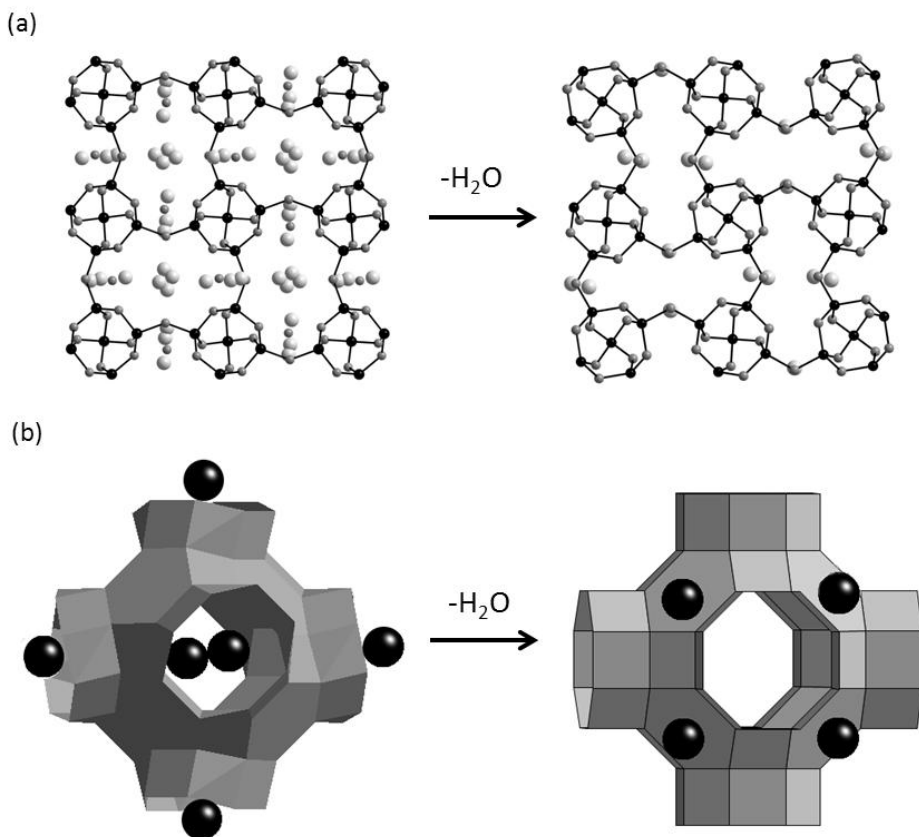


Figure 16. Zeolite frameworks can be flexible: in (a) the framework of natrolite distorts upon dehydration of the K^+ -form and in (b) at high temperature removal of water hydration from the Cd^{2+} ion in zeolite Rho results in migration of Cd^{2+} to 6MR sites in the α -cage and symmetry change of the framework.

If, in place of removal of water by heating, zeolites are put under high pressures (~ 1 GPa) by water-containing media, then reversible and irreversible structural changes can occur. For sodium aluminosilicate natrolite, for example, reversible hydration results initially in volume expansion as water molecules are taken up by the

structure, whereas in a sodium gallosilicate natrolite irreversible hydration results in a significant rearrangement of extra framework cations.⁶⁹

Many examples are known where cation migration and framework motion results from the adsorption of molecules other than water, and over wide temperature and pressure ranges. The flexible small pore sodium natrolite, for example, opens to take up CO₂ at 110°C at 1.5 GPa of CO₂.⁷⁰

5.3 Modification of the framework composition

The strong acidity of zeolites, together with their regular structure, is responsible for their widespread use as catalysts. The acidity derives from Brønsted acid sites, bridging hydroxyls, as well as Lewis acidic extra framework aluminium species. The preparation of zeolites with both types of acid sites is possible by the deammoniation of ammonium exchanges zeolites. As well as resulting in loss of ammonia and preparation of protonic form the process results in loss of framework aluminium, which is readily observed by solid state ²⁹Si and ²⁷Al MAS NMR (Magic-Angle Spinning Nuclear Magnetic Resonance). For zeolites with high Al contents, this usually results in loss of the structure. For some of these, with intermediate Si/Al ratios, the H-form produced by this process can be stabilized by deammoniating under ‘deep-bed calcination’ conditions, or by heating under high H₂O vapor pressures, or ‘steaming’. Under these conditions, it is possible for Si to migrate to fill some of the vacancies and the framework Si/Al ratio to be increased while the crystal structure is retained. This migration of silicon results in the development of secondary mesoporosity, which improves molecular diffusion in these materials. This approach is applicable to many zeolites, including most importantly zeolite Y, where ultrastabilised Y prepared in this way is sufficiently stable to withstand the extreme conditions of catalysis and regeneration found in fluidized bed catalytic crackers. Figure 17 illustrates the NMR spectra observed during the same process occurring during the steaming of zeolite Rho.

The details of the mechanism of dealumination have been widely investigated, particularly by solid state NMR. Spectroscopy on samples allowed to rehydrate after heating reveals the presence of at least three types of Al species in dealuminated zeolites in addition to tetrahedral framework Al. These are shown in the spectra of dealuminated Rho in Figure 17. Very similar spectra have been observed for dealuminated Y zeolite. The extra Al signals can be attributed to octahedral Al (possibly 2 signals), fivefold coordinated Al and tetrahedral extra-framework Al species (EFAL) which do not have the high symmetry of those within the framework sites and give broad signals.

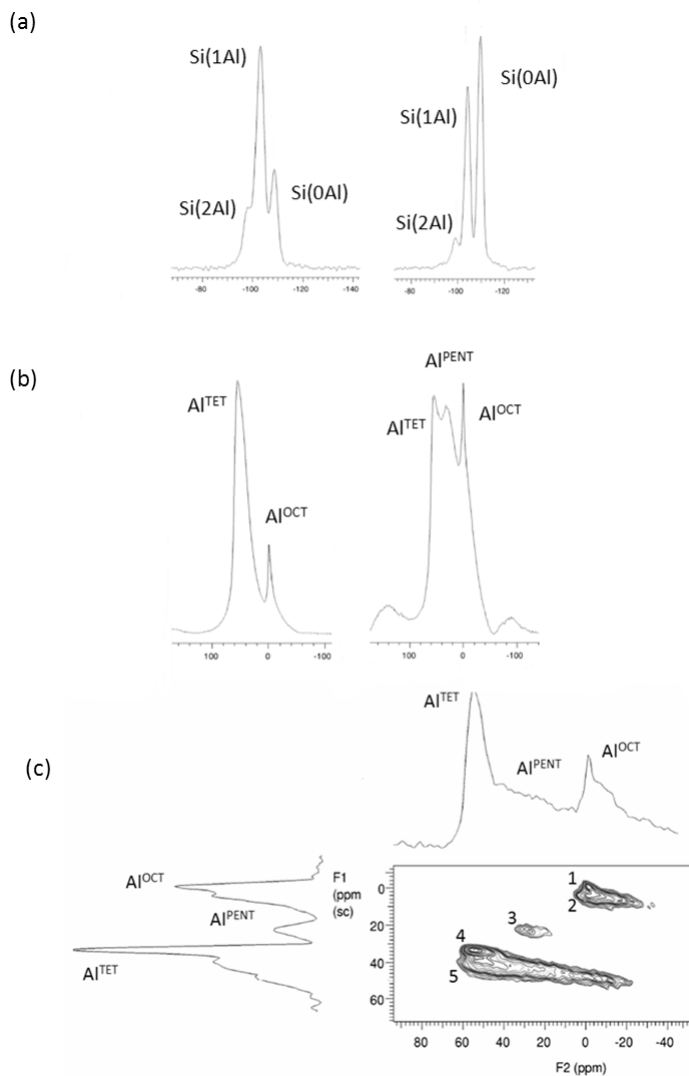
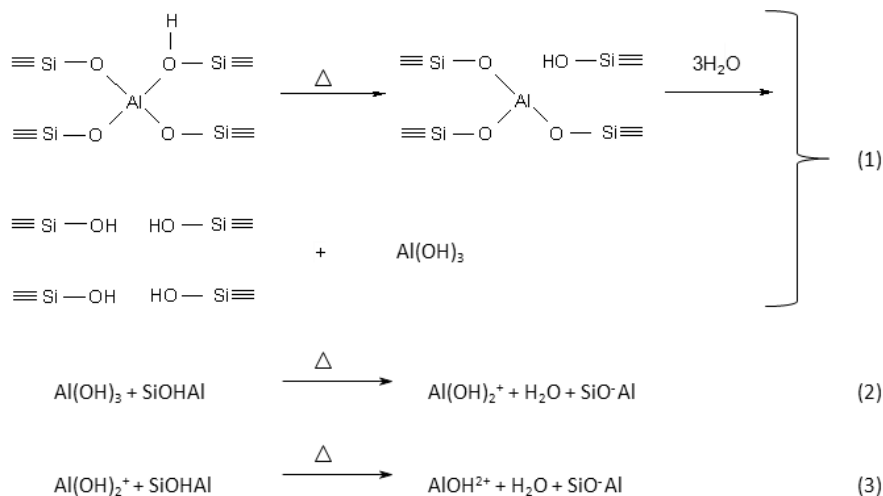


Figure 17. (a) ^{29}Si MAS NMR, (b) ^{27}Al MAS NMR and (c) $3Q$ ^{27}Al MAS NMR of H-Rho before (left) and after (right) intensive dealumination (a) reveals an increased framework Si/Al ratio of 3.9 to 7.1, and (b) and (c) the change in a significant part of the Al from framework tetrahedral site to extra framework 6-fold, 5-fold and 4-fold (OCT, PENT, TET) coordinated species. (M. Lozinska, unpublished results).



Scheme 1. Suggested mechanism of dealumination following deammoniation at heating to high temperature.⁷¹

Two recent studies shed light on the nature of these additional species. Combined *in situ* X-ray diffraction and spectroscopy⁷¹ indicate that during the deammoniation of zeolite Y some Al (< 10%) is lost from framework sites and migrates to site I' in the sodalite cage (Figure 6b). The major part of the dealumination occurs upon cooling and rehydration, however, when the occupancy of the sodalite cage site I' increases. This corresponds to migration of around 30% of the original framework Al there. In a separate study,⁷² state-of-the-art ²⁷Al NMR of samples steamed at different temperatures (500 – 700 °C) and measured after cooling and rehydration reveal that the EFAL signals develop in the progression: octahedral, five-fold, tetrahedral, and that these can be attributed to Al(OH)₃, Al(OH)₂⁺ and AlOH²⁺ species coordinated to oxygen atoms bound to framework Al species, according to Scheme 1. These species are thought to be able to be further coordinated by water molecules, so that the tetrahedral EFAL is (ZeoO)₂Al(OH)(OH₂). Taken all together, a picture arises of Al species removed from the lattice in two stages, during deammoniation and also during rehydration and hydrolysis at defect sites upon cooling. These Al species which remain bound to the lattice, and can adsorb water molecules, can have 6, 5 or 4-fold coordination, depending on the severity of the dealumination conditions.

In some cases, such as zeolite L, structures are not amenable to ultrastabilisation of this kind. Furthermore, it is very difficult to remove all Al in this way, even from zeolite Y. To prepare Y with very high Si/Al ratio, or as a pure silica, chemical treatment is required, either with SiCl_4 in the gas phase or with ammonium hexafluorosilicate in solution,^{73,74} giving direct replacement of Al with Si. Direct substitutions of this kind can give hydrophobic materials without defects or mesopores.

Similarly, trivalent B^{3+} and Ga^{3+} cations leave the zeolitic framework during hydrothermal treatment. Indeed, both are removed more easily than Al. The process has been particularly well studied in borosilicates, such as B-Beta, due to the amenability of ^{11}B and ^{29}Si to NMR. Boron is observed to move from tetrahedral to trigonal coordination upon preparation in the H-form, and is then removed from framework positions by stepwise hydrolysis of B-O-Si bonds.⁷⁵ It can be removed as boric acid when the solid is put into contact with aqueous solution. In addition, these cations can be replaced by other cations via solution reactions: in this way boron can be replaced by aluminium, imparting stronger acidity.

As described previously, germanosilicates have become of great interest because of the effect of inclusion of germanium in the crystallization of novel structures with large pores and low framework densities. However, germanium is expensive, and germanosilicates have low hydrothermal stability because Ge readily leaves framework sites. For these reasons, Gao et al⁷⁶ investigated the solution replacement of Ge by Al in solution, and found that around 50% of the Ge of a germanosilicate zeolite Beta C could be replaced by framework Al by treatment with polyaluminiumhydroxide chloride solution, whilst leaving the organic SDA within the pores (i.e. without calcination). The extent to which this is possible for other germanosilicates is under investigation.

Although most efforts in modification of the framework composition have concentrated on the framework cations, there has also been success in replacing a large fraction of the framework oxygen atoms of zeolite Y with NH groups by high temperature treatment with ammonia, whilst retaining crystallinity and porosity. The progress of this reaction is readily monitored by ^{29}Si NMR, and it is found that the replacement of Si-O-Al to give Si-NH-Al is favored over the replacement of Si-O-Si to give Si-NH-Si at 750 – 800 °C, but there is no preference at higher temperatures.⁷⁷ Once prepared, these solids are kept dry to prevent reaction upon adsorption of water.

6. Summary and Outlook

The structural variety and compositional range of zeolites has increased greatly from that of the known aluminosilicate zeolites and their earliest synthetic analogues, as a result of a major synthetic effort lasting over 40 years. Also,

appreciation of the direct link between application and structure has driven an examination of the structure of these solids on the long and short range as detailed and intense as for any family of materials. Challenges remain, however, including the important targets of stable materials with pore sizes above 1 nm, enantiopure, chiral zeolites and structures with well- defined location of aluminium framework cations,⁷⁸ and consequently active site distributions. In addition, there is considerable current interest in the preparation of zeolites with characteristic morphologies, including nanoparticles⁷⁹ (for example as precursors for thin films) or as thin sheets a few unit cells deep, separated by mesoporous galleries.⁸⁰ The related discovery that some zeolites form via layered precursors,⁸¹ which can be isolated and delaminated and the laminae re-assembled, offers other routes to high surface area catalysts with ordered zeolite-type behaviour. Taken together, these areas offer new and important fields of investigation into zeolite structural chemistry.

References

- [1] Breck, D. W., *Zeolite Molecular Sieves*, Wiley, New York (1974)
- [2] *Handbook of Porous Solids* Eds. Schüth, F., Sing, K. S. W. and Weitkamp, J. Wiley-VCH, New York (2002).
- [3] *Handbook of Zeolite Science and Technology*, Eds. Auerbach, S. M., Carrado, K. A. and Dutta, P. K., Marcel Decker, New York (2003).
- [4] *Introduction to Zeolite Science and Practice Studies in Surface Science and Catalysis* Eds. Čejka, J., van Bekkum, H., Corma A., & Schüth, F., Ch. 5, 137-179 (2007).
- [5] Wright, P. A. *Microporous Framework Solids* RSC Publishing, Cambridge (2008)
- [6] *Zeolites and Catalysis: Synthesis, Reactions and Applications* Eds. Čejka, J., Corma, A., and Zones, S. I. Wiley-VCH (2010).
- [7] Liebau, F. *Structural Chemistry of Silicates: Structure, Bonding and Classification*, Springer-Verlag, Berlin, pp. 14-30 (1985).
- [8] Wragg, D. S., Morris, R. E. and Burton, A. W. Pure silica zeolite-type frameworks: A structural analysis. *Chem. Mater.* **20**, 1561-1570 (2008).
- [9] de Man, A. J. M., van Santen, R. A. The relation between zeolite framework structure and vibrational spectra. *Zeolites* **12**, 269-279 (1992).
- [10] Treacy, M. M. J., Rivin, I., Balkovsky, E., Randall, K. H. and Foster, M. D. Enumeration of periodic tetrahedral frameworks. II. Polynodal graphs. *Micropor. Mesopor. Mater.* **74**, 121-132 (2004).
- [11] Database of Zeolite Structures, Structure Commission of the International Zeolite Association, <http://www.izastructure.org/databases/>

- [12] Baur, W. H. *Am. Mineral.* **49**, 697-704 (1964).
- [13] Delprato, F. et al. Synthesis of new silica-rich cubic and hexagonal faujasites using crown ether-based supramolecules as templates. *Zeolites*, **10**, 546-552 (1990).
- [14] Newsam, J. M., Treacy, M. M. J., Vaughan, D. E. W., Strohmaier, K. G. and Mortier, W. J. The structure of zeolite ZSM-20 - mixed cubic and hexagonal stackings of faujasite sheets. *J. Chem. Soc., Chem. Commun.* 493-495 (1989).
- [15] Czjzek, M., Jovic, H., Fitch, A. N., and Vogt, T. Direct determination of proton positions in D-Y and H-Y zeolites samples by neutron powder diffraction. *J. Phys. Chem.*, **96**, 1535-1540 (1992).
- [16] Adams, C. J., Araya, A., Cunningham, K. J., Franklin, K. R. and White, I. F. Measurement and prediction of Ca-Na ion-exchange equilibrium in maximum aluminium P (MAP), a zeolite with the GIS framework topology. *J. Chem. Soc., Faraday Trans.* **93**, 499-503 (1997).
- [17] Gaffney, T. R. Porous solids for air separation. *Curr. Opin. Solid State Mater. Sci.* **1**, 69-75 (1996).
- [18] Barrer, R. M. *Hydrothermal chemistry of zeolites*, Acad. Press, London, 1982.
- [19] Newsam, J. M., Treacy, M. M. J., Koetsier, W. T. and de Gruyter, C. B. Structural characterisation of zeolite Beta. *Proc. Roy. Soc. Lond. A*, **420**, 375-405 (1988).
- [20] Kokotailo, G. T., Lawton, S. L., Olson, D. H. and Meier, W. M. Structure of synthetic zeolite ZSM-5 *Nature*, **272**, 437-438 (1978).
- [21] Briscoe, N. A., Johnson, D. W., Shannon, M. D., Kokotailo, G. T. and McCusker, L. B. The framework topology of zeolite EU-1. *Zeolites*, **8**, 74-76 (1988).
- [22] Shannon, M. D., Casci, J. L., Cox, P. A. and Andrews, S. J. Structure of the 2-dimensional medium-pore high-silica zeolite NU-87. *Nature* **353**, 417-420 (1991).
- [23] Hong, S. B. et al. : Synthesis, structure solution, characterization, and catalytic properties of TNU-10: A high-silica zeolite with the STI topology. *J. Am. Chem. Soc.* **126**, 5817-5826 (2004).
- [24] Lobo, R F. and Davis, M. E. CIT-1 - a new molecular sieve with intersecting pores bounded by 10-rings and 12-rings. *J. Am. Chem. Soc.* **117**, 3764-3779 (1995).
- [25] Dorset, D. L., Weston, S. C. and Dhingra, S. S. Crystal structure of zeolite MCM-68: A new three-dimensional framework with large pores *J. Phys. Chem. B*, **110**, 2045-2050 (2006).
- [26] Simancas, R. et al. Modular Organic Structure-Directing Agents for the Synthesis of Zeolites. *Science*, **330**, 1219-1222 (2010).
- [27] Lobo R. F. et al. Characterisation of the extra-large-pore zeolite UTD-1. *J. Am. Chem. Soc.* **119**, 8474-8484 (1997).

- [28] Burton, A. et al. SSZ-53 and SSZ-59: Two novel extra-large pore zeolites. *Chem. Eur. J.*, **9**, 5737-5748 (2003).
- [29] Gramm, F. et al. Complex zeolite structure solved by combining powder diffraction and electron microscopy *Nature* **444**, 79-81 (2006).
- [30] Baerlocher, C. et al. Structure of the polycrystalline zeolite catalyst IM-5 solved by enhanced charge flipping. *Science*, **315**, 1113-1116 (2007).
- [31] Derouane, E. G., Gabelica, Z. A novel effect of shape selectivity - molecular traffic control in zeolite ZSM-5. *J. Catal.* **65**, 486-489 (1980).
- [32] Shannon, R. D. Revised effective ionic radii and systematic studies of interatomic distances in halides and chalcogenides. *Acta Cryst.*, **A32**, 751-767 (1976).
- [33] Cambor, M. A., Villaescusa, L. A. and Diaz-Cabanas, M. -J. Synthesis of all-silica and high-silica molecular sieves in fluoride media. *Top. Catal.* **9**, 59-76 (1999).
- [34] Baerlocher, C. et al. Ordered silicon vacancies in the framework structure of the zeolite catalyst SSZ-74. *Nature Mater.* **7**, 631-635 (2008).
- [35] Corma, A., Rey, F., Rius, J., Sabater, M. J., and Valencia, S. Supramolecular self-assembled molecules as organic directing agent for synthesis of zeolites. *Nature*, **431**, 287-290 (2004).
- [36] Cambor, M.A., Corma, A. and Valencia, S. Spontaneous nucleation and growth of pure silica zeolite-beta free of connectivity defects. *Chem. Commun.* 2365-2366 (1996).
- [37] Strohmaier, K. G. and Vaughan, D. E. W. Structure of the first silicate molecular sieve with 18-ring pore openings, ECR-34. *J. Am. Chem. Soc.* **125**, 16035-16039 (2003).
- [38] McCusker, L. B., Grosse-Kunstleve, R. W., Baerlocher, Ch., Yoshikawa, M. and Davis, M. E. Synthesis optimization and structure analysis of the zincosilicate molecular sieve VPI-9 *Micropor. Mater.* **6**, 295-309 (1996).
- [39] Park, M. B., Cho, S. J. and Hong, S. B. Synthesis of aluminosilicate and gallosilicate zeolites via a charge density mismatch approach and their characterisation. *J. Am. Chem. Soc.* **133**, 1917-1934 (2011).
- [40] Perego, C., Carati, A., Ingallina, P., Mantegazza, M. A. and Bellussi, G. : Production of titanium containing molecular sieves, and their application in catalysis *Appl. Catal. A*, **221**, 63-72 (2001).
- [41] Blasco, T. et al. Unseeded synthesis of Al-free Ti-beta zeolite in fluoride medium: A hydrophobic selective oxidation catalyst *Chem. Commun.* 2367-2368 (1996).
- [42] Anderson, M. W. et al. Structure of the microporous titanosilicate ETS-10. *Nature*, **367**, 347-351 (1994).

- [43] Corma, A., Nemeth, L. T., Renz, M. and Valencia, S. Sn-zeolite beta as a heterogeneous chemoselective catalyst for Baeyer-Villiger oxidations. *Nature*, **412**, 423-425 (2001).
- [44] Conradsson, T., Dadachov, M. S. and Zou, X. D. Synthesis and structure of $(\text{Me}_3\text{N})_6[\text{Ge}_{32}\text{O}_{64}](\text{H}_2\text{O})_{4.5}$, a thermally stable novel zeotype with 3D interconnected 12-ring channels. *Micropor. Mesopor. Mater.* **41**, 183-191 (2000).
- [45] Corma, A., Navarro, M. T., Rey, F., Rius, J. and Valencia, S. Pure polymorph C of zeolite beta synthesized by using framework isomorphous substitution as a structure-directing mechanism: *Angew. Chem. Int. Ed.* **40**, 2277-2280 (2001).
- [46] Paillaud, J. L., Harbuzaru, B., Patarin, J. and Bats, N. Extra-large-pore zeolites with two-dimensional channels formed by 14 and 12 rings. *Science*, **304**, 990-992 (2004).
- [47] Corma, A., Diaz-Cabanas, M. J., Jorda, J. L., Martinez, C. and Moliner, M. High-throughput synthesis and catalytic properties of a molecular sieve with 18- and 10-member rings. *Nature*, **443**, 842-845 (2006).
- [48] Jiang, J. X., Yu, J. H. and Corma, A. Extra-Large-Pore Zeolites: Bridging the Gap between Micro and Mesoporous Structures. *Angew. Chem. Int. Ed.* **49**, 3120-3145 (2010).
- [49] Brunner, G. O. and Meier, W.M Framework density distribution of zeolite-type tetrahedral nets. *Nature*, **353**, 146-147 (1989).
- [50] O'Keeffe, M. and Yaghi, O. M. Germanate zeolites: Contrasting the behavior of germanate and silicate structures built from cubic T_8O_{20} units (T = Ge or Si). *Chem. Eur. J.* **5**, 2796-2801 (1999).
- [51] Sun, J. L. *et al.* The mesoporous chiral zeolite. *Nature*, **458**, 1154-1157 (2009).
- [52] Wilson, S. T., Lok, B. M., Messina, C. C., Cannan, T. R. and Flanigen, E. M. Aluminophosphate molecular sieves - a new class of microporous crystalline solids. *J. Am Chem. Soc.* **104**, 1146-1147 (1982).
- [53] Davis, M.E., Saldarriaga, C., Montes, C., Garces, J. and Crowder, C. A molecular sieve with eighteen-membered rings. *Nature*, **331**, 698-699 (1988).
- [54] Cora, F. *et al.* Modelling the framework stability and catalytic activity of pure and transition-metal doped zeotypes. *J. Solid State Chem.* **176**, 496-529 (2003).
- [55] Wright, P. A. *et al.* Synthesis and structure of a novel large-pore magnesium containing aluminophosphate (DAF-1). *J. Chem. Soc., Chem. Commun.* 633-635 (1993).
- [56] Chen, J. S. *et al.* SAPO-18 catalysts and their Bronsted acid sites. *J. Phys. Chem.* **98**, 10216-10224 (1994).
- [57] Stocker, M. Methanol-to-hydrocarbons: catalytic materials and their behaviour. *Micropor. Mesopor. Mater.* **29**, 3-48 (1999).

- [58] Yamamoto, K. and Tatsumi, T. ZOL: A new type of organic-inorganic zeolite containing organic framework. *Chem. Mater.* **20**, 972-980 (2008).
- [59] Lee, Y. J., Lee, Y. M. and Seoung, D. Natrolite may not be a 'soda-stone' any more: Structural study of fully K-, Rb- and Cs-exchanged natrolite. *Am. Mineral.* **95**, 1636-1641, (2010).
- [60] Albert, B. R. and Cheetham, A. K. A synchrotron X-ray powder diffraction study of highly crystalline low-silica zeolite P during Na-Ca ion exchange. *Micropor. Mesopor. Mater.* **34**, 207-211 (2000).
- [61] Lightfoot, P., Woodcock, D. A., Maple, M. J., Villaescusa, L. A. and Wright, P. A. The widespread occurrence of negative thermal expansion in zeolites. *J. Mater. Chem.* **11**, 212-216 (2001).
- [62] Fyfe, C. A., Kennedy, G. J., Kokotailo, G. T., Lyster, J. R. and Fleming, W. W. The effect of temperature on the Si-29 Magic Angle spinning NMR spectrum of highly siliceous ZSM-5. *J. Chem. Soc., Chem. Commun.* 740-742 (1985).
- [63] Greaves, G. N., Meneau, F., Majerus, O., Jones, D. G. and Taylor, J. Identifying vibrations that destabilize crystals and characterize the glassy state. *Science*, **308**, 1299-1302 (2005).
- [64] Dooryhee, E. *et al.* A study of cation environment and movement during dehydration and reduction of nickel-exchanged zeolite Y by X-ray absorption and diffraction *J. Phys. Chem.* **95**, 4514-4521 (1991).
- [65] Wright, P. A. *Microporous Framework Solids* RSC Publishing, Cambridge (2008), pp. 242-243.
- [66] Shin, J. *et al.* PST-1: A synthetic small-pore zeolite that selectively adsorbs H₂. *Angew. Chem. Int. Ed.* **48**, 6647-6649 (2009).
- [67] Parise, J. B., Xing, L. and Corbin, D. R. Flexibility of the zeolite Rho framework - relocation of cadmium accompanying transformation of the unit cell at high temperatures *J. Chem. Soc. Chem. Commun.* 162-163 (1991).
- [68] Parise, J. B., Gier, T. E., Corbin, D. R. and Cox, D. E. Structural changes occurring upon dehydration of zeolite Rho - A study using neutron powder diffraction and distance-least-squares structural modelling. *J. Phys. Chem.* **88**, 1635-1640 (1984).
- [69] Lee, Y., Vogt, T., Hriljac, J. A., *et al.* Non-framework cation migration and irreversible pressure-induced hydration in a zeolite. *Nature.* **420**, 485-489 (2002).
- [70] Lee, Y.; Liu, D., Seoung, D., *et al.* Pressure- and heat-induced insertion of CO₂ into an auxetic small-pore zeolite. *J. Am. Chem. Soc.* **133**, 1674-1677 (2011).
- [71] Agostini, G. *et al.* In situ XAS and XRPD parametric Rietveld refinement to understand dealumination of Y zeolite catalyst. *J. Am. Chem. Soc.* **132**, 667-678 (2010).

- [72] Yu, Z. *et al.* Insights into the dealumination of zeolite HY revealed by sensitivity-enhanced ^{27}Al DQ-MAS NMR spectroscopy at high field. *Angew. Chem. Int. Ed.* **49**, 8657-8661 (2010).
- [73] Beyer, H. K. *et al.* Preparation of high-silica faujasites by treatment with silicon tetrachloride. *J. Chem. Soc., Farad. Trans I*, **81**, 2889-2901 (1985).
- [74] Skeels, G. W. and Breck, D. W. in *Proc. 6th Int. Zeol. Conf.*, Eds. Olson, D. and Bisio, A., Butterworths, Guildford, 1984, pp. 87.
- [75] Koller, H., Fild, C. and Lobo, R.F Variable anchoring of boron in zeolite beta. *Micropor. Mesopor. Mater.* **79**, 215-224 (2005).
- [76] Gao, F. *et al.* Framework stabilisation of Ge-rich zeolites via post-synthesis alumination. *J. Am. Chem. Soc.* **131**, 16580-16586 (2009).
- [77] Dogan, F. *et al.* Searching for microporous, strongly basic catalysts: experimental and calculated ^{29}Si NMR spectra of heavily nitrogen-doped Y zeolites. *J. Am. Chem. Soc.* **131**, 11062-11079 (2009).
- [78] Pinar, A. B., Garcia, R., Gomez-Hortiguela, L., *et al.* Synthesis of open zeolite structures from mixtures of tetramethylammonium and benzylmethylalkylammonium cations: a step towards driving aluminium location in the framework. *Top. Catal.* **53**, 1297-1303 (2010).
- [79] Tosheva, L., Valtchev, V. P. Nanozeolites: Synthesis, crystallization mechanism, and applications. *Chem. Mater.* **17**, 2494-2513 (2005).
- [80] Choi, M., Na, K., Kim, J., *et al.* Stable single-unit-cell nanosheets of zeolite MFI as active and long-lived catalysts. *Nature*. **461**, 246-249 (2009).
- [81] Ogino, I., Nigra, M. M., Hwang, S. J., *et al.* Delamination of layered zeolite precursors under mild conditions: synthesis of UCB-1 via fluoride/chloride anion-promoted exfoliation. *J. Am. Chem. Soc.* **133**, 3288-3291 (2011).

Basic principles of zeolite synthesis

Manuel MOLINER

Instituto de Tecnología Química, Universidad Politécnica de Valencia-Centro Superior de Investigaciones Científicas (UPV-CSIC), Valencia, E-46022, Spain

Abstract

Zeolites are microporous materials with large impact in the chemical industry. The combination of excellent physical-chemical properties, high thermal stability, and the capability of tailoring their textural properties (such as size and shape of pores and cavities) offer an excellent number of opportunities to apply those materials in industrially relevant chemical processes. In this chapter, a general overview of the most interesting achievements in zeolite manufacture in the last sixty years is presented.

1. Introduction

Zeolites are microporous materials formed by TO_4 tetrahedra ($\text{T}=\text{Si}, \text{Al}\dots$), interconnected by the oxygen atoms, creating pores and cavities with uniform size and shape in the molecular dimension range ($\sim 3\text{-}15 \text{ \AA}$). This particular characteristic allows discriminating molecules with precisions less than 1 \AA .¹ Then, the opportunity to create zeolitic structures with different framework topology, and also different chemical composition have allowed their application in diverse areas, such as separation, gas adsorption, ion exchange and catalysis, and more recently, biomedicine and electronics.²

Since the very first description of hydrothermal synthesis of zeolites achieved in the laboratory by Barrer in 1940s,^{3,4} the scientific and industrial interest in the field increased. A large number (close to 200) of different new structures have been discovered since then.⁵

Principally, zeolites can be synthesized in aqueous media under hydrothermal conditions (temperatures between 100°C and 200°C) in the presence of organic and/or inorganic cations and a mobilizing agent. A large number of variables influences the hydrothermal crystallization of molecular sieves, and determines the kinetics and the final crystalline phases formed. Despite the important efforts to rationalize the preparation of zeolites,⁶ the connection between the structure formed and the initial synthesis variables is not fully understood due to the complexity of the synthesis mechanism and the metastable nature of zeolites.


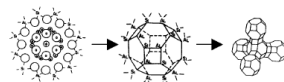
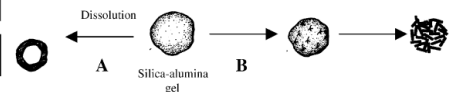
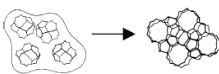

In the present chapter, a general overview of the basic principles in zeolite synthesis is presented. First, proposed synthesis mechanisms are quickly summarized, followed by a revision of the determinant variables and their influence on zeolite

crystallization. Finally, some considerations for the potential scale-up of zeolites in commercial production are presented.

2. Zeolite synthesis mechanisms

Several mechanisms have been proposed for the zeolite growth since the discovery of the first synthetic zeolite in a laboratory. As a general approximation, they are based on a phase transformation of the initial reactants in amorphous form towards a crystalline microporous product, by means of solution-mediated crystallization or solid transformation. A very nice review discussing the principal proposed mechanisms has been reported by Cundy and Cox.⁷ Next, the main zeolite synthesis mechanisms are briefly introduced.

Table 1. Zeolite growth mechanisms described in the literature. Taken from ref^[7]

Authors (Ref)	System Studied	Scheme
a) Barrer ⁸	Low silica phases	
b) Flanigen ⁹	Na-A, Na-X	
c) Kerr ¹⁰	Na-A	Amorphous solid $\xrightarrow{\text{fast}}$ soluble species(S) (S) + nuclei(or zeolite crystals) $\xrightarrow{\text{slow}}$ zeolite A
d) Zhdanov ¹¹	Na-A, Na-X	<div style="display: flex; justify-content: space-around; align-items: center;"> <div style="border: 1px solid black; padding: 2px;">Amorphous solid phase</div> <div style="font-size: 2em;">↔</div> <div style="border: 1px solid black; padding: 2px;">Liquid phase</div> </div> <div style="display: flex; justify-content: space-around; align-items: center; margin-top: 5px;"> <div style="border: 1px solid black; padding: 2px;">Accumulation of zeolite crystals</div> <div style="font-size: 2em;">←</div> <div style="border: 1px solid black; padding: 2px;">Formation of nuclei</div> </div>
e) Derouane ¹⁴⁻¹⁵	Na, TPA-Si-ZSM-5	<div style="display: flex; align-items: center;"> <div style="border: 1px solid black; padding: 2px; margin-right: 5px;">ZSM-5 nuclei</div> <div style="margin-right: 5px;">↓</div> <div style="border: 1px solid black; padding: 2px; margin-right: 5px;">Zeolite crystallites</div> <div style="margin-right: 10px;">←</div> <div style="text-align: center;"> <p>Dissolution</p>  <p>A Silica-alumina gel B</p> </div> </div>
f) Chang ¹⁶	Na, TPA-Si-ZSM-5	
g) Davis ¹⁷⁻¹⁸	TPA-Si-ZSM-5	

The first possible mechanism for zeolite synthesis was proposed by Barrer et al.⁸ In this early work, they discussed that the aluminosilicates are created by secondary building units, as rings of polyhedra, and not from additions of individual Al or Si tetrahedra (see Table 1a). Years later, Flanigen et al. depicted a complementary

mechanism, where primarily, the crystal growth takes place in the solid phase.⁹ They claimed the formation of a nucleus, where the zeolite growth occurs by means of polymerization and depolymerization reactions performed by the excess of hydroxide ions (see Table 1b).

In 1966, Kerr introduced the hypothesis of the solution-mediated growth mechanism where the amorphous solid is dissolved to soluble species by the sodium hydroxide, leading to deposition of zeolite crystals from those species in solution (see Table 1c).¹⁰ Following the same solution-mediated hypothesis, Zhdanov also reported that zeolite growth takes place from solution phase, but he described a dynamic equilibrium of the amorphous with the liquid phase, that allows the release of soluble species forming the nuclei and the later crystals (see Table 1d).¹¹

The introduction of quaternary ammonium cations as organic structure directing agents (OSDA) in the zeolite synthesis, allowed the preparation of new zeolite structures, as Beta¹² and ZSM-5.¹³ Then, those organic molecules showed new opportunities to study the zeolite growth mechanism. In this sense, Derouane et al. proposed two different pathways depending on the silica source used for the ZSM-5 preparation.^{14, 15} When polymeric silica was employed, they described a “mechanism A”, where small number of nuclei grew following a solution-based scheme (similar to Zhdanov description). In contrast, if monomeric silicates were used, they claimed a “mechanism B”, where large number of nuclei creates small microcrystallites by solid phase transformation (see Table 1e). Chang and Bell, nicely showed the effect of the OSDA in zeolite formation.¹⁶ An initial complex is formed by water molecules around the OSDA, followed by an isomorphous substitution of those water molecules by silicates, forming a clathrate-like silicate. Finally, nucleation occurs by assembling those units in the final crystals (see Table 1f). Davis et al. also showed the initial formation of pre-organized inorganic-organic composites (< 3nm) that leads to the aggregation of those species (see Table 1g).^{17, 18}

The different zeolite formation mechanisms presented provide very interesting information as an initial point in order to try to rationalize the zeolite synthesis. However, the large number of chemical reactions, equilibria, and solubility variations that occur in the gel results in a very complex process. Thus, the stabilization and determination of any zeolite precursors depending on the initial synthesis conditions is a difficult task. The presence of different heteroatom sources, inorganic cations, organic cations with different charge-flexibility-size, mineralizing agents, concentrated-diluted gel, temperature... make very complicate the capacity of controlling the first stage of synthesis at the atomic scale (nucleation) and the subsequent crystal growth. Therefore, despite the control and understanding of the synthesis mechanisms remain the main challenges in zeolite

synthesis, the scientists have achieved numerous guidelines to direct the manufacture of certain types of structures during the last fifty years. Next, the main principles of different chemical variables in the synthesis gel are introduced.

3. Principal chemical variables affecting zeolite synthesis

3.1 Mineralizing agent

The mineralizing agent is the chemical specie that allows increasing the solubility of the silicate or aluminosilicate species, among others, in the synthesis gel by means of dissolution and precipitation.¹⁹ The mineralizing agent acts as a catalyst in those processes, which is consumed during the dissolution of species, and recovered after the zeolite crystallization.

The most extended mineralizing agent is the OH⁻. The hydroxyl anion increases the solubility of silicon and aluminium sources, directing the formation of soluble silicate and aluminate anions [Si(OH)_{4-n}O_nⁿ⁻, Al(OH)₄⁻].

The use of OH⁻ as mineralizing agent, when no OSDA is present in the synthesis gel, usually directs the formation of aluminium-rich zeolites. As an example, aluminium-rich zeolite A (LTA) and zeolite X (FAU) are achieved at pH greater than 12.^{20, 21} In those cases, typically, the OH⁻ source is an alkali-metal hydroxide (NaOH, KOH...), and large amount of positive charges are introduced in the final crystalline solid by those extra-framework small inorganic cations. They must be balanced by the presence of large number of aluminium atoms in the framework. As it will be described later, the introduction of a trivalent atom in the framework, such as Al, introduces a negative charge in the inorganic framework. In contrast, when an OSDA, such as an amine or a quaternary ammonium salt, is introduced in the synthesis gel, the Si/Al ratio is increased. High silica zeolites can be achieved because the organic molecules are filling the zeolite void volume, inserting less positive charges in the final solid, and therefore, less aluminium atoms in the framework are required.^{22, 23}

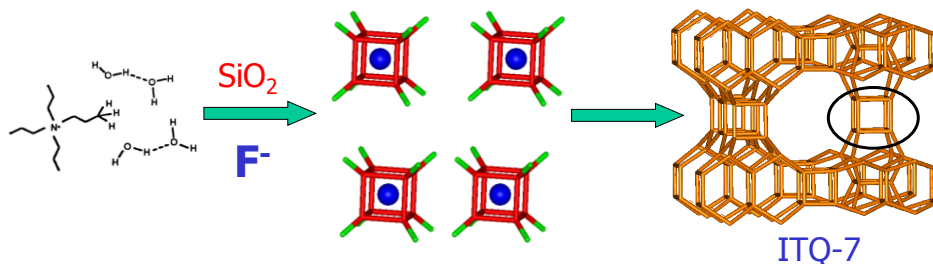


Figure 1. Directing effect of the fluoride anions towards small cages, such as D4R.³³

When the synthesis is carried out at high temperature and high pHs (>10) using OH^- as mineralizing agent, high solubility of species are obtained, but also some thermal stability problems of the OSDA can be observed. In those conditions, the quaternary ammonium cations can suffer the well-known Hoffman degradation. The introduction of fluoride anions as mineralizing agents was a breakthrough in zeolite synthesis. It was first described by Flanigen and Patton in 1978.²⁴ In this case, some fluoro complexes species (TF_6^{n-} , where T is Si, Al...) are formed in the synthesis gel.

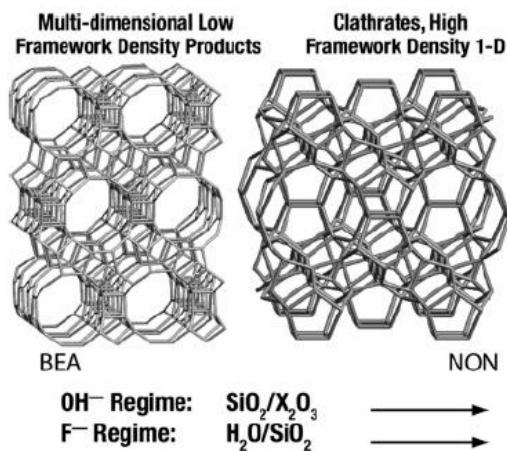


Figure 2. Product selectivity in high silica zeolites depending on the mineralizing agent used in the synthesis. X_2O_3 refers to trivalent lattice substitutes of silicon. Taken from^[34]

One advantage of fluoride route synthesis versus the traditional alkaline one is that the former can be performed at near neutral (or slightly alkaline) pH, increasing the stability of the organic molecules used as OSDA, because their degradation by the Hoffman mechanism is avoided.²⁵ In general, high-silica zeolites synthesized at high pH have a large amount of connectivity defects, due to the requirements for balancing the positive charges of the OSDA molecules precluded in the zeolite pores and cavities.²⁶ However, high-silica zeolites prepared in F^- media present less number of defects than the materials synthesized in OH^- media. This is because fluoride anions direct the formation of small cages (such as double four member rings, D4R, see Figure 1),²⁷ remaining inside of these cages in the final solid and balancing the positive charges of the OSDA. Moreover, the synthesis of zeolites in F^- media tends to form larger crystals than alkaline-mediated preparation. As consequence, the preparation of more perfect crystals in fluoride media (large crystals and less defects-containing) will affect their hydrophobicity/hydrophilicity properties, and then, their adsorption and catalytic properties.²⁸ Since fluoride

media route was reported, several new zeolitic structures have been synthesized.^{29,30,31,32,33}

Recently, Zones and co-workers have reviewed³⁴ the relation between the mineralizing agent used in the synthesis of high-silica zeolites and the zeolite framework density (FD). The FD can be related with the void volume, and therefore, with the micropore volume of zeolites (the lower the FD, the larger the void volume). They have observed low-density zeolite solids when high lattice substitution of silicon (Al, Zn, Be, B) is performed in hydroxide media.³⁵ The general trend in fluoride media is the achievement of open-framework lattices (low framework densities) under concentrated reaction conditions.³⁶ Those observations are shown in the Figure 2.

3.2 Organic structure directing agent (OSDA)

3.2.1 General concepts

As described above, the first zeolites were synthesized in alkaline media. They crystallized as aluminium-rich zeolites (Si/Al close to 1) due to the presence of large amount of extra-framework sodium atoms. Nevertheless, in 1961, the OSDA is introduced for the first time in zeolite synthesis by Barrer et al.²² The use of tetraalkylammonium cations allowed increasing the framework Si/Al ratio, determined by the OSDA incorporated into the zeolite.²³ As it can be seen in Figure 3, less positive charges are introduced by the organic molecule than by the small inorganic cations in the SOD cage, requiring less anionic charges in the zeolite framework. Therefore, the organic molecule can determine the amount of trivalent elements in the zeolite framework, but also the structural characteristics, such as pore dimensions and cavities, depending on shape, size, hydrofobicity, and number of charges of the OSDA molecule.

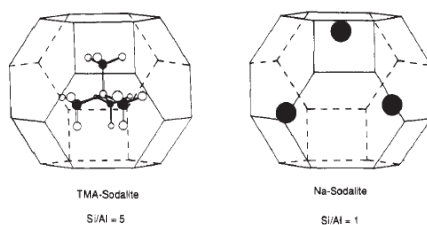


Figure 3. Schemes of tetramethylammonium cation (left) or sodium cations (right) into the sodalite cage. Taken from^[1]

Amines and quaternary ammonium ions are the most frequently used OSDA in zeolite synthesis. The OSDA increases the thermodynamic stability in the organic-

inorganic system during the nucleation step, by means of interactions with the zeolitic framework. There are no covalent bonds between organic and inorganic in this composite, but the assembly process occurs by weak interactions such as van der Waals forces,^{37, 38} showing the structural directing effect. The ideal correlation between the shape and size of the OSDA and the framework cavity is known as “template” effect. Two excellent examples of “template” structure direction are the synthesis of ZSM-18 using the triquat as OSDA,³⁹ and MCM-61 synthesis using the 18-Crown-6 molecule.⁴⁰

The relationships between OSDA properties and the characteristics of cages and pores of formed zeolites have been studied.⁴¹ Gies and Marler⁴² found that sixty-one molecules can be used to control the structure of the clathrasils. They showed that large molecules direct the formation of clathrasils with large cages, while small molecules direct the crystallization of clathrasils with small cages. Moreover, Nakagawa and Zones increased the size of the structure directing agent,⁴³ showing that when the size of the OSDA is increased, the product selectivity changes from a clathrasil to a microporous, large-pore zeolite. Furthermore, if the geometry is changed from cyclic to linear molecules, there is a transition from clathrasils to microporous molecular sieves with 10-ring pores,^{44,45} and the evolution from linear to branched organic molecule allows getting three-dimensional 10-ring (MFI) instead of one-dimensional 10-ring (ZSM-48).⁴¹

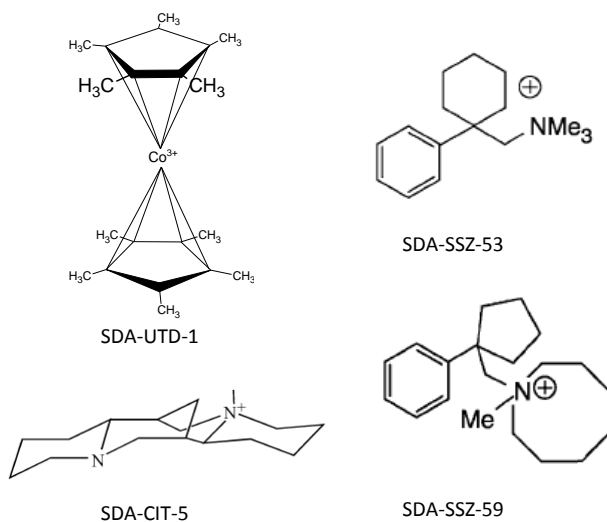


Figure 4. OSDA used for synthesizing the extra-large zeolites UTD-1, CIT-5, SSZ-53, and SSZ-59.

In general, the selectivity of the OSDA towards a zeolite is correlated with the size of the molecule. If the number of carbon and nitrogen atoms in the structure directing molecule increases, the quantity of structures obtained is reduced.⁴¹ Therefore, the specificity as “template” increases when it evolves from small and flexible to large and rigid molecules.

3.2.2 Rigid OSDA to synthesize extra-large pore zeolites and chiral zeolites

The synthesis of extra-large pore zeolites (pores with more than 12 T atoms) is highly desired in catalysis for their potential application in the reactivity of large molecules. The use of relatively large and rigid OSDAs (see Figure 4) was thought to be the adequate strategy to synthesize extra-large pore zeolites. Following this methodology, some extra-large pore zeolites with 14-ring openings were synthesized (UTD-1, CIT-5, SSZ-53, SSZ-59).^{46,47,48,49} However, as it will be shown in the section 3.4.3, the main achievements in the synthesis of extra-large pore molecular sieves have been accomplished with the introduction of Ge in the synthesis gel.

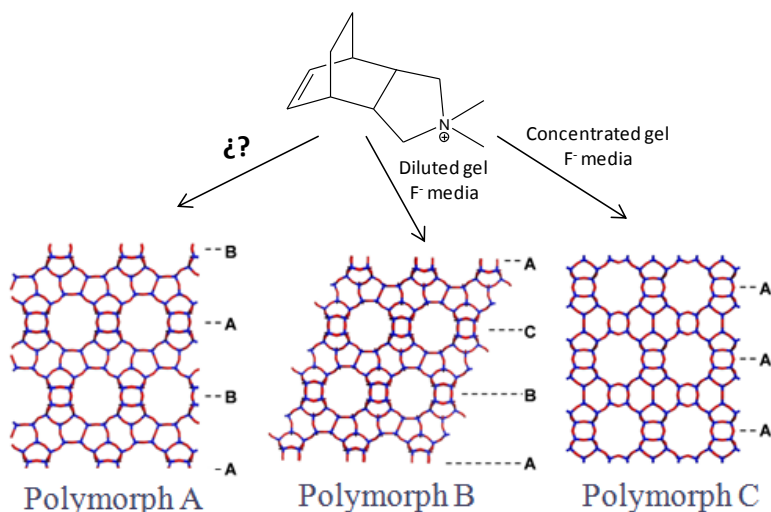


Figure 5. Chiral OSDA used in the synthesis of the pure silica polymorph B and C of Beta zeolite.

Another important goal in zeolite synthesis is the design of chiral solids that can perform enantioselective separation and catalysis. It is believed that in order to synthesize a chiral zeolite, a chiral OSDA must be employed.¹ The idea is to transmit the geometry and chirality of the organic molecule to the inorganic

framework, creating a true “templating” model. Then, rigid and large chiral OSDA should be designed to direct the formation of chiral zeolites. However, up to now, a true “template” capable to transmit its chirality to the framework has not been discovered. A very interesting case is the Beta zeolite.⁵⁰ This molecular sieve is formed by an intergrowth of two polymorphs, A and B, with an enrichment of 55% and 45%, respectively. The polymorph A has a helical pore along the *c* axis. Since the discovery of Beta zeolite structure, the achievement of the pure polymorph A has become one of the main challenges in zeolite synthesis. Together with the polymorphs A and B, it was proposed a third polymorph, C that contains larger void volume than the others.⁵⁰ Very recently, the preparation of the almost pure all-silica polymorph B and polymorph C using the same chiral OSDA at different synthesis conditions has been reported (see Figure 5).^{51,52} Then, the combination of the adequate size to direct the crystallization of different polymorphs of Beta zeolite and its chirality would confer to this OSDA (or related molecules) the adequate characteristics to be a good candidate to “template” the desired polymorph A of Beta zeolite under specific synthesis conditions.

Additionally, a new molecular sieve (ITQ-37) has been described in the last years showing a chiral extra-large framework.⁵³ For the preparation of this zeolite, an organic molecule with four chiral centers has been used (see Figure 6). However, in this case, the enormous helical channels are achieved by the presence of connectivity defects in the structure, and therefore the “true organic-template effect” cannot be claimed.

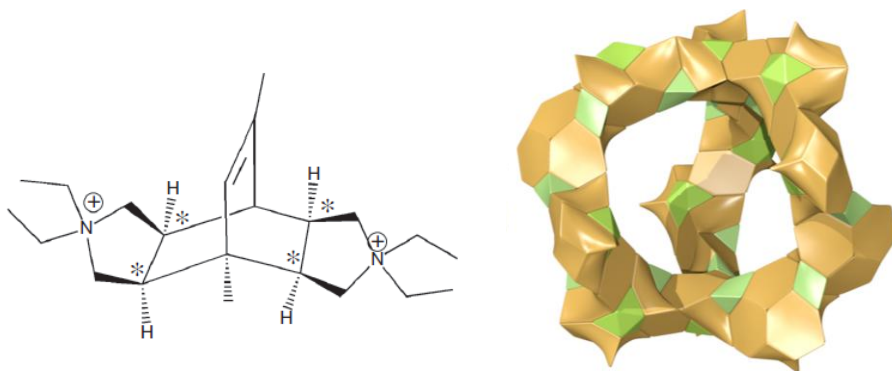


Figure 6. (Left) OSDA used for the ITQ-37 zeolite showing four chiral centers (asterisks), (Right) Chiral structure of the ITQ-37. Taken from^{153]}

These are only two examples in the investigation towards the design of chiral molecular sieves. The scientists have to increase the efforts in the preparation of

this type of solids by their enormous potential impact in different fields, as chemistry, pharmacy, and biology.

3.2.3 Free-combustion OSDA: the recyclability concept applied to zeolite synthesis

As it has been described, the use of the OSDA in the zeolite synthesis introduces some benefits, such as controlling the shape and size of pores and cavities, or the aluminium distribution in the framework. However, the elimination of the organic content in the final solid usually requires high temperature combustion that destroys this high-cost component. The development of novel methodologies avoiding the destruction of the most expensive component in the zeolite manufacture is required. In this sense, Davis et al. have designed a very intelligent approach, creating OSDAs that can be disassembled in the zeolite pore after crystallization, and can be used again by reassembly.⁵⁴

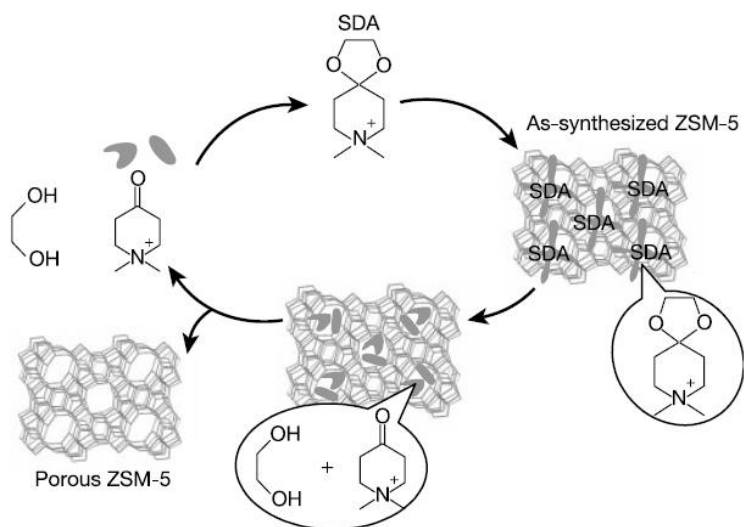


Figure 7. Schematic representation of the free-combustion methodology. Taken from^[54].

Cyclic ketal was chosen as OSDA, because it remains stable at zeolite synthesis conditions (high pH), and can be cleavable at low pH, where the zeolite is not destroyed. Several zeolites have been successfully synthesized with this methodology, such as ZSM-5, ZSM-11, and ZSM-12.^{55,56}

3.2.4 Cooperative structure directing agents

As it was mentioned, the synthesis of large pore zeolites requires the use of bulky OSDAs. Sometimes, the crystallization process cannot be energetically favorable because during the nucleation, the OSDA requires to assemble large number of TO_4 . In this sense, the rational design of zeolites by using a combination of small organic molecules with bulkier OSDAs would allow creating cooperative structure directing effects, where each type of organic molecule will show a precise task. The small cation could direct the small cage formation, and the bulk OSDA could assemble the final structure (see Figure 8). Following this technology, the synthesis of the FER zeolite has been reported by Perez-Pariente et al. in a very nice series of papers.^{57,58,59} Interestingly, they have shown that depending on the combination of organic molecules, the distribution of the acid sites in the structure can be populated between the ferrierite cage accessible through 8-ring windows and the 10-ring channel.^{60,61} A very good correlation between the acid site accessibility and catalytic activity has been achieved in the isomerization reaction of *m*-xylene and conversion of *n*-butene.⁶⁰ The same interesting correlation has been observed for the low-temperature carbonylation of dimethyl ether (DME) with carbon monoxide (CO).⁶²

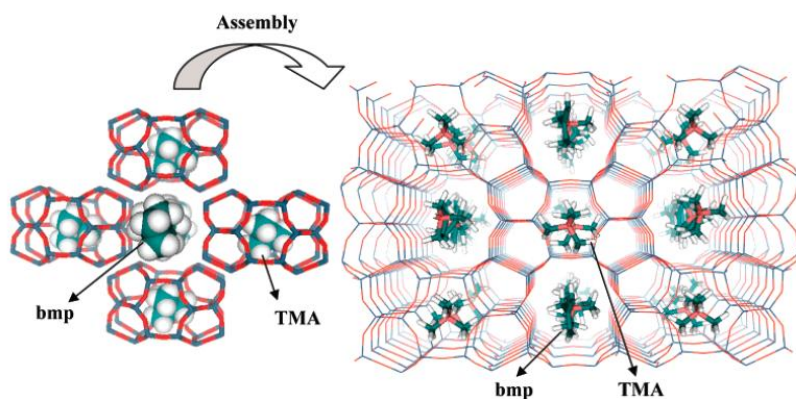


Figure 8. Scheme of the ferrierite containing two different OSDA. Taken from^[57]

3.2.5 Phosphorous derived OSDAs

Large variety of quaternary ammonium salts have been used as OSDA.^{41,63,64} However, those molecules can suffer the Hoffman degradation reaction at high pH and temperature. As a new concept, the use of tetraalkylphosphonium cations has been introduced in the zeolite synthesis in the last years (see Figure 9-left). Those compounds are more thermally stable than tetraalkylammonium molecules, and allow their use in more severe preparation conditions. As a consequence, three new

zeolite structures have been discovered by using phosphonium cations, ITQ-27,⁶⁵ ITQ-34,⁶⁶ and ITQ-40.⁶⁷

Another interesting advance in the OSDA design has been introduced by the use of phosphazene-derivatives. They can be synthesized by blocks similar to Legos, with a large variety of substituents, creating nearly unlimited synthesis options. Moreover, phosphazenes can mobilize silica, and also have the adequate polarity and stability. Their enormous basicities allow to the phosphazenes reacting with water, forming the corresponding hydroxides (see Figure 9-right). Boggsite zeolite has been synthesized for the first time by using this methodology.⁶⁸ This material shows the appropriated structure for aromatic alkylation reactions, thanks to the combination of 12 and 10-ring channels.

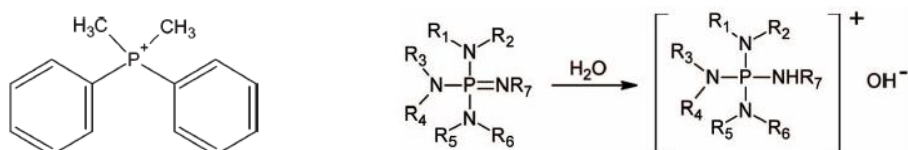


Figure 9. Example of a tetraalkylphosphonium cation (diphenyldimethylphosphonium) used in zeolite synthesis (left), and scheme of formation of a general phosphazanium hydroxide (right).

3.3 Solvent

The most used solvent in zeolite synthesis is water. The main characteristics of water are the non-toxicity, low cost, good thermal stability and conductivity. Also, water helps to the mineralizing agent in the dissolution of species needed for the crystallization, and can act as template in association with other templating species¹⁹

Despite the large benefits of using water as solvent, some examples can be found in the literature in non-aqueous systems. In a nice communication, Bibby and Dale hypothesized that silica can complex with many organic molecules, such as hydroxy- and amine-compounds^{69,70} Therefore, many organic solvents would be available for the synthesis of silicates in non-aqueous systems. Following this hypothesis, they synthesized the silica-sodalite structure from non-aqueous systems with ethylene glycol and propanol.⁶⁹ Expanding this initial work, other related sodalite structures have been synthesized in presence of ethanolamine or ethylenediamine.^{71,72}

The introduction of ionic liquids in zeolite synthesis by Morris et al. as a new preparation method instead of using water as solvent has been a very attractive discovery in the last years.⁷³ Ionic liquids act as both solvent and OSDA. They are

very good solvents because they are ionic and, present enough polarity to dissolve many types of inorganic salts required in zeolite synthesis.⁷⁴ Moreover, ionic liquids (imidazolium) are chemically very similar to the usual quaternary ammonium cations used as OSDA in the traditional zeolite synthesis. However, the most exciting property of ionic liquids is the very low vapour pressure. Then, at elevated temperatures, the ionic liquid produces no autogenous pressure,⁷⁵ permitting the manufacture of zeolites at ambient pressure (see a comparison between ionothermal and hydrothermal methodologies in Figure 10 left).⁷⁶ Moreover, the ionic liquid can be recovered and recycled after the synthesis procedure for a further use. Following this novel methodology, several new zeotype materials have been discovered (see some examples in Figure 10 right).^{73,77,78,79}

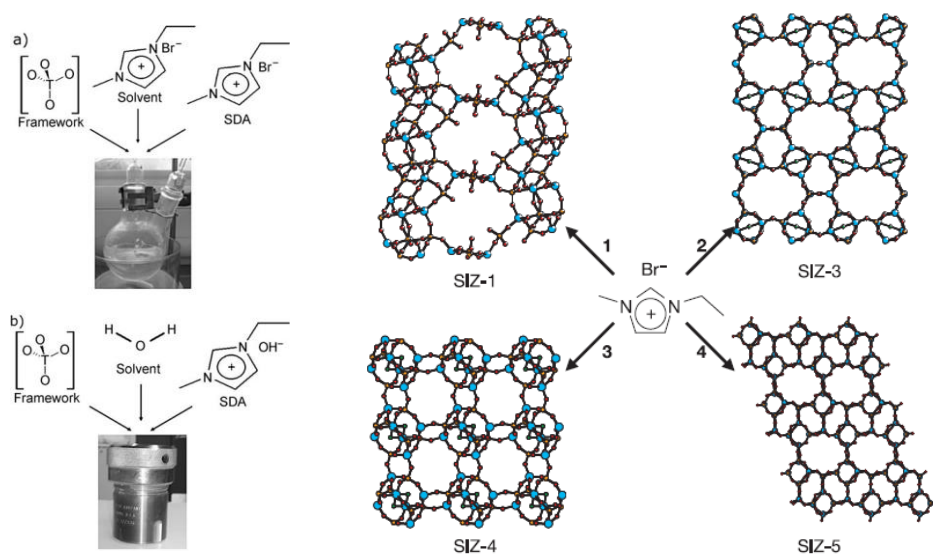


Figure 10. Comparison of ionothermal and hydrothermal zeolite synthesis (left), and some examples of zeotypes synthesized by using ionic liquids (right). Taken from^[76,73]

3.4 Other heteroatoms (T atoms)

The introduction of a T element different to Si in the zeolite structure requires that the oxidation state must be compatible with the TO₄ tetrahedra-related framework. The incorporation of elements with high or low oxidation states is complicated because the high formal charge would be difficult to be balanced (the oxidation state should be between +2 and +5). The Pauling's first rule, related with the ionic

bond in tetrahedral coordination, must be accomplished (R_{Tn+}/R_{O2-} between 0.225 and 0.414). Finally, the final chemical composition must present an overall charge reduced to one TO_2 unit between -1 and 0.¹⁹ The most common elements found in zeolitic structures are summarized in Table 2.

Up to now, we have shown the structure directing effects in zeolite synthesis showed by the OSDA and the fluoride anions. Nevertheless, the addition of T atoms other than Si is able to direct the formation of different zeolites even when the same OSDA is used.⁸⁰ Specific T atoms also can present an inorganic directing effect towards specific small rings or cages, such as 3- and 4-rings. These rings affect the angles and bond distances of T-O-T in the framework structure, changing the relative framework stability. As it has been described by Zones et al. the enthalpy of formation of all-silica structures increases when some atoms are placed in crystallographic positions with small angles (less than 140°).⁸¹ Piccione et al. has also reported that all-silica zeolites with double four-member rings cages (D4R) show less stability than other zeolites without this type of cages.^{82,83} Then, the structure stabilisation of materials containing highly tensioned T-O-T angles by introduction of specific heteroatoms different to Si is determinant, as shown next.

Table 2. Most common elements with their oxidation state that can perform the isomorphic substitution of Si in the tetrahedral zeolite framework.

Oxidation state			
II	III	IV	V
Be	Al	Ge	P
Zn	B	Sn	
Mg	Ga	Ti	

An attractive case in zeolite synthesis is the achievement of zeolites with extra-large pores. As we have described earlier, the preparation of very open structures with pores larger than 12-rings, opens new opportunities in the catalysis of large molecules. In this sense, Brunner and Meier reported a theoretical correlation between the minimum framework density and the size of the smallest ring in the structure, concluding that extra-large pore zeolites should contain 3- and 4-rings in their structure.⁸⁴

3.4.1 Beryllium, zinc and magnesium

It has been described that Be^{2+} , Mg^{2+} , and Zn^{2+} in the zeolite framework introduces the required flexibility in one of the tetrahedral atoms of the 3-ring to stabilize the structure. The isomorphic substitution of those divalent atoms instead of Si in the

framework, produces two negative charges that must be balanced principally by the inorganic or organic cations (Na^+ , K^+ , Ca^{2+} , OSDA...) found in the synthesis gel. The first synthesis attempts were focused in the introduction of beryllium in the gel, because many beryllosilicate minerals have shown numerous 3-rings.² Then, several beryllosilicates were synthesized containing 3-rings in their structure, as lovdarite, OSB-1 and OSB-2 (see Table 3).^{85,86} Interestingly, the OSB-1 material shows an extra-large system of 14-ring channels with numerous 3-rings in its structure. Then, as predicted by Brunner and Maier, the extra-large pore zeolites should contain small rings. Unfortunately, this material shows very low stability, and also, beryllium is highly toxic.

Other non toxic heteroatoms, such as Mg and Zn that can direct the formation of 3-rings were studied in zeolite synthesis. A series of zincosilicates containing 3-rings were prepared by Davis et al., as VPI-7, VPI-9, and VPI-10.^{87,88, 89} Also, a similar zincosilicate to VPI-7, RUB-17, was synthesized by Gies et al.⁹⁰ In the case of Mg, some crystalline silicates can be prepared with 3-ring in their structure, but they are dense phases.⁹¹

Table 3. Beryllium- and zinc-containing zeolitic structures with large number of 3-rings. Taken from¹²¹

Material	Composition	Pore size
Lovdarite	Beryllosilicate	9-ring
OSB-1	Beryllosilicate	14-ring
OSB-2	Beryllosilicate	8-ring
VPI-7	Zincosilicate	9-ring
RUB-17	Zincosilicate	9-ring
VPI-9	Zincosilicate	8-ring
VPI-10	Zincosilicate	9-ring

3.4.2 Boron and aluminium

The effect of the introduction of B or Al in the synthesis gel is not the same. There are many examples in the literature where the phase selectivity is different under the same synthesis conditions when the trivalent atom is changed, such as the cases of SSZ-31 and SSZ-33.⁴¹ This can be related to modifications of distances and angles around the substituted site. The incorporation of B in the zeolite framework implies a more severe deformation of the structure than from the Al introduction.⁹²

The presence of trivalent atoms in tetrahedral coordination in the framework is very important in catalysis. The trivalent insertion creates a negative charge in the framework, that is compensated by a proton after calcination of the OSDA-zeolites (synthesized using an organic molecule as OSDA), or after NH_4^+ exchange and posterior calcination in M^+ -zeolites (synthesized using alkaline cations).

Then, the aluminium substitution in the framework creates a strong Brønsted acid site which permits the application of zeolites in numerous processes that require acid catalysts.⁹³ In contrast, boron zeolites show weaker Brønsted acidity in comparison to the aluminosilicates. However, this can turn into a great advantage considering catalytic processes that require mild solid acid acids.^{94, 95} In addition, the synthesis of borosilicates provides an interesting post-synthetic route for the manufacture of aluminosilicates that cannot be prepared by direct synthesis form.⁹⁶

3.4.3 Germanium

The introduction of Ge does not produce any change in the zeolite charges, and germanates usually present D4R in their structures, where the germanium is tetrahedrally coordinated.^{97,98} If all T atoms in a D4R cage are Si^{4+} , the T-O-T angles are close to 145° . This can be relaxed if Ge is introduced, due to the larger distance of Ge-O compared to Si-O, and therefore the Ge-O-Si angle is smaller.⁶ Theoretical calculations have shown that the stability of D4R units increases when Si^{4+} is substituted by Ge^{4+} .⁹⁹

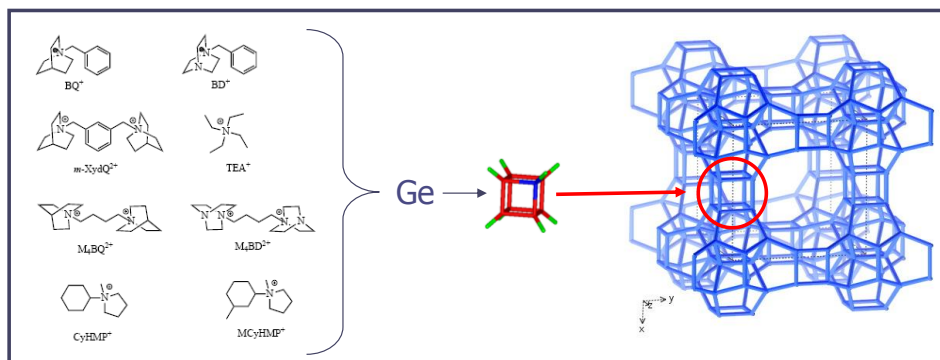


Figure 11. Inorganic structure directing effect of Ge towards BEC (ITQ-17) structure even when different OSDAs were used.

Following this theory, it was possible to synthesize for the first time the silicogermanate form of the polymorph C of Beta zeolite (BEC).¹⁰⁰ That polymorph was predicted by Newsam. et al.,⁵⁰ and it was the unique of the Beta family

polymorphs with D4R in their structure. As it can be seen in Figure 11, the inorganic structure directing effect of Ge towards the BEC structure is extraordinary, and the silicogermanate structure is achieved even when different OSDAs are used.

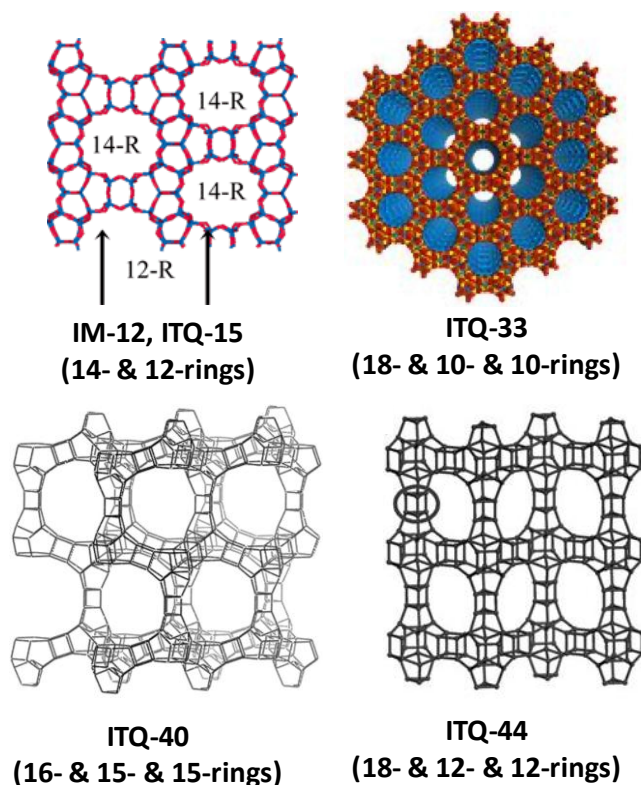


Figure 12. New silicogermanates synthesized with extra-large pore systems.

As predicted by Brunner and Meier,⁸⁴ the syntheses of several new silicogermanates containing small rings with extra-large pore systems have been accomplished when Ge has been introduced in the synthesis gel (see Figure 12). IM-12 and ITQ-15 were the first extra-large zeolites with a bi-directional pore system formed by intersecting 14- and 12-MR, containing D4R cages.^{101,102} ITQ-33 is a silicogermanate with straight extra-large pore channels with circular openings of 18-rings, interconnected by 10-ring channels. This attractive topology confers unique catalytic properties for catalytic cracking of vacuum gasoil.^{103,104} Also, two new silicogermanates, ITQ-40 and ITQ-44, have been recently reported with extra-

large channel systems, 16x15x15 and 18x12x12 respectively, containing for the first time double three rings (D3R) in their structure.^{67,105}

3.4.4 Titanium and tin

The isomorphous substitution of Ti into the zeolite framework in tetrahedral coordination produces interesting selective oxidation catalysis. The first titanosilicate reported was the TS-1.¹⁰⁶ This material is isostructural to the aluminosilicate MFI, with 10-ring channels, and shows high activity and selectivity in oxidation reactions when H₂O₂ is used as oxidant (such as aromatic hydroxylations, epoxidation of alkenes...).¹⁰⁷ This catalyst is the best when small molecules are reacted. However, when large size olefins should be reacted, larger pores are required. Ti-Beta is the most successful large pore catalyst synthesized.¹⁰⁸ The potential of controlling the crystal size and the hydrophilic/hydrophobic character of its external surface offers unique properties in selective oxidation reactions. Other large pore titanosilicates have been reported, as Ti-YNU-1¹⁰⁹ and Ti-ITQ-17.¹¹⁰

The inclusion of tin in the zeolite structure permits the creation of isolated Lewis-type acidic centres which are very useful for catalytic purposes. In this sense, the unique capacity of the isolated tin in tetrahedral coordination to activate the carbonyl groups has been demonstrated.¹¹¹ The discovery of the Sn-containing Beta zeolite has been recognized as very active in the Baeyer-Villiger oxidation reaction for the transformation of ketones in esters using H₂O₂ as oxidant.¹¹² The Sn-Beta has also been showed as an excellent catalyst for the selective reduction of carbonyl compounds with alcohols (Meerwin-Ponndorf-Verley reaction).¹¹³ Very recently, some new interesting applications of Sn-Beta in biomass transformations to get valuable products have been described.^{114,115,116}

4. Commercial production of zeolites and final remarks

Despite the large number of zeolite structures discovered (close to 200),⁵ only 10% of them are in commercial production (see Table 4). The most part of chemical processes that require a zeolitic catalyst are covered by the use of only five zeolites: FAU, Beta, ZSM-5, MOR, and FER.¹¹⁷ This can be explained because the preparation of those materials does not require high costs (expensive OSDAs are not used), and they show a broad spectrum of framework topologies and physical-chemical properties (small, medium, or large pores; large cavities; different acidities...) that allow their application in different type of catalytic processes.

Some of the new structures that have been recently reported in the literature show better activities or selectivities than the commercial zeolites, but in the scale-up of their manufacture it is mandatory the study of their commercial viability. In this way, costs are not only introduced by the use of expensive raw materials (complex

OSDA, or expensive elements such as Ge), but also synthesis time, filtration (waste management), synthesis yield, environmental permissions, and safety considerations.¹¹⁷ Moreover, scientific and industrial collaborations between zeolite manufacturers and application developers are required in order to improve the technology required to introduce a new material in commercial applications.^{117,118}

Table 4. List of zeolites reported in commercial production. Taken from^[117]

FAU	ZSM-22	SAPO-34	MCM-22
Beta	ZSM-23	SSZ-13	TS-1
ZSM-5	ZSM-12	RHO	LTL
MOR	ZSM-48	SAPO-11	UZM-8
FER			

During the last sixty years, scientists have performed many efforts in order to rationalize the synthesis of zeolites, as it has been shown along this chapter. It has been possible to synthesize different type of structures modulating their physicochemical properties, by rationalizing the synthesis variables, such as OSDA, inorganic cations, mineralizing agents, other heteroatoms, solvents... Now, the reduction of manufacture costs in the design and synthesis of new or known structures is compulsory for their industrial application. Some examples of new approaches have been reported in this line. Recently, some zeolites have been synthesized in OSDA-free media: Beta,^{119, 120} ZSM-12,¹²¹ ZSM-34,^{122, 123} and RUB-13.¹²⁴ The removal of the OSDA from the synthesis media will reduce the economical costs of manufacture. Also, some examples of OSDA recyclability have been introduced, as the free combustion methodology (presented in section 3.2.3) and the use of ionic liquids as solvent and OSDA (presented in section 3.3). The recyclability of the OSDA will allow the reuse of these expensive organic molecules during several synthesis cycles, reducing the total economical costs. Finally, the replacement of most of the OSDA in the synthesis gel by less-expensive pore filler (more than 80% of the original OSDA can be replaced by an inexpensive quaternary ammonium salt) will permit large economical savings in a possible zeolite commercial production.¹²⁵ Then, new chemical concepts must be introduced in zeolite synthesis, in order to boost the design of “low-cost” zeolites with very interesting and novel properties.

References

- [1] Davis, M. E. & Lobo, R. F. Zeolite and Molecular Sieve Synthesis. *Chem. Mater.* **4**, 756 (1992).
- [2] Davis, M. E. Ordered porous materials for emerging applications. *Nature.* **417**, 813 (2002).
- [3] Barrer, R. M. Synthesis of a zeolitic mineral with chabazite-like sorptive properties. *J. Chem. Soc.* 127 (1948).
- [4] Barrer, R. M, Hinds, L. & White, E. A. The hydrothermal chemistry of silicates. Part III. Reactions of analcite and leucite. *J. Chem. Soc.* 1466 (1953).
- [5] International Zeolite Association (IZA), www.iza-online.org.
- [6] Corma, A. & Davis, M. E. Issues in the synthesis of crystalline molecular sieves: towards the crystallization of low framework-density structures. *ChemPhysChem.* **5**, 304, (2004).
- [7] Cundy, C. S. & Cox, P. A. The Hydrothermal Synthesis of Zeolites: Precursors, Intermediates and Reaction Mechanism. *Microp. Mesop. Mater.* **82**, 1 (2005).
- [8] Barrer, R. M., Baynham, J. W., Bultitude, F. W. & Meier, W. M. Hydrothermal chemistry of the silicates. Part VIII. Low-temperature crystal growth of aluminosilicates, and of some gallium and germanium analogues. *J. Chem. Soc.* 195 (1959).
- [9] Flanigen, E. M. & Breck, D. W. *137th Meeting of the ACS, Division of Inorganic Chemistry*, Cleveland (OH), (1960).
- [10] Kerr, G. T. Chemistry of Crystalline Aluminosilicates. I. Factors. Affecting The Fomation of Zeolite A. *J. Phys. Chem.* **70**, 1047 (1966).
- [11] Zhdanov, S. P. in *Molecular Sieve Zeolites* eds E.M. Flanigen, & L.B. Sand. ACS Adv. Chem. Ser., **101**, 20 (1971).
- [12] Wadlinger, R. L., Kerr, G.T. & Rosinski, E. J. Catalytic composition of a crystalline zeolite. *US Patent 3,308,069* (1967).
- [13] Argauer, R. J. & Landolt, G. R. Crystalline zeolite ZSM-5 and method of preparing the same. *US Patent 3,702,886* (1972).
- [14] Derouane, E. G., Detremmerie, S., Gabelica, Z & Blom, N. Synthesis and characterization of ZSM-5 Type Zeolites 1. Physicochemical Properties of Precursors and Intermediates. *Appl. Catal.* **1**, 201 (1981).
- [15] Gabelica, Z., Blom, N. & Derouane, E. G. Synthesis and Characterization of ZSM-5 Type Zeolites. III. A Critical Evaluation of the Role of Alkali and Ammonium Cations. *Appl. Catal.* **5**, 227 (1983).
- [16] Chang, C. D. & Bell, A. T. Studies on the mechanism of ZSM-5 formation. *Catal. Lett.* **8**, 305 (1991).

-
- [17] Burkett, S. L. & Davis, M. E. Mechanism of Structure Direction in the Synthesis of Si-ZSM-5: An Investigation by Intermolecular $1\text{H}-29\text{Si}$ CP MAS NMR. *J. Phys. Chem.* **98**, 4647 (1994).
- [18] Burkett, S. L. & Davis, M. E. Mechanism of Structure Direction in the Synthesis of Pure-Silica Zeolites. 2. Hydrophobic Hydration and Structural Specificity. *Chem. Mater.* **7**, 1453 (1995).
- [19] Guth, J. L. & Kessler, H. in *Catalysis and zeolites: Fundamentals and Applications*. eds J. Weitkam, & L. Puppe. Springer-Verlag. Berlin (1999). Chapter 1, pp. 1.
- [20] Milton, R. M. Molecular sieve adsorbents. *US Patent 2,882,243* (1959).
- [21] Milton, R. M. Molecular sieve adsorbents. *US Patent 2,882,244* (1959).
- [22] Barrer, R. M. & Denny, P. J. Hydrothermal chemistry of the silicates. IX. Nitrogenous aluminosilicates. *J. Chem. Soc.* 971 (1961).
- [23] Baerlocher, Ch. & Meier, W. M. Synthesis and crystal structure of tetramethylammonium sodalite. *Helv. Chim. Acta.* **52**, 1853 (1969).
- [24] Flanigen, E. & Patton, R. L. Silica polymorph. *US Patent 4,073,865* (1978).
- [25] Barret, P. A., Cambor, M. A., Corma, A., Jones, R. H. & Villaescusa, L. A. Synthesis and Structure of As-Prepared ITQ-4, A Large Pore Pure Silica Zeolite: The Role and Location of Fluoride Anions and Organic Cations. *J. Phys. Chem. B.* **102**, 4147 (1998).
- [26] Koller, H., Lobo, R. F., Burkett, S. L. & Davis, M. E. $\text{SiO}_2 \cdot n\text{H}_2\text{O}$ Hydrogen Bonds in As-Synthesized High-Silica Zeolites. *J. Phys. Chem.* **99**, 12588, (1995).
- [27] Kessler, H. Direct effect of fluoride in the synthesis of molecular sieves with new characteristics and of the first twenty-membered ring microporous solid. *Mater. Res. Soc. Symp. Proc.*, **233**, 47, (1991).
- [28] Blasco, T., Cambor, M. A., Corma, A., Esteve, P., Guil, J. M., Martinez, A., Perdigon-Melon, J. A. & Valencia, S. Direct Synthesis and Characterization of Hydrophobic Aluminum-Free Ti-Beta Zeolite. *J. Phys. Chem.*, **102**, 75, (1998).
- [29] Guth, J. L., Kessler, H., Bourgogne, M., Wey, R. & Szabo, G. Synthesis and use of aluminosilicate-type zeolites. *Fr. Patent*, 2,567,868 (1986).
- [30] Kessler, H., Patarin, J. & Schott-Daric, C. The opportunities of the fluoride route in the synthesis of microporous materials. *Stud. Surf. Sci. Catal.*, **85**, 75, (1994).
- [31] Estermann, M., McCusker, L. B., Baerlocher, C., Merrouche, A & Kessler, H. A synthetic gallophosphate molecular sieve with a 20-tetrahedral-atom pore opening. *Nature*, **352**, 320, (1991).
- [32] Cambor, M.A., Corma, A., Lightfoot, P., Villaescusa, L. A. & Wright, P. A. Synthesis and structure of ITQ-3, the first pure silica polymorph with a two-

- dimensional system of straight eight-ring channels. *Angew. Chem., Int. Ed.*, **36**, 2659, (1997).
- [33] Villaescusa, L. A., Barret, P. A. & Cambor. ITQ-7: a new pure silica polymorph with a three-dimensional system of large pore channels. *Angew. Chem., Int. Ed.*, **38**, 1997, (1999).
- [34] Zones, S. I., Burton, A. W., Lee, G. S. & Olmstead, M. M. A Study of Piperidinium Structure-Directing Agents in the Synthesis of Silica Molecular Sieves under Fluoride-Based Conditions. *J. Am. Chem. Soc.*, **129**, 9066, (2007).
- [35] Zones, S. I. & Hwang, S-J. The inorganic chemistry of guest-mediated zeolite crystallization: a comparison of the use of boron and aluminum as lattice-substituting components in the presence of a single guest molecule during zeolite synthesis. *Micropor. Mesopor. Mater.* **58**, 263, (2003).
- [36] Zones, S. I., Hwang, S-J., Elomari, S., Ogino, I., Davis, M. E. & Burton, A. W. The fluoride-based route to all-silica molecular sieves; a strategy for synthesis of new materials based upon close-packing of guest-host products. *Comp. Rend. Chim.*, **8**, 267, (2005).
- [37] Lefebvre, F., Sacerdote-Peronnet, M. & Mentzen, B. F. Silicon-hydrogen interactions in sorbent/sorbate complexes studied by silicon-29 CP-MAS-NMR. The MFI/4 p-xylene system. *C.R. Acad. Sci. Paris, Ser.2*, **316**, 1549, (1993).
- [38] Burkett, S. L. & Davis, M. E. Mechanisms of Structure Direction in the Synthesis of Pure-Silica Zeolites. 1. Synthesis of TPA/Si-ZSM-5. *Chem. Mater.* **7**, 920, (1995).
- [39] Ciric, J. Synthetic zeolite ZSM-18. *U.S. Patent 3,950,496*, (1976).
- [40] Shantz, D. F., Burton, A. & Lobo, R. F. Synthesis, structure solution, and characterization of the aluminosilicate MCM-61: the first aluminosilicate clathrate with 18-membered rings. *Microporous Mesoporous Mater.* **31**, 61, (1999).
- [41] Lobo, R. F., Zones, S. I. & Davis, M. E. Structure-direction in zeolite synthesis. *J. Includ. Phen. Mol. Rec.*, **21**, 47, (1995).
- [42] Gies, H. & Marler, B. The structure-controlling role of organic templates for the synthesis of porosils in the system silica/template/water. *Zeolites*, **12**, 42, (1992).
- [43] Nakagawa, Y. & Zones, S. I. in *Synthesis of Microporous Materials*. Eds. Robson, H. Van Nostrand Reinhold. New York (1992) Vol. 1.
- [44] Nakagawa, Y. & Zones, S. I. Manufacture of intermediate-pore size zeolites ZSM-5 and zeolites theta 1 using neutral amines in the absence of a quaternary ammonium compound, and the zeolites obtained. *WO96/29285*, (1996).

-
- [45] Moini, A., Schmitt, K. D. & Polomski, R. F. Pentamethyl diethylene triamine and its quaternary cations as directing agents in zeolite synthesis: Monitoring the stability of directing agents under hydrothermal conditions. *Zeolites*, **18**, 2, (1997).
- [46] Freyhardt, C. C., Tsapatsis, M., Lobo, R. F., Balkus, K. J. & Davis, M. E. A high-silica zeolite with a 14-tetrahedral-atom pore opening. *Nature* **295**, 381, (1996).
- [47] Wagner, P., Yoshikawa, M., Tsuji, K., Davis, M. E., Lovallo, M. & Tsapatsis, M. CIT-5: a high-silica zeolite with 14-ring pores. *Chem. Commun.*, 2179, (1997)
- [48] Elomari, S. A. & Zones, S. I. Synthesis of novel zeolites SSZ-53 and SSZ-55 using novel organic templating agents derived from nitriles. *Stud. Surf. Sci. Catal.* **135**, 479, (2001).
- [49] Burton, A. W., Elomari, S. A., Chen, C.-Y., Medrud, R. C., Chan, I. Y., Bull, L. M., Kibby, C., Harris, T. V., Zones, S. I. & Vittoratos, E. S. SSZ-53 and SSZ-59: Two novel extra-large pore zeolites. *Chem.-A Eur. J.*, **9**, 5737, (2003).
- [50] Treacy, M. M. J. & Newsam, J. M. Two new three-dimensional twelve-ring zeolite frameworks of which zeolite beta is a disordered intergrowth. *Nature.*, **332**, 249, (1988).
- [51] Cantín, A., Corma, A., Díaz-Cabañas, M. J., Jorda, J. L., Moliner, M. & Rey, F. Synthesis and characterization of the all-silica pure polymorph C and enriched polymorph B intergrowth of zeolite beta. *Angew. Chem. Int. Ed.*, **45**, 8013 (2006).
- [52] Corma, A., Moliner, M., Cantín, A., Diaz-Cabañas, M. J., Jordá, J. L., Zhang, D., Sun, J., Jansson, K., Hovmöller, S. & Zou, X. Synthesis and Structure of Polymorph B of Zeolite Beta. *Chem. Mater.*, **20**, 3218, (2008).
- [53] Sun, J., Bonneau, C., Cantín, A., Corma, A., Diaz-Cabañas, M. J., Moliner, M., Zhang, D., Li, M. & Zou, X. The ITQ-37 mesoporous chiral zeolite. *Nature.*, **458**, 1154, (2009).
- [54] Lee, H, Zones, S. I. & Davis, M. E. A combustion-free methodology for synthesizing zeolites and zeolite-like materials. *Nature.*, **425**, 385, (2003).
- [55] Lee, H, Zones, S. I. & Davis, M. E. Zeolite Synthesis Using Degradable Structure-Directing Agents and Pore-Filling Agents. *J. Phys. Chem. B.*, **109**, 2187, (2005).
- [56] Lee, H, Zones, S. I. & Davis, M. E. Synthesis of molecular sieves using ketal structure-directing agents and their degradation inside the pore space. *Microp. Mesop. Mat.*, **88**, 266, (2006).
- [57] Pinar, A. B., Gomez-Hortiguera, L. & Perez-Pariente, J. Cooperative Structure Directing Role of the Cage-Forming Tetramethylammonium

- Cation and the Bulkier Benzylmethylpyrrolidinium in the Synthesis of Zeolite Ferrierite. *Chem. Mater.*, **19**, 5617, (2007).
- [58] Marquez-Alvarez, C., Pinar, A. B., Garcia, R., Grande-Casas, M. & Perez-Pariente, J. Influence of Al distribution and defects concentration of ferrierite catalysts synthesized from Na-free gels in the skeletal isomerization of n-butene. *Top. Catal.*, **52**, 1281, (2009).
- [59] Pinar, A. B., Garcia, R. & Perez-Pariente, J. Synthesis of ferrierite from gels containing a mixture of two templates. *Collect. Czech. Chem. Commun.*, **72**, 666, (2007).
- [60] Pinar, A. B., Marquez-Alvarez, C., Grande-Casas, M. & Perez-Pariente, J. Template-controlled acidity and catalytic activity of ferrierite crystals. *J. Catal.*, **263**, 258, (2009).
- [61] Gomez-Hortiguera, L., Pinar, A. B., Cora, F. & Perez-Pariente, J. Dopant-siting selectivity in nanoporous catalysts: control of proton accessibility in zeolite catalysts through the rational use of templates. *Chem. Commun.*, **46**, 2073, (2010).
- [62] Roman-Leshkov, Y., Moliner, M. & Davis, M. E. Impact of Controlling the Site Distribution of Al Atoms on Catalytic Properties in Ferrierite-Type Zeolites. *J. Phys. Chem. C*, **115**, 1096, (2011).
- [63] Burton, A. W., Zones, S. I. & Elomari, S. The chemistry of phase selectivity in the synthesis of high-silica zeolites. *Curr. Opin. Colloid Interface Sci.*, **10**, 211, (2005).
- [64] Jackowski, A., Zones, S. I., Hawng, S. J., & Burton, A. W. Diquaternary Ammonium Compounds in Zeolite Synthesis: Cyclic and Polycyclic N-Heterocycles Connected by Methylene Chains. *J. Am. Chem. Soc.*, **131**, 1092, (2009).
- [65] Dorset, D. L., Kennedy, G. J., Strohmaier, K. G., Diaz-Cabañas, M. J., Rey, F. & Corma, A. P-Derived Organic Cations as Structure-Directing Agents: Synthesis of a High-Silica Zeolite (ITQ-27) with a Two-Dimensional 12-Ring Channel System. *J. Am. Chem. Soc.*, **128**, 8862, (2006).
- [66] Corma, A., Diaz-Cabañas, M. J., Jorda, J. L., Rey, F., Sastre, G. & Strohmaier, K. A Zeolitic Structure (ITQ-34) with Connected 9- and 10-Ring Channels Obtained with Phosphonium Cations as Structure Directing Agents. *J. Am. Chem. Soc.*, **130**, 16482, (2008).
- [67] Corma, A., Diaz-Cabañas, M. J., Jiang, J., Afeworki, M., Dorset, D. L., Soled, S. L. & Strohmaier, K. G. Extra-large pore zeolite (ITQ-40) with the lowest framework density containing double four- and double three-rings. *Proc. Natl. Acad. Sci. U.S.A.*, **107**, 11935, (2010).

-
- [68] Simancas, R., Dari, D., Velamazán, N., Navarro, M. T., Cantin, A., Jorda, J. L., Sastre, G., Corma, A. & Rey, F. Modular Organic Structure-Directing Agents for the Synthesis of Zeolites. *Science.*, **330**, 1219, (2010).
- [69] Bibby, D. M. & Dale, M. P. Synthesis of silica-sodalite from nonaqueous systems. *Nature.*, **317**, 157, (1985).
- [70] Iler, R. K. in *The Chemistry of Silica*. Wiley. New York (1979).
- [71] Braunbarth, C. M., Behrens, P., Felsche, J., van de Goor, G., Wildermuth, G. & Engelhardt, G. Synthesis and characterization of two new silica sodalites containing ethanolamine or ethylenediamine as guest species: $[\text{C}_2\text{H}_7\text{NO}]_2[\text{Si}_6\text{O}_{12}]_2$ and $[\text{C}_2\text{H}_8\text{N}_2]_2[\text{Si}_6\text{O}_{12}]_2$. *Zeolites.*, **16**, 207, (1996).
- [72] Braunbarth, C. M., Behrens, P., Felsche, J. & van de Goor, G. Phase transitions and thermal behavior of silica sodalites. *Solid State Ionics.*, **101-103**, 1273, (1997).
- [73] Cooper, E. R., Andrews, C. D., Wheatley, P. S., Webb, P. B., Wormald, P. & Morris, R. E. Ionic liquids and eutectic mixtures as solvent and template in synthesis of zeolite analogues. *Nature.*, **430**, 1012, (2004).
- [74] Antonietti, M., Kuang, D. B., Smarsly, B. & Zou, Y. Ionic liquids for the convenient synthesis of functional nanoparticles and other inorganic nanostructures. *Angew. Chem., Int. Ed.*, **43**, 4988, (2004).
- [75] Ludwig, R. & Kragl, U. Do we understand the volatility of ionic ligands?. *Angew. Chem., Int. Ed.*, **46**, 6582, (2007).
- [76] Morris, R. E. Ionic liquids and microwaves-making zeolites for emerging applications. *Angew. Chem., Int. Ed.*, **47**, 442, (2008).
- [77] Parnham, E. R. & Morris, R. E. Ionothermal synthesis using a hydrophobic ionic liquid as solvent in the preparation of a novel aluminophosphate chain structure. *J. Mater. Chem.*, **16**, 3682, (2006).
- [78] Parnham, E. R. & Morris, R. E. The Ionothermal Synthesis of Cobalt Aluminophosphate Zeolite Frameworks. *J. Am. Chem. Soc.*, **128**, 2204, (2006).
- [79] Parnham, E. R. & Morris, R. E. Ionothermal Synthesis of Zeolites, Metal-Organic Frameworks, and Inorganic-Organic Hybrids. *Acc. Chem.Res.*, **40**, 1005, (2007).
- [80] Helmkamp, M. M. & Davis, M. E. Synthesis of porous silicates. *Annu. Rev. Mater. Sci.*, **25**, 161, (1995).
- [81] Petrovic, I., Navrotsky, A., Zones, S. I. & Davis, M. E. Thermochemical study of the stability of frameworks in high silica zeolites. *Chem. Mater.*, **5**, 1805, (1993).
- [82] Piccione, P. M., Laberty, C., Yang, S., Cambor, M. A., Navrotsky, A. & Davis, M. E. Thermochemistry of Pure-Silica Zeolites. *J. Phys. Chem. B*, **104**, 10001, (2000).

-
- [83] Piccione, P. M., Woodfield, B. F., Boerio-Goates, J. A., Navrotsky, A. & Davis, M. E. Entropy of Pure-Silica Molecular Sieves. *J. Phys. Chem. B*, **105**, 6025, (2001).
- [84] Brunner, G. O. & Meier, W. M. Framework density distribution of zeolite-type tetrahedral nets. *Nature*, **337**, 146, (1989).
- [85] Ueda, S., Koizumi, M., Baerlocher, Ch., McCusker, L. B. & Meier, W. M. *7th Int. Zeolite Conf.*, Tokyo, Poster Paper 3C-3 (1986).
- [86] Cheetham, A. et al. Very openmicroporous materials. From concept to reality. *Stud. Surf. Sci. Catal.135*, Paper 05-O-05 (Elsevier, 2001).
- [87] Annen, M. J., Davis, M. E., Higgins, J. B. & Schlenker, J. L. VPI-7: the first zincosilicate molecular sieve containing three-membered T-atom rings. *J. Chem. Soc. Chem. Commun.* 1175, (1991).
- [88] McCusker, L., Grosse-Kunstleve, R. W., Baerlocher, Ch., Yoshikawa, M. & Davis, M. E. Synthesis optimization and structure analysis of the zincosilicate molecular sieve VPI-9. *Microporous Mater.* **6**, 295, (1996).
- [89] Grosse-Kunstleve, R. W. *Zeolite Structure Determination From Powder Data: Computer-based Incorporation of Crystal Chemical Information. PhD thesis*, Swiss Federal Inst. Technol., Zurich (1996).
- [90] Rohrig, C. & Gies, H. A new zincosilicate zeolite with nine-ring channels. *Angew. Chem., Int. Ed.* **34**, 63, (1995).
- [91] Hazen, R. M., Yang, H., Finger, L. W. & Fursenko, B. A. Crystal chemistry of high-pressure BaSi₄O₉ in the trigonal (P3) barium tetragermanate structure. *American Mineralogist.* **84**, 987 (1999).
- [92] Valerio, G., Plevert, J., Goursot, A. & di Renzo, F. Modeling of boron substitution in zeolites and implications on lattice parameters. *Phys. Chem. Chem. Phys.* **2**, 1091 (2000).
- [93] Corma, A. From microporous to mesoporous molecular sieve materials and their use in catalysis. *Chem. Rev.* **97**, 2373 (1997).
- [94] Millini, R., Perego, G & Bellussi, G. Synthesis and characterization of boron-containing molecular sieves. *Top. Catal.* **9**, 13 (1999).
- [95] Chen, C. Y., Zones, S. I., Hwang, S. J. & Bull, L. M. In *Proceedings: 14th International Zeolite Conference*. Eds. Van Steen, E., Callanan, L. & Claeys, M. 1547, (2004).
- [96] Chen, C. Y. & Zones, S. I. In *Proceedings: 13th International Zeolite Conference*. Eds. Galarmeau, A., di Renzo, F., Fajula, F. & Vadrine, J. Elsevier, Amsterdam, paper 11-P-16, (2001).
- [97] O'Keefe, M. & Yaghi, O. M. Germanate zeolites: contrasting the behavior of germanate and silicate structures built from cubic T₈O₂₀ units (T = Ge or Si). *Chem. Eur. J.*, **5**, 2796, (1999).

-
- [98] Villaescusa, L. A., Lighfoot, P. & Morris, R. E. Synthesis and structure of fluoride-containing GeO_2 analogues of zeolite double four-ring building units. *Chem. Commun.*, **19**, 2220, (2002).
- [99] Blasco, T., Corma, A., Díaz-Cabañas, M. J., Rey, F., Vidal-Moya, J. A. & Zicovich-Wilson, C. M. Preferential Location of Ge in the Double Four-Membered Ring Units of ITQ-7 Zeolite. *J. Phys. Chem. B*, **106**, 2637, (2002).
- [100] Corma, A., Navarro, M. T., Rey, F., Rius, J. & Valencia, S. Pure polymorph C of zeolite beta synthesized by using framework isomorphous substitution as a structure-directing mechanism. *Angew. Chem., Int. Ed.*, **40**, 2277, (2001).
- [101] Corma, A., Díaz-Cabañas, M. J., Rey, F., Nicolopoulos, S. & Boulahya, K. ITQ-15: The first ultralarge pore zeolite with a bi-directional pore system formed by intersecting 14- and 12-ring channels, and its catalytic implications. *Chem. Commun.*, 1356, (2004).
- [102] Paillaud, J. L., Harbuzaru, B., Patarin, J. & Bats, N. Extra-Large-Pore Zeolites with Two-Dimensional Channels Formed by 14 and 12 Rings. *Science*, **304**, 990, (2004).
- [103] Corma, A., Díaz-Cabañas, M. J., Jorda, J. L., Martinez., C. & Moliner, M. High-throughput synthesis and catalytic properties of a molecular sieve with 18- and 10-member rings. *Nature*, **443**, 842, (2006).
- [104] Moliner, M., Díaz-Cabañas, M. J., Fornes, V., Martinez., C. & Corma, A. Synthesis methodology, stability, acidity, and catalytic behavior of the 18×10 member ring pores ITQ-33 zeolite. *J. Catal.*, **254**, 101, (2008).
- [105] Jiang, J., Jorda, J. L., Diaz-Cabanias, M. J., Yu, J. & Corma, A. The Synthesis of an Extra-Large-Pore Zeolite with Double Three-Ring Building Units and a Low Framework Density. *Angew. Chem., Int. Ed.*, **49**, 4986, (2010).
- [106] Perego, C., Bellussi, G., Como, C., Taramasso, M., Buonomo, F. & Exposito, A. Titanium-silicalite: a novel derivative in the pentasil family. *Stud. Surf. Sci. Catal.*, **28**, 129, (1986).
- [107] Bellussi, G. & Rigutto, M. S. in *Advance zeolite science and applications*. Eds. Jansen, J. C., Stocker, M., Karge, H. G. & Weitkamp, J. Elsevier. Amsterdam. (1994).
- [108] Blasco, T., Cambor, M. A., Corma, A., Esteve, P., Martinez, A., Prieto, C. & Valencia, S. Unseeded synthesis of Al-free Ti- β zeolite in fluoride medium: a hydrophobic selective oxidation catalyst. *Chem. Commun.*, 2367, (1996).
- [109] Fan, W., Wu, P., Namba, S. & Tatsumi, T. A titanosilicate that is structurally analogous to an MWW-type lamellar precursor. *Angew. Chem., Int. Ed.*, **43**, 236, (2003).

- [110] Moliner, M., Serna, P., Cantin, A., Sastre, G., Díaz-Cabañas, M. J. & Corma, A. Synthesis of the Ti-Silicate Form of BEC Polymorph of β -Zeolite Assisted by Molecular Modeling. *J. Phys. Chem. C.*, **112**, 19547, (2008).
- [111] Boronat, M., Corma, A. & Renz, M. Mechanism of the Meerwein-Ponndorf-Verley-Oppenauer (MPVO) Redox Equilibrium on Sn- and Zr-Beta Zeolite Catalysts. *J. Phys. Chem. B.*, **110**, 21168, (2006).
- [112] Corma, A., Nemeth, L. T., Renz, M & Valencia, S. Sn-zeolite beta as a heterogeneous chemoselective catalyst for Baeyer-Villiger oxidations. *Nature.*, **412**, 423, (2001).
- [113] Corma, A., Domine, M. E., Nemeth, L. T. & Valencia, S. Al-Free Sn-Beta Zeolite as a Catalyst for the Selective Reduction of Carbonyl Compounds (Meerwein-Ponndorf-Verley Reaction). *J. Am. Chem. Soc.*, **124**, 3194, (2002).
- [114] Moliner, M., Roman-Leshkov, Y. & Davis, M. E. Tin-containing zeolites are highly active catalysts for the isomerization of glucose in water. *Proc. Natl. Acad. Sci. U.S.A.*, **107**, 6164, (2010).
- [115] Roman-Leshkov, Y., Moliner, M., Labinger, L. A. & Davis, M. E. Mechanism of Glucose Isomerization Using a Solid Lewis Acid Catalyst in Water. *Angew. Chem., Int. Ed.*, **49**, 8954, (2010).
- [116] Holm, M. S., Saravanamurugan, S. & Taarning, E. Conversion of Sugars to Lactic Acid Derivatives Using Heterogeneous Zeotype Catalysts. *Science.*, **328**, 602, (2010).
- [117] Zones, S. I. *Translating New Materials Discoveries in Zeolite Research to Commercial Manufacture.*, doi: 10.1016/j.micromeso.2011.03.039 (2011).
- [118] Schmidt, F. New catalyst preparation technologies - observed from an industrial viewpoint. *Appl. Catal A: Gen.*, **221**, 15, (2001).
- [119] Xie, B., Song, J., Ren, L., Ji, Y., Li, J. & Xiao, F. S. Organotemplate-Free and Fast Route for Synthesizing Beta Zeolite. *Chem. Mater.*, **20**, 4533, (2008).
- [120] Kamimura, Y., Chaikittisilp, W., Itabashi, K., Shimojima, A., & Okubo, T. Critical Factors in the Seed-Assisted Synthesis of Zeolite Beta and "Green Beta" from OSDA-Free Na^+ -Aluminosilicate Gels. *Chem. Asian J.*, **5**, 2182, (2010).
- [121] Iyoki, K., Kamimura, Y., Itabashi, K., Shimojima, A., & Okubo, T. Synthesis of MTW-type zeolites in the absence of organic structure-directing agent. *Chem. Lett.*, **39**, 730, (2010).
- [122] Zhang, L., Yang, C., Meng, X., Xie, B., Wang, L., Ren, L., Ma, S., & Xiao, F. S. Organotemplate-free syntheses of ZSM-34 zeolite and its heteroatom-substituted analogues with good catalytic performance. *Chem. Mater.* **22**, 3099, (2010).

- [123] Wu, Z., Song, J., Ji, Y., Ren, L. & Xiao, F. S. Organic Template-Free Synthesis of ZSM-34 Zeolite from an Assistance of Zeolite L Seeds Solution. *Chem. Mater.* **20**, 357 (2008).
- [124] Yokoi, T., Yoshioka, M., Imai, H. & Tatsumi, T. Diversification of RTH-Type Zeolite and Its Catalytic Application. *Angew. Chem, Int. Ed.*, **48**, 9884, (2009).
- [125] Zones, S. I. Preparation of Molecular Sieves Using a Structure Directing Agent and An N, N, N-Triakyl Benzyl Quaternary Ammonium Cation. *U. S. Patent 20080075656*, (2008).

Crystal Structure Analysis in Zeolite Science

Hermann GIES, Bernd MARLER
Ruhr-Universität Bochum, 44780 Bochum, Germany

Abstract

Crystal structure analysis has had a major impact on the development of zeolite science. Structure solution of zeolite materials reveals their particular properties, inspiring synthesis and application oriented work. The review sheds light on classic examples, amongst others on the structure solution of MFI-type material and its consequences for zeolite research. On the other hand, the development of structure solution from powder X-ray pattern (P-XRD) and the development of high resolution instruments in particular has been driven by the strong demand from the zeolite community. Recent crystal structures of zeolite materials solved like ITQ-33, ITQ-37 or the family of interlayer expanded zeolites should have considerable impact on future developments. Finally, the increasing influence of electron crystallography is discussed. The advent of electron diffraction tomography and its automated data acquisition allows structure solution from nano crystals. Successful examples of structure determination of zeolite materials have been presented in literature, indicating that the technique will supersede the P-XRD analysis, at least for structure determination.

1 Historical perspective: The Impact of Structure Analysis on Zeolite Science

The determination and analysis of the crystal structures of micro- and mesoporous materials has had important impact on the development of microporous materials and also on their applications. The most valuable and obvious information that can be gained from diffraction experiments, is the atomically resolved crystal structure, its geometry, i.e. the framework structure, the pore opening and volume, the connectivity of channels, and its composition including the distribution of active centres in the framework. X-ray diffraction is the most widely used technique for structure elucidation using single crystal (SC-XRD) and powder diffraction (P-XRD) data for the analysis. Over time, zeolite science tremendously benefited from the technical development in diffraction experimentation and data analysis with regard to solving and refining ever more complicated crystal structures. But zeolite materials also played a key role as trigger in this advances in instrumentation serving as challenging materials for case studies, notably in the field of structure solution and structure refinement from P-XRD data. Powder diffraction has been

used alone and in combination with electron diffraction and imaging, and Rietveld analysis in the structure refinement. In general, all text books on zeolite science contain one chapter on the structure of zeolite frameworks to illustrate the close relationship between structure and property of this class of materials. Some more recent ones are given as reference¹⁻⁴.

Dehydration/rehydration and ion exchange properties of zeolites were already known prior to the first crystal structure analysis published in 1930 by Taylor (analcime, ANA)⁵ and **Pauling** (sodalite (SOD)⁶, cancrinite (CAN), natrolite (NAT) and scapolite)⁷, who **commented in his paper that "our determination of the structure of a zeolite leads to a simple explanation of their most characteristic property"** (Fig. 1).

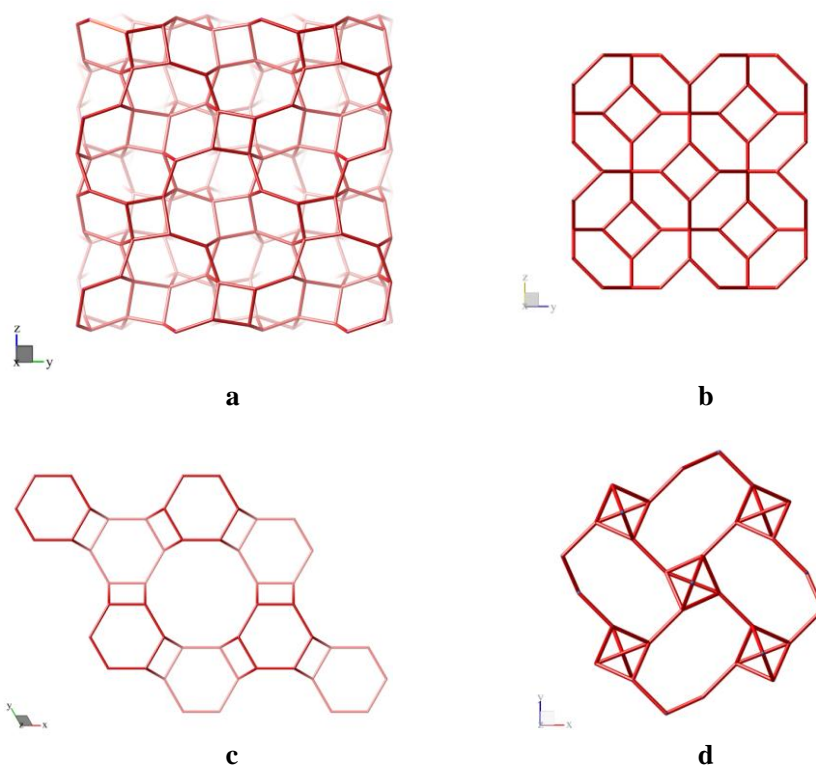


Fig. 1: Projections of the framework structures of the first zeolites of which the crystal structures were determined in 1930: a) analcime, b) sodalite, c) cancrinite, and d) natrolite.

With these findings, the rational exploitation and commercial application of useful properties started. In 1956 the crystal structures of zeolite A (LTA)⁸ and one year

later zeolite faujasite (FAU)⁹ were solved, again having enormous influence on the further development of sorptive and ion exchange properties. Another milestone in structure analysis represents the solution of the structure of zeolite ZSM-5 (MFI)^{10,11}. Internal knowledge of the crystal structure by the Mobil Cooperation prior to publication (U.S. patent 3,702,866 (1972)) led to significant economical advantages boosting structure analysis inside companies but also in academia.

The structure determination of ZSM-5, which was successful only by combining SC-XRD, P-XRD and electron diffraction, is a turning point with respect to the techniques applied. Until then, zeolite structures had been solved from single crystal data. Thereafter, for almost all synthetic zeolites powder data had to be used.

A most interesting case of the impact of structure analysis on applications is the structure solution of zeolite beta. In 1967, Mobile cooperation filed the patent (U.S. Patent 3,308,069). However, because of its structural disorder, the P-XRD diagram of beta looked as if the crystallinity of the material was poor and contained an amorphous fraction. This led to the neglect of further characterization and testing studies, although sorption data indicated high porosity similar to zeolite Y. Only in 1989, the structure was solved and immediately after, zeolite beta became one of the most interesting and commercially important microporous materials for catalytic applications.

Recent examples of the impact of structure analysis on the development of microporous materials are the evolution of coordination polymers, in the beginning exemplified by the invention of MOF-5, and of the introduction of interlayer expanded zeolites (IEZ). The structure solution of MOF-5 unambiguously revealed the bonding network and the microporous structure of the metal-organic framework and, at the same time, inspired chemists in the systematic exploration of this class of materials¹². Today we know more than 100 structure variants; its number is still expanding dynamically with exciting new crystal structures. For potential applications, the knowledge of their structure and properties is very important. Very recently, structure elucidation of interlayer expanded zeolites was reported. The synthesis method of interlayer expansion uses hydrous layer silicates as precursor materials to built three dimensional framework silicates interconnecting the layers with silylation reagents. In this way expanded channel structures of variable diameter are created and functionalized T-centres are introduced, allowing for the fine tuning of structural and chemical properties of the expanded product. Although the silylation procedure of IEZ exercises little control on the general crystallinity of the product, structure analysis proved that the IEZ-materials are locally well ordered with uniform pores and periodic framework structure^{13,14}. For IEZ materials also, the future will show whether or not the information on structural details will help to develop useful microporous materials for applications in sorption, separation or catalysis.

2 Fundamentals in structure analysis

In general, we distinguish between local and global structure, or, typical for solids, between local or long range order. Spectroscopic techniques reveal local order probing energetics of the atom or the atomic environment. IR yields information on the bonding interactions, NMR on the influence of the coordination chemistry on magnetic state of the nucleus probed, EXAFS on the geometry around a nucleus excited to emit photoelectrons which interact with the coordination sphere and, thus modulate the absorption spectrum, etc. **In order to elucidate the long range order, i.e. the crystal structure, describing the arrangement of atoms in the whole crystal, diffraction experiments are required.**

The basic physical process of the diffraction experiment is described as photon-electron interaction in the most widely used X-ray diffraction experiment, electron-electron interaction for electron diffraction and neutron-nucleus interaction for neutron diffraction, leading, in the elastic case, to atoms as centres of radiation creating a three dimensional interference pattern with information on the metric and symmetry of the unit cell (angular information, d-spacings) and its chemical content and atom positions (intensity information, structure factor). **The structure information obtained in a conventional diffraction experiment is the result of the superposition of all scattered waves thus averaging geometric and compositional information in time and space.**

The most frequently used experimental techniques for materials identification and structure analysis are single crystal and powder X-ray diffraction experiments. In all material science and catalysis laboratories X-ray instrumentation is nowadays standard. Electron microscopy is mainly used for high resolution imaging and local analysis of structural features. Instrumentation is more expensive and still is a technique reserved for experts. However, with the advent of electron precession tomography in electron crystallography, single crystal diffraction data from kinematic experiments became available rendering electron crystallography into a powerful tool for structure determination from nano-crystals¹⁵. Single crystal diffraction experiments yield well resolved diffraction intensities from every (hkl)-lattice plane of the crystal. In general, there are many more intensities, i.e. independent observations from a single crystal experiment than there are parameters to determine for the description of the crystal structure. Good data sets yield a 20-fold over-determination. However, since the measured intensity of a reflection is proportional to the absolute squared structure factor, the crystallographic "Phase Problem" arises, preventing the direct solution of the crystal structure. Therefore, for a successful structure determination based on diffraction data, a set of structure factors is necessary which has atomic resolution (d_{\min} ca. 1 Å) with individual factors calculated from correct intensities and having correct phases.

$$I \sim |F|^2; \Rightarrow \text{sign}(F) \text{ undetermined}; F_{hkl} = \sum_{j=1}^n f_j e^{2\pi i(hx+ky+lz)}$$

I = measured Intensity

F = structure factor for every lattice plane (hkl)

f = atomic form factor for every atom j in the unit cell on position x, y, z

If no single crystals are available, powder X-ray diffraction experiments are carried out for materials characterization and structure analysis. The powder experiment superimposes the scattered intensity from three dimensional space in one dimension. This leads to systematically superimposed or partly overlapping reflections in the powder pattern which might additionally contain extra peaks from crystalline or diffuse background from non-crystalline impurities in the sample. Conventional analysis of powder X-ray data, therefore, characterizes the averaged crystal structure of the bulk sample. This requires manipulation of the experimental data set, e.g. background correction, before structure analysis is carried out.

As already mentioned above, electron crystallography has amplified the power of single crystal structure analysis extending the range of crystals to be studied to nano-crystals making use of kinematic intensity data acquired using electron diffraction tomography. This allows for the analysis of conventional powder samples and using single crystal techniques for structure solution. Because of the limited resolution of the electron diffraction data set as it can be recorded presently, the refinement of the crystal structure is performed consecutively using X-ray diffraction data. However, if electron diffraction tomography experiment becomes available to the general community, structure solution from powder diffraction data becomes obsolete, at least for those materials which are stable under TEM-conditions.

Solving crystal structure nowadays is performed either with direct methods and its variants, using reciprocal space information (diffraction experiments), or "ab initio" in direct space using partial information on the structure of the material (typical bond length and angles, coordination numbers, force field parameters or fragments of the structure) to generate a multitude of structure models, e.g. with Monte Carlo techniques. These models are subsequently used to compute diffraction diagrams. Those are refined against an experimental powder X-ray data set for evaluation. Whereas reciprocal space direct methods are extremely time-efficient and assumption-less, ab initio structure analysis in direct space uses brute force computation-power to check the multitude of model structures proposed. In general, direct methods require atomic resolution in the experimental intensity data set (Sheldrick's rule), ab initio direct space techniques have no such limitation. The

complementarity of the structure solution techniques, recently, has led to the combination of reciprocal space direct methods for finding solutions of a partial structure which then can be used for direct space modeling.

Structural studies can be divided into two disciplines, structure solution and structure refinements. Structure solution still requires detailed understanding of crystallography and the particular technique applied. If the crystallinity of the material is perfect, structure solution is much facilitated. Therefore, spending time on improving synthesis conditions for providing the best possible material for structure solution always is a worthwhile investment. The refinement of the crystal structure, on the other hand, is a problem of finding the best possible model to describe the experimental data set. For reference type materials, high resolution in the intensity data set is required to obtain accurate structure models. Those are of extreme value as standards and also the best possible basis for theoretical-computational modelling studies. The structure commission of the IZA has undertaken the task to evaluate and survey structural work providing the zeolite community with expert-evaluated structural information in its data base of zeolite frameworks¹⁶.

Looking at structure analysis from a practical point of view, there are many extremely helpful details and informations which can be drawn from the knowledge of the crystal structure in atomic resolution, in particular in applied zeolite sciences. **There is no other discipline in materials science where structure - property relation is so evident and important than in microporous materials.** Therefore, structure analysis should become routine in application oriented laboratories to answer questions like structural integrity of the sample, sorbate-framework interaction, pore filling, etc. For all scientist, there are data bases with public domain software for all purposes of structure analysis, structure determination, structure refinement and also structure visualisation, which are user-friendly and almost self-explanatory. Still, the most important precondition for the analysis is that pure, homogeneous material is available, which has been characterized with complementary techniques, and, finally, carefully measured intensity data.

However, current practice is that structure analysis is mainly preformed on materials which fulfil the technical criteria of the highest standards of specialized crystallographic journals. Many materials of interest, however, are of only modest crystallinity, i.e. limiting diffraction intensities to 2Θ -values of less than 45° for Cu-K α radiation, and to resolution of $d_{hkl} \geq 2.5 \text{ \AA}$, respectively, far from atomic resolution (ca. 1 \AA). Analyses of these materials is not performed. Still, the structure is characteristic of the material and the specific information on the structural details is contained in the diffraction data set. Since every structure factor contains the information of all atoms of the crystal structure, a valuable description of the structural details is still possible, even if residuals are of lesser quality and accuracy

and precision is limited. The result of the structure refinement reflects the best possible fit of the structure model to the diffraction data set and describes real structural features of the particular material. This statement is meant to stimulate and encourage more structural studies also of those materials of limited quality which often are used in practical applications.

The most frequently used technique to perform a structure analysis based on P-XRD data is the Rietveld method. As precondition, a structure model and an indexed powder diagram, yielding the metric and symmetry of the unit cell, is required. Assuming analytical profiles for the intensities in the powder diagram and measuring the powder diagram in step scan mode, the simulated powder diagram is refined against the experimental one by optimizing the geometry of the structure model of the material. There are numerous public domain "Rietveld"-programs for structure analysis such as FULLPROF, RIETAN, GSAS, BGMN, etc. which can be used for this purpose. Those can be obtained from the Sinchris database supported by the international union of crystallography (URL: <http://www1.iucr.org/sinchristop/logiciel/> or by searching for the program in the internet). In order to comply with international standards of crystal structure analysis the user manuals of the respective Rietveld program are very useful. In addition, there are recommendations and guidelines collected by internationally renown experts providing very helpful strategic and technical advice for beginners and advanced scientists alike. If the material is identified, a structure model can be retrieved from the structure data base and loaded from the cif-file into the refinement software for a full pattern Rietveld structure analysis.

3 Selected examples of solution and refinement of zeolite structures and their impact on the science of microporous materials retrieved from literature.

This paragraph is intended to comment on milestones of structure analyses in zeolite science which have had major impact on the future development in the field of microporous materials concerning synthesis and synthesis strategies, sorption and separation, catalysis and modern applications. For full details on the specific topic, it is recommended to read the original communications. The selection is strongly biased as far as the particular examples are concerned, however, there is no doubt that elucidation of zeolite crystal structures reveals the structure property relationship and has inspired the development of zeolite science tremendously.

3.1 Zeolites ZSM-5 and silicalite-1, MFI framework type

The structure solution of ZSM-5 constituted a major achievement in zeolite science. The material ZSM-5 was patented in 1972 (patent filed in 1967) by Mobil Corporation¹⁷, its structure in the all silica form was first published in February 1978 by the Union Carbide zeolite group¹⁰ and one month later by the Mobile

Corporation zeolite group¹¹, both in *Nature*, reflecting the strong competition in the field and the high value of the structural information. The structure solution reported was performed on single crystal data of the calcined material. In the original paper by Flanigen et al. it is already reported that the crystal was twinned and, obviously, had undergone phase transition to lower, monoclinic symmetry (Fig. 2). The following up paper by Kokotailo et al. gives no details on the structure analysis, however, the technical problems concerning a proper structure refinement are commented on as "we have determined their structure by model building, single crystal and powder X-ray diffraction data". The crystal structure of MFI-type materials remained for a long time the most complicated zeolite crystal structure which is also documented in a series of structure refinements following the original structure reports. In particular the late Henk v. Koningsveld showed in a series of structure analyses that the ferroelastic phase transition leads to a slightly distorted monoclinic symmetry of the unit cell^{18;19}, that sorbates order periodically in the MFI-channel system^{20;21}, and that, dependent on the amount of sorbate, phase transitions occur leading to several MFI-type materials in distinct, sorbate-specific symmetries^{21;22;23}.

Structure analysis from X-ray diffraction in combination with TEM microscopy revealed even more structural details which were most important for application of the materials as refining and fine chemical catalyst. The typical twinning of crystals of MFI-type materials does not affect the porosity and the dimensionality of the channel system, and, therefore, has no impeding influence on applications. This is also true for the intergrowth with MEL-type material in the pentasil family²⁴.

The visualisation of the crystal structure in combination with data from nitrogen adsorption, chemical analyses, NMR-spectroscopy etc. substantiated the 10-ring pore dimension and the 3-dimensional diffusion pathway of the pores in the material, even if twinning or intergrowth occurs. Based on the knowledge of its crystals structure, MFI-type materials became the most researched and studied zeolites in the following years. Successful and important applications in the field of catalysis followed and emphasized the importance and the impact of structure analysis. Structure analysis of as synthesized tetrapropylammonium-silicalite, TPA-silicalite, very convincingly underlined the concept of structure directing by organic templates, the structure directing agents, SDA. The intimate correspondence of the molecular geometry of the SDA and the channel geometry in the silicate framework of ZSM-5²⁵ certainly inseminated chemists working in synthesis of zeolites and subsequently lead to the discovery of numerous zeolite materials, the most important ones are ZSM-12²⁶, ZSM-22²⁷, ZSM-23²⁸, and ZSM-48²⁹.

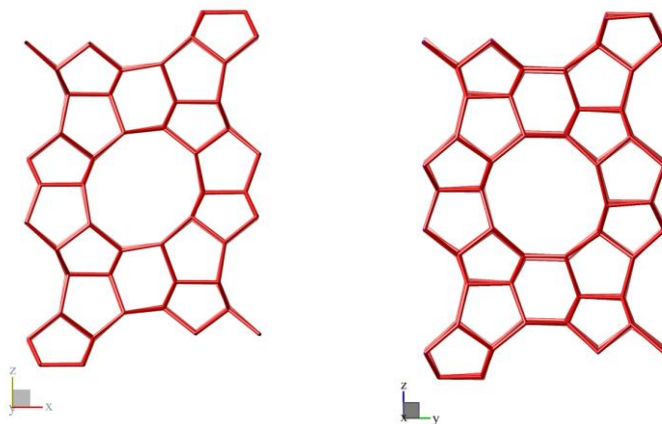


Fig. 2: Projections of the orthorhombic (l) and monoclinic (r) MFI framework along the straight channel. Watch the subtle differences due to the symmetry change.

3.2 Zeolite β and the search for a chiral zeolite framework

The original patent on zeolite β was filed in 1964 and granted in 1967 to the Mobil Oil Corporation. Only 24 years after filing the patent, structure models were published in literature by Newsam et al.³⁰ and Higgins et al.³¹ (Fig. 3). As already mentioned, the lack of interest in the material was caused by the unusual X-ray powder pattern showing broad and sharp reflections indicating complex material. In addition, the resolution in the P-XRD pattern and the obvious crystallinity of the material was low suggesting poor performance in applications typical for zeolites.

In the course of structure determination, TEM experiments, diffraction and imaging, played a crucial role. Despite its poor powder diagram, TEM images of the zeolite revealed its crystalline nature, however, there was disorder in the stacking sequence of layer-like building units. Underlying disorder of stacking, Newsam et al. succeeded in solving the structure and simulating the powder pattern. This led to the characterisation of the material and revealed its unperturbed 3-dimensional 12-ring pore system. In the same year Higgins et al. showed that there are ordered simplest end-members using the beta-sheet, one of which has a chiral framework structure, polymorph A, having space group symmetry $P4_122$ or $P4_322$. Not only the revelation of the crystal structure of beta immediately led to applications and commercialisation but also the search for the chiral ordered end member material started. Based on the SDA-synthesis approach, for more than a decade, synthesis chemists tried to achieve the goal without success. The refinement of synthesis conditions stimulated by the knowledge of the crystal structure and the very

successful SDA-based synthesis protocol led to the isolation of polymorph B^{32:33} and polymorph C^{34:35}. However, an enrichment or even pure polymorph A, the chiral variety, as bulk materials was never obtained.

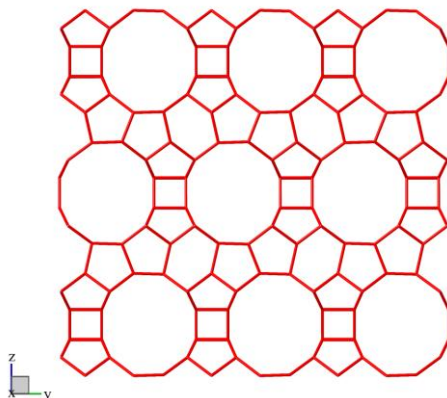


Fig. 3: Zeolite beta, polymorph A seen along [100].

In contrast to the exhaustive synthesis attempts chasing for the chiral zeolite framework, application oriented research transformed the material from a laboratory curiosity into a valuable industrial catalyst very quickly, after the crystal structure was known and confirmed that zeolite beta has a three dimensional, interconnected pore system. Again, the visualisation of the framework structure inspired the zeolite science community in all disciplines leading to year-long extensive studies of the many beta materials which have been synthesized meanwhile. The latest progress in the field is the template-free synthesis of zeolites beta which has few structural defects challenging the SDA-concept and turning beta into an even more interesting material for industrial applications³⁶.

3.3 The clathrasil octadecasil and the F⁻-synthesis of zeolites

The fluoride route in zeolite synthesis had been introduced in order to use other mineralization media than the basic hydroxyl anion. The first example obtained via the fluoride route was silicalite-1, the all silica analogue of zeolite ZSM-5. It was known that fluoride binds to silicon and might also stabilise higher coordination states of Si than four, however, the role of fluoride during zeolite synthesis was not recognized. The crystal structure analysis of the clathrasil octadecasil for the first time revealed that fluoride occupies the double-four-ring unit thus stabilising the AST-framework type which is of rather low framework density (Fig. 4)³⁷. The structure refinement from single crystal data immediately also explained the unusual chemical shift values in the 19-F MAS NMR spectra at ~ -40 ppm as fluoride entity in the double-four-ring confinement, D4R-confinement. Later, in

NMR experiments monitoring the synthesis of zeolite ITQ-7, it has been shown that the signal characteristic for the fluoride anion in the D4R-confinement shows up long before the crystalline material could be detected in P-XRD-experiments³⁸.

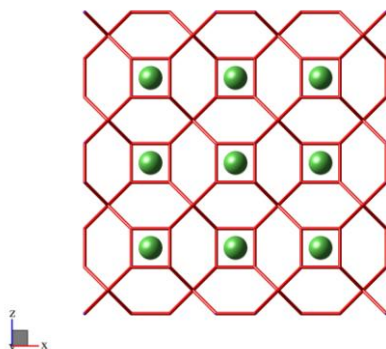


Fig. 4: AST framework showing the fluoride anion occupying the D4R.

Based on this insight, in particular Avelino Corma and his group very successfully used fluoride as mineralizer and structure director for the synthesis of many new silicate zeolite framework types all containing the D4R-unit as characteristic structural feature. These are the framework structure types and the type materials which have been obtained by the synthesis groups of the Instituto de Tecnología Química, ITQ, where the fluoride route was developed and D4R-units are part of the framework structure: ISV (ITQ-7)³⁹, ITW (ITQ-12)⁴⁰, ITH (ITQ-13)⁴¹, BEC (beta polymorph C or ITQ-17)³⁵, IWW (ITQ-22)⁴², IWR (ITQ-24)⁴³, IWS (ITQ-26)⁴⁴, IWV (ITQ-27)⁴⁵, ITR (ITQ-34)⁴⁶, -ITV (ITQ-37)⁴⁷, and IRR (ITQ-44)⁴⁸. In addition, the all silica LTA (ITQ-29)⁴⁹ was also obtained using fluoride as one of the structure directors. The long list of different and new framework structure types were not exclusively obtained by the fluoride SDA but in combination with other molecular SDA, most often organic amines, and by the addition of Ge as substituent for Si on T-positions. However, for the successful synthesis, fluoride was essential and the prime intention of the synthesis chemists was to stabilize D4R-units as they were first detected in octadecasil, AST framework type. Interestingly, before the fluoride anion was established experimentally in the D4R-unit, it was speculated from theoretical calculations that the sodium cation should fit inside the D4R and thus stabilize the structure. After some controversy, new simulation studies consolidated the experimental result and also found the stabilizing influence of the fluoride anion⁵⁰.

The octadecasil example very nicely shows the impact of basic research on the progress of science. The clathrasil octadecasil with 6-rings as largest pore openings has no typical ion exchange or sorption properties. There is also no catalytic activity since it is a neutral material and molecules can not enter through the 6-ring

window. Only the realization of the role of fluoride during synthesis as manifested in the crystal structure as the experimental growth protocol and its generalization in a specific synthesis strategy turned the structure analysis of the AST-framework type into a key experiment in zeolite science.

3.4 Direct methods and the solution of zeolite crystal structures from P-XRD data, from sigma-2 to the most complicated case: ITQ-22, framework code IWW

Crystal structure analysis has contributed tremendously to zeolite science. The ultimate need to visualise the materials atomic arrangement in order to rationalize synthesis parameters and physical and chemical properties of the microporous material has also fuelled the development of structure solution techniques and methods. Zeolitic materials most often are obtained as crystalline powders. In the past 25 years the advance of structure solution from X-ray powder diffraction data is strongly correlated with zeolite science. At any time, the most complicated structures solved from P-XRD data were microporous materials continuously shifting the degree of complexity higher and higher. Since the advent of high resolution powder diffractometers at synchrotron radiation sources, the refinement of crystal structures and later also the solution of crystal structures from powder X-ray diffraction data was pioneered by zeolite crystallographers. Various strategies were developed always involving most advanced instrumentation available at synchrotron light sources. In order to benefit from a high resolution powder diffractometer, materials of highest possible crystallinity are required facilitating the indexing of the pattern and data collection up to high Q-range in reciprocal space. Structure determination heavily relies on careful analysis of the materials metric and symmetry as well as on the precise extraction of intensities for as many reflections as possible. The information on the material in diffraction experiments is obtained from reciprocal space and should be complemented by spectroscopic, thermal or sorption experiments confirming the diffraction data analysis. It all started with the structure solution of the clathrasil sigma-2, framework code SGT⁵¹, which was the first zeolite framework type determined from P-XRD using direct methods. Although of no obvious useful zeolitic property, the successful structure determination motivated zeolite crystallographers tackling more and more complicated structures. Whereas most groups in zeolite crystallography used a complementary combination of methods like XRD, TEM, NMR and modelling for structure solution, the group of J. Rius focused on diffraction information only and improved the power of the original direct methods introducing the modulus sum function⁵² as implemented in structure solution program XLENS. Nowadays, direct methods are very efficient and, given the right input information, the solution or at least the partial solution is obtained within seconds. Completing the partial model and refining the crystal structure from P-XRD data using the Rietveld technique is a time demanding and slow process (Fig. 5).

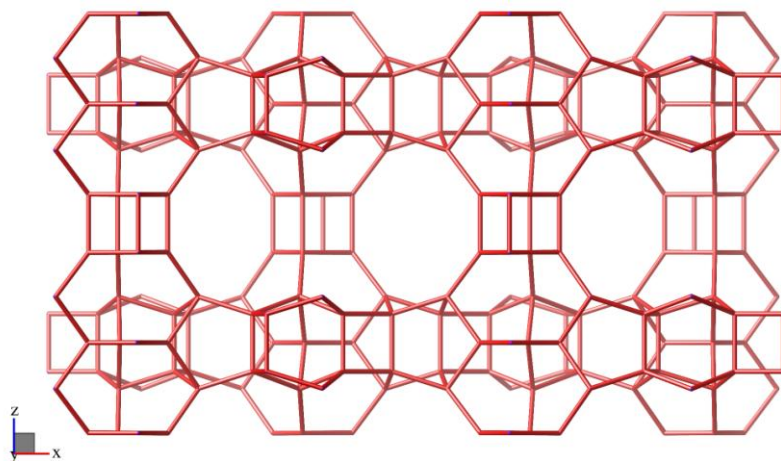


Fig. 5: Projection of zeolite ITQ-22 (IWW) along $[010]$. The D4R can be seen connecting layer-like complex building units.

The crystal structure of zeolite ITQ-22 with 16 inequivalent T-sites on framework positions is the most complicated structure solved from P-XRD and direct method application only⁴². It is the first material with 12-, 10-, and 8-ring channels which intersect. The material shows important shape selective properties in catalysis introduced through the channel hierarchy. From the synchrotron based P-XRD data set the unit cell dimensions and symmetry were retrieved and based on the extracted intensities almost all 16 T-atom positions were resolved. Assuming a three-dimensional four-connected net the structure was completed by adding O-atoms in between two T-centers and inserting $[TO_4]$ -units in structure gaps. The full pattern refinement finally confirmed the correctness of the structure model.

3.5 Combining TEM and P-XRD in reciprocal space and searching direct space: The structure of TNU-9, framework code TUN

Another step of complexity constitutes the solution of the structure of zeolite TNU-9⁵³. With 24 symmetry independent atoms on T-sites the unit cell volume is almost twice as big as in ITQ-22. Despite best quality data from the P-XRD experiment and using search techniques from FOCUS in direct space⁵⁴, no solution was obtained in the beginning. From additional electron diffraction and imaging data, structural information of the material had been obtained from projections along the channel axes. In addition, phases of reflections have been determined from these experiments. Adding this as starting information into the structure solution process using the full data set from P-XRD, the crystal structure was solved and refined using the Rietveld technique (Fig. 6). As can be learned from the original publication the process of structure solution was a very time-consuming process,

not only in setting up the physical collaboration between electron crystallography and powder diffraction but also in achieving the goal. In the successful final computer run, 16 days of cpu-time were required just for structure solution. The successive Rietveld refinement still laid ahead. The proportion of time needed for reciprocal space structure solution, as e.g. for ITQ-22, and direct space techniques is typical. Despite basic, but partial structure information from diffraction analysis is provided, the search in direct space using the FOCUS-approach is extremely costly. As perspective for the future, however, direct space modelling will become ever more competitive as computer power increases. With improved code and modern equipment one might cut cpu-time to one day or less today.

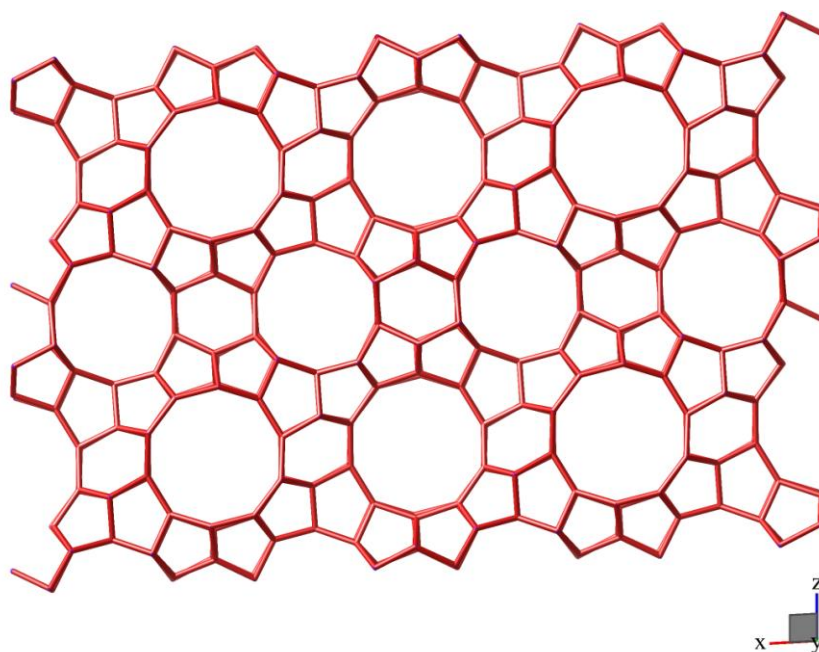


Fig. 6: Projection of the framework structure of zeolite TNU-9 (TUN) along $[010]$.

3.6 Extending the approach of the combination of complementary techniques using reciprocal and direct space: P-XRD, electron crystallography, charge flipping and structure envelope: The structure of IM-5, framework code IMF

IM-5 was an enigma for more than 10 years before in 2007 its structure was solved⁵⁵. Similar to the preceding material TNU-9, IM-5 has 24 symmetrically distinct T-atoms on T-sites in the unit cell. Different from the FOCUS-approach, direct space becomes involved through the charge flipping algorithm. In a recursive

way, electron density distribution in direct space obtained from refined phase values of structure factors in reciprocal space is repartitioned and back-transformed in new phases for structure factors in reciprocal space. In addition, partial information about the crystal structure was obtained from electron diffraction experiments leading to phase information for ca. 95 reflections. Feeding this information into the charge flipping structure solution process using intensity information from the extracted P-XRD data, the crystal was retrieved. The final electron density map obtained from the charge flipping calculations precisely represents the tetrahedral network of the microporous material (Fig. 7). The material has an unusual 2D 10-ring channel system which is connected through a larger cavity. Thus the material has potential catalytic activity and shape selectivity which should reflect the structural peculiarities.

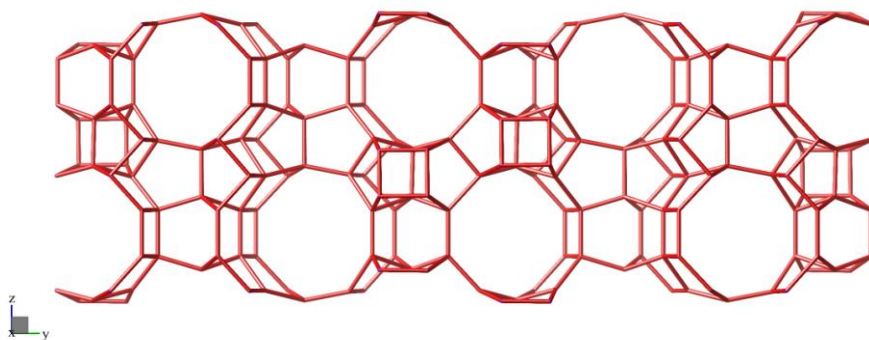


Fig. 7: Projection of the framework of zeolite IM-5 (IMF) seen along [100].

The advancement made with the introduction of charge flipping in the structure solution process is the efficiency with which direct space information is extracted and positively used and fed into the refinement of the structure factor phases. Still, as precondition materials of highest quality are required for the diffraction experiment, thus limiting structure solution.

3.7 New, exciting structures solved recently: ITQ-33 and ITQ-37 (framework code -ITV)

Following the strategies described above and developing the techniques to perfection, the structures of these two exciting materials were solved. The new structures clearly are of lower structural complexity, however, the materials exhibit exceptional structural properties which might inspire application oriented research. ITQ-33, which has no framework code so far, has an intersecting 10- by 18-ring channel system⁵⁶. The hierarchical channel system shows very interesting catalytic properties which are rationalized by the unusual structural features (Fig. 8, 1).

Finally ITQ-37⁴⁷ which is a mesoporous, crystalline zeolite with a 30-ring channel has the lowest framework density of all zeolite framework types. The very large pore volume of the germanosilicate and its chiral framework structure will possibly allow for new applications (Fig. 8, r).

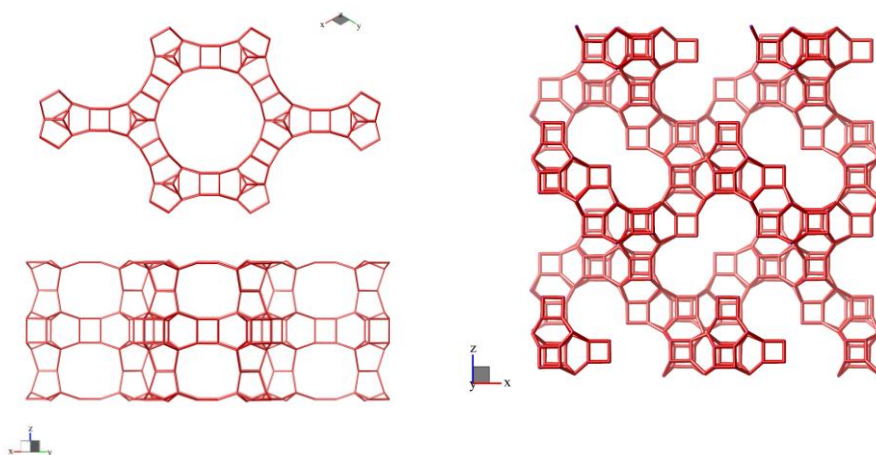


Fig. 8: Structure plots of ITQ-33 (l) and ITQ-37 (ITV) (r), two exiting new materials

3.8 Recent advances in structure analysis affecting zeolite science in the future: the breakthrough of electron crystallography

A major breakthrough in structure determination is the introduction of the automated electron diffraction tomography in combination with the precession technique in electron crystallography. Kolb and co-workers showed, also using zeolite materials as examples, that reliable intensity data can be extracted automatically from electron diffraction experiments of nano crystals and be processed as single crystal intensity data using direct methods for structure solution¹⁵. The most complicated crystal structures could be solved directly from TEM experiments using nano crystalline powder materials without further involvement of complementary X-ray experiments. This advancement in electron crystallography instrumentation supersedes crystal structure solution from P-XRD data and opens new vista in structural science of nano crystalline materials including zeolites.

3.9 Zeolite materials of limited crystallinity, are they left out?

All examples of structure solution and refinement described before required materials of perfect crystallinity. However, many materials exist which are of limited crystal quality. Still, their crystal structures are of interest for reasons of synthesis and application oriented research strategies. As examples two studies are mentioned describing zeolite crystal structure determinations from diffraction data of limited resolution. In these examples, standard direct methods failed and computer assisted model building was involved as important tool. RUT framework type belongs to the clathrasil family and could never be obtained as well crystallized material. Considering the $[\text{SiO}_4]$ -unit as invariant and connecting those to a 3-dimensional 4-connected silicate framework, the requirements of "atomic resolutions" are shifted to larger values. Introducing the new limits into the structure solution software, the RUT crystal structure was solved (Fig. 10)⁵⁷. From the distribution of T-centers, which showed up in the electron density map, the silicate framework could be built. Finally, the structure was refined from P-XRD data using the Rietveld method.

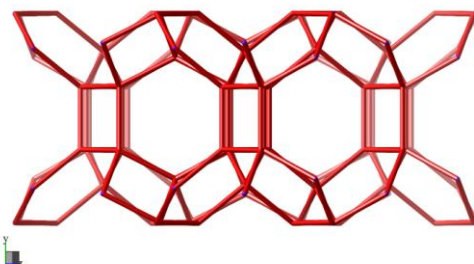


Fig. 9: Structure plot of RUB-10 (RUT).

Recently, interlayer expanded zeolites were introduced as post synthesis derivatives of layered precursors. The materials are homogeneous, however, their crystallinity is low since the bridging linker-unit introduced flexibility into the framework. An example is the material IEZ-RRO (Fig. 11). Knowing the crystals structure of the precursor and also the molecular structure of the linker, a structure model can be derived and used as starting model for the Rietveld analysis of the P-XRD data. Because there is no strict periodicity in the framework of the IEZ-material, reflections in the powder diagram are broadened. In addition, stacking disorder might be present in the sample, further complicating the analysis. Still, it is worthwhile to carry out the structure refinement in order to obtain the most detailed information about the structure from experimental analysis¹⁴. This is the best precondition for simulation studies using structure modelling.

Wherever limited crystallinity is an inherent property of the material or electron beam sensitive materials degrade in the TEM, direct space ab initio methods come into play. With information on the spacegroup symmetry, chemical composition, information on building blocs or structural subunits from IR- or NMR-spectroscopy, structure models can be generated using e.g. Monte-Carlo techniques and tested against the P-XRD diagram. There are commercial programs such as TOPAS and ENDEAVOUR and public domain programs such as FOX or FULLPROF which particularly address inorganic materials and are well suited to solve zeolite structures.

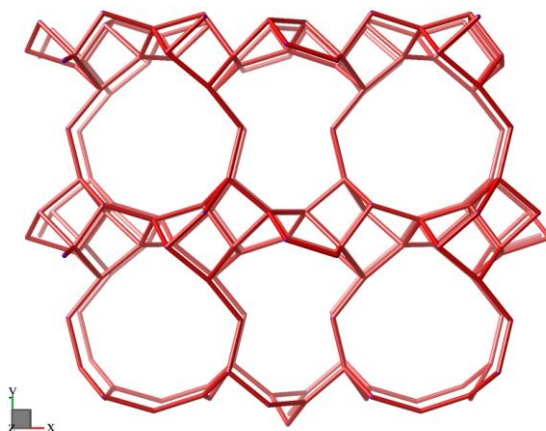


Fig. 10: Projection of the framework of interlayer expanded zeolite (IEZ) of RRO type along [001].

3.10 Zeolite structures not contained in the data base

There is a number of crystal structures published in literature which is not contained in the data base of zeolite framework types. Prominent examples are ITQ-21⁵⁸ or RUB-23⁵⁹. Although the materials qualify as typical zeolites, the structure commission rejected the assignment of a structure code because of technical reasons. The inventors were asked to improve their structure analysis and answer particular questions. Since this did not happen until now, no code was assigned. This is particularly pity for ITQ-21 since it is the parent structure for other materials, e.g. ITQ-26 (IWS)⁴⁴, where a code has been assigned.

4 Conclusions

The survey on zeolite structures, selecting some prominent examples which had and will have impact on the development of zeolite sciences, should provide historical

and actual information on the state of structural zeolite sciences. As mentioned in 3.8, it is expected that electron crystallography will take over the role of powder X-ray crystallography in the future. In this sense, the review also highlights the achievements of P-XRD and sets the starting point for the new electron crystallography era in zeolite sciences. Extrapolating from the past, TEM equipment with precession instrumentation will substitute for the synchrotron experiment in the future, however, the technique still needs experts until automation will substitute them.

References

- [1] Szostak, R. Handbook of molecular sieves. Springer. New York (2006).
- [2] Cejka, J. Introduction to Zeolite Molecular Sieves. Elsevier Science BV. Amsterdam (2007).
- [3] Xu, R.; Pang, W.; Yu, J. H.; Huo, Q. S.; Chen, J. S. Chemistry of zeolites and related porous materials. Wiley & Sons (Asia). Singapore (2007).
- [4] Wright, P. A. Microporous framework solids. The Royal Society of Chemistry; Thomas Graham House. Cambridge (2008).
- [5] Taylor, W. The structure of analcite ($\text{NaAlSi}_2\text{O}_6 \cdot \text{H}_2\text{O}$). *Z Kristallogr* **74**, 1–19 (1930).
- [6] Pauling, L. The structure of sodalite and helvite. *Z Kristallogr* **74**, 213–225 (1930).
- [7] Pauling, L. The structure of some sodium and calcium aluminosilicates. *Proc Natl Acad Sci* **16**, 453–459 (1930).
- [8] Reed, T.B.; Breck, D.W. Crystalline Zeolites. 2. Crystal structure of synthetic zeolite, type-A. *J Am Chem Soc* **78**, 5972–5977 (1956).
- [9] Nowacki, W.; Bergerhoff, G. Die Kristallstruktur des Zeolithes Faujasit. *Acta Crystallogr* **10**, 761–762 (1957).
- [10] Flanigen, E.; Bennett J.M.; Grose R.W.; Cohen J.P.; Patton R.L.; Kirchner R.M.; Smith J.V. Silicalite, a new hydrophobic crystalline silica molecular sieve. *Nature* **271**, 512–516 (1978).
- [11] Kokotailo, G.T.; Lawton, S.L.; Olson, D.H.; Meier, W.M. Structure of the synthetic zeolithe ZSM-5. *Nature* **272**, 437–438 (1978).
- [12] Eddaoudi, M.; Li, H.; Yaghi, O. Highly porous and stable metal-organic frameworks: Structure design and sorption properties. *J Am Chem Soc* **122**, 1391–1397 (2000).

- [13] Ruan, J.F.; Wu, P.; Slater, B.; Terasaki, O. Structure elucidation of the highly active titanosilicate catalyst Ti-YNU-1 *Angew Chem Int Ed* **44**, 6719–6723 (2005).
- [14] Gies, H.; Müller, U.; Yilmaz, B.; Tatsumi, T.; Xie, B.; Xiao, F.-S.; Bao, X.; Zhang, W.; Vos, D. de. Interlayer Expansion of the Layered Zeolite Precursor RUB-39: A Universal Method To Synthesize Functionalized Microporous Silicates *Chem Mater* **23**, 2545–2554(2011).
- [15] Kolb, U.; Gorelik, T.; Mugnaioli, E. Automated Diffraction Tomography Combined With Electron Precession: A New Tool for Ab Initio Nano structure Analysis. *Materials Research Society Symposium Proceedings* **1184**, 11–23 (2009).
- [16] Baerlocher, C.; McCusker, L.B. Database of Zeolite Structures. URL: <http://www.iza-structure.org/database/>
- [17] Argauer, R.J.; Landolt, G.R. Crystalline zeolite ZSM-5 and method of praring the same. U.S. pat. 3702886, (1972)
- [18] van Koningsveld, H.; Jansen, J. C.; van Bekkum, H. The monoclinic framework structure of zeolite H-ZSM-5 - Comparisoin with the orthorhombic framework of as synthesized ZSM-5. *Zeolites* **10**, 235-242(1990).
- [19] van Koningsveld, H.; Jansen, J. C.; van Bekkum, H. The orthorhombic monoclinic transition in single crystals of zeolite ZSM-5. *Zeolites* **7**, 564–568 (1987).
- [20] van Koningsveld, H.; Tuinstra, F.; van Bekkum, H.; Jansen, J.C. The location of para-xylene in a single-crystal of zeolite H-ZSM-5 with a new sorbate induced, orthorhombic framework symmetry. *Acta Crystallogr B* **45**, 423–431 (1989).
- [21] van Koningsveld, H.; Jansen, J. C.; van Bekkum, H. The location of p-dichlorobenzene in a single crystal of zeolite H-ZSM-5 at high sorbate loading. *Acta Crystallogr B* **52**, 140–144 (1996).
- [22] Stroble, H.; Fyfe, C.A.; Kokotailo, G.T.; Pasztor, C.T.; Bibby, D.M. High-symmetry, high-temperature zeolite lattice structures. *J Am Chem Soc* **109**, 4733–4734 (1987).
- [23] Fyfe, C.A.; Stroble, H.; Gies, H.; Kokotailo, G.T. High resolution solid-state NMR investigation of the nature of the interaction between organic substrates and the zeolite ZSM-5 lattice. *Can J Chem* **66**, 1942–1947 (1988).

- [24] Ohsuna, T.; Terasaki, O.; Nakagawa, Y.; Zones, S. I.; Hiraga, K. Electron microscopic study of intergrowth of MFL and MEL: Crystal faults in B-MEL. *J Phys Chem B* **101**, 9881–9885 (1997).
- [25] Price, G.; Pluth, J.; Smith, J.V.; Bennett, J.; Patton, R. Crystal-structure of tetrapropylammonium fluoride silicalite. *J Am Chem Soc* **104**, 5971–5977 (1982).
- [26] LaPierre, R.B.; Rohrman, A.C.; Schlenker, J.L.; Wood, J.D.; Rubin, M.K.; Rohrbaugh, W.J. The framework topology of ZSM-12 - A high silica zeolite. *Zeolites* **5**, 346–348 (1985).
- [27] Kokotailo, G.T.; Schlenker, J.L.; Dwyer, F.G.; Valyocsik, E.W. The framework topology of ZSM-22 - A high silica zeolite. *Zeolites* **5**, 349–351 (1985).
- [28] Rohrman, A.C.; LaPierre, R.B.; Schlenker, J.L.; Wood, J.D.; Valyocsik, E.W.; Rubin, M.K.; Higgins, J.B.; Rohrbaugh, W.J. The framework topology of ZSM-23 - A high silica zeolite. *Zeolites* **5**, 352–354 (1985).
- [29] Schlenker, J.L.; Rohrbaugh, W.J.; Chu, P.; Valyocsik, E.W.; Kokotailo, G.T. The framework topology of ZSM-48 - A high silica zeolite. *Zeolites* **5**, 355–358 (1985).
- [30] Newsam, J.M.; Treacy, M.M.; Koetsier, W.T.; DeGruyter, C.B. Structural characterisation of zeolite-beta. *Proc Royal Soc London Series A-Math Phys Eng Sci* **420**, 375 (1988).
- [31] Higgins, J.B.; LaPierre, R.B.; Schlenker, J.L.; Rohrman, A.C.; Wood, J.D.; Kerr, G.T.; Rohrbaugh, W.J. The framework topology of zeolite-beta. *Abstr Pap Am Chem Soc* **196**, 24 (1988).
- [32] Corma, A.; Moliner, M.; Cantin, A.; Diaz-Cabanias, M.J.; Lorda, J.L.; Zhang, D.; Sun, J.; Jansson, K.; Hovmoller, S.; Zou, X. Synthesis and structure of polymorph B of zeolite beta. *Chem Mater* **20**, 3218–3223 (2008).
- [33] Kadgaonkar, M.D.; Kasture, M.W.; Bhange, D.S.; Joshi, P.N.; Ramaswamy, V.; Kumar, R. NCL-7, A novel all silica analog of poly morph B rich member of BEA family: Synthesis and characterization. *Microporous Mesoporous Mat* **101**, 108–114 (2007).
- [34] Conradsson, T.; Dadachov, M.; Zou, X. Synthesis and structure of $(\text{Me}_3\text{N})_6[\text{Ge}_{32}\text{O}_{64}](\text{H}_2\text{O})_{4.5}$, a thermally stable novel zeotype with 3D interconnected 12-ring channels. *Microporous Mesoporous Mat* **41**, 183–191 (2000).

- [35] Corma, A.; Navarro, M. T.; Rey, F.; Rius, J.; Valencia, S. Pure polymorph C of zeolite beta synthesized by using framework isomorphous substitution as a structure-directing mechanism. *Angew Chem Int Ed* **40**, 2277–2280 (2001).
- [36] Xie, B.; Song, J.; Ren, L.; Ji, Y.; Li, J.; Xiao, F.-S. Organotemplate-free and fast route for synthesizing Beta zeolite. *Chem Mater* **20**, 4533–4535 (2008).
- [37] Caullet, P.; Guth, J.L.; Hazm, J.; Lamblin, J.M.; Gies, H. Synthesis, characterization and crystal structure of the new clathrasil phase octa decasil. *European J Sol State Inorg Chem* **28**, 345–361 (1991).
- [38] Song, J. Q.; Marler, B.; Gies, H. Synthesis of ITQ-7 with a new template molecule and its crystal structure analysis in the as synthesized form. *CR Chim* **8**, 341–352 (2005).
- [39] La Villaescusa; Barrett, P. A.; Cambor, M. A. ITQ-7: A new pure silica polymorph with a three-dimensional system of large pore channels. *Angew Chem Int Ed* **38**, 1997–2000 (1999).
- [40] Barrett, P. A.; Boix, T.; Puche, M.; Olson, D. H.; Jordan, E.; Koller, H.; Cambor, M. A. ITQ-12: a new microporous silica polymorph potentially useful for light hydrocarbon separations. *Chem Commun* **2003**, 2114–2115 (2003).
- [41] Corma, A.; Puche, M.; Rey, F.; Sankar, G.; Teat, S. J. A zeolite structure (ITQ-13) with three sets of medium-pore crossing channels formed by 9- and 10-rings. *Angew Chem Int Ed* **42**, 1156–1159 (2003).
- [42] Corma, A.; Rey, F.; Valencia, S.; Jorda, J.L.; Rius, J. A zeolite with interconnected 8-, 10- and 12-ring pores and its unique catalytic selectivity. *Nature Materials* **2**, 493–497 (2003).
- [43] Castaneda, R.; Corma, A.; Fornes, V.; Rey, F.; Rius, J. Synthesis of a new zeolite structure ITQ-24, with intersecting 10- and 12-membered ring pores. *J Am Chem Soc* **125**, 7820–7821 (2003).
- [44] Dorset, D.L.; Strohmaier, K.G.; Kliewer, C.E.; Corma, A.; Diaz-Cabanias, M.J.; Rey, F.; Gilmore, C.J. Crystal Structure of ITQ-26, a 3D Framework with Extra-Large Pores. *Chem Mater* **20**, 5325–5331 (2008).
- [45] Dorset, D.L.; Kennedy, G.J.; Strohmaier, K.G.; Diaz-Cabanias, M.J.; Rey, F.; Corma, A. P-derived organic cations as structure-directing agents: Synthesis of a high-silica zeolite (ITQ-27) with a two-dimensional 12-ring channel system. *J Am Chem Soc* **128**, 8862–8867 (2006).

- [46] Corma, A.; Diaz-Cabanas, M.; Jorda, J.; Rey, F.; Sastre, G.; Strohmaier, K. A zeolitic structure (ITQ-34) with connected 9- and 10-Ring channels obtained using phosphonium cations as structure directing agents. *J Am Chem Soc* **130**, 16482. (2008).
- [47] Sun, J.; Bonneau, C.; Cantin, A.; Corma, A.; Diaz-Cabañas, M.; Moliner, M.; Zhang, D.; Li, M.; Zou, X. The ITQ-37 mesoporous chiral zeolite *Nature* **458**, 1154–1157 (2009).
- [48] Jiang, J.; Jorda, J.; Diaz-Cabañas, M.; Yu, J.; Corma, A. The synthesis of an extra-large-pore zeolite with double three-ring building units and a low framework density *Angew Chem Int Ed*, **49**, 4986–4988 (2010).
- [49] Corma, A.; Rey, F.; Rius, J.; Sabater, M. J.; Valencia, S. Supramolecular self-assembled molecules as organic directing agent for synthesis of zeolites. *Nature* **431**, 287–290 (2004).
- [50] George, A. R.; Catlow, C. R. A computational study of the role of F-ions in the octadecasil structure. *Zeolites* **18**, 67–70 (1997).
- [51] McCusker, L. The ab initio structure determination of Sigma-2 (a new clathrasil phase) from synchrotron powder diffraction data. *J Appl Crystallogr*, **21**, 305–310 (1988).
- [52] Rius, J.; Frontera, C. Application of the constrained S-FFT direct-phasing method to powder diffraction data. XIII. *J Appl Crystallogr* **40**, 1035–1038 (2007).
- [53] Gramm, F.; Baerlocher, C.; McCusker, L.B.; Warrender, S.J.; Wright, P. A.; Han, B.; Hong, S. B.; Liu, Z.; Ohsuna, T.; Terasaki, O. Complex zeolite structure solved by combining powder diffraction and electron microscopy. *Nature* **444**, 79–81 (2006).
- [54] Grosse-Kunstleve, R.W.; McCusker, L.B.; Baerlocher, C. Powder diffraction data and crystal chemical information combined in an automated structure determination procedure for zeolites. *J Appl Crystallogr*, **30**, 985–995 (1997).
- [55] Baerlocher, C.; Gramm, F.; Massueger, L.; McCusker, L.B.; He, Z.; Hovmoeller, S.; Zou, X. Structure of the polycrystalline zeolite catalyst IM-5 solved by enhanced charge flipping. *Science* **315**, 1113–1116 (2007).
- [56] Corma, A.; Diaz-Cabanas, M. J.; Luis Jorda, J.; Martinez, C.; Moliner, M. High-throughput synthesis and catalytic properties of a molecular sieve with 18- and 10-member rings. *Nature* **443**, 842–845 (2006).

- [57] Gies, H.; Rius, J. Ab-initio structure determination of zeolite RUB-10 from low resolution X-ray powder diffraction data. *Z Kristallogr* **210**, 475–480 (1995).
- [58] Corma, A.; Diaz-Cabanas, M.; Martinez-Triguero, J.; Rey, F.; Rius, J. A large-cavity zeolite with wide pore windows and potential as an oil refining catalyst. *Nature* **418**, 514–517 (2002).
- [59] Park, S. H.; Daniels, P.; Gies, H. RUB-23: a new microporous lithosilicate containing spiro-5 building units. *Micropor Mesopor Mat* **37**, 129–143 (2000).

Synchrotron based in situ X-ray techniques for the characterisation of nanoporous solids

Gopinathan Sankar*, Kerry Simmance, Andrew J. Smith and Martin Martis

¹*Department of Chemistry, University College London, 20 Gordon Street, London WC1H 0AJ, United Kingdom*

Abstract

Here we describe the use of *in situ* and *ex situ* characterisation methods employed for the study of nanoporous solids, in particular targeted towards the understanding of (a) the nucleation and growth processes that take place during hydrothermal crystallization, (b) electronic and geometric changes that take place during the activation of nanoporous catalytic materials and (c) structural modifications during the activation and catalytic processes. To achieve this end, it is necessary to employ appropriate suite of techniques, in particular, time-resolved X-ray diffraction, X-ray absorption spectroscopy and small-angle X-ray scattering techniques. All these techniques have their own merits and limitations in providing detailed information on changes in the structure, which will be discussed. With the recent developments in these synchrotron radiation based techniques, it is possible to combine them appropriately to determine the structure of nano porous materials. Examples from zeolites and metal ions substituted aluminophosphates are given here.

1. Introduction

Over the last decade advancement in the area of characterisation of nanoporous materials has taken place employing a variety of techniques¹⁻⁷. Characterisation of microporous materials is essential in understanding their physical properties, their structure–application relationships, why certain structures favour specific reactions, and for a greater knowledge into the design of new materials. Synchrotron radiation techniques play a crucial role in the precise characterisation of zeolitic solids. In particular, X-ray diffraction (XRD), X-ray absorption spectroscopy (XAS), small angle X-ray scattering, total scattering (also called high energy X-ray diffraction (HEXRD)) and energy dispersive X-ray diffraction (EDXRD)⁸. Advancement in X-ray optics and detector technology allowed, not only the development of time-resolved techniques but also combination of many of these techniques along with appropriate optical spectroscopic methods. Although

each technique has its own advantage in providing specific information about the porous solids, at the same time all of them have their own limitations. Thus by combining methods⁹⁻¹⁰ it is possible to overcome such limitations and advance our understanding in; (a) overall structure, (b) local structure around hetero-atoms, (c) medium-range order structure, (d) particle size and shape in growing systems, and (e) electronic structure. Here each of the techniques strengths and limitations, and their power in understanding; (i) the crystallization process of zeolitic solids, (ii) generation of active sites, and (c) structural changes during catalytic processes, will be described.

2. Brief description of synchrotron radiation techniques

Advances in recent decades have seen the development in the use of synchrotron radiation, which produces X-rays with a much higher brilliance, in the range of 1×10^6 , compared to a laboratory water-cooled anode or rotating anode. In general X-rays from a synchrotron radiation source are particularly useful, since they have (a) easy tunability of wavelength/energy and (b) high-intensity. Thus techniques utilizing this radiation are wide ranging, and can cover the determination of structure from macroscopic to microscopic length scales, by employing appropriate methods. The four techniques which are vital for the characterisation of zeolitic solids are

- (i) X-ray diffraction (XRD) (both angle and energy dispersive modes)
- (ii) X-ray absorption spectroscopy (both X-ray absorption near edge structure (XANES) and extended X-ray absorption near edge structure (EXAFS))
- (iii) Small angle X-ray scattering (SAXS)
- (iv) Total scattering or high energy diffraction (HEXRD)

X-ray diffraction provides very unique information and it is commonly used for the study of zeolitic solids, in particular to determine the phase purity of the material synthesized. More advanced XRD measurements and analysis can provide very detailed structural information and is widely used to determine the structure of the zeolitic solid produced from hydrothermal methods¹¹⁻¹⁵. If single crystals are available, single crystal diffraction methods are used¹⁶⁻¹⁷, since the higher information content makes structure solution much easier. However, in many cases only powder samples are available and in such cases high-resolution powder diffraction are used to determine the overall structure of the solid^{11,13,15}. Although powerful in determining the overall structure of the zeolitic solid, which is very important to design shape selective catalytic reactions, this technique has a few limitations. In particular, if the material contains atoms with similar scattering cross-sections, for example silicon and aluminium, it is difficult differentiate their

location. Similarly, if the materials contain small amounts of hetero-atoms, for example, 1 wt. percent of titanium in silicate based system, it is difficult to determine the structure and location of the titanium ions; some diffraction experiments suggests that the lattice parameter expands when titanium ions are present in the framework¹⁸. Thus it is necessary to use additional techniques to determine the structure of those hetero-atoms responsible for functional properties.

X-ray absorption spectroscopy can provide complementary information to that of XRD⁹⁻¹⁰. In particular this technique is atom-specific and does not depend on the long-range order, as XRD does, and can provide detailed electronic and local structure of specific metal ions. This technique is widely used in the area of characterising catalytic materials, since it does not depend on the concentration of the element of interest and can be used for several elements. The main limitations are that the energy range commonly available does not allow the study of elements with low atomic numbers; although silicon and aluminium XAS have been carried out, it requires special equipments and conditions to perform those experiments.

Total scattering or HEXRD is a diffraction technique carried out at short wavelengths (high energy X-rays) to obtain a large q-range, so that Fourier transformation of the total scattering data can provide a radial distribution function which can be used to determine various atom-atom correlations present in a system¹⁹⁻²⁰. This technique does not depend on the symmetry present in the solid and can be used to determine the structure of ordered and disordered (poorly crystalline and amorphous) materials. Depending on the available data range (q-range), it is possible to extract near neighbour information of up to *ca.* 10Å. However, the major limitation is that extracting precise structural information can be complicated since all atom-correlations will be present in the radial distribution function.

Small-angle X-ray scattering methods are very useful for gaining information that has length-scales in the range of 10 to 100 nm^{8,21-35}. This technique is powerful in determining the size and shape of particles present in a matrix or solution and widely used to investigate the nature of particles present in colloidal solutions. Although informative about the shape and size of particles, very little or no structural information can be gained using this technique.

Despite the individual limitations of all these techniques, the strengths of individual methods are utilized extensively in the area zeolitic science. In addition, now many methodologies are being developed to analyse data obtained from all these techniques together in a combined manner so that a unique structure solution can be obtained. In particular, software for the analysis of combined XRD/XAS, XRD/HEXRD data are beginning to become available. Similarly, molecular modelling techniques can act as a common platform to combine the data analysis with all these techniques.

Here, examples of the study of formation of zeolite A using combined SAXS/XRD and HEXRD, formation of active sites in cobalt substituted aluminophosphate using combined XRD/XAS and infra-red spectroscopy, and monitoring the changes during catalytic conversion of methanol to olefin using XRD will be used to demonstrate the power of time-resolved in situ X-ray techniques in the study of nanoporous materials.

3. Formation of nanoporous materials

Preparation of novel nanoporous materials are, at present, an important field of research, in particular, towards the production of materials with new pore structures. Several investigations have been carried out in an attempt to understand the mechanism involved in the production of microporous materials. Despite the continued efforts in understanding the formation of these zeotype solids, due to the complexity of the formation process, the mechanisms are not completely understood and it has been recognized that it is necessary to understand the crystallisation mechanism in detail to synthesize nanoporous materials by rational design. Several attempts have been made in the past to unravel the complex mechanism of the zeolite formation, both computationally and experimentally employing both *in situ* and *ex situ* methods. In particular, NMR, dynamic light scattering and small angle X-ray scattering (SAXS) techniques were employed to investigate the formation of zeolite A. Silicalite-1 (MFI), from a clear solution with tetrapropylammonium (TPA^+) cation as a structure directing agent (SDA), has been studied using *in situ* small-angle and wide-angle X-ray scattering (SAXS and WAXS) techniques^{8,21-40}. Mintova et al studied the synthesis of nanosized aluminosilicate LTA from a colloidal solution, with tetramethylammonium (TMA^+) cations as SDA, and showed the steps of the generation and the densification of precursor particles to nanosized LTA by high resolution transmission electron microscopy (HRTEM)³⁹⁻⁴⁰. More recently, Fan et al reported the study of formation of zeolite A from clear solution and the study showed that, depending on the content of sodium hydroxide 5 nm particles were observed to form prior to the crystallisation of zeolite A^{4,26-27}.

To study the formation of crystalline materials, in particular prior to the formation of ordered structure, it is necessary to use techniques, for example SAXS or X-ray absorption spectroscopy. When combined with X-ray diffraction, these techniques become unique for the study of materials crystallizing from a clear solution or a gel. However, XAS is limited to the study of materials containing elements that has absorption energy higher than 5 KeV; more recently, Al K-edge XAS studies have been performed⁴¹, but restricted to a single technique, since it is difficult to combine with XRD technique at low energies.

3.1 SAXS/WAXS

Here we show an example of the use of SAXS/WAXS technique to determine the size and shape of the particle present prior and during crystallization of Zeolite A (from clear solution)²⁶⁻²⁷. Study of zeolite A was carried out using a solution containing

11.25 SiO₂ : 1.8 Al₂O₃ : 13.4 (TMA)₂O : 1.2 NaOH : 700 H₂O.

This solution was aged for 2 h prior to introduction in to a specially designed *in situ* cell (see figure 1). This *in situ* cell was placed in an electrically pre-heated (to a specific temperature, 100°C) stage which was mounted on the beam line such a way that X-ray can pass through the solution without any interference of other components (see figure 1). This cell has been used for several other X-ray techniques as well, in particular for combined XRD/XAS, SAXS/WAXS, HRPD/XAS/Raman in several beam lines. *In situ* SAXS/WAXS measurements were started as soon as the cell containing the gel was introduced and they were performed at Station 6.2 at Daresbury Laboratory. A sample to detector distance of 3.5 m and 1.3 m were used in order to cover different scattering ranges to gain information over a range of *ca.* 1 to 100 nm; the data were recorded using a wavelength of 1.4 Å. High-quality SAXS and WAXS patterns were collected simultaneously at every 2 min. The scattering from water was subtracted as the background. The scattering pattern of a standard sample (wet rat tail collagen) and the diffraction pattern of NaA zeolite were used to calibrate the patterns of SAXS and WAXS, respectively. SAXS data were analysed using the XOTOKO program available at Daresbury Laboratory. Time-resolved stacked SAXS and WAXS patterns are shown in Figure 2 (a) and (b), respectively. The SAXS data shown here are processed to remove the background by subtracting the SAXS pattern of water. It is clear from figure 2(a) a broad hump appears in the SAXS pattern after heating the clear solution for about 16 min. This hump spreads over a *q* range of *ca.* 0.7 and 0.4 nm⁻¹ which corresponds to *ca.* 5 and 15 nm with centre of the hump at *ca.* 10 nm (calculated using the equation $d = 2\pi/q$, where *q* is $(4\pi\sin\theta)/\lambda$). The position of the maximum point of the hump moves to a lower *q* value with time; the hump centered around *ca.* $q = 0.79 \text{ nm}^{-1}$ ($d = 8 \text{ nm}$), measured after 16 minutes of the reaction moves to *ca.* $q = 0.48 \text{ nm}^{-1}$ ($d = 13 \text{ nm}$) at 32 min. Particle size estimated from the position of the broad hump clearly shows that it has increased from 8 nm to 13 nm over a period of 16 minutes. WAXS patterns recorded simultaneously during the SAXS measurements did not show any Bragg reflection.

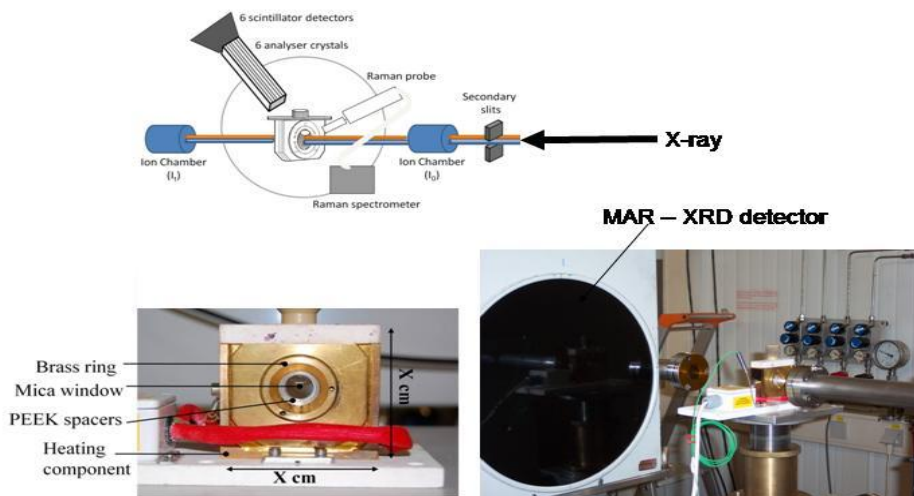


Figure 1. A schematic diagram of a typical setup used in in situ combined techniques; here in (a) scheme for the combined XRD/XAS/Raman setup used in Swiss Norwegian beam line at ESRF is shown. In (b) a photograph of the in situ cell used for study of the crystallization process of zeolitic solid is shown, which consists of a heating stage and a block made of brass. PEEK spacers were used along with two mica windows (50 micron in thickness and 25mm diameter) for X-rays to enter and exit the system. The heating block can be maintained at temperatures upto ca. 200°C. In (c) photograph of the setup used for combined XRD/XAS measurements is shown. This cell is also used in combined SAXS/WAXS studies.

After 42 min of the hydrothermal reaction, although the intensity of the broad hump appears to have decreased slightly, its position ($q = 0.44 \text{ nm}^{-1}$ ($d = 15 \text{ nm}$)) remained closely similar to the earlier observation made at ca 32 min, suggesting that the particle size has not significantly changed. More interestingly, an oscillatory pattern appears in the low q region of the SAXS patterns recorded after 32 mins, which also coincides with the appearance of reflections in the WAXS pattern. We fitted this oscillatory part of the data assuming a cubic morphology (confirmed through SEM measurements) and determined the particle size of the material formed during the crystallisation process.

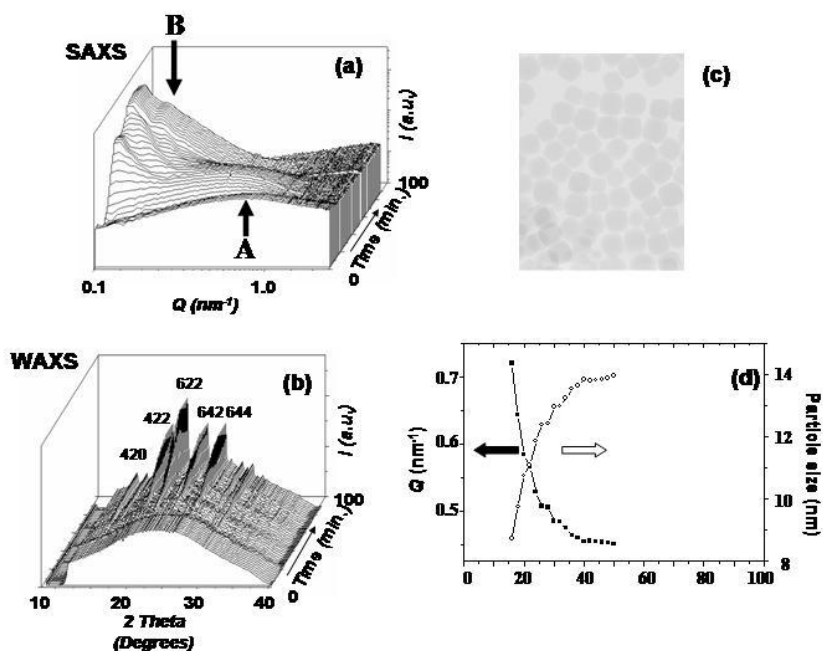


Figure 2. SAXS/WAXS patterns during the formation of zeolite A. (a) SAXS and (b) WAXS recorded simultaneously. (c) shows the TEM picture of the zeolite after hydrothermal treatment of 30 minutes. In (d) we show the variation in particle size estimated from SAXS and change in the Q value of feature A (in (a)).

We also carried out a series of experiments using a short sample to detector distance (1.3 meters) thus changing the scattering vector range that can be observed. The advantage with the short sample detector distance is that, the q -range is in such a way that both SAXS pattern and part of the Bragg scattering can be observed with the same detector. Typical stacked plot, recorded during the crystallisation of zeolite A from a clear solution is shown in Figure 2(d). Here we can see clearly several changes in the small angle region, in particular formation of a broad hump similar to the one observed using a long sample to detector distance, described above. A Bragg peak related to crystalline zeolite A starts to appear at high q region (marked as X in figure 2(d)) after about 35 mins of crystallisation. In order to show that the changes in the SAXS is not an artifact of the experimental setup, we also collected SAXS/WAXS patterns for solution containing only one of the starting material, either alumina or silica source. (The data were recorded under identical

conditions to that of the solution containing ingredients that produces zeolite A). Both these patterns did not show any change in the scattering, which include the presence of a hump in the initial stages, that corresponds to the formation of specific particles prior to crystallisation and the typical oscillatory behaviour observed during the formation of zeolite crystals. More importantly there were no Bragg peaks associated with the formation zeolite A or any other phase in both SAXS and WAXS patterns. Thus it is clear from the features seen in the SAXS patterns it can be concluded that they are due to the particles that are formed prior to the formation of crystalline zeolite A.

3.2 HEXRD

Although SAXS/WAXS studies provided information on the particle size, shape prior to crystallization, kinetics of formation of zeolite A particle and the homogeneity of nano-sized zeolite particles, it was not possible to extract information on the atomic-architecture of the growing amorphous phase prior to the formation of crystalline product. In order obtain information on the structure of amorphous intermediate, it is necessary to use HEXRD (as mentioned earlier, it is difficult to carry out XAS at the Al or Si K-edge and also they provide only short range order information which can be obtained from NMR with least difficulty)¹⁹⁻²⁰. Attempt to use *in situ* methods failed, since the amount of water present in the solution is higher than the aluminosilicate solid and thus the scattering contribution from water prevented us from obtaining any structural details of aluminosilicate precursors; O-O scattering dominated the RDF. Hence we extracted the solid from the solution after carrying out hydrothermal synthesis over a specific period of time and conducted HEXRD experiments at BL04B2 beam line at SPRING8, Japan. In a typical experiment, *ca.* 200 mg of the zeolite A powder extracted after 30 minutes of hydrothermal reaction was pressed into a pellet and the data were collected at 0.2 Å to obtain good quality data up to *ca.* 25Å⁻¹. A typical example of the data conversion from the raw data to S(q) to G(r) is shown in figure 3(top). For comparison, crystalline zeolite A sample was also measured. Total scattering data of both these samples and the respective RDF are shown in Figure 3 (bottom). It is clear from RDF that all of the first neighbours were very similar, as one would expect, and the peaks above 3.5 Å, although they appear similar, shifted to a lower R value. Analysis of the total scattering data using reverse Monte Carlo (RMC) procedure revealed that there are fewer 4 membered rings. However, the similarity of the shape of the RDF suggests that the interconnectivity leading to the formation of double 4 rings is incomplete and because of this, the diffraction pattern looks amorphous. Based on the analysis, we believe the pore structure, resembling that of final product is formed prior to crystallization. This supports the SAXS/WAXS data that solid-solid transformation takes place, as suggested by Mintova et al.

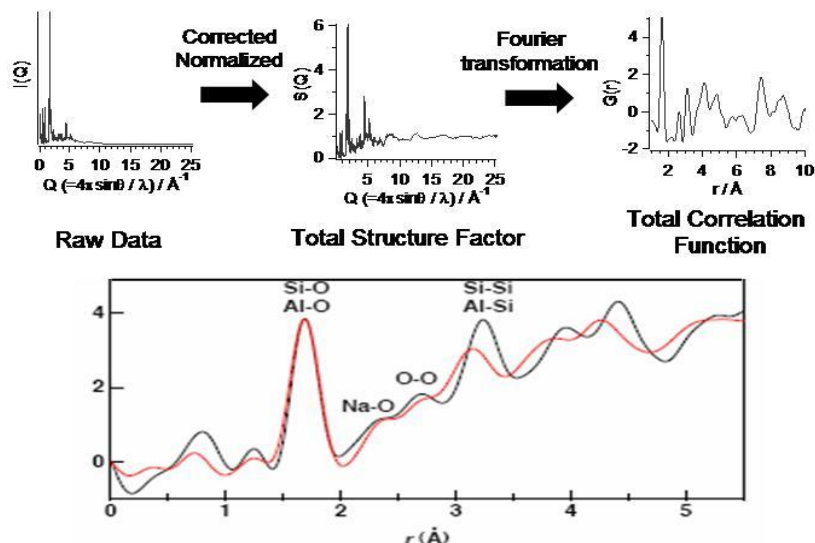


Figure 3. On the top, a typical analysis of the HEXRD data is shown and conversion from raw data to $S(Q)$ before Fourier transforming to $G(r)$. On the bottom, comparison of crystalline zeolite A with amorphous zeolite A, recorded using samples extracted after 30 minutes of hydrothermal treatment.

3.3 Combined XRD/XAS

As mentioned earlier, it was difficult to carry out combined XAS and diffraction methods on aluminosilicate material. However, this method can be applied to a variety of systems, in particular the ones containing iron or germanium containing silicate systems. This method is also ideal for a variety of metal ions substituted aluminophosphates. Here we show two examples of monitoring the formation of templated Ge-silicalite and CoAlPO-5 systems.

Ge Silicalite: Germanium has received a lot of interest recently due to its ability to increase zeolite nucleation and crystal growth rates. In addition it has been shown that Ge(IV) ions promote the formation of 4 membered rings. Here we present the results of an *in situ* combined quick extended X-ray absorption fine structure (QuEXAFS) and X-ray diffraction (XRD) study of the crystallisation of Ge-silicalite. Germanium K-edge QuEXAFS was used to monitor the changes in the local coordination geometry during the crystallization process with a time resolution on the order of a minute. Combining this with XRD, we can correlate changes in the germanium environment with the progress of crystallisation.

Samples of amorphous $\text{GeO}_2\text{-SiO}_2$ xerogel were prepared using a two step sol-gel technique similar to that of Serrano et al.⁴²⁻⁴⁵. The silicon precursor (tetraethylorthosilicate, TEOS) was hydrolysed using 0.05 M HCl. Germanium dioxide was added to the sol and stirred until clear (Si/Ge ratio \approx 30). Basic condensation of the sol was then achieved by addition of tetrapropylammonium hydroxide. The resulting gel was dried overnight at 100°C to remove water and ethanol liberated by hydrolysis of the TEOS. The resulting xerogel was ground to a fine powder and impregnated with 20% TPAOH solution (1.6g TPAOH solution per 1g xerogel). Crystallisation was carried out in the same *in situ* hydrothermal cell described previously in this chapter. Combined Ge K-edge QuEXAFS and XRD experiments were conducted at BM29 at the ESRF. A sample of TPAOH-impregnated xerogel was charged into the hydrothermal cell and heated to 180°C. Ge K-edge EXAFS spectra and XRD patterns were collected alternately throughout the crystallization. XRD data collected sequentially, below the Ge K-absorption edge, showed the presence of amorphous phase prior to crystallization (see figure 4). In order to determine the local structure around germanium, EXAFS data was analysed in detail. To do so, it was necessary to construct a model structure and refine the structural parameters to determine the local structure of Ge(IV) prior and during crystallisation process. The local environment of germanium during the crystallisation is uncertain. Because of this, we constructed a series of 5 model environments (See figure 4) which were based on the likely chemistry of germanium. Each cluster contains a central excited germanium atom. The first coordination shell consists of 4 tetrahedrally arranged oxygen atoms while the second coordination shell contains 0-4 germanium atoms with the remainder being silicon. This covers the range of possible germanium environments, from pure GeO_2 (model E) to an isolated germanium atom embedded in a silica matrix (model A). Fitting the data in k-space ($3.3 \leq k \leq 11$) showed model C gave the best fit to the experimental data throughout the crystallisation (figure 4c shows a typical fit). This is interpreted as an average environment for germanium, containing 2 Si and 2 Ge atoms in the second shell, which does not change significantly during the crystallisation process. Hydrolysis of TEOS with TPAOH has been shown to produce a range of monomeric and oligomeric silica species. The EXAFS data suggest that during sol-gel processing, GeO_2 dissolves and becomes incorporated within silica oligomers. Furthermore, analysis of the Debye-Waller factor of the second shell, a measure of the disorder of these atoms, shows a significant reduction in disorder over the first 30-40 minutes of the crystallisation (see figure 4d). This suggests that the local environment around germanium is determined before the onset of crystallisation, as the first Bragg peaks become apparent at around 60 minutes (see figure 4a).

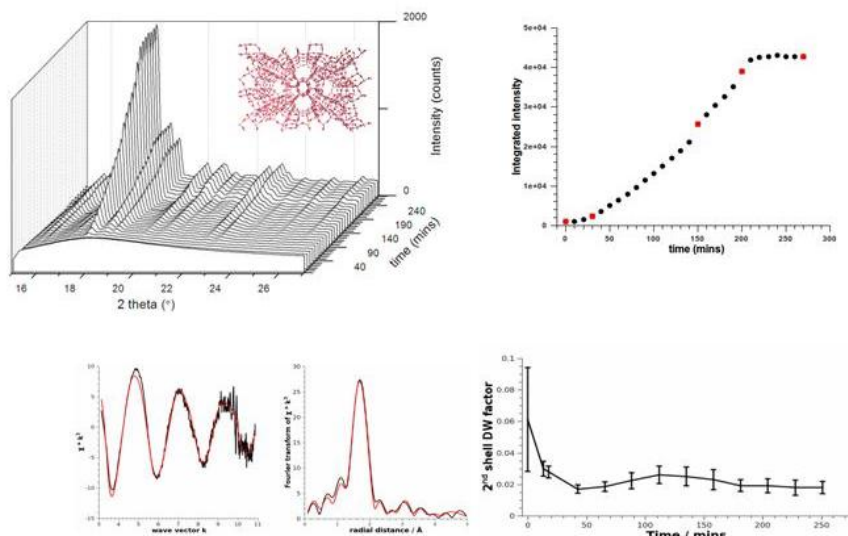


Figure 4. On the top left we show the time-resolved XRD pattern recorded during crystallisation of Ge-silicalite using combined XRD/XAS technique. On the top right we show the variation of integrated intensity of the main reflection with time. On the bottom left, Ge K-edge EXAFS and associated Fourier transform of the final data set is shown. On the bottom right, we show the variation in static disorder (Extracted from the analysis of the EXAFS data) associated with Ge-O bond distance, which reflects the formation of more ordered species upon crystallisation compared to the starting material in the gel.

CoAlPO-5: *In situ* studies of CoAlPO-5 have been carried out extensively^{8,24,46-50}; the main reasons being that this system is easy to synthesize in a relatively short amount of time (only a few hours) and several organic templates can promote the formation of this material. This system can present as a good example for understanding the crystallization process of aluminophosphates from gel. Most of the previous studies utilized combined XRD/XAS technique (at the Co K-edge) by measuring sequentially, as in the previous example of Ge Silicalite. However, with the recent advances in the speed at which the monochromator can move between energies and detector technology, it was possible to develop a simultaneous measurement of XRD and XAS data without losing much time-resolution which is critical for understanding the crystallization process. In addition, sequential measurements are important to avoid a large background due to fluorescence effects

when XRD is measured at energies above the absorption edge; we used a MAR detector to collect XRD data which did not suffer these effects and collected only the XANES data at the Co K-edge in a recent experiment to avoid a large variation in wavelength.

The formation of CoAlPO-5 system in the presence of methylcyclohexylamine (MCHA), which is known to form only the AlPO-5 structure over a wide range of temperature, pH and chemical composition, was followed. In figure 5 we show a stacked plot of the XRD data recorded simultaneously with XAS during the crystallisation process at 160°C. All the peaks can be indexed to the AFI structure, with the first signs of crystallisation developing after 1 hour.

The background-subtracted and normalised XANES data as a function of crystallisation time is also presented in figure 5. Our data shows a change in the white line intensity, corresponding to an electric dipole-allowed 1s-4p transition, over synthesis time. It is well-known that the white line feature is not only affected by electronic factors, but also by the coordination environment of the metal resulting through the presence of multiple scattering effects; for example, octahedral coordination has linear O-Co-O bonds giving rise to large white line intensity compared to a tetrahedrally coordinated Co. Thus, the decrease in the intensity of the white line absorption peak is indicative of an overall change in the cobalt(II) coordination from an octahedral to a tetrahedral environment. The intensity of the white line absorption peak decreases via a two stage step.

The first stage, an initial sharp decrease in the intensity of the white line peak (region I) before becoming relatively stable for a short time (region II), suggests a transformation from regular octahedral coordination, in which the Co(II) ions are surrounded by water molecules, to a less symmetrical pseudo-octahedral coordination $[\text{CoO}_4(\text{H}_2\text{O})_2]^{2+}$ or $[\text{CoO}_5(\text{H}_2\text{O})]^{2+}$, in which some of the coordinating oxygen atoms bridge between two cations (P(V)-O-Co(II)). Previously such a change in intensity was thought to arise from the presence of a mixture of octahedral and tetrahedral coordination^{28,51-52}. However, we discount this possibility, since if a direct octahedral-tetrahedral transformation takes place, the intensity would decrease continuously over the reaction time, rather than staying constant for a short period (region II). Previous UV-Vis spectroscopy studies also observed a cobalt(II) pseudo-octahedral species⁵¹. The second stage, a gradual decrease in the white line intensity over a 48 minute time interval (region III) before remaining constant (region IV), indicates the conversion of Co(II) ions in a pseudo-octahedral environment to one with tetrahedral coordination (region IV) in which all the coordinating oxygen atoms bridge between cobalt(II) and phosphorus(V). It should be noted that there was no change in the position of the white line feature, indicative of the oxidation state of cobalt(II) remaining the same throughout the formation of the AlPO product.

The pre-edge feature, a dipole-forbidden $1s \rightarrow 3d$ transition, which is affected by pure electric quadrupole coupling and a change in geometric contribution, can also be examined to follow a change in the coordination environment of the probing atom. A change from a symmetric cobalt(II) octahedral to a non-symmetric tetrahedral environment results in an overlap of the oxygen 2p orbital with the cobalt(II) 3d orbital, these metal 3d orbitals become more p in character due to the shortening of the bond distances and gives rise to a pre-edge feature in the XANES data. A plot of the normalized pre-edge (7.708 keV for cobalt) intensity as a function of time is presented in Figure 5, and supports a two-stage transformation from octahedral to tetrahedral Co(II) via a pseudo-octahedral intermediate. It should be noted that the small pre-edge feature observed at the onset of the reaction may be due to some distortions around the octahedral Co(II) environment.

The integrated intensity of the white line feature and the intensity of the 211 Bragg reflection as a function of crystallisation time are shown in figure 5. It should be noted that on comparison of the integrated area under a number of single AFI reflections during the *in situ* experiment revealed crystallization curves which were generally superimposable over the duration of the experiment, indicating an isotropic growth on all crystallographic planes. The combined simultaneous XAS/XRD results reveal that Co(II) ions are incorporated into the structure during the crystal formation; a transformation of Co(II) in an pseudo-octahedral coordination to a tetrahedral environment is revealed at the same time that Bragg reflections are observed in the XRD pattern. This is in contrast to previous investigations, which have been based on sequential instead of simultaneous XRD/XAS methods; a study by Grandjean et al.²⁸ revealed that Co(II) ions, present in an octahedral coordination, are converted to tetrahedral coordination just prior to the crystallisation of CoAlPO-5. In addition, an *in situ* UV-Vis study together with XRD revealed the presence of intermediate pseudo-octahedral Co(II) species in the initial synthesis stages (as mentioned previously)⁵¹, however this study could not distinguish if Co(II) ions converted to tetrahedral coordination just prior to or during crystallization. It is important to note that both the previous studies referred to used triethylamine as the organic template, which is well-known to produce a CHA phase as a competing material, under certain conditions⁵⁰. Although the CHA phase was not observed during the crystallization process (within the limits of XRD detection), the use of this template may have a different effect on the Co(II) ions. For example, an *ex situ* XRD/diffuse reflectance spectroscopy (DRS) study on the formation of MeAlPOs observed a pseudo-octahedral Co(II) species during the formation of CoAlPO-5 (AFI), however, this species was not present during the formation of CoAlPO-34 (CHA)⁵². Our study is unique, since MCHA was used as the organic template in the synthesis, which produces only the AFI structure (over a wide range of pH, temperature and with a variety of metal ions) without any competing phases.

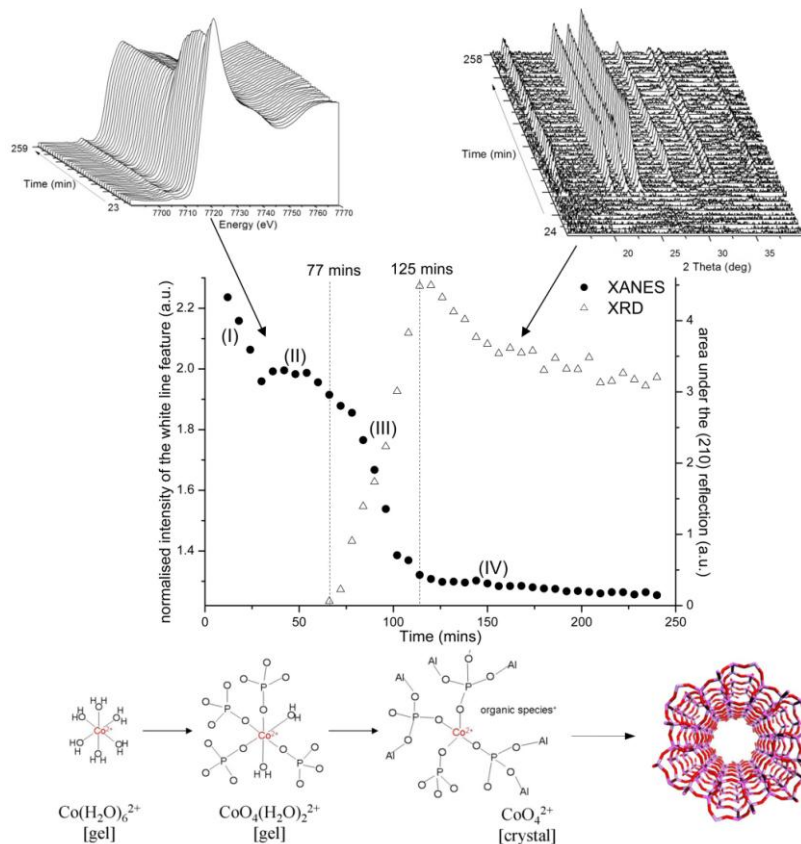


Figure 5. On the top left, we show the Co K-edge XANES and XRD on the top right recorded ‘simultaneously’ during the hydrothermal synthesis of CoAlPO-5 from an amorphous gel. In the middle, variation in the normalised intensity of the white line feature along with the growing intensity of the major reflection in the XRD, with time is shown. In the bottom we schematically describe the mechanism that takes place prior to the formation of crystalline AFI material.

4. Formation of active sites and their reactivity in nanoporous materials

Combined XRD/XAS for the study of activation of nanoporous catalyst and investigation of redox chemistry: Another area of considerable interest in zeolitic

solid is the conversion of as-synthesized nanoporous material to an active catalyst for catalytic reaction. Here, some of them rely simply on the retention of oxidation state and generation of acid sites (due to presence of lower valent metal ions). However, majority of the transition metal ions containing system undergoes redox reactions or change in coordination geometry which can be followed using in situ combined XRD/XAS techniques. This is important, since it will provide vital information on the stability of microporous structure (some solids lose its microporous structure upon calcinations which is important for shape selective reactions and others may not undergo appropriate redox reactions). Several examples have been reported in the literature on this topic. Here we take two examples to demonstrate the power of this combined technique to show the formation of active sites in titanium substituted silicalite (TS-1) and cobalt substituted aluminophosphate (CoAlPO-34).

4.1 In situ XAS

Titanium-containing nanoporous materials attract much interest because of their remarkable catalytic properties in various oxidation reactions⁵³⁻⁵⁵. Titanosilicate materials are shown to catalyze oxidation reactions in the presence of hydrogen peroxide H_2O_2 (as an oxidant) where only water is given off as the by-product. Therefore such materials act as catalysts in ‘green’ reaction systems. Hence, Titanosilicate is one of the well studied system using both *in situ* and *ex situ* techniques. The main concern in this system is the presence of titanium in the framework tetrahedral site⁵⁶⁻⁶¹. Several studies utilized UV-VIS spectroscopy and XANES (at the Ti K-edge) to confirm the presence of Ti(IV) ions in the framework tetrahedral site. In particular, Ti K-edge XANES has been shown to be sensitive to local coordination geometry and has been used extensively to determine the active and reactive sites. One of the main draw backs is that conducting a successful diffraction measurement during this measurement is difficult, since Ti K-edge falls at low energies and obtaining diffraction pattern close to this energy with good intensity and resolution is not straight forward; for this reason the majority of studies are focused on the measurement of XAS data. In figure 6 we show the Ti K-edge XANES data recorded during activation of TS-1 in the presence of dry air and its reaction with water molecules. The experiments were performed at BM26A, DUBBLE beam line, at ESRF. In a typical experiment, 100 mg of the catalyst was pelletized and loaded into the *in situ* cell (see figure 6). The sample was heated at 5 °C per minute to 500 °C and cooled to room temperature. Subsequent to this *in situ* activation, water vapour was introduced (water is well known to react with Ti centre and it is used as probe molecule to understand the reactivity of Ti centres and the nature of hydrophobic character of the titanosilicate catalysts; higher the hydrophobicity, the selectivity for epoxidation is found to be high).

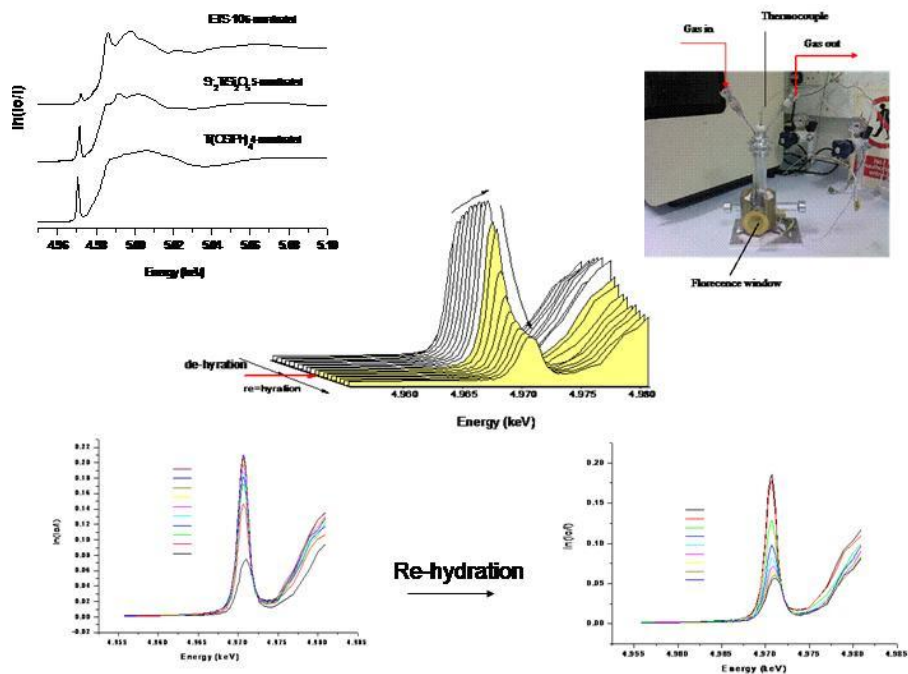


Figure 6. On the top left we show Ti K-edge XANES of three model compounds representative of 4, 5 and 6 coordinated species. On the top right, picture of a typical in situ cell used for the study of TS-1. In the middle, a 3D stacked plot of the normalized Ti K-edge XANES is shown, in particular highlighting the pre-edge part of the data. Bottom left shows the variation in the pre-edge intensity recorded during the dehydration (calcinations process) and rehydration of the same solid is shown on the right.

In figure 6, we show a typical Ti K-edge XANES spectra of model compounds and shows characteristic pre-edge features which are different depending on the coordination geometry. The order of intensity is; Ti (4 coordinated) > Ti (5 coordinated) > Ti (6 coordinated). This, in combination with the plot of pre-edge intensity vs its energy position, can be used to determine the coordination of real systems^{56,58}. In figure 6 (bottom) we also show the temperature resolved XANES data recorded during calcinations and reaction with water molecule. It is clear that the intensity increases during calcinations process which indicates removal of water molecule. However, the intensity of the pre-edge of the as-synthesised TS-1 is

already higher than typical octahedrally coordinated titanium species suggesting the presence of hydrophobic titanium centres. The small increase can be interpreted as species which has water coordination. Upon re-hydration, the intensity of the pre-edge decreases, much below the starting material suggesting molecules are able to access the pores (upon removal of organic template) thereby reacting with titanium centres. This method has been successfully used to interpret the activity and selectivity for titanosilicate in the conversion of cyclohexene to cyclohexene oxide.⁵⁶

4.2 Combined XRD/XAS

First we show the use of combined XRD and XAS technique to follow the redox chemistry of CoAlPO-34 catalysts and subsequently show the use of recently developed high-resolution powder diffraction coupled with time-resolved measurement to follow the changes in the structural parameters of SAPO-34 during activation and catalytic conversion of methanol to olefin.

Combined XRD and XAS techniques have been used over the last decade to determine the local and long-range structure of many microporous materials¹⁰. CoAlPO-34 is of particular interest since they convert methanol to selectively olefins and more importantly it is shown to be very specific to oxyfunctionalise linear alkanes⁶²⁻⁶³. In figure 7 we show the combined XRD and Co K-edge XAS recorded during calcinations process of CoAlPO-34, in air. Changes in the cell parameter reveal a decrease in the overall volume which could be due to either a decrease in the Co-O bond distance due to a change in the oxidation state or due to negative thermal expansion seen in these materials. Co K-edge XAS clearly showed that there is a shift in the edge position and also a decrease in the Co-O distance; a plot of the variation in the Co-O distance with temperature is shown below the stacked XAS plot which is a clear indication of the change in oxidation state. Thus by combining the two techniques it was possible to clearly show that Co(II) is oxidised to Co(III) while retaining the overall Chabasite structure.

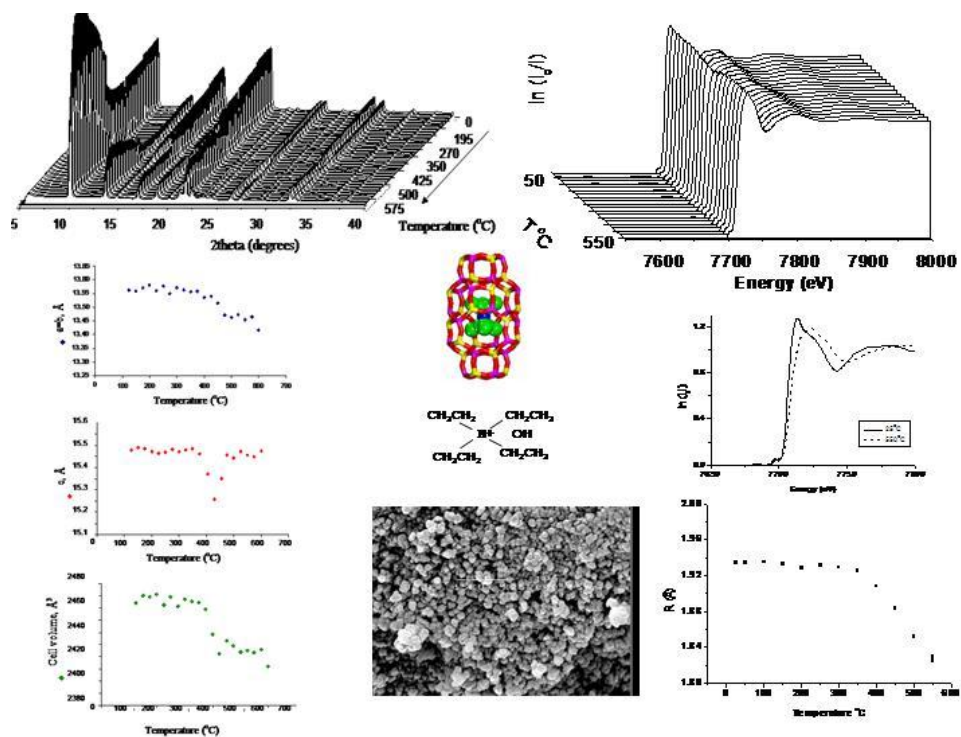


Figure 7. On the right stacked XRD plot (top) and the respective lattice parameters during calcinations of CoAlPO-34 synthesized in presence of tetraethyl ammonium hydroxide. It is clear from the XRD plots that the structure is stable during the calcinations procedure. The changes in intensity and possible structural modification were analyzed in detail and given below the XRD pattern. It is clear from the obtained from the analysis of the XRD data are shown. In the middle, typical CHA structure (With an organic template), the template used and a SEM picture of the solid produced are shown. On the right stacked Co K-edge XAS data (top), start and end data of the CoAlPO-34 obtained during calcinations and the variation in Co-O distance obtained from the detailed analysis of the EXAFS data, with temperature are shown.

4.3 In situ high resolution X-ray diffraction

More recent, high-resolution powder diffraction data conducted during the activation of SAPO-34 indeed show promising results during activation and catalytic reaction (please note that there are no redox metal ions present in this system and further more, earlier studies were conducted using a position sensitive detector with much poorer resolution). In figure 8 we show the stacked XRD plot of SAPO-34 recorded during calcinations and reaction with methanol at 400°C. Both plots clearly show the stability of the structure and more importantly, the lattice parameters are seen to decrease during initial calcinations. This is likely to be due to the contraction of the lattice, which has been shown to exist for these systems⁶⁴⁻⁶⁵. However, in presence of methanol, it is clear that the lattice parameter expands with reaction time. This is suggested to be due to the build up of coke during catalysis⁶⁶.

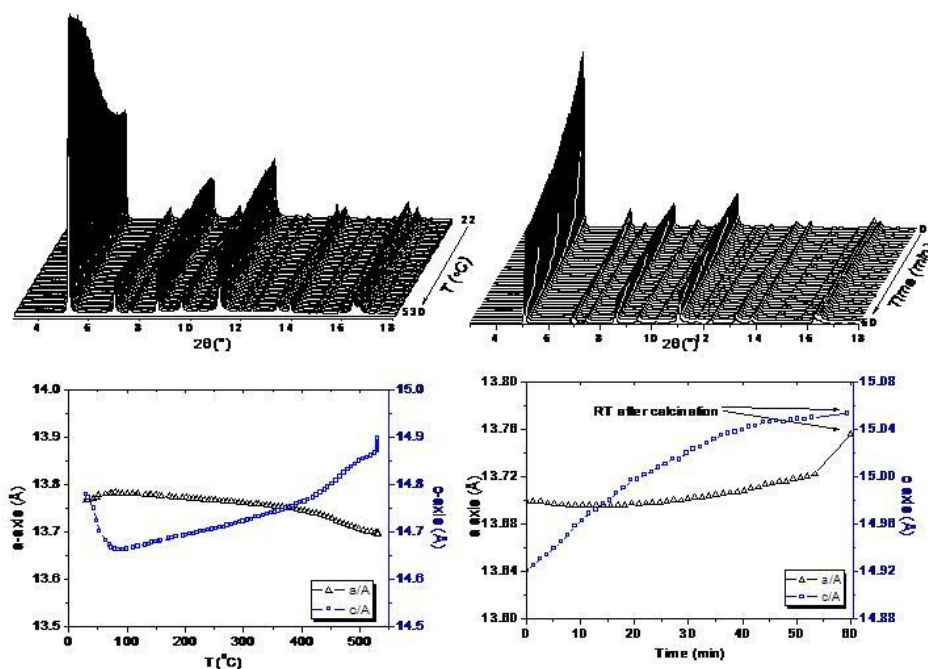


Figure 8. Stacked XRD data of SAPO-34 recorded during calcination in air using a capillary reactor. On the right we show the stacked XRD data recorded during the catalytic reaction of methanol over SAPO-34 at 400°C. Variation in the lattice parameter extracted from the respective data are shown at the bottom.

5. Summary

In summary, synchrotron radiation techniques have been powerful in following the formation of nanoporous solids, determining the oxidation of metal ions that creates the catalytic functionality in the framework, stability of the nanoporous materials which are known to be thermally metal stable and more recently the structural modification that takes place during activation and catalytic processes. With the advancement in the time-resolution and detection capabilities, it is possible to determine a wide range of length scales from macropores to particles to atomic architecture. The wide availability of the facility couple with the various techniques, it is now becoming routine to exploit these advancements to the study of nanoporous materials.

References

1. Beale, A. M., Jacques, S. D. M. & Weckhuysen, B. M. Chemical imaging of catalytic solids with synchrotron radiation. *Chemical Society Reviews* 39, 4656-4672.
2. Blasco, T. Insights into reaction mechanisms in heterogeneous catalysis revealed by in situ NMR spectroscopy. *Chemical Society Reviews* 39, 4685-4702.
3. O'Brien, M. G., Beale, A. M. & Weckhuysen, B. M. The role of synchrotron radiation in examining the self-assembly of crystalline nanoporous framework materials: from zeolites and aluminophosphates to metal organic hybrids. *Chemical Society Reviews* 39, 4767-4782.
4. Fan, F. T., Feng, Z. C. & Li, C. UV Raman spectroscopic study on the synthesis mechanism and assembly of molecular sieves. *Chemical Society Reviews* 39, 4794-4801.
5. Newton, M. A. & van Beek, W. Combining synchrotron-based X-ray techniques with vibrational spectroscopies for the in situ study of heterogeneous catalysts: a view from a bridge. *Chemical Society Reviews* 39, 4845-4863.
6. Bordiga, S., Bonino, F., Lillerud, K. P. & Lamberti, C. X-ray absorption spectroscopies: useful tools to understand metallorganic frameworks structure and reactivity. *Chemical Society Reviews* 39, 4885-4927.
7. Ivanova, II & Kolyagin, Y. G. Impact of in situ MAS NMR techniques to the understanding of the mechanisms of zeolite catalyzed reactions. *Chemical Society Reviews* 39, 5018-5050.
8. Sankar, G. & Bras, W. Insights into the formation of microporous materials by in situ X-ray scattering techniques. *Catalysis Today* 145, 195-203 (2009).

9. Sankar, G., Thomas, J. M. & Catlow, C. R. A. Combining X-ray absorption with X-ray diffraction for the structural elucidation of catalysts. *Topics in Catalysis* 10, 255-264 (2000).
10. Sankar, G. & Thomas, J. M. In situ combined X-ray absorption spectroscopic and X-ray diffractometric studies of solid catalysts. *Topics in Catalysis* 8, 1-21 (1999).
11. Baerlocher, C. & McCusker, L. B. in *From Zeolites to Porous Mof Materials - the 40th Anniversary of International Zeolite Conference, Proceedings of the 15th International Zeolite Conference* (eds. Xu, R., Gao, Z., Chen, J. & Yan, W.) 657-665 (2007).
12. Xie, D., Baerlocher, C. & McCusker, L. B. Combining precession electron diffraction data with X-ray powder diffraction data to facilitate structure solution. *Journal of Applied Crystallography* 41, 1115-1121 (2008).
13. McCusker, L. B., Baerlocher, C., Grosse-Kunstleve, R., Brenner, S. & Wessels, T. Solving complex zeolite structures from powder diffraction data. *Chimia* 55, 497-504 (2001).
14. Grosse-Kunstleve, R. W., McCusker, L. B. & Baerlocher, C. Powder diffraction data and crystal chemical information combined in an automated structure determination procedure for zeolites. *Journal of Applied Crystallography* 30, 985-995 (1997).
15. McCusker, L. B. Zeolite Crystallography - Structure Determination in the Absence of Conventional Single-Crystal Data. *Acta Crystallographica Section A* 47, 297-& (1991).
16. Sankar, G., Wyles, J. K. & Catlow, C. R. A. On the nature and location of organic template molecules and their effect on the stability and redox properties of microporous CoAlPO-34 catalyst. *Topics in Catalysis* 24, 173-184 (2003).
17. Sankar, G. et al. Structure of templated microcrystalline DAF-5 (Co_{0.28}Al_{0.72}PO₄C₁₀H₂₀N₂) determined by synchrotron-based diffraction methods. *Chemical Communications*, 117-118 (1998).
18. Lamberti, C. et al. Ti location in the MFI framework of Ti-silicalite-1: A neutron powder diffraction study. *Journal of the American Chemical Society* 123, 2204-2212 (2001).
19. Wakihara, T. et al. Intermediate-range order in mesoporous silicas investigated by a high-energy X-ray diffraction technique. *Chemistry Letters* 37, 30-31 (2008).
20. Wakihara, T. et al. A new approach to the determination of atomic-architecture of amorphous zeolite precursors by high-energy X-ray diffraction technique. *Physical Chemistry Chemical Physics* 8, 224-227 (2006).

21. Aerts, A. et al. Modelling of synchrotron SAXS patterns of silicalite-1 zeolite during crystallization. *Physical Chemistry Chemical Physics* 13, 4318-4325.
22. Caremans, T. P. et al. Investigation of Nanoparticles Occurring in the Colloidal Silicalite-1 Zeolite Crystallization Process Using Dissolution Experiments. *Chemistry of Materials* 22, 3619-3629.
23. Aerts, A. et al. Investigation of the Mechanism of Colloidal Silicalite-1 Crystallization by Using DLS, SAXS, and Si-29 NMR Spectroscopy. *Chemistry-a European Journal* 16, 2764-2774.
24. Sankar, G., Okubo, T., Fan, W. & Meneau, F. New insights into the formation of microporous materials by in situ scattering techniques. *Faraday Discussions* 136, 157-166 (2007).
25. Tompsett, G. A., Panzarella, B. A., Conner, W. C., Bennett, S. & Jones, K. W. In situ SAXS and WAXS of zeolite microwave synthesis. *Nuclear Instruments & Methods in Physics Research Section B-Beam Interactions with Materials and Atoms* 261, 863-866 (2007).
26. Fan, W., Ogura, M., Sankar, G. & Okubo, T. In situ small-angle and wide-angle X-ray scattering investigation on nucleation and crystal growth of nanosized zeolite A. *Chemistry of Materials* 19, 1906-1917 (2007).
27. Fan, W. et al. In situ observation of homogeneous nucleation of nanosized zeolite A. *Physical Chemistry Chemical Physics* 8, 1335-1339 (2006).
28. Grandjean, D., Beale, A. M., Petukhov, A. V. & Weckhuysen, B. M. Unraveling the crystallization mechanism of CoAPO-5 molecular sieves under hydrothermal conditions. *Journal of the American Chemical Society* 127, 14454-14465 (2005).
29. Yang, S. Y. & Navrotsky, A. Early-stage reactions in synthesis of TPA-silicalite-1: Studies by in situ calorimetry, SAXS, and pH measurements. *Chemistry of Materials* 16, 3682-3687 (2004).
30. Yang, S. Y., Navrotsky, A., Wesolowski, D. J. & Pople, J. A. Study on synthesis of TPA-silicalite-1 from initially clear solutions of various base concentrations by in situ calorimetry, potentiometry, and SAXS. *Chemistry of Materials* 16, 210-219 (2004).
31. Smaïhi, M., Barida, O. & Valtchev, V. Investigation of the crystallization stages of LTA-type zeolite by complementary characterization techniques. *European Journal of Inorganic Chemistry*, 4370-4377 (2003).
32. de Moor, P., Beelen, T. P. M., van Santen, R. A., Beck, L. W. & Davis, M. E. Si-MFI crystallization using a "dimer" and "trimer" of TPA studied with small-angle X-ray scattering. *Journal of Physical Chemistry B* 104, 7600-7611 (2000).
33. de Moor, P. et al. Imaging the assembly process of the organic-mediated synthesis of a zeolite. *Chemistry-a European Journal* 5, 2083-2088 (1999).

34. de Moor, P., Beelen, T. P. M., van Santen, R. A., Tsuji, K. & Davis, M. E. SAXS and USAXS investigation on nanometer-scaled precursors in organic-mediated zeolite crystallization from gelling systems. *Chemistry of Materials* 11, 36-43 (1999).
35. deMoor, P., Beelen, T. P. M. & vanSanten, R. A. SAXS/WAXS study on the formation of precursors and crystallization of silicalite. *Microporous Materials* 9, 117-130 (1997).
36. Cundy, C. S. & Cox, P. A. The hydrothermal synthesis of zeolites: Precursors, intermediates and reaction mechanism. *Microporous and Mesoporous Materials* 82, 1-78 (2005).
37. Cundy, C. S. & Cox, P. A. The hydrothermal synthesis of zeolites: History and development from the earliest days to the present time. *Chemical Reviews* 103, 663-701 (2003).
38. Shi, J. M., Anderson, M. W. & Carr, S. W. Direct observation of zeolite a synthesis by in situ solid-state NMR. *Chemistry of Materials* 8, 369-375 (1996).
39. Mintova, S., Olson, N. H. & Bein, T. Electron microscopy reveals the nucleation mechanism of zeolite Y from precursor colloids. *Angewandte Chemie-International Edition* 38, 3201-3204 (1999).
40. Mintova, S., Olson, N. H., Valtchev, V. & Bein, T. Mechanism of zeolite a nanocrystal growth from colloids at room temperature. *Science* 283, 958-960 (1999).
41. Beale, A. M. et al. Monitoring the coordination of aluminium during microporous oxide crystallisation by in situ soft X-ray absorption spectroscopy. *Chemical Communications*, 4410-4412 (2006).
42. Serrano, D. P. & van Grieken, R. Heterogenous events in the crystallization of zeolites. *Journal of Materials Chemistry* 11, 2391-2407 (2001).
43. Serrano, D. P., Van Grieken, R., Sanchez, P., Sanz, R. & Rodriguez, L. Crystallization mechanism of all-silica zeolite beta in fluoride medium. *Microporous and Mesoporous Materials* 46, 35-46 (2001).
44. Melero, J. A., van Grieken, R., Serrano, D. P. & Espada, J. J. Crystallization mechanism of Al-TS-1 synthesised from amorphous wetness-impregnated Al₂O₃-TiO₂-SiO₂ xerogels: role of aluminium species. *Journal of Materials Chemistry* 11, 1519-1525 (2001).
45. Serrano, D. P. et al. Crystallization mechanism of Al-Ti-beta zeolite synthesized from amorphous wetness impregnated xerogels. *Journal of Materials Chemistry* 9, 2899-2905 (1999).
46. Simmance, K., Sankar, G., Bell, R. G., Prestipino, C. & van Beek, W. Tracking the formation of cobalt substituted ALPO-5 using simultaneous in situ X-ray diffraction and X-ray absorption spectroscopy techniques. *Physical Chemistry Chemical Physics* 12, 559-562.

47. Middelkoop, V., Jacques, S. D. M., O'Brien, M. G., Beale, A. M. & Barnes, P. Hydrothermal/autoclave synthesis of AlPO-5: a prototype space/time study of crystallisation gradients. *Journal of Materials Science* 43, 2222-2228 (2008).
48. Muncaster, G. et al. On the advantages of the use of the three-element detector system for measuring EDXRD patterns to follow the crystallisation of open-framework structures. *Physical Chemistry Chemical Physics* 2, 3523-3527 (2000).
49. Rey, F. et al. Synchrotron-based method for the study of crystallization: Templated formation of CoALPO-5 catalyst (vol 7, pg 1435, 1995). *Chemistry of Materials* 8, 590-590 (1996).
50. Rey, F. et al. Synchrotron-Based Method for the Study of Crystallization - Templated Formation of Coalpo-5 Catalyst. *Chemistry of Materials* 7, 1435-1436 (1995).
51. Weckhuysen, B. M., Baetens, D. & Schoonheydt, R. A. Spectroscopy of the formation of microporous transition metal ion containing aluminophosphates under hydrothermal conditions. *Angewandte Chemie-International Edition* 39, 3419-+ (2000).
52. Weckhuysen, B. M., Rao, R. R., Martens, J. A. & Schoonheydt, R. A. Transition metal ions in microporous crystalline aluminophosphates: Isomorphous substitution. *European Journal of Inorganic Chemistry*, 565-577 (1999).
53. Ratnasamy, P., Srinivas, D. & Knozinger, H. in *Advances in Catalysis*, Vol 48 1-169 (2004).
54. Notari, B. in *Advances in Catalysis*, Vol 41 253-334 (1996).
55. Tatsumi, T., Nakamura, M., Negishi, S. & Tominaga, H. Shape-Selective Oxidation of Alkanes with H₂O₂ Catalyzed by Titanosilicate. *Journal of the Chemical Society-Chemical Communications*, 476-477 (1990).
56. Welch, A. et al. Epoxidation of cyclohexene over crystalline and amorphous titanosilicate catalysts. *Catalysis Letters* 105, 179-182 (2005).
57. Barker, C. M. et al. On the structure and coordination of the oxygen-donating species in Ti up arrow MCM-41/TBHP oxidation catalysts: a density functional theory and EXAFS study. *Physical Chemistry Chemical Physics* 4, 1228-1240 (2002).
58. Thomas, J. M. & Sankar, G. The role of synchrotron-based studies in the elucidation and design of active sites in titanium-silica epoxidation catalysts. *Accounts of Chemical Research* 34, 571-581 (2001).
59. Oldroyd, R. D., Sankar, G., Thomas, J. M. & Ozkaya, D. Enhancing the performance of a supported titanium epoxidation catalyst by modifying the active center. *Journal of Physical Chemistry B* 102, 1849-1855 (1998).

60. Maschmeyer, T., Rey, F., Sankar, G. & Thomas, J. M. Heterogeneous Catalysts Obtained by Grafting Metallocene Complexes onto Mesoporous Silica. *Nature* 378, 159-162 (1995).
61. Sankar, G. et al. Probing Active-Sites in Solid Catalysts for the Liquid-Phase Epoxidation of Alkenes. *Journal of the Chemical Society-Chemical Communications*, 2279-2280 (1994).
62. Thomas, J. M., Raja, R., Sankar, G. & Bell, R. G. Molecular-sieve catalysts for the selective oxidation of linear alkanes by molecular oxygen. *Nature* 398, 227-230 (1999).
63. Thomas, J. M., Raja, R., Sankar, G. & Bell, R. G. Molecular sieve catalysts for the regioselective and shape-selective oxyfunctionalization of alkanes in air. *Accounts of Chemical Research* 34, 191-200 (2001).
64. Amri, M. & Walton, R. I. Negative Thermal Expansion in the Aluminum and Gallium Phosphate Zeotypes with CHA and AEI Structure types. *Chemistry of Materials* 21, 3380-3390 (2009).
65. Lightfoot, P., Woodcock, D. A., Maple, M. J., Villaescusa, L. A. & Wright, P. A. The widespread occurrence of negative thermal expansion in zeolites. *Journal of Materials Chemistry* 11, 212-216 (2001).
66. Wragg, D. S., Johnsen, R. E., Norby, P. & Fjellvag, H. The adsorption of methanol and water on SAPO-34: in situ and ex situ X-ray diffraction studies. *Microporous and Mesoporous Materials* 134, 210-215.

Theoretical Methods in Zeolite Chemistry

Luis GÓMEZ-HORTIGÜELA

Instituto de Catálisis y Petroleoquímica-CSIC. c/ Marie Curie 2. 28049. Madrid. Spain.

Abstract

Theoretical methods represent currently a very powerful tool to study zeolite properties that cannot or are very difficult to be addressed by experimental techniques, providing a valuable methodology to understand at an atomic-level different issues in zeolite chemistry related to their structure, synthesis and applications, complementary to the information gained by experimental studies. This chapter aims to describe the different computational-based methodologies that are currently used, the procedure of setting up a calculation as well as some examples of applications of these methodologies to understand particular problems in zeolite science. Rather than to give a fundamental understanding of the computational methods or a review of their many applications, the ultimate goal of this chapter is to provide a general overview of the fundamentals that a zeolite researcher non-expert in theoretical methods should know in order to apply these computational methodologies for his own interests.

1. Introduction

During the last years, the knowledge on zeolite materials has greatly augmented by the development and application of advanced physico-chemical characterisation techniques devoted to the understanding of the synthesis, structure and applications of these materials, including high-resolution X-Ray Diffraction, Magic-Angle Solid State Nuclear Magnetic Resonance and High-Resolution Electron Microscopy. Besides, new synthetic strategies, especially the use of increasingly-complex structure-directing agents (SDA) [1] and/or solvents other than water such as ionic liquids [2], have enabled the discovery of a large number of new zeolite structures. One of the main aims in zeolite science is the development of a detailed understanding of the structures and processes taking place in zeolite systems at an atomic scale. Although such advanced characterisation techniques have led to a great impact on that knowledge, there are several limitations that they cannot overcome. For instance, knowledge of the location of guest molecules (being SDA molecules or other sorbates) within zeolite structures is usually difficult to gain experimentally since it requires a high-ordering of the guest molecules within the zeolite system and good-quality crystals; location of dopants within zeolite networks is also difficult to study by experimental techniques due to the very

similar scattering power of Si and the dopant atoms (generally Al). Besides, due to the long-range nature of diffraction techniques, the experimental solution of structures gives “averaged” model structures, but cannot provide atomic-detailed information on short-range defects like dopants or connectivity defects. On the other hand, there is a lot of interesting energetic information that cannot be gained (or is very difficult) directly by physico-chemical techniques, such as diffusivities, interaction energies between guest molecules and zeolite hosts, or enthalpies and activation barriers in catalytic reactions. Moreover, a rational interpretation of the collected experimental observations is sometimes difficult to achieve, which has in cases led to the design of experiments on a “trial and error” basis. This information can instead be gained from computational simulation techniques, which have proved to be an essential complementary tool for the understanding of zeolite science.

Over the last years, the rapid development of physical-chemistry theories, combined with a vast increase in computer power due to technological advancements, has transformed computer simulation into a new area of knowledge in science which aims to apply fundamental theory to study complex systems in an effective way [3]. Computational science has provided with a large number of modelling tools which can assist in the interpretation of the experimental observations, and therefore can provide a rational guide in the design of new experiments, leading to a much more efficient research strategy. To achieve this, a close contact between experiments and theoretical studies must exist, which are complementary to each other. Computational simulations rely on a number of assumptions and simplifications that must be validated against experimental information in order to trust on the information they provide. Therefore, the most effective use of computational models is in complement to experimental studies, although in recent years modelling methods have become increasingly predictive [4].

This chapter is intended to give a general overview of the most widely used computational models and methodologies for readers who are interested in zeolite science, but who are non-experts on modelling techniques. Only qualitative information on the methods, models and techniques will be presented, avoiding complex mathematical formulations. The ultimate goal will be to familiarise a zeolite scientist non-expert in theoretical chemistry with the methods and the information that can be gained from these modelling tools and to face him with the main decisions that will have to tackle when applying these methods. First, the types of computational methods that are used to study zeolite systems will be presented, followed by the most common simulation techniques employed to study different problems. Then the models available to describe the zeolite system will be described, as well as the main choices that one has to face when preparing a computational study. Finally, some of the most common applications will be briefly commented, focusing especially on the use of Molecular Mechanics Methods.

2. Computational Methods

The computational methods that are used to study any chemical or biological system, including zeolites, are divided in two main categories: i) methods that do not explicitly consider electrons in the system, which are based on Classical Mechanics, and are usually referred to as Molecular Mechanics Methods (MM), and ii) methods that explicitly consider electrons in the systems, which are based on Quantum Mechanics (QM), and involve the solution of the Schrödinger equation at some level of approximation; these methods are commonly referred as Electronic Structure Methods.

2.1 Molecular Mechanics Methods

Molecular Mechanics Methods (hereafter these methods will be denoted as MM), also referred as interatomic potential methods, are based on Classical Mechanics. The main assumption of these methods is given by the Born-Oppenheimer approximation, which enables to express the potential energy of a system as a function of the nuclear coordinates of the components that conform the system. Typically, all-atomistic Molecular Mechanics are used, where each atom is simulated as a single particle, and is assigned a constant net charge, which can be derived by different methodologies, usually from Quantum Chemistry calculations.

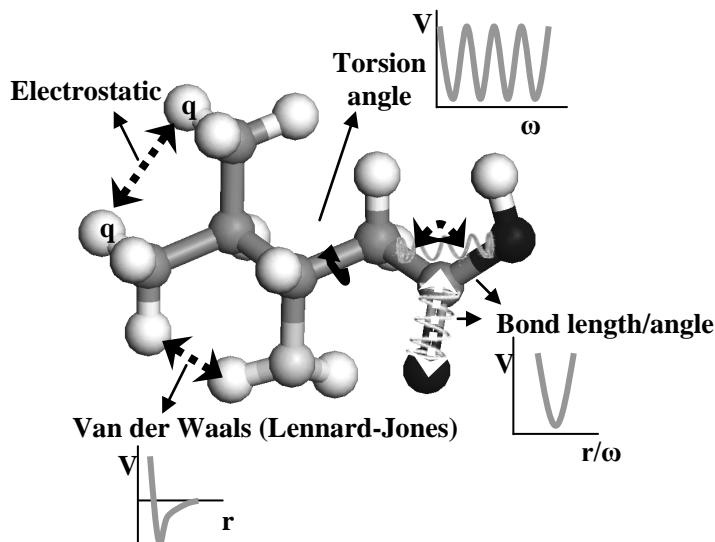


Figure 1. Schematic representation of typical energy terms in a common force-field.

These methods are based on interatomic potentials, which are parametrised analytical functions that represent the potential energy of a system as a function of

the nuclear coordinates of its components (generally atoms) –i.e. of the configurational space. The fundament of these methods is that bonds have optimum bond lengths and angles to which all the molecular systems tend to adjust. Roughly speaking, this can be seen as if the atoms are linked by springs with the optimum configuration corresponding to the equilibrium values (see Figure 1). The analytical representation of the potential energy is known as force-field, and gives the potential energy of a system in a given conformation as a sum of individual terms which account for different molecular parameters. Typical molecular force-fields include intramolecular terms for bond lengths (two-body term, i.e. terms depending on two atoms) and bond angles (three-body term), which are usually modelled as harmonic potentials centred around equilibrium values, torsion angles (four-body term), usually cosine functions, and intra/intermolecular terms to account for non-bonded interactions, including Van der Waals, which is typically modelled using a 6-12 Lennard-Jones potential, meaning that attractive forces fall off with distance as r^{-6} and repulsive forces as r^{-12} . Finally, the intra/intermolecular electrostatic interactions are modelled by the Coulomb energy. Hence, the potential energy function is expressed as the sum of all those terms calculated for all possible combination of atoms (Eq. 1):

$$V = E_{\text{total}} = \Sigma E_{\text{bond}} + \Sigma E_{\text{angle}} + \Sigma E_{\text{torsion}} + \Sigma E_{\text{vdW}} + \Sigma E_{\text{electrostatic}} = \\ \Sigma \frac{1}{2} K_r (r - r_{\text{eq}})^2 + \Sigma \frac{1}{2} K_\theta (\theta - \theta_{\text{eq}})^2 + \Sigma \frac{1}{2} K_\omega [1 - \cos(n\omega - \delta)] + \Sigma [(A_{ij} \cdot r_{ij}^{-12}) - (B_{ij} \cdot r_{ij}^{-6}) + (q_i q_j / r_{ij})] \\ \text{(Eq. 1)}$$

This analytical expression of the potential energy is commonly used for molecular systems, where intramolecular flexibility is essential to accurately model them. Additionally, “improper torsional” terms may be added, for instance to enforce the planarity of aromatic rings, and “cross-terms” that account for couplings of different internal variables, such as bond angles and lengths. However, zeolite lattices are represented as ionic models (Born model), where these additional terms are not an essential requirement, and in this case the potential energy is just a function of the Coulomb energy and the short-range interactions, which comprise non-bonded repulsive (or Pauli) terms, and a term to represent van der Waals interactions and contributions due to covalency [4]; often two-body terms are supplemented by angle-dependent terms (three-body term). A common analytical expression for the potential energy of a zeolite (summing for all i-j pairs), which is commonly referred as lattice energy, is (Eq. 2):

$$V_{ij}(r) = q_i q_j / r + A_{ij} \cdot \exp(-r/\rho) - C \cdot r^{-6} + \frac{1}{2} K_\theta (\theta - \theta_{\text{eq}})^2 \quad \text{(Eq. 2)}$$

The Coulomb energy is obtained by summing the electrostatic interactions between all the charged atoms of the system. This sum is difficult to converge on real space; however, if partially transformed into reciprocal space, as the Ewald method

proposes [5,6], a convergent summation more easily to handle is achieved. The Ewald method is therefore used in the majority of lattice energy calculations.

The bond in zeolite materials has an intermediate nature between covalent and ionic. Indeed, the ionicity can vary as a function of the tetrahedral atoms conforming the network; for instance, bonds in all-silica zeolites have a stronger covalent nature, while bonds in aluminophosphate networks are better described in terms of Al^{3+} and PO_4^{3-} ions ionically bonded [7]. However, it is generally accepted to model all these zeolite systems with an ionic model (Born model), in which covalent effects are included as part of the short-range interactions. When modelling ionic systems as zeolites, it is generally required to include a term to account for the polarisability of the ions, especially for the anions. The most widely used model for describing polarisability is represented by the *shell* model [8], which models the polarisable ion in terms of a core, which contains all the mass of the ion with a particular charge, linked by a spring constant to a massless shell which represents the polarisable valence shell electrons, with a different charge; the distinct charges of the core and the shell involves that the distance between both entities, which is determined by the spring constant, describes the development of a dipole. Short-range interactions are usually required to act with shells for a good description of the model.

As previously mentioned, Molecular Mechanics Methods are based on the so-called force-fields, which include the form and a library of parameters of the analytical functions that describe the potential energy of a system. A force-field defines a set of parameters for each type of atom, depending not only on the type of element but also on its chemical nature. For example, a force field would include distinct parameters for an oxygen atom in a carbonyl group (with the characteristic bond lengths and angles of a double bond) or in a hydroxyl group (with a single bond); these different types of atoms are defined as force-field types. The variable parameters in a force-field include equilibrium bond lengths and angles and dihedral angles, force-constants, repulsive and attractive constants, etc. These parameters may be determined either by empirical fitting methods, in which the value of the parameters are systematically varied through a least squares fitting procedure in order to reproduce experimental data available; alternatively, Quantum-Chemistry methods may also be used to calculate interactions between the species and the parameters are set accordingly to reproduce these interactions. A large number of different force-fields is currently available for studying different types of systems, including organic, biological or inorganic systems. However, sets of parameters and functional forms of the potential energy are defined to be self-consistent within a specific force-field. Therefore, because the functional forms of the potential terms vary largely on different force-fields, the parameters from one force-field should in principle not be transferred to others. In fact, very often force-

fields are parametrised to specifically model in an accurate way a particular type of system, for instance proteins or zeolites.

2.2 *Electronic Structure Methods*

Electronic Structure Methods are based on Quantum Mechanics (hereafter QM will make reference to these methods), and require an electronic treatment in order to solve the Schrödinger equation of a system. For achieving this, several approximations have to be done, and the large size of zeolite systems generally involves an increase of the simplifications that one has to assume. Nowadays, there are mainly two different types of methodologies in Quantum Chemistry, traditional “*ab initio*” methods, which include Hartree-Fock (HF) and post-HF methods to consider the electron correlation, and methods based on Density Functional Theory (DFT), which are currently the most widely used methods for studying zeolites, due to the development of efficient exchange-correlation functionals and their lower computational cost, enabling the study of increasingly-larger systems. A brief and very simplified description of these methods will be given here; for details of these methodologies, the reader is referred to specialised books and reviews [9-14].

In HF methods, electron-electron interactions are treated with the model of independent electrons, in which the electrons move in the average potential created by other electrons. The one-electron wave functions, corresponding to molecular orbitals, are expressed using a potential where the electron-electron interaction is derived from the electrostatic interaction with other electrons distributed in the other one-electron wavefunctions. The wavefunction is then described as a product (in fact, as a Slater determinant in order to ensure the antisymmetry of the wavefunction) of one-electron functions (orbitals). The best set of orbitals is determined by the variational principle, i.e. the orbitals that give the lowest energy. Since the other electrons are described by their respective orbitals, the HF equations depend on their own solutions, and so must be solved iteratively [14]. The main consequence of this approximation is that there is a certain probability of having two electrons at the same position. This leads to the error known as correlation energy. HF theory only accounts for the average electron-electron interactions, and consequently neglects the correlation between electrons. It is not the scope of this chapter to give a detailed description of the HF methodology, but only of its implications on the study of zeolite materials; more detailed discussions are available in [15,16]. Applicability of HF methods is severely restricted due to the neglect of the electron correlation, although it has been found to give reasonable structures but not reaction energies. There are several post-HF methods that account for the electron correlation. Coupled-Cluster methods (CC) are based on a cluster expansion of the wave function, since HF is the best single determinant wave function; usually, only single and double excitations (CCSD) are considered, although triple excitations are sometimes also included, but treated at the

perturbation theory level (CCSD(T)). This methodology can only be applied to very small systems (usually of the order of 10 atoms), and therefore are prohibitive to use for zeolites. However, results obtained with this reliable methodology for small systems can be used to assess the reliability of other Electronic Structure methods. Møller–Plesset perturbation theory is the only post-HF method that can be applied to zeolites, considering terms up to the second order (MP2), although this method usually overestimates the correlation energy [16]. In summary, HF methods are not very widely used in zeolite science due to the high cost associated to post-HF methods and the large size of zeolite systems. Nevertheless, HF and post-HF methods are still the method of choice to obtain accurate information about non-periodic systems.

Semi-empirical quantum chemistry methods are based on the Hartree-Fock method, but make additional approximations and obtain some parameters derived from empirical data. They are important in computational chemistry for treating large molecules where the full Hartree-Fock method without the approximations is too expensive; semi-empirical calculations are much faster than their *ab initio* counterparts. The use of empirical parameters allows some inclusion of electron correlation effects into the methods. Their application, however, is limited to systems for which these parameters exist.

In DFT methods, the properties of a many-electron system are determined by using functionals, i.e. a mathematical entity that associates a number to a function, which in this case is the electron density depending on the spatial coordinates (only three coordinates), thus reducing the many-body problem of N electrons with $3N$ coordinates to 3 coordinates (the x , y and z coordinates of which the electron density depends). Hohenberg and Kohn showed that the ground-state energy and other properties of a system are uniquely determined by the electron density [17]: there exists a one-to-one correspondence between the electron density of a system and the energy. DFT methods are based on one-electron orbitals (the so-called Kohn-Sham orbitals) to represent the density, and on the application of the variational principle [16]. In DFT, the many-body problem of interacting electrons in an external potential is reduced to a tractable problem of non-interacting electrons moving in an effective potential that generate the same density as the system of interacting particles. The effective potential includes the external potential and the effects of the Coulomb interactions between the electrons, the exchange and correlation interactions. Modeling the latter two interactions becomes the main problem in DFT, since the form of the exchange-correlation functional is not known and must be approximated. There are a number of exchange-correlation functionals in the literature; the most commonly used are those based on the Local Density Approximation (LDA) [18-20], which is the simplest approximation in which the exchange-correlation functional depends only on the electron density, the General Gradient Approximation (GGA) [21,22], in which exchange-correlation

depends also on the gradient of the electron density, and Hybrid functionals [23] that, apart from depending on the electron density and its gradient, they partially introduce the exact exchange calculated with a HF treatment of the orbitals.

DFT calculations are notably less demanding than traditional *ab initio* methods in terms of computational resources, and much larger systems, such as zeolites, can be routinely studied at a relatively low computational cost with reasonable reliability; hence DFT is the main Electronic Structure Method that is currently applied to the study of zeolite systems. One of the main reasons why DFT is so widely used in the study of periodic systems is the possibility to implement efficient methods to solve the equations employing plane waves. However, despite this important advantage, one has to be aware of several limitations of the DFT formulation. For example, DFT methods give an incorrect description of the effect of dispersion interactions. This is particularly important when studying the interaction between guest species and zeolite hosts. Nevertheless, there are approaches to overcome this limitation, as is the inclusion of a parametrized long-range dispersion term in the DFT method [24]. Another important limitation of DFT is the underestimation of the band gap (usually it gives values of the band gap which are 50% lower than the experimental values).

3. Simulation Techniques

There are several simulation procedures that can be applied with either of the methods described above, i.e. with Molecular Mechanics or Electronic Structure Methods. These include Energy Minimisation (EM), Molecular Dynamics (MD) and Monte-Carlo (MC) simulations.

3.1 Energy Minimisation (EM)

Also known as Geometry Optimisation, Energy Minimisation (EM) procedures are used to compute the equilibrium configuration of a system. Stable configurational states of a system correspond to minima in the potential energy surface (PES) (Figure 2). Starting from a non-equilibrium geometry, EM procedures vary structural parameters to move atoms so as to reduce the net forces on the atoms until they become negligible. By definition, EM does not include the effect of temperature. The trajectories of the atoms during a minimisation procedure do not make any physical sense, i.e. one can only obtain a final state of the system that corresponds to a local minimum on the PES.

The algorithms based on gradients are the most popular methods for EM. The basic idea is to move atoms by the total net forces acting on them. The force on atoms is calculated as the negative gradient of the total potential energy of the system. Therefore, atoms are moved in the configurational space towards regions that reduce the potential energy (black arrows in Figure 2), until a configuration with

zero gradient is achieved. EM methods are useful to obtain minima, but are severely limited as the minimisation procedure only leads to minima that are local to the initially specified configuration. Let us clarify this by an example: if one starts with a configuration like (1) or (2) (Figure 2), the minimisation procedure –which always goes towards lower energies– will inevitably lead to the local minimum X. However, one is usually interested in the global minimum (Y in Figure 2), but this cannot be reached from (1) or (2) configurations due to the presence of activation barriers that cannot be overcome by a minimisation procedure –it cannot go towards higher energies. Global minimum Y could only be achieved if one starts from configurations like (4) or (5). There are global minimisation methods that try to overcome this limitation and will be discussed below. Another problem is the existence of saddle points (Z in Figure 2) where the gradient is also zero but do not represent true minima in the PES. More sophisticated methods condition the second derivative matrix to be of the correct form for a true minimum, that is, with no negative eigenvalues, ensuring the convergence to a true minimum and avoiding saddle points. Energy minimisation techniques provide, in any case, a very powerful tool if approximate structures to the one sought are available.

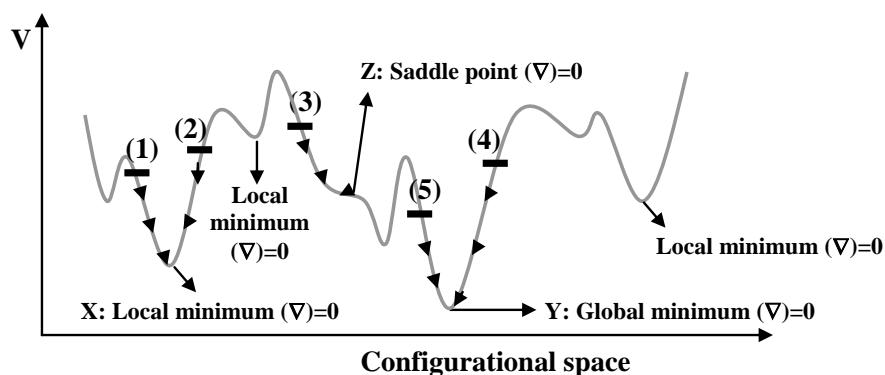


Figure 2. Schematic representation of a potential energy surface (PES) as a function of the configurational space. Different configurations which satisfy the condition of zero gradient are shown: several local minima (X; note that not all local minima are labelled), global minimum (only one, Y) and saddle points (Z).

3.2 Molecular Dynamics

Despite the great advances in physico-chemical characterisation techniques, it is very difficult to get time-dependant information of complex systems from experimental studies, especially due to the short time-scale of the atomic processes going on. Explicit dynamical information can be gained, however, from Molecular

Dynamics (MD) simulations. This technique solves, by an iterative numerical procedure, the Newtonian equations of motion of the system as a function of the forces acting on them, the latter being calculated using a given potential (from MM or Electronic Structure methods).

Let us consider a Taylor expansion of the position of a particle at time t , $r(t)$ (Eq. 3):

$$1) r(t+\Delta t) = r(t) + v(t)\Delta t + \frac{1}{2} a(t)\Delta t^2; \text{ and } 2) r(t-\Delta t) = r(t) - v(t)\Delta t + \frac{1}{2} a(t)\Delta t^2 \text{ (Eq. 3)}$$

where $v(t)$ and $a(t)$ are the velocity and acceleration, respectively, at a given time t . Summing the two equations gives (Eq. 4):

$$r(t+\Delta t) = 2r(t) - r(t-\Delta t) + a(t)\Delta t^2; \text{ where } a(t) = F(t)/m \quad (\text{Eq. 4})$$

where the acceleration $a(t)$ is derived from the forces acting on the particle, and the force itself is obtained from the derivative of the potential energy given by the particular method [4]. This equation is solved repeatedly at consecutive Δt , after which the particle coordinates and velocities are updated using the classical equations of motion, thus giving a trajectory of the particles of the system as a function of time. The essence of any MD simulation is the choice of the time-step (Δt), which must be small enough, typically 10^{-15} seconds (1 femtosecond), as to ensure the conservation of the energy (forces) during that time-step. Assuming a good description of the potential energy, the main limitation of MD simulations is the short time that can be sampled in the simulation, usually in the range of nanoseconds. This time-scale is enough to study particular molecular processes, but not for others that are slower, such as slow diffusion processes of large molecules.

There are several ensembles to perform MD simulations. In the microcanonical ensemble (NVE), the number of particles (N), volume (V) and the total energy of the system, defined as the sum of the potential and kinetic energies, is conserved. It corresponds to an adiabatic process with no heat exchange. In the canonical ensemble (NVT), apart from N and V , the temperature is conserved, while in the NPT ensemble, the pressure rather than the volume is conserved. Depending on the conditions that one wants to simulate, one of the different ensembles will be used. In MD simulations of zeolite systems, the NVE and NVT ensembles are the most widely employed. In both cases, an initial equilibration period is usually carried out, after which production of results starts.

MD simulations can be performed at a given temperature. This provides a way to overcome activation barriers in order to reach global minima, as long as enough temperature is given to the system as to increase its energy and overcome such energy barriers. A particular case of MD simulations aimed to find global minima is the so-called “simulated annealing” (SA) procedure. The name comes from annealing in metallurgy, a technique which involves heating and controlled cooling of a material to increase the size of its crystals and reduce their defects. High

temperatures cause the atoms to become free from their initial positions (a local minimum in the PES) and move randomly through states of higher energy; the slow cooling facilitates finding configurations with lower energy than the initial one. The same principle is applied in computational chemistry to find the global minimum of a system starting from a configuration not close to it (Figure 3). The system changes its configuration randomly when the temperature is high, but progressively towards lower energies as the temperature decreases. The high temperatures provide the systems with enough energy as to overcome energy barriers, enabling them to become free from the initial local minimum and thus move towards more stable minima in the PES. In SA simulations, the system is heated up to a temperature and then decreased slowly, and a certain time of MD simulation is performed at each temperature allowing the system to relax and explore the configurational space, going towards lower-energy, possibly the global, minima. However, one can never be sure that the global minimum has been certainly achieved, and consequently several cycles of SA-MD simulations are usually performed, taking finally the most stable configuration of all the cycles. Usually a final Energy Minimisation is performed to get the final configuration.

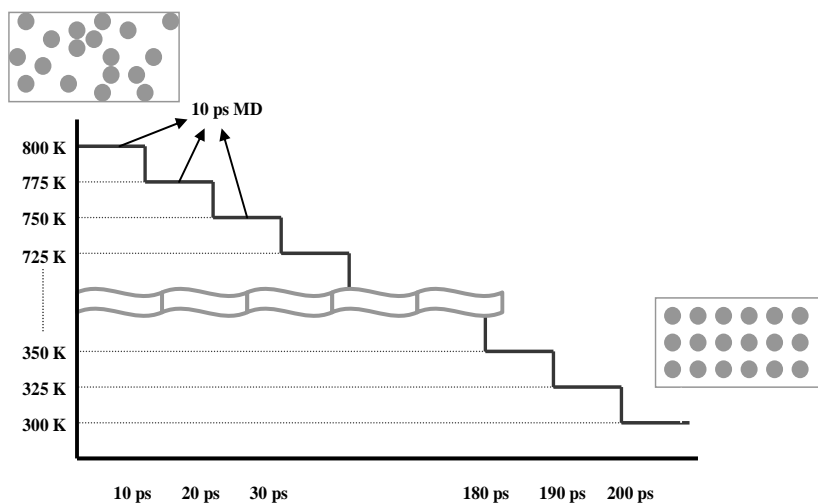


Figure 3. Schematic representation of a simulated annealing MD simulation.

3.3 Monte-Carlo simulations

Monte-Carlo (MC) simulations are based on statistical mechanics and consist of generating a representative set of configurations of a system from which average properties can then be calculated. Starting from an initial configuration, the

simulation proceeds via the generation of new configurations through random moves (translation or rotations) of the particles of the system (hence the name Monte-Carlo, with the random nature of the method making reference to the Monte-Carlo Casino). Each new configuration can be then accepted or rejected according to a certain probability, generally using the Metropolis algorithm [25], which weights the probability of acceptance according to a Boltzmann distribution obtained using the energy change caused by the new configuration. The probability of acceptance (P) of a new configuration is given by the following expression (Eq. 5):

$$P = \min \{1, e^{-\Delta E/kT}\} \quad (\text{Eq. 5})$$

The Metropolis criteria means that if the new configuration is more stable, i.e. ΔE is negative, then the new configuration is accepted and collected in the set. If the new configuration is less stable, then ΔE is positive, and there is a certain probability of accepting that configuration. A random number between 0 and 1 is generated and compared with $e^{-\Delta E/kT}$ (for positive ΔE , this always gives a number between 0 and 1), and the new configuration is accepted if such random number is lower than $e^{-\Delta E/kT}$. If ΔE is very high, i.e. the new configuration is much more unstable, $e^{-\Delta E/kT}$ will be very close to 0, and so the probability of having a random number between 0 and 1 smaller than $e^{-\Delta E/kT}$ will be very small. On the contrary, if ΔE is low, $e^{-\Delta E/kT}$ will be higher (but always lower than 1), and then the probability of satisfying the condition will be higher. In practice, this means that moves leading to very unstable configurations are very unlikely to be accepted, whilst moves driving to configurations just slightly more unstable have a certain probability of being accepted. Once a significant number of configurations has been generated, average properties can be calculated. This methodology is able to overcome activation barriers since there is a certain probability of driving the system towards higher energies, and thus is a useful methodology to search for global minima.

In Canonical Monte-Carlo simulations (NVT), the number of particles, the volume and the temperature are fixed (this is usually referred as “fixed loading”). This is useful for example to compute heats of adsorption at particular uptakes, or to study the occupation of the zeolite pores at a particular guest composition. In Grand Canonical Monte-Carlo methods, the chemical potential, volume and temperature are fixed, while the number of particles (N) is varied. In general, it is the pressure rather than the chemical potential that is specified; this ensemble is particularly useful to generate isotherms of adsorption by performing several MC simulations at different pressures. In this ensemble, not only translation and rotation of the particles are used for generating the new configurations, but also insertion/deletion of particles.

If studying complex systems, which in our case can be exemplified by adsorbing complex sorbate molecules in zeolite systems, the rate of generation of new

configurations might be extremely slow due to the low probability of acceptance. In this case, *biasing* Monte-Carlo techniques have been developed where the probability of energetically favourable moves is increased. Flexible and large sorbate molecules represent a particular challenge for MC simulations. These molecules are usually quite tightly adjusted within zeolite frameworks, and besides, the shape of the zeolite pore system usually determines the shape of the sorbate conformation in which it is adsorbed; hence, the rate of acceptance in normal MC simulations would be extremely small [4]. A new MC methodology, *configurational-bias* method [26-28], was developed in order to overcome these problems. In this methodology, the sorbate molecule to be inserted is grown, atom by atom, within the zeolite pores, instead of inserting the whole molecule at once, what would have a very low probability of acceptance. The simulation starts with the insertion of an atom or “seed”, and then the molecule is grown by addition of new atoms at a random location on a sphere of fixed radius (corresponding to the bond distance between those atoms) centred on the previous atom. The result of this type of methodology is that only the molecular conformations that fit within the zeolite channels are efficiently generated, thus increasing notably the rate of acceptance and hence the generation of the configurations. This method has been very successfully used to study the adsorption of large alkanes in all-silica zeolites [26-29].

These three types of techniques (EM, MD and MC) represent the main simulation tools that are commonly used to study zeolite systems, either with Molecular Mechanics or Electronic Structure Methods. The fundamentals of the techniques are the same regardless of the model used, although its implementation might require specific features depending on the method; for instance, Car-Parrinello developed a methodology for applying MD simulations with Electronic Structure Methods. In any case, it should be noted that this does not represent a complete list of simulation engines; there are other techniques used in zeolite systems. For instance, Genetic Algorithm Methods [3,30], useful for finding global minima, mimics the process of natural evolution: the energy landscape of a system is explored in which populations of candidate structures evolve through successive generations by exchanging features which are evaluated by a cost function. It is also important to mention the application of mathematical-geometrical procedures to generate hypothetical zeolite frameworks [4,31].

4. Zeolite Models

Depending on the type of problem one wants to study and the computational method to use (Molecular Mechanics or Electronic Structure Methods), as well as on the computational resources available, three different types of models can be employed for studying zeolite systems.

4.1 Periodic Models

A periodic model is the natural one to study crystalline materials such as zeolites. In this approach, the zeolite is represented by a unit cell that is periodically repeated by translation along the three crystallographic directions, applying periodic boundary conditions (PBC) (Figure 4, top left). This is the most reliable model to simulate a zeolite system since it includes long-range interactions and full topological effects, and hence, if possible, this is the model to use. The lower computational cost of Molecular Mechanics Methods based on interatomic potentials involves that these methods invariably use zeolite periodic models; however, the much larger computational demand of Electronic Structure Methods makes sometimes extremely expensive the use of these periodic models, forcing to use simpler models (see below).

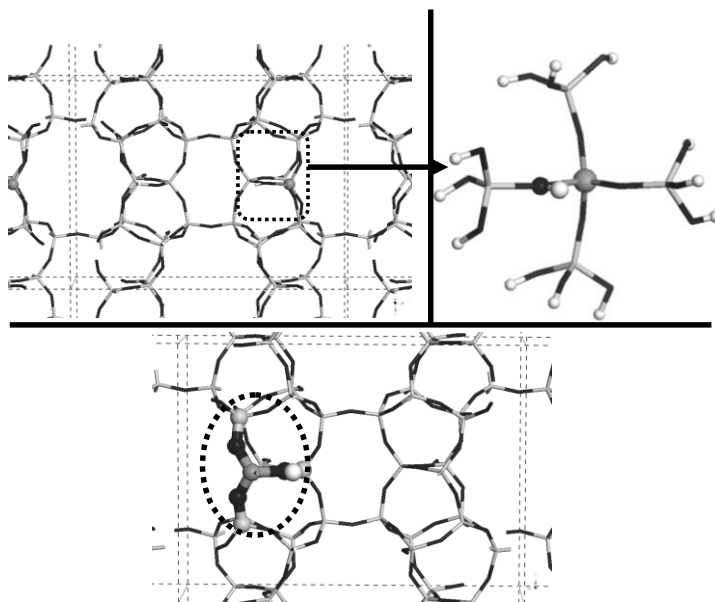


Figure 4. Types of zeolite models for FER with an Al dopant (grey ball) and associated H^+ (white ball): periodic (top left, showing the unit cell), cluster (top right, with terminating bonds as OH groups), and hybrid (bottom), with the part treated at QM level displayed as larger balls and sticks (highlighted by the circle), and the region modelled as MM as thinner sticks.

When using periodic models, one can take advantage of the symmetry of zeolites, where symmetry-equivalent atoms in a unit cell are treated as one, what can speed up notably the calculations; however, it is very often necessary to remove symmetry

operations (impose a P1 symmetry to the system) in order to enable an effective exploration of the configurational space without symmetry constraints. All zeolite structures available have a periodic model that contains the space group, the unit cell parameters and the atomic fractional coordinates.

4.2 Cluster Models

In cases, when using computationally-demanding Electronic Structure Methods, an entire periodic model of a zeolite is too large as to be tractable in an efficient way. Therefore, sometimes it is convenient to use cluster models of the zeolite structure, where the model is composed of several TO_4 units (where T denotes tetrahedral atoms, usually Si and Al) arranged in an equivalent fashion as they are in a zeolite structure in order to partially mimic its topology (see Figure 4-top right). Traditionally, cluster models have ranged from having 1 T atom up to 28-T atoms^[32]. The larger the number of T atoms used in the model, the better the description of a particular zeolite structure, at the expense of more computationally-demanding calculations. In order to provide real chemical species, dangling bonds generated at the borders of the cluster must be saturated; typically, O-atoms are saturated with H atoms, since Si and H have similar electronegativities (consider that terminal H atoms are replacing the hypothetical site of a Si atom in a zeolite). In general, three work approaches are used with cluster models: the geometry can be fixed at the experimental positions, it can be fully relaxed (although this can lead to geometries very different from that in the zeolite, and so this is not usually employed), or only certain atoms are relaxed [16]. In any case, cluster models have the disadvantage of imposing geometry constraints, and especially, they neglect long-range interactions in a zeolite framework, which can have a profound impact on the results. Cluster models were traditionally used in zeolite studies; however, the development of accurate DFT methods as well as the rapid increase in computer power have decreased their use in benefit of periodic or hybrid models which better describe zeolite systems. However, despite the limitations associated with these models, they still can be useful in order to apply highly-accurate and reliable post-HF methods to test the reliability of other less computationally-demanding QM techniques which are to be applied in periodic/hybrid models, by comparing results on the cluster model at different levels of theory.

4.3 Hybrid Models

Hybrid models, also known as embedded clusters or QM/MM models, were developed in order to overcome the main limitations of cluster models, i.e. the imposition of artificial geometry constraints and the neglect of long-range interactions and of long-range topological effects, while allowing for a good description, at a high level of theory, of a particular region of the model with special importance on the issue under study [33]. In these models, the system is

divided in two parts, an inner region (see Figure 4, bottom, large balls and sticks), containing the atoms of particular interest, which are treated at a high level of theory employing QM Methods, and the outer region (thinner sticks), which is described at a lower level of theory, typically with an MM model –this is why they are also called QM/MM models. The main problem of these models comes from how to account for cross-interactions between the border regions. These models allows for studying with high levels of theory a region involved in electronic processes, for instance an active site interacting with reactants, which is not valid to study under MM, while keeping the rest of the structure studied at a lower level of theory, thus permitting the inclusion of long-range effects, while notably decreasing the computational cost of the simulations compared with full periodic models.

5. Setting up a calculation

In this section, the main decisions that one has to tackle when facing a computational study of a particular problem will be briefly described. A scheme of the process of setting up a computational study, including the selection of the method, model and simulation technique, is described in Figure 5.

The first and main question that one has to address is related to the choice of the computational method: Molecular Mechanics or Electronic Structure Method? For selecting the method, one has to consider if electronic-related information or changes in the electronic configuration are important for our particular problem. For instance, spectroscopic information, or information related to the acid/basic or redox activity of active sites, chemical reactions, which usually involve bond breaking and formation, activation energies, reaction enthalpies, etc, can only be extracted from a model in which we have explicitly dealt with electrons in the system, i.e. an Electronic Structure Method should be used. Instead, there is other type of information that does not necessarily rely on the electronic configuration and can be studied by the computationally much cheaper MM methods, like the topology of zeolite structures or the physisorption of guest species, which is only due to Van der Waals and electrostatic interactions, usually reliably modeled by force-fields, remarkably the interaction of structure-directing agent (SDA) molecules with frameworks, or adsorption and/or diffusion of sorbate molecules within zeolite structures. In general, processes in which the main driving forces are Van der Waals interactions are usually accurately described with appropriate force-fields. In addition, when selecting the method to use, one has to be aware of the much more demanding nature of QM-related methods, which dramatically reduces the size of the systems to study efficiently as well as the simulation technique to employ, which should be much less demanding (usually Energy Minimisation).

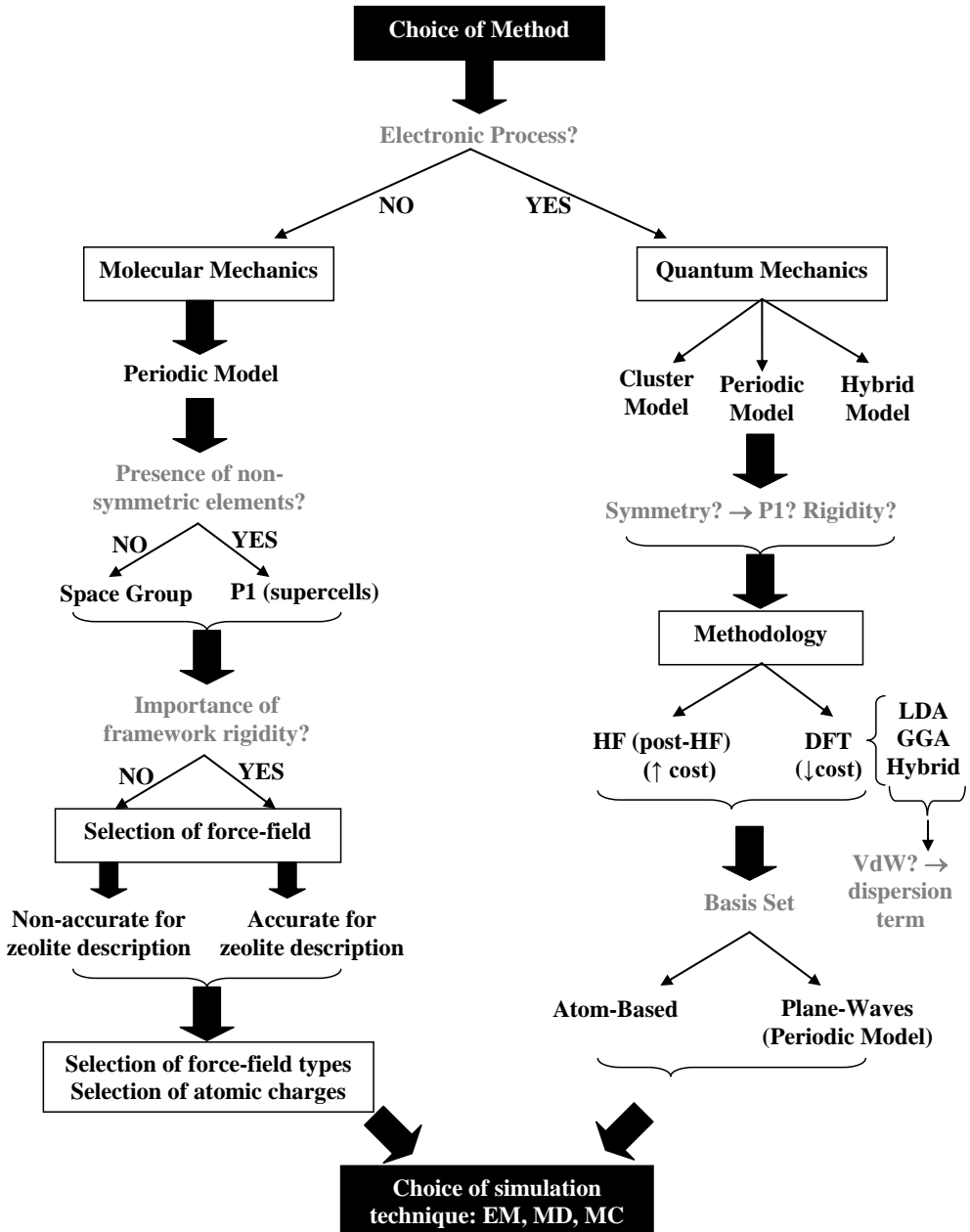


Figure 5. Schematic procedure for setting up a computational study.

If it is not an electronic process, one would use an MM method. Due to their low computational cost, MM methods always use periodic models of the zeolite system due to their higher reliability. A periodic model can make use of the symmetry of the zeolite structure to speed up the calculations; however, this imposes symmetry constraints that sometimes do not allow for a complete relaxation of the zeolite lattice. Besides, in this type of calculations one is usually interested on the interaction with guest species (SDA or sorbates), or the presence of dopants or other defects, whose usually non-long-range-ordered disposition with respect to the zeolite lattice cancels the existence of symmetry operations, and then forces the system to be set up in P1 space group (i.e. without symmetry constraints). Another feature that one has to select is the size of the zeolite system (in terms of unit cells along particular directions). This is important especially when studying the location of SDA molecules or other guest species, especially if these are large, since usually one single unit cell is not enough to site an organic molecule, or it does not enable a full relaxation of these guest species without periodic-image impositions, or if different guest loadings are to be studied, and also in MD simulations in order to prevent interactions between periodic images of the sorbate in consecutive unit cells. Usually supercells with P1 symmetry and composed of several primitive unit cells along the channel directions are used as zeolite models with MM methods. Once set up the model to simulate the zeolite system, the next question to address is whether to use a rigid or flexible framework. Keeping fixed the atomic coordinates of the zeolite framework atoms is an approximation that notably speeds up the calculations and enables a more efficient exploration of the energy landscape, for instance by using global minimization techniques, such as simulated annealing. Depending on the problem to study, this can be an acceptable assumption. For instance, when studying interactions between SDA molecules and zeolite frameworks, this is an assumption widely applied since, unless specific cases, the SDA molecules do not provoke a strong distortion of the zeolite framework. However, there are cases where distortion/vibrations of the framework are important; for instance, when studying interactions between guest molecules and dopant atoms embedded in the zeolite framework (e.g. Al substituting Si atoms), these dopants and their electrostatic interactions with the SDA molecules usually provokes a distortion of the zeolite framework; on the other hand, it has been demonstrated that diffusion of large molecules along zeolite channels are severely influenced by the vibrations of the zeolite atoms composing the channel rings [³⁴]. In these cases, the zeolite framework should be allowed to relax during the simulation.

Depending on whether one will use a rigid or flexible framework, different force-fields will be employed to model the potential energy of the system as a function of the configurational space. If rigid frameworks are to be used, general-purpose force-fields that include a large number of energy terms to provide a very good

description of the guest molecules and their interactions with the zeolite networks can be employed, such as *cvff* [35]. On the contrary, if flexible frameworks are required, the force-field to use should include an accurate description of the zeolite topology as well as of the molecular structure of the guest molecules and their interactions with the zeolite network. In this case, it is very common to use a combination of interatomic potentials, one that was initially parametrised to model the zeolite structure (Sanders et al. [36,37]) which makes use of the shell model to simulate the polarizability of the oxygen atoms and has been demonstrated to properly model the topology of zeolite structures [³⁸,³⁹], the potential by Kiselev et al. [40] to account for the intermolecular SDA-zeolite and SDA-SDA interactions, and the potential by Oie et al. [41] for modelling the intramolecular interactions between the organic atoms of the guest molecules. Such a combination of potentials has been shown to work properly for modelling host-guest systems of zeolites and organic species when framework flexibility is essential [42-44]. However, as previously mentioned, the use of combined potentials should not be taken as a general rule: it is not common to combine different potentials since the parameters are usually not transferrable. Finally, once selected the method and the zeolite model, the only thing left to do is to assign forcefield-types to the different atoms as a function of their chemical nature, and importantly, the atomic charges, that can be derived from Electronic Structure calculations or from other methods such as charge-equilibration [45].

If the electronic configuration is important in the case of study, one has to inevitably go to Electronic Structure Methods, despite their much larger computational cost. Nowadays, due to the rapid increase in computational power, the most widely models applied with Electronic Structure methodologies are the periodic and the hybrid model, while cluster calculations are used to assess the reliability of the QM methodology [16]. Again one has to address the choice of the use of symmetry, the supercell size, keeping in mind that these are much more computationally-demanding calculations (usually supercells of one or two primitive unit cells are used) and the approximation of fixed or flexible frameworks. HF (or post-HF to account for correlation energy) or DFT methodologies can be used to study zeolite systems. Nevertheless, the lower computational cost and the notable advancement in DFT functionals, as well as the application of hybrid functionals that include a part of the exact exchange calculated at HF level, has enormously increased the use of DFT methods to study zeolite systems, which currently are used on a routine basis. If periodic models are used, atom-centred or plane-wave basis sets can be used, each being employed by the different codes available. Besides, the number of electrons explicitly considered can be reduced by replacing the core electrons, which are not likely to be modified on the process under study, with pseudopotentials, increasing the computational efficiency.

When working with DFT methods, the form for the exchange-correlation functionals has to be selected. LDA methods are usually very poor to describe zeolites, especially energies, while GGA, and especially hybrid functionals such as the widely employed B3LYP, are much more reliable. Again one has to keep in mind that hybrid functionals require a larger computational cost. Finally, the main limitation of DFT methods is the lack of inclusion of dispersion interactions; nevertheless, if these are thought to be important in our system, current DFT methods allow for the inclusion of a parametrized long-range dispersion term [24].

Finally, there is also the possibility of using QM/MM methodologies, which combine the description of QM (Electronic Structure) and MM methods to particular regions of our zeolite system; in this case, the procedure to set up a calculation is essentially the same as described above, following both approaches, QM and MM. Special attention should be taken when deciding which atoms of the system are to be modelled with QM, and on the computational treatment of the boundaries between the two regions.

Once set up the method and zeolite model, the last task is to define the simulation technique to use, including Energy Minimisation (EM), Molecular Dynamics (MD) or Monte-Carlos (MC) simulations, depending on the problem to study. The main codes that are used to study zeolite systems include GULP (MM with flexible frameworks) [46], Discover or Forcite modules (MM with fixed frameworks) (within Materials Studio software) [47] or DLPOLY (for accurate MD simulations with force-fields) [48], while codes such as CRYSTAL (HF or DFT, atom-centred basis set) [49], CASTEP (DFT, plane waves basis set) [50] or DMol3 (DFT) [51], etc, perform an electronic treatment of the system. In subsequent sections, the main applications of these simulation techniques to address different cases of study in zeolite science will be briefly presented by describing some of the most widely used types of computational studies.

6. Studies Related to Zeolite Structure

Although strictly speaking is not a computational study, one very powerful tool of the computational programs is the visualization of zeolite frameworks. These are usually complex structures which very often are difficult to visualize in 3-dimensions, and general tools that are available in usual programs such as Material Studio [52], a software that compile a number of computational codes, facilitate the visualization of these structures, remarkably the calculation of free volumes to visualize the pore system of zeolites. As an example, Figure 6 displays the structure and the free volume of the complex zeolite MCM-22 (MWW structure type), which is composed of two independent systems of channels, and can be easily pictured by the free volume of the pores.

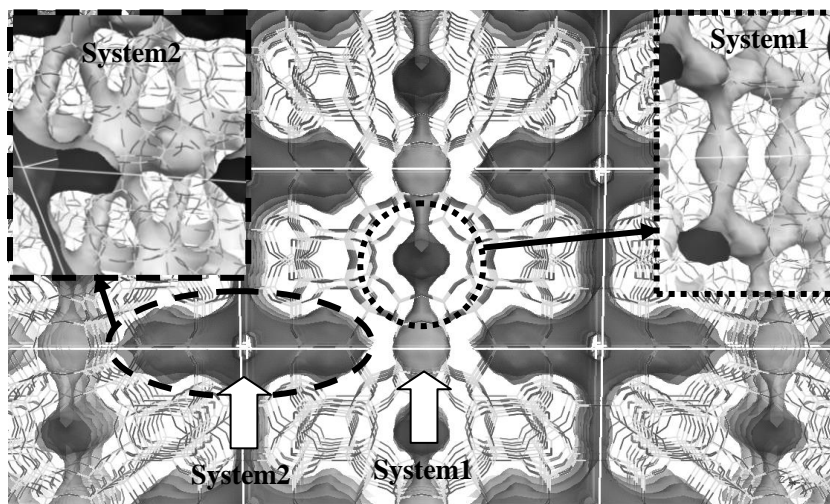


Figure 6. Structure of MCM-22, showing the free volume of the two channel systems; insets: detail of the cavities present on each system.

The existence of accurate interatomic potentials to describe the different zeolite topologies combined with the use of the shell model has provided a tool for accurate modelling the structure of zeolite frameworks. An early study helped in the solution of the structure of zeolite Nu87, which could not be solved by the available powder diffraction data [53]. Starting from an approximate model, energy-minimisation techniques generated a framework structure candidate, which was then refined by Rietveld refinement of the diffraction data and led to the satisfactory solution of the zeolite structure. Henson and Gale [54] performed a comparison of the experimental and energy-minimised structures and studied the meta-stability of pure-silica zeolites, finding a very good agreement and hence evidencing the reliability of interatomic potential techniques for the description of zeolite topologies. There are several potentials available for modelling zeolite materials. Not only perfectly crystalline zeolite structures, but also defects and crystal surfaces can be studied by these techniques [4]. A very common application of lattice-energy calculations is the study of the distortion generated by the presence of dopants in the zeolite network –especially Al substituting Si–, as well as the different stability of these dopant atoms sited on non-equivalent T sites and their relative distribution [55]. The main difficulty here is the large number of permutations of Si and Al atoms over the different T sites; however, new codes such as SOD [56] facilitate the study by finding symmetry relationships between the different distributions of dopants. The incorporation of Si atoms in aluminophosphate frameworks through

the different substitution mechanisms has also been studied by lattice-energy calculations [57]. Apart from dopant atoms embedded in the zeolite network, the location and stability of extra-framework cations like Na^+ or K^+ can also be reliably studied by MM models.

A very interesting computational application in the field of zeolite structures is the enumeration of hypothetical zeolite structures. One of the main investigations in zeolite science is related to the discovery of new zeolite structures. In this sense, the knowledge of hypothetical structures a priori by computational engines could efficiently aid in this search. Zeolite networks have well-defined structural features; they can be seen as 4-connected nets in which each vertex (the T-atom), is connected to its four closest neighbours via oxygen bridges. Therefore, it is possible to enumerate periodic 3-dimensional 4-connected nets by applying different mathematical approaches, using topological and geometric considerations [4]. Apart from simply generating hypothetical zeolite structures, their relative stability as a function of the topological features they contain can be studied. The generated hypothetical zeolite structures can be refined by lattice-energy minimisation techniques and their relative stability studied. It was observed that, as expected, higher densities lead to more stable structures [58]. Zwijnenburg et al. [59] found that there seems to exist a maximum mean ring size of six; hence, ring sizes larger than 6 must be compensated for by the simultaneous presence of smaller rings, providing a basis for the early empirical observation of Brunner and Meier that low-density zeolites tend to contain small 3- and 4-rings [60]. These types of studies have allowed gaining new insights into the complex relationships between zeolite structure and feasibility.

Electronic Structure Methods, especially based on DFT, can also be applied to structure determination. When comparing with experimental results, DFT methods in general provide structures with a good accuracy. Depending on the functionals, LDA tends to slightly underestimate and GGA to overestimate bond lengths; hybrid functionals perform significantly better [16]. DFT methods for structure determination are especially important when electronic effects are important, like for example coordination of extraframework Cu cations to framework oxygen atoms [61]. Another important application of Electronic Structure Methods is the study of spectroscopic properties, which in general cannot be studied by MM methods (unless vibrational spectra using very accurate force-fields). One of the main studies in this field is the calculation of NMR characteristics. Solid State NMR is a very powerful technique in structure-elucidation of zeolites, but the spectra can sometimes be very complex as to assign every signal to a particular chemical species. In this way, QM methods can be used to calculate NMR shifts and help in the assignment of the experimentally observed signals [62].

7. Studies Related to Zeolite Synthesis

One of the main applications of computational models is the study of the location and interactions of the organic structure directing agents (SDA) with the zeolite framework they direct [1]. Understanding and rationalizing the role played by these organic molecules in the synthesis of zeolite-like materials is a long-time sought goal in zeolite research. Usually, the efficiency of organic molecules to direct a particular zeolite structure is related to the interaction energy they develop, which includes the effect of the two main features that characterize the efficiency of an SDA, the space-filling ability and the adjustment between the molecular shape of the SDA and the channel walls of the zeolite. The interactions that are established between SDA molecules and zeolite frameworks are non-bonded in nature, Van der Waals and electrostatic interactions. Therefore, for this particular problem, MM methods based on interatomic potentials are invariably used. SDA molecules are usually quaternary ammonium cations, and their positive charge is compensated by the zeolite network through the presence of low-valent dopants such as Al substituting for Si, or the presence of negatively-charged connectivity defects. The modeling of the zeolite framework including explicitly these negatively-charged defects is difficult, especially by the large number of possible distributions. A commonly employed solution is to uniformly distribute all the negative charge required for charge-balance along all the T sites, treating each T site as an average species; this would represent a model with a random distribution of the negatively-charged defects. This assumption is generally valid to study the location and interaction of SDA molecules with zeolite frameworks, but of course gives no information on Si/Al distributions depending on the SDA molecule.

A pioneering work by Lewis et al. [63] demonstrated the reliability of MM methods to investigate the location and structure-directing efficiency of organic molecules in the synthesis of several zeolite structures. They observed that for achieving a good agreement between the experimental and computational observations, in terms of location and structure-directing efficiency, packing interactions, e.g. intermolecular interactions between consecutive organic molecules, must be accounted for in the model. They proposed –and provided evidence– that the structure-directing efficiency of an organic molecule to direct the synthesis of a particular zeolite framework can be expressed in terms of the interactions developed between them, which represent a measure of the adjustment between the pore volume of zeolites and the shape of the organic molecule, i.e. of the template effect. An example of this template effect is given by the location of the triquataternary ammonium ion used as SDA for the synthesis of ZSM-18, where a clear structural relationship between the organic molecule and the zeolite internal surface can be appreciated (see Figure 7).

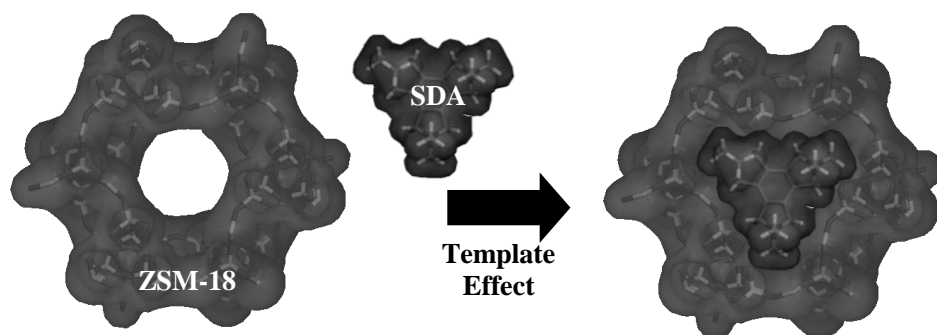


Figure 7. Template effect of the triquat (SDA) in the synthesis of ZSM-18.

The typical way of locating the organic SDA molecules within a zeolite framework and calculating the non-bonded interactions is to insert the organic molecules in a large enough model of the microporous framework and determine their most stable location by means of different simulation techniques, including Monte-Carlo, Molecular Dynamics (simulated annealing) and Energy Minimization methodologies. Freeman et al. [64] developed a computational methodology which consisted of an initial insertion of the organic molecules through MC techniques, followed by a search of the global minimum by simulated annealing procedures, and finally the energy of the system was minimized. In this way, molecular mechanics calculations of the non-bonded interactions have been generally used to understand and, in certain cases, to predict [65] the structure directing ability of organic molecules. Indeed, this type of methodologies has enabled the rational design of organic molecules for a desired zeolite framework. For instance, Sastre et al. [65] searched for a specific SDA for ITQ-7. ITQ-7 structure is closely related to the C polymorph of zeolite Beta, and it is difficult to discriminate between the two structures during the synthesis. By calculating the interaction energies of different molecules with the two related structures, the authors were able to find a SDA that fits much better in the ITQ-7 structure than in the C polymorph, and thus zeolite ITQ-7 could be experimentally obtained without impurities of polymorph C. In the same line of rational design, one interesting approach, called *de novo* design, was developed by Lewis et al by using computational tools [66]. The authors developed a procedure by which an SDA molecule is computationally grown in the void space of a desired zeolite from different organic fragments previously defined. Van der Waals interactions are in last term a quantification of the fit between SDAs and frameworks, and hence they were used to control the growth of the organic species within the zeolite. In this way, organic SDA molecules in which van der Waals interactions with a certain microporous framework are maximised can be a priori designed. This methodology was experimentally validated. In recent times, more

sophisticated models for computationally studying structure-directing effects have been developed, by taking into account the inclusion of other guest species (solvent molecules) or the stability of the SDA molecules in the gels, which have been observed to be necessary for accurately predicting the organic content of zeolite materials [67]. Furthermore, the influence of the SDA molecules on the location of the Al dopant atoms has also been studied [68], finding that NH_x groups of the SDAs able to form H-bonds with framework oxygen atoms tend to attract Al to their vicinity.

Another important field of study is in the mechanisms of zeolite synthesis and structure-direction. Catlow et al. addressed this issue by applying Electronic Structure methodologies to the synthesis of LEV-type structure [69]. They found that silica fragments that are part of the zeolite networks are not stable in water solution; they collapse upon attack of water molecules due to their hydrophobic nature, reducing as much as possible the contact surface with water molecules. Organic SDAs provide the driving force by which the inorganic species can be stabilized to allow the formation of the metastable crystalline structure: SDAs shield the inorganic fragments from the solvent and therefore prevent collapse of the more open fragments. A similar concept of shielding was demonstrated by Caratzoulas et al. by performing MD studies based on MM methods of water solutions in the presence of tetramethylammonium (TMA) and the octamer ($\text{Si}_8\text{O}_{20}^{8-}$) and hexamer ($\text{Si}_6\text{O}_{15}^{6-}$) silicate species [70,71]. They found that the stability of the silicate species was strongly correlated to the ability of the SDAs, TMA in this case, to adsorb onto their surfaces, reinforcing the theory that one of the roles of SDAs is to protect the siloxane bonds (Si–O–Si) from being attacked by water molecules, i.e. from hydrolysis.

8. Studies Related to Zeolite Applications

Computational simulations have also provided a valuable tool to understand at an atomic level applications where zeolite materials are widely used, including adsorption, diffusion and catalysis. As in the case of SDAs, simulation techniques based on global minima search engines are efficient to locate adsorption sites within a zeolite framework. Moreover, adsorption isotherms of sorbate molecules can be simulated through Grand Canonical (constant NPT) MC simulation techniques, provided a good description of the host-guest interactions is available in the force-field. The configurational-bias MC method, described previously, has been very successful in simulating the adsorption of linear and branched alkanes in all-silica zeolites, finding a very good agreement with the experimental observations [26--29].

MD simulations are particularly useful to study the diffusion of guest molecules through the pore systems of zeolites, an issue very important both in catalytic and

molecular sieve applications of zeolites. In this case, the main problem is when studying large molecules with slow diffusion processes, which might require very long simulation times not affordable in current computers; in these cases, other techniques such as transition state theory or kinetic MC may be more useful. MD simulations might be performed with rigid or flexible frameworks. It was observed that for studying small molecules such as methane [72], the use of flexible frameworks, which involves a much higher computational cost, led to small differences in the diffusivities found compared to rigid frameworks. However, Sastre et al. found that for larger molecules such as benzene and propylene (in MCM-22), a good agreement with experiments could only be achieved if using flexible frameworks [34], evidencing that framework flexibility is important when the sorbate molecules have similar dimensions as those of the zeolite pores.

Finally, one of the main applications of computational models is the study of catalytic properties, reaction mechanisms and energy barriers in reactions catalyzed by doped-zeolites, containing acid or redox active sites. Of course this type of simulations inevitably involves the use of QM models because of the essential implication of electrons in catalysis, with DFT being the most widely applied methodology. The large computational cost associated to these QM studies usually involves the use of the simpler Energy-Minimisation engines, although in certain cases more sophisticated techniques such as MC or MD (Car-Parrinello MD) are used. One of the most important applications is in the study of complex heterogeneous catalytic reaction mechanisms and activation barriers. In this case, to obtain activation barriers, transition-state search engines that look for maxima in the PES, points that are characterized by having all the frequency modes positive but one –corresponding to the reaction coordinate– must be used. Hybrid-DFT methods usually perform reasonably well in these systems, although sometimes it is necessary to include an additional term to account for dispersion interactions [73]. Car-Parrinello MD simulations have been used to study complex PES in the methanol-to-hydrocarbon reaction [74]. Recently we have performed a hybrid-DFT study to unravel the complex mechanism of the catalytic oxidation of hydrocarbons catalyzed by transition-state metal-doped aluminophosphates zeotypes, giving results in good agreement with the experimental observations [75].

9. Conclusions

This chapter provides a general overview of the computational methods, simulation techniques and zeolite models that are currently applied in order to study zeolite systems. The increasing power of high-performing computers combined with the rapid development of computational methodologies has provided a very powerful tool to study, at an atomic level, zeolite problems that are difficult to unravel experimentally, giving very important information complementary to that obtain from experiments that can significantly aid in the interpretation of experimental

data and provide a rational guide for the design of future experiments. Molecular Mechanics and Electronic Structure Methods can be routinely applied to different problems in zeolite science, ranging from the study of zeolite structures, zeolite syntheses and zeolite applications. Depending on the type of problem to study, a different methodology, in terms of computational method, model and simulation technique, will be employed. Due to the large number of approximations assumed in these computational calculations, a close contact with experiments is inevitably required in order to validate the reliability of the calculations performed. The continuing growth in both computational technology as well as in the techniques applied will likely increase the contribution of this type of studies to the understanding of the complex phenomena involved in the chemistry of zeolites, providing a perfect match with the knowledge gained by experimental techniques, especially in those issues where experiments cannot reach the information.

Acknowledgements

The author acknowledges Dr. Furio Corà and Prof. C. Richard A. Catlow for their long-time guidance in the application of computational methodologies to the study of zeolites, and Dr. Said Hamad for revising this manuscript.

References

- [1] Pérez-Pariente, J. & Gómez-Hortigüela, L. in *Zeolites, from model materials to industrial catalysts* eds J. Čejka, J. Pérez-Pariente, W. J. Roth. Ch. 3, 33-62 (2008).
- [2] Cooper, E. R., Andrews, C. D., Wheatley, P. S., Webb, P. B., Wormald, P. & Morris R. E. Ionic liquids and eutectic mixtures as solvent and template in synthesis of zeolite analogues. *Nature* **430**, 1012-1016 (2004).
- [3] Catlow, R., Bell, R., Corà, F., French, S. A., Slater, B. & Sokol, A. Computer modeling of inorganic materials. *Annual Reports on the Progress on Chemistry, Section A* **101**, 513-547 (2005).
- [4] Catlow, R., Bell, R., Corà, F. & Slater, B. in *Introduction to Zeolite Science and Practice – Studies in Surface Science and Catalysis* eds Jiří Čejka, Herman van Bekkum, Avelino Corma, & Ferdi Schüth) Ch. 19, 659-700 (2007).
- [5] Ewald, P. P. The calculation of optical and electrostatic grid potential. *Annalen der Physik* **64**, 253-287 (1921).
- [6] Tosi, M.P. Cohesion of ionic solids in the Born model. *Solid State Physics* **16**, 1-120 (1964).
- [7] Corà, F., Alfredsson, M., Barker, C. M., Bell, R. g., Foster, M. D., Saadoune, I. Simperler, A. & Catlow, C. R. A. Modeling the framework stability and catalytic

- activity of pure and transition metal-doped zeotypes. *Journal of Solid State Chemistry* **176**, 496-529 (2003).
- [8] Dick B. G. & Overhauser, A. W. Theory of the dielectric constants of alkali halide crystals. *Physical Reviews* **112**, 90-103 (1958).
- [9] Sauer, J. Molecular-models in abinitio studies of solids and surfaces- from ionic crystals and semiconductors to catalysts. *Chemical Reviews* **89**, 199-255 (1989).
- [10] *Modelling of Structure and Reactivity in Zeolites* ed C. Richard A. Catlow. Academic Press, London (1992).
- [11] Sauer, J. Ugliengo, P., Garrone E. & Saunders, V. R. Theoretical study of Van der Waals Complexes at surface sites in comparison with the experiment. *Chemical Reviews* **94**, 2095-2160 (1994).
- [12] Koch, W. & Holthausen, M. C. *A Chemist's Guide to Density Functional Theory*. Wiley-VCH, Weinheim (2000).
- [13] *Computer Modelling of Microporous Materials* eds C. R. A. Catlow, R. A. v. Santen, B. Smit (eds.) Elsevier, Amsterdam, 2004.
- [14] *Introduction to Computational Chemistry*. F. Jensen. Ed. Wiley; Second Ed. (2007).
- [15] Van Santen, R. A., van de Graaf, B. & Smit, B., in *Studies in Surface Science and Catalysis* **137**, Ch. 10, 419-466 (2001).
- [16] Nachtigall, P. & Sauer, J., in *Introduction to Zeolite Science and Practice – Studies in Surface Science and Catalysis* eds Jiří Čejka, Herman van Bekkum, Avelino Corma, & Ferdi Schüth) Ch. 20, 701-736 (2007).
- [17] Hohenberg, P. & Kohn, W. Inhomogeneous electron gas. *Physical Reviews B* **B136**, 864 (1964).
- [18] Kohn, W. & Sham, L. J. Self-consistent equations including exchange and correlation effects. *Physical Reviews A* **140**, 1133 (1965).
- [19] Vosko, S. H., Wilk, L. & Nusair, M. Accurate spin-dependent electron liquid correlation energies for local spin-density calculations-A critical analysis. *Canadian Journal of Physics* **58**, 1200-1211 (1980).
- [20] Dirac, P. A. M. Note on exchange phenomena in the Thomas atom. *Proceedings of the Cambridge Philosophical Society* **26**, 376-385 (1930).
- [21] Becke, A. D. Density-Functional Exchange energy approximation with correct asymptotic behavior. *Physical Reviews A* **38**, 3098-3100 (1988).
- [22] Lee, C. Yang, W. & Parr, R. G. Development of the Colle-Salvetti correlation energy formula into a functional of the electron density. *Physical Reviews B: Condensed Matter* **37**, 785-789 (1988).
- [23] Becke, A. D. Density-Functional Thermochemistry. 3. The role of exact exchange. *Journal of Chemical Physics* **98**, 5648-5652 (1993).

- [24] Grimme, S. Accurate description of van der Waals complexes by density functional theory including empirical corrections. *Journal of Computational Chemistry* **25**, 1463-1473 (2004).
- [25] Metropolis, N., Rosenbluth, A. W., Rosenbluth, M. N., Teller, A. H. & Teller, E. Equation of state calculations by fast computing machines. *Journal of Chemical Physics* **21**, 1087-1092 (1953).
- [26] Smit, B. & Siepmann, J. I. Computer simulations of the energetics and siting of N-alkanes in zeolites. *Journal of Physical Chemistry* **98**, 8442-8452 (1994).
- [27] Smit, B. & Siepmann, J. I. Simulating the adsorption of alkanes in zeolites. *Science* **264**, 1118-1120 (1994).
- [28] Vlugt, T. J. H., Martin, M. G., Smit, B., Siepmann, J. I. & Krishna, R. Improving the efficiency of the configurational-bias Monte Carlo algorithm. *Molecular Physics* **94**, 727-733 (1998).
- [29] Maginn, E. J., Bell, A. T. & Theodorou, D. N. Sorption thermodynamics, siting, and conformation of long N-alkanes in silicalite as predicted by configurational-bias Monte-Carlo integration. *Journal of Physical Chemistry* **99**, 2057-2079 (1995).
- [30] Woodley, S. M., Catlow, C. R. A., Battle, P. D. & Gale, J. D. The prediction of inorganic crystal framework structures using excluded regions within a genetic algorithm approach. *Chemical Communications* 22-23 (2004).
- [31] Klinowski, J. Hypothetical molecular sieve frameworks. *Current Opinion in Solid State & Materials Science* **3**, 79-85 (1998).
- [32] Boronat, M., Zicovich-Wilson, C. M., Viruela, P. & Corma, A. Cluster and periodic calculations of the ethene protonation reaction catalyzed by theta-1 zeolite: Influence of method, model size, and structural constraints. *Chemistry A European Journal* **7**, 1295-1303 (2001).
- [33] Sauer J., Sierka, M. Combining quantum mechanics and interatomic potential functions in ab initio studies of extended systems. *Journal of Computational Chemistry* **21**, 1470-1493 (2000).
- [34] Sastre G., Catlow, C. R. A. & Corma, A. Diffusion of benzene and propylene in MCM-22 zeolite. A molecular dynamics study. *Journal of Physical Chemistry B* **109**, 5187-5196 (1999).
- [35] Dager-Osguthorpe, P., Roberts, V. A., Osguthorpe, D. J., Wolff, J., Genest, M. & Hagler, A. T. Structure and energetics of ligand-binding to proteins-escherichia-coli dihydrofolate reductase trimethoprim, A drug-receptor system. *Proteins: Structure, Functions, and Genetics* **4**, 31-47 (1988).
- [36] Sanders, M. J., Leslie, M. & Catlow, C. R. A. Interatomic potentials for SiO₂. *Journal of the Chemical Society, Chemical Communications* 1271-1273 (1984).
- [37] Jackson, R. A. & Catlow, C. R. A. Computer Simulation Studies of Zeolite Structure *Molecular Simulation* **1**, 207-224 (1988).

- [38] Henson, N. J., Cheetham, A. K. & Gale, J. D. Theoretical calculations on silica frameworks and their correlation with experiment. *Chemistry of Materials* **6**, 1647-1650 (1994).
- [39] Henson, N. J., Cheetham, A. K. & Gale, J. D. Computational studies of aluminum phosphate polymorphs. *Chemistry of Materials* **8**, 664-670 (1996).
- [40] Kiselev, A. V., Lopatkin, A. A. & Shulga, A. A. Molecular statistical calculation of gas-adsorption by silicalite. *Zeolites* **5**, 261-267 (1985).
- [41] Oie, T., Maggiora, T. M., Christoffersen, R. E. & Duchamp, D. J. Development of a flexible intramolecular and intermolecular empirical potential function for large molecular-systems. *International Journal of Quantum Chemistry, Quantum Biology Symposium* **8**, 1-47 (1981).
- [42] Combariza, A.F., Sastre, G. & Corma, A. Molecular Dynamics Simulations of the Diffusion of Small Chain Hydrocarbons in 8-Ring Zeolites. *Journal of Physical Chemistry C* **115**, 875-884 (2011).
- [43] Sastre, G., Cantin, A., Diaz-Cabanas, M. J. & Corma, A. Searching organic structure directing agents for the synthesis of specific zeolitic structures: an experimentally tested computational study. *Chemistry of Materials* **17**, 545-552 (2005).
- [44] Sastre, G., Leiva, S., Sabater, M. J., Gimenez, I., Rey, F., Valencia, S. & Corma, A. Computational and experimental approach to the role of structure-directing agents in the synthesis of zeolites: The case of cyclohexyl alkyl pyrrolidinium salts in the synthesis of beta, EU-1, ZSM-11, and ZSM-12 zeolites. *Journal of Physical Chemistry B* **107**, 5432-5440 (2003).
- [45] Rappe, A. K. & Goddard, W. A. Charge equilibration for molecular dynamics simulations. *Journal of Physical Chemistry* **95**, 3358-3363 (1991).
- [46] Gale, J. D. GULP: A computer program for the symmetry-adapted simulation of solids. *Journal of the Chemical Society, Faraday Transactions* **93**, 629-637 (1997).
- [47] Forcite and Discover modules, Material Studio, version 5.5. Accelrys Inc. San Diego, CA, 2008.
- [48] Smith, W. & Forester, T. R. DL_POLY_2.0: A general-purpose parallel molecular dynamics simulation package. *Journal of Molecular Graphics* **14**, 136-141 (1996).
- [49] Dovesi, R., Saunders, V.R., Roetti, C., Orlando, R., Zicovich-Wilson, C.M., Pascale, F., Civalieri, B., Doll, K., Harrison, N. M., Bush, I. J., D'Arco, Ph. & Llunell, M. CRYSTAL06. University of Torino, Torino, 2006.
- [50] Segall, M. D., Lindan, P. L. D., Probert, M. J., Pickard, C. J., Hasnip, P. J., Clark, S. J. & Payne, M. C. Structure Resolution of Ba₅Al₃F₁₉ and Investigation of Fluorine Ion Dynamics by Synchrotron Powder Diffraction, Variable-Temperature Solid-State NMR, and Quantum Computations. *Journal of Physics: Condensed Matter* **14**, 2717-2744 (2002).

- [51] Delley, B. An all-electron numerical-method for solving the local density functional for polyatomic molecules. *Journal of Chemical Physics* **92**, 508-517 (1990).
- [52] Material Studio, version 5.5. Accelrys Inc. San Diego, CA, 2008.
- [53] Shannon, M. D., Casci, J. C., Cox, P. A. & Andrews, A. Structure of the 2-dimensioal medium-pore high-silica zeolite Nu-87. *Nature* **353**, 417-420 (1991).
- [54] Henson, N. J., Cheetham, A. K. & Gale, J. D. Theoretical calculations on silica frameworks and their correlation with experiment. *Chemistry of Materials* **6**, 1647-1650 (1994).
- [55] Ruiz-Salvador, A. R., Gomez, A., Lewis, D. W., Rodriguez-Fuentes, G. & Montero, L. Silicon-aluminium distribution in dehydrated calcium heulandite. *Physical Chemistry Chemical Physics* **1**, 1679-1685 (1999).
- [56] Grau-Crespo, R., Hamad, S., Catlow, C. R. A. & de Leeuw, N. H. Symmetry-adapted configurational modelling of fractional site occupancy in solids. *Journal of Physics-Condensed Matter* **19**, ArtN 256201 (2007).
- [57] Sastre, G., Lewis, D. W. & Catlow, C. R. A. Modeling of silicon substitution in SAPO-5 and SAPO-34 molecular sieves. *Journal of Physical Chemistry B* **101**, 5249-5262 (1997).
- [58] Foster, M. D., Simperler, A., Bell, R. G., Friedrichs, O. D., Paz, F. A. A. & Klinowski, J. Chemically feasible hypothetical crystalline networks. *Nature Materials* **3**, 234-238 (2004).
- [59] Zwijnenburg, M. A. Bromley, S. T., Jansen, J. C. & Maschmeyer, T. Toward understanding the thermodynamic viability of zeolites and related frameworks through a simple topological model. *Chemistry of Materials* **16**, 3809-3820 (2004).
- [60] Brunner, G. O. & Meier, W. M. Framework density distribution of zeolite-type tetrahedral nets. *Nature* **337**, 146-147 (1989).
- [61] Nachtigallova, D., Nachtigall, P. & Sauer, J. Coordination of Cu⁺ and Cu²⁺ ions in ZSM-5 in the vicinity of two framework Al atoms. *Physical Chemistry Chemical Physics* **3**, 1552-1559 (2001).
- [62] Profeta, M., Mauri, F. & Pickard, C. J. Accurate first principles prediction of O¹⁷ NMR parameters in SiO₂: Assignment of the zeolite ferrierite spectrum. *Journal of the American Chemical Society* **125**, 541-548 (2003).
- [63] Lewis, D. W., Freeman, C. M. & Catlow, C. R. A. Predicting the templating ability of organic additives for the synthesis of microporous materials. *Journal of Physical Chemistry* **99**, 11194-11202 (1995).
- [64] Freeman, C. M., Catlow, C. R. A., Thomas, J. M. & Brode, S. Computing the location and energetics of organic-molecules in microporous adsorbents and catalysts-a hybrid approach applied to isomeric butenes in a model zeolite. *Chemical Physics Letters* **186**, 137-142 (1991).

- [65] Sastre, G., Cantin, A., Diaz-Cabañas, M. J. & Corma, A., Searching organic structure directing agents for the synthesis of specific zeolitic structures: an experimentally tested computational study. *Chemistry of Materials* **17**, 545-552 (2005).
- [66] Lewis, D. W., Willock, D. J., Catlow, C. R. A., Thomas, J. M. & Hutchings, G. J. De novo design of structure-directing agents for the synthesis of microporous solids. *Nature* **382**, 604-606 (1996).
- [67] Gómez-Hortigüela, L., Hamad, S., López-Arbeloa, F., Pinar, A. B., Pérez-Pariente, J. & Corà, F. Molecular insights into the self-aggregation of aromatic molecules in the synthesis of nanoporous aluminophosphates: a multilevel approach. *Journal of the American Chemical Society* **131**, 16509-16524 (2009).
- [68] Gómez-Hortigüela, L., Pinar, A. B., Corà, F. & Pérez-Pariente, J. Dopant-siting selectivity in nanoporous catalysts: control of proton accessibility in zeolite catalysts through the rational use of templates. *Chem. Comm.* **46**, 2073-2075 (2010).
- [69] Catlow, C. R. A., Coombes, D. S., Lewis, D. & Pereira, J. C. G. Computer modeling of nucleation, growth, and templating in hydrothermal synthesis. *Chemistry of Materials* **10**, 3249-3265 (1998).
- [70] Caratzoulas, S., Vlachos, D. G. & Tsapatsis, M. Molecular dynamics studies on the role of tetramethylammonium cations in the stability of the silica octamers $\text{Si}_8\text{O}_{20}^{8-}$ in solution. *Journal of Physical Chemistry B* **109**, 10429-10434 (2005).
- [71] Caratzoulas, S., Vlachos, D. G. & Tsapatsis, M. On the role of tetramethylammonium cation and effects of solvent dynamics on the stability of the cage-like silicates $\text{Si}_6\text{O}_{15}^{6-}$ and $\text{Si}_8\text{O}_{20}^{8-}$ in aqueous solution. A molecular dynamics study. *Journal of the American Chemical Society* **128**, 596-606 (2006).
- [72] Demontis, P., Suffritti, G. B., Fois, E. S. & Quartieri, S. Molecular Dynamics studies on zeolites. 6. Temperature-dependence of diffusion of methane in silicalite. *Journal of Physical Chemistry* **96**, 1482-1490 (1992).
- [73] Tuma C. & Sauer, J. Treating dispersion effects in extended systems by hybrid MP2 : DFT calculations - protonation of isobutene in zeolite ferrierite. *Physical Chemistry Chemical Physics* **8**, 3955-3965 (2006).
- [74] Haase, F., Sauer, J. & Hutter, J. Ab initio molecular dynamics simulation of methanol adsorbed in chabazite. *Chemical Physics Letters* **266**, 397-402 (1997).
- [75] Gómez-Hortigüela, L., Corà, F., Sankar, G., Zicovich-Wilson, C. M. & Catlow, C. R. A. Catalytic Reaction Mechanism of Mn-Doped Nanoporous Aluminophosphates for the Aerobic Oxidation of Hydrocarbons. *Chemistry A European Journal* **16**, 13638-13645 (2010).

Adsorption Properties of Zeolites

Philip A. BARRETT^{1*} and Neil A. STEPHENSON¹

¹*Praxair Inc., 175 East Park Drive, Tonawanda, New York 14150, USA*

Abstract

Commercial adsorbents types, application examples, manufacturing methods and modification means are outlined and discussed in the context of the success enjoyed by zeolites in commercial adsorbent applications. A large number of modification techniques have been developed and applied to create new zeolite adsorbents. As a result, a high degree of compositional variation has been realized within the comparatively small sub-set of commercially or naturally available structure types. This ability to alter composition has contributed to the current level of success enjoyed by zeolites in adsorption applications. Two case studies are provided to showcase the application of some of these modifications to develop advanced adsorbents in large volume for commercial deployment.

1. The Success of Zeolites in Commercial Adsorption Applications

The potential of zeolites to function as adsorbents in gas separation processes was one of their more easily recognizable features. A seminal paper by R.M. Barrer in 1938 confirmed the sorption of polar and non-polar molecules and the molecular sieving properties of these solids¹. Arguably, the next significant development on the road to development of commercial zeolite adsorbents came with the discovery of synthetic zeolites and importantly, convenient methods to produce them from common raw materials by Milton, Breck, Flanigen and others at Union Carbide in 1940's and 1950's². This pioneering work at Union Carbide opened up the pathway to obtaining zeolites in the large quantities required for commercial use. The next step was to scale-up these lab synthesis processes, learn how to shape these products into agglomerated forms and build manufacturing facilities where all of these unit operations (synthesis, forming, calcination/activation) can be conveniently performed in sequence³. With these manufacturing developments completed, the reigns were handed back to the academic and industrial communities to begin adding to, modifying and improving on these first-generation commercial zeolite adsorbents. Activity in this area has grown substantially since these humble beginnings in with millions of pounds of adsorbent produced annually across the globe. Processes across multiple and industries employ zeolite adsorbents today

with new applications emerging almost annually⁴. Reasons behind this continued success and the themes explored in this article include:

1. Sufficient structures have been commercialized at reasonable cost
2. The adsorption properties for a given zeolite type are readily tunable enabling different types of adsorption process (i.e. Pressure Swing Adsorption (PSA), Temperature Swing Adsorption (TSA), Vacuum Swing Adsorption (VSA))
 - a. For many of these structures, a range of $\text{SiO}_2/\text{Al}_2\text{O}_3$ ratios is available enabling a first level of adsorption property tuning
 - b. Convenient forms of materials modification including ion-exchange and impregnation are applicable and provide a second level of adsorption property tuning
3. Simple agglomeration techniques including extrusion and bead making processes work well, enabling easy deployment in packed-bed systems
4. All the main adsorbent bases are covered within the zeolite family, including physisorbents, chemisorbents and molecular sieves (kinetic separation)
5. Excellent structural stability, and tolerance to the “rough and tumble” of practical industrial applications (i.e. in process lifetimes > 10 years are common)
6. Toxicology, safe handling and disposal means are known

The success alluded to above encompasses a breadth concentration ranges of the adsorbate species themselves⁵. Purification and bulk separations are routinely performed at small (L/min of product) to very large (millions of scft/day) scales to serve critical market segments including medical, refining, power generation, steel and other heavy industry, as well as food and beverage, to name but a few⁶. Zeolites are effective in both liquid and gas phase separation processes and can manage streams containing both percent and even trace contaminant levels, offering potential to reduce these impurities to low ppb levels or better, if required. To build-up and support this level of accomplishment, a significant body of academic and industrial work has been established covering both microscopic and macroscopic levels of understanding. These developments include advanced simulation methods to model and engineer the full separation or purification process⁵, experimental methods to measure adsorption properties with high levels of precision⁷. In addition, many fundamental studies have been completed elucidating microscopic details such as the location and function of the adsorption sites, diffusion studies in all types of pore and structure, as well as recipes to make and modify adsorbent compositions and properties. This large bank of data and understanding has placed zeolite adsorbents in a very strong and sustainable

position and, as a result, when new applications are under development, zeolites are almost always selected amongst the first candidates for screening.

For all of these reasons, zeolites will continue to be successful in the commercial adsorption field and will not be easily displaced by, for instance, newer classes of porous solid. Instead, it is more likely that these new classes of adsorbent will supplement the zeolites in commercial use and/or find their own niche applications, where cost is less of a driver and their unique properties play. In the proceeding sections of this review, we will introduce the most commonly used zeolite adsorbents, and showcase some of their compositional and structural properties. Next, we will describe the basics of adsorbent manufacturing and in particular, bead forming and extrusion methods of agglomeration that are of special relevance to packed-bed adsorption processes. An understanding of the capabilities of adsorbent manufacturing at commercial scales is important, since investment in new capital equipment can be hard to justify. This means the most must be made of existing methods of adsorbent production, at least in the near term. Thereafter we will review several of the commonly employed modification strategies which have been developed to enhance zeolite separation performance using examples chosen from the literature to demonstrate the effects. Finally, we will conclude this chapter with two case studies to convey some key learning's that were enabling from the perspective of solving the problems required to meet the performance targets of their respective commercial applications.

2. Overview of Common Commercial Zeolite Adsorbents

Thanks to the devoted efforts of a great many zeolite chemists and mineralogists, upwards of a 100 different structure types are known today⁸. However, only a comparatively small fraction of these have been commercialized (Table 1). Even within this commercial subset of zeolites certain structures, especially zeolites A, X and Y, tend to dominate in terms of end users applications in the adsorption area⁹.

The data in Table 1 shows that both synthetic and natural structures are available. The natural structures are more limited, as expected in terms of available $\text{SiO}_2/\text{Al}_2\text{O}_3$ ratio and to some extent, in pore size range as well. Amongst the synthetic zeolites, there is more choice in both $\text{SiO}_2/\text{Al}_2\text{O}_3$, as well as pore size with so called small, medium and large pore structures and high, medium and low $\text{SiO}_2/\text{Al}_2\text{O}_3$ ratios varieties all being available. Amongst the reasons for the commercialization of these structures, in preference to other known zeolites, is ease of synthesis for the man-made materials, and availability and accessibility for the natural mined zeolites. The low $\text{SiO}_2/\text{Al}_2\text{O}_3$ zeolites A, X, Y, P and medium $\text{SiO}_2/\text{Al}_2\text{O}_3$ zeolite L, mordenite and synthetic chabazite are produced from organic template free recipes, at comparatively low hydrothermal pressures and temperatures and importantly, short crystallization times¹⁰. Amongst the higher

SiO₂/Al₂O₃ zeolites, ZSM-5 and Beta are examples of the more readily attainable materials and have been produced from many different recipes and under a wide range of conditions ¹⁰. This is helpful to commercial producers who need to consistently manufacture pure products to well defined specifications and gives them options to control costs and scale-up these products.

Table 1. Commercial Zeolites and Their Basic Structural Properties.

Zeolite	IZA Code ⁸	SiO ₂ /Al ₂ O ₃	Pore Size Range (Å)	Use
A	LTA	2	3-5	Widespread
X	FAU	2-2.5	8	Widespread
Y	FAU	3-1000	8	Moderate
P	GIS	2	3	Widespread
Mordenite	MOR	12-200	6-7	Moderate
ZSM-5	MFI	25-1000	5-5.5	Moderate
Beta	BEA	25-200	5.5-6.5	Moderate
Zeolite L	LTL	6	7	Limited
Ferrierite	FER	18	4-5	Limited
Clinoptilolite*	HEU	5.5-11	Variable	Moderate
Chabazite**	CHA	2.8-4	3.5-4	Limited

*Natural zeolite-mined, **Natural and synthetic

Of the natural zeolites, clinoptilolite is the most widely available and often occurs together with chabazite deposits. Multiple regions of the world have significant natural zeolite resources and ~4 million tons are mined each year ^{11,12}. The wider availability of these two natural zeolites gives them a significant advantage, in terms of their application as adsorbents in commercial systems. As a word of caution, following the work of Ackley ¹², natural zeolites are not necessarily low cost options, since significant costs are incurred in making them useful for adsorption applications. At a minimum, there are transportation costs, washing and potentially ion-exchange treatments, to clean them up and adjust/homogenize the composition, in addition to particle sizing and thermal activation steps, to remove moisture and other removables prior to use. As a result, natural zeolites, as with any of the above commercial zeolites or prospective adsorbent candidates, should be selected based on their unique properties for the target separation and ranked on a price and performance basis.

Table 2. Important Industrial Adsorbents and Example Applications.

Zeolite Type	Commercial Products	SiO ₂ /Al ₂ O ₃	Cations	Application Examples
A	3A	2	K > 70%	EtOH Dehydration, Drying
	4A	2	Na > 99%	Desiccant, Medical O ₂ , other PSA, Natural Gas Processing
	5A	2	Ca > 70%	H ₂ PSA, Medical O ₂ , VPSA O ₂ , Natural Gas Processing
X	13X	2-2.5	> 99% Na	Air Prepurification
	LiX	2-2.5	> 88% Li	VPSA O ₂ , Medical O ₂
	AgX	2-2.5	> 80% Ag	CO, H ₂ abatement
	BaX		Ba, K	p-xylene recovery
	CaX	2.5-2.0	> 70% Ca	H ₂ PSA, N ₂ O removal, O ₂ VPSA
Y	NaY	3-5	>99% Na	Desulfurization, *HC Separation
	HY	20-1000	H ⁺	Desulfurization, HC Separation
Mordenite	Small/ Large Port	5	Na	Desulfurization, HC Separation
Clinoptilolite	TSM-140/ CS400	6	Mixed (Na, K, Ca, Mg)	N ₂ O Removal

*Where HC = Hydrocarbon

In Table 2, a summary of the typical commercial zeolite adsorbent products is presented, together with short descriptors of the chemical composition and example applications. A brief study of the information in Table 2 will quickly draw the readers' attention to the fact that the majority of the key adsorbents for the industrial gas business are essentially low silica zeolites, in general possessing SiO₂/Al₂O₃ ratios < 5. The higher SiO₂/Al₂O₃ zeolites, which are commonplace amongst industrial zeolite catalysts, have found niche applications in adsorption processes, with the focus being in hydrocarbon and/or desulfurization applications. In the commercially available low silica zeolite family, those belonging to the A and X types have the greatest number of currently available products. The primary differentiator between these different products is the type of extra-framework cation, and for the zeolite X family, the SiO₂/Al₂O₃ ratio. The use of ion-exchange techniques to alter the adsorption properties of these A and X, and to a lesser extent

zeolite Y adsorbents, has proven to be the most successful method of adsorbent modification, in current commercial use. A basic outline of commercial manufacturing methods is described in the next section and is important since, commercialization of new adsorbents rarely justify the redesign of existing manufacturing facilities and/or processes. As a result, a preferred approach is to work within the existing equipment limitations and/or use modification techniques, including ion-exchange methods, to fine tune the properties of an adsorbent.

3. Basics of Commercial Adsorbent Manufacturing

Commercial adsorbent manufacturing is itself an art and the challenges posed by the multi-step nature of the process have been solved in different ways by different suppliers. The basic steps however, tend to be common from supplier to supplier and represent the framework to work within, with respect to the production of new zeolite adsorbent compositions. A schematic of the basic manufacturing steps is provided in Figure 1. The goal in all of these subtly different manufacturing processes is the same, high quality products at high throughput with minimal yield losses. Nearly all adsorbent manufacturing processes begin with a zeolite synthesis stage. The purpose is to produce high purity zeolite powder, in a comparatively short timeframe, at good yield. In general, the low silica zeolites can be synthesized with ambient pressure synthesis reactors, whereas the higher $\text{SiO}_2/\text{Al}_2\text{O}_3$ structure types, including zeolite Beta and to some extent ZSM-5, require reactors capable of being operated to greater hydrothermal pressures. A number of commercial synthesis reactors are described in the patent literature, often differentiated by the means of delivering the heat required to effect crystallization, as well as the means of agitation which can be critical to the product purity.

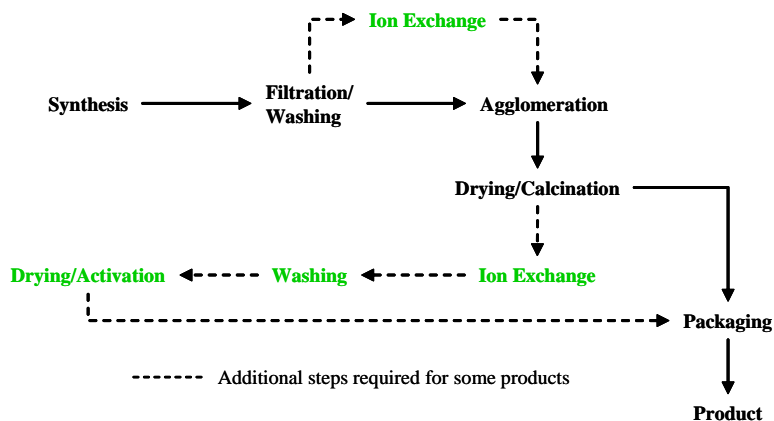


Figure 1. Principle Steps in Adsorption Manufacturing Processes.

After synthesis, the zeolite powder must be washed free of any synthesis residues dried until friable and harvested for the agglomeration stages. In some manufacturing processes, ion-exchange and/or other modifications are performed on the zeolite powder directly, prior to agglomeration. This is especially convenient for products that do not require very high levels of ion-exchange (i.e. 50-70%) and wherein the modification is facile (i.e. favorable ion-exchange isotherm) and non-hazardous.

The next key portion of the manufacturing processes (see Figure 1) is agglomeration. There are multiple agglomeration methods in commercial use, with the most common methods being extrusion and bead-forming. In both of these processes, a mixing step is usually performed upfront with the goal of adding additional components including a binding agent, whose function is essentially to act as a “glue” and impart strength to the final product, and any required processing additives (e.g. extrusion aids). In the case of extrusion, the product from the mixing stage is usually a wet paste, which is then fed to an extruder and shaped into rod-like particles by being forced mechanically through a die of a given size. Commonly, the abrasive nature of zeolite powders makes this process difficult without the use of extrusion aids to add the required plasticity and therefore enable them to be passed through the die with sufficient ease. Common dies have holes at 1/8th or 1/16th inches which sets the particle diameter. The length of the extrudates can be controlled by natural breakage or often by the use of a chopper, affixed to the outlet of the extruder, which is set to rotate at a selected speed and thus produce extrudates of a controlled length.

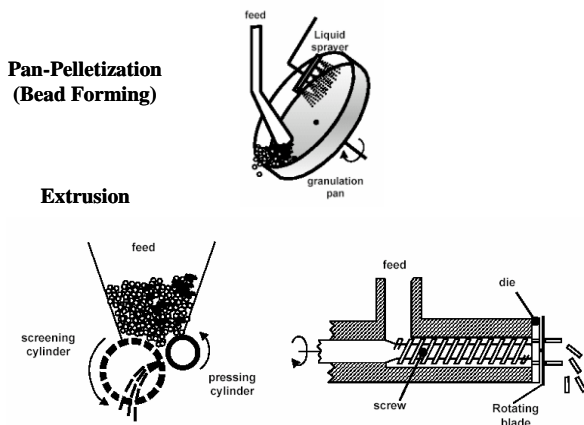


Figure 2. Common Apparatus for Zeolite Agglomeration.

Bead forming processes, on the other hand, rely on rotational motion, and snow-ball like growth, to form products with a high degree of sphericity. Typical pieces of equipment for bead-forming include pan-granulators, where a rotating inclined pan is used to shape and round the products, as well as mixing methods, such as Nauta forming wherein, rotational motion is applied in two axes and the use of a conical shaped bowl all help produce spherical particles. The number of forming methods is quite extensive and interested parties are encouraged to read a review article by Pfenninger⁹. The goal of any of these agglomeration methods is to produce particles of a target size range with acceptable yields and throughput. Another requirement is that the newly agglomerated zeolite particles possess enough intrinsic strength to survive the solids handling, typically required to convey them to the next stage of processing namely drying and calcination.

The drying and calcination step for some products is the final step in the manufacturing process. In this phase of production, the now agglomerated zeolite particles are subjected to a steadily increasing temperature regime, so as to remove any removable components including moisture, as well as thermally set the binding agent. For the majority of the products in Table 2, clay binding agents are employed^{3,9}. The aluminosilicate nature of common clays, as well as their high density of surface hydroxyls, makes them very compatible with zeolites and capable of producing final products which have acceptable physical strength characteristics (typically represented by crush strength and attrition values). Good particle strengths are required to permit adsorption vessels to be loaded and in service lifetimes upwards of 10 years to be realistically achieved. The term binder setting is used to mean the chemical fusing of the binder with the zeolite crystallites and/or other binder particles, so as to form a “bonded” network, which both encapsulates the zeolite crystallites (low attrition) and prevents the particle from being easily broken by impact. The binder setting chemistry typically requires temperatures > 600°C which often run close to the thermal stability limits of the zeolites themselves. This is one reason that the drying and calcination step is a very critical step in the manufacturing process^{13,14}. The keys to success are careful temperature ramping and control, as well as the provision of adequate amounts of a suitable purge gas, whose function is to sweep away moisture and other removables continuously, so as to avoid the creation of hydrothermal conditions which can damage the zeolite structure and render it less effective in the target application. The goal of the drying and calcination step is to make physically strong products and lower the residual moisture content to levels of 1 wt% or less, to open up and access the micropores (internal surface area) and adsorption sites (see below), without doing excessive damage to the zeolite thermally, hydrothermally or otherwise.

4. Common Modification Methods

Given the often limited range of compositions available from basic synthesis, it is not unusual to see this basic manufacturing process augmented with additional steps, with the usual goal of making compositional changes to the as-synthesized zeolite. In Table 3, a summary of the common techniques available for adsorbent modification is presented together with some examples and descriptors regarding the typical outcome of applying a given method. In terms of current commercial adsorbents, arguably the most important modification methods used are ion-exchange, altering the $\text{SiO}_2/\text{Al}_2\text{O}_3$ ratio of the framework by synthesis or by post-synthesis modification and forming binderless adsorbents by caustic digestion treatments on agglomerated particles. Impregnation methods have found some utility as well but, typically for adsorbent compositions for specific niche applications. The modification methods are described in more detail in sections 4.1-4.7.

Table 3. Common Modification Methods Applied to Zeolite Adsorbents

Modification	Chemical Impact	Adsorption Impact	Example
Ion-exchange	Non-Framework Composition	Equilibrium Isotherms and Zeolite Pore Size	LiX, CaX, & 3A, 4A, 5A
$\text{SiO}_2/\text{Al}_2\text{O}_3$ by Synthesis	Framework Composition	Equilibrium Isotherms	NaX2.5, NaX2.3, NaX2.0
Impregnation	Non-Framework Composition	Equilibrium Isotherms and zeolite pore size	Cu(I)Y CO Adsorbent
Dealumination	Framework Composition	Equilibrium Isotherms	High Silica Low Polarity Adsorbents
Desilication	Framework Composition	Equilibrium Isotherms	Mesoporous Zeolites
Alumination/ Zincation	Framework Composition	Equilibrium Isotherms	Increasing Adsorbent Polarity
Framework Substitution	Framework Composition	Equilibrium Isotherms	Ge, Ga Insertion
Binder Conversion	Macropore/ Mesopore	Adsorption Kinetics & Equilibrium Capacity	Binderless X and A Zeolites

4.1 Ion-exchange

One of the most successful methods of compositional adjustment is the use of ion-exchange to completely or partially replace the cation(s) from synthesis, with others which have been selected to fit the application. This method has been widely adopted industrially, largely in part due to the comparative simplicity of ion-exchange processes¹⁵. Direct liquid contact with a salt solution containing the new cation is all that is necessary to achieve some degree of ion-exchange. Often, the cations present for the negative framework charge compensation, are the strongest adsorption sites (centers of highest charge density). Therefore, ion-exchanging one type of cation with another serves to adjust the number, position and type of adsorption sites present in the zeolite and has a great impact on the adsorption properties, as a result. In a practical sense, ion-exchange can be carried out on either powders or agglomerated particles, which offers some flexibility to adsorbent manufacturers to find an optimum for their processes and equipment. An example of the profound effect on the adsorption properties of different cations, is given in Figure 3 wherein isotherms of N₂ at 27°C are plotted for the Na, Ca and Li form of zeolite X. In each of these cases, the degree of ion-exchange is > 99% by chemical analysis and the SiO₂/Al₂O₃ ratio is the same in each case. It is clear from Figure 3 that NaX has the lowest affinity for N₂ adsorption of the three materials with the Li and Ca forms clearly adsorbing more N₂ at equivalent pressure. This is understood by the higher mass-to-charge ratio of Li and Ca which leads to a stronger interaction with the N₂ quadrupole moment^{16,17}.

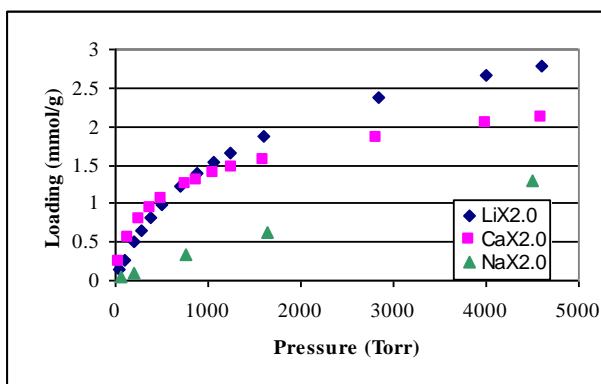


Figure 3. Adsorption Isotherms at 27°C for Na, Li and Ca forms of Zeolite X.

Adjustment of cation type to influence the uptake of one gas over another (often denoted by the term selectivity) has been successfully applied to bulk phase separations, as well as purifications. Ion-exchange methods are used to prepare LiX, CaX and CaA adsorbents for air separation and/or H₂ recovery by pressure

swing adsorption¹⁸. Mixed ion-exchange adsorbents including rare-earth and Li cation blends have also been prepared by ion-exchange and proposed by others for air separation applications, in particular¹⁹.

The preceding examples made use of ion-exchange methods to alter the equilibrium adsorption properties of a given zeolite. However, ion-exchange techniques can also be used to adjust the pore sizes and create or enhance molecular sieving properties. The most well-known and industrially relevant example of the use of ion-exchange to tune the zeolite micropore size is the 3A, 4A and 5A series of adsorbents. From direct synthesis, the Na form is obtained having a pore size of $\sim 4\text{\AA}$ (hence, the designator 4A). Ion-exchanging the as-synthesized form with at least 50-70% K, creates a pore size closer to $\sim 3\text{\AA}$. Alternatively, replacing the Na cations in the 4A by 50-70% Ca provides a pore size $\sim 5\text{\AA}$. In these examples, a combination of the cationic radii and cation position is responsible for the effective micropore size. In the as-synthesized and dehydrated 4A, Na cations reside in 2 primary positions, on the 6 membered rings (6MR) of the Sodalite cages, around the periphery of the main cage, as well as singularly occupying one of the 8MR windows leading into the supercage. The position of the sodium and its cationic radii lead to an effective pore size of $\sim 4\text{\AA}$. Introducing 50-70% K by ion-exchange, leads to primary replacement of the Na cations in the 8MR. The larger cationic radii of the potassium effects a reduction of the pore size to $\sim 3\text{\AA}$. The ion-exchange of Ca^{2+} for Na^+ functions a little differently. The preferred position of the Ca is found to be the 6MR of the Sodalite cages and the higher valence of the Ca, leads to 8MR windows which are cation-free and thereby enable the full 8MR pore size of $\sim 5\text{\AA}$, in the zeolite 5A case. This zeolite A example teaches an important lesson with regard to the need to understand both the crystal structure of the adsorbents, as well as the position and site preference of the different cations. As taught in the LiX case study (see section 5.1), the newly exchanged cations may take unwanted positions in the structure, as opposed to favorable positions where positive changes to the adsorption properties can be realized.

4.2 Impregnation

Impregnation is routinely used to prepare catalyst compositions, including zeolite catalysts, but in the zeolite adsorption area it is not as widely employed as a mainstream method for adsorbent modification. That said, there are some encouraging examples of adsorbent compositions whereby impregnations methods have been successfully utilized to increase the working capacity and in particular, to increase or change the selectivity from one component to another. In carbonaceous adsorbents, as well as silica gels and aluminas, impregnation is quite commonly used to tune the adsorption properties. For example, Chao et al²⁰ impregnate activated carbon adsorbents with dispersed halide salts to increase their selectivity for removal of Hg compounds present in flue gas and Prichett et al²¹ teach base

modified aluminas for enhancing the CO₂ and water removal capacity over untreated aluminas for air pre-purification. A zeolite example that highlights the power of impregnation to alter the adsorption properties is the impregnation of zeolite Y by CuCl, reported by Xie et al²². In this work, the authors show that zeolite NaY prior to impregnation is selective for CO₂ over CO. After impregnation with a near monolayer of Cu(I) salt, the selectivity is now reversed in favor of CO. This copper salt impregnated zeolite Y has been successfully used in commercial scale plants to recover CO at purities above 99% from syngas streams²². Impregnated zeolite adsorbents have been proposed for nuclear remediation applications to selectively capture radioactive Cs from liquid wastes²³, as well as removal of sulfur compounds, especially from transportation fuels and sources²⁴.

Another use of impregnation, which is quite distinct from the above examples, is pore size modification to create new specific molecular sieves for size-based separations. Examples, in the open literature of increased CO₂/CH₄ and H₂/CH₄ selectivities from pore-mouth modified ZSM-5 and other zeolites, suggest that this may be a viable modification method for size-based separations²⁵.

4.3 Dealumination/Desilication

Dealumination, like impregnation has been routinely used to modify zeolite catalyst compositions. A large number of dealumination agents and methods have been proposed in the literature^{10,26}, all having the effect of changing the SiO₂/Al₂O₃ ratio of the framework, as well as influencing the zeolite acidity, channel surfaces, and even the pore sizes. Given the correspondence of the equilibrium adsorption properties of an adsorbent with the chemical, structural and electronic properties of the adsorbent surface, a modification such as dealumination will naturally alter the properties of the product versus the as-synthesized parent form. The impact as taught by Stach et al²⁷ for adsorption of hydrocarbons on dealuminated zeolites X and Y is lower heats of adsorption due to a reduction in the energetic heterogeneity of the adsorbent. Similar conclusions of lower adsorption strength and surface heterogeneity of dealuminated zeolites have been reported for water and other vapors. Hence, as a strategy to decrease the adsorbent polarizability and/or increase the adsorbent hydrophobicity, dealumination is a tried and tested method. In terms of industrial practice, the authors are not aware of any large-scale adsorption applications using dealuminated zeolites, at the present time.

Desilication refers to the selective removal of Si from the zeolite lattice. Given the wide number of different reagents and pretreatment conditions that have successfully removed Al from the zeolite lattice, it is easy to imagine the Si species are harder to selectively remove. However, a number of reports teach the selective removal of framework Si using base solutions. Reports of successful desilication of zeolites A, X and ZSM-5 are published by several groups²⁸. The interest from the

standpoint of adsorption applications is the relatively new reports of the generation of intracrystalline mesoporosity in zeolites by desilication post-synthesis treatments. The same authors show the benefit of enhanced uptake kinetics of large hydrocarbon species in desilicated ZSM-5, versus the un-modified parent material²⁹. The use of desilication has also been advocated as part of a strategy to prepare zeolites with hierarchical pore structures, which offer the benefit of reduced micropore mass transfer limitations. In most common gas separations, the main transport resistances are macropore limitations in agglomerated adsorbent particles³⁰. But, in micropore limited separations such as water softening, adding some mesoporosity to shorten the effective transport length is, in principle, a good strategy to improve the separation efficiency. That said, the commercial impact of internal mesoporosity generation to adsorption applications remains to be determined and quantified.

4.4 Framework SiO₂/Al₂O₃ Ratio

A commercially successful method of adsorbent property modification is adjustment of the framework SiO₂/Al₂O₃ ratio by direct synthesis. This is commercially attractive since, the adjustment can be performed in a single step within the synthesis stage of the basic manufacturing scheme, and unlike dealumination or desilication does not necessarily add steps to the production process, or require new raw materials. Moreover, direct synthesis methods offer excellent control of the framework composition, as well as minimizing defect concentrations. Aggressive post-synthesis methods, such as dealumination, can leave behind connectivity defects which change the adsorption surface charge distribution and chemistry and therefore, impact the adsorption properties, as a result. The drawback of the direct synthesis approach is simply the limited range of SiO₂/Al₂O₃ ratios that are accessible, currently by known synthesis methods. The Faujasite zeolites X and Y are among those most commonly modified in this way. In fact, many commercial suppliers offer zeolite X products at three different SiO₂/Al₂O₃ ratios namely 2.5, 2.3 and 2.0. These different SiO₂/Al₂O₃ products are made by direct synthesis using different synthesis recipes in each case. In adsorption terms, the significance of these changes to the zeolite X SiO₂/Al₂O₃ ratio is the change in number of the extra-framework cations, particularly those accessible to the gas molecules which act as primary adsorption sites within the structure. An example of the impact of changing the SiO₂/Al₂O₃ ratio from 2.5 to 2.0 for Li ion-exchanged zeolite X, at similar Li ion-exchange levels is shown in Figure 4. It is evident that the N₂ capacity is increased by decreasing the SiO₂/Al₂O₃ ratio of the zeolite X.

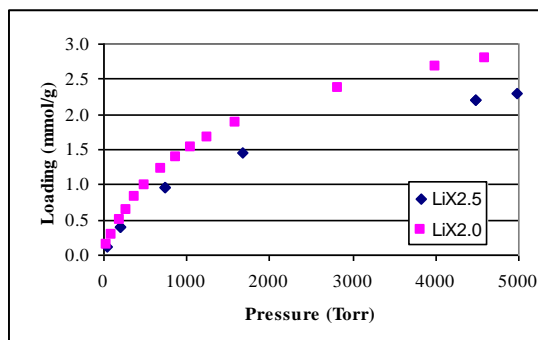


Figure 4. Adsorption Isotherms at 27°C for Li ion-exchanged X2.5 and X2.0.

Commercially, changes to the $\text{SiO}_2/\text{Al}_2\text{O}_3$ ratio have also been successfully applied to air prepurification processes to remove at least CO_2 from air streams using Na forms of zeolite X³¹, as well as purification of hydrogen using Ca ion-exchanged zeolite X adsorbents³², amongst others. A recent example of tuning the adsorption strength by modification of the framework $\text{SiO}_2/\text{Al}_2\text{O}_3$ ratio of zeolite A is provided by Palomino et al³³. They showed that the selectivity for CO_2/CH_4 separation is enhanced by decreasing the Al content of the zeolite A to alter the isotherm shape from near rectangular to more linear. This serves to increase the working capacity for CO_2 recovery under process relevant conditions. This concept is illustrated in Figure 5.

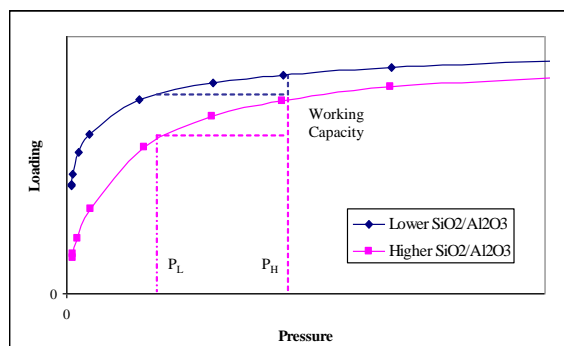
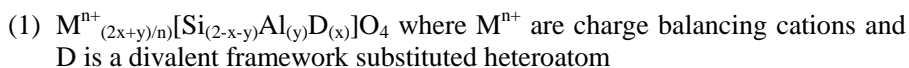


Figure 5. Concept of tuning isotherm shape to increase adsorption working capacity under process (adsorption-regeneration) conditions.

4.5 Framework Zincation/Alumination

Alumination post-synthesis treatments have been used to prepare adsorbents having elevated Al contents compared to their parent as synthesized forms. The main intent of alumination processes is to insert Al atoms into the zeolite framework to decrease the $\text{SiO}_2/\text{Al}_2\text{O}_3$ ratio beyond the ranges achieved by known synthesis methods. As with dealumination, a variety of post-synthesis treatments and reagents have been proposed for alumination reactions. Common reagents include AlCl_3 vapor and/or mild hydrothermal treatments with NaAlO_2 or KAlO_2 solutions. Adsorption data on aluminated zeolites is somewhat scarce. Kuznicki et al.³⁴ showed that alumination of a natural chabazite zeolite successfully decreased the $\text{SiO}_2/\text{Al}_2\text{O}_3$ ratio and increased the ion-exchange capacity supporting a successful post-modification. In our own work, we successfully aluminated a number of zeolites including offretite and chabazite but found that CO_2 and N_2 adsorption capacities were not increased, as a result of this modification. The interpretation was that any new cation sites generated by the alumination treatment were not accessible to the CO_2 or N_2 adsorbates³⁵. A number of authors have proposed mechanisms for alumination that involve hydroxyl nests and defects in the framework, suitable for insertion of the new framework Al species³⁶. If defect concentrations are important then alumination without formation of non-framework Al species may difficult to achieve practically and this could represent another reason for the low impact of this kind of modification on the adsorption properties of common zeolites.

As well as Al, other framework substitutions have been attempted, perhaps most notably using Zn (zincation). The premise of introducing a divalent heteroatom in place of tetravalent Si in the zeolite lattice is an enticing one from the perspective of generating additional adsorption sites by increasing the net negative charge on the adsorbent framework through substitution. This is evident through the generalized formula for this type of divalent framework substituted zeolites:



The interest among the adsorption community is to prepare a Zn containing adsorbent such that Lowenstein's rule is still obeyed and the number of extraframework cations is increased with respect to the pure aluminosilicate framework. Some progress towards this end was realized by MacDougall et al.³⁷, who reported successful incorporation of Zn by both post-synthesis and direct synthesis approaches. Adsorption studies with common gases were used to demonstrate that these Zn-containing zeolites had good adsorption properties. Since these disclosures, a number of studies including computational works³⁸ have supported the good stability of the Zn framework atoms. However, with current synthesis methods, only low levels of Zn substitution appear to be achievable which

is performance controlling. The difficulty to insert large amounts of Zn into the framework may be a consequence of the longer Zn-O bond and the additional lattice strain that is created. The benefit of attempting zincation or alumination remains in trying to create new low silica materials. These have been difficult to obtain in recent times, largely due to the absence of new synthesis pathways for stable frameworks with high net negative charge.

4.6 Framework Substitution (Synthesis)

Another class of modification methods reviewed herein from an adsorption standpoint, is compositional variations that are achievable primarily through, direct synthesis approaches. Although alumination and zincation methods described above impact the adsorbent framework composition, these modifications are most commonly applied to previously synthesized zeolite structures. However, successful incorporation of other heteroatoms, including gallium and germanium have been achieved by identifying suitable reagents and conditions and applying hydrothermal synthesis techniques. More recently, synthesis recipes have been developed that allow framework oxygen atoms to be replaced by bridging methylene groups³⁹, opening up further possibilities for framework compositional modification of adsorbents. In terms of adsorption however, these kinds of framework substitution have yet to reveal some unique properties that can justify their cost. Another issue is stability of the heteroatom structures and whether or not they are compatible with the adsorbent manufacturing processes described above, as well as the requirements of the application. To the best of our knowledge, there are no commercial adsorption processes using heteroatom substituted zeolites. The benefit they may yet bring is through their different bond lengths and angles which could in turn lead to new positions for the non-framework cations and/or new distributions for these cation sites, versus the aluminosilicate parent structure.

Another twist on the use of synthesis methods to add new components to a zeolite composition is the premise of occlusion or encapsulation. The goal here is to use synthesis techniques to selectively add components to fill specific areas of the zeolite structure. An example of this effect is provided by Johnson et al⁴⁰ who showed that phosphate occluded ZK-21 materials could be prepared by adding some phosphorus reagents to the synthesis gel. The products were characterized by MAS NMR techniques from which it was shown that phosphate species had been selectively incorporated into the Sodalite cages of ZK-21. The authors were able to demonstrate that the P-occluded ZK-21 structures had higher Henry's law selectivities for N₂/O₂ than the non-occluded reference sample. The enhancement of the adsorption properties reported in this study was attributed to a blocking effect and/or a redistribution of the framework charge. The main advantage of the use of this synthesis approach, over an impregnation method (see Section 3.2) is the high

specificity obtained for the location of the occluded species in a single preparation step.

4.7 Binderless Adsorbents

A tried and tested commercial adsorbent improvement strategy is to make binderfree adsorbent compositions. Section 3 highlighted that most adsorbents are deployed commercially in some agglomerated form with beads and pellets being the most common morphologies. During the bead and pellet making process, binding agents are employed to give some intrinsic strength to the final products. The most common binding agents are clays. The clays, themselves being aluminosilicate materials, are very compatible with the zeolite compositions and give products with high strength and manageable levels of attrition (dust caused by particle-particle or particle vessel contact). In typical adsorbent compositions, the binder content is around 12-20 wt% and has been shown to act as an inert with respect to the adsorption properties of the agglomerated zeolite. Therefore, as a consequence of the need for a binding agent, the effective zeolite content is reduced to 80-88%, depending on the binder amount, and therefore the equilibrium adsorption properties are decreased with respect to the 100% zeolite case.

Some types of clay can be post-converted into active zeolite adsorbent and as a result, the equilibrium adsorption capacity is enhanced relative to the binder containing version. The accepted method, to create a substantially binder-free adsorbent, is called caustic digestion and the most commonly used clay suitable for this binder conversion process is kaolin. In the generalized manufacturing process for binderless adsorbents, beads or pellets are formed and dried and calcined. The agglomerated zeolite particles are rehydrated and treated with strong caustic solutions (up to 6M) ⁴¹ under mild temperature conditions, during which time, the clay is essentially dissolved and recrystallized into new zeolite material. The treatment must be carefully controlled to avoid dissolution or damage to the original zeolite, as well as to control the type of new zeolite that is obtained from the clay conversion. Depending on the conditions, the kaolin based component can be converted to X or A zeolites. Usually, if the starting zeolite is type X, then target phase from the clay binder conversion process is also type X. There are a few specialty products where X/A composites are prepared using this caustic digestion process. The binder-free zeolite adsorbent, if well-prepared, will have a higher adsorption capacity than the clay containing version, as a consequence of the higher zeolite content. The drawback of binderless adsorbents is their higher cost, due to the additional manufacturing steps and raw material requirements. Another downside is that the strength properties of the binder-free adsorbent particles are sometimes diminished compared to the binder containing materials. Hence, for

applications where strong adsorbent particles are required, binderless materials may not be the right choice.

Another documented advantage of binderless adsorbents is enhanced adsorption kinetics. The importance of adsorption uptake and release rates is discussed in section 5.1 for the air separation application using Li ion-exchanged zeolite X. The caustic digestion-binder conversion process can lead to an improvement in the macropore structure of the agglomerated particles. Many gas separation processes, including air separation are known to be macropore rate limited, with the diffusion inside the zeolite micropores being orders of magnitude faster than within the macropores created by the stacking of the zeolite crystallites, inside the bead or pellet (Figure 6.). The caustic digestion process can alter the particle porosity characteristics of the agglomerated adsorbent and at the same time, improve the adsorption kinetics. This dissolution-recrystallization is proposed to reduce the quantity of undesirable pores⁴¹.

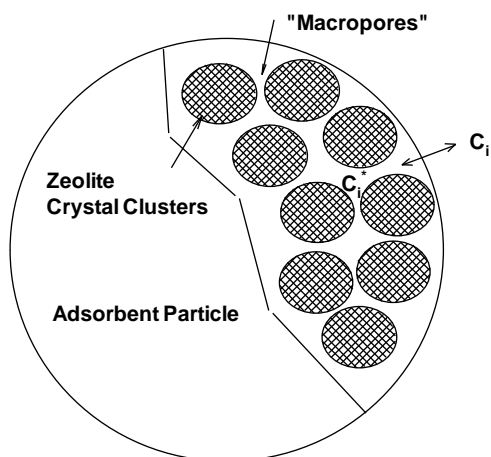


Figure 6. Anatomy of an adsorbent particle.

5 Case Studies

To bring this review to a close, two case studies of commercially successful adsorbent developments are presented to reiterate the themes of this article concerning the great flexibility of zeolites to meet the needs of both bulk separations and purifications. The bulk separation example is the development of high performance LiX adsorbents for vacuum pressure swing (VPSA) air separation. Secondly, selective removal of ppm levels of CO from an air stream using Ag-exchanged zeolite X is used to illustrate an adsorptive purification. In

these case studies, elements of adsorbent design and modification are reviewed together with the key learning's that contributed to their commercial success.

5.1 Case Study-Air Separation using Li-Exchanged Zeolite X

Adsorption technology for non-cryogenic air separation already has a rich history of development, since its early inception in the 1960's ⁴. A production niche was identified for adsorption technology to provide oxygen volumes in the neighborhood of 100 TPD at < 95% purity. The most commonly used process cycle is a vacuum pressure swing cycle where vessels containing adsorbent are cycled between a feed pressure around 1.5 bar and regenerated by vacuum. A two-bed system schematic is illustrated in Figure 7, although 1-bed systems are also practiced commercially.

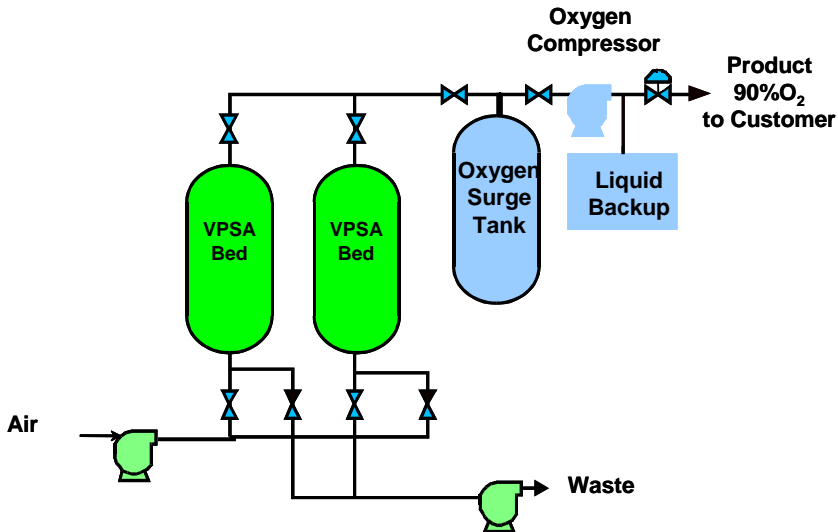


Figure 7. Schematic of 2-Bed VPSA O₂ system

In terms of the preferred adsorbent for air separation using VPSA technology, Li ion-exchanged zeolite X, is strongly preferred. The favorable isotherm characteristics of the LiX zeolite were recognized by Chao ⁴² who taught that effective adsorbents for this process need to have high N₂/O₂ selectivity and high N₂ working capacities, as measured under process relevant conditions (i.e. calculated at the feed and vacuum pressures expected in commercial systems). In the examples

and data presented in this seminal Chao disclosure ⁴², the impact of the %Li and the significance of the SiO₂/Al₂O₃ ratio of the zeolite X were taught. Firstly, regarding the impact of ion-exchange, a series of samples were prepared using the same base zeolite X (SiO₂/Al₂O₃ = 2.5) and the degree of Li exchange was varied between 0-100% and for each sample a single point N₂ loading was measured at 23°C and 700 Torr. The findings are reproduced in Figure 8, where it can be seen that there is a rapid change in equilibrium N₂ capacity for ion-exchange levels above ~80%. Lowering the SiO₂/Al₂O₃ ratio of the zeolite X framework further enhances the N₂ capacity and N₂/O₂ selectivity values calculated under practical pressures and temperatures. The best performing adsorbent was that having a SiO₂/Al₂O₃ ratio of 2 and a Li ion-exchange level of 99%.

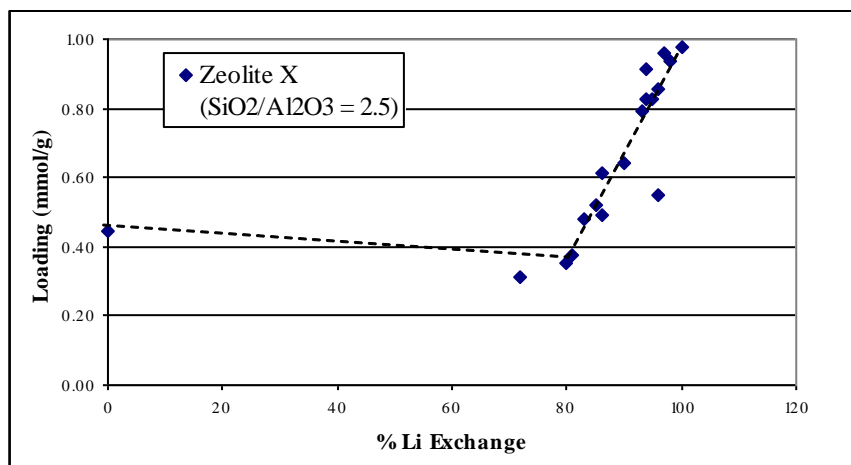


Figure 8. Trend of N₂ Capacity (700 Torr, 23 °C) with %Li in zeolite X2.5 ⁴²

These promising practical results for LiX adsorbents were enough to justify the development of manufacturing processes to produce them economically, in bulk for commercial deployment ^{9,43}. Meanwhile, this interesting trend of %Li versus N₂ loading was analyzed by various groups using characterization tools such as X-ray and neutron diffraction, ⁷Li MAS NMR ⁴⁴, and by carefully designed adsorption experiments. Molecular simulation techniques also played a role in elucidating structural information about the LiX adsorbent ⁴⁵. The net understanding gained from these and related studies has led to a detailed understanding of the role of Li cations in effecting this separation, as well as their specific location in the zeolite X

structure. The structural characterization of zeolite X ($\text{SiO}_2/\text{Al}_2\text{O}_3 = 2$) in its highly Li form (>99% Li), revealed 3 distinct positions for the Li cations in the dehydrated LiX zeolite (Figure 9). The adsorption data of Chao can be rationalized by the filling of these sites, and their respective preferences for the Li cations.

The zeolite X structure can be thought of conceptually as the stacking of Sodalite cages through a 6-ring, which creates a hexagonal prism and the well known zeolite X supercage⁸. The understanding we have gained showed that at low Li ion-exchange levels, the sites denoted SI' (top and bottom of hexagonal prism) are filled initially, together with the SII sites located on the faces of the 6-ring of the Sodalite cage. The final sites to be filled, as the %Li is increased towards 100%, are those denoted SIII/SIII' which are located within the zeolite X supercage and are associated with the 4-rings (SIII near the face of the 4-ring and SIII' denote a position near the edge of 2 distinct 4-rings).

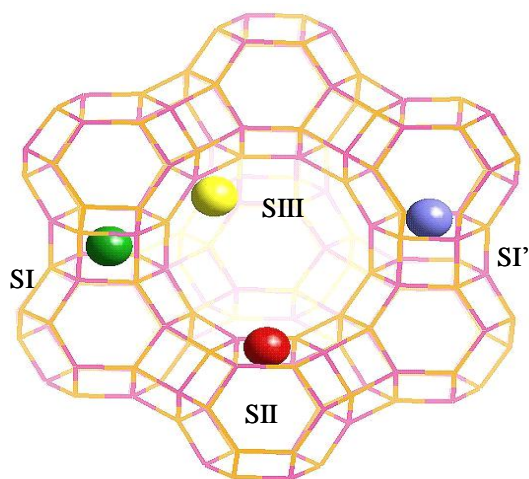


Figure 9. Cage-view of Zeolite X with cation sites marked.

From the structural chemistry work, it was clear that any Li cations on the SI' site buried deep inside the small zeolite X sub-cages, are not in a position to serve as adsorption sites. The SIII/SIII' positions are in the supercage and are the most under-coordinated sites and therefore likely to be primary sites for adsorption. Less obvious however, was whether or not the SII sites on the single 6-rings around the periphery of the main supercage are sufficiently exposed to contribute as secondary adsorption sites. Neutron diffraction studies had cast some doubt on the degree of exposure of these SII Li sites, showing them to be well solvated by the surrounding

framework oxygen atoms⁴⁴. However, this uncertainty was addressed by the use of O₂ and N₂ as probe gases in ⁷Li MAS NMR experiments, carried out by Lobo and co-workers⁴⁶, wherein it was shown that the signals from Li cations in the SI and SII positions did not change when exposed to O₂ and N₂ gases. On the other hand, the SIII lines moved significantly downfield due to the paramagnetism of the O₂ molecule, confirming that only the SIII/SIII' sites are actively participating in the O₂/N₂ separation. The excellent selectivity to N₂ from Li cations is understood as deriving from a combination of the favorable mass-to-charge ratio of Li over other group I cations, as well as the stronger quadrupole moment of N₂ versus O₂^{16,17,45}.

The first part of this case study on air separation using Li exchanged zeolite X has yielded some key learning with respect to adsorbent optimization and equilibrium adsorption performance enhancement:-

- SiO₂/Al₂O₃ ratio had significant impact on the adsorbent working capacity and selectivity for N₂/O₂
- The impact of %Li also needed to be understood and utilized in order to generate a higher number of Li cations in exposed positions
- Credible adsorbent manufacturing methods needed to be developed to manage the comparatively high cost of Li compared to other Group I and II cations
- Characterization tools played a role in understanding the position occupied by Li preferentially and the ability of these different sites to interact with the O₂ and N₂ feed gases

In this second part of this case study, the role of adsorption kinetics in dictating and improving the performance of VPSA air separation processes using LiX adsorbents having favorable SiO₂/Al₂O₃ ratios and %Li, is described. A common strategy employed by many segments of the chemicals industry to decrease costs is to intensify the process. A useful definition of process intensification is to reduce the size of a chemical (or other) plant needed to achieve a given production objective⁴⁷. In our terms, this means reducing the amount of adsorbent and sometimes the associated equipment size, in order to still produce the required amount of O₂ at the target purity of at least 90%. A common way to begin process intensification is to shorten the cycle time. However, without improving the adsorption kinetics, merely reducing cycle time decreases the amount of equilibrium zone in the adsorption bed with respect to the mass transfer zone, and therefore decreases the bed utilization (Figure 10). A preferred strategy is to try and preserve the ratio of equilibrium to mass transfer zone (L_{MTZ}/L_{Bed}) and thereby sustain the adsorption bed efficiency, at the now shorter cycle time. In order to achieve this, the size of

the mass transfer zone must be decreased (i.e. generate more equilibrium zone through faster adsorption kinetics).

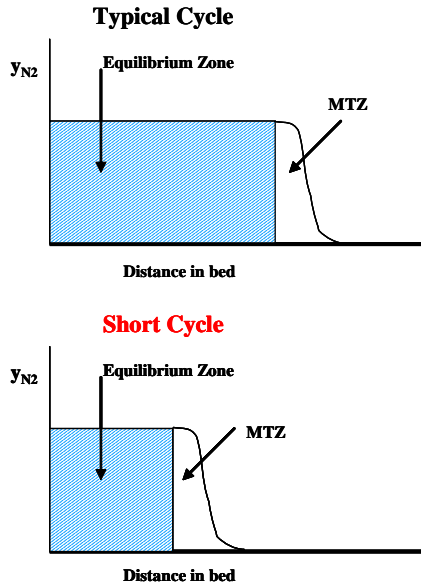


Figure 10. Effect of Shorter Cycle Time.

Since micropore and to some extent mesopore diffusion limitations, would be addressed in a different manner to low macropore diffusivities, a prerequisite to enhancing the kinetics of an adsorbent is understanding what are the controlling mass transfer resistances. A common manifestation of macropore diffusion limitations is that there is a significant influence of particle size of the beads or pellets used on the mass transfer coefficient of the process. This behavior is evident for VPSA air separation processes using LiX zeolite. In order to improve the mass transfer coefficient of the process, according to relation (2) there are three possibilities, increase the bead or pellet porosity, decrease the particle size and/or increase the macropore diffusivity. With the exception of macropore diffusivity, the other “handles” have drawbacks associated with them. In the case of increasing the particle porosity, the offsetting feature is increasing the void space in the bed, in which gas is stored but not separated. Decreasing the particle size has its problems as well, since smaller particles can lead to pressure drop issues, they are more easily fluidized and can be physically weaker (lower crush strength and attrition resistance

than larger particles) which can lead to low in-process lifetimes. The best and most challenging approach is enhancement of the macropore diffusivity.

$$k_i = \frac{15\varepsilon_p(1-\varepsilon_b)D_{pi}}{r_p^2} \quad (2)$$

(where K_i = Mass Transfer Coefficient, ε_p = particle porosity, ε_b = bed porosity, r_p = particle radii and D_{pi} = pore diffusivity)

The concept of improving the macropore diffusivity involves improving the pore architecture of the agglomerated adsorbent particle. Chao, for instance, describes the concept of a trunk and tributary system within the bead or pellet, which provides some level of organization and can thereby reduce the tortuosity and improve the macropore diffusivity⁴¹. One of the most compelling improvement pathways for enhancement of the adsorbent kinetics has been the implementation of the binder conversion technology (see Section 4.7). A number of authors have identified the presence of a binding agent as a cause of increased diffusion resistance. Hirano et al specifically call out the plate-like morphology of many clay binding agents, as being detrimental to gas diffusion into and out of the agglomerated adsorbent particle. The binder conversion process enhances the macropore diffusion by removing these “clay barriers” and generating in their place discrete growths of new zeolite material. As shown by Chao, the adsorbent compositions after binder conversion had both a larger mean pore diameter, as well as a higher adsorption rate⁴¹. These rate and porosity enhancements give some support to the “macropore cleaning” action of the caustic digestion treatment. The benefit of these rate enhanced adsorbents on the VPSA air separation process has been shown by Ackley to enable significant process intensification with worthwhile reductions in adsorbent bed size factor and appreciable improvements in O₂ recovery achieved³⁰. It is important to realize that the process efficiency improvements in air separation by VPSA technologies have come about through a combination of the equilibrium adsorption property improvements described in the first part of this case study, with the rate enhancements described in this section. Discoveries such as these have enabled adsorption based air separation technology to keep pace with developments in other areas including cryogenic systems and preserve their place in the commercial marketplace, ahead of these competing alternatives.

5.2 Case Study-Trace CO removal from air streams

In many industries and especially the electronics industry, ultra high purity gases are required with contaminant levels suppressed to low ppb levels. Adsorption technologies have proven to be effective in reducing ppm levels of common air contaminants, including CO and H₂, to these low ppb concentrations thereby enabling these stringent purity targets to be met. In this case study, we will describe how well-manufactured Ag exchanged zeolite X adsorbents can successfully remove CO present at concentrations of < 50 ppm from air streams and meet the purity requirements of the electronics industry¹⁴. Considering the properties of the CO molecule and including the moderately strong dipole and quadrupole moments relative to either the N₂ or O₂ matrix gases, it is tempting to think that this would be an easy separation, compared to the LiX air separation example described above, which relies on a small difference in quadrupole moments for N₂ and O₂. However, the main challenge in this trace purification example is provided by the overwhelming concentration difference between the CO at ppm levels and the air matrix. As a result of this extreme competition, a preferred approach to adsorbent selection and screening is to use experiments which include the competition effects arising from the co-adsorption of the matrix gases. On a lab scale, breakthrough style experiments are an appropriate means of carrying out these kinds of adsorbent evaluation^{4,14}. In a breakthrough test, an adsorbent bed is packed with agglomerated particles of the candidate material and is contacted with a feed gas which contains representative concentrations of the respective matrix and target contaminants, at pressures, temperature and flow rates chosen to reflect the conditions of the real process. At the outlet of the bed an analyzer, in this case for CO, monitors the exit concentration and enables a concentration versus time curve to be recorded. By analysis of these data, the adsorbent capacity and performance can be extracted. A good adsorbent is one which achieves at least the target CO removal requirements and sustains this for a long period of time (i.e., time to “breakthrough” is long).

In a first attempt to identify an adsorbent for this ppm level of CO removal from an air stream, conventional zeolites which are already used in air pre-purification processes, primarily for CO₂ removal, were investigated for their ability to remove CO. Breakthrough experiments were conducted with 2 ppm CO in air at a temperature and pressure of 283K and 100 psig, respectively, at a feed molar flux of 79 mol/m²-s. A zeolite 13X, effective for ppm CO₂ removal was chosen and tested under the above conditions with the result obtained showing immediate CO breakthrough. Other zeolites, including LiX, chabazite and clinoptilolite, all offered insufficient levels of CO removal. The approach taken next was to look for a modification means to supplement the basic physisorption characteristics of the above zeolites with some chemisorption specificity for CO. A number of reports on Cu, Ag and Au exchanged zeolites had evidenced the ability of these species to

form π -complexes with CO⁴⁸. The unknown was whether or not these π -complexes are sufficiently strong to selectively remove ppm levels of CO from the air stream under the pressure and temperature constraints of the purification process. Of the three cation types identified in the literature, Au was rejected for cost reasons and Cu was disfavored due to the difficulty to form the required Cu(I) species in high concentration and the likelihood of their reoxidation to Cu(II) under the temperature swing regeneration conditions of an air pre-purifier. Hence, breakthrough experiments were performed on Ag exchanged zeolite X with good results obtained from lab prepared samples. The measured breakthrough times were now in the order of hours not minutes, suggesting that the π -complexation was indeed helping to achieve greater CO working capacities, over and above the physisorbents tested previously.

Table 4. CO Working Capacities for Ag and non Ag exchanged adsorbents.

Adsorbent	Descriptor	¹ Tb @100 ppb CO (min)	² CO Working Capacity (mmol/g)
NaX2.5	Commercial Sample	Immediate	N/A
LiX2.0	Commercial Sample	<2	2.5× 10 ⁻⁵
Clinoptilolite	Commercial Sample	<2	1.4× 10 ⁻⁵
AgX2.5	Lab Sample	798	0.13
AgX2.5	Commercial Sample 1	330	0.051
AgX2.5	Commercial Sample 2	72	0.012
AgX2.5	Improved Drying	384	0.060
AgX2.5	Improved Washing	552	0.089
AgX2.5	Full Production Campaign	430	0.067

¹Tb = breakthrough time for 2ppm CO in synthetic air, P = 100 psig, 283K

²CO Working Capacity at 0.012 Torr¹⁴

Multiple samples of AgX were obtained from a commercial supplier and evaluated in our breakthrough test system. One of the clear conclusions from testing different lots of commercially produced material was the existence of significant variation in the CO working capacity from sample to sample (Breakthrough times to 100 ppb CO varied from 330 to 72 minutes). Such a large performance variation in commercially produced material is not necessarily uncommon, but from the

standpoint of designing an adsorption system, is not tolerable. Efforts were therefore placed on understanding the sources of manufacturing damage and providing suitable fixes. The quality of the basic zeolite X, to which the Ag is added by ion-exchange, was evaluated and found to be acceptable. The first avenue for improvement we explored was making improvements to the drying and calcination process. By installing a drier capable of reducing the dewpoint of the air used for the drying and calcination to less than -10°C and ensuring that an adequate amount of dry purge gas was used, a modest improvement in the CO working capacity was achieved. Next the Ag exchange and washing steps were evaluated and found to be another source of inconsistent performance. By taking commercial samples after the ion-exchange step and re-washing and re-activating them, a considerable improvement in performance was observed. A summary of the impact of these adsorbent and manufacturing improvements is given in Table 4. Finally, these manufacturing improvements were applied to a commercial production campaign with each lot of material produced having CO working capacities above the best original commercial sample prior to any manufacturing process enhancements. Whilst the performance is still below the lab made samples, the lot-to-lot consistency is now at least sufficient to design an adsorption process and have confidence that it will work to specification.

The key learning from this second case study is around the mechanics of providing a commercially viable solution to an adsorption problem or need:-

- Adsorbent screening with commercial products as a first step
- Turned to the open literature to identify paths forward
- Applied these “leads” to commercially available precursors
- Performance evaluations under process relevant conditions and with inclusion of co-adsorption effects
- Recognized manufacturing issues related to product consistency and worked to narrow the gap between lab and full production scale samples
- Established a consistent manufacturing method capable of acceptable performance minimums to enable an adsorption bed and process design

6.0 Conclusion

Zeolite pioneer Edith Flanigen concluded her review of the first twenty five years of molecular sieve technology with the comment that “the zeolite future looks bright”². It is very pleasing to be able to say that this is still the case today. In recent times, adsorbent developments have come more through modification of existing materials and less through commercialization of new structures. The number of modification methods continues to grow and provides the adsorption community with new tools

to adjust both equilibrium and rate properties and thereby obtain new high performance adsorbent compositions. Improvements can come by way of working capacity, working selectivity, as well as though enhanced adsorption kinetics. To guarantee commercial success, cost and manufacturability constraints must be recognized and adhered to at all times.

References

- [1] Barrer, R. M. The sorption of polar and non-polar gases by zeolites. *Proceedings of the Royal Society of London* **167**, 392-420 (1938).
- [2] Flanigen, E. M. Molecular sieve technology-the first twenty five years. *Pure & Applied Chemistry* **52**, 2191-2211 (1980).
- [3] Breck, D. W. Zeolite molecular sieves, *Wiley-Interscience, New York* **1**, 725-755 (1974).
- [4] Yang, R. T. Adsorbents: fundamentals and applications. *John Wiley & Sons*, **1**, 1-6 (2003).
- [5] Moscou, L. The zeolite scene. *Studies in Surface Science and Catalysis*, **58**, 1-12 (1991).
- [6] Kerry, F. G. Industrial gas handbook: gas separation and purification, *Taylor & Francis Group*, **1**, 273-287 (2007).
- [7] Webb, P. A. & Orr C, Analytical methods in fine particle technology, *Micromeritics Instrument Corporation*, **Ch. 3** 53-155 (1997).
- [8] Baerlocher, Ch. McCusker, L.B. & Olson D. H. Atlas of zeolite framework types, *Elsevier* **6th Ed.** (2007).
- [9] Pfenninger, A. Manufacture and use of zeolites for adsorption processes, in *Molecular sieves-science and technology*, *Springer*, **2**, 163-198 (1999).
- [10] Szostak, R. Fundamentals of synthesis in Molecular sieves, *Springer* **2nd Ed.** Ch. 4, 75-120 (1998).
- [11] Sand, L. B. & Mumpton, F. A. Natural zeolites occurrence, properties and use. *Pergamon Press* (1978).
- [12] Ackley, M. W. Rege, S. U. & Saxena, H. Application of natural zeolites in the purification and separation of gases. *Microporous and Mesoporous Materials*, **61**, 25-42, (2003).
- [13] Coe, C. G. & Kuznicki, S. M. Polyvalent ion exchanged adsorbent for air separation. U.S. Patent 4, 481, 018 (1984).
- [14] Ackley, M. W. & Barrett, P.A. Silver-exchanged zeolites and methods of manufacture therefor. U.S. Patent 7, 455, 718 (2008).
- [15] Townsend, R. P. & Harjula, R. Ion exchange in molecular sieves by conventional techniques. *Molecular sieves science and technology*, **3**, 1-42 (2002).

- [16] Shen, D. Bulow, M. Jale, S.R. Fitch, & F.R. Ojo, A. F. Thermodynamics of nitrogen and oxygen sorption on zeolites LiLSX and CaA. *Microporous & Mesoporous Materials*, **48**, 211-217 (2001).
- [17] Yoshida, S. Hirano, S. & Nakano, M. Nitrogen and oxygen adsorption properties of ion-exchanged LSX zeolite. *Kagaku Kogaku Ronbunshu*, **30**, 461-467 (2004).
- [18] Sircar, S. Application of gas separation by adsorption for the future. *Adsorption Science & Technology*, **19**, 347-366 (2001).
- [19] Bulow, M. Jale, S.R., Ojo, A.F. Fitch, & F.R. Shen, D. Sorption equilibria of nitrogen and oxygen on Li, Re-LSX zeolite for oxygen PVSA processes. *Studies in Surface Science & Technology*, **154**, 1961-1970 (2004).
- [20] Chao, C. & Pontonio, S.J., Catalytic adsorbents for mercury removal from flue gas and methods of manufacture therefor. U.S. Patent 0204418 (2006).
- [21] Prichett, D.A. Meikle, R.A. Golden, T.C. Kalbassi, M.A. Taylor, F.W. Raiswell, C. J. & Mogan, J. L. Co-formed base treated aluminas for water and CO₂ removal. U.S. Patent 0037702 (2007).
- [22] Xie, Y. Zhang, J. Qiu, J. Tong, X. Fu, J. Yang, G. Yan, H. & Tang, Y. Zeolites modified by CuCl for separating CO from gas mixtures containing CO₂. *Adsorption*, **3**, 27-32 (1996).
- [23] Motojima, K. Kawamura, F. Process for producing zeolite adsorbent for treating radioactive liquid waste with the zeolite adsorbent. U.S. Patent 4,448,711 (1984).
- [24] Velu, S. Ma, X & Song, C. Selective adsorption for removing sulfur from jet fuel over zeolite based adsorbents. *Industrial & Engineering Chemistry Research*, **42**, 5293-5304 (2003).
- [25] Jasra, R. V. Chintansinh, & D. Jince, S. Process for the preparation of a molecular sieve adsorbent for the size/shape selective separation of air. U.S. Patent 0192437 (2004).
- [26] Beyer. H.K. Dealumination techniques for zeolite. *Molecular Sieves Science & Technology*, **3**, 203-256 (2002).
- [27] Stach, H. Lohse, U. Thamm, H. & Schirmer, W. Adsorption equilibria of hydrocarbons on highly dealuminated zeolites. *Zeolites*, **6**, 74-90 (1986).
- [28] Groen, J. C. Peffer, L. A. A. Moulijn, & J. A. Perez-Ramirez, J. On the introduction of intracrystalline mesoporosity in zeolites upon desilication in alkaline medium. *Microporous & Mesoporous Materials*, **69**, 29-34 (2004).
- [29] Groen, J. C. Zhu, W. Brouwer, S. Huynink, S. J. Kapteijn, F. Moulijn, J. A. & Perez-Ramirez, Direct demonstration of enhanced diffusion in mesoporous ZSM-5 zeolite obtained via controlled desilication. *Journal of American Chemical Society*, **129**, 355-360 (2007).
- [30] Ackley, M. W. & Leavitt, F. W. Rate enhanced gas separation. U.S. Patent 6,500,234 (2002).

- [31] Ojo, A. F. Fitch, F. R. Bulow, M. Removal of carbon dioxide from gas streams. U.S. Patent 5,531,808 (1996)
- [32] Baksh, M. S. A. Ackley, M. W. Pressure swing adsorption process for the production of hydrogen. U.S. Patent 6,340, 382 (2002).
- [33] Palomino, M. Corma, A. Rey, F. & Valencia, S. New insights on CO₂-methane separation using LTA zeolites with different Si/Al ratios and a first comparison with MOFs. *Langmuir*, **26**, 1910-1917 (2010).
- [34] Kuznicki, S. M. & Whyte, J. R. Ion-exchange agent and use thereof in extracting metals from aqueous solutions. U.S. Patent 5,071,804 (1991).
- [35] Barrett, P.A. Huo, Q. & Stephenson, N. A. Recent advances in low silica zeolite synthesis. *Studies in Surface Science & Catalysis*, **170**, 250-257 (2007).
- [36] Wu, P. Komatsu, T. & Yashima, T. IR and MAS NMR studies on the incorporation of aluminium atoms into defect sites of dealuminated mordenite. *Journal of Physical Chemistry*, **99**, 10923-10931 (1995).
- [37] MacDougall, J.E. Braymer, T.A. & Coe, C. G. Zincoaluminosilicates of the FAU structure. U.S. Patent 6,136,069 (2000).
- [38] Shubin, A. A. Zhidomirov, G. M. Kanansky, V. B. & van Santen, R. A. DFT cluster modeling on molecular and dissociative hydrogen adsorption on Zn²⁺ ions displacing aluminium in the framework of high silica zeolites. *Catalysis Letters*, **90**, 137-142 (2003).
- [39] Su, B. L. Roussel, M. Vause, K. Yang, X. Y. Gilles, F. Shi, L. Leonova, E. Eden, M. & Zou, X. Organic group-bridged hybrid materials with a Faujasite X zeolite structure (ZOF-X). *Microporous & Mesoporous Materials*, **105**, 49-57 (2007).
- [40] Johnson, L. M. & Miller, M. M. P occlusion in LTA: an approach for enhancing N₂ adsorption properties. *Studies in Surface Science & Catalysis*, **135**, 1 (2001).
- [41] Chao, C. & Pontonio, S. J. Advanced adsorbent for PSA, U. S. Patent 6,425,940 (2002).
- [42] Chao, C. Process for separation nitrogen from mixtures thereof with less polar substances. U.S. Patent 4,859, 217 (1989).
- [43] Leavitt, F. W. Lithium recovery. U.S. Patent 5,451,383 (1995).
- [44] Feuerstein, M. & Lobo, R. F. Characterization of Li cations in zeolite LiX by solid state NMR spectroscopy and neutron diffraction. *Chemistry of Materials*, **10** 2197-2204 (1998).
- [45] Jale, S. R. Bulow, M. Fitch, F. R. Perelman, N. & Shen, D. Monte carlo simulation of sorption equilibria for nitrogen and oxygen on LiLSX zeolite. *Journal of Physical Chemistry B*, **104**, 5272-5280 (2000).

- [46] Feuerstein, M. Accardi, R. J. & Lobo, R. F. Adsorption of nitrogen and oxygen in the zeolites LiA and LiX investigated by ^6Li and ^7Li MAS NMR spectroscopy. *Journal of Physical Chemistry B*, **104** 10282-10287 (2000).
- [47] Reay, D. Ramshaw, C. & Harvey A. Process intensification: engineering for efficiency, sustainability and flexibility. *Butterworth-Heinemann*, **Ch. 2** 21-44, (2008).
- [48] Yang, R. T. Hernandez-Maldonado, A. J. & Yang, F. H. Desulfurization of transportation fuels with zeolites under ambient conditions. *Science*, **301**, 79-81 2003).

Basic concepts in zeolite acid-base catalysis

Johannes A. LERCHER and Andreas JENTYS

Technische Universität München, Department of Chemistry and Catalysis Research Center, Garching, 85748, Germany

Abstract

While the use of zeolites as catalysts makes up only for a smaller part of their overall utilization, crystalline molecular sieves constitute a very large fraction of solid catalysts used today. The lecture will attempt to outline the basic features that make zeolites attractive for large volume applications in refining and petrochemistry. The combination of the confines of the nanopores and the control of the nature and concentration of active sites allow realizing advanced catalytic reactions. While Brønsted acid sites are used for most of the large volume refining applications, also (redox active) Lewis acid sites have considerable importance for chemical transformations and emission clean up. The interaction of the nano pores with the reacting molecules allows to concentrate reactants and to promote reaction pathways also via entropic control. The narrow variation of the size of the zeolite channels allows for a particular material to control access, the transition state and the diffusion of products from the active sites inside the zeolite.

1. Introduction

The present contribution should not be seen as review, but rather as text accompanying the respective lecture in the post congress course. Much of the material has been presented in previous reviews from our group and has been rearranged and updated to reflect current opinions. Readers are referred to these papers¹⁻³ and the references within these reviews for a more comprehensive overview the topics covered.

Zeolites are widely used as solid catalysts or catalyst components in petroleum refining and chemical synthesis because their unique properties and the possibility to tailor the microporous material with respect to the concentration and nature of catalytically active sites and their immediate environment⁴⁻⁶. This includes controlling the access of molecules to the catalytically active sites⁷, a property usually associated only with enzymes. In turn, it has the inherent disadvantage that it restricts the size of molecules that can be reacted in molecular sieves and that the transport to these sites can become the rate limiting step. It should be mentioned at this point that molecules are claimed to be able to react at the pore entrance, when

being too bulky to enter⁸⁻¹⁰. As the density of pore entrances is strictly related to the size of the primary crystal, significant efforts have been undertaken to create a secondary pore structure in order to maximize the pore openings and to minimize also the time span a reacting molecule has to pass through a zeolite crystal^{11,12}. It has also been shown over the last 20 years that zeolites in a certain stage of crystallization can be delaminated into crystalline sheets^{13,14}. Such sheets can be arbitrarily stacked or pillared enhancing the space for molecules to react, while maintaining the well-defined crystalline environment of the catalytically active site. This allows stabilizing Brønsted acid sites in a more open environment, conceptually generating the access also for very large molecules.

While theoretically a very large number of structures is possible¹⁵, only few are currently applied in industry¹⁶. These structures include large pore materials such as faujasite, mordenite and zeolite Beta, medium pore zeolites such as ZSM-5 and MCM-22, as well as narrow-pore materials such as ferrierite and ZSM-22. In addition, zeolite structures in which transition metal cations such as Ti have been substituted for tetrahedral lattice atoms¹⁷ and microporous aluminum phosphate zeotypes¹⁸ are also used in large-scale. The reasons for this relatively low number are associated with cost factors in industrial synthesis and with the fact that most of the existing structures can be tuned in a way that they are highly suitable for required applications.

The popularity of the use of molecular sieves as key catalyst components has been caused by three unique properties of zeotype molecular sieves: (i) The high concentration of active sites in comparison with mixed oxides induced by the crystalline structure results in very active catalysts. (ii) The defined pore structure controls sorption of reactants and products and allows so preferring and excluding reactants from being converted and/or products to be formed or transported out of the pores exerting steric constraints (shape selectivity), i.e., to control reaction rates via transition entropy. (iii) The active site and the environment of that site can be designed on the atomic level for example by ion exchange or chemical functionalization of the framework.

The ability to have a higher concentration of active sites in zeolites compared to high surface area mixed oxides relates to the fact that in these latter oxides the surface terminating the bulk structure tends to reconstruct in a way that minimizes the exposure of active acid and base sites. In contrast, the pores of zeolites are part of the crystalline structure, in which active sites are generated by substituting tetrahedrally coordinated cations. Thus, the acid and base sites result from the charge imbalances of the framework atoms.

The well-defined pore size not only controls the concentration and thermodynamic state of sorbed molecules, but also the access to the pore system. The contributions of enthalpy and entropy in the sorbed state also determine the relative

concentrations of mixtures of reactants and products under reaction conditions. Local steric constraints allow influencing the strength of interaction between the substrate and the catalyst¹⁹ and open a way to adjust the surface chemical properties. Adding cations or functional groups within the zeolite pores opens the possibility to realize bifunctional catalysis exerting the action of two sites on one substrate molecule to be converted. While we are still witnessing only the beginning of such developments, the proximity of sites within zeolite pores is able to induce the activation of refractory molecules such as alkanes even at ambient temperature²⁰. This indicates that zeolite catalysis is subtly controlled by several factors. It is influenced by the specificity of the acid and base sites and their strengths of interaction with the reactants and products, determined by their acid and base strengths and in case of Lewis acid sites also their hardness. It is on the other hand also controlled by the access of the reactant to a particular site and the possibility to desorb the products, a property which is called transport controlled shape selectivity²¹. Finally, it is influenced by the constraints in the sorbed as well as in its transition state. This can cause deceleration by limiting bulky transition states²² as well as acceleration of reaction pathways by providing a large difference between the entropy in the ground state and in the transition state²³.

The advantage of zeolite catalysis is also accompanied by an inherent disadvantage. Catalytic chemistry inside a zeolite pore can be understood to occur in a microscopically small tubular reactor or a bundle of interlinked tubular reactors in which the active sites are distributed over the whole reactor. It is obvious that in such an environment it is difficult, if not impossible, to avoid sequential reactions of the same type.

In the present contribution, we will first describe the relation between the chemical composition as well as the structure of the zeolite and the nature and concentration of the catalytically active sites. This will be followed by outlining the way molecules interact with these active sites. The catalytic transformation of hydrocarbons and increasingly more basic molecules (alcohols and amines) on Brønsted acid sites will be at the core. Discussing the options and limitations of shape selectivity will complete the discussion on mechanisms in zeolite catalysis. While this is certainly a personal choice, it is hoped that it may serve as guideline, how to design and synthetically realize other zeolite catalyzed reactions.

2. Acid and base sites in zeolites

2.1 Nature and origin of strong Brønsted acid sites

Molecular sieves consist of a three-dimensional network of metal-oxygen tetrahedra (and to a lesser extent also octahedra) that provides a regularly sized micropore structure, in which the acid and base sites are structurally included^{24,25}. Acid sites

result from the imbalance between the metal and the oxygen formal charge in this smallest building unit. This is seen most clearly in the case of zeolites, which comprise of a three-dimensional network of Si-O tetrahedra. Formally, the 4+ charge on the Si cation and the 2- charge on the oxygen anion leads to neutral tetrahedra, as every oxygen belongs to two of such units. Thus, a framework consisting of only Si-O tetrahedra is neutral and may possess acid properties only through defects in such a structure. If a Si⁴⁺ cation is substituted by Al³⁺ the formal charge on that tetrahedron changes from neutral to -1. This negative charge is balanced by a metal cation or a proton forming a Lewis or a Brønsted acid site, respectively²⁶. Note that the bare, negatively charged tetrahedron constitutes the corresponding base. Depending upon the charge on the metal cation/proton and the oxygen, the acidic or basic properties of the molecular sieves will be dominating and consequently it will be called a solid acid or base²⁷.

The differences in the charge of these primary building units determine the concentration of the acid and base sites. Their strength depends primarily on the overall chemical composition of the framework, but more subtle factors such as the nature of the metal cations at exchange sites and the lattice type may also exert an influence^{28,29}. Especially for zeolites containing a high concentration of aluminum the nature of the exchangeable cation incorporated influences the polarizability and the effective charge of framework oxygen atoms. Thus, adjusting the combination of chemical composition, (partial) cation exchange and the molecular sieve structure can lead to a wide variety of chemical properties. Overall, the concentration of aluminum in the framework is directly proportional to the concentration of acid sites and the polarity of the framework and to a first approximation indirectly proportional to the strength of acid sites. For a given chemical composition of the zeolite, the polarity of the lattice increases with decreasing framework density³⁰. These relationships between the chemical composition, the crystal structure and the acid/base properties of molecular sieves have been studied extensively and were thoroughly reviewed³¹⁻³⁴.

2.2 Evidence for uniformity and distribution of acid sites in molecular sieves

The Brønsted acid sites of high silica zeolites such as ZSM-5 exhibit uniform acid strength and uniform catalytic activity. This has been unequivocally demonstrated for two acid catalyzed reactions, i.e., protolytic cracking and m-xylene isomerization. Haag *et al.*³⁵ demonstrated that the rate of n-hexane cracking is directly proportional to the concentration of aluminum in the framework (see Fig. 1). n-Hexane cracking is a monomolecular reaction under the conditions chosen, catalyzed by strong Brønsted acid sites only. Interestingly, also the rate of n-hexene cracking, a reaction that should be catalyzed by much weaker acid sites, also varies linearly with the concentration of strong Brønsted acid sites. However, such relationships strongly suggest, but do not prove that only one type of sites

exists in HZSM-5. A distribution of strong sites may exist and lead to linear relations between site concentrations and catalytic activity as long as the distribution of site strength does not change with the concentration of aluminum in the zeolites framework.

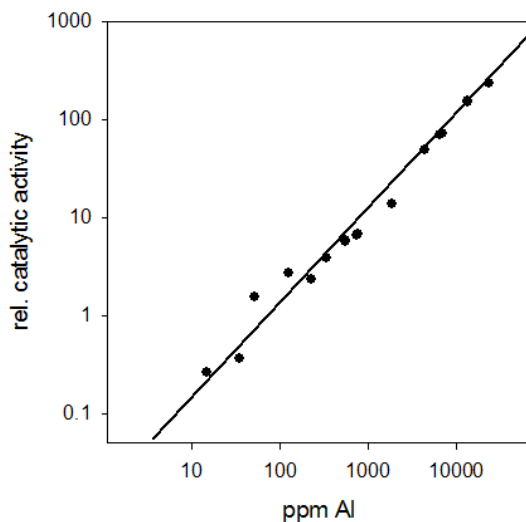


Figure 1: Hexane cracking activity as function of the Si/Al ratio for HZSM-5³⁵

The presence of Brønsted acid sites of equal strength in one particular sample of HZSM-5 has been demonstrated by Mirth *et al.*³⁶ for m-xylene isomerization using *in situ* IR spectroscopy to determine the concentration of sorbed reactants (shown in Fig. 2). Through a variation in the partial pressure of m-xylene the reaction rate was shown to be directly proportional to the concentration of acid sites covered, indicating that all acid sites converted m-xylene to o- and p-xylene with the same rate per proton. It should be noted that due to the operating conditions (steric limitations in the accessibility, diffusional limitations, etc.) not all acid sites of the ZSM-5 samples may actually participate in the reaction. The aspects of the shape selectivity that also influence activity in a complex way will be discussed in a later section.

It should be emphasized at this point that such uniform properties of acid sites are usually restricted to high silica zeolites or, in general, to molecular sieves with a low density of acid sites. With materials of higher acid site concentrations (such as zeolite Y and X) sites with distinct differences in the acid strength have been

observed³⁷. These differences were attributed mainly to the existence of neighboring acid sites that produce a local situation not unlike to that of H₂SO₄, in which two protons with differing acid strength exist.

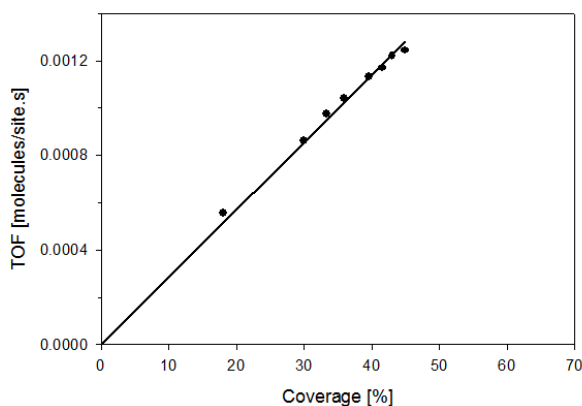


Figure 2: Reaction rate for isomerization of *m*-xylene to *o*- and *p*-xylene as function of the coverage of acid sites for HZSM-5

A large number of papers, however, report very broad distributions of acid sites in all zeolitic materials (see, e.g.,³⁸⁻⁴¹). Such observations stem partly from the fact that not only structurally defined strong Brønsted acid sites are present in the materials investigated. The higher the concentration of defects, the more they will influence directly (by being acid sites of medium strength) and indirectly (by altering the site strength of the strong Brønsted acid sites) the properties of the materials investigated. An excellent example for this is the catalytic activity for the protolytic cracking of *n*-hexane over partially alkali exchanged “clean” and “mildly steamed” HZSM-5³⁵. It is obvious that in the latter case few very active Brønsted acid sites exist, while over two thirds of the acid sites show markedly lower activity.

The presence of neighboring acid sites appears to be important, when bimolecular reaction steps are involved in the reaction network. Hydride transfer reactions in alkane/alkene transformations depend in a nonlinear fashion on the varying concentrations of acid sites. Post *et al.*⁴² showed elegantly that the rates of these bimolecular reactions depend upon the square of the concentration of the acid sites, while the rates of the monomolecular reactions (protolytic cracking) depended linearly on the proton concentration⁴³. The observation should not be interpreted so that two protonated species have to react, but rather that a higher concentration of acid sites also results in a higher concentration of reactants in the pores, which in

turn favors the bimolecular reactions. It should also be noted that the higher concentration of aluminum leads to a more polar and less covalent lattice, which also would improve the stabilization of the alkoxy group to be formed⁴⁴.

The direct role of Lewis acid sites in hydrocarbon conversions is less understood. Karge *et al.*⁴⁵ have shown that La³⁺ ion exchanged zeolites that do not contain hydroxyl groups are catalytically inactive for ethylbenzene disproportionation suggesting that protons are indispensable for carbon-carbon bond rearrangement reactions. On the other hand, several reactions have been reported (the absence of hydroxyl groups is not certain in all those cases) that are well-catalyzed by trivalent metal cation exchanged zeolites⁴⁶. The role of the metal cation, however, appears to lie in these instances in mediating the acid strength and modifying the adsorption.

3. Sorption of reactants and products in zeolite pores

Many of the unique catalytic properties result from the proximity of the molecule and the surrounding zeolite wall, which is in essence a nanoreactor made from quartz (SiO₂) having active sites (bridging SiOHAl groups) at particular locations. The proximity allows substantial contributions of short-range dispersion forces, which dominate over specific chemical interactions for almost all larger molecules. While this is not confined to zeolites, the regularity of the pores makes the sites more accessible than in other irregular porous oxides.

For the case of a proton containing zeolite one can differentiate between directed chemical bonds (at the active sites) and the bonding resulting from the London dispersion forces. The direct interaction results from localized chemical bonds that range in strength from dipole induced hydrogen-bridge bonding with alkanes to the formation of a cation with strong bases such as ammonia. The interaction resulting from the London dispersion forces summarizes all forms of non-localized interactions, similar in nature to the bonds that give rise to the non-ideal behavior of a real gas. The partition between these two forces depends on the size of the molecule, the fit between the sorbed molecule and a particular pore, as well as the strength of the acid-base interaction allowing an optimal arrangement between the sorbed molecule and the active site.

For zeolites it is possible to estimate the different contributions by comparing sorption in a zeolite with and without aluminum in the lattice (e.g., with and without Brønsted acid sites). Fig. 3 shows the dependence of the heat of sorption of n-alkanes on their chain length. The initial heat of sorption increases linearly with the chain length for ZSM-5 and zeolite Y^{47,48}, which is attributed to the linear increase of the London dispersion forces with the size of the alkane. Two observations are notable, i.e., (i) the increment with which the heat of sorption increases per carbon atom is larger for the medium pore ZSM-5 material than for the large pore zeolite Y and (ii) the presence of strong Brønsted acid sites increases

the heat of sorption by 7-10 kJ mol⁻¹. The larger contribution of the latter term for ZSM-5 suggests that it was the stronger acid of the two studied. The larger increment of the heat of adsorption per carbon atom for this material, however, suggests that the narrower pore interacts stronger with the hydrocarbon than the wider one⁴⁸.

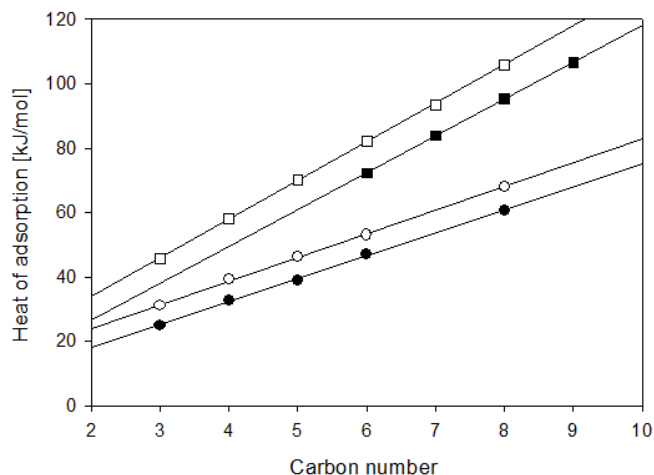


Figure 3: Heat of sorption of *n*-alkanes on (□) HZSM-5, (■) ZSM-5 (siliceous), (○) H-FAU and (●) FAU (siliceous)

It is impressive to see that the contribution of the Brønsted acid sites to the overall heat of adsorption is small compared to the contribution of the dispersion forces indicating that sorption, but not catalysis, of hydrocarbons is governed by physisorption. Please note, how subtle the accessibility of Brønsted acid sites, for example, influences the two contributions to sorptive bonding. While the direct interaction of *n*-hexane via charge induced hydrogen bonding is approximately 10 kJ/mol for HZSM-5, this contribution is only 2 kJ/mol for benzene. Despite it is the sorbent with the higher base strength⁴⁹, its larger size prevents the molecule from attaining the minimum distance of hydrogen bonding. It should also be mentioned at this point that metal cations (especially those with a larger radius and with a higher charge) induce a much stronger polarization of the hydrocarbons and, hence, a much stronger interaction⁵⁰

The sorption in the pores reduces also the degrees of freedom for the sorbed molecules, which is manifested in a decrease of the entropy compared to its state in the gas phase. This is mainly due to the reduction of at least one translation degree of freedom in the transfer to the adsorbed state. In consequence, stronger bonding should lead to a more pronounced reduction of the translational degrees of freedom

and consequently of the sorbate entropy. Indeed, it can be seen that with increasing chain length of the alkane (increasing heat of sorption) also the entropy in the sorbed state decreases, following a linear relation. For a given heat of adsorption, however, the loss of entropy decreases with the pore size of the molecular sieve⁴⁷. This indicates that for larger pore materials the hydrocarbon retains more configurational entropy and loses in consequence less entropy compared to its state in the gas phase. This influence of the pore size decreases with the size of the molecule suggesting that for methane the role of the pore size would be very limited.

It has to be emphasized this point that the compensation between adsorption entropy and the entropy suggests that with increasing reaction temperature the situation may occur that differences in adsorption enthalpy are overcompensated, i.e., the zeolite showing the higher adsorption enthalpy has a lower coverage of adsorbed molecules. Bhan and Iglesia have shown in this context that for HZSM-5 the thermodynamic data of hydrocarbon sorption extrapolated to typical reaction temperatures suggest an equal coverage for in alkanes between three and eight carbon atoms, while at room temperature the coverages of propane and n-hexane were nearly two orders of magnitude apart⁵¹.

For catalysis, these observations suggest that the different rates of reactions found with zeolites of varying pore size for reactions such as alkane cracking are certainly influenced by the concentration of the reactants in the pores of the zeolites, but that this effect depends on the adsorption entropy and enthalpy. It has been reported that the true energy of activation of monomolecular cracking of alkanes is not only identical for a large number of alkanes in one molecular sieve, but also that with different molecular sieves such as zeolites Y or HZSM-5 the same energy of activation is found⁵². The constancy of the true activation energy results from the compensation between apparent energy of activation and the heat of adsorption. As at least for HZSM-5 also the same coverage for the various alkanes has been observed, the drastic variations in the observed rate (a linear increase in rate with the carbon number of the alkane) indicates an important influence of the transition entropy. In turn, recent computational results point to the fact that indeed entropy will play a major role in determining the catalytic conversion of alkanes and that extrapolation of thermodynamic data are possible over substantial temperature spans⁵³.

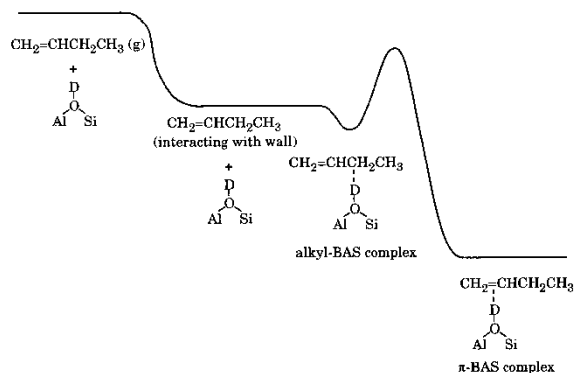
Such strong effects are, however, not confined to molecules that are fully taken up into the pores of the zeolites, but also appear to play a role with molecules that cannot fully penetrate the zeolites pore. Such molecules may adsorb and react at the pore entrance^{54,55}. Under such circumstances, however, the relation between entropy and enthalpy is rather complex leading to rather strong coverage dependent effects⁵⁶.

4. Acid catalyzed reactions

4.1. Activation of alkanes and alkenes by formation of carbocations

The success of zeolite catalysis is closely linked to the ability of the microporous materials to catalyze the conversion of alkanes and alkenes with a much higher efficiency than amorphous mixed oxides of equal chemical composition⁵⁷. While the contributions to cracking has been very substantial over several decades, it is surprising that only now a general understanding as to how zeolites act begin to emerge.

The activation of an alkene appears to be a rather facile reaction. If an olefin is contacted with a zeolite at ambient temperature immediately an alkoxy group is being formed. These alkoxy groups tend to be rather susceptible for alkylation by another olefin resulting in a rapidly growing alkoxy chain⁵⁸. It is however surprising that at low temperatures (150 K) alkenes are adsorbed in zeolites such as ZSM-5 *via* dispersion induced bonding on the saturated part of the molecule⁵⁹. Only upon warming to temperatures above 170 K the carbon-carbon bond interacts *via* hydrogen bonding with the Brønsted acidic hydroxyl groups (see Scheme 1).



Scheme 1: Adsorption of 1-Butene on deuterium exchanged ZSM-5⁵⁹

Upon further heating it may be expected that the hydrogen-bonded alkene would be protonated forming an alkoxy group. The alkoxy group constitutes the ground state of the carbenium ion, which is the active species in the transformations. The size of the carbocation and the zeolite pore determine which of the two is stabilized. For the narrow pore zeolite, Tuma and Sauer have shown recently by elaborate DFT calculations (and in contrast to earlier estimates⁶⁰) that a *tert* butoxy carbenium ion is only a meta-stable intermediate on ferrierite. It is 60 kJ/mol less stable than

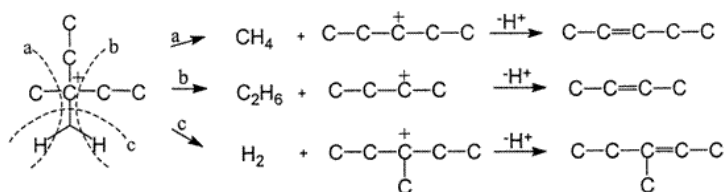
adsorbed isobutene and also 24 and 51 kJ/mol less stable than tert-butoxide and isobutoxide, respectively⁶¹. The lifetime of the carbenium ion will depend on the barriers separating it from the more stable reactant and surface products. Experimentally, it might only be detected by techniques that are able to access the 60 μ s lifetime, which explains that earlier NMR spectroscopic measurements found carbenium ions only to be stable for sterically constrained sorbents with a much higher base strength⁶².

The activation of an alkane is significantly more difficult. In principal, three routes have been postulated, i.e., (i) hydride abstraction to form a carbenium ion, (ii) the addition of a proton to form a carbonium ion and (iii) radical cleavage of a C-H bond leading to a hydrogen deficient radical hydrocarbon fragment. These elementary reactions steps are endothermic with increasing energies of activations in the sequence of mentioning.

Hydride transfer and hydride abstraction occur preferentially under mild conditions. In the initial step the carbenium is formed by abstraction of a hydride either by a Lewis acid site⁶³ or more likely by another carbenium ion in the zeolite⁶⁴. Such carbenium ions are formed, *e.g.*, by protonation of trace olefins present in the alkane feed. It has been shown empirically that hydride transfer reactions are favored in zeolite catalysts containing rare earth element cations such as La³⁺ or extra framework alumina and which have a low silica alumina ratio^{65,66}. The catalytic activity of zeolites for alkane activation *via* that route does not coincide with the acid strength of the material. For hydride abstraction *via* metal cations the stabilization of the metal-hydride and the route of release of the abstracted hydrogen are most important. The difficulty to describe this reaction pathway completely and the resulting controversial discussion in the literature stem from the fact that only a few of such sites suffice to start hydride transfer reactions among hydrocarbon molecules. Recent results with LaX zeolites show that alkanes with two *tert* carbon atoms are being dehydrogenated at ambient conditions by exposed La³⁺ cations²⁰.

The rate of hydride transfer between carbenium ions (alkoxy groups in the ground state) and alkanes increases with the concentration of Brønsted acid sites in the zeolites following a second order kinetics⁶⁷. The unexpectedly high order is the result of two factors, the strengthening of the carbon oxygen bond in the alkoxy group and the increased concentration of alkane molecules in the zeolites pores. Theoretical calculations⁶⁸ indicate that in addition to the chemical effects described above, also the bulky transition state between the incoming alkane and the alkoxy group (carbenium ion) will play an important role. Thus, large pore zeolites such as zeolite Y show higher tendency for hydride transfer than medium pore zeolites such as HZSM-5⁶⁹.

The direct protonation of an alkane by a proton in liquid super acids at low temperatures has been known from the work of Olah for some time, before Haag and Dessau⁷⁰ postulated in a landmark paper that also in zeolites alkanes may be directly protonated to form a “surface stabilized” carbonium ions. The proposal was based on the interpretation of the decay pattern of the carbonium ions formed as transition states in zeolites similar to that depicted in Scheme 2.



Scheme 2: Schematic reaction pathways for carbonium ion decay (protolytic cracking) of a protonated 3-methylpentane together with principal transition states for dehydrogenation and cracking

Because the reactive decay of the carbonium ion leads to breaking of the C-C or C-H bonds at the insertion point of the proton, the reaction has been named protolytic cracking. The typical products are alkanes, hydrogen and primary carbenium ions, which can isomerize or desorb as alkenes. These products correspond to those observed from the collapse of a $C_6H_{15}^+$ ion in a mass spectrometer.

In contrast to the super acid chemistry in the liquid phase, the formation of the carbonium ions appears with zeolites only to be significant at higher temperatures (above 723 K). Also in contrast to the stable carbonium ions in liquid super acids, theoretical studies suggest that carbonium ions in zeolites exist only in a transition state. Thus, it can be concluded that the catalytic manifestation only at high temperatures is a consequence of the thermodynamic equilibrium between the ground state (a hydrogen bonded alkane molecule) and the transition state. Various recent *ab initio* calculations show that (i) the transition state for the various decay routes (dehydrogenation, cracking) differ markedly, i.e., that the reaction pathways are controlled by individual carbonium ions and (ii) that the framework of the zeolite exerts some stabilization to the carbonium ion. It should be mentioned at this point that the rate of protolytic cracking it appears to be governed at least to important degree by the difference of the transition entropy between the ground state and the (late) transition state²³.

At this point the alternative position of McVicker *et al.*⁷¹ and Corma *et al.*⁷² that the alkane activation occurs via the formation and the subsequent decay of a radical cation should be mentioned. The strongest argument for such a route is the fact that

the formation of radical cations is not proportional to the concentration of acid sites, but rather to the presence of extra framework aluminum. Interestingly, experiments by Narbeshuber *et al.*⁷³ showed that a non-catalytic dehydrogenation occurs at short times on stream and that this route is related to the presence of extra framework alumina.

4.2. Reactions involving carbon-carbon bond scission in aliphatic compounds

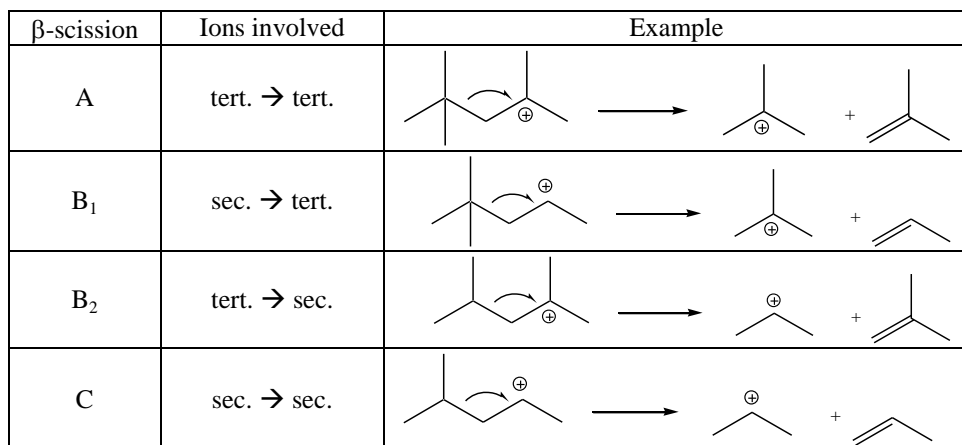
Overall, three major mechanistic pathways can be distinguished for catalytic alkane and alkene cracking, i.e., protolytic cracking of carbonium ions, β -cracking of carbenium ions and cracking that is preceded by some degree of oligomerization of reactants and/or products (oligomerization cracking). The importance of a particular reaction route depends upon the reaction conditions and the zeolite used.

Monomolecular (protolytic) cracking dominates at low conversions, high reaction temperatures, low reactant pressures and with medium and small pore zeolites that have a low concentration of Brønsted acid sites. All these conditions favor a low concentration of reactants in the pores and impede hydride transfer. The decay of the carbonium ion into an alkane and a smaller carbonium ion, which is the central elementary step in protolytic cracking, has already been discussed with respect to the activation of alkane molecules. Thus, only two aspects should be mentioned here. First, results with n-alkanes in various zeolites suggest that the true energy of activation of cleaving the carbon-carbon bond is equal for all bonds in the molecule and that the overall rate depends on the concentration of reactants in the pores and the transition entropy. The selectivity of the C-C bond scission shows a marked compensation effect between the individual barrier of breaking a particular bond and the transition entropy decreasing in magnitude as the proton is attached to a more central bond. Thus, also selectivity is markedly determined by entropic effects⁷⁴.

Cracking of a carbenium ion leads to the formation of an alkene and a smaller carbenium ion. The carbon-carbon bond cleaved is located in β -position to the carbon atom bearing the positive charge (β -cracking). When the smaller carbenium ion donates the proton back to the zeolite, an olefin is formed. Alternatively, the carbenium ion can abstract a hydride ion from an alkane leading to desorption of an alkane and the formation of a new carbenium ion. Thus, for alkanes that cracking route proceeds *via* a chain mechanism⁷⁵. The overall process is governed by the stability of the carbenium ions in the initial and final states of the reaction. As shown also by theoretical calculations, the difference in the stability of the carbenium ions determines the true energies of activation for the elementary step of the carbon-carbon bond cleavage. Thus, when only considering the initial state, cracking of a carbenium ion with the positive charge at a tertiary carbon will be faster than cracking of a carbenium ion with the positive charge at a secondary or

primary carbon atom. Similarly, the ease of reaction decreases in the sequence tertiary > secondary > primary carbenium ion formed.

Note that this is related to the influence of the Polanyi relationship between the initial and final state upon the true energy of activation. The energy of activation usually increases with increasing the energy level of the final state. Therefore, the rate for reactions starting from a tertiary carbenium ion and ending with a tertiary carbenium ion (Type A) is faster, than the reaction starting from and ending with a secondary carbenium ion (Type C). The possible reaction pathways for the reaction are depicted in Scheme 3. Note that these rather simple assumptions for the mechanism lead to a surprisingly good prediction of the cracking selectivity observed⁷⁶.



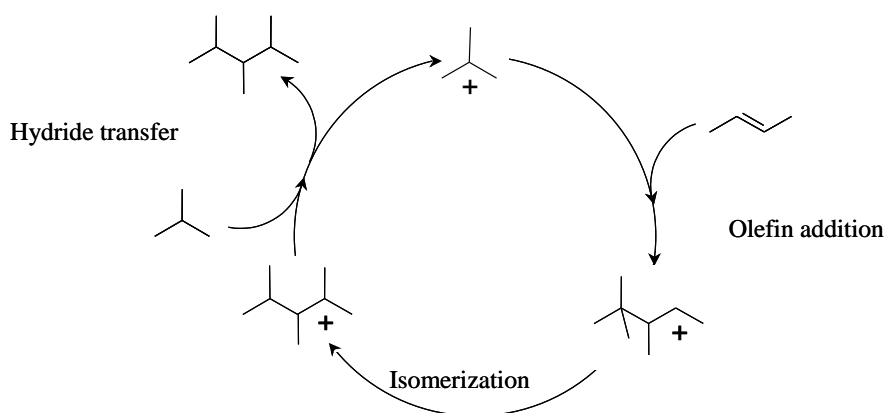
Scheme 3: β -scission mechanism for secondary and tertiary alkylcarbenium ions

Especially at higher reactant partial pressures this reaction route is gradually replaced by a cracking mechanism that includes substantial oligomerization preceding the cracking process. Clear evidence for such a route comes from labeling studies that show complete scrambling of carbon labeled olefinic products of cracking⁷⁷. The importance of the mechanism increases with higher partial pressure, higher conversion and lower reaction temperature. While that route is important for accounting for the product distribution in some cases, the basic chemistry related to cracking is identical with that observed in β -cracking.

4.3. Reactions involving formation of carbon-carbon bonds in aliphatic compounds

Following the principles of microscopic reversibility, zeolites are also suitable catalysts for the alkylation of alkanes, alkenes and aromatic molecules with alkenes. Owing to the lower temperature of reaction the desorption step is often difficult in these reactions, especially as the product of the reaction is stronger adsorbed than the reactants.

The most demanding reaction is the alkylation of isobutane with light alkenes leading to the formation of a complex mixture of branched alkanes^{78,79}. The main reaction cycle occurring during alkylation consists of olefin addition to a tertiary butoxy group/carbenium ion, isomerization *via* methyl and hydride shift reactions of the resulting C₈ alkoxy group and hydride transfer from isobutane to the C₈ alkoxy group, which then desorbs as the corresponding isooctane (see Scheme 4).



Scheme 4: Principal catalytic cycle in the alkylation of iso-butane with n-butene

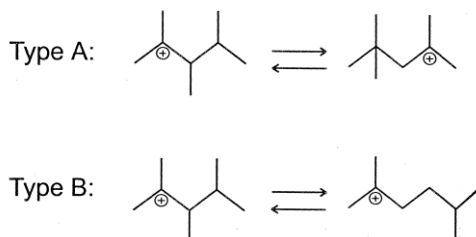
The reaction is initiated by the sorption of n-butene on a Brønsted acid site followed by olefin addition and hydride transfer (i.e., a n-butene dimerization followed by hydride transfer from isobutane) or by adsorption of n-butene on the Brønsted acid site, followed by hydride transfer producing an n-butane molecule and a tertiary butoxy group. The lifetime of the catalyst is determined by the relative rates of olefin addition and hydride transfer⁸⁰. The rate of hydride transfer is intrinsically influenced by the stability of the carbenium ion (in turn controlled by the chemical composition of the molecular sieve) and the steric hindrance through the micropore environment. The slower the hydride transfer (relative to the olefin addition) the more likely multiple alkylation, leading to C₁₂ or C₁₆ carbenium ions, becomes. The hydride transfer to these molecules is increasingly slow, therefore, they cannot

desorb and, thus, will block the particular site. Note that the rate of hydride transfer will also influence the isomer distribution, as methyl shift reactions will lead to product distributions closer to the chemical equilibrium⁸¹.

4.4. Reactions involving carbon-carbon bond rearrangements

As for cracking, the catalytic activity for isomerization is strongly related to the concentration of strong Brønsted acid sites. The catalysts are mostly dual functional, i.e., they contain a metal to facilitate the dehydrogenation of alkanes and isomerized alkenes. Thus, the reacting species are alkenes, their concentration being dependent on the operating conditions. As isomerization and β -cracking share the same intermediates (i.e., alkoxy groups or carbenium ions) the reactions are interlinked. A higher lifetime of the carbenium ion, usually associated with a stronger acid site, leads to more pronounced cracking and less isomerization. This implies that the reaction rate constant for cracking is lower than for isomerization.

Skeletal isomerization of alkanes can be grouped in two categories⁸², one that results in a positional shift of the branching and the other that increases or reduces the number of branches, for more extended reviews please consult, e.g., refs.⁸³⁻⁸⁵. Both processes combine (facile) hydride shift reactions and the formation of a cyclopropyl ring, but differ insofar as in the type A isomerization only ring closure and opening occurs, while in the type B reaction also a corner to corner proton jump occurs (see Scheme 5). The transition state complex for this latter reaction appears to be energetically significantly higher than that for reaction pathway A. Thus, changes in the branching will only occur under more severe conditions than the methyl shift isomerization. The pore size and shape of zeolites has a marked influence on the isomerization and subsequent cracking, which can be attributed to the strain to form and break the ring in the zeolite pores⁸⁶.



Scheme 5: Classification of skeletal rearrangements of alkylcarbenium ions

4.5. Nucleophilic substitution and addition reactions

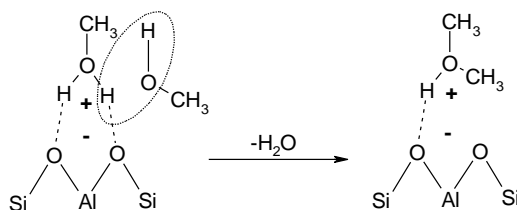
Nucleophilic substitution and addition reactions follow two mechanistic pathways, i.e., the two-step nucleophilic substitution (S_{N1}) and the one step process (S_{N2}). In the former route, the highly polar intermediate species or, in the limiting case, the carbocation is stabilized by the catalyst, while in the latter a transition state comprising the substituent and the leaving group is formed in a concerted fashion.

Direct evidence for stable carbocation intermediates is limited to the most basic substrates. The course of the reaction is determined by the chemical nature of the leaving and the substituting group, the zeolite in acid strength, the influence of co-reactants and the availability of space for the reaction to take place. The majority of the nucleophilic substitutions involve the replacement of an -OH group with a -NH₂, -NR₂, -S, -SH, -SR, and -OR group.

Often, the resulting product interacts more strongly with the molecular sieve than the reactant. In these cases, the reaction is desorption controlled and requires either a reactant to desorb (adsorption assisted desorption) or a gaseous/liquid co-catalyst that also facilitates desorption of the products without participating in the reaction. Note that for liquid phase reactions the solvent can assume the role of the co-catalyst.

Formation of ethers from alcohols

The experimentally and theoretically well studied dimethylether formation from methanol is an excellent example, how the reaction conditions influence the reaction mechanism, i.e., whether the reaction proceeds along the S_{N1} or the S_{N2} pathway⁸⁷⁻⁹⁰. Temperature programmed reaction studies of methanol conversion over HZSM-5 suggest that three reaction routes to dimethylether exist, i.e. *via* an alkoxonium cation and *via* two alkoxy pathways. At low temperatures the reaction proceeds *via* an Eley-Rideal type mechanism. In the transition state one methanol molecule forms a methoxonium ion, water leaves the molecule and simultaneously another weakly sorbed methanol binds to the methyl group forming protonated dimethylether (see Scheme 6). The protonated dimethylether donates the proton back to the zeolite and desorbs.



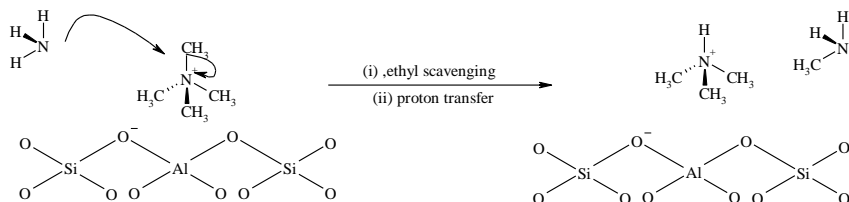
Scheme 6: Formation of dimethylether from methanol

As the reaction temperature increases, part of the methanol molecules are transformed into methoxy groups replacing the proton in bridging (SiOHAl) and terminal (SiOH) hydroxyl groups. These methoxy groups react with weakly associated methanol to form dimethylether under the simultaneous restitution of the hydroxyl group. While the methoxy group is covalently bound to the zeolite framework, its reactivity increases with the acid strength of the hydroxyl group it replaces⁹¹. Thus, methoxy groups at bridging hydroxyl groups produce dimethylether at lower temperatures than methoxy groups at terminal hydroxyl groups.

Computational chemistry by Blazowski and van Santen suggest that the pathway to form dimethylether *via* a methoxonium ion is energetically favored over the pathway *via* methoxy groups⁹². The S_{N2} reaction involves a complex transition state. For a successful reaction, four elementary steps have to proceed in a concerted manner, i.e., (i) formation of a methoxonium ion by proton donation from the zeolite, (ii) cleavage of water from the methoxonium ion and formation of a methylcarbenium ion, (iii) binding of the methyl carbenium ion to the second methanol molecule to form protonated dimethylether and (iv) donation of the proton back to the zeolite. Stabilization of the methoxonium ion by the catalyst would lead to a less complex transition state and, hence, one might expect the intrinsic rates of the reaction to be higher.

Reactions of alcohols with ammonia

Amination of alcohols follows a mechanistic pathway similar to etherification⁹³. Like for the ether formation the mechanism varies as a function of the active site and the reaction temperature used. For the purely Brønsted acidic zeolites the basicity of the reactants dictates that at the start of the reaction ammonia is present in the molecular sieve as ammonium ions. The alkyl group reacts with the ammonium ion forming water as the leaving group and an alkylammonium ion⁹⁴. The alkylammonium ions, however, cannot desorb under the reaction conditions, i.e., temperatures of 625 K. Thus, the alkylamines released into the gas phase stem either from a further nucleophilic substitution in which the alkyl group of the alkylammonium ion is scavenged by weakly adsorbed ammonia or the desorption of the alkylammonium ion is aided by the simultaneous formation of an ammonium ion (see Scheme 7). Both reaction pathways have been found to be important under typical reaction conditions. High selectivity to mono- and dialkylamines is achieved with surface modification of the zeolites by coating with silica overlayers⁹⁴. In the resulting materials trimethylamines can be formed, but cannot leave the pores and react *via* disproportionation to the smaller mono- and dimethylamines.



Scheme 7: Proposed mechanism for the removal of methyl amines by scavenging with ammonia

Formation of alkylamines by addition of ammonia to olefins

Catalysis for the addition of alkenes and ammonia requires the alkene to be activated by the Brønsted acid site of the zeolite, which is only possible if the acid sites are not completely blocked by ammonium ions. Examples include the amination of ethene with H-Y, H-erionite and H-mordenite at reaction temperatures between 500 and 550 K⁹⁵. At higher temperatures, nitriles tend to be formed. The reaction of isobutene with ammonia is successfully catalyzed with B-ZSM-5⁹⁶. In order to favor alkene adsorption, mild reaction temperatures and high pressures of alkenes are favorable in addition to moderate to weak acid sites⁹⁷.

4.6. Electrophilic substitution on the aromatic ring

The reactions are characterized by the attack of an electron deficient species, i.e., one with a positive partial charge, a carbocation or a radical on an aromatic ring, preferably on the carbon atom with the highest negative charge. The generation of such species occurs *via* several pathways, amongst which protonation, hydride abstraction and cleavage of polar groups are the most important ones.

Coordinative bonding between the π -electrons of the aromatic ring and the electrophile occurs frequently in the first step. Recent spectroscopic evidence for such an intermediate was reported for the methylation⁹⁸. The aromatic ring must only be weakly held by the zeolite in order not to decrease the availability of the π -electrons. Subsequently, one carbon atom of the ring interacts with the electrophile prior to the actual substitution. In the presence of a substituent on the ring, the carbon atom position at which the interaction with the electrophile occurs will depend on the inductive effects from the ring substituent. For electron donating substituents the preferred carbon atoms to accept the electrophile are those in ortho- and para-position to the substituent group.

The overall reactivity of the aromatic ring depends upon the nature of the substituent. Electron donating properties of the substituents increase the availability of π -electrons at the aromatic ring, while the electron withdrawal properties reduce it. In that respect alkyl-, hydroxyl-, alkoxy-, or amine groups increase the reactivity, while in the presence of halogen or nitro groups the reactivity is reduced. The reactivity of heterocycles also depends upon whether or not the ring has a π -electron excess. This results in pyrrole and thiophene being more reactive than benzene, while pyridine is less reactive.

Friedel-Crafts type alkylation of benzene by alkenes involves the initial formation of a framework associated carbenium ion, formed by protonation of the sorbed olefin. The chemisorbed alkene is covalently bound to the zeolite in the form of an alkoxy group and the carbenium ion formed exists only in the transition state⁹⁹. As would be expected from conventional Friedel-Crafts alkylation, the reaction rate over acidic molecular sieves increases with the degree of substitution of the aromatic ring (i.e., tetramethyl > trimethyl > dimethyl > methyl > unsubstituted benzene). However, the spatial restrictions induced by the pore size and geometry frequently inhibit the formation of large multi-substituted products.

The alkylation of benzene or toluene with light olefins is generally performed with zeolite catalysts¹⁰⁰ (ZSM-5, Beta, MCM-22, mordenite) having rather high Si/Al ratios. The shape selective properties depend critically on the specific alkylation processes. While for alkylation of toluene with ethene the shape selectivity to para-substituted products is most important, single alkylation and catalyst stability dominates for cumene synthesis¹⁰¹.

The alkylation of toluene with methanol over H-ZSM-5 proceeds at low temperatures *via* a protonated methanol species in the transition state¹⁰² and weakly coadsorbed toluene as classically predicted for Friedel-Crafts alkylation. The reaction rate is directly proportional to the concentration of the chemisorbed methanol in the presence of excess toluene. Alkylation leads preferentially to ortho- and para- substituted products, which rapidly isomerize in the zeolite pores. Specific reaction conditions and tailoring of the catalyst pore structure help that para- substituted products are preferentially produced^{103,104}. The reasons for this selectivity and the methods for optimizing the catalyst performance will be discussed in a later section. The catalysis appears to be completely controlled by the Brønsted acid sites with the role of the Lewis acid sites being marginal¹⁰⁵.

In contrast to the alkylation with alcohols, nitration of aromatic compounds requires very strong acid sites to stabilize the NO_2^+ cation, which is an important intermediate in liquid phase nitration. Several nitrating agents such as HNO_3 , NO_2 and N_2O_4 have been successfully applied using mainly dealuminated mordenites or faujasites and elevated pressures^{106,107}. The stability of the zeolites is a major problem in the highly acidic reaction medium. A combination of high crystallinity

and sufficient extra-zeolite surface area (the presence of extra-framework material) was found to be beneficial for stabilizing the catalysts.

5. Shape selectivity

Shape selectivity can be induced by differences in the diffusivities of the reactants and/or the products or by steric constraints of the transition state. A schematic representation of the three groups of shape selectivity, i.e., the limitations of the access of some of the reactants to the pore system (reactant selectivity), the limitation of the diffusion of some of the products out of the pores (product selectivity) and constraints in forming certain transition states (transition state selectivity) are shown in Fig. 4.

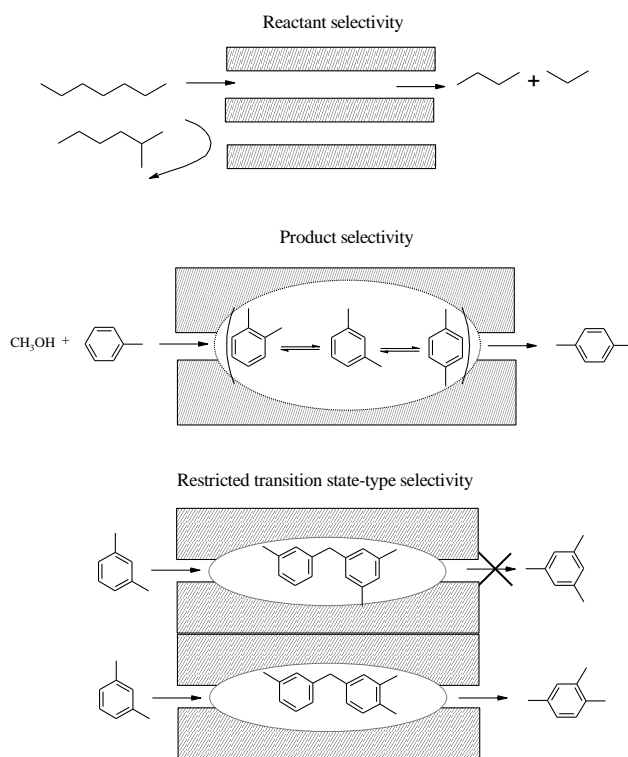


Figure 4: Schematic representation of the three types of shape selectivity

Differentiation between the latter two is difficult as the kinetic results may be disguised, when the overall rate is influenced by the rates of diffusion. *In situ* IR and NMR spectroscopy have contributed much to our understanding of these complex phenomena. The examples given here should only illustrate what can be achieved by employing a zeolite and why the pathway of a particular reaction is influenced. For further reading several excellent reviews exist¹⁰⁸⁻¹¹⁰.

The first example of shape selectivity was reported by Weisz¹¹¹ for the dehydration of an n-butanol/iso-butanol mixture over LTA type zeolites. Because of its larger

minimum kinetic diameter iso-butanol is excluded from entering the zeolite pores, while n-butanol is easily dehydrated to butene. This demonstrated that the catalytically active sites are inside the zeolite pores and that the pores are able to realize a well-defined cutoff point with respect to the minimum kinetic diameter of the reacting molecules. This principle of size exclusion was frequently used in hydrocarbon processing to remove linear hydrocarbons from a mixture of hydrocarbons (e.g., selectoforming¹¹²).

One of the most discussed cases of shape selectivity involving transition state selectivity or product diffusional constraints is the production of p-xylene over chemically modified ZSM-5 zeolites¹¹³. Processes utilizing the shape selectivity include the alkylation of toluene with methanol, xylene isomerization and selective toluene disproportionation. Toluene alkylation by methanol occurs *via* methoxonium ions at low temperatures and *via* methyl carbenium ions at high temperatures. Initially toluene is alkylated preferentially in o- and p- position of toluene, but all three isomers appear to be kinetic primary products as shown by *in situ* IR spectroscopy¹¹⁴. The high para-selectivity is coupled with rapid a isomerization of the xylenes. The diffusion constant of p-xylene is about 10^3 times higher than that of m-xylene¹¹⁵. In an idealized model one would, therefore, expect to find the xylenes in their equilibrium concentrations in the ZSM-5 pores. *In situ* IR spectroscopy indicates that m- and o-xylene as well as trimethylbenzenes are preferentially retained. Combining the rate constants for the isomerization of the individual xylene isomers and the concentrations of the products in the ZSM-5 pores, shows that the selectivity to p-xylene is high, when the rate of internal isomerization exceeds drastically the overall rate of alkylation. Thus, the results indicate that the secondary isomerization is important for the shape selective production of p-xylene.

The isomerization of m-xylene is in contrast a good example of transition state selectivity. Irrespective of the temperature and coverage, (a particular sample of) ZSM-5 showed a product ratio of p- to o-xylene of 2:1. In the zeolite pores, only m-xylene was found to be sorbed in appreciable quantities. Thus, the reaction rate appears not to be influenced by the preferred retention of one of the products. The selectivity must consequently be governed by the differences in the transition states of the two products. As this ratio also did not vary with the reaction temperature, the different selectivities must be caused by differences in the transition entropy. Considering the identical energies of activation and the identical heats of adsorption of all isomers the larger kinetic diameter of the transition state of the m-o xylene transformation is concluded to require more specific configurations in the ZSM-5 channels, i.e., lower transition entropy. Note that similar effects have been observed for hydrocarbon conversions¹¹⁶.

Blocking the pore mouth and reducing the diffusivities of the xylenes, e.g., by chemical vapor deposition of ethoxysilanes or by selectively coking the channels does not change the overall catalytic pathway for toluene methylation, but enhances the para selectivity^{117,118}. However, zeolites prepared in that way deactivate, which has to be balanced with higher reaction temperatures required to open new reaction channels (dealkylation, transalkylation, and disproportionation). This allows the desorption of products from the pores as the longer residence times lead to polymethylated benzenes, which are unable to leave the zeolite pores and would eventually block all acid sites.

A more complex problem is the shape selective alkylation of multi-nuclear aromatic compounds. For example 4,4'-diisopropylbiphenyl can be produced from propene and biphenyl in high yields over dealuminated mordenite¹¹⁹ obtained by severe acid leaching, which resulted in a catalyst with a Si/Al ratio of 1300 containing large mesopores. This post synthesis modification converted the mono dimensional channel structure of mordenite into a three dimensional structure, in which the micropores are connected by micro and mesopores generated in the leaching procedure. It is concluded that the mesopores are indispensable for efficient mass transport of the bulky molecules and that dealumination reduces coke formation and unselective alkylation in the para-meta positions.

Also condensed aromatic molecules such as 2-methylnaphthalene (2-MN) and 2,6-dimethylnaphthalene (2,6-DMN) can be selectively produced by isomerization and disproportionation of 1-methylnaphthalene (1-MN) or by direct alkylation of naphthalene over non-modified zeolites. The observed reactivity for the isomerization of 1-MN and 2-MN over H-ZSM-5, H-ZSM-11, H-beta, H-mordenite and H-Y led Weitkamp *et al.*¹²⁰ to propose that product shape selectivity dominates, while Fraenkel *et al.*¹²¹ suggest that cavities at the external surface containing strong Brønsted acid sites are responsible for the selectivity. The idea has been followed up by Derouane, proposing nest-like structures to be important¹²². However, Neuber and Weitkamp¹²³ showed that even the more bulky molecules can enter the zeolite pores. While the role of the external and internal acid sites is not completely resolved, the combination of silylation and poisoning experiments for xylene isomerization suggest that external acid sites do not markedly contribute to the reaction pathway for such large molecules.

The role of pore mouth catalysis for shape selectivity has been strongly debated^{124,125}. It has been shown that product patterns points to the fact that only the acid sites at the entrance of small pore materials such as erionite, ZSM-22 and Theta-1 are catalytically active. The isomer distribution suggests that branching of n-alkanes occurs in approximately the distance between two pore openings. Sorption of branched alkanes on these materials demonstrates that the acid sites

involved in such catalysis, are located not directly at the pore entrance, but just inside the zeolite channel¹²⁶.

6. Concluding remarks

Our understanding of zeolite synthesis, characterization and catalysis has dramatically emerged over the last decades. Especially the combination of advanced physicochemical characterization and computational chemistry has helped to better understand elementary processes and the requirements to catalyze them efficiently. I hope that the short outline on zeolite acid-base catalysis has helped to raise interest in going deeper into this fascinating chemistry.

Especially reactions involving hydrocarbon conversions and processing renewable feedstock will see zeolite catalysts as a key component of future sustainable technology. Knowledge-based design of catalysts will help to achieve these goals and will markedly contribute securing our energy future.

References

- [1] J. A. Lercher and A. Jentys, in *Handbook of Porous Solids*, p. 1097, F. Schüth, K. S. W. Singh and J. Weitkamp Eds., Wiley-VCH, Weinheim (2002).
- [2] J. A. Lercher and A. Jentys, in *Dekker Encyclopedia of Nanotechnology*, p. 633 (2004).
- [3] J. A. Lercher, A. Jentys, and A. Brait, *Molecular Sieves - Science and Technology* **6**, p.153 (2008).
- [4] S. M. Csicsery, *Zeolites* **4**, 202 (1984).
- [5] J. Weitkamp, *Solid State Ionics* **131**, 175 (2000).
- [6] A. Corma and H. Garcia, *J. Chem. Soc., Dalton Trans.* 1381 (2000).
- [7] F. R. Ribeiro, F. Alvarez, C. Henriques, F. Lemos, J. M. Lopes and M. F. Ribeiro, *J. Mol. Catal. A* **96**, 245 (1995).
- [8] J. A. M. Arroyo, G. G. Martens, G. F. Froment, G. B. Marin, P. A. Jacobs and J. A. Martens, *App. Catal. A*, **192**, 9 (2000).
- [9] P. Andy, D. Martin, M. Guisnet, R. G. Bell and C. R. A. Catlow, *J. Phys. Chem. B* **104**, 4827 (2000).
- [10] T. L. M. Maesen, R. Krishna, J. M. van Baten, B. Smit, S. Calero and J. M. C. Sanchez, *J. Cata.*, **256**, 95 (2008).

-
- [11] J. Perez-Ramirez, C. H. Christensen, K. Egeblad, C. H. Christensen and J. C. Groen, *Chemical Society Reviews*, **37**, 2530 (2008).
- [12] C. Fernandez, I. Stan, J.P. Gilson, K. Thomas, A. Vicente, A. Bonilla and J. Perez-Ramirez, *Chem.-Eur. J.* **16**, 6224 (2010).
- [13] A. Corma, V. Fornes, S. B. Pergher, T. L. M. Maesen and J. G. Buglass, *Nature* **396**, 353 (1998).
- [14] A. Corma, V. Fornes, J. M. Guil, S. Pergher, T. L. M. Maesen and J. G. Buglass, *Microp. Mesop. Mater.* **38**, 301 (2000).
- [15] D. Majda, F. A. A. Paz, O. D. Friedrichs, M. D. Foster, A. Simperler, R. G. Bell and J. Klinowski, *J. Phys. Chem. C* **112**, 1040 (2008).
- [16] J. E. Naber, K. P. DeJong, W. H. J. Stork, H. P. C. E. Kuipers and M. F. M. Post, *Stud. Surf. Sci. Catal.*, **84**, 2197 (1994).
- [17] B. Notari, *Stud. Surf. Sci. Catal.* **37**, 413 (1987).
- [18] E. M. Flanigen, L. Patton and S. T. Wilson, *Stud. Surf. Sci. Catal.* **37**, 13 (1988).
- [19] B. Onida, B. Bonelli, L. Borello, S. Fiorilli, F. Geobaldo and E. Garrone, *J. Phys. Chem. B* **106**, 10518 (2002).
- [20] C. Sievers, A. Onda, A. Guzman, K. S. Otillinger, R. Olindo and J. A. Lercher, *J. Phys. Chem. C* **111**, 210 (2007).
- [21] G. Sastre and A. Corma, *J. Mol. Catal. A-Chem.* **305**, 3 (2009).
- [22] L. I. Devriese, J. A. Martens, J. W. Thybaut, G. B. Marin, G. V. Baron and J. F. M. Denayer, *Microp. Mesop. Mater.* **116**, 607 (2008).
- [23] R. Gounder and E. Iglesia, *J. Am. Chem. Soc.* **131**, 1958 (2009).
- [24] D. W. Breck, *Zeolite Molecular Sieves, Structure, Chemistry and Use*, J. Wiley & Sons, New York, 1974, p 29.
- [25] V. B. Kazansky, *Stud. Surf. Sci. Catal.* **85**, 251 (1994). (and references cited therein).
- [26] J. Ward, *J. Catal.* **9**, 231 (1967).
- [27] K. Tanabe, M. Misono, Y. Ono and H. Hattori, *Stud. Surf. Sci. Catal.* **51**, 142 (1989).
- [28] W. J. Mortier, *J. Catal.* **55**, 138 (1978).
- [29] K. P. Schröder, J. Sauer, M. Leslie, C. R. A. Catlow and J. M. Thomas, *J. Chem. Phys. Lett.* **188**, 320 (1992).

- [30] K. A. van Genechten and W. J. Mortier, *Zeolites* **8**, 273 (1988).
- [31] D. Barthomeuf, *Catalysis by Zeolites*, Elsevier, Amsterdam, 1980, p.56.
- [32] J. A. Rabo and G. C. Gajda, *Catal. Rev.* **31**, 385 (1989).
- [33] R. A. van Santen, *Stud. Surf. Sci. Catal.* **85**, 273 (1994).
- [34] G. Sastre, V. Fornes and A. Corma, *J. Phys. Chem. B* **2000**, 104, 4349.
- [35] R. M. Lago, W. O. Haag, R. J. Mikovsky, D. H. Olson, S. D. Hellring, K. D. Schmitt and G. T. Kerr, Proc. of the 7th International Zeolite Conference, Amsterdam, 1986, p. 677.
- [36] G. Mirth, J. Cejka and J. A. Lercher, *J. Catal.* **139**, 24 (1993).
- [37] P. A. Jacobs and J. Uytterhoeven, *J. Chem. Soc., Faraday Trans. I* **69**, 359 (1973).
- [38] P. D. Hopkins, J. T. Miller, B. L. Meyers, G. J. Ray, R. T. Roginski, M. A. Kuehne and H. H. Kung, *App. Catal. A* **136**, 29 (1996).
- [39] C. Costa, J. M. Lopes, F. Lemos and F. R. Ribeiro, *J. Mol. Catal. A* **144**, 221 (1999).
- [40] T. L. M. Maesen and E. P. Hertzberg, *J. Catal.* **182**, 270 (1999).
- [41] G. Sastre, V. Fornes and A. Corma, *J Phys: Chem. B*, **106**, 701 (2002).
- [42] A. H. F. Wielers, N. Vaarkamp and M. F. M. Post, *J. Catal.* **127**, 51 (1991).
- [43] W. O. Haag, R. M. Dessau and R. M. Lago, *Stud. Surf. Sci. Catal.*, **60**, 255 (1990).
- [44] R. M. Lago, W. O. Haag, R. J. Mikovsky, D. H. Olson, S. D. Hellring, K. D. Schmitt and G. T. Kerr, *Stud. Surf. Sci. Catal*, **28**, 677 (1986).
- [45] H. G. Karge, G. Borbély, H. K. Beyer and G. Onyestyak, Proceedings of the 9th International Congress on Catalysis, M. J. Philips, M. Ternan (Eds.) 1988, Vol I, p.396.
- [46] R. Carvajal, P.-J. Chu and J. Lunsford, *J. Catal*, **125**, 123 (1990).
- [47] F. Eder, M. Stockenhuber and J. A. Lercher, *J. Phys. Chem. B* **101**, 5414 (1997).
- [48] F. Eder and J. A. Lercher, *J. Phys. Chem.* **101**, 1273 (1997).
- [49] A. Jentys, R. R. Mukti, H. Tanaka and J. A. Lercher, *Microp. Mesop. Mater.*, **90**, 284 (2006).
- [50] C. Sievers, A. Onda, R. Olindo and J. A. Lercher, *J. Phys. Chem. C* **111**, 5454 (2007).
- [51] A. Bhan, R. Gounder, J. Macht and E. Iglesia, *J. Catal.* **253**, 221 (2008).

- [52] J. A. van Bokhoven, M. Tromp, D. C. Koningsberger, J. T. Miller, J. A. Z. Pieterse, J. A. Lercher, B. A. Williams and H. H. Kung, *J. Catal.* **202**, 129 (2001).
- [53] B. de Moor, M. F. Reyniers, J. A. Lercher and G. Marin, *J. Phys. Chem. C* **115**, 1204 (2011).
- [54] J. A. M. Arroyo, G. G. Martens, G. F. Froment, G. B. Marin, P. A. Jacobs and J. A. Martens, *App. Catal. A* **192**, 9 (2000).
- [55] M. C. Claude and J. A. Martens, *J. Catal.* **190**, 39 (2000).
- [56] J. A. Z. Pieterse, S. Veefkind-Reyes, K. Seshan and J. A. Lercher, *J. Phys. Chem. B* **104**, 5715 (2000).
- [57] C. J. Plank and E. J. Rosinski, *Chem. Eng. Progr. Symp. Ser.* **73**, 26 (1967).
- [58] M. Boronat, P. Viruela and A. Corma, *J. Phys. Chem. A* **102**, 982 (1998).
- [59] J. N. Kondo, F. Wakabayashi, and K. Domen, *J. Phys. Chem B* **102**, 2259 (1998).
- [60] C. Tuma and J. Sauer, *Angew. Chemie, Int. Ed.* **44**, 4769 (2005).
- [61] C. Tuma, T. Kerber and J. Sauer, *Angew. Chem. Int. Ed.* **49**, 4678 (2010).
- [62] J. F. Haw, W. Song, D. M. Marcus and J. B. Nicholas, *Acc. Chem. Res.* **36**, 317 (2003).
- [63] A. Brait, A. Koopmans, K. Seshan, H. Weinstabl, A. Ecker and J. A. Lercher, *Ind. Eng. Chem. Res.* **37**, 873 (1998).
- [64] K. A. Cumming and B. W. Wojciechowski, *Catal. Rev. Sci. Eng.* **38**, 101 (1996).
- [65] V. B. Kazansky, M. V. Frash and R. A. van Santen, *Appl. Catal.* **146**, 225 (1996).
- [66] B. A. Williams, S. M. Babitz, J. T. Miller R. Q. Snurr and H. H. Kung, *Appl. Catal. A* **177**, 161 (1999).
- [67] A. F. H. Wielers, M. Vaarkamp and M. F. M. Post, *J. Catal.* **127**, 51 (1991).
- [68] S. R. Blaszkowski and R. A. van Santen, *Topics Catal.* **4**, 145 (1997).
- [69] V. B. Kazansky, M. V. Frash and R. A. van Santen, *Appl. Catal.* **146**, 225 (1996).

- [70] W.O. Haag and R.M. Dessau, Proceedings of the 8th International Congress on Catalysis, Dechema, Frankfurt am Main, 1984, p 305.
- [71] G. B. McVicker, G. M. Kramer and J. J. Zemiak, *J. Catal.* **83**, 286 (1983).
- [72] A. Corma, *Stud. Surf. Sci. Catal.* **49**, 49 (1989).
- [73] T. Narbeshuber, A. Brait, K. Seshan and J. A. Lercher, *J. Catal.* **172**, 127 (1997).
- [74] T. Narbeshuber, H. Vinek and J. A. Lercher, *J. Catal.* **157**, 388 (1997).
- [75] A. Corma and A. V. Orchillés, *Microp. Mesop. Mater.* **35-36**, 21 (2000).
- [76] B. C. Gates, J. R. Katzer and G. C. A. Schuit, in *Chemistry of Catalytic Processes*, Mc Graw-Hill New York, 1979, p.1.
- [77] D. W. Werst, P. Han, S. C. Choure, E. I. Vinokur, L. Xu, A. D. Trifunac and L. A. Eriksson, *J. Phys. Chem. B* **103**, 9219 (1999).
- [78] A. Corma and A. Martinez, *Catal. Rev.-Sci. Eng.* **35**, 483 (1993).
- [79] J. Weitkamp, Y. Traa, in *Handbook of Heterogeneous Catalysis*, G. Ertl, H. Knözinger, J. Weitkamp (Eds.), Wiley-VCH, Weinheim, 1997, p.2039.
- [80] A. Feller and J. A. Lercher, *Adv. in Catalysis* **48**, 229 (2004).
- [81] A. Feller and J. A. Lercher, *J. Catal.* **216**, 313 (2003).
- [82] D. M. Brouwer and H. Hogeveen, *Recul. Trav. Chim. Pays-Bas.* **89**, 211 (1970).
- [83] H. Pines, in *The Chemistry of Hydrocarbon Conversions*, Academic Press, New York, 1981.
- [84] A. Corma, *Chem. Rev.* **95**, 559 (1995).
- [85] D. S. Santili and B. C. Gates, in *Handbook of Heterogeneous Catalysis*, G. Ertl, H. Knözinger, J. Weitkamp (Eds.), Wiley-VCH, Weinheim, 1997, p.123.
- [86] J. A. Martens and P. A. Jacobs, *Zeolites* **6**, 334 (1986).
- [87] T. R. Forester and R. F. Howe, *J. Am. Chem. Soc.* **109**, 5076 (1987).
- [88] W. W. Kaeding and S. A. Butter, *J. Catal.* **61**, 155 (1980).
- [89] G. Mirth and J. A. Lercher, *Stud. Surf. Sci. Catal.* **61**, 437 (1991).
- [90] J. A. Lercher, G. Mirth, M. Stockenhuber, T. Narbeshuber and A. Kogelbauer, *Stud. Surf. Sci. Catal.* **90**, 147 (1994).

- [91] L. Kubelkova, J. Novakova and K. Nedomova, *J. Catal.* **124**, 441 (1990).
- [92] S. R. Blaszkowski and R. A. van Santen, *J. Am. Chem. Soc.* **118**, 5152 (1996).
- [93] Ch. Gründling, G. Eder- Mirth and J. A. Lercher, *Res. Chem. Int.* **23**, 25 (1997).
- [94] C. Grundling, G. Eder-Mirth and J. A. Lercher, *J. Catal.* **160**, 299 (1996).
- [95] M. Deeba, M. E. Ford and T.A. Johnson, *J. Chem. Soc., Chem. Comm.* **8**, 562 (1987).
- [96] V. Taglieber, W. Hölderich, R. Kummer and W. D. Mross, German Pat., DE 3327000 A1, 1983, assigned to BASF AG.
- [97] M. Lequite, F. Figueras, C. Moreau and S. Hub, *J. Catal.* **163**, 255 (1996).
- [98] G. Mirth and J. A. Lercher, *J. Phys. Chem.* **95**, 3736 (1991).
- [99] T. Xu, D. H. Barich, P. D. Torres, J. B. Nicholas and J. F. Haw, *J. Am. Chem. Soc.* **119**, 396 (1997).
- [100] J. S. Beck and W. O. Haag, , in *Handbook of Heterogeneous Catalysis*, G. Ertl, H. Knözinger, J. Weitkamp (Eds.), Wiley-VCH, Weinheim, 1997, p. 2123.
- [101] G. Meima, *Cattech* **3**, 5 (1998).
- [102] G. Mirth and J. A. Lercher, *J. Catal.* **132**, 244 (1991).
- [103] G. Mirth, J. Cejka, J. Krtil and J. A. Lercher, *Stud. Surf. Sci. Catal.* **88**, 241 (1994).
- [104] J. Cejka, N. Zilkova, B. Wichterlova, G. Eder-Mirth and J. A. Lercher, *Zeolites* **17**, 265 (1996).
- [105] H. Vinek, M. Derewinski, G. Mirth, J. A. Lercher, *Appl. Catal.* **68**, 277 (1991).
- [106] L. E. Berteau, H. W. Kouwenhoven and R. Prins, *Stud. Surf. Sci. Catal.* **84**, 1973 (1994).
- [107] A. Kogelbauer and H. W. Kouwenhoven, in *Fine Chemicals through Heterogeneous Catalysis*, R.A. Sheldon, H.van Bekkum (Eds.), Wiley-VCH, Weinheim, 2001, p. 123.
- [108] A. Corma, *Chem. Rev.* **95**, 559 (1995).

- [109] S. I. Zones and T. V. Harris, *Microp. Mesop. Mater.* **35-36**, 31 (2000).
- [110] C. R. Marcilly, *Topics in Catal.* **13**, 357 (2000).
- [111] P. B. Weisz and V. J. Frilette, *J. Phys. Chem.* **64**, 382 (1960).
- [112] N. Y. Chen, J. Maziuk, A. B. Schwartz and P.B. Weisz, *Oil Gas Journal* **66**, 154 (1968).
- [113] W. W. Kaeding, C. Chu, L. B. Young, B. Weinstein and S. A. Butter, *J. Catal.* **67**, 159 (1981).
- [114] G. Mirth and J.A. Lercher, *J. Catal.* **147**, 199 (1994).
- [115] G. Mirth, J. Cejka and J. A. Lercher, *J. Catal.* **139**, 24 (1993).
- [116] T. F. Narbeshuber, H. Vinek and J. A. Lercher, *J. Catal.* **157**, 388 (1995).
- [117] S. Zheng, A. Jentys and J. A. Lercher, *J. Catal.* **241**, 304 (2006).
- [118] S. J. Reitmeier, O. C. Gobin, A. Jentys and J. A. Lercher, *J. Phys. Chem. C* **113**, 15355 (2009).
- [119] G. S. Lee, J. J. Maj, S. C. Rocke and J. M. Garcés, *Catal. Lett.* **2**, 243 (1989).
- [120] J. Weitkamp and M. Neuber, *Stud. Surf. Sci. Catal.* **60**, 291 (1990).
- [121] D. Fraenkel, M. Cherniavsky, B. Ittah and M. Levy, *J. Catal.* **101**, 273 (1986).
- [122] E. Derouane, *J. Catal.* **100**, 541 (1986).
- [123] M. Neuber and J. Weitkamp, *Stud. Surf. Sci. Catal.* **49**, 425 (1989).
- [124] W. Souverijns, J. A. Martens, G. F. Froment and P. A. Jacobs, *J. Catal.* **174**, 177 (1998).
- [125] C. S. Laxmi Narasimhan, J. W. Thybaut, G. B. Marin, P. A. Jacobs, J. A. Martens, J. F. Denayer and G. V. Baron, *J. Catal.* **220**, 399 (2003).
- [126] J.A.Z. Pieterse, S. Veefkind-Reyes, K. Seshan, and J. A. Lercher, *J. Phys. Chem. B*, **104**, 5715 (2000).

Zeolites in refining and petrochemistry

Roberto MILLINI

*eni s.p.a. – refining & marketing division, San Donato Milanese Research Center,
Via F. Maritano 26, I-20097 San Donato Milanese (Milano – Italy)*

Abstract

Oil refining and petrochemistry are important industrial sectors where zeolites find a widespread use as heterogeneous acid catalysts and molecular sieves. The role and the increasing importance of zeolite catalysts is examined through the illustration of selected examples of consolidated processes: the Fluid Catalytic Cracking (FCC), one of the most important process in the modern refinery, and the synthesis of cumene, the intermediate in the production of phenol. Finally, the synthesis of 2,6-dimethylnaphthalene by alkylation of naphthalene and methylnaphthalene is reported as an example of emerging technology, whose development is strongly related to the use of new zeolite catalysts.

1. Introduction

“One can safely say that the impact of zeolites in science and technology in the last 50 years has no precedents in the field of materials and catalysis”: this sentence opens the Preface of a very recent book edited by Jiří Čejka, Avelino Corma and Stacey Zones¹. Nobody can disprove this sentence, since the introduction of zeolites in several industrial processes has brought important economical and environmental benefits. They replaced low-selective and harmful mineral acids and chloro-containing catalysts in several industrial processes, improving the yields and selectivities of the reaction, the quality of the products, the overall life of the catalyst (which is easily regenerable several times before being disposed), the energy consumption.

Refining and petrochemical industries have taken the major advantages from the introduction of zeolites as demonstrated by the fact that these sectors employ more than 90% of the industrial zeolite catalysts. In the common view, it is expected that the innovation in these areas proceeds through the optimization and incremental improvements of the existing processes rather than through the achievement of radical breakthroughs. Nevertheless, in the last few years, the situation has changed as a consequence of some trend-breaking events. The impressive growth of several countries (the so called BRICs above the others), favored by the globalization of the markets, has in fact induced an acceleration of goods and energy consumption with

the consequent negative effects on the price of raw materials and energy sources and on the environment. In particular, the increase of the costs of goods and energy as well as the severe regulations introduced by several countries for reducing the impact of the anthropogenic activity on the environment have induced a strong pressure to the industry. In this context, to satisfy the needs of the market and of the regulations, refining and petrochemical industries are requested to introduce innovative processes based on the use of more efficient and environmental friendly catalysts able to produce a given product with higher selectivity (lower by-product production) and lower energy requirements respect to the existing ones.

Due to their peculiar properties, zeolites are the ideal candidates for being employed as catalysts in refining and petrochemical processes and research in these fields takes advantage of the enormous mass of work done in the synthesis of new structures, in the modification of known materials, in the catalytic testing for the preparation of new products. In this chapter, it is highlighted the importance of zeolites in supporting technology innovation in refining and petrochemical industry.

2. The Zeolite Catalysts

197 zeolite framework types and 22 disordered zeolite framework (i.e. intergrowths of two or more different but structurally related frameworks), officially recognized by the Structure Commission of the International Zeolite Association², and several different microporous phases with a still unknown structure constitute the actual portfolio of microporous structures. Not only a framework type is different respect to any other in terms of pore architecture and size, but it can exist in different variants (in terms of type of framework constituents and relative composition). Literarily thousands of materials with different properties are therefore available, offering the possibility to the researcher to select the most suitable ones for the desired application.

Though several materials with different framework topology and composition have been tested as acidic, basic or oxidation catalysts in a variety of reactions, only a few of them have reached a commercial stage and are currently applied in refining and petrochemical industries. In 1999, Tanabe & Hölderich have published an interesting survey of the industrial processes based on the use of solid acid-base catalysts, highlighting the primary role played by zeolites³. They found that a total of 127 industrial processes employ 180 solid catalysts, of which 74 include at least a zeolite phase. A more detailed view of the survey results indicated that only a few framework types are effectively used, being MFI, FAU, MOR and Beta the most extensively employed³. Vermeiren & Gilson, who confirmed the prevalent use of the above reported zeolite structures and explicitly reported the other framework types employed, recently drew a more detailed overview on the commercial processes using zeolite-based catalysts⁴.

The worldwide consumption of synthetic zeolites is estimated at 1.7 – 2 million metric tons per year with a product worth amounting to ca. 1.8 billion USD in 2004⁵. Synthetic zeolites are mainly applied as detergent, adsorbents and desiccators, the overall consumption amounting to \varnothing 86% on a volume basis and \varnothing 73% on a value basis. Catalysts represent only \varnothing 14% of the overall volume but \varnothing 27% of the value, a clear indication that zeolite-based catalysts are more sophisticated and complex to synthesize than the zeolite materials used for other applications (e.g. LTA-type for detergent). In 2004, the market of synthetic zeolites for catalytic applications amounted to 241 ktons, corresponding to 665 ktons of final (i.e. shaped) catalysts⁵. Among them, the FCC catalysts, which alone account for + 90% of the overall synthetic zeolite consumption, take the lion's share. The lower contribution (on a volume basis) to the overall yearly consumption of the zeolite catalysts employed in other refining and petrochemical processes is not a sign of their scarce interest. It is instead related to characteristics of the different processes and to the overall life of the catalyst. In the case of FCC, for instance, there is the necessity to integrate frequently the inventory for replacing the spent catalyst, while for other processes it is not required because of the longer life of the catalyst.

3. Zeolites for Oil Refining

Oil refining is one of the most important industries worldwide, because it is where the crude oil, which has no value to the consumers, is transformed into products that can be used in the marketplace. A large number of excellent monographs covering in great details the complex world of oil refining are available⁶⁻⁸ and the interested reader can refer to them for a complete overview.

A modern oil refinery is constituted by a complex pool of different processes (Figure 1), which involve both physical separations (e.g., distillations, adsorptions, extractions) and chemical transformations (e.g., coking, hydrocracking, FCC, alkylations, etc.), necessary to efficiently transform the feedstock in useful product. What schematized in Figure 1 is just an example, since the actual configuration of a refinery depends on the needs. The refineries are classified according to their complexity, measured worldwide by the Nelson Complex Index (NCI). Developed in years 1960s and calculated by the Oil & Gas Journal annually, the NCI measures of the ability of a given refinery to adjust its production to the quality of feedstock and to the demand of finished products. Being referred to the crude distillation unit, a high NCI indicates a large secondary processing capacity, which generates more high-value products and higher refining margins respect to refineries of lower complexity. It is clear that a refinery of high complexity is equipped for facing the challenging problem induced by the evolution of the products demand with the continuous worsening of the quality of the feedstock in terms of API gravity (increase of molecular weight), metal (e.g. V, Ni) and heteroatoms (S and N) content.

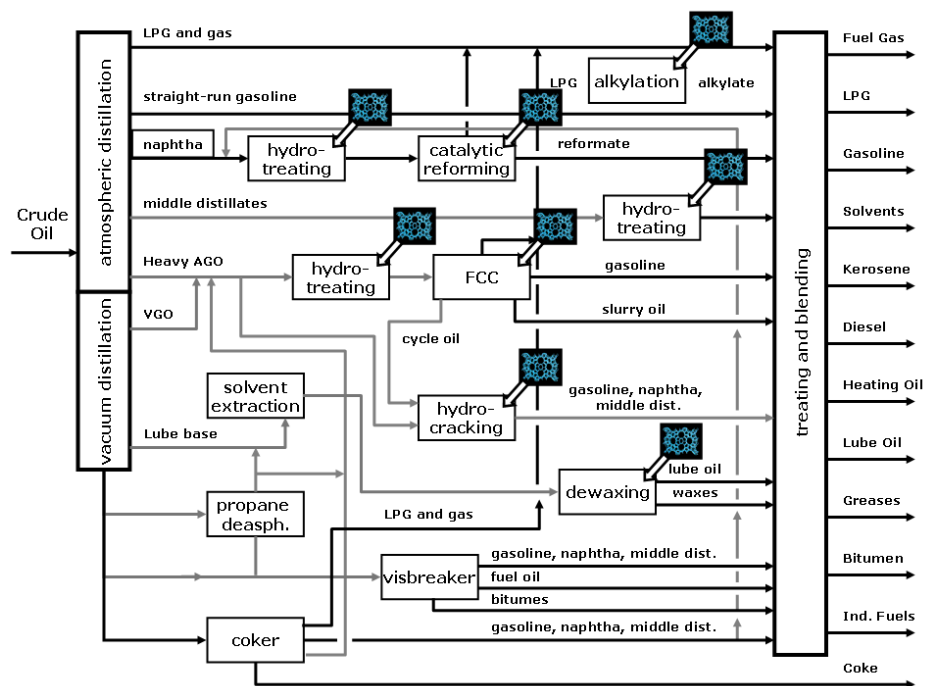


Figure 1. Modern oil refinery scheme indicating the processes employing zeolite-based catalysts.

The unit operations which mostly contribute to increase the complexity of a refinery are the cracking units, in particular the Fluid Catalytic Cracking (FCC) necessary to convert vacuum distillates and residues into more valuable products, mainly gasoline. Since its introduction in refinery, FCC represents the key technology because for decades it contributed to satisfy the increasing demand of gasoline. Today, this trend seems to be less adequate than in the past, particularly in Europe, where since the year 2000, the demand for diesel fuel is steadily increasing, with a continuous decline of the demand of gasoline. This trend is described in Figure 2, where the evolution of the demand of petroleum products in Europe in the period 2000 – 2020 is projected⁹. Such a situation (well evidenced in Figure 2 by the increase of the ratio middle distillates/gasoline) implies, already today, a net imbalance in Europe between demand and production of fuels, with a surplus production of gasoline which is exported in US and a deficit in diesel covered by the import from Asia. Obviously, unpredictable events may modify such a situation; for instance, the recent economic and financial crisis has had a negative impact on the European refining industry, which is now pressed to increase its competitiveness and to recover the loss of refining margins occurred in the last few years.

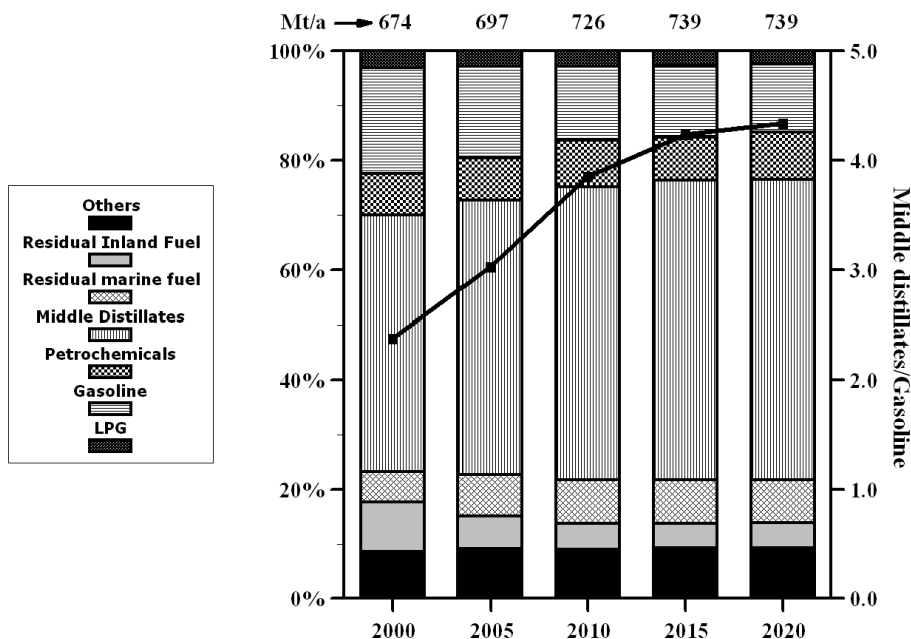


Figure 2. Evolution of products demand in Europe (source CONCAWE) ⁹.

To reach these objectives the modification/improvement of the refining technologies is necessary and, surely, the key factor is represented by the development of better performing catalysts, in particular zeolites-based catalysts used in several refining processes (Figure 1). Due to the limited space allotted, only the already introduced FCC process will be here treated in details, since it is the key technology in a refinery and the improvement of the zeolite-based catalyst employed may decisively contribute to solve the imbalance between demand and production of gasoline and diesel.

3.1 Fluid Catalytic Cracking (FCC)

The history of the catalytic cracking started some 90 years ago, when A. McD. McAfee (Gulf Refining Co.) claimed the use of AlCl_3 as cracking catalyst ¹⁰. A significant milestone in the history of this process was the introduction of heterogeneous catalysts such as activated clays ¹¹ and silica-aluminas ¹² made by E. J. Houdry in years 1930's. They proved to be more advantageous respect to AlCl_3 , but with an important drawback: the rapid deactivation of the catalyst due to the deposition of coke on the surface. The problem was successively solved with the development of new reactors and processes, including the semi-continuous cracking

operations (Thermofor Catalytic Cracking¹³) and, finally, the continuous cracking in fluidized bed reactor (FCC)¹⁴, the latter being the ancestor of the actual technology.

For 20 years the FCC process employed amorphous silica-alumina catalysts and only in 1964 the modern time of crystalline zeolite-based catalysts began¹⁵, practically in the same period in which Union Carbide patented the synthesis of Y zeolite¹⁶. The introduction of highly active zeolite-based catalysts can be rightfully considered as the real breakthrough in the development of the FCC process. In fact, zeolites have become the key component of FCC catalysts either as active phase or as additive for specific applications¹⁷. Besides, they have also allowed the development of the full-riser cracking, in which the contact time of the feedstock with the catalyst amounts to just a few seconds. Before treating in details the actual catalyst and the recent results of the research in this field, it is useful to describe briefly the overall FCC configuration.

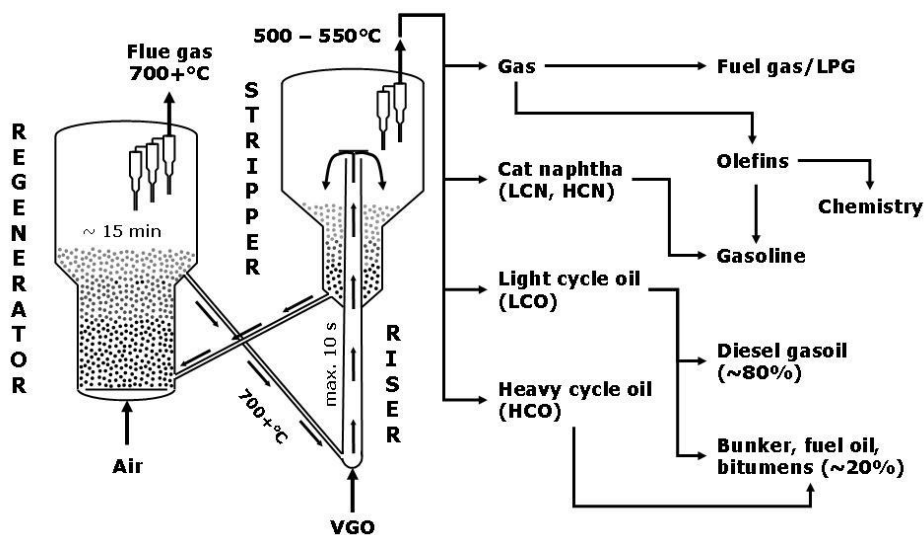


Figure 3. Simplified FCC configuration and typical distribution of the products.

The cracking reaction is endothermic and increases the number of moles of products respect to the feed. It is therefore favored at high temperature and low pressure. Furthermore, the catalyst undergoes coking very rapidly and should be frequently regenerated. The FCC configuration schematized in Figure 3 takes into account these few concepts: the preheated feed (vacuum gas-oil, VGO) is fed at the bottom of the riser (the reactor) where it is mixed with the catalyst. The endothermic cracking reactions occur in the riser where the volume expansion helps

the mix catalyst/feed to move upwards very rapidly (2 – 10 s). Then, the mix is sent to the stripper where the hydrocarbons are separated from the coked catalyst, which is finally steam-stripped from the adsorbed volatile products. The stripped coked catalyst is finally sent to the regeneration unit, where the coke is burned off with air for 10 – 15 min; the regenerated catalyst, at a temperature of 700+°C due to the exothermal combustion of coke, returned to the bottom of the riser ready for a new cycle.

Figure 3 also reports a scheme of the products typically generated by FCC and their finally destination use. Whereas the relative yields depend on the characteristics of the feed (e.g. paraffinic or aromatic) and of the catalytic system, all the streams have a defined use but olefins, cracking naphtha and LCO are the most valuable streams. Such a complex pool of products is the result of the secondary reactions (isomerization, cyclization, dehydrogenation, H-transfer) summarized in Figure 4, which occur together with the cracking⁴.

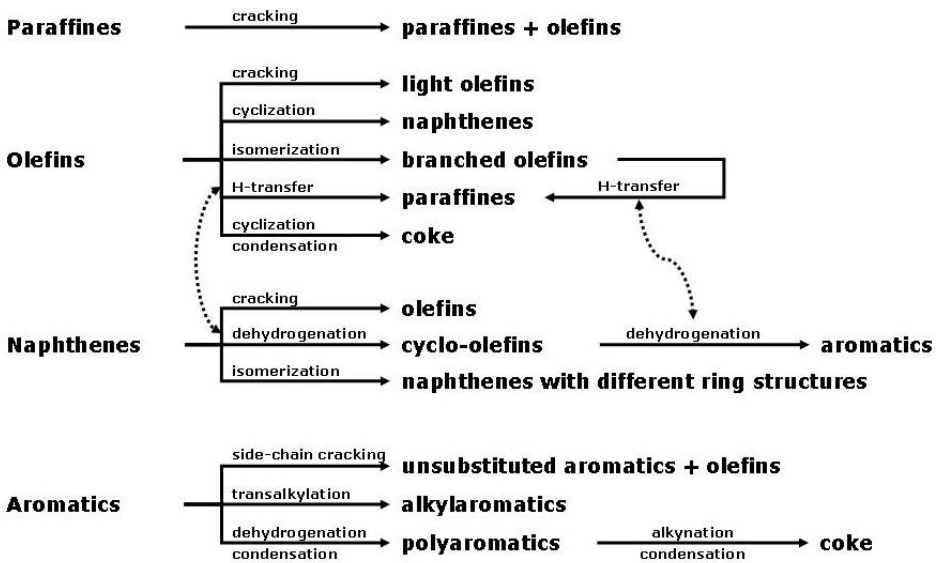


Figure 4. Main reactions occurring in the FCC process⁴.

With the exception of cracking, the most important reaction in this scheme is probably the H-transfer because it influences the distribution of the products. Essentially, the H-transfer reaction favors the redistribution of hydrogen among the saturated (or partially saturated) and unsaturated molecules, through hydride and proton transfers. For instance, a naphthene molecule may successively transfer

hydrides to olefins activated by the acid site to yield aromatic and paraffinic molecules¹⁸. This is important because aromatics and paraffins are more stable than naphthenes and olefins and their formation helps to increase the yield of gasoline. In this context, zeolites proved to be more efficient than the amorphous silica-alumina catalysts in maximizing the gasoline output, because the reaction occurs in the restricted space provided by the pores, favoring the bi-molecular pathway involving the H-transfer.

Zeolite Y, originally used as FCC catalyst, showed this effect but with some drawbacks. First of all, the high density of acid sites favors the H-transfer reaction yielding gasoline with low octane number due to the low concentration of olefins. Furthermore, the zeolite structure proved to be unstable under the steaming conditions present both in the stripper and in the regenerator, undergoing severe dealumination and massive crystallinity loss. In this way, the catalytic properties of Y zeolite may be affected by the formation of debris of alumina removed by the framework, which, from one side, increase the production of fuel gas and coke (as in the case of amorphous silica-alumina catalysts), from the other reduce the pore accessibility¹⁷.

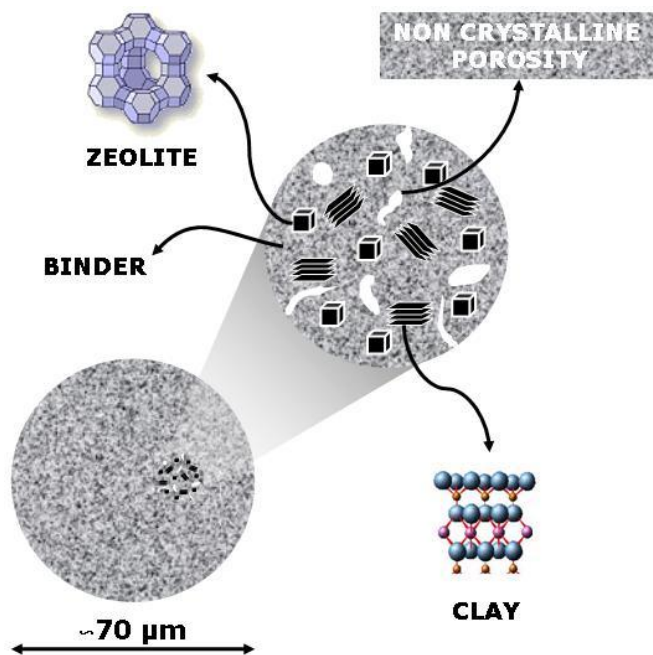


Figure 5. Schematic representation of a FCC catalyst.

These evidences stimulated the research, with the aim to improve the catalytic performances of zeolite Y and of the overall FCC catalyst. The long but, we would say, exciting way leading to the high-performance FCC catalysts available today is spangled with several important milestones, summarized in the following^{4,17}:

- incorporation of rare-earths (RE = La, Ce, etc., not necessarily as pure components) by ion-exchange in Y zeolite; RE allow the fine tuning of the acidic properties of Y zeolite, reducing the H-transfer reactions and coke formation, and increasing the resistance of the zeolite towards steam dealumination;
- development of manufacturing processes of ultra-stabilized Y zeolite (USY) which include appropriate dealumination conditions and successive silicon migration/incorporation to stabilize the defect sites; the lower Si/Al ratio in the framework assures higher stability under steaming, depressing in the same time the H-transfer reactions and coke formation;
- incorporation of RE in USY by ion-exchange for tuning the acidic properties of the zeolite catalyst.

Several other improvements of the catalyst have been achieved during the last decades, leading to the current FCC catalysts, a complex mixture of different components, each of them with a peculiar role. How an FCC catalyst is made?

The FCC catalyst

A schematic representation of a FCC catalyst is shown in Figure 5. It consists of spherical particles of ϕ 70 μm average diameter (20 – 120 μm range), suitable for the application in the fluidized circulating reactor. A deeper insight into the particles evidences that zeolite is only one of the components, the crystals being dispersed in an active matrix of alumina or silica alumina, together with clay particles. A fundamental characteristic of the FCC catalyst is represented by the porosity. The size of the pores of zeolite Y (12-membered ring opening with free dimensions of ϕ 7.5 \AA , interconnecting large spherical supercages with free diameter of ϕ 12.5 \AA) limits the accessibility of the molecules to the active sites. It is therefore necessary to tune the porosity of the silica-alumina matrix during the preparation procedure to generate porosity spanning from macro- to meso- to micropores. Figure 6 shows a scheme describing the ideal hierarchical pore architecture of a FCC catalyst¹⁹.

The improvements of the FCC catalyst achieved during the last 40 years have regarded not only the zeolite phase but even the other components, because differently from what observed in other shaped catalyst used, e.g., in petrochemical processes, the matrix is not merely a binder but also displays catalytic activity towards heavy molecules. The formation of macro- and mesoporosity is, therefore, necessary both for assuring the diffusion of the fluid within the catalyst particle, for providing the space necessary for cracking large molecules and, last but not least,

for protecting the catalyst from the detrimental effect of the metals (Ni and V above all) contained in the feed.

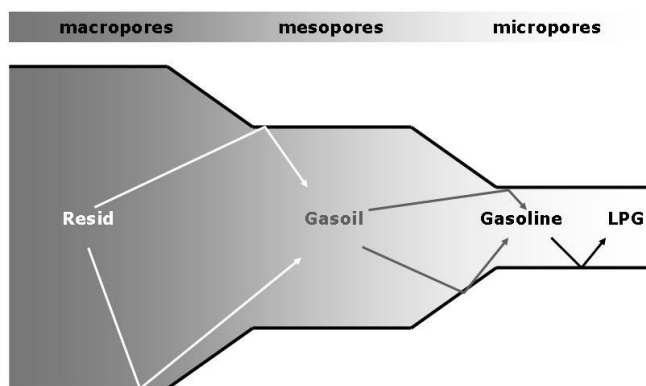


Figure 6. Schematic representation of the pore architecture of a FCC catalyst.

The hierarchical pore architecture schematized in Figure 6 is important because one of the challenges in FCC technology is the increase of the bottom cracking, i.e. the conversion of the fraction of the FCC feed with boiling point $> 430^{\circ}\text{C}$. It is constituted by molecules too large to pass through the pore openings of zeolites and their conversion requires the presence of active sites on the surface of the matrix²⁰. The non-zeolitic porosity has different catalytic effects, summarized in the following:

- mesopores ($d < 100 \text{ \AA}$) develop high specific surface area (SSA) and a large number of active sites; they strongly contribute to the bottom cracking activity but even to the selectivity towards coke and H_2 ;
- meso- and macropores in the range $100 < d < 1000 \text{ \AA}$ have relatively high SSA and display good bottom cracking activity but low selectivity towards coke and H_2 ;
- macropores ($d > 1000 \text{ \AA}$) contribute only marginally to the overall activity because of their very low SSA.

It is clear that mesopores represent an important feature of the FCC catalyst because they increase the possibility to crack heavy molecules, increasing the bottom cracking activity. However, when the mesopores are generated in the active matrix, the advantages associated to the increase of the bottom cracking activity are negatively compensated by the increase of coke and H_2 selectivity. The suitable modification of the characteristics of the matrix may limit the undesired reactions, provided that proper actions are taken for maintaining (or better, increasing) the

bottom cracking. One of them, recently proposed, is represented by the use of mesoporous Y zeolite. This zeolite usually crystallizes in form of μm -sized crystals, a feature which limits somewhat the mass transport in their interior. As a result, only the external part of the crystals is involved in the catalytic reaction with the net result of a low degree of catalyst utilization ²¹. A strategy for increasing the intracrystalline diffusion of molecules in the whole crystal comprises the synthesis of zeolites with hierarchical pore architecture. This was done by J. Garcia-Martinez, who developed a post-synthesis method for generating a complex network of mesopores in zeolite Y crystals, by hydrothermal treatment of preformed USY with an alkaline solution containing a surfactant (e.g. hexadecyltrimethylammonium bromide). In this way, the zeolite reconstructs itself in form of μm -sized crystals with open and extended mesoporosity obtained by burning off the surfactant molecules ²². When employed as FCC, the mesoporous Y zeolite displays better performances than USY in gasoline, bottom cracking and coke selectivity ²².

The overall composition of the FCC catalyst is determined also by other factors, including the necessity to handle the heavy metals (mainly Ni and V) present in the feed in form of metal organic complexes. This problem becomes more and more important because of the need to treat heavier feeds, which generally contain increasing concentrations of metal.

Nickel is an effective dehydrogenation catalyst, promoting the formation of H_2 and coke when present on the FCC catalysts. The early solution of this problem comprises the addition of small amounts of Sb compounds to the feed in order to favor the formation of Ni-Sb alloys substantially inactive in the dehydrogenation reaction ²³. More interestingly, the passivation of Ni can be achieved by exploiting the tendency of the oxide (NiO) to form solid solutions with alumina to form nickel aluminates of general formula $\text{Ni}_x\text{Al}_2\text{O}_{3+x}$ (with $0 \leq x \leq 1$), themselves characterized by very low dehydrogenation activity. Therefore, the problems induced by the deposition of Ni have been tackled by designing alumina-based binders able to passivate Ni, reducing its contribution to H_2 and coke formation.

Even vanadium represents a serious problem for FCC catalysts because, in addition to the promotion of undesired reactions, it has dramatic effects on the stability of the zeolite component. Oxidation of vanadium produces V_2O_5 , which is distributed over the entire catalyst because of its high volatility. It is transformed to H_3VO_4 by reaction with water and it is this acid which irreversibly reacts with Al atoms of the zeolite to give AlVO_4 and leading to the collapse of the zeolite structure ²⁴. The presence of Na ions, residue of the ion-exchange of the fresh zeolite and/or present in the feed, enhances the effect of vanadium. All these problems can be mitigated by adopting some measures, including the use of more stable zeolites (i.e. with lower Al and Na contents), the addition of V traps, i.e. components (e.g. MgO, CaO, SrO, La_2O_3) able to form stable vanadates.

Additives of the FCC catalyst

Till now, it has been examined the main components of a FCC catalyst. However, another important aspect deserves the attention: the use of additives. The addition of other components to the already complex FCC catalyst derives from specific needs, such as to promote the combustion, to increase the desulfurization, to enhance octane number of the gasoline and the olefins yield, to improve the bottom cracking. The use of these additives obviously depends on the feedstock characteristics as well as the products demand but particularly interesting are those based on zeolites.

Zeolite additives are often used for enhancing the octane number. This need derives from the fact that the gasoline output from FCC contains significant amounts of n-alkane and n-alkene molecules, characterized by significantly lower octane number respect to branched alkanes/alkenes and aromatics. The octane-enhancing can be achieved if n-alkanes/alkenes are preferentially removed, e.g. by selectively cracking them over zeolite catalyst displaying reactant shape selectivity properties. To do that, medium pore zeolite such as ZSM-5, very active in selective cracking but less prone to promote H-transfer reactions, proved to be efficient because of its ability to adsorb the linear hydrocarbons only and cracking them to lighter species²⁵. In other words, the octane number enhancement is due to the increased contents of branched hydrocarbons and aromatics, but the overall yield of gasoline is obviously reduced. However, the selective cracking leads to the production of light olefins (propylene and butenes), which are useful by-products. They can be feed to the alkylation unit (if present) to produce alkylates suitable for being added to the gasoline cut.

FCC is also a source of light alkenes used as raw materials in petrochemical processes and their production, where required, can be maximized by using zeolite additives. Corma *et al.* examined the influence of the pore topology of several zeolites on the cracking of n-heptane, selected as a model molecule in the gasoline range²⁶.

They found that the paraffins/olefins ratio increases as the void space dimensions increases (Figure 7) and provided useful indications about the distribution of the products (e.g. branched vs. linear) on the different zeolites. In particular, they confirmed that to maximize the propylene yield, zeolites with 9- and 10-membered ring openings would be preferred. ZSM-5 is one of them and it is used today as propylene additive in dedicated FCC units.

Another important issue concerns the possibility to use zeolite additives for enhancing the bottom cracking. Due to the lack of zeolite structures with pore openings large enough to allow the adsorption of heavy molecules, the idea would be to exploit the acid sites present on the surface or close to the pore mouths, for cracking part of the large molecules. This is possible, provided that the crystals are

small enough to maximize the external surface area, thus providing a sufficiently large number of active sites available for the reaction.

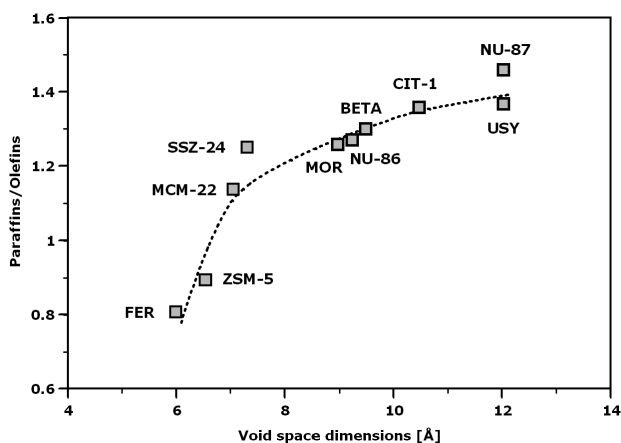


Figure 7. Paraffins/Olefins ratio in the cracking products of *n*-heptane as a function of the void space dimensions (adapted from ²⁶).

This concept has recently been verified when the Eni's proprietary material ERS-10 was tested as an additive of a commercial FCC catalyst ²⁷. The interesting disordered ERS-10 structure is an intergrowth of zeolites NON, EUO and NES ²⁸. The peculiarity of this phase is the presence of egg-shaped 14-MR openings, which offer the possibility to increase the conversion of heavy molecules. As a matter of fact, compared to the base case (i.e. the commercial catalyst without additives) the addition of just 3 wt% of ERS-10 resulted in the significant increase of the conversion to LPG and gasoline and to a significant increase of the bottom cracking ²⁷. These results, obtained in a fixed bed micro-activity test (MAT) unit, require further investigations on more complex units. Nevertheless, they are interesting because demonstrate that it is possible to exploit new zeolite structures as specific additives of the FCC catalyst.

New zeolites in FCC

The increasing availability of new zeolite structures with different pore architecture and composition has stimulated an extensive research with the aim to identify microporous materials which might replace zeolite Y, maintaining or better improving its catalytic performances. When considering the size of the molecules present in the feedstock, it is clear that the ideal candidates belong to the families of the large (12MR) and extra-large pore (14MR+) zeolites.

Very promising results have been obtained with different zeolites. For instance, a

patent filed in 1987 claimed the use of zeolite Beta and ZSM-20 (with the FAU-EMT intergrowth structure) as FCC catalysts able to enhance the octane number of gasoline²⁹. Zeolite Beta, in particular, displays high cracking activity and low H-transfer ability, producing high octane number gasoline³⁰. Its tendency to produce more gasses and coke during the cracking of gasoil can be reduced by tuning the crystallite size; in its optimized formulation, zeolite Beta produces almost the same gasoline yield as USY, but much greater amounts of propylene and butenes, which can be used for either producing gasoline alkylate and MTBE or re-addressed to petrochemical processes³¹. It was successively found that it is convenient to embed the zeolite Beta crystals in an amorphous silica-alumina matrix³²; in this way, zeolite Beta is stabilized towards de-alumination and consequent structure collapse which occurs during the treatment at high temperature³³.

Other interesting examples, among the several ones available in the literature, were reported by the group of Avelino Corma, very active in the synthesis and catalytic testing of new zeolites. The first example concerns ITQ-21, a large pore zeolite characterized by a 3D channel system, with circular 12MR openings, and large cages at their intersection³⁴. ITQ-21 proved to be effective in the cracking of Arabian Light vacuum gas-oil and more active than USY and zeolite Beta. In particular, it produces higher propylene yields in the gas fraction than USY. The olefins concentration in gasoline is the lowest with ITQ-21, but the octane number is the highest. These results indicate that, thanks to the peculiar pore architecture and framework composition, ITQ-21 might replace zeolite Y in the FCC catalyst formulation, because it produces higher propylene yield and less H-transfer products³⁴. The second more recent example is related to ITQ-33 zeolite. Its 3D pore architecture comprises 18MR linear channels, interconnected to a 2D system of 10MR channels³⁵; in other words, ITQ-33 is an example of extra-large pore zeolite and the large free dimensions of the 18MR channels (12.2 Å) is in principle very favorable for FCC applications (see above). The catalytic cracking tests of Arabian Light vacuum gas-oil confirmed that the peculiar pore architecture of ITQ-33 positively influences the products distribution. Furthermore, if combined with ZSM-5, it produces much higher diesel and propylene yield, with lower gasoline, than the combination USY/ZSM-5 does³⁵.

In summary, the possibility to replace zeolite Y in the FCC catalyst formulation exists, but there is a major drawback hampering that: the cost of the zeolites. Synthetic zeolites are usually obtained by time-consuming hydrothermal treatment under autogeneous pressure of a mixture containing, at least, the sources of silica and alumina and a specific organic additive (SDA), which is burned off from the crystallized product. On the contrary, zeolite Y is synthesized in a faster manner by treating a fully inorganic mixture at a moderate temperature. Consequently, its cost is much lower than the other zeolites, at least one order of magnitude lower than zeolite Beta, which among the zeolites cited above, is the only commercially

available. Furthermore, in the case of ITQ-21 and ITQ-33, the crystallization require the presence of germanium, even in large amounts ($\text{Si/Ge} = 2$, in the case of ITQ-33³⁵). Ge increases dramatically the cost of the final materials, rendering their possible industrial application at least questionable. In spite of these interesting results, it is likely that Y-type zeolites will maintain their specific role in the formulation of FCC catalyst for a long time.

4. Zeolites for Petrochemistry

Petrochemical is another important industrial sector worldwide where zeolites catalysts are frequently used. Compared to oil refining, where zeolites are used in a few conversion units (mainly in FCC), petrochemical industry takes more advantages of the peculiar properties of the zeolite catalysts. The reason is simple: oil refining processes are addressed to the transformation of complex hydrocarbon feedstocks into a broad range of similar products, with less stringent requirements in terms of reaction selectivity of the catalyst.

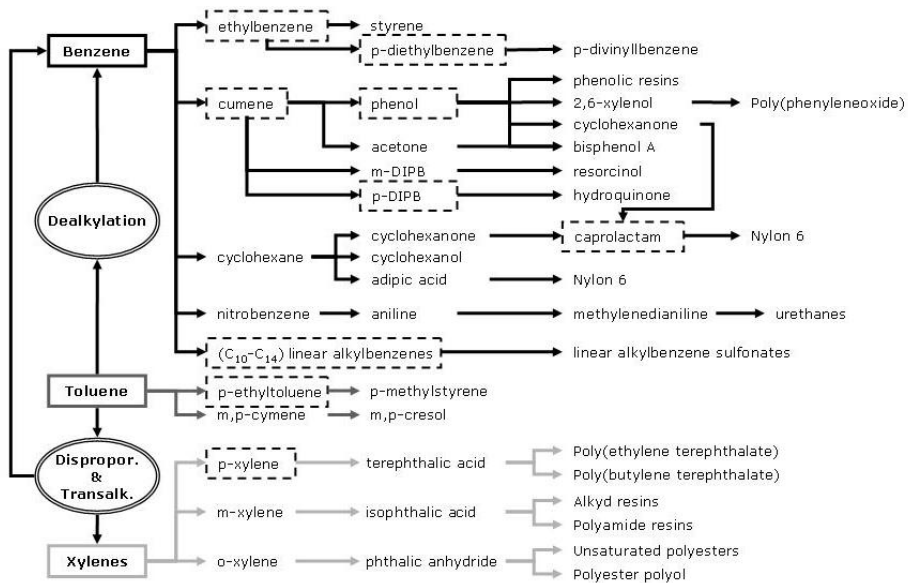


Figure 8. General overview of the products obtained from BTX. The intermediates produced with zeolite catalysts are marked with a dotted box

On the contrary, a petrochemical process is essentially based on the transformation of a well defined feedstock into a desired well defined product. In this case, the reaction selectivity is obviously of primary importance. The petrochemicals

building blocks (olefins, aromatics and syngas) are produced by different processes: steam reforming of various oil fractions or natural gas, catalytic reforming, FCC. When operated in the conditions which maximize olefins and aromatics production, the latter represent a sort of interface between refinery and petrochemistry, providing opportunities for both industries³⁶. Aromatics (benzene, toluene, xylenes, BTX), together with olefins, are the main feedstocks for petrochemistry. Their availability is increasing as a consequence of the new legislative limits on aromatics concentrations in fuels, which impose to switch their application from fuels to petrochemicals. Figure 8 illustrates a general, though not complete, overview of the products obtained by BTX building blocks: it is impressive the number and the variety of intermediated and final products produced, particularly if one considers that the worldwide demand of benzene, toluene and xylenes amounts to 41, 21 and 41 million tons per year, respectively. Zeolite-based catalysts are employed not only for toluene dealkylation to benzene and disproportionation/transalkylation to xylenes and benzene, but even in several processes for the production of important intermediates (dotted boxes in Figure 8). Most of them are produced by alkylation of benzene and toluene with olefins (e.g. ethylene and propylene to ethyl- and i-propylbenzene, or cumene, respectively), acid catalyzed reactions originally performed in the presence of strong mineral acids (HF, H₂SO₄) or Lewis acids (AlCl₃). Several drawbacks, however, arise from the use of these homogeneous acid catalysts: the low selectivity towards the desired product, the dangerous manipulation and transport, the corrosiveness, the difficult, energy-consuming and expensive separation and disposal. The use of solid acid catalysts may avoid all these problems, providing undoubted advantages in terms of selectivity, safety, regenerability, environmental compatibility, ... Among solid acids, zeolites are often preferred because they fully meet these requirements, particularly for what concerns their shape selectivity properties, which can be defined, in a simplified view, as the combination of catalysis with the molecular sieve effects³⁷. Several examples of development of new or improved industrial processes based on the use of zeolite catalysts exist and the interested reader can refer to the interesting reviews available in the literature^{3,4,38-41}. The aim of this contribution is therefore to show how the zeolite catalysts are developed focusing the attention on a couple of significant examples rather than to merely summarize all the main existing processes. In particular, the processes for the synthesis of cumene, an important intermediate for the synthesis of phenol and other intermediates (Figure 8) and 2,6-dimethylnaphthalene (an intermediate for the preparation of the high performance polyethyleneterephthalate, PEN, polyester) are considered in the following. Before entering in the details of these processes it is, however, useful to spend few words on the different steps involved in the development of a heterogeneous catalyst.

4.1 Catalyst development

The development of an industrial heterogeneous catalyst is a quite complex process; it involves several different steps requiring a multi-disciplinary knowledge (Figure 9). Multi-disciplinary because it requires competences in the synthesis of materials, in their accurate characterization and catalytic testing, in the formulation and shaping according to the reactor technology: fixed bed, fluidized bed, slurry, etc.

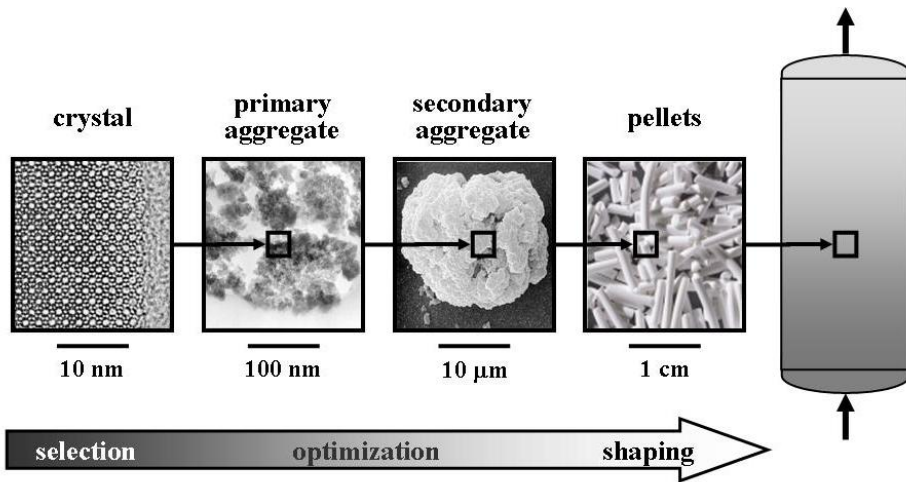


Figure 9. The catalyst development cycle.

The entire cycle is usually time consuming and therefore expensive, often requiring several years for developing the idea in an industrial application. Nevertheless, the key of success is represented by the accurate control of all the steps involved in the development cycle, the entire costs being recovered in a short time when the process is applied at an industrial level.

4.2 Synthesis of cumene

Originally employed as an octane enhancing component of gasoline, cumene is currently an intermediate in the synthesis of phenol; the worldwide yearly production amounts to 8 million metric tons, accounting for around 17% of the overall benzene demand, the second most important after the synthesis of ethylbenzene, which consumes ca. 50% of the benzene produced for petrochemical applications.

The synthesis of cumene involves the alkylation of benzene with propylene via the secondary carbocation generated by the interaction with the Brønsted acid site

(Figure 10). Several side and consecutive reactions, potentially affect this apparently simple reaction: successive alkylation of cumene to di- (DIPBs) and tri-isopropylbenzenes (TIPBs) (which can be considered useful by-products since they can be converted to cumene by transalkylation with benzene), secondary isomerization of cumene to n-propylbenzene (nPB), oligomerization of propylene to higher olefins, which in turn can undergo cracking and isomerization and even alkylate aromatics to produce higher alkylbenzenes (Figure 10). In this scenario, it is easy to understand that an industrial process, to be successful, should imply the use of conditions which limit the side- and consecutive reactions (e.g. working with a high benzene/propylene ratio to limit poly-alkylation and propylene oligomerization) together with a selective catalyst able to maximize the yield of cumene.

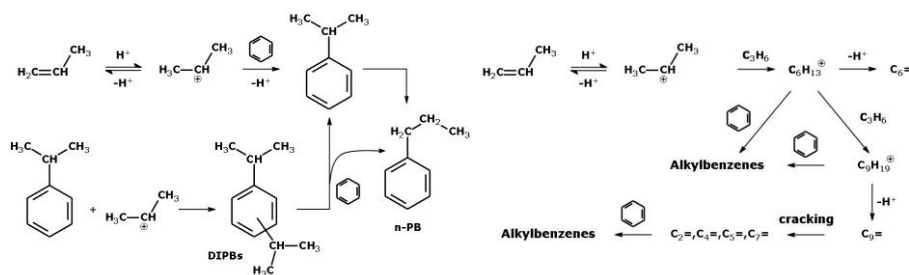


Figure 10. Acid catalyzed reactions involved in the synthesis of cumene.

The evolution of the cumene processes is somehow related to that of ethylbenzene, since the catalytic systems developed are often employed in the production of both intermediates.

Cumene was initially produced with sulfuric acid as homogeneous catalyst; this process was replaced soon by the UOP technology, which makes use of solid phosphoric acid (SPA) as a heterogeneous catalyst⁴². This process is still the most diffused in cumene production (at least as a number of installations), in spite of the significant progresses recently achieved. The first one concerned the development of the Monsanto-Lummus technology based on $\text{AlCl}_3\text{-HCl}$ catalyst⁴³; a few plants were, however, realized with such a technology because of the serious drawbacks related to the use of a homogenous catalyst.

The possibility of substituting these catalysts with environmental friendly, non-corrosive and regenerable materials such as zeolites has been evaluated since the mid of years 1960s, when Minachev et al.⁴⁴ and Venuto et al.⁴⁵ used X and Y zeolites for the alkylation of benzene with light olefins in the gas phase. ZSM-5 catalyst, employed in the Mobil-Badger ethylbenzene technology, was also tested in

the gas-phase alkylation of benzene with propylene but the results were unsatisfactory because of the high production of the undesired n-propylbenzene, probably due to the high temperature necessary to overcome the constraints imposed to diffusion of cumene by the narrow 10MR channels of MFI, and of the rapid decay of the catalyst due to the oligomerization of propylene with the formation of heavy products in the pore⁴⁶. ZSM-5 proved to be poorly active also in liquid-phase alkylation of benzene with propylene⁴⁷, indicating that the most suitable catalysts for cumene synthesis should be selected among the large pore zeolites. As a matter of fact, during the years 1990s new industrial processes based on the use of such kind of zeolites were developed.

In particular, CDTech proposed the use of a Y-type catalyst operating in a catalytic distillation column reactor, a system with good catalytic performances⁴⁸, but not commercially diffused. The 3-DDM cumene process developed by Dow-Kellog is based on dealuminated mordenite catalyst; dealumination is necessary to connect in some way the otherwise modimensional 12MR channel into a three-dimensional porous system, with enhanced performances and stability⁴⁹. UOP, from its side, developed the Q-Max process, probably based on zeolite Beta as a catalyst⁵⁰. The Mobil-Raytheon cumene technology, operating with a fixed bed reactor system, makes use of MCM-22 as a catalyst⁵¹. This is interesting because MCM-22 is a medium pore zeolite, but its peculiar structure characteristics render it suitable for applications in reactions requiring large pore systems. This aspect will be treated later in details. Finally, EniChem (now Polimeri Europa) also developed an alkylation technology based on the use of zeolite Beta as a catalyst⁵². The proprietary PBE-1 catalyst is employed both in ethylbenzene and cumene productions.

Zeolite Beta was selected among different zeolite candidates (mordenite, ERB-1, USY and ZSM-12) on the basis of the results of the catalytic tests performed at 150°C with molar ratio benzene/propylene = 7⁵³. Zeolite Beta showed to be the most efficient catalyst in terms of overall selectivity to cumene and by-products production (Figure 11). In the successive optimization activity, the framework composition and crystal/aggregate morphology were accurately tuned in order to improve the overall catalytic performances of the catalyst.

Attention was finally devoted to the shaping of the catalyst, performed by mixing the zeolite powder with a selected binder (e.g. γ -Al₂O₃) and extruding the mixture in form of pellets of the desired shape and dimensions. The formulation and shaping conditions were accurately selected in order to maximize the extra-zeolite porosity, without losing the crushing strength of the pellets. Girotti *et al.* demonstrated that the extra-zeolite porosity is an important feature of the final catalyst because it influences the life of the catalyst, which increases as the overall pore volume of the pellets increases (Figure 12)⁵⁴.

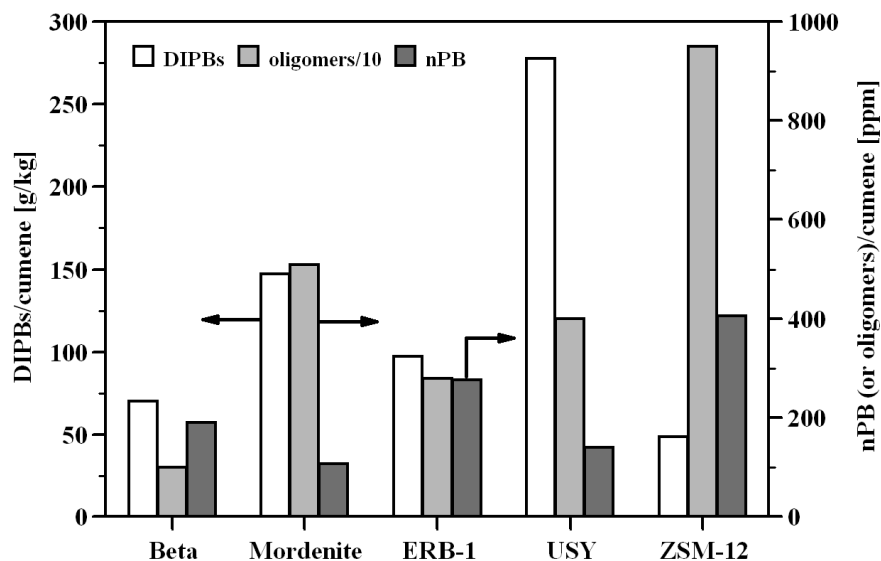


Figure 11. By-product selectivities in benzene alkylation with propylene over large pore zeolite⁵³. The data related to oligomers are divided by 10.

Coming back to the catalyst selection, molecular mechanics and dynamics calculations performed to support the experimental investigations gave interesting results. In particular, calculations of the minimum energy pathway (MEP) indicated that cumene diffuses substantially unhindered through the pore systems of *BEA, MOR, FAU and MTW, in agreement with the experimental results⁵³. On the contrary, the same calculations performed on MWW evidenced what Perego *et al.* defined as an unusual behavior. In fact, the high energy barriers, hampering the diffusion of cumene through the two MWW pore systems (both having 10MR openings), were in contrast with the excellent catalytic behavior of this zeolite, much closer to that of large pore zeolites⁵³.

The reasons of the unexpected catalytic performances in cumene synthesis were found examining the peculiar pore architecture of MWW structure, which is made up by two non-interconnected systems: one formed by large supercages (a sort of cylinder 18 Å long and 7.1 Å wide) interconnected by slightly elliptical 10MR windows, the other by sinusoidal channels also with 10MR apertures⁵⁵.

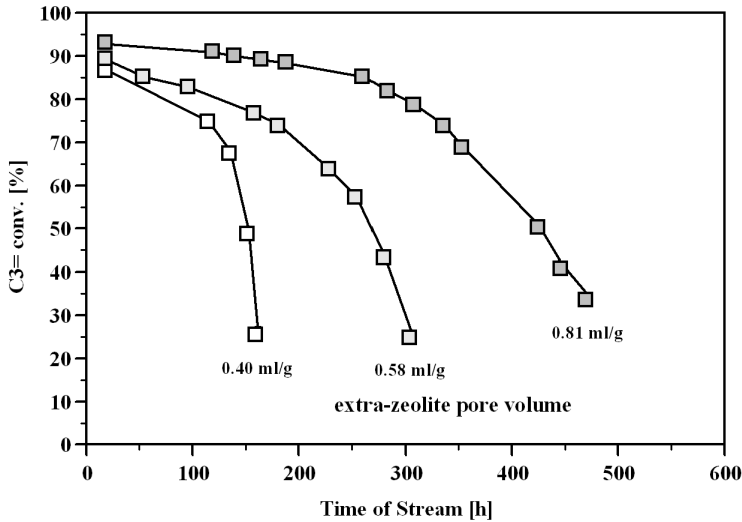


Figure 12. Propylene conversion as a function of extra-zeolite pore volume in extruded zeolite Beta catalysts⁵⁴.

MWW-type zeolites have another peculiarity: their formation occurs through the initial crystallization of a 2D layered precursor in which the layers (one unit cell thick, $\varnothing 25 \text{ \AA}$, containing the sinusoidal channel system and large pockets, the emi-supercages, on the external surface) are aligned vertically but not covalently connected along the crystallographic (001) direction⁵⁶. The calcination at $T > 270^\circ\text{C}$ leads to the formation of the 3D ordered MWW structure through the condensation of the silanol groups located on the surface of the layers. In this way, the second pore system (containing the supercages) forms, while on the [001] surface of the platelet-like crystals are still present the emi-supercages, circular pockets having a free diameter of 7.1 \AA . It is in these emi-supercages where cumene and DIPBs form, under a steric control but without diffusion limitations (Figure 13)⁵³. On the contrary, the rather narrow pore sizes prevent the diffusion of cumene in the pore system containing the large cages so that, even if formed, it is retained in the supercages. Sastre *et al.* later confirmed this hypothesis on the basis of accurate molecular dynamics simulations⁵⁷.

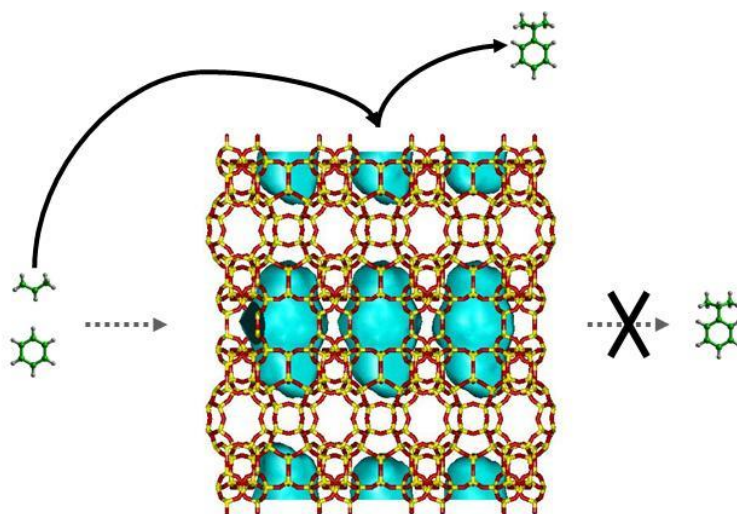


Figure 13. Structure of MWW highlighting the space occupiable by cumene.

Together with Beta, MWW-type zeolites are excellent catalysts for cumene production⁵⁸ but, according to the mechanism reported above, it is clear that only a minor part of the entire catalyst (i.e. the [001] surface of the crystals) is involved in the reaction. To increase the accessibility of the internal surface of MWW zeolite, different approaches were developed, thanks to peculiar features of this system recently summarized by Roth & Dorset⁵⁹. The most interesting involves the swelling and the successive delamination of the precursor, as described by Corma *et al.* for the preparation of ITQ-2⁶⁰. Respect to the 3D structure (MCM-22), the delamination process improves the accessibility of the active sites without affecting their catalytic activity, as demonstrated in different reaction tests. On the same concept is based the synthesis of MCM-56⁶¹ and more recently of UZM-8⁶². The latter has been claimed to display better catalytic activity in cumene synthesis than MCM-22 and MCM-56⁶³.

Several other zeolite structures have been tested in the alkylation reaction of aromatics with light olefins. For a number of reasons (e.g. difficult synthesis procedure, high costs), none of them will replace in a near future Beta and MCM-22 as catalysts for the industrial production of cumene. Nevertheless, some very promising results have been reported stimulating the research in the field.

One above the others concerns the already cited ITQ-33 zeolite, which was reported to be more stable than Beta in the benzene alkylation with propylene⁶⁴. Due to the presence of extra-large 18MR pores, the selectivities towards poly-alkylated

products (DIPBs and even TIPBs) are much higher than with Beta zeolite catalyst, but this is not considered a detrimental effect because of the presence of transalkylation units in the cumene industrial processes. More interesting is the very low selectivity to nPB (< 100 ppm), much better than the other commercial processes⁶⁴. Hence, a very promising catalyst but, again, with a serious drawback: its synthesis still requires a large amount of germanium (Si/Ge = 2 in the synthesis mixture^{35,64}). Only when an optimized procedure for the synthesis of Ge-free ITQ-33 will be developed, the potentiality of this zeolite in refining and petrochemical processes will be fully explored.

4.3 Synthesis of 2,6-dimethylnaphthalene (2,6-DMN)

The present petrochemical industry consists of consolidated productions, whose improvement is limited to the development of new more efficient catalysts, and the cumene production illustrated above is a clear example. The evolution of petrochemistry is strongly linked to the development of technologies which represent, for instance, alternative routes to the production of given chemicals respect to the existing ones. Vermeiren & Gilson⁴ identify a number of emerging technologies based on the use of zeolite catalysts, which include the skeletal isomerization of butenes and pentenes, the selective cracking of C_{4+} olefins to propylene, the methylation of toluene to xylenes, the one-step synthesis of styrene *via* side-chain alkylation of toluene with methanol, the methanol to olefins (MTO) process, etc.

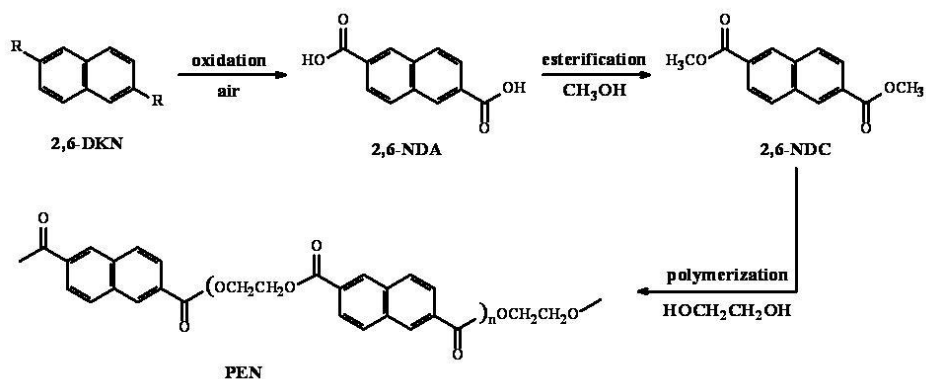


Figure 14. Synthesis of polyethylene-naphthalate (PEN).

Innovation, however, means also new products with improved properties respect to the existing ones and the production of 2,6-dimethylnaphthalene (2,6-DMN) certainly constitutes a clear example. 2,6-DMN is a key-intermediate in the synthesis of polyethylene-naphthalate (PEN, Figure 14) which, compared to other

thermoplastic polyester (e.g. PET), has improved thermal, mechanical and gas barrier properties.

2,6-DMN is preferred to other 2,6-dialkyl-derivatives (e.g. diethyl- or diisopropyl-naphthalene) because no C atoms are lost during the oxidation step. Its availability and high costs, however, still represent serious obstacles to the mass production of PEN. Different synthesis routes to 2,6-DMN have been proposed⁶⁵, but today only BP-Amoco produces it on a relatively large scale (30 kton/y), through the rather complex 4-step process shown in Figure 15. Interestingly, this process makes use of zeolites catalysts in two different steps: the cyclization of 5-*o*-tolylpentene and the final isomerization of 1,5-DMN to 2,6-DMN with zeolite Beta.

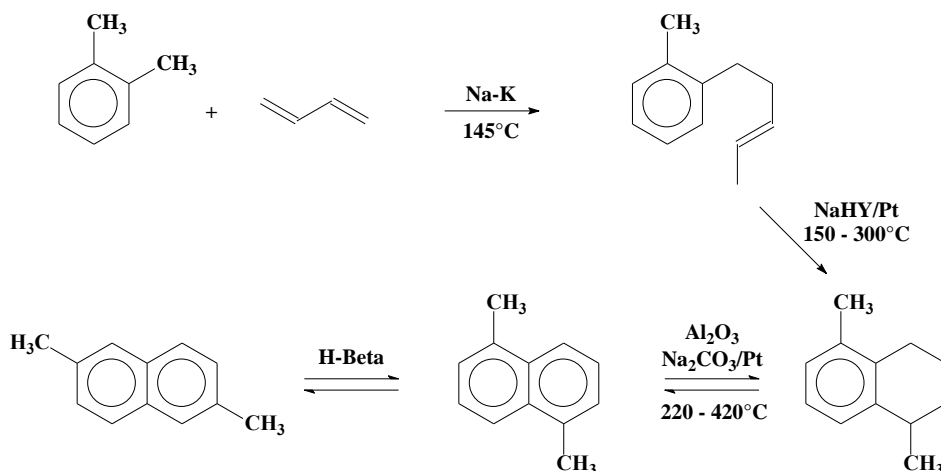


Figure 15. The BP-Amoco process for the production of 2,6-DMN.

From the industrial point of view, the synthesis of 2,6-DMN through the alkylation of naphthalene (NAPH) or methyl-naphthalene (MN) would be a simpler and more desirable synthesis route. In 1992, researchers at Teijin claimed a 2-step process in which naphthalene is firstly reacted with an isomeric DMN mixture to produce MNs; at the same time the amount of 2,6-DMN increases as a consequence of the isomerization of DMNs. Successively, MNs are methylated with methanol to produce a 2,6-DMN enriched product⁶⁶. The yields are low and that imposes extensive recycling with consequent high production costs. More recently, a process combining the Mobil's synthesis technology based on the use of MCM-22 catalyst for the methylation of NAPH and MNs and the Kobe Steel's DMNs separation technology promised to reduce the costs of producing 2,6-DMN⁶⁷. The process proved to be effective when using 2-MN as pure feedstock since a ratio 2,6-/2,7-DMN = 2.3 (well above the thermodynamic value of φ 1) was obtained. However,

the same ratio dropped down to 1.2 – 1.5 when a mixture of MN isomers is fed and that significantly reduces the economics of the entire process⁶⁷.

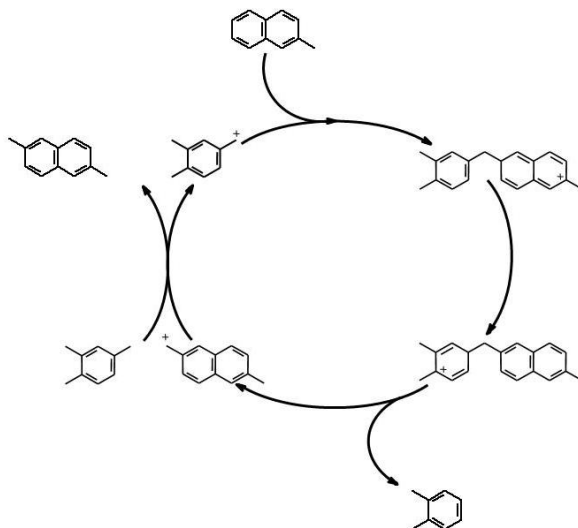


Figure 16. Proposed mechanism for the methylation of 2-MN with TMB.

Several research groups have exploited the possibility to use zeolite catalysts for developing an efficient process able to produce 2,6-DMN in high yields and with DMN isomers distribution far from the equilibrium either by direct alkylation with methanol (with or without paraffinic or aromatic solvents) or by disproportionation of MNs. A variety of different zeolite structures, including ZSM-5, ZSM-11, ZSM-12, mordenite, Y, beta, MCM-22 and NU-87 have been tested in different conditions⁶⁸⁻⁸⁰, but the most interesting results were obtained by using ZSM-12 in the presence of 1,2,4-trimethylbenzene (TMB) as solvent/reagent, together with methanol⁸¹. ZSM-12 was selected among different medium (MFI and EUO) and large-pore (*BEA, MOR, MAZ, FAU, LTL, OFF and MTW) zeolites by using modeling tools based on molecular mechanics and dynamics⁸². Starting from the mechanism proposed for the reaction, which involves TMB as alkylating agent (Figure 16), the minimum energy pathways for the diffusion of NAPH, MN and selected DMN isomers (1,5-, 1,6-, 2,6- and 2,7-DMN, taken as representative of the different steric situations) in the different zeolite models were computed. The results indicated that medium pore zeolites are not good candidates for the reaction, due to the high energy barriers hampering the diffusion of MN and DMN isomers. On the contrary, the behavior of large pore zeolites depends on the architecture and effective size of the pore openings; some of them (MOR, MAZ, *BEA and FAU) were predicted to be completely unselective allowing to diffuse substantially

unhindered even the molecules bearing $-\text{CH}_3$ in α position (Figure 17). They can be used in the isomerization of 1,5- and 1,6-DMN to 2,6-DMN (in reality zeolite Beta is used for this reaction in the last step of the BP-Amoco process, Figure 15) The others showed significant differences in the MEPs, with high energy barriers hampering the diffusion of the bulkiest molecules. The case of MTW (ZSM-12) was particularly interesting because 2,6-DMN was predicted to diffuse substantially unhindered in the linear but puckered 12MR channels, while all the MN and DMN isomers with at least a $-\text{CH}_3$ in α position together with 2,7-DMN were not (Figure 17). In other words, MTW was predicted to have marked product shape selectivity properties, features confirmed by the catalytic tests. ZSM-12 gave, in fact, the highest 2,6-DMN yields with a 2,6-/2,7-DMN ratio in the range 2.0 – 2.6, well above the thermodynamic value of $\varphi 1$ obtained with the other zeolites. The unique catalytic performances of ZSM-12 were further explained by the fact that it possesses also transition state shape selectivity properties since it provides the highest stabilization of the 1,2-diarylmethane intermediate molecules leading to 2-MN, 2,6-DMN and 2,7-DMN (Figure 16) and their formation can be considered more probable than for those involved in the formation of molecules with a $-\text{CH}_3$ in α position⁸².

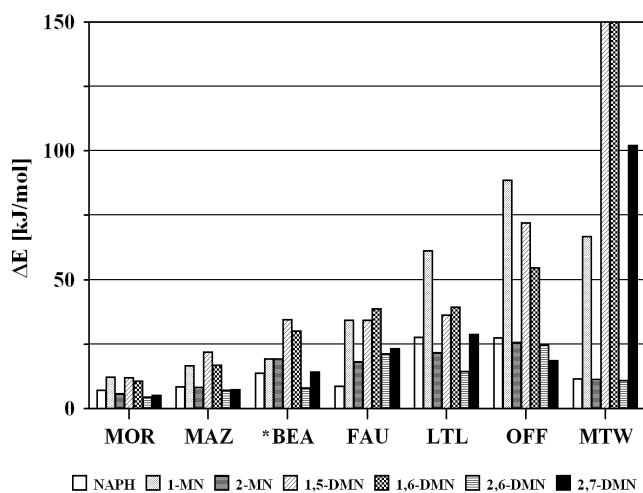


Figure 17. Energy barriers for the diffusion of molecules in large pore zeolites⁸².

The tests performed at a pilot plant level using a low value refinery stream containing naphthalene and methynaphthalenes confirmed the good preliminary

data, with high selectivity towards 2,6-DMN (ϕ 30% to be compared with the thermodynamic data of 12.8%), high yields (> 60%) of useful isomers (1,5- and 1,6-DMN should be considered useful products because they can be isomerized to 2,6-DMN with an acid catalyst, such as zeolite Beta) and, overall, a very favorable 2,6-/2,7-DMN ratio, constantly above 2. These interesting results demonstrated the effectiveness of the process, ready to be scaled to the industrial production once the favorable conditions will permit it.

5. Conclusions

From the examples here reported it is clear that zeolites have found important applications as acid catalysts in several refining and petrochemical processes. Their peculiar structural properties together with the possibility to tune their composition and morphology render them unique among the variety of different materials available for catalytic applications. The benefits for huge industrial sectors such as oil refining and petrochemistry are undoubted and they are not only economic, since the development of zeolite catalysts has allowed the replacement of the harmful, dangerous and corrosive mineral acids in several processes. Environment takes therefore great advantages from the use of zeolite catalysts, whose activity and selectivity contribute to reduce the energy demand and the by-product production.

This is not, however, the end of the story: the industry has to face important challenges imposed by the worsening of the quality of the feedstocks, by the evolution of the market demand and by the more and more pressing environmental legislation. In this context, research plays a primary role. From one side, the continuous discovery of new zeolite structures with novel pore architecture and characteristics, increases the portfolio of materials available. From the other, the deeper and deeper collaboration between academia and industry generates new ideas and technologies necessary for assuring the development of these important industries.

References

- [1] Čejka, J., Corma, A. & Zones S. in *Zeolite and Catalysis. Synthesis, Reactions and Application* Vol. 2 (eds J. Čejka, A. Corma & S. Zones), Wiley-CVH, Weinheim, Preface, xiii-xvi (2010).
- [2] Database of Zeolite Structures: <http://www.iza-structure.org/databases> as in April 2011.
- [3] Tanabe, K. & Hölderich, W. F. Industrial application of solid acid-base catalysts. *Appl. Catal. A: General* **181**, 399-434 (1999).
- [4] Vermeiren, W. & Gilson, J.-P. Impact of zeolites on the petroleum and petrochemical industry. *Top. Catal.* **52**, 1131-1161 (2009).
- [5] Davis, S. & Inoguchi, Y. *Zeolites Chemical Economic Handbook*, SRI Consulting (2009).

- [6] Speight, J. G. & Özüm B. *Petroleum Refining Processes*, Marcel Dekker Inc., New York, (2002).
- [7] *Handbook of Petroleum Processing* (eds D. S. J. Jones & P. R. Pujadó), Springer, Dordrecht (2006).
- [8] Fahim, M. A., Al-Sahhaf, T. A. & Elkilani, A. S. *Fundamentals of Petroleum Refining*, Elsevier, Amsterdam (2010).
- [9] CONCAWE Report no. 8/08 (December. 2008). *Impact of Product Quality and Demand Evolution on EU Refineries at the 2020 Horizon*. p. 8, <http://www.concawe.org/Content/Default.asp?PageID=31>.
- [10] McAfee, A. McD. Manufacture of Gasoline. *U.S. Patent 1,405,054*, (1922), assigned to Gulf Refining Company.
- [11] Houdry, E. J. Process and Apparatus for the Treatment of Heavy Oils and the like for the Conversion thereof into Lighter Products. *U.S. Patent 1,957,648* (1934), assigned to Houdry Process Co.
- [12] Houdry, E. J. Catalytic Materials and Process of Manufacture. *U.S. Patent 2,078,945* (1937), assigned to Houdry Process Co.
- [13] Houdry, E. J. Operation of Catalytic Plants. *U.S. Patent 2,387,267* (1945), assigned to Houdry Process Co.
- [14] Campbell, D. L., Martin, H. Z., Murphree, E. V., & Tyson, C. W. Method of and Apparatus for Contacting Solids and Gases. *U.S. Patent 2,451,804* (1948), assigned to Standard Oil Development Co.
- [15] Plank, C. J., & Rosinski, E. J. Catalytic Cracking of Hydrocarbons with a Crystalline Zeolite Catalyst Composite. *U.S. Patent 3,140,249* (1964), assigned to Socony Mobil Oil Corp.
- [16] Breck, D. W. Crystalline Zeolite Y. *U.S. Patent 3,130,007* (1964), assigned to Union Carbide Corp.
- [17] Biswas, J. & Maxwell, I.E. Recent Process- and Catalyst-Related Developments in Fluid Catalytic Cracking. *Appl. Catal.* **63**, 197-258 (1990).
- [18] Corma, A. & Martinez, A. *Stud. Surf. Sci. Catal.* **157**, 337-366 (2005).
- [19] O'Connor, P. & Humphies, A. P. Accessibility of functional sites in FCC. *Prep. - Am. Chem. Soc. Div. Petrol. Chem.* **38**, 598-603 (1993).
- [20] Bellussi, G., Carati, A. & Millini, R. Industrial potential of zeolites in *Zeolite and Catalysis. Synthesis, Reactions and Application* Vol. 2 (eds J. Čejka, A. Corma & S. Zones), Wiley-VCH, Weinheim, 449-491 (2010).
- [21] Pérez-Ramírez, J., Christensen, C. H., Egeblad, K., Christensen, C. H., & Groen, J.C. Hierarchical zeolites: enhanced utilisation of microporous crystals in catalysis by advances in materials design. *Chem. Soc. Rev.* **37**, 2530-2542 (2008).
- [22] Garcia-Martinez, J. Methods for making mesostructured zeolitic materials. *U.S. Patent Application 2008/0132874 A1* (2008), assigned to Rive Technology, Inc.

- [23] Nielsen, R. H., & Doolin, P. K. Metal passivation in Fluid Catalytic Cracking: Science and Technology. *Stud. Surf. Sci. Catal.* **76**, 339-384 (1993).
- [24] Habib, E. T. Jr., Zhao, X., Yaluris, G., Cheng, W. C., Boock, L. T., & Gilson, J.-P. in *Zeolites for Cleaner Technologies* (eds M. Guisnet & J.-P. Gilson) Ch. 5, Imperial College Press, London (2002).
- [25] Dwyer, F. G., & Degnan, T. F. Shape selectivity in catalytic cracking in Fluid Catalytic Cracking: Science and Technology. *Stud. Surf. Sci. Catal.* **76**, 499-530 (1993).
- [26] Corma, A., González-Alfaro, V., & Orchillés, A. V. The role of pore topology on the behaviour of FCC zeolite additives. *Appl. Catal. A: General* **187**, 245-254 (1999).
- [27] Bellussi, G., Millini, R., Rizzo, C., & Colombo, D. Cracking process and enhanced catalysts for said process. *WO Patent 2009/147496* (2009), assigned to eni s.p.a.
- [28] Zanardi, S., Cruciani, G., Carluccio, L. C., Bellussi, G., Perego, C., & Millini, R. Framework topology of ERS-10 zeolite. *Angew. Chem. Intern. Ed.* **41**, 4109-4112 (2002).
- [29] Edwards, G. C., & Peters, A. W. Cracking catalysts with octane enhancement. *European Patent 243,629* (1987), assigned to W. R. Grace & Co.
- [30] Corma, A., Fornés, V., Montón, J. B., & Orchillés, A. V. Catalytic activity of large-pore high Si/Al zeolites: Cracking of heptane on H-Beta and dealuminated HY zeolites. *J. Catal.* **107**, 288-295 (1987).
- [31] Bonetto, L., Cambor, M. A., Corma, A., & Pérez-Pariente, J. Optimization of zeolite- β in cracking catalysts. Influence of crystallite size. *Appl. Catal. A: General* **82**, 37-50 (1992).
- [32] Kubicek, N., Vaudry, F., Chiche, B. H., Hudec, P., Di Renzo, F., Schulz, P., & Fajula, F. Stabilization of Zeolite Beta for FCC Application by embedding in maorphous Matrix. *Appl. Catal. A: General* **175**, 159-171 (1998).
- [33] Millini, R., Perego, C., Parker Jr., W. O., Flego, C., & Girotti, G. Stability upon Thermal treatment of Coked Zeolite Beta. *Stud. Surf. Sci. Catal.* **154**, 1214-1221 (2004).
- [34] Corma, A., Díaz-Cabañas, M. J., Martínez-Triguero, J., Rey, F. & Rius, J. A large-cavity zeolite with wide pore windows and potential as an oil refining catalyst. *Nature (London)* **418**, 514-517 (2002).
- [35] Corma, A., Díaz-Cabañas, M. J., Jordá, J. L., Martínez, C. & Molíner, M. High-throughput synthesis and catalytic properties of a molecular sieve with 18- and 10-member rings. *Nature (London)* **443**, 842-845 (2006).
- [36] Degnan, T. F. Jr., Application of zeolites in petroleum refining. *Top. Catal.* **13**, 349-356 (2000).
- [37] Weitkamp, J., Ernst, S. & Puppe, L. Shape-selective catalysis in zeolites in *Catalysis and zeolites - Fundamentals and applications*, Ch. 5 (eds J.

- Weitkamp & L. Puppe), Springer, Berlin, 327-376 (1999).
- [38] Blauwhoff, P. M. M., Gosselink, J. W., Kieffen, E. P., Sie, S. T. and Stork, W. H. J. Zeolites as catalysts in industrial processes in *Catalysis and zeolites - Fundamentals and applications*, Ch. 7 (eds J. Weitkamp & L. Puppe) Springer, Berlin, 437-538 (1999).
- [39] Perego, C. & Ingallina, P. Recent advances in the industrial alkylation of aromatics: new catalysts and new processes. *Catal. Today* **73**, 3-22 (2002).
- [40] Perego, C. & Pollesel, P. Advances in aromatic processing using zeolite catalysts in *Advances in nanoporous materials*. Vol. 1 (ed S. Ernst), Ch. 2, Elsevier, Amsterdam, 97-150 (2009).
- [41] Al-Khattaf, S., Ali, M. A. & Čejka, J. Recent developments in transformation of aromatic hydrocarbons over zeolites in *Zeolite and Catalysis. Synthesis, Reactions and Application* Vol. 2 (eds J. Čejka, A. Corma & S. Zones) Ch. 20, 623-648 (2010).
- [42] Ipatieff, V. N. & Schaad, R. E. Alkylation of benzene. *U.S. Patent 2,382,318* (1945) assigned to UOP Co.
- [43] Applegath, F., Du Pree, L. E., MacFarlane, A. C. & Robinson J. D. Alkylation Process. *U.S. Patent 3,848,012* (1974), assigned to Monsanto Co.
- [44] Minachev, K. R., Isakov, Y. I. & Garanin, V. I. Alkylation of aromatic hydrocarbons on synthetic zeolites. *Doklady Akademii Nauk. SSSR* **165**, 831-839 (1965).
- [45] Venuto, P. B., Hamilton, L. A., Landis, P. S. & Wise, J. J. Organic reactions catalyzed by crystalline aluminosilicates: 1. Alkylation reactions. *J. Catal.* **5**, 81-98 (1966).
- [46] Kaeding, W. W. & Holland, R. E. Shape-selective reactions with zeolite catalysts: VI. Alkylation of benzene with propylene to produce cumene. *J. Catal.* **109**, 212-216 (1988).
- [47] Bellussi, G., Pazzuconi, G., Perego, C., Girotti, G. & Terzoni, G. Liquid-phase alkylation of benzene with light olefins catalyzed by β zeolites. *J. Catal.* **157**, 227-234 (1995).
- [48] Ercan, C., Dautzenberg, F. M., Yeh, C. Y. & Barner, H. E. Mass-transfer effects in liquid-phase alkylation of benzene with zeolite catalysts. *Ind. Eng. Chem. Res.* **37**, 1724-1728 (1998).
- [49] Garcés, J. M., Olken, M. M., Lee, G. J., Meima, G. R., Jacobs, P. A. & Martens, J. A. Shape selective chemistries with modified mordenite zeolites. *Top. Catal.* **52**, 1175-1181 (2009).
- [50] Gajda, G. J. & Gajek, R. T. Modified zeolite Beta, processes for preparation and use thereof. *U.S. Patent 5,522,984* (1996) assigned to UOP.
- [51] Cheng, J. C., Fung, A. S., Klocke, D. J., Lawton, S. L., Lissy, D. L., Roth, W. J., Smith, C. M. & Walsh, D. E. Process for preparing short chain alkyl aromatic compounds. *U.S. Patent 5,453,554* (1995) assigned to Mobil Oil

- Corp.
- [52] Perego, C., Amarilli, S., Bellussi, G., Cappellazzo, O. and Girotti, G. Development and industrial application of a new β zeolite catalyst for the production of cumene. *Proceedings of the 12th International Zeolite Conference*, Vol. 1 (eds M. M. J. Treacy, B. K. Marcus, M. E. Bisher & J. B. Higgins), Materials Research Society, Warrandale, 575-582 (1999).
- [53] Perego, C., Amarilli, S., Millini, R., Bellussi, G., Girotti, G. & Terzoni, G. Experimental and computational study of beta, ZSM-12, Y, mordenite and ERB-1 in cumene synthesis. *Microporous Mater.* **6**, 395-404 (1996).
- [54] Girotti, G., Cappellazzo, O., Bencini, E., Pazzuconi, G. & Perego, C. Catalytic composition and process for the alkylation and/or transalkylation of aromatic compounds. *Eur. Patent Appl.* 847,802 (1997) assigned to EniChem S.p.A.
- [55] Leonowicz, M.E., Lawton, J.A., Lawton, S.L. & Rubin, M.K. MCM-22: a molecular sieve with two independent multidimensional channel systems. *Science* **264**, 1910-1913 (1994).
- [56] Millini, R., Perego, G., Parker Jr., W. O., Bellussi, G. & Carluccio, L. Layered structure of ERB-1 microporous borosilicate precursor and its intercalation properties towards polar molecules. *Microporous Mater.* **4**, 221-230 (1995).
- [57] Sastre, G., Catlow, C. R. A. & Corma, A. Diffusion of benzene and propylene in MCM-22 zeolite. A molecular dynamics study. *J. Phys. Chem. B* **103**, 5187-5196 (1999).
- [58] Corma, A., Martínez-Soria, V & Schnoefeld, E. Alkylation of benzene with short-chain olefins over MCM-22 zeolite: catalytic behavior and kinetic mechanism. *J. Catal.* **192**, 163-173 (2000).
- [59] Roth, W. J. & Dorset, D. L. Expanded view of zeolite structures and their variability based on layered nature of 3-D frameworks. *Microporous Mesoporous Mater.* **142**, 32-36 (2011).
- [60] Corma, A., Fornes, V., Pergher, S. B., Maesen, Th. L. M. & Buglass, J. G. Delaminated zeolite precursor as selective acidic catalysts. *Nature (London)* **396**, 353-356 (1998).
- [61] Fung, A. S., Lawton, S. L. & Roth, W.J. Synthetic layered MCM-56, its synthesis and use. *U. S. Patent 5,362,697* (2005), assigned to Mobil Oil Co.
- [62] Jan, D.-Y., Miller, R. M., Koljack, M. P., Bauer, J. E., Bogdan, P. L., Lewis, G. J., Gajda, G. J., Koster, S. C., Gatter, M. G. & Moscoso, J. G. Hydrocarbon conversion processes using catalysts comprising UZM-8 and UZM-8HS compositions. *U. S. Patent 7,091,390* (2006) assigned to UOP LLC.
- [63] Schmidt, R., Jan, D.-Y & James, R. Alkylation of aromatics with high activity catalyst. *U.S. Patent Appl.* 2010/0160704 A1 (2010) filed by Honeywell/UOP.
- [64] Moliner, M., Díaz-Cabañas, M. J., Fornés, V., Martínez, C. & Corma, A. Synthesis methodology, stability, acidity, and catalytic behavior of the 18 % 10 member ring pores ITQ-33 zeolite. *J. Catal.* **254**, 101-109 (2008).

- [65] Lillwitz, L. D. Production of dimethyl-2,6-naphthalenedicarboxylate: precursor to polyethylene naphthalate. *Appl. Catal.* **221**, 337-358 (2001).
- [66] Sunitami, K. & Shimada, K. Preparation of 2,6-dimethylnaphthalene. *Jap. Patent 4,013,637* (1992) assigned to Teijin Ltd.
- [67] Motoyaki, M., Yamamoto, K., McWilliams, J. P. & Bundens, R. G. Process for preparing dialkylnaphthalenes. *U.S. Patent 5,744,670* (1998) assigned to Kobe Steel Ltd./Mobil Oil Co.
- [68] Fraenkel, D., Cherniavsky, M., Ittah, B. & Levy, M. Shape-selective alkylation of naphthalene and methylnaphthalene with methanol over H-ZSM-5 zeolite catalysts. *J. Catal.* **101**, 273-283 (1986).
- [69] Weitkamp, J. & Neuber, M. Shape selective reactions of alkylnaphthalenes in zeolite catalysts. *Stud. Surf. Sci. Catal.* **60**, 291-301 (1991).
- [70] Kikuchi, E., Mogi, Y. & Matsuda, T. Shape selective disproportionation of methylnaphthalene on ZSM-5 catalyst. *Collect. Czech. Chem. Commun.* **57**, 909-919 (1992).
- [71] Komatsu, T., Araki, Y., Namba, S. & Yashima, T. Selective formation of 2,6-dimethylnaphthalene from 2-methylnaphthalene on ZSM-5 and metallosilicates with MFI structure. *Stud. Surf. Sci. Catal.* **84**, 1821-1828 (1994).
- [72] Popova, Z., Yankov, M. & Dimitrov, L. Methylation, isomerization and disproportionation of naphthalene and methylnaphthalenes on zeolite catalysts. *Stud. Surf. Sci. Catal.* **84**, 1829-1835 (1994).
- [73] Loktev, A. S. & Chekriy, P. S. Alkylation of binuclear aromatics with zeolite catalysts. *Stud. Surf. Sci. Catal.* **84**, 1845-1851 (1994).
- [74] Pu, S.-B. & Inui, T. Synthesis of 2,6-dimethylnaphthalene by methylation of methylnaphthalene on various medium and large-pore zeolite catalysts. *Appl. Catal. A: General* **146**, 305-316 (1996).
- [75] Pu, S.-B. & Inui, T. Influence of crystallite size on catalytic performances of HZSM-5 prepared by different methods in 2,7-dimethylnaphthalene isomerization. *Zeolites* **17**, 334-339 (1996).
- [76] Anunziata, O. A. & Pierella, L. B. Transalkylation of naphthalene with mesitylene over H-ZSM-11 zeolite. *Catal. Lett.* **44**, 259-263 (1997).
- [77] Gläser, R., Li, R., Hunger, M., Ernst, S. & Weitkamp, J. Zeolite HNU-87: synthesis, characterization and catalytic properties in the shape-selective conversion of methylnaphthalenes. *Catal. Lett.* **50**, 141-148 (1998).
- [78] Park, J.-N., Wang, J., Hong, S.-I & Lee, C. W. Effect of dealumination of zeolite catalysts on methylation of 2-methylnaphthalene in a high-pressure fixed-bed flow reactor. *Appl. Catal. A: General* **292**, 68-75 (2005).
- [79] Wu, W., Wu, W., Kikhtyanin, O. V., Li, L., Toktarev, A. V., Ayupov, A. B., Khabibulin, J. F., Echevsky, G. V. & Huang, J. Methylation of naphthalene on MTW-type zeolites. Influence of template origin and substitution of Al by Ga.

- Appl. Catal. A: General* **375**, 279-288 (2010).
- [80] Zhang, C., Guo, X., Song, C., Zhao, S. & Wang, X. Effects of steam and TEOS modification on HZSM-5 zeolite for 2,6-dimethylnaphthalene synthesis by methylation of 2-methylnaphthalene with methanol. *Catal. Today* **149**, 196-201 (2010).
- [81] Pazzuconi, G., Perego, C., Millini, R., Frigerio, F., Mansani, R. & Rancati, D. Process for the preparation of 2,6-dimethylnaphthalene using a MTW zeolitic catalyst. *U. S. Patent 6,147,270* (2000) assigned to Enichem S.p.A.
- [82] Millini, R., Frigerio, F., Bellussi, G., Pazzuconi, G., Perego, C., Pollesel, P. & Romano, U. A priori selection of shape-selective zeolite catalysts for the synthesis of 2,6-dimethylnaphthalene. *J. Catal.* **217**, 298-309 (2003).

Emerging Applications of Zeolites

Jean-Pierre Gilson*, Olivier Marie, Svetlana Mintova and Valentin Valtchev
*Laboratoire Catalyse & Spectrochimie, ENSICAEN, Université de Caen, CNRS, 6
bd Maréchal Juin, 14050, Caen, France*

Abstract

The field of emerging applications of zeolites is very broad and our depth of its present knowledge varies greatly. We illustrate its important and yet untapped potential in a series of fields linked to cleaner energy technologies and energy savings. While many academic or industrial findings (inventions) are reported, only a few will appear on the market as innovations. However they will benefit from the enormous body of knowledge accrued over the years in the more classical and mature applications.

1. Introduction and Scope

Most reviews and tutorials on zeolites rightly focus on their past, present and potential successful applications in catalysis and separation in oil refining, petro- and fine-chemicals processing. They are covered in the chapters 8 and 9 of this monograph. Zeolites brought to these fields spectacular advances either by disruptive innovations (FCC, Luboils processing...) or numerous incremental improvements (FCC...) ¹⁻². Here, as choices have to be made to limit the size of the topic, we will focus on four areas where their potential has not yet been tapped or the first applications have just emerged:

- 1) The processing of renewable (*i.e.* biomass) and synthetic (*i.e.* derived from syngas) feedstocks to produce cleaner energy and chemicals in the form of transportation fuels and green(er) power
- 2) The curative post-treatment of pollutants generated by stationary and mobile sources
- 3) The unconventional uses of zeolites related to energy savings based on zeolite films and layers for *a)* membrane and *b)* sensing applications.

In all these areas, once laboratory inventions will prove to be potentially and sustainably useful at an affordable cost, they will probably become innovations at a fast pace since they will benefit from the know-how already gathered in the more mature fields. It is however certain that new challenges in the transformation of new

inventions to innovations will appear and will test the creativity of scientists and engineers.

2. Processing of Renewable and Alternative Feedstocks

2.1 Introduction and new challenges

Emerging, *i.e.*, renewable and alternative (heavy oils, coals) feedstocks all contain oxygen compounds and their composition is best described at the hand of the so called “van Krevelen” diagrams ¹, Figure 1.

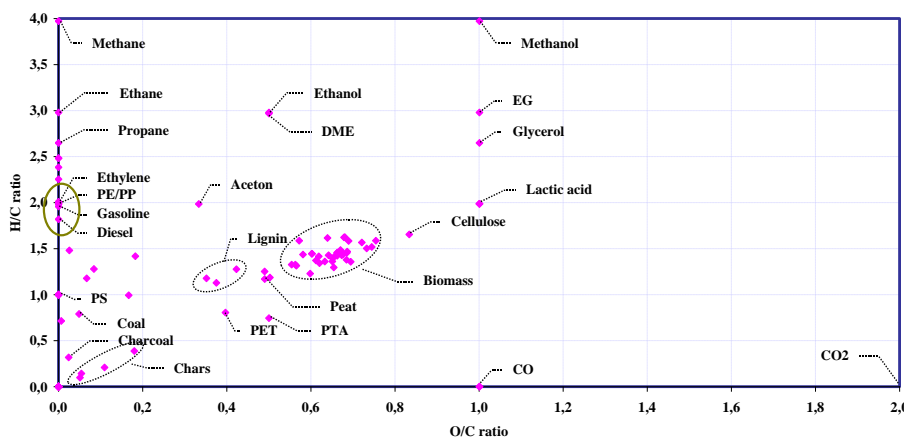


Figure 1. Typical “van Krevelen” diagram of emerging feedstocks and commodity products (encircled). Reprinted with permission from ref 1. Copyright 2009 Springer.

While scientists and engineers involved in catalysis often focus on the feedstocks and their transformation processes to chemicals or fuels, the complexity and multidisciplinary character of the challenges should be recognized. A commercially successful finished fuel (*i.e.* additivated) will have to meet simultaneous demands, as there is an intimate interplay between the fuel and its combustion process ³:

- a high volumetric energy density, necessary to achieve a high mileage, as summarized (for mass energy density !) in Figure 2. In that respect, oxygenates suffer from a penalty compared to pure hydrocarbons.
- be fungible with existing fuels as *i*) these will still largely dominate the markets for many (tens of) years, *ii*) the cost to maintain separate distribution networks is unaffordable. Oxygenates present many additional drawbacks (vapor pressure, water solubility, corrosion, plastic swelling, combustion...) along the whole

distribution and combustion chain. For these and other reasons, ethanol is for instance limited to low concentration blends (5-10 % by volume), namely E5-E10. - the drivability of cars powered by internal combustion engines, in constant evolution, requires the use of different molecules at different stages of the driving cycle (cold and warm start, high and constant speeds...) and a capacity to adjust to the various driving styles (“Vroom” factor). Complex hydrocarbon mixtures are therefore the most preferred and flexible fuels.

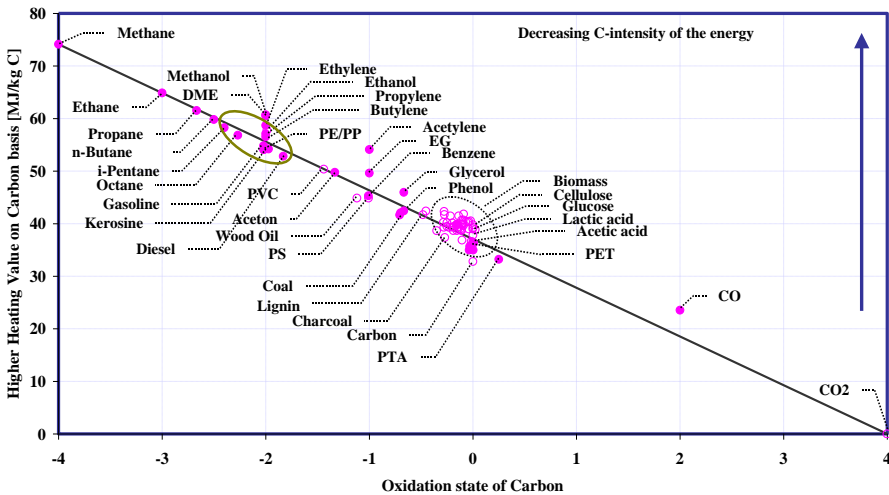


Figure 2. Energy content against oxidation state of Carbon in emerging feedstocks and commodity products (encircled): HHV stands for high heating value. Reprinted with permission from ref 1. Copyright 2009 Springer.

Figure 2 highlights that emerging fuels range from single molecules, *i.e.* chemicals (methanol, ethanol, dimethylether, butanol...) to transportation fuels “look-alike” (*e.g.* green diesel⁴). The above indicates that the preferred new fuels will be hydrocarbons and efficient de-oxygenation will be the key step in their large scale production⁵. This is an area where zeolites could play an important role as processes using zeolites will consume less hydrogen than the hydroprocessing routes⁶⁻⁷; the latter operate with a high partial pressure of hydrogen on classical or modified hydrotreating catalysts.

Common sense indicates that biofuels could benefit from economies of scale and reduced capital expenditures by being produced in existing refineries and ideally in existing units (co-processing); further cost benefits would come from blending and distributing them with fossil fuels.

Finally, catalysts scientists and engineers should recognize that if green power is used in the transformation processes (Figure 3), part of this "greenery" should be allocated to the product therefore avoiding the fallacy to push at any cost, every green carbon atom from the feedstocks to a Product (Fuel). This last point further highlights the need to perform life cycle analyses (LCA) on every new invention ⁴.

2.2 Biomass processing with zeolites

Figure 3 summarizes the different routes and processes studied today for the insertion of liquid hydrocarbon biofuels in the current pool of transportation fuels (ca. C₅₋₁₂ for gasoline, ca. C₉₋₁₆ for jet fuel, ca. C₁₀₋₂₀ for diesel). In addition, multi-branched molecules are required (octane number specification) in gasoline while mono-branched are required in diesel and jet fuel, (cetane number and cold flow properties specifications). A rapid analysis of Figure 3 indicates that two major processing routes emerge: *i*) fermentation and *ii*) thermal (pyrolysis and gasification).

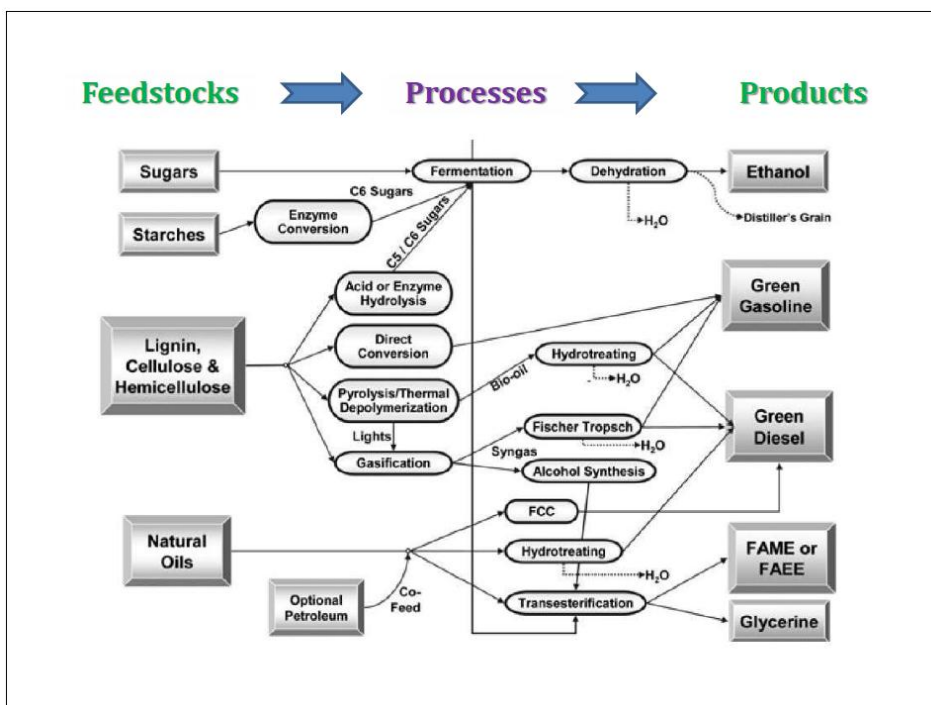


Figure 3. Overview of biofuels production: feedstocks, processes and products. Adapted from ref 4.

2.2.1 Pioneering work

Researchers at Mobil found shortly after the ZSM-5 discovery that due to its unique shape selectivity it could transform almost any hydrocarbon and oxygenates in a mixture limited to *ca.* 10-11 carbon atoms⁸, *i.e.* in the gasoline range. This finding led to the commercial development of the Methanol to Gasoline (MTG) and later to the Methanol to Olefins (MTO) processes. It also highlighted that any oxygenated feedstock could be transformed in mixtures of hydrocarbons (paraffins, olefins, naphthenes and aromatics). They also defined a very useful index⁹, EHI (Effective hydrogen Index),

$$(H/C)_{\text{eff}} = (H - 2O - 3N - 2S) / C$$

H, C, O, N and S are the relative atomic ratios of hydrogen, carbon, oxygen, nitrogen and sulfur of the feedstocks on an anhydrous basis. The efficiency of the conversion of any heteroatom containing feedstock increases with its EHI and is linked to its coking. Methanol has an EHI of 2 while pyrolysis oils (*vide infra*) have EHI typically below 0.5. These values are easily obtained by elemental analysis of the feeds. We will describe below some selected processes where zeolites could play a role, moving from the raw feedstock conversion to the transformation of extracts or side products more akin to fine chemicals processing.

2.2.2 Catalytic fast pyrolysis

Pyrolysis is a process where biomass is heated in the absence of oxygen at moderate temperatures (*ca.* 400°C) and with residence times of the order of 15-30 minutes¹⁰. It is a relatively cheap process that produces gases, liquids and a residual solid (char). If the operating conditions are changed to higher temperatures (*ca.* 500°C), faster heating rates and shorter contact times (< 1 s), the product is predominantly a liquid and the process called Fast Pyrolysis¹¹. Both processes are non-catalytic and therefore only operating conditions can steer its selectivity. In the case of Fast Pyrolysis, zeolite catalysts were introduced to better steer the selectivity to more desirable products. The results are mixed but interesting. The main features of such a process are:

- a pyrolysis oil yield around 45-50% compared with 75% when no catalyst (*e.g.* an FCC catalyst) is present
- a parallel increase of gas and char indicative of overcracking and coke deposition induced by the zeolite
- a higher hydrocarbon content of the pyrolysis oil and therefore a lower oxygenate content highlighting that catalytic deoxygenation in the presence of zeolite produces water instead of CO₂

More details are available elsewhere¹², but it is obvious that while zeolites bring beneficial effects to the Fast Pyrolysis Process, much remains to be done to increase

liquid yield, decrease coke and generate products with the required (blending) properties for transportation fuels. ZSM-5, described above is also used in such a process¹³. It is expectedly found that aromatics are produced by ZSM-5 because of its hydrogen transfer capability. Even if simpler feedstocks are used such as sugars (glucose), coke remains an issue and again ZSM-5 emerges as the most promising zeolite tested (Y, Beta)¹⁴. These processes are emerging since they compete with well-established, highly efficient (carbon and energy) ones already deployed by the oil industry¹⁵. Further progress will come from a rational design of the zeolite catalysts; in the studies reported so far, zeolites were taken “off the shelf” for proof of principle purposes. This is typically an area where academic creativity and industrial reality (process constrains and products specifications) can benefit from each other.

2.2.3 Pyrolytic oils upgrading

Pyrolytic oils can be upgraded by hydroprocessing^{6, 16, 17}, but catalyst stability and hydrogen consumption are, among others, important issues having a negative impact of the process economics. As expected from the pioneering work at Mobil described above, zeolites demonstrated their potential in scouting studies of pyrolysis oils. ZSM-5 appears the most promising catalyst but produces highly aromatic products¹⁸. Such a feedstock is an example of the penalty associated with a low EHI $(H/C)_{\text{eff}}$, *i.e.* a high coke make. Again, a rational design of the catalyst, paying much attention to minimizing its coking tendency could improve significantly the yields of desired products. However, such a process will have to demonstrate superior performances and cost advantage over two obvious competitors: *i)* the direct use of pyrolysis oils to fire stationary power generators¹⁹ and *ii)* co-processing in FCC units⁴. These alternatives present the important advantage of using existing equipment (lower capital demand) and offer the option to use pyrolysis oils blended with classical (fossil) oil fractions as feedstocks, albeit after some process modifications.

An integrated approach presented recently by Vispute et al.²⁰ could prove quite appealing. In a series of steps combining hydrogenation and zeolite processing, the selectivity to various petrochemical products (aromatics, olefins, monohydric alcohols and diols) can be tuned as a function of the market demand. The strategy is to offer to the zeolite processing catalyst the feedstock with the best possible $(H/C)_{\text{eff}}$. However as the feedstocks derived from pyrolysis oils are quite complex, all concepts derived from laboratory data need to be validated with real feedstocks tested under representative conditions.

2.2.4 Co-processing in FCC

This option is obviously favored by oil refiners and in addition to the advantages described above it allows the refiner to better control the supply chain of its fuels and petrochemicals. The FCC unit is very flexible: it is designed to process a wide variety of feedstocks and can be tuned to produce either fuel (gasoline but also

middle distillates) or contribute to the olefins and, to a lesser extent, aromatics pool of the petrochemical industry¹. As in the case of Catalytic Fast Pyrolysis (2.2.2 above) and pyrolysis oils upgrading with zeolites (2.2.3. above), the exploratory studies point to problems, including the need for a partial hydrodeoxygenation pretreatment to allow miscibility with oils fractions^{21,22}. Even with such a pretreatment, enhanced coking in the FCC unit occurs; it was rationalized by Huber and Corma on the basis of the new pathways opened by the presence of oxygenated molecules²³. It is therefore critical to perform more fundamental studies to focus on the details of the transformation of such complex feedstocks. A welcome example is a franco-portuguese study on the influence of phenol and guaiacol on n-heptane and methycyclohexane transformations on ZSM-5 under near FCC conditions²⁴. Some of the take home messages are the following:

- the slow diffusion of phenol inside the pores of the zeolite increases its residence time and therefore its coking tendency
- phenol has a different effect on paraffinic and naphthenic feeds
- guaiacol tends to react more on the zeolite external surface than phenol, due to its larger size

These pieces of information point to some tools for a more rational design of dedicated catalysts, *i.e.* to better tune the adsorption of oxygenates (change the zeolite hydrophobicity...), minimize diffusion (small but stable crystallites), induce Al gradients in the zeolite (position more active sites at the outer surface of zeolite crystals by using hierarchical materials where the toxic oxygenates would not compete with hydrocarbons inside the micropores, engineer the amorphous matrix, etc.). In addition, a combination of processes could maximize the yield of desired products. In a first step, carbon could be expelled in the form of CO₂ to increase the (H/C)_{eff} followed by another catalytic step where oxygen would be removed as H₂O. The catalysts used in such a process would need a very precise design. Again, as the feedstocks derived from pyrolysis oils are quite complex, all concepts derived from laboratory data need to be validated with real feedstocks tested under representative conditions.

2.2.5 Chemicals

The transformation of sugars by isomerization, their conversion to lactates, their dehydration to furanic compounds and the dehydration of ethanol and glycerol processing have been recently extensively reviewed by Taarning *et al.*¹⁰. Some of the routes lead to interesting bending components in gasoline (5-hydroxymethylfurfural [HMF], 2,5-dimethylfuran [DMF]...) or are green gasoline routes (ethanol to gasoline [ETG] process, a near cousin of the methanol to gasoline [MTG] process). In this field, two remarks are warranted:

- zeolites could play an increasing role as adsorbents in the energy efficient separation of various high value chemicals like glucose/fructose: processes like the

UOP Sarex (zeolite X) could receive a second life²⁵. They can operate as standalone units or in tandem with a catalytic conversion, as practiced in petrochemistry (xylene isomerization...) and oil refining (light paraffin isomerization)¹

- the adsorption processes described above operate in the aqueous phase and zeolites are known to suffer from leaching problems under these conditions. While techniques exist to mitigate it²⁶, they should be validated and eventually adjusted for each aqueous stream to purify.

2.3 Processing of syngas derived products by zeolites

In the so-called syngas route, a mixture of CO/H₂ is produced either by gasification (non-catalytic) or steam reforming (catalytic process). In particular, the gasification process can accommodate biomass wastes either alone or mixed with solids derived from fossil resources. The syngas produced is then, after adjusting its CO/H₂ ratio by the water gas shift reaction, transformed catalytically in a wide variety of chemicals or fuels by some of the most well established processes of the chemical industry (e.g. ammonia and methanol syntheses). Methanol in particular is already capable of producing some interesting chemicals and fuels.

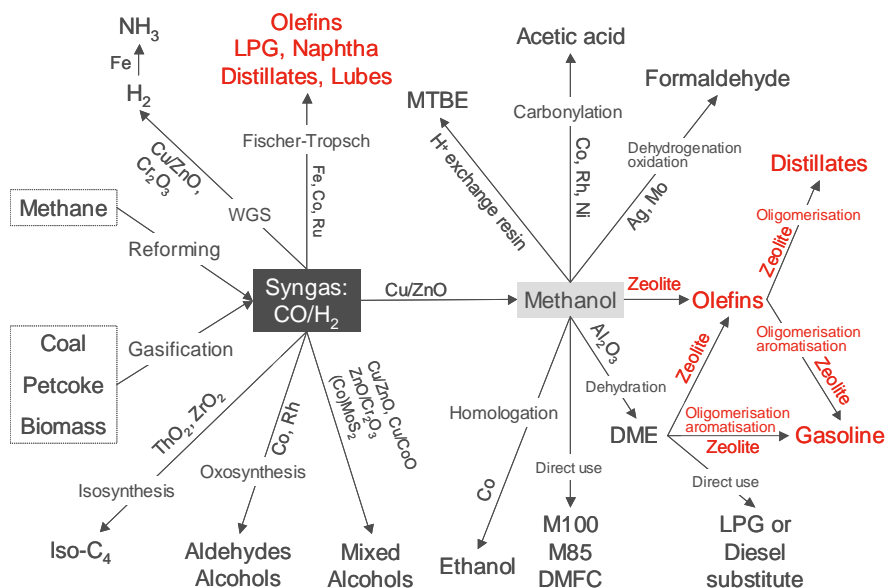


Figure 4. Products of synthesis gas and possible chemical transformations: text in red indicates where zeolites have high potential to contribute. Reprinted with permission from ref 1. Copyright 2009 Springer.

This route is not a very efficient process¹⁵ and the derived products should have a strategic value.

2.3.1 Zeolites in Fischer-Tropsch liquids upgrading

The patent²⁷ and open literature^{28, 29} indicate that the most preferred catalysts for the upgrading of Fischer-Tropsch (FT) liquids are bi-functional. The almost pure waxes are hydrocracked in middle distillates and luboils; the resulting products need to be slightly isomerized in order to maintain a good balance between their cold flow properties and other specifications (cetane number for diesel and viscosity index for luboils). The very high purity of FT waxes enables to work with the so-called “ideal” bi-functional catalysts where the metallic function is provided by Pt and the acid function by an acidic catalyst. The rate determining step then is the carbonations rearrangements that follow a fast dehydrogenation of paraffins on the Pt particles. While dedicated amorphous silica-alumina catalysts perform very well, zeolites have potential in these reactions. However, great care has to be taken to insure that the adsorption of very long molecules is not favoring their overcracking. Nanocrystalline zeolites with large pores and a tri-dimensional network (FAU, BEA...) dispersed in an active matrix could play an important role in lowering the temperature of reaction and avoiding the production of aromatics, thermodynamically favored around 340°C. In addition, composites made of multiple zeolites (intimate mixtures of large and intermediate pore zeolites promoting mono-branching) could further improve the quality of the products as in luboils hydroprocessing. Finally, the metal/acid balance of the working catalysts should be further investigated as the presence of small amounts of oxygenates could alter a catalyst developed for oxygenates free feedstock³⁰. These interesting fine tuning exercises could be met with properly designed zeolites or zeolite composites.

2.3.2. Zeolites in the conversion of methanol to hydrocarbons

The large scale production of methanol is a well-proven and optimized process. Although methanol as such can be used as a fuel or blended with gasoline, its preferred mode of incorporation is as an oxygen free hydrocarbon (2.1 above). Fortunately, routes for its transformation are known and some have been practiced commercially at large scale while others are offered for commercialization. The Methanol to Gasoline process (MTG) developed by Mobil (now ExxonMobil)² uses the well-known ZSM-5. It suffers from a high aromatic selectivity and in particular 1,2,4,5-tetramethylbenzene (durene) is the source of problems due to its high melting point. A variant of the MTG process, methanol to olefins (MTO) is also commercialized. A first unit (600 KTPA of olefins), licensed by the Dalian Institute of Chemical Physics (DMTO) to the coal company Shenhua Group Holdings of China came on stream in August 2010 and operated successfully since. Many other processes of a similar nature are available¹ and new units are likely to

come on stream using gas or coal, the latter mainly in China. The lower olefins ($C_{2,3}$) can be polymerized by well-established processes to polyethylene or polypropylene (MTP process) or oligomerized to gasoline of middle distillates. It is possible to produce gasoline by oligomerization (e.g. EMOGASTM from ExxonMobil²) to replace advantageously older Silica mounted Phosphoric Acid (SPA) technologies by a greener zeolite (ZSM-5) catalyst. Further oligomerization to diesel fuel is still problematic and not commercially successful so far. It is due to the nature of the reaction and maybe other zeolites need to be scouted.

As a result of excellent academic research with advanced tools, a better understanding of the MTG, MTO and related chemistry emerges. A few important advances merit a mention due to their ability to:

- Study hydrocarbons trapped inside the zeolite micropores by a technique developed by the Poitiers school^{31,32} where the zeolite is dissolved and the hydrocarbon retained extracted. This opens the door to a molecular level characterization of complex mixtures by advanced analytical techniques
- Monitor the surface of a working catalyst, the so called *operando* spectroscopy. This technique allows also to correlate the effect of reactants, products and poisons to the active sites and their location^{33,34}
- Build a coherent picture of the effects of all parameters in influencing the reaction chemistry, such as the hydrocarbon pools mechanisms³⁵ to explain the various selectivity obtained on different zeolites (e.g. ZSM-5 and ZSM-22)

The deeper insight in the coking mechanism and the knowledge that coke is located preferentially on specific sites of the zeolite surface^{33,34,36} will pave the way for next generation catalysts. Hierarchical materials should play a key role in these next generations, as already shown in preliminary experiments³⁷.

2.4 Direct conversion of light alkanes

Zeolite based technologies to transform light alkanes (C_{1-4} paraffins) are available. For instance propane and butane can be transformed in aromatics and hydrogen on a Ga/ZSM-5 zeolite operating in a circulating bed reactor of the CCR type¹. The process, jointly developed by BP and UOP, Cyclar, has been licensed to Saudi Arabia for petrochemical applications. However, the Holy Grail of C_1 chemistry, the direct transformation of methane to higher hydrocarbons (olefins, aromatics) remains an elusive goal. The first report of the direct transformation of methane to aromatics and hydrogen using Molybdenum loaded ZSM-5³⁸ attracted a lot of attention and generated much research activity, in academia and industry¹. This non-oxidative transformation takes place at 700 °C on Mo-ZSM-5 at atmospheric pressure but is limited by thermodynamics (12 – 24 % conversion at 700 – 800 °C respectively) and plagued by coking. After an induction period where no products are observed benzene is produced with selectivity around 80% at conversions of 8-

10%. While a better understanding of the reaction mechanism and coking resulted from years of intense research, the process is still far from commercialization. So, while extremely appealing, the direct transformation of methane using this non-oxidative route and all other alternatives remain a (grand) challenge³⁹ for science and technology.

3 Zeolites in Pollution Abatement

Because the severity of environmental specifications is always increasing, pollution abatement technologies are required to mitigate the emissions of mobile (transport industry) and stationary sources (process industries and power generation). Due their exceptional intrinsic properties (strong ad(b)sorbents, molecular sieves, efficient catalysts) zeolites are among the materials most applied. For example, during the last five years period, more than 100 papers/patents per year were published dealing with the application of zeolites for pollution control. Therefore, it is impossible to provide a short and exhaustive overview in this chapter, instead only a brief survey of the recent and significant developments in NO_x removal is presented here. The 2008 review by Sobalik⁴⁰ indicates that zeolite catalysts are ready for industrial application.

3.1 NO_x abatement from stationary sources

Because it is recognized that CO₂ contributes to the greenhouse effect, measures were taken to force the industrialized countries to limit its emission. Recently, nitrogen protoxide (N₂O) was officially recognized in the United States to possess a global warming capacity 300 times superior to that of CO₂. As a consequence, the N₂O removal will become a major concern, especially for nitric acid production plants but we will not develop this point here to better focus on the NO and NO₂ abatement. Various stationary sources of NO_x emissions are encountered in industry. Energy production is a prerequisite for industrial development and most often it is generated by the combustion of fossil sources. Thermal power plants are thus major contributors to NO_x emission along with many other industrial sectors such as cement, glass, etc. A process currently applied for NO_x abatement from stationary sources is the zeolite based Selective Catalytic Reduction (SCR) with ammonia but, as it is also the main technology developed for automotive sources, it will be discussed in the next section.

3.1.1. NO_x removal from thermal power plants via methane

Energy production by natural combustion is becoming more popular. It is therefore interesting to develop a process which would be able to limit the NO_x emission using methane (the major component in natural gas) instead of ammonia (via urea) as a reducing agent. Most of the studies in this field use cobalt based zeolite catalysts. As reported by Smeets *et al.*, the preparation and the cobalt loading greatly

influences the CH₄ SCR performances. High loadings lead to oxidic Co species active in methane direct combustion with oxygen thus limiting the NO_x reduction extent⁴¹. Most publications report a major role for NO₂⁴², which oxidizes to nitrates, further reacting with CH₄ to yield nitroso and nitromethane (CH₃NO and CH₃NO₂)⁴³ as displayed in Figure 5. The later compound would then quickly react with nitrosonium (NO⁺)⁴⁴ according to the following reaction: NO⁺Z⁻ + CH₃NO₂ → N₂ + H⁺Z⁻ + H₂O + CO₂. In order to examine the effect in real conditions, a rare earth promoted Pd-MOR under a representative exhaust gas feed is examined, and it showed an initial decay of the activity, indicated by a 15% loss of NO_x conversion. Detailed analysis indicated that sulfur species from the odorant added to the natural gas provoked the partial poisoning of the catalyst surface was presented⁴⁵.

3.1.2. Other hydrocarbons (HC's) as alternative reducing agent.

Propane⁴⁶ and propene were extensively studied as possible NO_x reducing agents, however, we will focus here on iso-butane (i-C₄) whose tertiary hydrogen is more readily activated⁴⁶. An interesting approach was developed to prepare Fe-MFI catalysts with strongly different Brønsted acidity but with similar Fe content and structure (as confirmed by UV-Vis and EPR spectroscopy). They revealed dramatic differences in NO_x conversion implying a key role of Brønsted acidity in the reaction mechanism through i-C₄ activation⁴⁷. Regarding the mechanism for HC's SCR with C_nH_{2n+2} or C_nH_{2n} with n>1, a general consensus exists on the involvement of primary nitroalkane (RNO₂)⁴⁸ converted to cyanide (-CN), further oxidized to isocyanate (-NCO) and finally hydrolyzed to NH₃ which constitutes the final strong NO_x reducing agent⁴⁹⁻⁵¹.

Finally, original studies using acetylene (C₂H₂) as an efficient reducing agent are worth mentioning. A mechanism also involving isocyanate species was proposed to take place on H-MOR zeolite where the addition of molybdenum considerably increased the amount of bridging nitrate species. The parallel increase of the NO_x removal suggests the latter reacts with C₂H₂ to provide the isocyanate intermediate⁵². Similarly, a stable and active catalyst was obtained upon the introduction of Zr into H-ZSM-5 zeolite. The obtained catalyst gives promising results: 89% NO conversion to N₂ at 350°C in a flow containing 1600 ppm NO, 800 ppm C₂H₂, and 9.95% O₂⁵³. One could argue that acetylene is not readily available and should be first produced and further transported to the stationary source. However, this study suggests an interesting potential application for automotive polluted gas abatement since on boarding of solid calcium carbide as C₂H₂ precursor [CaC₂ + 2 H₂O → C₂H₂ + Ca(OH)₂] would be much safer than on-boarding ammonia precursors⁵⁴.

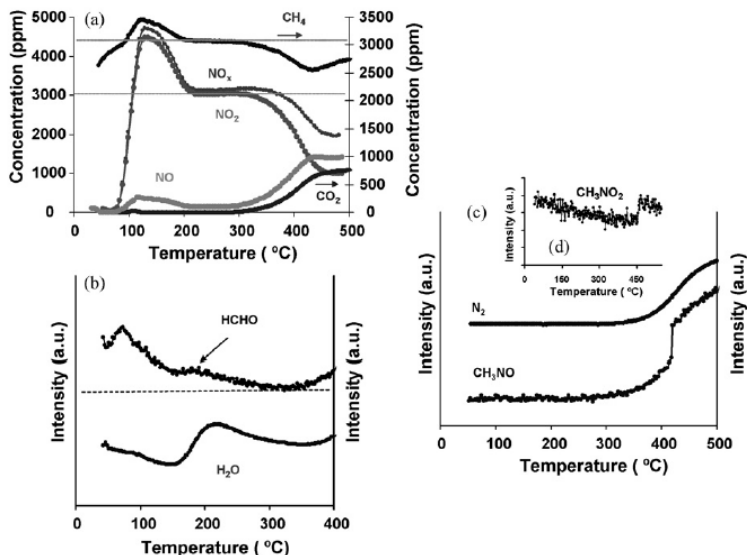


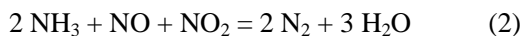
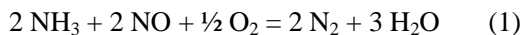
Figure 5. TPSR profiles with 3000 ppm NO_2 and 3000 ppm CH_4 in He; total flow of 250 mL min^{-1} ; $\text{GHSV} = 45,000 \text{ h}^{-1}$: (a) NO_x , NO , NO_2 , CH_4 and CO_2 ; (b) HCHO and H_2O ; (c) CH_3NO and N_2 ; (d) CH_3NO_2 evolution profiles, reproduced from ref. ⁴³, with permission of the copyright holders.

3.2 NO_x abatement from mobile sources

Although ammonia SCR has been used for years in stationary sources with VO_x/TiO_2 based catalysts and more recently with zeolites, the recent rise of zeolite based catalysts is a consequence of ever stringent specifications on the amount of emitted NO_x , unburnt HC's, CO_2 and particles. Diesel and lean-burn gasoline engines present the main advantage to lower the CO_2 emission but their NO_x emissions need to be reduced in the presence of a high excess of oxygen. As a consequence, the use of a strong reducing agent such as NH_3 (mainly arising from urea decomposition) appeared as an efficient alternative to overcome the drawbacks associated to the concurrent Lean NO_x Trap process (*i.e.* fuel overconsumption and high sulphur sensitivity).

3.2.1. Some proposed NH_3 SCR mechanisms.

The chemical reaction between ammonia and NO_x species is often divided into two main equations describing the (1) standard SCR and (2) fast SCR reactions:



The standard SCR reaction is kinetically less favourable than the fast SCR reaction, however the NO_x emitted from a Diesel or lean burn engine contain nitrogen monoxide as the main component ($> 80\%$). As a consequence, the SCR catalysts require a redox function; in the case of zeolites it is provided by transition metal ions (TMI). It is generally accepted that the rate determining step for the standard SCR reaction is the NO to NO_2 oxidation. However, there is up to now, no real consensus regarding the way NO_x and ammonia react together. For example, a comparative study between Cu/NaZSM5 and Cu/HZSM5 indicates that the Cu/NaZSM5 significantly higher NO_x conversion could be attributed to the promoting effect of Na^+ cations on the formation of nitrite and nitrate intermediates species⁵⁵. Over similar Cu-ZSM5 catalyst, a mechanism involving a reaction between adsorbed NO_2 and NH_3 , the subsequent formation of HNO_2 and HNO_3 and the final reduction to N_2 or N_2O is consistent with the kinetic modelling of a broad set of experimental conditions for which NH_3 inhibition was observed at low temperature⁵⁶. This NH_3 blocking effect on the fast SCR catalytic mechanism at low temperature was also observed with a state-of-the-art commercial Fe-zeolite and further examined in dedicated transient reactivity runs. Evidence was provided that such a blocking is associated with a strong interaction between NH_3 and surface NO_3^- preventing these nitrates⁵⁷ from reacting with NO to yield NO_2^- . Ammoniate nitrite indeed selectively decomposes into N_2 in a broad range of temperatures while ammonium nitrate forms solid salts deposits at $T^\circ < 160^\circ\text{C}$ and decomposes non-selectively to N_2 and N_2O . The low temperature loss of SCR efficiency in presence of NO_2 is thus also often suggested to occur via NH_4NO_3 accumulation inside the microporous volume. However when temperature rises above 200°C , the introduction of an ammonium nitrate aqueous solution to a typical $\text{NO}_x + \text{NH}_3$ SCR feed is reported to greatly improve the NO_x removal efficiency. The dosed oxidizing additive (nitrates) indeed plays the role of NO_2 in the fast SCR reaction with the advantage that the SCR boosting effect is no longer determined by the activity of the upstream oxidation catalyst⁵⁸.

The previous studies report a major role of adsorbed NO_x species in the SCR mechanism. On another hand, the observation of the catalyst surface under duty reveals that NH_4^+ species are the most abundant adsorbed species while no adsorbed NO_x is detected in reaction condition. Furthermore, an excellent correlation between the amounts of NH_3 adsorbed species and the NO_x reduction efficiency strongly suggests ammonium species as the main active species⁵⁹⁻⁶⁰. As adsorbed ammonia seems to play an important role in SCR, we would like to underline the necessity for the development of reliable kinetic models to properly estimate its corresponding heat of adsorption. In a very recent paper, micro

calorimetry was used to provide coverage-dependent activation energy for NH_3 desorption from Cu-BEA zeolite⁶¹.

According to the above, it seems quite ambitious to establish a 'universal' detailed reaction path since both the interaction of NH_3 with adsorbed NO_x or the interaction of NO_x with adsorbed ammonia seem possible. Nevertheless, the presence in the final N_2 reaction product of one nitrogen atom coming from the ammonia molecule and the other one from a NO_2 molecule was clearly proved via isotopic exchange experiment⁶².

3.2.2 Influence of feed composition (H_2O , unburnt HC's, SO_2)

In the case of automotive engines with frequent emission gas composition changes, a reliable kinetic model is required in order to control the urea injection. For this purpose, a real feed gas composition should be considered and both the individual effect of any compound together with possible cross reactions should be taken into account. Regarding the water effect, in the low temperature range, H_2O not only competes with ammonia for adsorption sites but also interacts with ammonium species⁶³. Over Fe-ZSM5, an inhibiting effect of water on the NO oxidation capability was also proposed⁶⁴.

Concerning the effect of traces of unburnt HC's, it was observed over a commercial Fe-ZSM5 sample that among propene, toluene and decane, the heaviest molecule representative of the Diesel fuel had the main inhibiting effect especially in the low temperature range where it poisons adsorption sites for ammonia⁵⁹.

The presence of SO_2 in the automotive exhaust gas engine is known to severely poison the basic NO_x trap catalysts and it is thus useful to test the sulphur resistance of the alternative zeolite based SCR catalysts. An aged Fe-FER zeolite with a 2.5wt% iron loading was thus tested for the accepted SCR rate determining step NO to NO_2 oxidation in presence of SO_2 . The figure 6 clearly indicates that iron sulphates progressively accumulate on the surface at the expense of iron nitrosyl [$\text{Fe}^{2+}(\text{NO})$]. The concomitant analysis of the gas phase reveals that the NO_2 production tends to zero when sulphates are formed and no more Fe^{2+} sites are available for NO adsorption⁶⁰.

This study illustrates that even if sulphur resistant SCR zeolites exist, the control of the location of the active red-ox sites is fundamental since the development of TMI oxide clusters upon aging provokes catalyst poisoning through sulphate formation.

3.2.3. Iron versus copper based zeolites.

As reported above, the most popular TMI in zeolite based SCR catalysts are iron and copper and the question of which offers the best performances is still debated. Girard *et al* combined Cu-zeolite with Fe-zeolite for their complementary performances⁶⁵. Cu-zeolite catalysts are indeed generally known for their efficient

NO_x reduction at low temperature with little or no NO_2 , but tend to selectively oxidize NH_3 to N_2 above 400°C , leading to poor NO_x conversion at elevated temperatures. Fe-zeolite catalysts provide on the contrary a very efficient NO_x conversion at temperatures as high as 600°C or higher, but are not as efficient as Cu-zeolite catalysts at lower temperature in the absence of NO_2 .

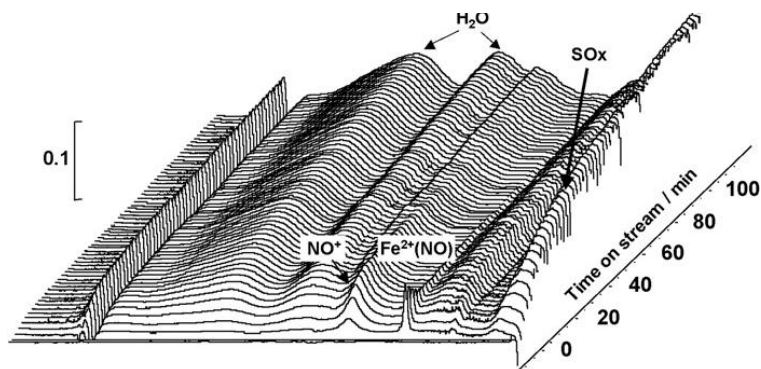


Figure 6. Evolution of the catalyst: IR surface spectra during the NO -to- NO_2 reaction at 433 K with SO_2 over the 2.5 wt% Fe-FER. Reproduced from ref. ⁶⁰, with permission of the copyright holders.

The key question is the precise nature of the active redox sites. A great number of studies has indeed been devoted to the characterization of the transition metal cations located in/on zeolites in order to identify their most active local structure and optimize their amount at the preparation stage. We report here only on the characterization of iron but the conclusions are applicable to copper sites. The main issue with iron lies in the proper identification of the proportion of cations with different oxidation state in one sample. EPR or UV-VIS spectroscopies only properly detect Fe^{3+} sites and probe molecule adsorption such as NO monitored by FTIR spectroscopy are only sensitive to Fe^{2+} sites. As a consequence, the correlation between catalytic activity and the amount of specific Fe^{3+} or Fe^{2+} site could lead to the biased conclusion that they are the active sites. Mössbauer spectroscopy is the technique of choice since it can simultaneously quantify Fe^{3+} and Fe^{2+} ions. Figure 7 represents the Mössbauer spectrum of a Fe-FER zeolite in which Fe^{2+} accounts for around 90% of the total iron species in a freshly prepared sample ⁶⁶.

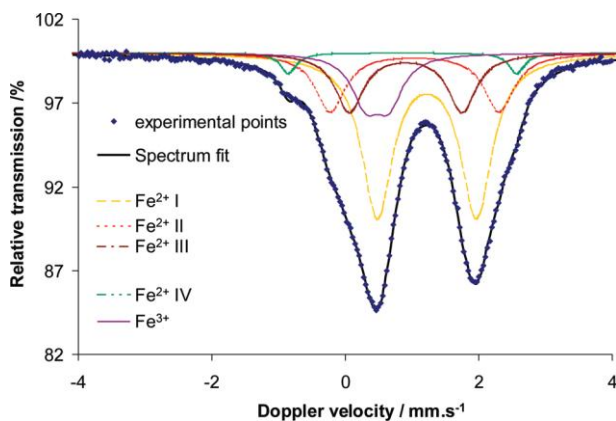


Figure 7. Mössbauer spectrum of the “as-prepared” sample 1.5^{57}Fe-FER recorded at 298K and the corresponding optimized curve fitting with five components.

Reproduced from ref. ⁶⁶ with permission of the copyright holders.

After an oxidizing treatment under O_2 , a major fraction of Fe^{2+} was converted to Fe^{3+} while a minor fraction of the latter was further reversibly converted to Fe^{2+} under a reducing atmosphere. This result is very important since only sites that may easily and reversibly change their oxidation state are good candidates for active sites in catalytic redox reactions ⁶⁷.

Finally, the reader is advised to carefully read the details when literature data seem a priori contradictory, since many parameters may affect the conclusions. Among them, one can only briefly cite, the influence on the active sites of: *i*) the preparation conditions, *ii*) the TMI loading, *iii*) the zeolite structure (numerous recent patents), *iv*) the Si/Al ratio, *v*) the Al distribution, etc.

3.2.4. The automotive SCR catalyst real life.

When used in automotive applications, SCR catalysts are shaped as monoliths and integrated in an integrated exhaust treatment system where NO_x , soot and unburnt HC's should be removed. Noble metal based Diesel Oxidation Catalyst (DOC) and Diesel Particulate Filter (DPF) are associated to the SCR block in the complete catalytic process. The periodic regeneration of the DPF by combustion of the accumulated soot provokes important exotherms which impact all catalysts. In a classical configuration, the DOC catalyst is located upstream from the SCR one. A recent study of the SCR performance after the thermal aging of the whole catalytic chain, showed two primary degradation mechanisms. The first one, linked to the zeolite deterioration, leads to loss of surface area, zeolite dealumination, and Fe_2O_3

crystal growth while the second one is associated with the presence of Pt traces on the front section of the SCR catalyst originating from the DOC. Evidence of this Pt deposit was provided by the high NH_3 oxidation levels (80% conversion at 400°C), coinciding with the decreased performance⁶⁸. A poisoning effect by phosphorus deposits from lubricant additives was also recently evidenced⁶⁹. Incomplete urea hydrolysis may also lead to solid deposits onto the zeolite surface preventing the access of reactants to the SCR active sites. A proposal to circumvent this phenomenon is to position the urea injector upstream of the DPF, itself upstream the SCR catalyst⁷⁰. Recent developments in zeolite hydrothermal stability even permit to directly place the SCR zeolite washcoat on the DPF with improved resistance to the regeneration step. Furthermore, the on-board ammonia production may be an interesting alternative to on boarding a heavy ammonia precursor. For this purpose, the combination of NOx-trap and SCR catalysts in a double-bed configuration is a current promising investigation way⁷¹.

4. Zeolite Films for Energy Saving Applications

Synthetic zeolites are usually produced as a fine crystalline powder. Prior to their use, the powder is agglomerated into spheres, tablets and extrudates by the addition of non-zeolitic binders. The binding additives provide the zeolite agglomerates with high mechanical strength and attrition resistance. However, since the binders are typically present in amounts of up to 50 wt. % they dilute the active phase and can block the zeolite pores. Thus, the preparation of binderless zeolite agglomerates with high mechanical stability and open structures to ensure short diffusion paths is of great technological importance. There are also a number of applications where a composite material comprising a thin zeolite film is required in order to achieve new functionality⁷². In the following sections, the developments in the preparation of supported zeolite films for separation, membrane reactors, fuel cell devices and chemical sensors will be considered.

4.1. Zeolite membranes

A membrane is an intervening phase acting as an active or passive barrier between gases or liquids adjacent to it under a driving force. In general the separation processes are widely used in the industry since the chemical conversions are often incomplete. Thus the membrane technology is the most attractive separation method because its low cost, selectivity and in the case of inorganic membranes the high thermal, mechanical and chemical stability. Over the past 20 years the development of zeolite-based membranes has attracted considerable research efforts^{73,74}. The great expectations related with zeolites as separation media are based on their selectivity that could be used to separate molecules with difference in size below 1 Å^{75,76}. Besides the unraveled selectivity, the particular properties of zeolite membranes that attracted the attention of academic and application scientists are: (i)

long-term stability at high temperature, (ii) resistance to harsh environments, (iii) resistance to high pressure drop, (iv) inertness of microbiological degradation, (v) easy cleanability and catalytic activation. The interest in zeolite membranes is also related with the nowadays requirements for the minimization of energy consumption and cleaner technologies^{77,78}. Detailed information can be found in the current literature and several excellent reviews dealing with the subject of zeolitic membranes^{79,80}. In the present overview we will briefly consider different types of zeolite membranes and the main areas of their application.

4.1.1 Supported polycrystalline zeolite membranes

The preparation of zeolite membranes has been studied actively during last two decades. In the early nineties the research was oriented to the preparation of self-supported zeolite membranes. Intergrowth zeolite films were prepared on temporary supports like teflon⁸¹ or cellulose⁸². Aqueous - air or aqueous -organic interfaces have also been employed in order to grow self supported zeolite films⁸³. This route for preparation of zeolitic membranes has been rapidly abandoned because of the poor mechanical characteristics of free standing zeolite films. Consequently the major part of zeolite membrane research was devoted to the supported membranes. The approach consists in *in situ* hydrothermal crystallization of a relatively thin film on pre-shaped porous support that provides the mechanical resistance of the zeolite membrane (Figure 8). Amongst different types of inorganic materials the most often employed supports are porous alumina, titania, zirconia, metals, glasses and carbon.

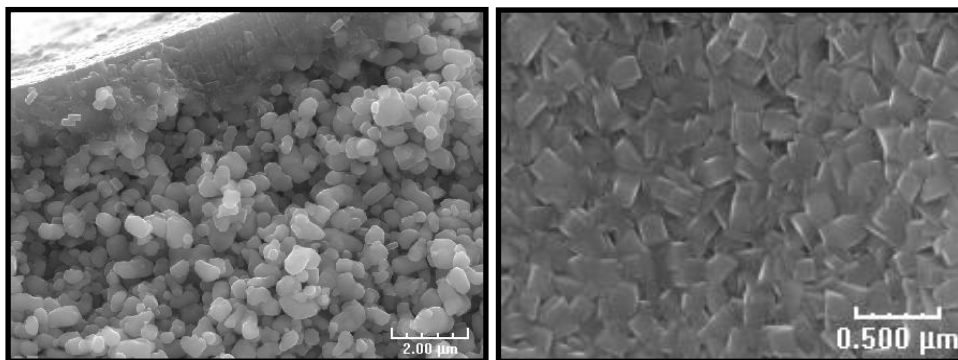


Figure 8. Side (left) and top (right) views of a silicalite-1 membrane grown on sintered alumina support.

The continuity, homogeneity, intactness and lack of cracks and pinholes are essential for the separation performance of supported zeolite films. The contact between the support and the zeolite layer is of paramount importance for the properties of the growing zeolite films. The nucleation and crystal growth on the support can be self-induced or promoted by a preliminary functionalization of the support. In the second case the seeding is the most widely used approach, although a number of different approaches have been developed through the years. Most efforts have been devoted to the development of approaches that allow a uniform deposition of zeolite seeds on the supports. Upon hydrothermal treatment with an appropriate synthesis mixture the seeds induce homogeneous crystallization yielding continuous zeolite films with a good adhesion to the substrate.

The seeding approach is first reported by Tsapatsis and co-workers^{84,85}. The method is based on the application of aluminum hydroxide as a binder. Another method, which is probably the most widely used in the zeolite film preparation, is based on the electrostatic adsorption of zeolite nanoseeds⁸⁶. Namely, the substrate surface is charge modified by a cationic polymer, negatively charged colloidal zeolite crystals are then adsorbed and the seeds are induced to grow into a continuous dense film by hydrothermal treatment with a fresh synthesis solution or gel⁸⁷. Colloidal zeolite crystals have also been deposited on flat supports by spin-coating^{88,89}. The thickness of the spin-on films can be controlled to a certain extent by increasing the spin-coating steps. However, although being smooth, the films are composed of discrete non-intergrown crystals, which might be a drawback for some applications. Continuous films of the deposited by spin-coating seeds may be obtained by a secondary crystal growth. It is worth mentioning that this approach is applicable to flat supports only. Preformed zeolite crystals have also been deposited onto three dimensional supports (beads and fibers) by laser ablation^{90,91}. These crystals upon hydrothermal treatment grow into continuous films. Despite the merits of the laser ablation method, the technique is quite exotic and cannot be applied in many research laboratories. Another unconventional method to attach positively charged colloidal zeolite crystals (the zeta potential being controlled by the pH of the media) is by electrophoretic deposition⁹².

Table 1 summarizes the most commonly employed zeolite framework types in the preparation of membranes. As can be seen the most important from industrial point of view zeolitic materials have been prepared in the form of intergrown films for membrane purposes. The available zeolite membranes vary in both composition and pore size thus offering the opportunity to adapt the membrane module to the particularities of the separation process. Besides the pore size the availability of different zeolite types allows to control hydrophilic/hydrophobic properties of the membrane. For instance, a silicon rich zeolite membrane (silicalite-1) is inert and hydrophobic, while an aluminum rich zeolite membrane (NaX, NaA) is hydrophilic. The incorporation of foreign atoms in the zeolite framework also changes

hydrophilic / hydrophobic properties and might affect the transport of molecules through the channels. The most often used cations for isomorphous substitutions of Si and/or Al in zeolite membranes are Ga, B, Fe, V and Ti. The charge balancing cations that compensated the unsaturated charges of zeolite framework represent another tool to physically restricted and chemically modify the characteristics of zeolite membranes.

Table 1. Zeolite framework types prepared in the form of supported zeolite films for membrane uses.

Framework type	Zeolite	Framework cation	Pore openings (Å)
CHA	SAPO-34	Al, P, Si	3.8
DDR	Deca-dodecasil 3R	Si	4.4 x 3.6
DON	UTD-1	Si	10.0 x 7.5
FAU	NaX	Si, Al	7.4
FAU	NaY	Si, Al	7.1
LTA	NaA	Si, Al	4.2
MFI	Silicalite-1	Si	5.6 x 5.3; 5.5 x 5.1
MFI	ZSM-5	Si, Al	5.6 x 5.3; 5.5 x 5.1
MOR	Mordenite	Si, Al	7.0 x 6.5; 5.7 x 2.6

Prior to discuss different separations on zeolite-based membranes the mechanism of transport is worthy to be addressed. Zeolite membranes discriminate molecular mixtures on the basis of molecular sieving or surface diffusion mechanism^{93,94}. More precisely the mechanisms of separation through zeolite membranes can be recapitulated to: (i) molecular sieving; (ii) diffusion-controlled and (iii) adsorption-controlled permeation. In general, the separation with small pore zeolites is namely based on molecular sieving, where the discriminated molecules are larger than the pore size. Diffusion- and adsorption-controlled permeation governs the separation mechanism when the size of the pores is larger than the molecules to be separated.

The simplest example of a separation unit for flat membrane testing is presented on Figure 9. It should be mentioned that a serious problem in membrane utilization is the sealing of zeolite-ceramic composites, especially in the case of tubular modules. The gas-tight, high temperature sealing of tubular zeolite membranes remains an issue that is difficult to address on an industrial scale^{95,96}.

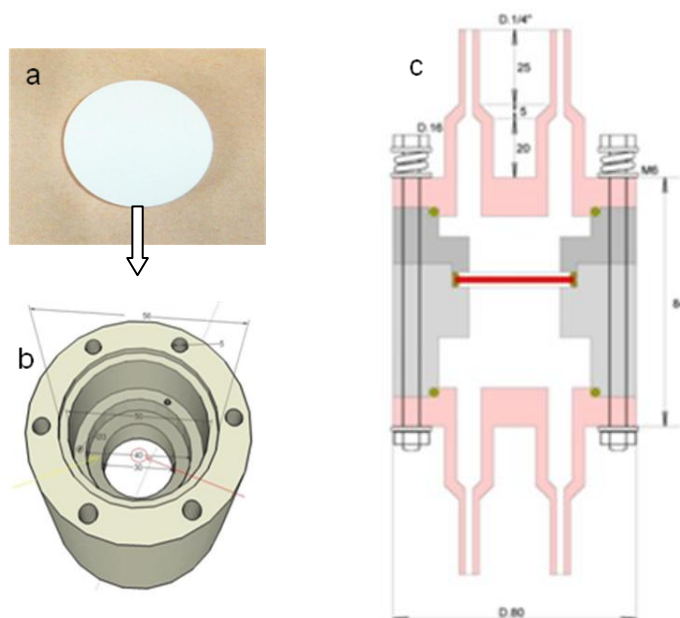


Figure 9. Optical micrograph of a flat alumina support comprising a zeolite film (see Figure 8) (a); top view of membrane holder (b); and a cross section of the entire membrane reactor (c).

Zeolite membranes are used in two main groups of separation, that is, gas-vapor and liquid-liquid. Both groups are important from industrial and environmental points of view. For instance, the CO₂ separation from different gas mixtures is amongst the most serious environmental problems nowadays. On the other hand, the H₂ is clean energy career and with high potential market. Consequently numerous studies have been performed to extract hydrogen from H₂/N₂, H₂/O₂, H₂/CH₄ and multi component gas mixtures. Liquid-liquid separation on zeolite membranes is a promising alternative of such an energy-intensive process as the distillation. Different alcohols (methanol-, ethanol-, propanol-, butanol-, etc.) - water mixtures

were subjected to separation by zeolite membranes. The first breakthrough was the commercialization of a LTA-type zeolite membrane for production of water-free ethanol by Mitsui & Co. Ltd., Japan^{97,98}. The water/ethanol separation factor is about 10000. This unit proved the feasibility of the preparation of defect-free large scale tubular (1 m length) zeolite membranes. On the other hand, the great efforts put on the preparation of zeolite membrane able to provide satisfactory xylene isomers separation was not achieved. Lately, the achievements of Tsapatsis group in the preparation of *b*-oriented MFI-type membrane⁹⁹ and grain boundary defect elimination by rapid thermal processing¹⁰⁰ bring back the optimism for successful industrial application of the MFI-type membrane in this important process.

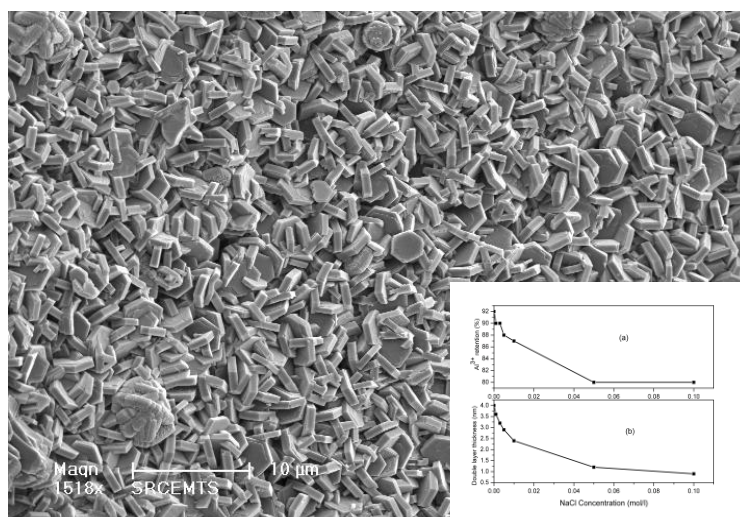


Figure 10. Top view of EMT-type film grown on alumina support. Inset: Al^{3+} retention (a) and double layer thickness (b) as a function of NaCl concentration.

Zeolite membranes are also considered as interesting alternative of polymer membranes in water purification. Reverse osmosis is currently the most important desalination technology, which is expected to grow continuously¹⁰¹. Theoretically, hydrated ions can be completely excluded by zeolite membranes with pore opening smaller than the size of the hydrated ion. Silicalite-1 (MFI-type) membranes showed 77 % salt rejection, but the water flux was relatively low ($0.003 \text{ m}^3 \text{ m}^{-2} \text{ day}^{-1}$)¹⁰². Large pore zeolite (EMT-type) membrane has been used in brackish water purification¹⁰³. The characteristic feature of the membrane was the high water permeability of relatively thin ($\sim 2 \text{ } \mu\text{m}$) zeolite layer (Figure 10). Nanofiltration experiments were performed with $Al(NO_3)_3$ as ionic solute at varying ionic strength

(different NaCl concentration) and different molecular weight ethylene glycols (EG) and polyethylene glycols (PEG) as non-ionic solutes. This membrane demonstrated high retention of (Figure 10, inset) and non-ionic species from aqueous solutions. In summary, the zeolite membranes are expected to overcome the challenges that polymer membranes cannot face. The active research on zeolite membrane preparation has already more than 20 years history with the goal to transfer the unique intrinsic properties of zeolites to membrane modules. However, the expectations that zeolite membranes could achieve a better performance in respect to polymer membranes, complemented by excellent thermal and chemical resistance, are still not realized. The preparation of zeolite membranes, in particular on a large scale, remains a challenge. The major disadvantages of zeolite membranes are poor processability and mechanical stability, very often poor fluxes and technical difficulties related with sealing at high temperature. Substantially higher costs of zeolite membranes are also an obstacle to their large industrial utilization. Obviously, the processing methods will have to be further developed in order to ensure an industry application of supported zeolite membranes.

4.1.2 Zeolite-containing mixed-matrix membranes

Today when the polymeric membranes reached the limits of their performance and the zeolite membranes cannot meet the industrial requirements, an acceptable alternative is the mixed-matrix membrane. In a mixed-matrix membrane zeolite crystals are embedded in a polymer that is sealing the gap between zeolite particles with gas-tight matrix. Thus, the properties of the host matrix can be enhanced by the separation power of the filler. Such a composite membrane combines the advantages of a polymeric membrane as ease of processability, good mechanical stability, acceptable selectivity and low cost with the higher permeability and selectivity of a zeolite¹⁰⁴. In addition, the mixed-matrix membrane combines the solution-diffusion mechanism of a polymeric membrane and the molecular sieving ability of a zeolite. First attempt for preparation of such membrane was in 1950¹⁰⁵, and after that different groups periodically came back to this concept^{106,107}. From the mid-1980s a renaissance of the concept was observed related namely with the inventions of Kulprathipaja and co-workers^{108,109}. Small pore zeolites (LTA-¹¹⁰, CHA-¹¹¹, NSI-type¹¹²) are preferred in mixed-matrix membrane preparation. An important zeolite characteristic that favors the successful preparation of a mixed-matrix membrane is the particle size, as nanosized zeolite particles are more appropriate than their micron-sized counterparts^{113,114}. The interfacial problem between microporous filler and polymer matrix is another issue of concern, namely due to the poor wetting. This problem is not observed when the mineral filler is mesopores material¹¹⁵ or a zeolite containing mesopores¹¹⁶.

Today mixed-matrix membranes are expected to open new prospects for membrane technology in separation and purification processes. Similarly to supported zeolite membranes the mixed-matrix membranes are still not at the level that allows large industrial application. However, all necessary conditions are brought together and it is not risky to predict a breakthrough and recent industrial uses of zeolite-containing mixed-matrix membranes.

4.2 Zeolite membrane reactors

Combining zeolite catalytic activity and selectivity in a membrane reactor is an attractive concept that could open great prospects in chemical processing. The topic has been actively studied during last decade¹¹⁷. There are already a number of examples where zeolite membranes enhance chemical reactions. However, there are a few cases where the zeolite membrane is catalytically active. It is worth nothing that a classical catalyst commonly used in a reaction may not be good when applied to a membrane reactor. The latter was clearly demonstrated by Dalmon and co-workers in *i*-butane dehydrogenation in a fixed catalytic bed employing MFI-type membrane to separate hydrogen^{118,119}. The team from IRCE-Lyon revealed that the membrane reactor requires a specially designed catalyst possessing catalytic activity that matches to the permeation capability of the membrane¹²⁰. Thus the role of a zeolite membrane in catalytic reactors is limited to equilibrium displacement or selective removal of reaction rate inhibitors.

The number of reaction tested on zeolite membrane reactors is fairly large. The most promising results were obtained in de-hydrogenation, partial oxidation, isomerization or esterification. For instance, silicalite-1 (MFI-type) zeolite membrane was used in the catalytic de-hydrogenation of *i*-butane. In the conventional packed-bed experiment the thermodynamic equilibrium conversion was obtained, while in the zeolite membrane reactor *i*-butane conversion was 15 % higher, which was attributed to the hydrogen removal in the course of the reaction¹²¹. The latter led to two important consequences: (i) the reverse reaction had a lower rate, and (ii) hydrogenolysis was suppressed thus increasing the selectivity to *i*-butane. The esterification process provided another sound example of enhancement of chemical reaction by removing of an undesired reaction product. A hydrophilic zeolite (LTA-type) was employed to remove the product water formed in the reaction of oleic acid with ethanol¹²². More hydrophobic molecular sieves as zeolite T¹²³ and ZSM-5¹²⁴ have been employed in the esterification of acetic acid with ethanol. The water removal in the Fischer-Tropsch process by a zeolite membrane has also showed promising results^{125,126}.

Summarizing the above discussion one can say that the main function of zeolite membranes in a reactor is the extraction of small molecules like water or hydrogen, thus increasing the conversion and/or the yield. The zeolite membranes can also

enhance the selectivity of the reaction by controlling the traffic of the reactants to catalytically active phase¹²⁷.

Lately, a trend to decreasing the size and miniaturization of the reactors was observed. Micron-sized and even nano-sized zeolite-containing composites were employed in different catalytic transformations showing promising results. An interesting example was published by Yang et al., who synthesized dimethyl ether from syngas on zeolite encapsulated Cu-ZnO-Al₂O₃ beads¹²⁸. Each Cu-ZnO-Al₂O₃ bead was covered with a thin MFI-type zeolite shell. The zeolite-containing composite catalysts showed much better performance than a classical oxide catalyst. In a parallel experiment, the Cu-ZnO-Al₂O₃ beads were introduced into a reactor comprising a zeolite layer controlling the traffic of the reactants. Noteworthy, the composite catalyst (core – shell beads) showed better performance than the reactor comprising a zeolite membrane. This is a spectacular example of synergism between the zeolite membrane and the catalyst. Lai et al. reported an example of fine chemical reaction performed in a membrane microreactor where the removal of the by-product water during the reaction provided a 25 % improvement in the conversion¹²⁹. The microreactors geometry is not limited to spherical particles. For instance, Yeung and co-workers employed a microchannel reactor comprising a zeolite NaA membrane and CsNaX catalyst in the reaction between benzaldehyde and ethyl cyanoacetate to produce ethyl-2-cyano-3-phenylacrylate¹³⁰. A multichannel microreactor comprising TS-1 nanoparticles was used for continuous selective oxidation of aniline by hydrogen peroxide¹³¹. The list of examples could be further extended revealing a long lasting interest and high activity in this field. We believe that the interest in microreactors will continue to grow in the era of nanotechnology.

4.3 Zeolites and fuel cell devices

The growing energy demand is probably the most serious problem that faces the world at the beginning of new millennium. Fuel cell devices are considered as one of the most promising instruments for generation of clean and efficient energy. A fuel cell combines hydrogen and oxygen to produce electricity, releasing water and heat as by-product¹³². The principle difference between a fuel cell and a conventional battery is that the fuel cell is a thermodynamically open system that consumes reactants from external sources and thus the device can operate as long as the fuel is supplied.

A key element in a fuel cell is the electrolyte membrane that mediates the electrochemical reaction between the electrodes and provides a rapid and selective conduction of ions. At present, namely polymer-based membranes are commercialized and show satisfactory performance. However, they restrict the operation temperature to about 80 °C. Hence, different inorganic materials based

alternatives are considered, where the membrane could be solely inorganic or composite inorganic-organic one. Zeolites and molecular sieves are among the best candidates since their channels and cages are occupied by water or other solvents and cations that compensate the negative charge of the framework. Thus the ionic conductivity is an intrinsic property of zeolites that can be explored in the search of better performing fuel cells membranes. Recently Yeung and Han have revised the application of zeolites and molecular sieves in fuel cell applications¹³³. According to their analysis, the zeolites have advantages as electrolytes in respect to perfluorosulfonic polymers membranes in direct methanol fuel cells and could face the fuel crossover problems. They anticipate that in near future the composite polymer-zeolite membranes will develop rapidly. Further, the advances in the zeolite synthesis and fabrication of complex zeolite morphological constructions will certainly bring all zeolite layers to application in fuel cell devices.

5. Zeolite-based Chemical Sensors

Most efforts have been focused on the synthesis of permselective zeolite membranes for the separation of gas or liquid mixtures (see section 4). However, there has been a considerable amount of work toward the development of other applications for zeolites such as optical devices, films with low dielectric constant, gas/liquid sensors, etc. A comprehensive knowledge for preparation of zeolite crystals with desired shape, size, morphology and crystalline structure and future assembly in thin-to-thick films are of great help in the design of these novel applications. Moreover, the mechanical and thermal stability and physicochemical properties of the zeolites assembled in the films are of significant importance.

This section is dedicated on the use of zeolites for sensors preparation, which is directly related with the energy saving applications. The new developments in the field after 2005 will be reviewed¹³⁴.

5.1. Sensor fabrication

The chemical sensing process involves molecular recognition of a chemical species (analyte) and transduction of the chemical information into a measurable signal. Many factors must be addressed in designing of new sensors such as material's sensitivity, selectivity, reproducibility, reliability, level of development/demonstration/acceptance, ease of use, relevance to in-situ and real-time measurements, robustness etc. The wide varieties of detectors for analytes (gas/liquid) exist but they do not satisfy all the necessary requirements of high sensitivity, selectivity, long-term stability, fast response, and appropriate integration in measurable network. Some of the approaches for enhancing selectivity and sensitivity of the sensors toward specific analytes include: i) design of highly selective materials, ii) manipulation of interfacial architecture on the molecular scale, iii) monitoring the kinetics of the reaction in situations where kinetic control

is operative (thin films, small crystalline particles), iv) use of sensor arrays involving multiple coating/transducer sets, and v) sensor array with recordable response as a function of temperature or change of surrounding.

In this section the emphasis will be given to the design of highly selective materials, i.e., molecular sieves (zeolites). Many fabrication methods are used in the production of zeolite-based chemical sensors. Factors that must be considered when selecting the production technique include their expense, purity, porosity, reliability and reproducibility. Numerous studies have addressed the goal to obtain thin-to-tick layers of zeolites on various substrates such as noble and non-noble metals, glass, ceramics, silicon, and even biological substrates. Common techniques for preparation of sensors include (1) screen-printing, (2) sol-gel techniques, (3) dip and spin coatings, and (4) direct growth with and without pre-seeding of the substrates. Indeed, the completely controlled zeolite structures, fine-tuned chemical composition and ion-exchange capacity make them attractive as true shape-selective compounds^{134,135}. However, the slow diffusion in their micropores leads to sluggish reaction rates. To overtake these limitations, zeolite materials have been manufactured and assembled in the nanosized scale. Considerable progress has already been reached in this field by assembling zeolites in thin films either by controlled attachment on self-assembled monolayers followed by growth or by different patterning techniques¹³⁶⁻¹⁴³.

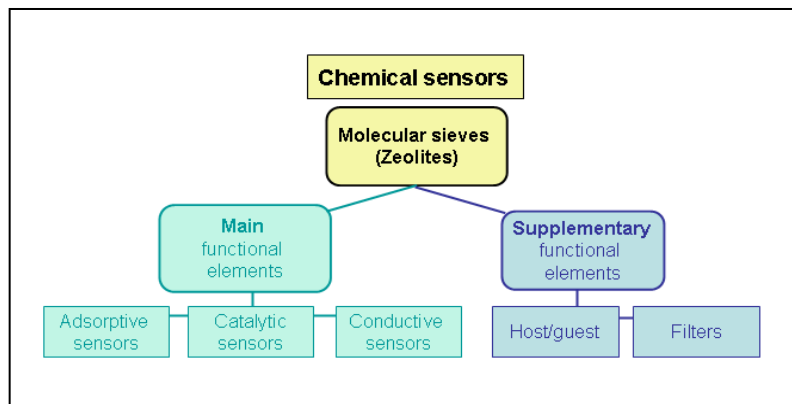


Figure 11. Classification of zeolite-based chemical sensors.

The versatility of zeolites with respect to pore structure, surface area, catalytic activity, particle dimensions and morphology is of particular interest for the sensor application. Their adsorption capacity, high-surface area and porosity, presence of mobile ions, and catalytic activity make them attractive candidates for chemical sensing/detection. In general the sensors have been categorized in four groups based primarily on the principal physics and operating mechanisms: (1) chromatography

and spectrometry, (2) electrochemical sensors, (3) mass sensors, and (4) optical sensors. Very detailed classification of gas sensor devices based on zeolites was presented by Moos et al.¹⁴⁴. The zeolite-based chemical sensors are divided in two groups depending on the respective role of the molecular sieves (Figure 11). The zeolite can act as a main functional element, which is the case for sensor principles relying directly on conductive, adsorptive, or catalytic properties of one specific type molecular sieve and its interaction with the analytes. The second group includes devices where the zeolites are supplementary or secondary elements. As an example, host-guest materials with active sites encapsulated within the zeolite pores are considered.

In the following section, the first group of sensors based on the specific properties of zeolites will be revised.

5.2. Adsorptive Sensors

The great variety of nano-structures and approaches for their depositions on two-dimensional supports result in wide number of reports describing their sensing applications. This is an active research area based on the need to obtain increasing amounts of data in chemical and food process streams as well as environmental monitoring. Applying selective molecular sieves is expected to increase considerably the performance and especially the selectivity towards one analyte versus others. The presence of charge-compensating cations such as alkaline, alkaline earth, protons, etc. within the inorganic frameworks adds ion exchange and selective properties. Moreover, the hydrophobic nature of pure silica materials or the hydrophilic nature of aluminosilicates makes these solids useful as specific adsorbents of organic molecules or water in gas or liquid phases.

A review paper on the uses of zeolites and zeolite-based materials for development of gas sensors has been published by Long¹⁴⁵. The potential of zeolites as high selective material towards specific gases is highlighted and white roads for further research are suggested.

The selective adsorption behaviour of zeolites is resulting in a measurable mass change. Therefore a great variety of gas sensors are developed using zeolite layers deposited on piezoelectric microbalances (QCM) or surface acoustic wave (SAW) devices. A large variety of molecular sieves has been deposited on sensor devices and a large number of analytes have been investigated¹³⁴.

For rapid equilibration of sensors with molecules in the gas phase, the diffusion path in the zeolite crystals has to be minimized¹⁴⁶. Nanosized ZSM-5 and LTA zeolite crystals were assembled on the gold electrodes of QCMs and the sorption isotherms of *n*- and *i*-butane were derived from frequency changes of the QCM. It is demonstrated that the response behaviour of the zeolite-based piezoelectric sensor

depends on the framework structure as well as on the size and shape of the analyte molecule. Selective sorption of *n*-butane in the LTA-type structure was shown, confirming the capability of producing a molecular sensor able to recognize and discriminate molecules within 1 Å.

Besides, LTA-type zeolite deposited on a magnetoelastic gas sensor was used for selective recognition of propylene and not propane. The high selectivity is based on the adsorption of propylene within the small pore molecular sieve¹⁴⁷.

The elastic properties of zeolite polycrystalline films under adsorption of different gases are also measured. The effect of adsorbed molecules on the mechanical properties of the zeolite film is determined. The adsorption of gases such as CO₂ and N₂, on faujasite nanocrystals induces changes in the elastic modulus of the zeolite film, and this has been used as a sensing parameter¹⁴⁸. Not only the mass but also the mechanical properties of zeolite crystals are changed with gas adsorption.

The zeolite sensor also proved to be more selective as it acts as a size and shape selective sensing element, essentially excluding potential interferents such as large hydrocarbon molecules, branched alcohols, *etc.* from reaching the sensor element and disrupting the nitrogen dioxide response¹⁴⁹.

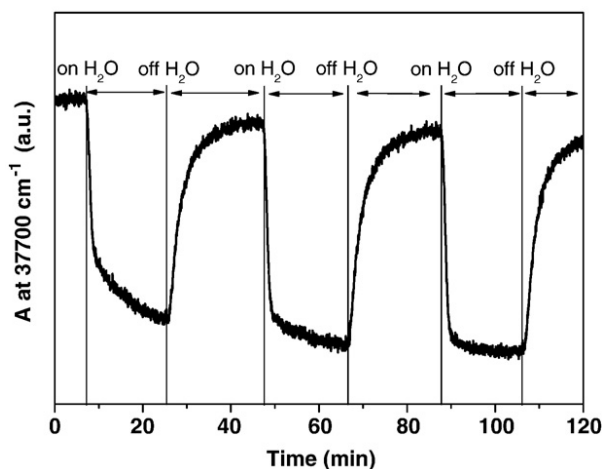


Figure 12. Sensing of water with AgH-ZSM-5.

Mostly pure zeolites without additional functionality have been used as size selective sensors for water, hydrocarbons, CO, NO_x, *etc.*¹⁵⁰. However, additional functionality in the zeolite sensors has been introduced via using their ion-exchange capacity. Thus different metals are introduced in the zeolite films and the selectivity

towards desired molecules has been stimulated. The preparation of chemically/thermally stable sensing material based on silicon-rich zeolites containing metal ion species suitable for sensor applications under severe conditions using AgH-ZSM-5 zeolites was demonstrated¹⁵¹. It is shown that the metal ion species with sensing properties are located in the channels of the silicon-rich zeolite. The adsorption/desorption of water within Ag-ZSM-5 is recorded by IR spectroscopy (Figure 12). The properties of Ag-ZSM-5 are completely reproducible for several days even at elevated temperatures, which opened the possibility of applying the Ag-zeolite as high-temperature sensors.

Humidity sensors based on LTA, BEA, AEI, and vanadium-doped MFI layers on QCM were also investigated¹⁵². Besides, selective sensors toward water or acetone for medical diagnosis are reported¹⁵³.

Recently, in our group different metal clusters (Ag, Pt, Pd, Cu, Cd, etc.) incorporated in confined environment (different types of zeolites) as gas sensors were studied. The porosity and accessibility to the metal clusters for detection of CO, NO_x, hydrocarbons and water vapors have been investigated. For the enhanced reactivity and selectivity at metal-containing porous interfaces, the transport properties of the self-organized materials are shown to improve considerably their sensing performance, especially in terms of selectivity and stability. The sensing toward different analytes on the metal-containing zeolites has been measured by in-situ IR spectroscopy (Figure 13). Additionally, the bi-functionality of the metal-containing zeolite sensors toward CO and alcohols has been demonstrated. Moreover, it is shown that the presence of water in the cell did not disturb the function of the gas sensors¹⁵⁴⁻¹⁵⁶.

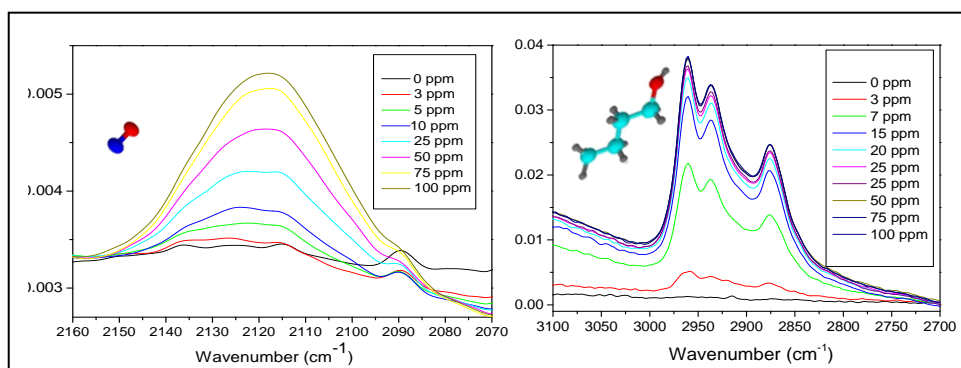


Figure 13. Simultaneous sensing of CO (left) and butanol (right) on Pt-Beta zeolite.

A large number of solid state sensors has been designed and brought to market for detection of hazardous, harmful, and toxic gases, in particular in safety, automotive, process control, or household applications¹⁵⁷. Safe detection of high energetic material such as 1,1-diamino-2,2-dinitroethylene (Fox-7) adsorbed in MFI zeolite by Raman and ¹³C NMR has been reported. The FOX-7 molecules are adsorbed within the MFI zeolites and the detection with spectroscopic methods is carried out safely, which is based on the sorption properties of the zeolites¹⁵⁸. By using materials with different pore structures and affinity toward hazardous and toxic gases, chemical sensors based on the selective sorption behaviour have been prepared.

A new chemically modified sensor based on a copper (II) doped zeolite was constructed (Cu²⁺/Y/ZMCPE)¹⁵⁹. It is demonstrated that this novel sensor could be used for the simultaneous determination of the pharmaceutically important compounds such as paracetamol and mefenamic acid. For the mefenamic acid, a linear correlation between oxidation peak current and analyte concentration over the range 0.3–100 μM with a detection limit of 0.04 μM, was obtained. The analytical performance of this sensor has been evaluated for the detection of paracetamol and mefenamic acid in human serum, human urine and in pharmaceutical products. Besides, the human blood glucose levels has been controlled through analyzing the acetone present in exhaled breath as a noninvasive method with the help of an electronic nose system based on QCM sensors. The amount of acetone vapor which is the marker of blood glucose (0.1-10 ppm) in human expiration was measured. In order for the QCM sensors to sense low levels of acetone concentration, a condenser containing zeolite absorbent ingredients is used. The QCM data from the breath is compared with blood glucose value¹⁶⁰.

MFI-type zeolite thin film deposited on long period fiber grating (LPFG) sensor was developed and tested for direct measurement of trace organic vapors¹⁶¹. The sensor measured the chemical vapor concentration by monitoring the molecular adsorption-induced shift of LPFG resonant wavelength in near IR region. Once the analyte molecules are adsorbed in the zeolite, the refractive index is changed. The sensor had a much faster response for isopropanol than for toluene as the former has a smaller molecular kinetic size and greater diffusivity in the MFI zeolite pores. The concept of physically and functionally integrating zeolite films with the LPFG offers new opportunities to develop a variety of chemical sensors for detection of chemical and biological molecular species with high sensitivities. The advantages of this type of sensors are operation simplicity, electromagnetic immunity, low backward reflection, and compactness, which are highly desirable for portable device applications.

In an alternative approach, optical devices were designed to measure the change in optical reflectivity upon adsorption of organic vapours. The concept of using

photonic crystals for label-free optical sensing has been proven. In recent years, color-tunable Bragg stacks composed of various materials, including hydrogels, inorganic materials such as silicon, titania, silica etc. have been designed and found responsive to a wide variety of analytes through optical thickness variations of their specific nanostructures¹⁶²⁻¹⁶⁴. To enhance the sensitivity and particularly the chemical selectivity of the Bragg stacks sensors towards solvent vapors and gases, highly porous layers based on $\text{TiO}_2/\text{SiO}_2$ multilayer as well as nanosized molecular sieves (colloidal zeolites) are utilized^{165,166}.

5.3. Catalytic sensors

The zeolites may behave as selective catalysts and are capable of discriminating between gas molecules on the basis of size and shape, allowing some gases through their structure, whilst not admitting others. Further, the zeolites behave in a chromatographic manner through variable diffusion characteristics. A mixture of gas may enter the zeolites pores, and the zeolite interior leads to a difference in diffusion speed. Finally the zeolites may perform a catalytic reaction involving the target gas, and this may lead to the production of one or more molecules that the sensor element may be more or less sensitive to. In the ideal case, this catalytic reaction will be specific to a particular analyte and lead to the production of multiple species that the sensor element is more sensitive, thus leading to a large enhancement in response signal for a given analyte with no chance of cross sensitivity.

The silicon-rich zeolites with a high degree of selectivity are of particular interest in the design of gas sensor devices with very low cross-interference. While sensitivity to broad classes of chemicals may be useful in many monitoring applications, it is less desirable in cases where the primary goal is the identification of target species within a mixture. One way of modifying the selectivity of a broadly active catalyst is to disperse it within a zeolite host, where access of a reactant to the catalyst becomes, among other things, a function of its steric dimensions relative to those of the host framework (Figure 14). With this fact in mind, sensor chips with combustion catalyst-containing zeolites were prepared and tested for their responses to reactive species¹⁶⁷. The effects of combustion catalyst-containing zeolites on the output signals of micromachined thin-film calorimeters demonstrates that sensitivity to different species can be notably altered depending on the pore size of the zeolite used. The equilibration time of the overall sensor system is far greater than that of the unmodified transducer. Most significantly, by varying the catalyst micropore size, the sensor can be made to respond more strongly to the smallest and fastest-diffusing hydrocarbons instead of those with the greatest carbon contents.

Beside, cataluminescence described by chemiluminescence emitted during the heterogeneous catalytic oxidation of organic vapours on the zeolites surface is used

to prepare optical sensor elements¹⁶⁸. The sensor devices for selective detection of acetaldehyde are based on Na- and Na/Cs- containing FAU zeolite. The selectivity towards acetaldehyde was attributed to the specific pore size of the zeolite and the steric effects. Moreover, the nature of the mobile ions has a crucial role for further development, since it has an impact on the acidity and catalytic activity of the zeolite. In an alternative approach zeolites are used for sensing application, and it was found that the propane sensor effect takes place at the zeolite/Au electrode and is controlled by bulk diffusion of propane into the pores of the zeolite¹⁶⁹.

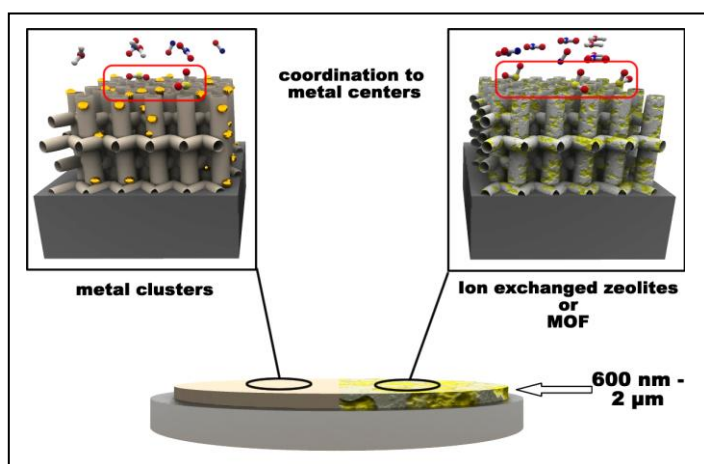


Figure 14. Enhanced reactivity and selectivity at metal-containing porous sensor: zeolites and metal organic framework type materials (MOF).

Tightening emission legislations for passenger cars and heavy duty vehicles in conjunction with the urgent need for fuel efficiency lead to leanly operated power train concepts, which are required novel exhaust gas after treatment methods like NO_x storage catalysts and ammonia selective catalytic NO_x reduction, or even to a combination of both¹⁷⁰⁻¹⁷². Several new exhaust sensors were suggested in the last years¹⁷³. The sensing devices have to provide three-fold functionality. It should be electrically conductive, catalytically selective, and electrochemically active. All functions should be highly long-term stable in the harsh environment of automotive or industrial exhausts. Therefore, an intensive material development process combining all these three functions in one complex material configuration is required.

A novel mixed gas sensor concept, in which the electrode functions are separated, is suitable for selective ammonia detection in the exhaust. A sensor with two equally conductive porous electrodes, one of which being covered by a porous

commercially available catalyst with a proven long-term stability in the exhaust was presented. Iron-containing zeolites (Fe-ZSM5) are used as electrode coating. The advantage of this concept is that the catalyst materials do not need to be electrically conductive but to provide the requested catalytic selectivity and long-term stable. The sensors are tested in a heated synthetic exhaust gas (10 vol.% O₂, 6.5 vol.% CO₂, and 7 vol.% H₂O), thus simulating an exhaust of an engine operated at an air-to-fuel ratio of ≈ 2 . NH₃; and nitrogen oxides (NO and/or NO₂) are added in different concentrations to the base gas. It is demonstrated that these mixed sensors with an additional catalyst layer as active materials have a high potential for ammonia detection.

5.4. Zeolite conductive sensors

The role of zeolite as an ionic conductor opens the interest to these materials for sensing application. The motion of extra-framework cations in response to an electric field is the basis of conductivity. In addition, the effect of different polar and nonpolar molecules adsorbed on the ionic conductivity of zeolites has been explored¹⁷⁴. The results from these studies have led to exploiting the change in ionic conductivity of zeolites in the presence of molecules and thus to the possibility of designing of new gas sensors¹⁷⁵. A large body of studies exists on the fundamental mechanism of the effect of ammonia on the conductivity of different types of zeolites at high temperatures. Study on the effect of ammonia on dehydrated zeolite BEA was carried out and an increase in the protonic bulk conductivity of the material is measured. These results are attributed to the adsorption of NH₃ molecules, which support the proton transport from one aluminum site within the zeolite framework to the next. Since the effect depends essentially on the amount of adsorbed NH₃, i.e., on the ammonia partial pressure pNH_3 , proton-conducting zeolites are promising candidates for conductometric or impedimetric ammonia sensors. The robust zeolite sensor is intended to be used for automotive exhaust gas applications, since no significant cross-interference of hydrocarbons, CO₂, CO, and O₂ was observed when they were operated at 420 °C¹⁷⁶. In a later study¹⁷⁷, a similar sensor concept using protonconducting H-MFI zeolite for conductometric amine detection was presented.

A highly selective hydrocarbon gas sensor based on Au interdigital electrodes covered with zeolite and chromium (III) oxide films is reported¹⁷⁸. The zeolite did not cover the semiconducting metal oxide as a catalytically active filter layer, while the Cr₂O₃ film is applied on top of an ion-conducting Pt-doped ZSM-5 zeolite film. Impedance spectra of such sensors showed high-frequency semicircles, which are assigned to the hydrocarbons ionic mobility within the zeolite bulk material. Measurements at fixed frequency in the gas dependent range show high sensitivity to different hydrocarbon gases and no cross sensitivity toward CO and H₂. This new sensing mechanism is attributed to the interface between zeolite and Cr₂O₃.

The effect of acidity and pore diameter of zeolites (MFI, MOR and BEA) on the detection of base molecules such as water, acetonitrile, ammonia, benzonitrile, pyridine, aniline, and triethylamine was investigated. For smaller molecules having diameter of less than 0.4 nm (water, acetonitrile, and ammonia), a good correlation was observed between the response and the proton affinity of base molecules. It was indicated that acid–base interaction is the major factor when molecular diameter is smaller than the zeolite pore diameter. As for larger molecules (benzonitrile, pyridine, aniline, and triethylamine) of which the molecular diameter is nearly the pore diameter of zeolites, the response magnitudes were lower than those of the smaller molecules. Quantification of adsorbed species by in situ FTIR revealed that the response magnitude for larger molecules significantly depends on the mobility of migrating species, which is controlled by relative size of molecules to zeolite pore diameter¹⁷⁹. The sensitivity of the MFI, MOR and BEA- zeolite sensors to various base molecules as a function of proton affinity, which can be regarded as a measure of base strength of the molecules has been investigated. The sensitivity generally increased with the increase in the proton affinity. This trend indicates that the acid–base interaction between the zeolite and the probe molecule is an essential factor for high sensitivity of the zeolite based sensors. In the case of NH₃ detection, the sensitivity is in the order of MOR > MFI > BEA, while the pore diameter is as MOR = BEA > MFI, which is suggesting major contribution of acid–base interaction between zeolites and probe molecules. In the case of large molecules such as pyridine and triethylamine, the sensitivity was strongly dependent on the type of zeolites (MOR > BEA > MFI) indicating the significant contribution of diffusion in detection of the larger molecules¹⁸⁰.

Sensor devices using the conductivity as a direct measure for analyte with different concentrations can be divided into two subgroups depending on the localization of that effect. The interaction involves either the entire bulk of the zeolite and takes place within the channels (pores), or it is confined mostly to the interface between the zeolite and the neighbouring phase¹⁸¹. A conductometric sensor concept for humidity and combustible gases has been developed. The working temperature for the conductive devices is in the range 40–110 °C¹⁸². Later, the same concept was applied to an impedimetric zeolite-based sensor for humidity detection in more severe environment¹⁸³. Here, the impedance of a Si-rich zeolite film was found to respond linearly and reversibly even to traces of humidity.

Impedance spectroscopy of Na⁺-exchanged zeolite Y was investigated in the presence of Dimethylmethylphosphonate (DMMP), which is a stimulant for the highly toxic organophosphate nerve agent Sarin. It was shown that the Na⁺ conductivity in zeolite decreased in the presence of DMMP vapour at the ppm-level. The surface of the zeolite has negligible effects on the decomposition of DMMP, while the intrazeolite cation motions facilitated by the DMMP reorientation are responsible for the decrease in the impedance. The cations with

larger size in the supercages showed an increase in impedance when exposed to DMMP, probably due to the repulsive interactions that counteract the ionic motion. The change in impedance of NaY can be used as a sensor for detection of organophosphates at elevated temperatures. Moreover, the selectivity to DMMP in the presence of CO, NH₃, and hydrocarbons such as methane and propane has been increased¹⁸⁴. A similar sensor concept for amine detection was developed. By measuring its impedance at elevated temperatures, selective ammonia sensor elements were obtained. Only comparatively high concentrations of NO₂ and propane have caused a small cross-interference, whereas the NO sensitivity was negligible for the sensor. In addition to bulk effects within the zeolite framework, interface effects between the zeolite and an adjacent material may cause a sensor response.

5.4.1. Conductive polymers doped with zeolites

Recently, there are interests in using conductive polymers as gas sensing materials, as alternatives to metal or metal oxides¹⁸⁵. Conductive polymers can offer a variety of advantages for sensor applications over the metallic or ceramics counterparts: they are relatively low cost materials and lighter. Additionally, the fabrication techniques are relatively simple and straightforward since there are no needs for clean room and high temperature processes. The conductive polymers can be deposited on various types of substrates and can be operated at lower applied voltage in many conditions. Moreover, the materials exhibit moderately fast reversible electrical conductivity changes when they are exposed to gases or vapours at room temperature. Finally, they have flexibility in molecular architectures such as side chain attachments, and modifications by charged or neutral particles either in the bulk or on the surface.

Combining the advantages of conductive polymer, poly(3-thiopheneacetic acid) and different zeolites has resulted in selective gas sensors¹⁸⁶. The effects of zeolite type, concentration, cation type on the electrical conductivity response of the composites were investigated. Zeolites LTL, Mordenite and Beta with nearly the same pore sizes but different Si/Al ratios have been used. It has been measured a negative electrical conductivity response and sensitivity which is occurred under H₂ exposure. The electrical conductivity sensitivity is increased with decreasing the Al content because of interactions between H₂ and the zeolite, and consequently a greater interaction between H₂ and the active sites on the polymer chain has occurred. Zeolite Beta has the highest electrical conductivity sensitivity due to the lowest amount of Al. However, the Li⁺ form has lower electrical conductivity sensitivity than those of the Na⁺ and K⁺ forms due to the higher electronegativity and a smaller ionic radius. The loading of Na⁺ cations causes a more loosely binding interaction between the cation and H₂ and correspondingly a more favourable interaction between H₂ and the conductive polymer. At higher zeolite

(Mordenite) content, the reduction of sensitivity value is suggested to arise from the diminishing of available active sites on the conductive polymer.

Similar investigation on electrical conductivity of Poly(Phenylene-vinylene)/Zeolite composites has been carried out¹⁸⁷. The interest in such sensors is explained by the combustion of petroleum products such as diesel oil, heating oil, and heavy fuel oil which generates pollutant emissions in the environment. For example, carbon monoxide causes chest pain in heart patients, headaches, nausea and reduced mental alertness, while sulfur dioxide can induce lung disease and breathing problems for asthmatics. Emissions of sulfur dioxide also lead to the deposition of acid rain and other acidic compounds. Moreover, these depositions change the chemical balance of soils which leads to the leaching of trace minerals and nutrients critical to vegetations. In addition to those toxic gases in the atmosphere, high energetic materials are of great concern. A safe detection of potential explosion (high energetic materials) *via* tailored gas sensors which can sense various volatiles of typical bomb chemicals cyclotrimethylenetrinitramine (RDX), trinitrotulene (TNT), and ammonium nitrate are needed. Conducting polymers such as poly(*p*-phenylenevinylene) (PPV) was used as a sensing material because PPV possesses good optical and electrical properties, and it can be synthesized by a relative simple technique. For such applications, molecular sieves with high sensitivity towards polar chemicals were considered. Zeolite Y was introduced into the polymer matrix and an increased sensitivity towards NH_4NO_3 was measured. The pure PPV is used to detect eight organic solvents (chloroform, acetone, ethanol, ethyl acetate, toluene, hexane, acetic acid, methanol, diethyl ether). Besides, a detection of NH_4NO_3 , which is commonly found in fertilizers and explosive material industries with PPV vapour, was reported.

5.5. Mixed zeolite/photopolymer gas sensors

The good optical compatibility between the zeolite nanoparticles and the water-soluble acrylamide-based polymer allows a versatile design of photopolymerizable nanocomposites with different properties by selecting the adequate type of zeolites. Nanoparticles doped polymers are the subject of intensive research investigations due to their unique, improved mechanical, electrical, optical and thermal properties. A substantial advantage in using zeolite nanoparticles as dopants is that the properties of the resulting polymer nanocomposites are tunable due to their hybrid nature. Also, because the zeolite nanoparticles are very small, they introduce lower scattering than the micron-sized particles used as reinforcing agents. Another advantage is that the loading requirements for nano-sized dopants are lower.

The nanocomposites containing different zeolite nanoparticles have demonstrated selective sensing behaviour toward toluene, water, linear and branched hydrocarbons, and they have been coated in either glass or plastic substrates and exposed directly to the environmental conditions. Besides, the optical properties of

the photopolymer layers combined with the zeolite nanoparticles have demonstrated irreversible sensing for water¹⁸⁸⁻¹⁹².

Transmission holographic grating sensor devices are designed and it was shown that the diffraction efficiency has changed permanently after exposure to high humidity (Figure 15).

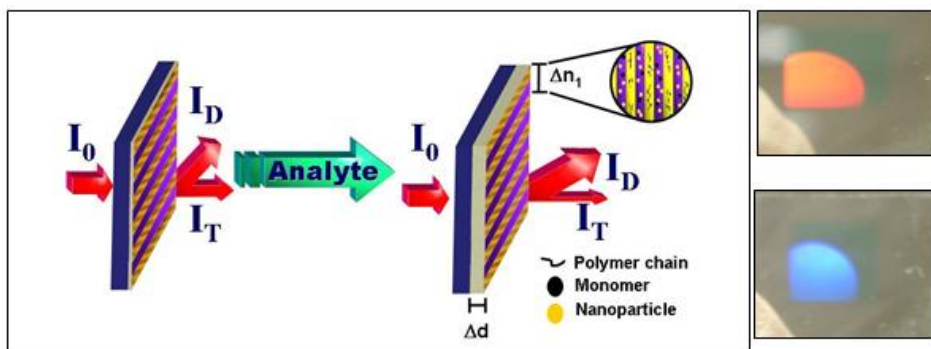


Figure 15. Principal scheme of zeolite/photopolymer sensors: irreversible change in colour due to adsorption and desorption of water.

In summary, advances have been made in the understanding of materials chemistry and materials processing for preparation of high selective and sensitive chemical sensors based on zeolites. Modification of selective and catalytic materials (zeolites) is an important development, and shows a further way in which the materials' science can be used to improve the specificity and response to a target analytes, while making sure the response of the film is not disrupted by a competing gas, humidity, high temperature. In the face of the growth in the number of studies dedicated to sensors, the zeolites are expected to play an ever increasing role in the design of next generation of sensor devices. In addition to improvements of the materials used for sensor, novel principles of measuring and manufacturing have been opened. For high-temperature gas sensing, real-time in-situ diagnosis of reactions and combustion processes are considered, while for low-temperature gas sensing indoor air control or medical applications are envisioned. The unique properties of zeolites make them ideal candidates for advanced gas sensing

6. General Conclusions

The use of zeolites in areas other than their historical debuts has emerged. It is driven by the need to meet ever tighter specifications on fuels, chemicals and energy efficiency in general. In order to meet these goals, molecular and atomic precision in the design of catalysts, adsorbents, sensors, films, etc., is required and

zeolite are unique materials in that sense. Some of their limitations, such as the diffusion restriction on large or polar molecules, are partially removed by the design of hierarchical materials for instance. The reasons for the early success of zeolites are known and have been analyzed by Degnan², in short they are:

- Early discovery (invention) and development (innovation)
- Scalability and affordable manufacturing costs
- Early structure resolutions
- Hydrothermal stability and regenerability
- Compositional and morphological versatility
- Understanding of the underlying chemistry and implication of molecular transport (catalytic engineering).

Most of these factors are still present and even strengthened by impressive advances in instrumentation and computer power, and they will be complemented by the skills and creativity of people coming from new fields.

The list of emerging applications considered in the present review is not exhaustive. Nevertheless it gives an idea about the diversity of potential uses of zeolites in both conventional and advanced applications. To this large variety of new promising applications one has to add the contribution of zeolites to energy saving processes, which is probably amongst the most serious challenges that faces modern society. Hence, it is not uncertain to predict a growing interest and new fascinating developments based on zeolite-type materials that go far beyond the traditional uses.

Acknowledgements

All of us thank the Conseil Régional de Basse-Normandie for important support in the field of zeolites. JPG wishes to thank the St-Nikon Foundation for unrelenting support over the years in the fields of zeolite and scientific management.

References

- [1] Vermeiren, W. & Gilson, J-P. Impact of Zeolites on the Petroleum and Petrochemical Industry. *Top Catal* **52**, 1131-1161 (2009)
- [2] Degnan, T. F. Recent progress in the development of zeolitic catalysts for the petroleum refining and petrochemical manufacturing industries. *Stud Surf Sci Catal* **170**, 54-65 (2007)
- [3] Guibet, J-C., *Fuels and Engines: Technology, Energy, Environment*. Editions Technip, Paris (1999)

- [4] Holmgren, J., Marinangeli, R., Marker, T. McCall, M., Petri, J., Czernik, S., Elliott, D. & Shonnard, D. Opportunities for Biorenewables. *Hydrocarbon Engineering*, June (2007)
- [5] Serrano-Ruiz, J. C. & Dumesic, J.A. *Energy Environ Sci* **4**, 83-99 (2011)
- [6] Huber, G. W., Iborra, S. & Corma, A. Synthesis of Transportation Fuels from Biomass: Chemistry, Catalysts, and Engineering. *Chem Rev* **106**, 4044-4098 (2006)
- [7] Popov, A., Kondratieva, E., Gilson, J-P., Mariey, L., Travert, A. & Maugé, F. IR Study of the Interaction of Phenol with Oxides and Sulided CoMo Catalysts for Bio-Fuel Hydrodeoxygenation. *Catal Today* doi:10.1016/j.cattod.2011.02.010
- [8] Weisz, P.B., Haag, W.O. & Rodewald, P.G. Catalytic production of high-grade fuel (gasoline) from biomass compounds by shape-selective catalysis. *Science* **206**, 57-58 (1979)
- [9] Chen, N.Y., Degnan, T.F. & Koenig, L.R. Liquid Fuels from Carbohydrates. *Chemtech* **16**, 506-511 (1986)
- [10] Taarning, E., Osmundsen, C.M., Yang, X., Voss, B., Andersen, S & Christensen, C.H. Zeolite-Catalyzed Biomass Conversion of Fuels and Chemicals. *Energy Environ Sci* **4**, 793-804 (2011)
- [11] Bridgwater, A.V., Meier, D. & Radlein, D. An Overview of Fast Pyrolysis of Biomass. *Org Geochem* **30**, 1479-1493 (1999)
- [12] Lappas, A.A, Samolada, M.C., Iatridis, D.K., Voutetakis, S.S. & Vasalos, I.A. Biomass Pyrolysis in a Circulating Fluid Bed Reactor for the Production of Fuels and Chemicals. *Fuel* **81**, 2087-2095 (2002)
- [13] Carlson, T.R., Vispute, T.P. & Huber, G.W. Green Gasoline by Catalytic Fast Pyrolysis of Solid Biomass Derived Compounds. *Chem Sus Chem* **1**, 397-400 (2008)
- [14] Carlson, T. R., Tompsett, G. A., Conner, W. C. & Huber, G.W. Aromatics Production from Catalytic Fast Pyrolysis of Biomass-derived Products *Top Catal* **52**, 241–252 (2009)
- [15] De Jong, K.P. Efficient Catalytic Processes for the Manufacturing of High Quality Transportation Fuels. *Catal Today* **29**, 171-178 (1996)
- [16] Furimski, E. Catalytic Hydrodeoxygenation. *Appl Cata A* **199**, 147-190 (2000)
- [17] Elliott, D.C. Historical Developments in Hydroprocessing Bio-oils. *Energy Fuels* **21**, 1792-1815 (2007)
- [18] Adjaye, J. D., Katikaneni, S.P.R & Bakhshi N.N. Catalytic Conversion of a Biofuel to Hydrocarbons: Effect of Mixtures of HZSM-5 and Silica-alumina Catalysts on Product Distribution. *Fuel Process Technol* **48**, 115–143 (1996)

- [19] Boucher, M.E., Chaala, A., Pakdel, H. & Roy, C. Bio-oils Obtained by Vacuum Pyrolysis of Softwood Bark as a Liquid Fuel for Gas Turbines. *Biomass Bioenergy* **19**, 337-361 (2000)
- [20] Vispute, T.P., Zhang, H., Sanna, A., Xiao, R. & Huber, G.W. Renewable Chemical Commodity Feedstocks from Integrated Catalytic Processing of Pyrolysis Oils. *Science* **330**, 1222-1227 (2010)
- [21] Lappas, A.A, Bezergianni S. & Vasalos I.A. Production of Biofuels via Co-processing in Conventional Refining Processes. *Catal Today* **145**, 55-62 (2009)
- [22] Domine, M.E, van Veen, A.C, Schuurman, Y. & Mirodatos, C. Coprocessing of Oxygenated Biomass Compounds and Hydrocarbons for the Production of Sustainable Fuel. *ChemSusChem* **1**, 179-181 (2008)
- [23] G. H. Huber, A. Corma, Synergies Between Bio- and Oil Refineries for the Production of Fuels from Biomass. *Angew Chem Int Ed* **46**, 7184-720 (2007)
- [24] Graça, I., Fernandes, A., Lopes, J.M., Ribeiro, M.F., Laforge, S., Magnoux, P. & Ramôa Ribeiro, F. Bio-oils and FCC Feedstocks Co-processing: Impact of Phenolic Molecules on FCC Hydrocarbons Transformation over MFI. *Fuel* **90**, 467-476 (2011)
- [25] Kulprathipanja, S. in *Zeolites in Industrial Separation and Catalysis* ed Kulprathipanja, S. Ch. 6, 203-228 (2010)
- [26] Kulprathipanja, S. Technique to Reduce the Zeolite Molecular Sieve Solubility in an Aqueous System, *US Patent* 4,431,456, assigned to UOP Inc. (1984)
- [27] van Ballegoy, C.M., Daamen, J.T., Gilson, J-P., Klazinga, A.H., Hoek, A. Process for the preparation of middle distillates. *EP* 537,815, assigned to Shell Int. Res. Mij. B.V. (1997)
- [28] Bouchy, C., Hastoy, G., Guillon, E. & Martens, J.A. Fischer-Tropsch Waxes Upgrading via Hydrocracking and Selective Hydroisomerization. *Oil & Gas Sci Tech – Rev IFP* **64**, 91-112 (2009)
- [29] Sie, S.T., Senden M.M.G., & Van Wechem H.M.H. Conversion of Natural Gas to Transportation Fuels via the Shell Middle Distillate Synthesis Process (SMDS). *Catal Today* **8**, 371-394 (1991)
- [30] Leckel, D. Selectivity Effect of Oxygenates in Hydrocracking of Fischer-Tropsch Waxes. *Energ Fuel* **21**, 661-667 (2007)
- [31] Guisnet, M., Costa, L. & Ribeiro, F.R. Prevention of Zeolite Deactivation by Coking. *J Mol Catal A* **305**, 69-83 (2009)
- [32] Guisnet, M. & Magnoux, P. Organic Chemistry of Coke Formation. *Appl Catal A* **212**, 83-96 (2001)

- [33] Thibault-Starzyk, F., Vimont, A. & Gilson, J-P. 2D COS IR Study of Coking in Xylene Isomerization on H-MFI Zeolite. *Catal Today* **70**, 227–241 (2001)
- [34] Fernandez, C., Stan, I. Gilson, J-P., Thomas, K., Vicente, A., Bonilla, A. & Perez-Ramirez, J. Hierarchical ZSM-5 Zeolites in Shape Selective Xylene Isomerization: Role of Mesoporosity and Acid Site Speciation. *Chem Eur J* **16**, 6224-6233 (2010)
- [35] Teketel, S., Olsbye, U., Lillerud, K-P., Beato, P. & Svelle, S. Selectivity Control Through Fundamental Mechanistic Insight in the conversion of methanol to hydrocarbons over zeolites. *Microporous Mesoporous Mater* **136**, 33-41 (2010)
- [36] Barbera, K., Bonino, F., Bordiga, S., Janssens, T.V.W & Beato, P. Structure Deactivation Relationship for ZSM-5 Catalysts Governed by Framework Defects. *J Catal* doi:10.1016/j.jcat.2011.03.016
- [37] Bjørgen, M, Joensen, F., Holm, M.S., Olsbye, U., Lillerud, K-P. & Svelle, S. Methanol to Gasoline over H-ZSM-5: Improved Catalytic Performance by Treatment with NaOH. *Appl Catal A* **345**, 43-50 (2008)
- [38] Wang, L., Tao, L., Xie, M., Xu, G. Huang, J. & Xu, J. Dehydrogenation and aromatization of methane under non-oxidizing conditions. *Catal Lett* **21**, 35-41 (1993)
- [39] Holmen, A. Direct Conversion of Methane to Fuels and Chemicals. *Catal Today* **142**, 2-8 (2009)
- [40] Sobalik, Z., Environmental catalysis with zeolites. *Zeolites*, 333 (2008)
- [41] Smeets, P. J., Meng, Q., Corthals, S., Leeman, H., Schoonheydt, R. A., Co-ZSM-5 catalysts in the decomposition of N₂O and the SCR of NO with CH₄: Influence of preparation method and cobalt loading. *Applied Catalysis, B: Environmental* **84** (3-4), 505 (2008)
- [42] Ferreira, A. P., Capela, S., Da Costa, P., Henriques, C., Ribeiro, M. F., Ribeiro, F. R., CH₄-SCR of NO over Co and Pd ferrierite catalysts: Effect of preparation on catalytic performance. *Catalysis Today* **119** (1-4), 156 (2007)
- [43] Capela, S., Catalao, R., Ribeiro, M. F., Da Costa, P., Djega-Mariadassou, G., Ribeiro, F. R., Henriques, C., Methanol interaction with NO₂: An attempt to identify intermediate compounds in CH₄-SCR of NO with Co/Pd-HFER catalyst. *Catalysis Today* **137** (2-4), 157 (2008)
- [44] Lonyi, F., Solt, H. E., Valyon, J., Decolatti, H., Gutierrez, L. B., Miro, E., An operando DRIFTS study of the active sites and the active intermediates of the NO-SCR reaction by methane over In,H- and In,Pd,H-zeolite catalysts. *Applied Catalysis, B: Environmental* **100** (1-2), 133 (2010)

- [45] Pieterse, J. A. Z., Top, H., Vollink, F., Hoving, K., Van den Brink, R. W., Selective catalytic reduction of NO_x in real exhaust gas of gas engines using unburned gas: Catalyst deactivation and advances toward long-term stability. *Chemical Engineering Journal (Amsterdam, Netherlands)* **120** (1-2), 17 (2006)
- [46] Zhao, D., Ingelsten, H. H., Skoglundh, M., Palmqvist, A. J., Catalytic and mechanistic study of lean NO₂ reduction by isobutane and propane over HZSM-5. *Journal of Molecular Catalysis A: Chemical* **249** (1-2), 13 (2006)
- [47] Schwidder, M., Santhosh Kumar, M., Bentrup, U., Perez-Ramirez, J., Brueckner, A., Gruenert, W., The role of Brønsted acidity in the SCR of NO over Fe-MFI catalysts. *Microporous Mesoporous Mater.* **111** (1-3), 124 (2008)
- [48] Liu, I. O. Y., Cant, N. W., The reactions of nitroalkanes over Cu-MFI and Fe-MFI catalysts under hydrocarbon-selective catalytic reduction conditions. *Journal of Catalysis* **230** (1), 123 (2005)
- [49] Chen, X., Yang, X., Zhu, A., Au, C. T., Shi, C., In situ DRIFTS study during C₂H₄-SCR of NO over Co-ZSM-5. *Journal of Molecular Catalysis A: Chemical* **312** (1-2), 31 (2009)
- [50] Haerelind, I., Hanna, P., Anders, S., Mechanistic Aspects of HC-SCR over HZSM-5: Hydrocarbon Activation and Role of Carbon-Nitrogen Intermediates. *Journal of Physical Chemistry B* **110** (37), 18392 (2006)
- [51] Capek, L., Novoveska, K., Sobalik, Z., Wichterlova, B., Cider, L., Jobson, E., Cu-ZSM-5 zeolite highly active in reduction of NO with decane under water vapor presence. Comparison of decane, propane and propene by in situ FTIR. *Applied Catalysis, B: Environmental* **60** (3-4), 201 (2005)
- [52] Li, G., Wang, X., Jia, C., Liu, Z., An in situ Fourier transform infrared study on the mechanism of NO reduction by acetylene over mordenite-based catalysts. *Journal of Catalysis* **257** (2), 291 (2008)
- [53] Wang, C., Wang, X., Xing, N., Yu, Q., Wang, Y., Zr/HZSM-5 catalyst for NO reduction by C₂H₂ in lean-burn conditions. *Applied Catalysis, A: General* **334** (1-2), 137 (2008)
- [54] Authors personal comment
- [55] Sultana, A., Nanba, T., Haneda, M., Hamada, H., SCR of NO_x with NH₃ over Cu/NaZSM-5 and Cu/HZSM-5 in the presence of decane. *Catalysis Communication* **10** (14), 1859 (2009)
- [56] Sjoevall, H., Blint, R. J., Olsson, L., Detailed kinetic modeling of NH₃ SCR over Cu-ZSM-5. *Applied Catalysis, B: Environmental* **92** (1-2), 138 (2009)
- [57] Grossale, A., Nova, I., Tronconi, E., Ammonia blocking of the "Fast SCR" reactivity over a commercial Fe-zeolite catalyst for Diesel exhaust aftertreatment. *Journal of Catalysis* **265** (2), 141 (2009)

- [58] Forzatti, P., Nova, I., Tronconi, E., Enhanced NH₃ Selective Catalytic Reduction for NO_x Abatement. *Angewandte Chemie, International Edition* **48** (44), 8366 (2009)
- [59] Malpartida, I., Marie, O., Bazin, P., Daturi, M., Jeandel, X., An operando IR study of the unburnt HC effect on the activity of a commercial automotive catalyst for NH₃-SCR. *Applied Catalysis, B: Environmental* **102** (1-2), 190 (2011)
- [60] Malpartida, I., Ivanova, E., Mihaylov, M., Hadjiivanov, K., Blasin-Aube, V., Marie, O., Daturi, M., CO and NO adsorption for the IR characterization of Fe²⁺ cations in ferrierite: an efficient catalyst for NO_x SCR with NH₃ as studied by Operando IR spectroscopy. *Catalysis Today* **149**, 295 (2010)
- [61] Wilken, N., Kamasamudram, K., Currier, N. W., Li, J., Yezerets, A., Olsson, L., Heat of adsorption for NH₃, NO₂ and NO on Cu-Beta zeolite using microcalorimeter for NH₃ SCR applications. *Catalysis Today* **151** (3-4), 237 (2010)
- [62] Li, G., Jones, C. A., Grassian, V. H., Larsen, S. C., Selective catalytic reduction of NO₂ with urea in nanocrystalline NaY zeolite. *Journal of Catalysis* **234** (2), 401 (2005)
- [63] Bazin, P., Alenda, A., Thibault-Starzyk, F., Interaction of water and ammonium in NaHY zeolite as detected by combined IR and gravimetric analysis (AGIR). *Dalton Transactions* **39** (36), 8432 (2010)
- [64] Kroecher, O., Devadas, M., Elsener, M., Wokaun, A., Soeger, N., Pfeifer, M., Demel, Y., Mussmann, L., Investigation of the selective catalytic reduction of NO by NH₃ on Fe-ZSM5 monolith catalysts. *Applied Catalysis, B: Environmental* **66** (3-4), 208 (2006)
- [65] Girard, J., Cavataio, G., Snow, R., Lambert, C., Combined Fe-Cu SCR systems with optimized ammonia to NO_x ratio for diesel NO_x control. *SAE International Journal of Fuels and Lubricants* **1** (1), 603 (2009)
- [66] Blasin-Aube, V., Marie, O., Saussey, J., Plesniar, A., Daturi, M., Nguyen, N., Hamon, C., Mihaylov, M., Ivanova, E., Hadjiivanov, K., Iron Nitrosyl Species in Fe-FER: A Complementary Mossbauer and FTIR Spectroscopy Study. *Journal of Physical Chemistry C* **113** (19), 8387 (2009)
- [67] Ivanova, E., Mihaylov, M., Hadjiivanov, K., Blasin-Aubé, V., Marie, O., Plesniar, A., Daturi, M., Evidencing three distinct FeII sites in Fe-FER zeolites by using CO and NO as complementary IR probes. *Applied Catalysis B: Environmental* **93** (3-4), 325 (2010)
- [68] Toops, T. J., Nguyen, K., Foster, A. L., Bunting, B. G., Ottinger, N. A., Pihl, J. A., Hagaman, E. W., Jiao, J., Deactivation of accelerated engine-aged and field-aged Fe-zeolite SCR catalysts. *Catalysis Today* **151** (3-4), 257 (2010)

- [69] Silver, R. G., Stefanick, M. O., Todd, B. I., A study of chemical aging effects on HDD Fe-zeolite SCR catalyst. *Catalysis Today* **136** (1-2), 28 (2008)
- [70] Han, P. H., Nam, G. U.; (Hyundai Motor Co., S. Korea), Apparatus for removing particulate matter and NO_x, Application: KR Patent No. 2007-125196 2009058427 (20071204. 2009)
- [71] Bonzi, R., Lietti, L., Castoldi, L., Forzatti, P., NO_x removal over a double-bed NSR-SCR reactor configuration. *Catalysis Today* **151** (3-4), 376 (2010)
- [72] Tosheva, L. & Valtchev, V. Supported and self-bonded molecular sieve structures. *C. R. Chimie* **8**, 475-484 (2005).
- [73] Noble, R.D. Silicalite-1 Composite Membranes. *Catalysis Today* **25**, 209-212 (1995).
- [74] Bein, T. Synthesis and applications of molecular Sieve layers and membranes. *Chemistry Materials* **8**, 1636-1653 (1996).
- [75] Den Exter, M.J., Jansen, J.C., van de Graaf, J.M., Kapteijn, F., Moulin, J.A. & van Bekkum, H. Zeolite-based membranes preparation, performance and prospects. *Studies Surface Science Catalysis* **102**, 413-454 (1996).
- [76] Matsukata, M. & Kikuchi, E. Zeolitic membranes: synthesis, properties, and prospects. *Bulletin Chemical Society Japan* **70**, 2341-2356 (1997).
- [77] McLeary, E.E., Jansen, J.C. & Kapteijn, F. Zeolite based films, membranes and membrane reactors: progress and prospects. *Microporous Mesoporous Materials* **90**, 198-220 (2006).
- [78] Caro, J. & Noack, M. Zeolite membranes – recent developments and progress. *Microporous Mesoporous Materials* **115**, 215-233 (2008).
- [79] Coronas, J., & Santamaria, J., Separations using zeolite membranes. *Separation Purification Methods* **28**, 127-177 (1999).
- [80] Tavolaro, A. & Drioli, E. Zeolites Membranes. *Advanced Material* **11**, 975-996 (1999).
- [81] Tsikoyiannis, J.G. & Haag, W.O. Synthesis and characterization of a pure zeolitic membrane. *Zeolites* **12**, 126-130 (1992).
- [82] Sano, T., Kiyozumi, Y., Maeda, K., Toba, M., Niwa, S. & Mazukami, F. New preparation method for highly siliceous zeolite films. *Journal Materials Chemistry* **2**, 141-142 (1992).
- [83] Tricoli, V., Sefcik, J. & McCormick, A.V. Synthesis of oriented zeolite membranes at the interface between two phases. *Langmuir* **13**, 4193-4196 (1997).
- [84] Tsapatsis, M., Lovallo, M., Okubo, T. & Davis, M. Synthesis and structure of ultrafine zeolite films. *Materials Research Society Symposium Proceedings* **371**, 21-26 (1995).

- [85] Lovallo, M.C. & Tsapatsis, M. Preferentially oriented submicron silicalite membranes. *Separations* **42**, 3020-3029 (1996).
- [86] Valtchev, V., Schoeman, B.J., Hedlund, J., Mintova, S., Sterte, J. Preparation and characterization of hollow Fibers of Silicalite-1. *Zeolites* **17**, 408-415 (1996).
- [87] Hedlund, J. Schoeman, B.J. & Sterte, J. Synthesis of ultra-thin silicalite-1 films by the seed film method. *Studies Surface Science Catalysis* **105**, 22032210 (1997).
- [88] Wang, H., Mitra, A., Huang, L., Yan, Y. Pure-silica zeolite low-*K* dielectric thin films. *Advanced Material* **10**, 746-749 (2001).
- [89] Mintova, S. & Bein, T. Microporous films prepared by spin-coating stable colloidal suspensions of zeolites. *Advanced Material* **13**, 1880-1883 (2001).
- [90] Balkus, K.J., Scott, A.S. Molecular sieve coatings on spherical substrates via pulsed laser deposition. *Microporous Mesoporous Material* **34**, 31-42 (2000).
- [91] Deng, Z. & Balkus, K.J. Pulsed laser deposition of zeolite NaX thin films on silica fibers. *Microporous Mesoporous Materials* **56**, 47-53 (2002).
- [92] Ke, C., Yang, W.L., Ni, Z., Wang, Y.J., Tang, Y., Gu, Y. & Gao, Z. Electrophoretic assembly of nanozeolites: zeolite coated fibers and hollow zeolite fibers. *Chemical Communications* 783-784 (2001).
- [93] Lin, Y.S., Kumakiri, I., Nair, B.N. & Alsyouri, H. Microporous inorganic membranes. *Sep. Purif. Meth.* **31**, 229-379 (2002).
- [94] Caro, J., Noack, M. & Kolsch, P. Zeolite membranes: from the laboratory scale to technical applications. *Adsorption* **11**, 215-227 (2005).
- [95] Liu, P.K.T., Sabol, H.K., Smith, G.W. & Ciora, R.J. *US Patent* 5611931 (2004).
- [96] Hanson, W.B. Structure and properties of ceramic composites joined by brazing. *Materials Technology* **14**, 53-56 (1999).
- [97] Morigami, Y., Kondo, M., Abe, J., Kita, H. & Okamoto, K. Large-scale pervaporation plant using tubular-type module with NaA membrane. *Separation Purification Technology* **25**, 251-260 (2001).
- [98] Okamoto, K., Kita, H., Horii, K., Tanaka, K. & Kondo, M. Zeolite NaA membrane: Preparation, single-gas permeation, and pervaporation and vapor permeation of water/organic liquid mixtures. *Industrial Engineering Chemistry Research* **40**, 163-175 (2001).
- [99] Lai, Z., Bonilla, G., Diaz, I., Nery, J.G., Sujaoti, K., Amar, M.A., Kokkoli, E., Terasaki, O., Thompson, R.W., Tsapatsis, M. & Vlachos, D. Microstructural optimization of a zeolite Membrane for organic vapor separation. *Science* **100**, 456-460 (2003).

- [100] Choi, J., Jeong, H.-K., Snyder, M.A., Stoeger, J.A., Masel, R.I. & Tsapatsis, M. Grain boundary defect elimination in a zeolite membrane by rapid thermal processing. *Science* **325**, 590-593 (2009).
- [101] Lee, K.P., Arnot, T.C. & Mattia, D. A review of reverse osmosis membrane materials for desalination-development to date and future potential. *Journal Membrane Science* **370**, 1-22 (2011).
- [102] Li, I., Dong, J. Nenoff, T.M., Lee, R. Desalination by reverse osmosis using MFI zeolite membranes. *Journal Membrane Science* **243**, 401-404 (2004).
- [103] Chowdhury, S.R., De Lamare, J., &Valtchev, V. Synthesis and structural characterization of EMT-type membranes and their performance in nanofiltration experiments. *Journal Membrane Science* **314**, 200-2005 (2008).
- [104] Liu, C., Kulprathipanja, S. in *Zeolites in Industrial Separation and Catalysis* (Ed. S. Kulprathipanja), Wiley-VCH, Ch. 11, 329-353 (2010).
- [105] Wyllie, M.R.J. & Pathode, H.W. The development of membranes from artificial cation-exchange materials with particular reference to the determination of sodium-ion activity. *Journal Physical Chemistry* **54**, 204-211 (1950).
- [106] Barrer, R.M., James, S.D. Electrochemistry of crystal-polymer membranes. Part I. Resistance measurements. *Journal Physical Chemistry* **64**, 417-422 (1960).
- [107] Robb, W.I. Thin silicone membranes-their permeation properties and some applications, *Annual NY Academy Science* **146**, 119-137 (1968).
- [108] Kulprathipanja, S., Funk, E.W., Kulkarni, S.S. & Chang, Y.A. *US Patent* 4735193 (1988).
- [109] Kulprathipanja, S., Neuzil, R.W. & Li, N.N. *US Patent* 4740219 (1988).
- [110] Moore, T.T., Vo, T., Mahanajan, R., Kulkarni, S., Hasse, D. & Koros, W.J. Effect of humidified feeds on oxygen permeability of mixed matrix membranes. *Applied Polymer Science* **90**, 1574-1580 (2003).
- [111] Zones, S.I., Yuen, I. & Miller, S.J. *US Patent* 6709644 (2004).
- [112] Gorgojo, P., Uriel, S., Tellez, C. & Coronas, J. Development of mixed matrix membranes based on zeolite Un-6(2) for gas separation. *Microporous Mesoporous Materials* **115**, 85-92 (2008).
- [113] Moermans, B., Beuckelaer, W.D., Vankalecom, I.F.J., Ravishankar, R., Martens, J.A. & Jacobs, P.A. Incorporation of nano-sized zeolites in membranes. *Chemical Communications* 2467-2468 (2000).

- [114] Wang, H., Holmberg, B.A. & Yan, Y. Homogeneous polymer-zeolite nanocomposite membranes by incorporating dispersible template-removed zeolite nanocrystals. *Journal Materials Chemistry* **12**, 3640-3643 (2002).
- [115] Reid, B.D., Ruiz-Trevino, F.A., Musselmann, I.H., Balkus, K.J. & Ferraris, J.P. Gas permeability properties of polysulfone membranes containing the mesoporous molecular sieve, MCM-41. *Chemistry Materials* **13**, 2366-2373 (2001).
- [116] Zhang, Y., Balkus, K.J., Musselmann, I.H. & Ferraris, J.P. Mixed-matrix membranes composed of mitrimid and mesoporous zeolite nanoparticles. in *15th International Zeolite Conference*, Beijing, Recent Progress Reports 145 (2007).
- [117] Coronas, J. & Santamaria, J. The use of zeolite films in small-scale and micro-scale applications. *Topics Catalysis* **29**, 29-44 (2004).
- [118] Casanave, D., Giroir-Fendler, A., Sanchez, J., Loutaty, R. & Dalmon, J.A. Control of transport properties with a microporous membrane reactor to enhance yields in dehydrogenation reactions. *Catalysis Today* **25**, 309-314 (1995).
- [119] Ciavarella, P., Moueddeb, H., Miachon, S., Fiaty, K. & Dalmon, J.A. Experimental study and numerical simulation of hydrogen/isobutane permeation and separation using MFI zeolite membrane reactor. *Catalysis Today* **56**, 253-264 (2000).
- [120] Ciavarella, P., Casanave, D., Moueddeb, H., Miachon, S. & Dalmon, J.A. Isobutane dehydrogenation in a membrane reactor. Influence of the operating conditions on the performance. *Catalysis Today* **67**, 177-184 (2001).
- [121] Illgen, U., Schäfer, R., Noack, M., Kölsch, P., Kühnle, A. & Caro, J. Membrane supported catalytic dehydrogenation of *n*-butane using MFI-type zeolite membranes. *Catalysis Communications* **2**, 339-345 (2001).
- [122] Jafar, J.J., Budd, P.M. & Highes, R. Enhancement of esterification reaction yield using zeolite A vapor permeation membrane. *Journal Membrane Science* **199**, 117-223 (2002).
- [123] Navajas, A., Mallada, R., Tellez, C., Coronas, J., Menendez, M. & Santamaria, J. Preparation of mordenite membranes for pervaporation of water-ethanol mixtures. *Desalination* **148**, 25-29 (2002).
- [124] Bernal, M.P., Coronas, J., Menendez, M. & Santamaria, J. Coupling of reaction and separation at the microscopic level: esterification processes in a H-ZSM-5 membrane reactor. *Chemical Engineering Science* **57**, 1557-1562 (2002).

- [125] Zhu, W., Gora, I., van der Berg, A.W.C., Kapteijn, F., Jansen, J.C. & Moulin, J.A., Water vapor separation from permanent gases by a zeolite 4A membrane. *Journal Membrane Science* **253**, 57-66 (2008).
- [126] Khajavi, S., Jansen, J.C. & Kapteijn, F. Preparation and performance of H-SOD membranes: a new synthesis procedure and absolute water separation. *Stud. Surf. Sci. Catal.* **170**, 1028-1035 (2007).
- [127] He, J., Yoneyama, Y., Xu, B., Nishiyama, N. & Tsubaki, N. Designing a capsule catalyst and its application for direct synthesis of middle isoparaffins. *Langmuir* **21**, 1699-1702 (2005).
- [128] Yang, G., Tsubaki, N., Shamoto, J., Yoneyama, Y. & Zhang, Y. Confinement effect and synergistic function of H-ZSM-5/Cu-ZnO-Al₂O₃ capsule catalyst for one-step controlled synthesis. *Journal American Chemical Society* **132**, 8129-8136 (2010).
- [129] Lai, S.M., Martin-Aranda, R., &Yeung, K.I. Knoevenagel condensation reaction in a membrane microreactor. *Chemical Communications* 218-219 (2003).
- [130] Lai, S.M., Ng, C.P., Martin-Aranda, R. & Yeung, K.I. Knoevenagel condensation reaction in a zeolite membrane reactor. *Microporous Mesoporous Materials* **66**, 239-252 (2003).
- [131] Wan, Y.S.S., Yeung, K.I. & Gavriilidis, A. TS-1 oxidation of aniline to azoxybenzene in a microstructured reactor. *Applied Catalysis A* **281**, 285-293 (2005).
- [132] Shao, Y.Y., Yin, G.P., Wang, Z.B. & Gao, Y.Z. PEMFC from low temperature to high temperature: material challenges. *Journal Power Sources* **167**, 235-242 (2007).
- [133] Yeung, K. L. & Han, W., in *Zeolites and Catalysis* (Eds. I. Cejka, A. Corma & S. Zones), Wiley-VCH, Ch. 26, 827-861 (2010).
- [134] Bein, T. & Mintova, S. Advanced applications of zeolites. *Zeolites and Ordered Mesoporous Materials: Progress and Prospects* (Eds. J. Cejka, H. van Bekkum) Elsevier, **157**, 263-288 (2005)
- [135] Urbitzondo, M. A., Pina, M. P. & Santamaria, Gas sensing with silicon-based nanoporous solids. J. in *“Ordered Porous Materials”* (Eds. V. Valtchev, S. Mintova, M. Tsapatsis) Elsevier, 387 (2009)
- [136] Torres, M., Gutiérrez, M., Lopez, L., Mugica, V., Gomez, R., Montoya & J. A. Controlled crystal growth of beta zeolite films on alumina supports. *Materials Letters* **62**, 1071-1073 (2008)

- [137] Mintova, S., Reinelt, M., Metzger, T. H., Senker, J. & Bein, T. Pure silica BETA colloidal zeolite assembled in thin films. *Chemical Communications* 326-327 (2003)
- [138] Chaikittisilp, W., Davis, M. E. & Okubo, T. TPA-Mediated conversion of silicon wafer into preferentially-oriented MFI zeolite film under steaming. *Chemistry of Materials* **19**, 4120-4122 (2007)
- [139] Wang, Z., Hedlund, J., Zhang, H. & Zou, X. Oriented films of epitaxial MFI overgrowths. *Microporous and Mesoporous Materials* **95**, 86-91 (2006)
- [140] Doyle, A. M., Rupprechter, G., Pfander, N., Schlogl, R., Kirschhock, C. E. A., Martens, J. A. & Freund, H.-J. Ultra-thin zeolite films prepared by spin-coating - Silicalite-1 precursor solutions. *Chemical Physics Letters* **382**, 404-409 (2003)
- [141] Vilaseca, M., Mateo, E., Palacio, L., Pradanos, P., Hernandez, A., Paniagua, A., Coronas, J. & Santamaría, J. AFM characterization of the growth of MFI-type zeolite films on alumina substrates. *Microporous and Mesoporous Materials* **71**, 33-37 (2004)
- [142] Sun, J., Zhu, G., Yin, X., Chen, Y., Cui, Y. & Qiu, S. Preparation of an ordered zeolite MFI film by epitaxial growth. *Chemical Communications* 1070-1072 (2005)
- [143] Wee, L. H., Tosheva, L., Wasilev, C. & Doyle, A. M. Influence of the dispersion medium on the properties of spin-coated Silicalite-1 films. *Microporous and Mesoporous Materials* **103**, 296-301 (2007)
- [144] Sahner, K., Hagen, G., Schönauer, D. & Reiß, S. Zeolites - Versatile materials for gas sensors. *Solid State Ionics* **179**, 2416-2423 (2008)
- [145] Xu, X. W., Wang, J. & Long, Y. C. Zeolite-based materials for gas sensors. *Sensors* **6**, 1751-1764 (2006)
- [146] Biemmi, E. & Bein, T. Assembly of nanozeolite monolayers on the gold substrates of piezoelectric sensors. *Langmuir* **24**, 11196-11202 (2008)
- [147] Baimpos, T., Kouzoudis, D. & Nikolakis, V. Use of a Zeolite LTA Film for the Selective Detection of Light Hydrocarbons. *Science of Advanced Materials* **2**, 215-218 (2010)
- [148] Baimpos, T., Giannakopoulos, I. G., Nikolakis, V. & Kouzoudis, D. Effect of gas adsorption on the elastic properties of faujasite films measured using magnetoelastic sensors. *Chemistry of Materials* **20**, 1470-1475 (2008)
- [149] Fine, G. F., Cavanagh, L. M., Afonja, A. & Binions, R. Metal Oxide Semiconductor Gas Sensors in Environmental Monitoring. *Sensors* **10**, 5469-5502 (2010)

- [150] Xiong, W. & Baker, M. D. Electrochemistry of zeolites on thickness shear mode oscillators. *Journal Physical Chemistry B* **109**, 13590-13596 (2005)
- [151] Sazama, P., Jirglová, H. & Dědeček, J. Ag-ZSM-5 zeolite as high-temperature water-vapor sensor material. *Materials Letters* **62**, 4239-4241 (2008)
- [152] Vilaseca, M., Yague, C., Coronas, J. & Santamaria, J. Development of QCM sensors modified by AlPO₄-18 films. *Sensors Actuators B-Chemical* **117**, 143-150 (2006)
- [153] Huang, H., Zhou, J., Chen, S., Zeng, L. & Huang, Y. P. A highly sensitive QCM sensor coated with Ag⁺-ZSM-5 film for medical diagnosis. *Sensors Actuators B- Chemical* **101**, 316-321 (2004)
- [154] Knoerr, R., Yordanov, I., De Waele, V., Mintova, S. & Mostafavi, M. Preparation of Colloidal BEA Zeolite Functionalized with Pd Aggregates as a Precursor for Low Dimensionality Sensing Layer. *Sensor Letters* **8**, 497-501 (2010)
- [155] Yordanov, I., Knoerr, R., De Waele, V., Mostafavi, M., Bazin, Ph., Thomas, S., Rivallan, M., Lakiss, L., Metzger, T. H. & Mintova, S. Elucidation of Pt Clusters in the Micropores of Zeolite Nanoparticles Assembled in Thin Films. *Journal Physical Chemistry C* **114**, 20974-20982 (2010)
- [156] Rivallan, M., Yordanov, I., Thomas, S., Lancelot, Ch., Mintova, S. & Thibault-Starzyk, F. Plasma Synthesis of Highly Dispersed Metal Clusters Confined in Nanosized Zeolite. *ChemCatChem* **2**, 1074-1078 (2010)
- [157] Yamazoe, N. Toward innovations of gas sensor technology. *Sensors Actuators B- Chemical* **108**, 2-14 (2005)
- [158] Majano, G., Mintova, S., Klapeotke, T. & Bein, T. High-density energetic material hosted in pure silica MFI-type zeolite nanocrystals. *Advanced Materials* **18**, 2440-2443 (2006)
- [159] Babaei, A., Khalilzadeh, B. & Afrasiabi, M. A new sensor for the simultaneous determination of paracetamol and mefenamic acid in a pharmaceutical preparation and biological samples using copper(II) doped zeolite modified carbon paste electrode. *Journal Applied Electrochemistry* **40**, 1537-1543 (2010)
- [160] Saraoglu, H. M. & Kocan, M. Determination of blood glucose level-based breath analysis by a Quartz Crystal Microbalance sensor array. *IEEE Sensors J* **10**, 104-109 (2010)
- [161] Zhang, J., Tang, X. L., Dong, J. H., Wei, T. & Xiao, H. Zeolite thin film-coated long period fiber grating sensor for measuring trace organic vapors. *Sensors Actuators B- Chemical* **135**, 420-425 (2009)

- [162] Kang, Y., Walish, J. J., Gorishnyy, T. & Thomas, E. L. Broad-wavelength-range chemically tunable block-copolymer photonic gels. *Nature Materials* **6**, 957-960 (2007)
- [163] Hidalgo, N., Calvo, M. E., Míguez, H. Mesostructured thin films as responsive optical coatings of photonic crystals. *Small* **5**, 2309-2315 (2009)
- [164] Lotsch, B. V., Knobbe, C. B. & Ozin, G. A. A step towards optically encoded silver release in 1D photonic crystals. *Small* **5**, 1498-1503 (2009)
- [165] Kobler, J., Lotsch, B. V., Ozin, G. A. & Bein, T. Vapor-sensitive Bragg mirrors and optical isotherms from mesoporous nanoparticle suspensions. *ACS Nano* **3**, 1669-1676 (2009)
- [166] Lotsch, B. V., Scotognella, F., Moeller, K., Bein, T. & Ozin, G. A. Stimuli-responsive Bragg stacks for chemo-optical sensing applications. *SPIE Proceedings* **7713** (2010)
- [167] Yasuda, K. E., Visser, J. H. & Bein, T. Molecular sieve catalysts on microcalorimeter chips for selective chemical sensing. *Microporous and Mesoporous Materials* **119**, 356-359 (2009)
- [168] Yang, P., Lau, C., Liang, J., Lu, J. Z. & Liu, X. Zeolite-based cataluminescence sensor for the selective detection of acetaldehyde. *Luminescence* **22**, 473-479 (2007)
- [169] Dubbe, A. Influence of the sensitive zeolite material on the characteristics of a potentiometric hydrocarbon gas sensor. *Solid State Ionics* **179**, 1645-1647 (2008)
- [170] Twigg, M. V. Progress and future challenges in controlling automotive exhaust gas emissions. *Applied Catalysis B: Environmental* **70**, 2-15 (2007)
- [171] Moos, R. & Schönauer, D. Review: Recent developments in the field of automotive exhaust gas ammonia sensing. *Sensors Letters* **6**, 808-811 (2008)
- [172] Moos, R. A brief overview on automotive exhaust gas sensors based on electroceramics. *International Journal of Applied Ceramic Technology* **2**, 401-413 (2005)
- [173] Schönauer, D., Wiesner, K., Fleischer, M. & Moos, R. Selective mixed potential ammonia exhaust gas sensor. *Sensors Actuators B- Chemical* **140**, 585-590 (2009)
- [174] Franke, M. E. & Simon, U. Solvate-supported proton transport in zeolites. *ChemPhysChem* **5**, 465- 472 (2004)
- [175] Sahner, K., Hagen, G., Schönauer, D., Reiß, S. & Moos, R. Zeolites - Versatile materials for gas sensors. *Solid State Ionics* **179**, 2416-2423 (2008)

- [176] Moos, R., Müller, R., Plog, C., Knezevic, A., Leye, H., Irion, E., Braun, T., Marquardt, K. & Binder, K. Selective ammonia exhaust gas sensor for automotive applications, *Sensors Actuators B- Chemical* **83**, 181-189 (2002)
- [177] Rodriguez-Gonzalez, L., Franke, M. & Simon, U. Electrical detection of different amines with proton-conductive H-ZSM-5. *Study Surface Science and Catalysis* **158**, 2049-2056 (2005)
- [178] Hagen, G., Dubbe, A., Fischerauer, G. & Moos, R. Thick-film impedance based hydrocarbon detection based on chromium(III) oxide/zeolite interfaces. *Sensors Actuators B- Chemical* **118**, 73-77 (2006)
- [179] Satsuma, A., Yang, D. J. & Shimizu, K. Effect of acidity and pore diameter of zeolites on detection of base molecules by zeolite thick film sensor. *Journal of Microporous and Mesoporous Materials* **141**, 20-25 (2011)
Journal of Microporous and Mesoporous Materials
- [180] Simon, U. & Franke, M. Electrical properties of nanoscaled host/guest compounds. *Journal of Microporous and Mesoporous Materials* **41**, 1-36 (2000)
- [181] Malkaj P., Dalas E., Vitoratos E. & Sakkopoulos S. pH electrodes constructed from polyaniline/zeolite and polypyrrole/zeolite conductive blends. *Journal of Applied Polymer Science* **101**, 1853-1856 (2006)
- [182] Schäfer, O., Ghobarkar, H., Steinbach, A. C. & Guth, U. Basic investigations on zeolite application for electrochemical analysis. *Fresenius J Anal Chem* **367**, 388-392 (2000)
- [183] Neumeier, S., Echterhof, T., Bölling, R., Pfeifer, H. & Simon, U. Zeolite based trace humidity sensor for high temperature applications in hydrogen atmosphere. *Sensors Actuators B- Chemical* **134**, 171-174 (2008)
- [184] Li, X. G. & Dutta, P. K. Interaction of Dimethylmethylphosphonate with Zeolite Y: Impedance-Based Sensor for Detecting Nerve Agent Simulants. *Journal of Physical Chemistry C* **114**, 986-994 (2010)
- [185] Chuapradit, C., Wannatong, L. R., Chotpattananont, D., Hiamtup, P., Sirivat, A. & Schwank J. Polyaniline/zeolite LTA composites and electrical conductivity response towards CO. *Polymer* **46**, 947-953 (2005)
- [186] Thuwachaowsoan, K., Chotpattananont, D., Sirivat, A., Rujiravanit, R. & Schwank, J. W. Electrical conductivity responses and interactions of poly(3-thiopheneacetic acid)/zeolites L, mordenite, beta and H-2. *Materials Science Engineering B* **140**, 23-30 (2007)
- [187] Kamonsawas, J., Sirivat, A., Niamlang, S., Hormnirun, P. & Prissanaroon-Ouajai, W. Electrical Conductivity Response of Poly(Phenylene-vinylene)/Zeolite Composites Exposed to Ammonium Nitrate. *Sensors* **10**, 5590-5603 (2010)

- [188] Leite, E., Naydenova, I., Mintova, S., Leclercq, L. & Toal, V. Photopolymerizable nanocomposites for holographic recording and sensor application. *Applied Optics* **49**, 3652-3660 (2010)
- [189] Leite, E., Babeva, Tz., Ng, E.-P., Toal, V., Mintova, S. & Naydenova, I. Optical Properties of Photopolymer Layers Doped with Aluminophosphate Nanocrystals. *Journal of Physical Chemistry C* **114**, 16767-16775 (2010)
- [190] Babeva, T., Todorov, R., Mintova, S., Yovcheva, T., Naydenova, I. & Toal, V. Optical properties of silica MFI doped acrylamide-based photopolymer. *Journal of Optics A: Pure and Applied Optics* **11**, 024015/1-024015/8 (2009)
- [191] Leite, E., Naydenova, I., Pandey, N., Babeva, T., Majano, G., Mintova, S. & Toal, V. Investigation of the light induced redistribution of zeolite Beta nanoparticles in an acrylamide-based photopolymer. *Journal of Optics A: Pure and Applied Optics* **11**, 024016/1-024016/9 (2009).
- [192] Alasi, N., Ikon, T., Ouco, N., Pran, R., Acin, E., A spectroscopy study of zeolites coating on Nikon lens. *Appl Optics* **77**, 6215-7777 (1977)

Zeolites as catalysts for fine chemicals synthesis and renewables conversion

Annelies PEETERS, Gerardo MAJANO, Bart STEENACKERS, An PHILIPPAERTS, Michiel DUSSELIER, Jan GEBOERS, Jan DIJKMANS, Stijn VAN DE VYVER, Bert F. SELS, Dirk E. DE VOS*¹

¹ *Centre for Surface Chemistry and Catalysis, Kasteelpark Arenberg 23, 3001 Leuven, Belgium*

Abstract

This review illustrates the potential that zeolites have in the conversion of organics to (intermediates for) fine chemicals and in the conversion of renewable resources. Examples are selected from the fields of aromatic functionalization, C-C, C-O and C-N bond formation, selective reduction and selective oxidation. The importance of shape selective effects is highlighted, as well as the rich possibilities that zeolites offer for designing bifunctional catalysts.

1. Introduction

While zeolite chemistry largely owes its development and economic importance to the fields of petrochemicals and base chemicals, it has been realized since the 1970s that zeolites offer tremendous potential for catalytic chemists looking for tailor-made catalysts for converting organic chemicals at a smaller scale. Zeolites can contain Brønsted or Lewis acid sites with well-controlled strength and in controlled amounts; they can also be functionalized with extra Lewis acid sites by isomorphous substitution of the framework, by ion exchange or by entrapment of complexes, and metal clusters of controllable size can be introduced, either in the inner pore volume or at the external surface. The wide variety of available topologies then adds the extra dimension of shape selectivity. Several early reviews excellently summarize the rich organic chemistry possible on zeolites¹⁻³; relevant zeolite effects on organic reactions were also the topic of a review paper by one of us at the occasion of a summer school of the International Zeolite Association⁴.

In this contribution, we illustrate the use of zeolites in a broad spectrum of organic conversions. Recent examples include new zeolite topologies, zeolites with controlled or hierarchical porosities, and zeolites with particular elements substituted isomorphously in the lattice. In a final section, selected examples of the use of zeolites for renewables utilization are given.

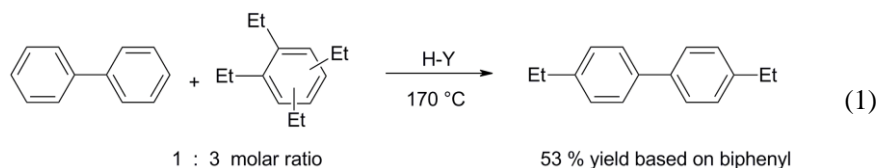
2. Zeolite effects in the synthesis of fine chemicals

2.1 Zeolites in electrophilic aromatic substitutions

a. Alkylation

One of the principal tools in the production of fine chemicals is the Friedel-Crafts alkylation, which currently covers large scale processes carried out over zeolites such as the production of ethylbenzene on H-ZSM-5, H-Beta or H-MCM-22, and the production of cumene on dealuminated H-mordenite. However, the most marked effects of shape selectivity in aromatic alkylation reactions have been observed using dinuclear aromatics such as biphenyl and naphthalenes.

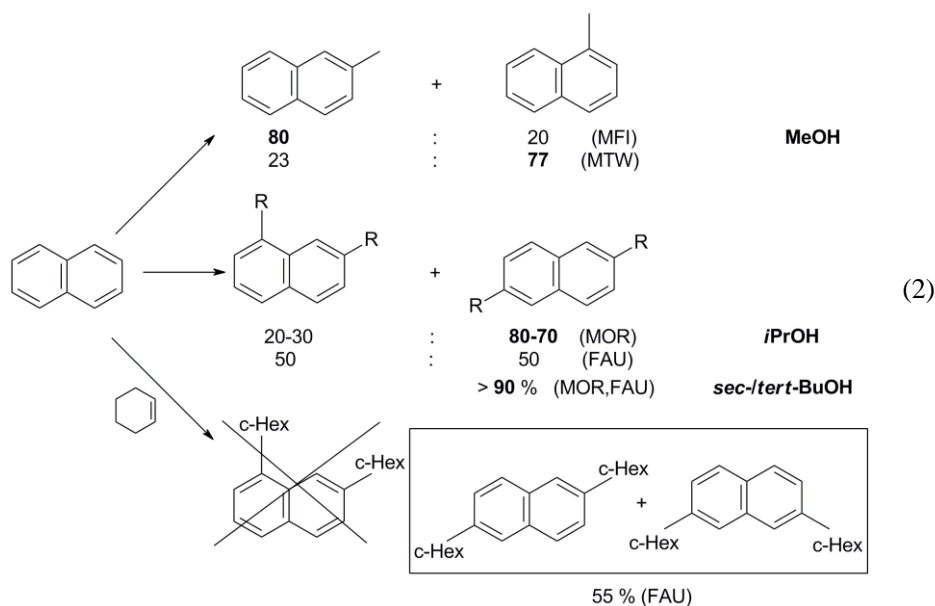
In the dialkylation of biphenyl with propylene, the desired *p,p'*-product is selectively formed inside the straight pores of a dealuminated mordenite and in diverse zeolites such as H-ZSM-5, H-CIT-5, H-SSZ-31 and H-SAPO-5,⁵⁻⁷ whereas the thermodynamically more stable *p,m'*-isomer is formed on the external acidic sites⁸. The selectivity can be increased using isobutene or 1-butene, as demonstrated with H-SSZ-31⁷; by contrast, ethylene is a more difficult alkylating agent to achieve shape selectivity, due to the limited steric constraints on the ethylated products in the pores^{8,9}. The desired *p,p'*-diethylbiphenyl (86 %) can be obtained by transalkylation with polyethylbenzenes over H-Y; however it is unlikely that shape selective effects play a role⁹:



The *p,p'*-dimethyl compound can be obtained using H-SAPO-11 and 4-methylbiphenyl as a starting reactant. The high selectivities (70-85 %) can be further enhanced in supercritical methanol, but the methylation quickly stops due to coke formation¹⁰.

The dependency of shape selectivity on the size and nature of the alkylating agent and the pore opening of the zeolite is effectively demonstrated by the studies on naphthalene alkylation (scheme 2). With MeOH as the alkylating agent, a medium pore zeolite like H-ZSM-5 is capable of hindering a double methylation and moreover favours the 2-isomer¹¹. Using isopropanol, H-MOR is shape selective for the 2,6-isomer, while an H-Y catalyst shows little discrimination between various dialkylated products¹². Finally, using cyclohexene or cyclohexylbromide as a

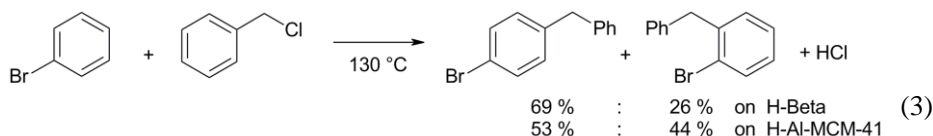
reactant and H-Y as a catalyst, the alkylation in the α -position is suppressed completely¹³⁻¹⁶. In the last case, however, the pore system is still incapable of differentiating the 2,6- from the 2,7-isomer which are obtained in the same amounts (29 and 26 %) but still prevail over the monoalkylated product (31 %)^{17,18}:



Similar behaviour has been seen for the alkylation of 2-methoxynaphthalene¹⁹. H-ZSM-5 is also selective for the conversion of 2-methyl- to 2,6-dimethylnaphthalene since both compounds can diffuse in the pores, but not the 2,7-isomer²⁰. The same products can be obtained via transmethylation of naphthalene or methylnaphthalenes with 1,2,4-trimethylbenzene over H-ZSM-12²¹.

Larger pore systems and easy accessibility are required for alkylation with large α -olefins, where the 2-arylalkanes are the target products for the production of biodegradable sulfonated surfactants. In the reaction of benzene with 1-dodecene, the selectivity for 2-phenyldodecane is much higher using dealuminated mordenite (80 %) or MCM-41/Beta composites (76 %) than with H-Beta or H-Y zeolites²²⁻²⁴. Similar trends were observed in toluene alkylation with 1-heptene²⁵. Transition state shape selectivity has been invoked to explain the selectivity on mordenite; but different degrees of olefin isomerization may also play a role. Alkylation of α -methylnaphthalene with C₁₁₋₁₂ olefins over H-Y and H-Beta has also been reported with good selectivities for the monoalkylated products^{26,27}.

Another case of shape selective alkylation is demonstrated by the benzylation of bromobenzene with benzyl chloride^{28,29} where the *p/o* ratio was 2.6 with H-Beta, while only 1.3 was achieved with mesoporous H-Al-MCM-41:



It is possible to carry out alkylations of bromobenzene over H-USY zeolite with less bulky bifunctional alkylating agents such as allyl alcohol and allyl acetate, but preferred sorption of these compounds causes a strong initial formation of side products which declines with time upon deactivation of the zeolite outer surface³⁰.

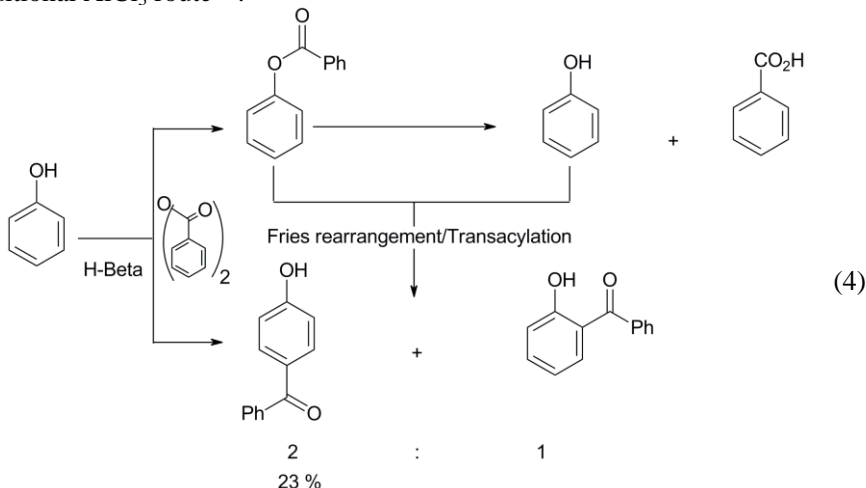
In order to reduce diffusion limitation effects inside the channel network, zeolites with additional mesoporosity have also been investigated in alkylation reactions with somewhat mixed results. Early experiments showed a marked increase in conversion and selectivity for alkylation of benzene with propanol over mesoporous H-Beta obtained with organic polymers as a mesostructuring co-template compared to the purely microporous material³¹. On the other hand a decline in conversion in the ethylation of benzene upon introduction of mesoporosity in Beta after synthesis with alkaline desilication was observed, which was attributed to shielding of strong acid sites during treatment³². However, mesoporous ZSM-5 synthesized with an amphiphilic organosilane showed conversions nine times higher (91 %) than a parent ZSM-5 sample for the benzylation of benzene with benzylalcohol³³. Alkaline treated ZSM-5 has shown remarkable performance in synthesis of ethylbenzene³⁴.

b. Acylation

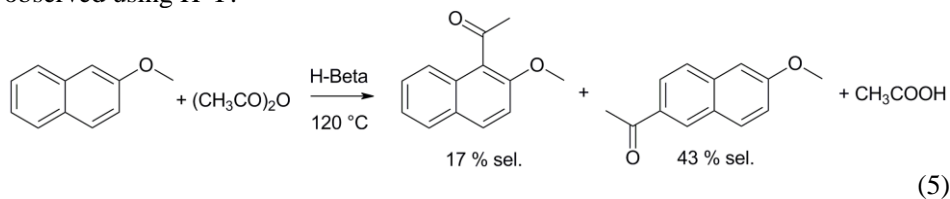
In spite of the limited enhancement of the regioselectivity using zeolites in the acetylation reactions of small molecules such as anisole and veratrole for industrially relevant processes, their main advantage still resides in their more environmentally benign nature compared to traditional AlCl_3 reactions. Pore size limitations for anisole acylation with large molecules such as octanoyl chloride can be overcome by using composite catalysts such as MCM-41/Beta which have shown an almost complete yield of the *para*-product after 1 h³⁵.

More marked in acylation are the influence of the Al-content and thus hydrophobicity and sorption properties of the active catalyst, which can be seen in the direct benzylation of phenol with benzoic anhydride to produce 4-hydroxybenzophenone (4-HBP). H-Beta and H-Y show a slightly higher conversion

of 95 % but several times better selectivity for 4-HBP (23.3 % yield) compared to the traditional AlCl_3 route ³⁶.

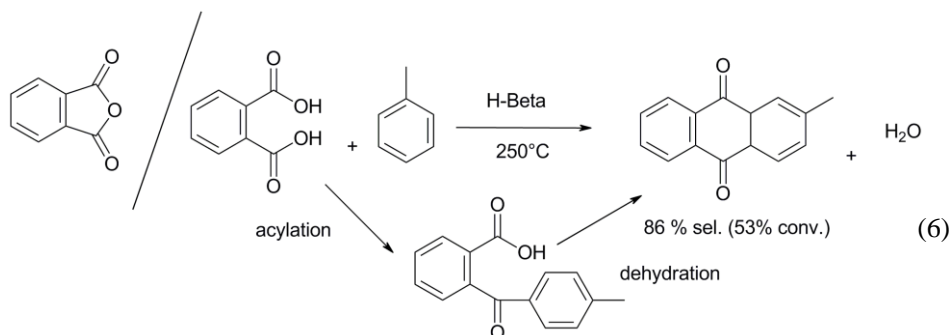


Product shape selectivity is more pronounced in the acetylation of larger substrates such as 2-methoxynaphthalene with acetic anhydride ³⁷⁻⁴¹. In the latter reaction the 1-acetyl isomer is kinetically favoured but the pharmaceutically relevant 6-acetyl isomer is formed almost exclusively on H-Beta by a combination of direct acetylation and intraporous intermolecular transacetylation of the 1-acetyl isomer due to slower diffusion and longer residence time inside the pores ⁴⁰, which is not observed using H-Y:



Transition-state shape selectivity effects can also be observed in the reaction of naphthalene with acetic anhydride over H-Beta while at the same time the hydrophobicity of decalin as solvent can be used for increasing the reaction rate ^{42,43}. Results for these reactions have been compared for H-Beta, and for the related structures H-ITQ-17, which is the pure C-polymorph of zeolite Beta, and for H-ITQ-7, which is a related material with slightly narrower pores. With the latter two materials, a higher selectivity to the 6-acetyl isomer is obtained, as the 1-acetyl isomer diffuses even more slowly through these structures than through Beta itself. However, the reactions with H-ITQ-7 and H-ITQ-17 also result in lower conversion values ^{40,41}.

A practical one-pot combination of acylation and dehydration of toluene has also been demonstrated over H-Beta, H-Y and H-MOR in order to produce 2-methylantraquinone in the liquid phase. Especially zeolite H-Beta showed a high selectivity for 2-methylantraquinone of 91 % with a yield of 61 %. It is interesting to note that the yield increases to 82 % when using phthalic acid instead of the anhydride as acylating agent ⁴⁴. In addition, nanosized H-Beta showed higher catalytic performance and a minimal increase in selectivity due to faster diffusion rates and slower deactivation:

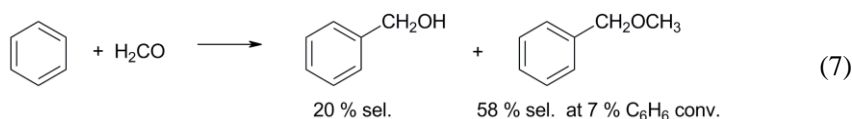


The beneficial effect of microwave irradiation on zeolite-catalyzed acylations has been demonstrated for reactions of aromatic ethers like 2,3-dihydrobenzofuran or anisole with carboxylic acids like hexanoic acid. Using H-Beta or H-Y as the catalysts, conversion values of 60 % were reached in 30 min at 190 °C, which is twice as much as in conventional reactions which were carried out in parallel ⁴⁵.

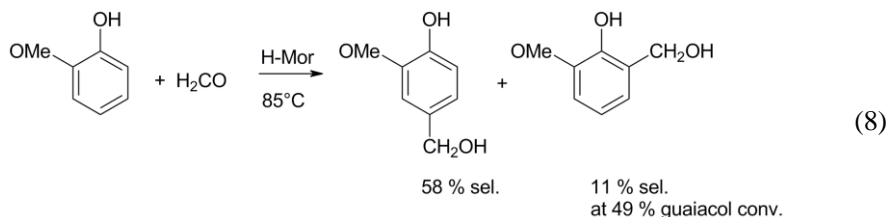
c. Hydroxyalkylation

Aromatics, in particular electron-rich ones, tend to form diarylalkanes upon reaction with aldehydes under acid catalysis. A common way to avoid this and to obtain the mono-hydroxyalkylated compound is to work with a large excess of the aldehyde. This was first demonstrated for the hydroxyalkylation of furfuryl alcohol with aqueous formaldehyde ^{46,47}.

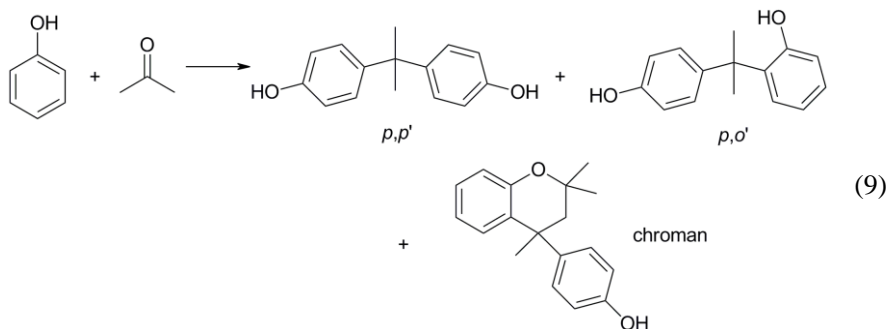
An elegant alternative way to achieve mono-hydroxyalkylation is to use a medium pore zeolite such as H-ZSM-5, which is able to restrict the double hydroxyalkylation. This has been demonstrated for the reaction of benzene with formaldehyde, with benzyl alcohol and benzyl methylether as main products, while on other zeolites the predominant product is diphenylmethane ⁴⁸:



A problem, from the technical point of view, is the use of formaldehyde as reactant, as the cheapest source of formaldehyde is an aqueous solution which may hinder adsorption of reactants onto the catalyst. This problem can be solved by the use of high-silica zeolites such as H-Beta and H-mordenites. This has been demonstrated in the synthesis of *para*-vanillol (3-methoxy-4-hydroxybenzyl alcohol), a precursor for the food aroma vanillin⁴⁹⁻⁵¹. This precursor can be obtained from the hydroxymethylation of guaiacol (2-hydroxyanisole). In addition, high formaldehyde content limits the further hydroxymethylation of the product. The effect of dealuminating H-mordenite has been well investigated and *p'/(o+p)* ratios of up to 85 % can be achieved^{50,52}. Such a level of selectivity cannot be achieved through the traditional route with sulphuric acid, which is solid proof for shape selectivity:



Another case of transition-state selectivity is found in the synthesis of bisphenol A starting from phenol and acetone. H-Beta and H-Y provide sufficiently large pore spaces in which the resulting *p,p'/(p,p' + o,p')* ratio amounts to 64-67 %, while the formation of chroman side products is completely suppressed due to their large size⁵³.



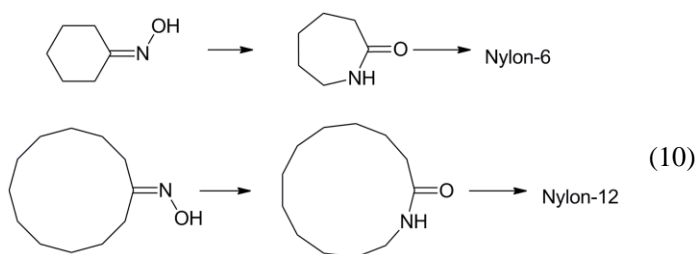
As with other reactions with large products, a problem shared by hydroxyalkylations is the resulting deactivation by pore clogging. Supercritical CO₂ as a solvent increases diffusion and thus doubles or triples the conversion in the reaction of anisole with H₂CO to the diarylmethane product, even if the reaction temperature was 60 °C for sc CO₂ and 110 °C for toluene⁵⁴. In the related synthesis of diaminodiphenylmethane from aniline and formaldehyde dealuminated zeolites, like ITQ-2, -6 and -18, couple reduced deactivation with selectivity control on the

structured outer surface⁵⁵. In this case conversions higher (99.5 %) than those over zeolite H-Beta have been obtained while maintaining not only selectivity towards the 4,4'-isomer (57 %) but also longer catalyst lifetime due to enhanced diffusion. A better 4,4'/(2,2'+2,4')-isomer ratio (6.71) can be achieved with mesoporous silicas but with more formation of oligomeric amines and faster deactivation⁵⁶.

2.2 Zeolites in acid-catalyzed rearrangement reactions

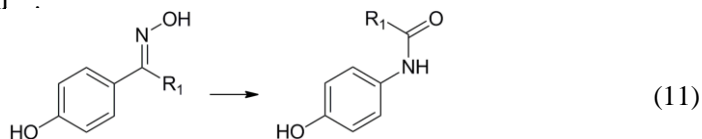
ϵ -Caprolactam, an important intermediate in the Nylon-6 production, can be obtained by the Beckmann rearrangement of cyclohexanone oxime (scheme 10, top). Zeolites have been developed to replace sulphuric acid as industrial catalyst. For example, a high-silica MFI zeolite in which the active sites are located at the pore mouths was synthesized for performing the rearrangement in the vapour phase⁵⁷. The active sites were identified as silanol nests. These weakly Brønsted acid sites were found to be excellent rearrangement catalysts. Very high selectivities were attained by blocking terminal silanols with methanol.

A variation of this process is the Beckmann rearrangement in the vapour phase of cyclododecanone oxime to ω -laurolactam, the monomer for the production of Nylon-12 (scheme 10, bottom). Here an acid treated [Al,B]-Beta zeolite was able to reach almost 100 % conversion and selectivity⁵⁸. T-atoms were removed from the *BEA framework by dealumination/deboronation with HNO₃, creating highly selective silanol nests with extremely weak Brønsted acidity. These sites were again found to catalyze the rearrangement in a superb manner. Even in a simple fixed bed set-up, coking of the catalyst occurred only to a very limited extent.



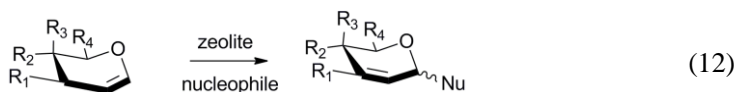
Besides for producing monomers for polyamides, the Beckmann rearrangement is also useful to prepare other high value chemicals, pharmaceuticals, fragrances etc. For example, *N*-acetyl-*p*-aminophenol, otherwise known as paracetamol, is an important analgesic drug which can be synthesized by a Beckmann rearrangement of 4-hydroxyacetophenone oxime, an acetophenone derivate (scheme 11). Delaminated ITQ-2 (Si/Al = 15) zeolites and mesoporous MCM-41(Si/Al=15)

aluminosilicates were found to have excellent activities and selectivities for paracetamol formation⁵⁹.



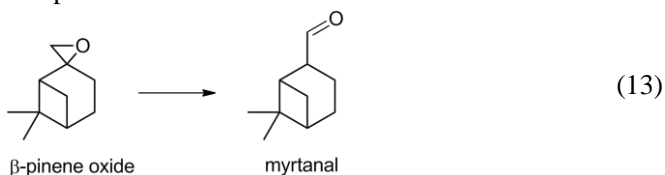
Tests with zeolites with different pore sizes yielded interesting information about the mechanism of this rearrangement. With several of the tested zeolites, *e.g.* Beta, USY, MCM-22 and ZSM-5, the activity decreased or remained constant when the size of the aromatic substituents, or their number increased. A transition-state geometrical constraint is imposed in the pores of these zeolites. This can be explained by the mechanism of the Beckmann rearrangement; the group that migrates is generally the aromatic group in the *anti* position to the hydroxyl group, which can be impeded from migration inside a zeolite pore. With mesoporous MCM-22 and ITQ-2, however, the activity increased together with the intrinsic reactivity of the oxime, regardless of the size of the aromatic substituents. The activity is controlled by electronic effects, rather than by steric effects. For the ITQ-2 catalyst, this indicates, as expected, that the reaction largely takes place on the well-exposed outer surface cups. When the size of the oxime was increased (bulkier R₁-group), the effect of the zeolite topology has a lower impact on the activity, but ITQ-2 and MCM-22 still remain the most active catalysts⁵⁹.

Also in carbohydrate chemistry, zeolites can be used as catalysts, for example, in the Ferrier rearrangement for the synthesis of 2,3-unsaturated glycols, which are versatile biological intermediates. From a range of catalysts, ultrastable Y zeolites (H-USY) were found to have superior activities⁶⁰. A commercial CBV-720 catalyst, which was obtained by steam treatment and leaching with mineral acid of the parent Y zeolite (CBV-300), was useful for formation of a broad range of *O*-, *S*-, *N*- and *C*-glycosides from acetyl-protected glycols. The high reactivity of the normally less reactive benzylated glycols with zeolite CBV-720 is a significant advantage over other known homogeneous and heterogeneous catalysts. The large pores of the steam treated and leached CBV-720 allow diffusion of the relatively large glycols and the reaction products to and from active sites:



Lewis acidity can be introduced into the framework of zeolites by isomorphous substitution of metals *e.g.* Zr, Sn, Ti, etc. Such a Zr-Beta was found to be an excellent catalyst for the isomerization of β -pinene oxide to myrtanal, with much

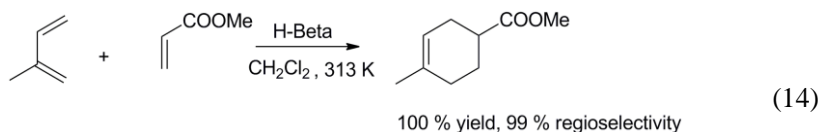
higher yields than for any other catalyst thus far reported⁶¹ (scheme 13). The high activity and selectivity (up to 94 %) were attributed to well-defined single Lewis acid sites, which can be obtained by tuning synthesis and post-synthesis treatment. Proper selection of the solvent was found to raise selectivity by balancing competitive adsorption of the product.



2.3 C-C bond formation reactions

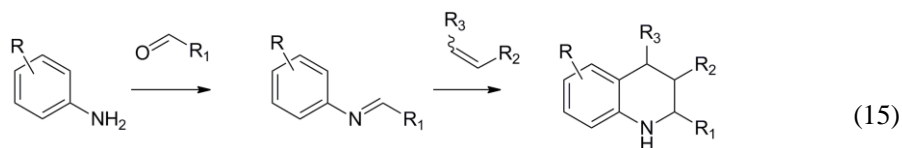
Diels-Alder reactions are C-C bond forming reactions most commonly catalyzed by Lewis acids. For instance, Cu(I) immobilized on a Y-zeolite is an excellent catalyst for the formation of 4-vinylcyclohexene from butadiene^{62,63}. Another example is ZnCl₂ supported on a NaY zeolite, which was found to be a highly regioselective catalyst for the reaction of myrcene with acrolein⁶⁴. But even in the absence of extra added Lewis acid functions, zeolites can accelerate Diels-Alder reactions.

The high activities and regioselectivities of zeolites in catalytic Diels-Alder reactions can be ascribed to many factors. For instance, the nature of the active site plays a prime role. Other factors, *e.g.* the stability of the products towards secondary reactions catalyzed by the zeolite, can be important as well. For instance, in the reaction of isoprene with methyl acrylate, a completely selective reaction is observed over zeolite H-Beta (Si/Al = 14.5)⁶⁵:



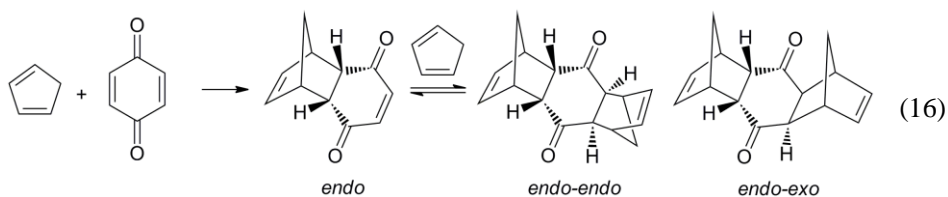
All other zeolites or Lewis acids which were tested yielded inferior results; with AlCl₃, the best homogeneous Lewis acid, the maximal yield was 83 %, with a regioselectivity of 95 %.

Special types of cycloadditions are finding their way to zeolite catalysis as well. For instance, the one pot [4+2] cyclocondensation of arylamines and aldehydes with alkenes, yielding high value quinoline derivatives is efficiently catalyzed by Sc(III) US-Y zeolite⁶⁶:



Contrarily, under the same conditions, a Cu(I) as well as a Cu(II)-USY zeolite were not effective as catalysts. An overall high *cis* stereoselectivity (up to 100 %) of R₁-R₃ groups was found in the adduct. This could be ascribed to the spherical shape of the cage of the USY zeolite, favouring more spherical (*cis*) rather than extended (*trans*) transition states.

Retro-Diels-Alder reactions can also be catalyzed by a Brønsted acidic zeolite. Gómez *et al.* (2005) studied the Diels-Alder-reaction of cyclopentadiene and *p*-benzoquinone, and found that the presence of more strongly acidic OH groups enhanced the competitive retro-Diels-Alder reaction, which lowered the selectivity for the *endo-endo* isomer⁶⁷:



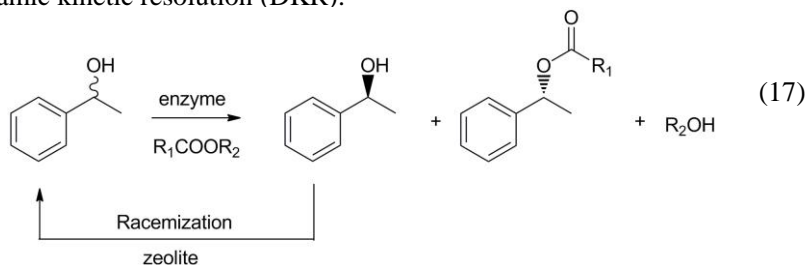
The *endo* monoadduct (formation of an *exo* monoadduct was not observed) could be regenerated in the presence of Brønsted acid sites from the *endo-endo* isomer. This occurred more easily than the regeneration from the *endo-exo* isomer, effectively increasing the amount of *endo-exo* monomer in the mixture. For instance, by generating stronger Brønsted acidity by introduction of aluminium in the framework of the highly selective Ti-ITQ-2 zeolite, the selectivity for the *endo-endo* isomer dropped. Demuynck *et al.* found that a H-Beta (Si/Al =12.5) was an excellent catalyst for the retro-Diels-Alder reaction of a range of cyclopentadiene cyclo-adducts in the presence of an active dienophile⁶⁸.

2.4 Acid-catalyzed racemization of secondary alcohols

Acid zeolites were screened for alcohol racemization reactions in aqueous solutions. H-Beta appeared to be the most promising catalyst of all tested zeolites for the racemization of benzyl alcohols⁶⁹. With acid resins as catalysts, lower activities were obtained. With aqueous solutions of homogeneous catalysts (HCl and pTSA) comparable results could only be obtained with high acid concentrations (0.5 M)

while lowering the concentration (0.1 M) gave much lower racemization activity than for H-Beta.

Racemization of alcohols requires strong Brønsted acid sites. The strength of the acid sites in zeolites increases with the Si/Al ratio, and in a series of Y zeolites, this resulted in increased racemization activity. With increasing Si/Al-ratio the hydrophobicity increases as well, leading to a preferred adsorption of the substrate and not of excess water, which also leads to a higher reactivity. Zhu and co-workers (2007) found that a Beta zeolite with low concentrations of Zr or Al is an excellent racemization catalyst, even in toluene⁷⁰. The racemization can be combined with an enzyme catalyzed transesterification with a lipase to yield enantiopure esters in a dynamic kinetic resolution (DKR):

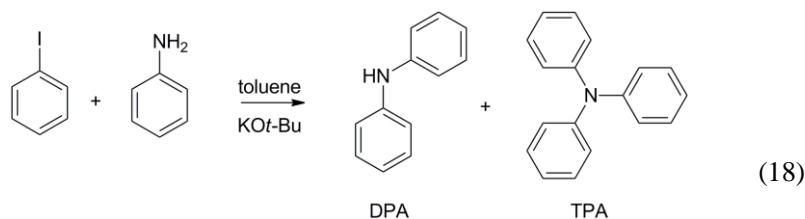


2.5 Formation of C-N bonds

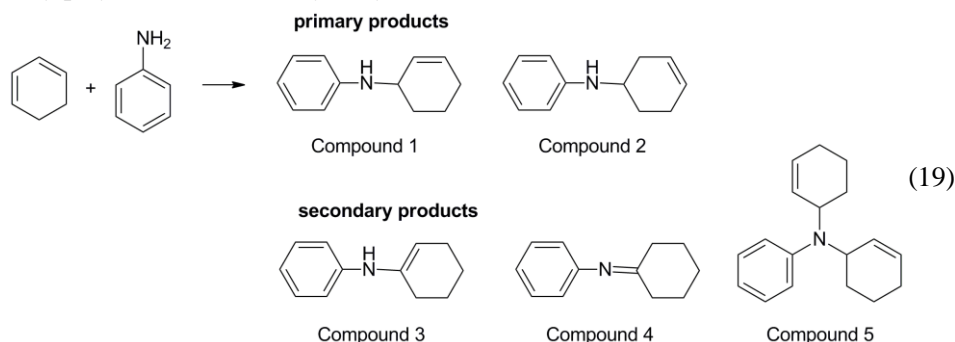
Amination can proceed through various routes using zeolite catalysts. Classical gas phase amination of alcohols can be performed shape selectively with zeolites. For example, the amination of methanol to valuable mono- and dimethylamines can be performed with high selectivity on small pore zeolites with cages that can be accessed via 8-membered ring windows (*e.g.* H-chabazite), on mordenites that have undergone special treatments to make them shape selective, etc⁷¹⁻⁷³. The undesired trimethylamine is unable to diffuse out of the pore channel. A new type of zeolite derived from layered silicates, Al-RUB-41, was recently found to be highly selective as well⁷⁴. This zeolite with RRO topology has appropriate channel dimensions (0.58 x 0.41 nm (8MR); 0.59 x 0.41 nm (10MR)) for shape selective amination of methanol, even if no cages are present in the material. High Si/Al ratios were found to increase selectivity, as well as lowering the amount of less selective acid sites on the outer surface by silylation.

For the amination of aryl halides, copper can be used, immobilized as phenantroline or bipyridine complexes in Y zeolites⁷⁵. Homogeneous copper catalysts were found to be active, but generally not selective. This example shows that by immobilization of an active homogeneous catalyst not only recovery of products, but also product selectivity can be improved. In the amination of aryl iodide with aniline catalyzed by a NaY zeolite with an encapsulated Cu(II) complex, a restricted transition state shape selectivity effect was proposed. Triphenylamine (TPA) can be generated

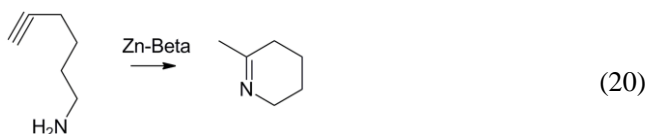
inside the zeolite cavities but is unable to diffuse out of the pores (scheme 18). The third phenyl group on aniline can be transferred to a new aniline molecule entering the pore, yielding diphenylamine (DPA) with high selectivity. With a mesoporous MCM-41, for instance, the selectivity is reversed: here TPA is able to diffuse out of the pores.



A third example of amination with zeolites is the hydroamination of 1,3-cyclohexadiene with H-Beta⁷⁶. Hydroamination is the direct addition of an amine to a C-C unsaturated bond. This is an attractive route to substituted amines from inexpensive alkene or alkyne feedstocks. Addition of aniline to 1,3-cyclohexadiene was studied, yielding a complex product spectrum (scheme 19). No reaction was observed in medium pore zeolites like H-ZSM-5. With large pore H-Y zeolites with faujasite supercages the double addition product is formed (compound 5). H-Beta, on the other hand, has the most efficient pore system, with 12-membered ring openings. Here, the desired products can diffuse out of the pores, while the double addition product is only formed in lower amounts. Ion exchange with Lewis acidic Zn²⁺ decreased the activity of the zeolites. Such an exchange effectively increases the Lewis acidity of the material, but at the same time the Brønsted acidity drops. This shows that the Brønsted acid sites are responsible for the catalytic activity. A molecular Brønsted acid (trifluoromethanesulfonic acid) however was not able to catalyze the reaction, indicating that a reaction intermediate is stabilized in the zeolite pores. Even then, Lewis acid sites resulting from aluminium in the material may play a role in the catalytic cycle.



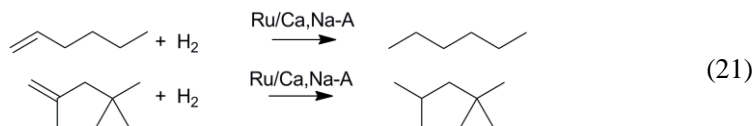
By contrast, when an alkyne is used in the hydroamination, the ion exchange of zeolite Beta with Zn^{2+} cations had a beneficial role on the reaction rate⁷⁷. For example, the intramolecular addition of an amine to a C-C triple bond was performed with high yields on a Zn-Beta, while homogeneous $\text{Zn}(\text{CF}_3\text{SO}_3)_2$ was less active (scheme 20). The higher activity was ascribed to the simultaneous presence of Brønsted and Lewis acid sites in Zn-Beta. H-Beta was much less active in this case, indicating that the active site for hydroamination is much dependent on the reactants used.



2.6 Hydrogenation reactions using metal-loaded zeolites

The molecular sieving properties of zeolite frameworks and the presence of potentially co-catalytic acid sites make metal-loaded zeolites excellent hydrogenation catalysts which allow intermolecular and even intramolecular selective double bond hydrogenation, as well as selective functional group reduction. Zeolite-catalyzed selective hydrogenation is well documented in gas phase reactions. For instance, acetylene can be selectively hydrogenated in an ethylene stream using a bimetallic PdAg/Na-Beta zeolite⁷⁸, in which case the selectivity is due to preferential adsorption of acetylene rather than to shape selectivity. On the other hand, *p*-xylene can be selectively hydrogenated in a xylene mixture on a modified Pt-ZSM-5⁷⁹. Linear olefin hydrogenation is favoured in the competitive hydrogenation of linear and branched olefins in small-pore zeolites such as Pd-loaded Rho or Pd-loaded ZK-5⁸⁰.

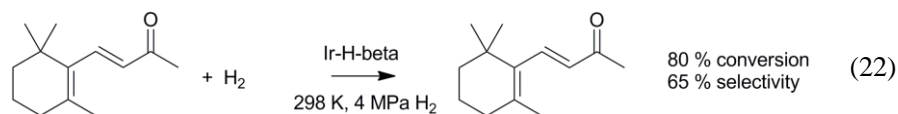
While reactant shape selectivity may not be industrially relevant, it often is a useful tool in the discrimination between active sites on the external surface and those within the zeolite structure. Altwasser *et al.* prepared ruthenium-containing small pore zeolites with LTA, KFI, MER and RHO topologies. After ion exchange with calcium nitrate, these zeolites were shape selective as was demonstrated for Ru/Ca,Na-A (LTA) with a Ru-loading of up to 4 wt% in the competitive hydrogenation of 1-hexene and 2,4,4-trimethyl-1-pentene⁸¹.



The literature contains many beautiful examples of zeolitic catalysts for liquid phase hydrogenation reactions as well. Using a Pt-loaded Na-Beta zeolite, the hydrogenation of a mixture of 1-decene and 5-decene almost exclusively results in hydrogenation of the 1-decene^{82,83}. It was suggested that the approach of the terminal double bond to the zeolite-entrapped metal cluster is easier. The zeolite framework can also play a part in enhancing the lifetime of the catalyst by preventing aggregation of supported metal nanoclusters. Furthermore, by controlling the zeolite synthesis, the support can be prepared in nanodimensions, resulting in a more active catalyst. In this way, Zahmakiran *et al.* reported the hydrogenation of neat benzene to cyclohexane under mild conditions (25 °C; 2.9 bar H₂). The use of Ru-nanoclusters stabilized by a nanozeolite FAU-framework resulted in unprecedented catalytic activity (initial TOF = 5430 h⁻¹) and lifetime (TTO = 177200)⁸⁴.

α,β -Unsaturated carbonyl compounds are valuable precursors for fine chemicals such as pharmaceuticals, agrochemicals and fragrances. Even though the hydrogenation of the C=C double bond is thermodynamically favoured, several catalysts have been designed which are able to exclusively reduce the carbonyl group. Cinnamaldehyde can be hydrogenated in high selectivity to cinnamyl alcohol when using Pt-Y⁸⁵ or Pt-Beta⁸⁶. The excellent selectivity towards the allylic alcohol

97 % selectivity at 50 % conversion for Pt-Y - is rationalized by restricted access of the C=C double bond to the metal surface. A related but more challenging reaction is the selective hydrogenation of β -ionone, a sterically hindered α,β -unsaturated ketone, to the unsaturated alcohol. Most catalysts that are successful in the hydrogenation of α,β -unsaturated aldehydes to primary alcohols fail to convert α,β -unsaturated ketones to secondary allylic alcohols but Ir-loaded Beta zeolites are suitable catalysts for this reaction. The chemoselectivity can be explained by a promoting effect of the acid functionality of the H-Beta on the Ir-particles⁸⁷. Moreover, this promoting effect is rather unique for zeolite H-Beta as the obtained selectivity with Ir/TiO₂ for example is much lower:



In another approach, using isopropanol as the reducing agent rather than hydrogen, the Meerwein-Ponndorf-Verley reduction of α,β -unsaturated aldehydes over Al-free Zr-zeolite Beta is a potential route to primary allylic alcohols. This way, cinnamaldehyde can be converted to cinnamyl alcohol in 97 % yield. The absence of Brønsted acid sites in the catalyst with isomorphous Zr substitution appeared to be crucial for achieving high chemoselectivity⁸⁸.

Synthesis of fine chemicals can be simplified by applying the so-called “one pot” concept which involves bifunctional catalysts that facilitate multiple consecutive reaction steps. A nice example hereof is the synthesis of menthol: citronellal cyclisation to isopulegol is followed by hydrogenation - at hydrogen pressures in the range of 3 to 20 bars - to menthol over Ir-Beta⁸⁹. Over Ni/Zr-Beta, menthol can even be synthesised starting from citral; hereby citral is initially hydrogenated to citronellal⁹⁰. The diastereoselectivity to the desired (\pm)-menthols is determined by the acid-catalyzed cyclisation step and amounts up to 75 % for Ir-loaded Al-Beta and 94 % for Zr-Beta, both at full conversion.

Finally, nitrobenzene can be transformed to *para*-aminophenol over Pt-zeolites in the gas phase. Nitrobenzene is first hydrogenated by Pt to β -phenylhydroxylamine which is in turn transformed into aminophenol by the acid sites of the zeolitic framework via the Bamberger rearrangement. Best results were obtained for Pt-ZSM-5: the selectivity for *para*-aminophenol was 42 % at 40 % conversion of nitrobenzene⁹¹.



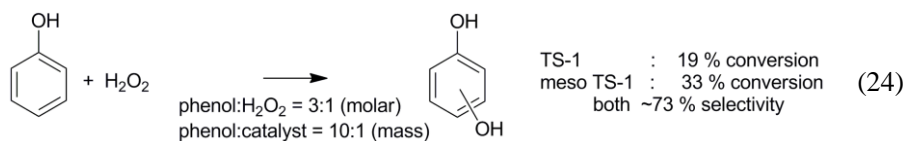
2.7 Zeolites as oxidation catalysts

Titanium-Silicalite-1 (TS-1) is by far the most useful and best understood shape selective zeolite oxidation catalyst up to date. TS-1 is a hydrophobic material, and therefore it for instance prefers olefins as adsorbates over more polar alcohol solvent molecules. As TS-1 is essentially Al-free, it contains only weak residual acidity, resulting in high selectivity for *e.g.* aliphatic epoxides from olefins. The active sites of TS-1 can be considered as tetrahedrally coordinated titanium in the MFI-lattice. TS-1 is currently used for three major types of oxidation reactions on industrial scale with the environmentally benign hydrogen peroxide as oxidant: olefin epoxidation, hydroxylation of phenols and ammoximation of ketones⁹². The dimensions of both the pore system and the TS-1 crystals play a key role in the performance of the catalyst for these reactions. Because of the limited pore size (5.5 Å), the scope of alkene epoxidation over TS-1 is largely limited to linear alkenes. 1-Hexene for example, is efficiently epoxidized while cyclohexene is not. In contrast to what might be expected however, TS-1 was found to be more selective for *cis*-alkenes in the epoxidation of an equimolar *cis/trans*-alkene mixture⁹³. In phenol hydroxylation, hydroquinone is assumed to be formed mainly inside the pores, while catechol is formed as a result of extraporous reaction⁹⁴. For cyclohexanone ammoximation it was found that the activity of TS-1 is strongly

influenced by the amount of framework titanium. As a possible explanation for this observation, it was proposed that the titanium content affected the unit cell parameters and thus the diffusion rate of the reagents inside the pores⁹⁵.

The development of TS-1 analogues with larger pore systems has received much attention in the scientific community. One approach is the incorporation of Ti in zeolites with more open frameworks. A well-known example of such materials is Ti-Beta, a large pore zeolite (6.4 -7.6 Å). Over Ti-Beta, epoxidation of branched and cyclic alkenes becomes feasible. The more hydrophilic nature of Ti-Beta favours ring opening of epoxides, resulting in the formation of diols and monoethers as the main products. Therefore, one option is to use acetonitrile as an alternative solvent; or the oxidant can be changed from hydrogen peroxide to *tert*-butyl hydroperoxide. Another example of a TS-1 analogue with more accessible active sites is Ti-MWW. Ti-MWW has a unique *trans*-selective behavior when it is used for the epoxidation of *cis/trans*-mixture of alkenes⁹⁶. Furthermore Ti-MWW catalyzes the epoxidation of allyl alcohol to glycidol more efficiently and selectively than TS-1⁹⁷. A characteristic feature of this material is the sinusoidal channel system which explains the remarkable epoxidation performance complementary to that of TS-1.

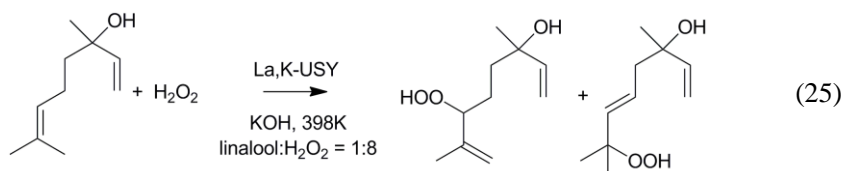
A different approach in the synthesis of Ti-containing molecular sieves with limited steric constraints, is the introduction of mesoporosity in the TS-1 structure. The success of such hierarchically structured TS-1 zeolites strongly depends on the used synthesis method. Reichinger *et al.* reported the CTAB-directed synthesis of a TS-1 analogue with a hexagonal mesopore system from a TS-1 seed-containing solution. This material outperformed TS-1 in the epoxidation of cyclohexene but failed completely when the epoxidation of 1-hexene was attempted. Most of the Ti sites appeared to have a six-fold coordination which might explain the reactivity difference with the original TS-1 material⁹⁸. Xin *et al.* used carbon black as a mesoporosity introducing agent and the obtained material - called meso TS-1 - showed similar selectivity but higher activity for phenol hydroxylation and methyl ethyl ketone ammoxidation than TS-1⁹⁹.



The relative absence of size restrictions is also apparent for the recently developed Sn-substituted Beta zeolites in Baeyer-Villiger oxidations with H₂O₂. Cyclohexanone and the much bulkier adamantanone are converted to the respective

lactones at about equally high rates and at > 98 % selectivity. The very high selectivity of Sn-Beta is attributed to the wide functional group tolerance of Sn peroxide species that might be formed and to the fact that the tetrahedrally coordinated Sn activates the carbonyl group but not H₂O₂. The inability of Sn-Beta to convert 2-*tert*-butylcyclohexane while 4-*tert*-butylcyclohexane is readily transformed into its lactone might point to the presence of shape selective effects. Another possible explanation for the lack of conversion of 2-*tert*-butylcyclohexane however, is the hindered access of the ketone group to the metal centre caused by the substituent in the *ortho*-position. Double bonds in the substrates are not epoxidized, indicating that this material is perfectly complementary with the aforementioned Ti-based catalysts¹⁰⁰.

Dark singlet oxygenation is an interesting alternative for the - often unsafe - photosensitized production of singlet oxygen. In dark singlet oxygenation, hydrogen peroxide is disproportionated by inorganic compounds into singlet oxygen and water¹⁰¹. In the presence of this reactive oxygen species, olefins are exclusively converted to allylic alcohols. Wahlen *et al.* attempted the dark singlet oxygenation by using La³⁺-exchanged zeolites. Dispersion of La on the zeolite lattice resulted in significantly higher oxygenation yields than when using *in situ* prepared La-hydroxide gel. Higher conversions were obtained with LaK-Y zeolites characterized by high Si/Al ratios (10-15) than with those with low ratios, suggesting that the adsorption properties of H₂O₂ and the substrate were of importance¹⁰².

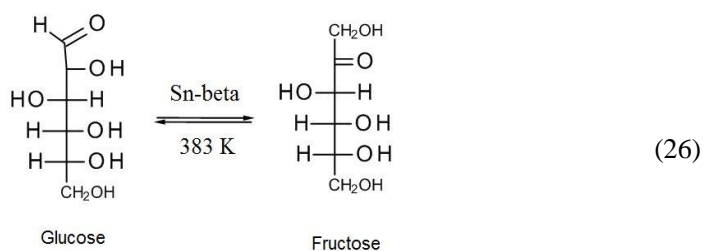


As a last example of zeolitic effects in oxidation reactions the use of zeolitically encapsulated noble metal catalysts is shortly discussed. Silicalite-1 encapsulated Ag and Pt nanoparticles were tested for aerobic alcohol oxidation. Their reactant selectivity, poison resistance and reusability greatly exceed those of commercially available catalysts such as Pt/SiO₂¹⁰³. Silicalite-1 encapsulated Au-nanoparticles on the other hand, were demonstrated to be reactant shape selective catalysts for the aerobic oxidation of benzaldehydes in methanol to their methyl esters. While benzaldehyde was readily converted to methyl benzoate, 3,5-di-*tert*-butylbenzaldehyde was unreactive¹⁰⁴.

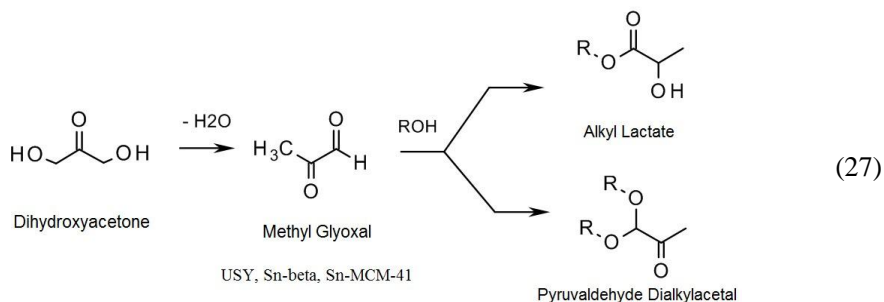
3. Zeolites for catalytic biomass conversion

3.1 Zeolites in carbohydrate chemistry

The isomerization of glucose to fructose is considered as an essential step for the selective production of fuels and chemicals from glucose or ultimately cellulose. Fructose is the keto isomer of glucose, and is more susceptible towards chemical reactions. Industrially, this reaction is carried out with immobilized biocatalysts. As enzyme-based processes not always lend themselves easily to an integrated multi-step approach, stable inorganic isomerization catalysts are preferred. Isomerization of glucose can be carried out with soluble bases. Moreau *et al.* presented high fructose selectivity at 25 % conversion for NaX and KX, but the catalysts were not stable in successive runs due to leaching of the metal cation¹⁰⁵. More recently, large pore zeolites containing Lewis acid sites, comprising of tin or titanium, proved to be very efficient^{106,107}. Moliner *et al.* were able to rapidly convert a 10 wt% glucose in water solution using Sn-Beta zeolite with Sn/glucose ratio of 50/1: 46 % glucose, 31 % fructose and 9 % mannose were obtained after 30 minutes at 383 K:



Another option is retro-aldol chemistry. For fructose this yields two trioses, *viz.* glyceraldehyde and dihydroxyacetone, which are very interesting C₃ building blocks. Janssens *et al.* were the first to report the zeolite catalyzed conversion of trioses¹⁰⁸. They reported acidic USY-zeolites to be effective for isomerization and esterification of dihydroxyacetone in alcoholic media yielding moderate amounts of alkyl lactate (scheme 27). The alkyl lactates and lactic acid find applications in cosmetics, the food industry, green solvents and are a vital building block for biodegradable PLA polymer synthesis.



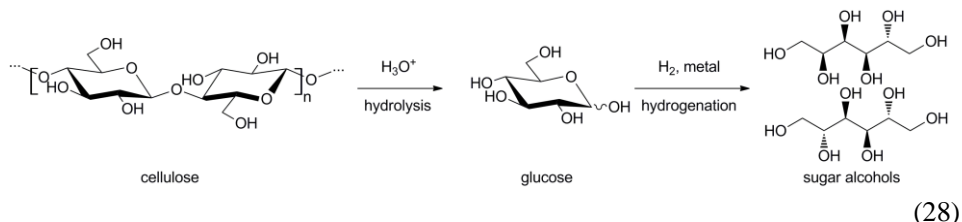
Following this pioneering work, detailed analysis and isotope labeling experiments showed the requirement of both Lewis and Brønsted acid sites. The latter preferably catalyzes the rate determining dehydration of trioses into methyl glyoxal, while the Lewis acid assists the further rearrangement according to a hydride shift (Meerwein-Ponndorf-Verley or intramolecular Cannizzaro reaction type) into alkyl lactate¹⁰⁹. Strong Brønsted acidity is unwanted as it converts methyl glyoxal into undesired dialkyl acetal. Synthesis of lactic acid is also possible in water, but the activity and the catalyst stability is lower¹¹⁰. Sn-Beta zeolite also successfully converts trioses into alkyl lactate with > 95 % selectivity^{111,112}. In search of other Lewis acid heterogeneous catalysts, Li *et al.* reported Ga₂O₃ and Sn-MCM-41 mesoporous materials¹¹³. The latter proved to be as selective and faster (per Sn) than Sn-Beta due the presence of both weak protonic silanols and isolated Sn sites.

Holm *et al.* reported the one step conversion of fructose and sucrose, a disaccharide of glucose and fructose, into alkyl lactates with Sn-Beta zeolites¹¹⁴. A yield of 64 % methyl lactate was reached with sucrose as feed in methanol over 20 hours at 433 K. Isomerization of glucose (if sucrose is used), retro-aldol, dehydration and the final hydride shift were catalyzed by one catalyst in the same pot. Single site tin was found to be more selective than less acidic Ti or Zr. If one considers the reaction pathway starting from glucose, this catalyst is thus able to mimic a one-pot synthetic glycolysis¹¹⁵.

3.2. Bio-based chemicals from cellulose with zeolites

Diminishing fossil fuel reserves, global climate changes and an increase in demand for energy, fuels and materials¹¹⁶ are inspiring a great deal of research into renewable energy and carbon¹¹⁷. The most promising renewable source of energy and chemicals in the short-to-medium term is biomass, in particular its main structural component lignocellulose, which makes up to 95 % of plant biomass¹¹⁸. Cellulose, a homopolymer of glucose units connected through β-1,4-glycosidic bonds, is the main component of lignocellulose, and as such its valorization is currently a research focal point. The main reaction to consider is cellulose hydrolysis to liberate glucose monomers. However, due to its structure cellulose is water insoluble and extremely resistant to chemical and enzymatic attack, making hydrolysis very slow, all the more since the low thermostability of glucose limits the reaction temperature.

A promising strategy to avoid this problem, known as hydrolytic hydrogenation, is the combination of hydrolysis with a simultaneous hydrogenation that converts the formed sugars to more stable sugar alcohols, enabling higher process temperatures (scheme 28)¹¹⁹. In many cases related compounds such as sorbitan and isosorbide are also formed through acid dehydration of sugar alcohols.



This bifunctional pathway was pioneered halfway through the 20th century by Russian researchers who used combinations of mineral acids and mostly Ru-based hydrogenation catalysts¹²⁰. Though mineral acids proved to be active and selective hydrolysis catalysts, reactor corrosion and the need for extensive neutralisation proved to be prohibitive for large-scale applications. Therefore, research attention shifted to the use of solid acids. The first successes were reported for conversion of oligosaccharides over Ru catalysts supported on montmorillonite and active carbon¹²¹. However, heavy Ru sintering considerably shortened catalyst lifetime. This problem was solved by supporting Ru catalysts on H-USY zeolites. With this system, a stable performance for at least 10 consecutive runs was reported, after which the catalyst could be regenerated to its initial activity by simple re-reduction of the Ru¹²². Furthermore, the use of a highly acidic support allowed the conversion of water soluble polysaccharides such as starch. Full conversion of 50 wt% starch feeds into > 99 % sugar alcohols in 1 h at 453 K was reported.

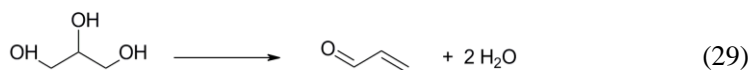
The water insoluble nature of cellulose impedes effective hydrolysis by intrazeolitic acid sites, as was shown by Fukuoka and Dhepe, who reported glucose yields under 4 % from cellulose after 24 h at 463 K with a range of common zeolites^{119a}. Recently, a solution to this accessibility problem was reported¹²³: by adding trace amounts of mineral acids (typically about 35 ppm) to a Ru/H-USY zeolite, full cellulose conversion to 93 % hexitols was achieved at 463 K. The minute concentration of mineral acid assists hydrolysis of cellulose to short soluble oligomers, which in turn are easily adsorbed by the zeolite and hydrolysed into glucose. Glucose is rapidly hydrogenated into sugar alcohols over the intraporous Ru particles. The low concentration of mineral acid should limit reaction corrosion and neutralisation waste.

Zeolites have also been demonstrated useful for the catalytic fast pyrolysis of cellulose¹²⁴. In this approach, biomass is heated quickly to high temperatures (973-1073 K) under inert atmosphere, forming vapours that are condensed to bio-oil. This bio-oil is of low value due to its high oxygenate content and its incompatibility with petroleum-derived oils. Interestingly, pyrolysis in presence of zeolites converts the vapors directly into aromatics, forming a product of much higher value. Typically, medium pore zeolites with a medium internal pore space and steric hindrance, such as ZSM-5, affords the highest yield in aromatics¹²⁵.

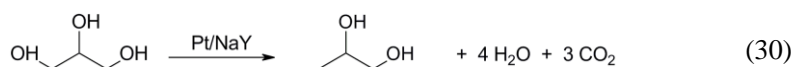
3.3 Catalytic conversion of glycerol

The ready availability of glycerol as a byproduct of the soap and biodiesel industry recently encouraged researchers to study the use of glycerol as a chemical commodity. Several review articles have already been written on the subject,¹²⁶⁻¹²⁹ with particular focus on glycerol oxidation, dehydration, hydrogenation, selective esterefication, chlorination and polyol formation. By subjecting glycerol to these catalytic transformations, products ranging from acrolein and acetol to lactic acid, as well as various hydrogenolysis products like propanediols can be obtained.

Acrolein has a large number of uses, *e.g.* as an intermediate for the production of acrylic acid and DL-methionine, as well as for the synthesis of various fine chemicals. Whereas the traditional industrial route involves oxidation of propene over complex multicomponent BiMoO_x-based catalysts, glycerol of renewable origin seems to be an attractive alternative for future acrolein production. The dehydration of glycerol over zeolite catalysts can occur both in the gas and liquid phase. At temperatures of 315-360 °C, it was shown that zeolites H-ZSM-11, H-ZSM-5 and H-Beta convert glycerol almost quantitatively with acrolein yields ranging from 73 to 81 %¹²⁹. Alternatively to the commonly used fixed-bed reactors, Corma *et al.* also demonstrated the opportunity of reacting gas-phase glycerol/water mixtures with zeolites in a continuous fluidized-bed reactor¹³⁰. At 350 °C and contact times of 0.5-2 s, they were able to obtain 61 % acrolein yield with a ZSM-5 based catalyst. The current acrolein selectivity for zeolite catalyzed dehydrations is slightly lower than those obtained when using less acidic metal oxides¹²⁷.



Another example of glycerol valorization with zeolites relies on the hydrogenolysis of glycerol to 1,2-propanediol via bifunctional heterogeneous catalysis¹³¹. The mechanism involves zeolite-catalyzed dehydration, followed by metal-mediated hydrogenation. A sustainable way to circumvent the need of externally added hydrogen involves the integration of a glycerol-based hydrogen production via catalytic aqueous-phase reforming. D'Hondt *et al.* presented a chemical route derived for the hydrogenolysis of glycerol in presence of Pt impregnated NaY zeolites in absence of external hydrogen supply, according to the following net reaction¹³²:



Under nonoptimized process conditions, preliminary results with glycerol under inert atmosphere are reported to yield up to 55 % 1,2-propanediol at 85 % conversion. A bimodal size distribution of the Pt particles is crucial to balance aqueous-phase reforming and hydrogenation towards maximum 1,2-propanediol yields and high H₂ efficiency¹³³.

3.4 Zeolite catalysis in Oleochemistry

a. Hydrogenation of FAMEs and vegetable oils using zeolite catalysts

The catalytic hydrogenation of vegetable oils is an important process in the food industry as it converts liquid vegetable oils into more stable oils or (semi-)solid fat products with desirable physical properties. Conventional hydrogenation processes yield besides hydrogenation also isomerization products, such as *trans* fatty acids¹³⁴. This *cis/trans* isomerization should be limited as some of these *trans* isomers, especially elaidate (C18:1 *trans*-9), are considered a risk factor in coronary heart diseases¹³⁵.

It has been shown that the pore size of the MFI topology enables discriminating between the bended *cis*- and the linear *trans* fatty acid chains¹³⁶. Hydrogenation experiments of equimolar methyl oleate (*cis*) and elaidate (*trans*) mixtures with a Pt/ZSM-5 catalyst selectively hydrogenates the *trans*-isomer, provided that Pt resorts inside the zeolite pores. Shape selectivity is obviously due to a difference in substrate diffusivity. The *cis/trans* preference has also been demonstrated in the hydrogenation of the bulkier triacylglycerols¹³⁷. Here, the story is somewhat different. As entire triacylglycerol molecules are unable to diffuse into the zeolite pores, the shape selective effect is limited to the pore mouth. Interestingly, the triacylglycerol preferably enters the pore mouth with the internal fatty acid chain. This has been demonstrated for the selective *sn*-2 hydrogenation of pure trioleate (OOO) into OSO (O is oleate; S is stearate). Pt/ZSM-5 catalyst also shows a stepwise reduction of polyunsaturates to the mono-unsaturated level with reduced formation of saturated fatty acids. The selectivity concepts are also observed in the hydrogenation of raw soybean oil¹³⁸. The hydrogenation process of soybean oil at low temperature and high hydrogen pressure in presence of shape selective Pt/ZSM-5 catalyst, results in a unique fat product with high thermal stability, high nutrition level (low contents of palmitate and high contents of mono-unsaturates, low *trans values*, and very plastic, suitable for many shortening applications).

b. Isomerization of FAMEs using zeolites

Next to hydrogenation reactions, also isomerization of FAMEs and vegetable oils has been investigated with zeolite catalysts. Two types of isomerizations are considered, *viz.* conjugation and skeletal rearrangement.

Conjugated vegetable oils are of high interest in industry as their conjugated double bonds are highly active in polymerization reactions. Traditionally conjugated vegetable oils are added to paints, varnishes and inks to improve their drying properties¹³⁹. Furthermore, conjugated linoleic acids (CLAs) are also used in the production of bio-plastics¹⁴⁰. In recent years, various positive health effects have been attributed to CLAs. However, from the different possible CLA isomers, only the beneficial health effects of the c9,t11, t10,c12¹⁴¹ and t9,t11 CLA isomers¹⁴² are known. Nowadays, CLAs are mainly produced by conjugation of oils high in linoleic acid, *viz.* soybean and safflower oil, using homogeneous base¹⁴³ or alternatively by dehydration of castor oil¹⁴⁴. Heterogeneous catalysts are more attractive as they can be easily recovered by filtration. The design of an efficient catalyst using metal loaded zeolites with high CLA selectivity is difficult because of a competing hydrogenation reaction¹⁴⁵. While many attempts failed due to too CLA productivity, only a recent Ru/Cs-USY catalyst with a high Si/Al ratio was able to compete with the homogeneous processes¹⁴⁶. Almost no hydrogenation products are formed, as the reactions can be carried out in inert atmosphere. Moreover, this catalyst shows a very high selectivity towards the biologically most active CLA isomers. A high Ru dispersion, the absence of strong acid sites and the high accessibility of the active sites for the bulky reagent molecules are the three most important criteria¹⁴⁷.

Alkyl-branched fatty acids are used in various industrial products, especially in the cosmetics and lubricant area¹⁴⁸. Nowadays, clay catalysts are used for this isomerization reaction, yielding complex mixtures of both alkyl-branched and dimeric fatty acids¹⁴⁹. When using a modified acid Ferrierite zeolite catalysts, very high yields and selectivities (> 85 %) for the branched fatty acids were obtained¹⁵⁰. In order to obtain these high yields and productivities the Si/Al ratio and the pretreatment procedure of the zeolite are crucial.

4. Conclusion

Zeolite chemistry continues to be a particularly fertile ground for designing new catalysts with optimized selectivity for the most diverse organic reactions. Intriguing opportunities are offered by new topologies, new types of functions that are introduced in the zeolites, or by enhanced control of diffusion of reactants and products. Despite the large molecular dimensions of many biomass-derived feedstock molecules, a proper tailoring of zeolite catalysts allows to successfully employ zeolites for the transformation of renewables to useful chemicals.

Acknowledgements

Several of us are grateful to IWT (BSt, JB) or to FWO (APe, SVDV, APh, MD) for a doctoral fellowship. The efforts of BSe and DDV in organic catalysis are supported by the IAP program of the Belgian Federal Government and by a Metusalem grant.

References

- 1 Hölderich, W. F. & Bekkum, H. v. in *Introduction to Zeolite Science and Practice, Stud. Surf. Sci. Catal.* Vol. 58 (eds E. M. Flanigen H. van Bekkum & J. C. Jansen) Ch. 16, 631-726 (Elsevier, 1991).
- 2 Espeel, P. H. *et al.* in *Catalysis and Zeolites* (eds Weitkamp J. & Puppe L.) 377-436 (Springer, 1999).
- 3 Venuto, P. B. Organic catalysis over zeolites: A perspective on reaction paths within micropores. *Microporous Mater.* **2**, 297-411, doi:Doi: 10.1016/0927-6513(94)00002-6 (1994).
- 4 De Vos, D. E. & Jacobs, P. A. Zeolite effects in liquid phase organic transformations. *Micropor. Mesopor. Mater.* **82**, 293-304, doi:DOI: 10.1016/j.micromeso.2005.01.038 (2005).
- 5 Meima, G. R., Lee, G. S. & Garces, J. M. in *Fine Chemicals through Heterogeneous Catalysis* (eds Roger Arthur Sheldon & Herman van Bekkum) Ch. 123-183, 123-183 (Wiley-VCH Verlag GmbH, 2007).
- 6 Brechtelsbauer, C. & Emig, G. Shape selective methylation of biphenyl within zeolites: An example of transition state selectivity. *Appl. Catal. A* **161**, 79-92, doi:Doi: 10.1016/s0926-860x(96)00382-1 (1997).
- 7 Ahedi, R. K., Tawada, S., Kubota, Y., Sugi, Y. & Kim, J. H. Shape-selective alkylation of biphenyl catalyzed by H-[Al]-SSZ-31 zeolite. *J. Mol. Catal. A* **197**, 133-146, doi:Doi: 10.1016/s1381-1169(02)00627-1 (2003).
- 8 Sugi, Y., Kubota, Y., Hanaoka, T.-a. & Matsuzaki, T. Zeolite Catalyzed Alkylation of Biphenyl. Where Does Shape-Selective Catalysis Occur? *Catalysis Surveys from Japan* **5**, 43-56, doi:10.1023/a:1012394525091 (2001).
- 9 Takeuchi, G., Shimoura, Y. & Hara, T. Selective transalkylation of biphenyl over solid acid catalysts. *Appl. Catal. A* **137**, 87-91, doi:Doi: 10.1016/0926-860x(95)00323-1 (1996).
- 10 Horikawa, Y., Uchino, Y., Shichijo, Y. & Sako, T. Shape-selective Methylation of 4-Methylbiphenyl to 4,4'-Dimethylbiphenyl with Supercritical Methanol over Zeolite Catalysts. *J. Japan Petr. Inst.* **47**, 136-142 (2004).
- 11 Hoeltmann, W., Collin, G., Neuber, M., Spengler, H. & Weitkamp, J. US patent US 4795847 (1989).

- 12 Derouane, E. G., Fellmann, J. D., Saxton, R. J., Wetreck, P. R. & Massiani, P. US patent US 5026942 (1991).
- 13 Wang, J., Park, J.-N., Park, Y.-K. & Lee, C. W. Isopropylation of naphthalene by isopropyl alcohol over USY catalyst: an investigation in the high-pressure fixed-bed flow reactor. *J. Catal.* **220**, 265-272, doi:Doi: 10.1016/s0021-9517(03)00212-4 (2003).
- 14 Cutrufello, M. G. *et al.* Liquid-phase alkylation of naphthalene by isopropanol over zeolites: Part III. Mordenites. *Appl. Catal. A* **241**, 91-111, doi:Doi: 10.1016/s0926-860x(02)00461-1 (2003).
- 15 Ferino, I. *et al.* Liquid-phase alkylation of naphthalene by isopropanol over zeolites: Part II: Beta zeolites. *Appl. Catal. A* **183**, 303-316, doi:Doi: 10.1016/s0926-860x(99)00074-5 (1999).
- 16 Sugi, Y. *et al.* The alkylation of naphthalene over three-dimensional large pore zeolites: The influence of zeolite structure and alkylating agent on the selectivity for dialkyl naphthalenes. *Catal. Today* **132**, 27-37, doi:DOI: 10.1016/j.cattod.2007.12.009 (2008).
- 17 Moreau, P. *et al.* Selective dialkylation of naphthalene with hindered alkylating agents over HM and HY zeolites under liquid phase conditions. *Catal. Today* **31**, 11-17, doi:Doi: 10.1016/0920-5861(96)00029-6 (1996).
- 18 Mravec, D. *et al.* Cyclohexylation of naphthalene over unmodified HY zeolites. *Catal. Lett.* **38**, 267-270, doi:10.1007/bf00806580 (1996).
- 19 Srinivas, N., Singh, A. P., Ramaswamy, A. V., Finiels, A. & Moreau, P. Shape-Selective Alkylation of 2-Methoxynaphthalene with tert-Butanol over Large-Pore Zeolites. *Catal. Lett.* **80**, 181-186, doi:10.1023/a:1015472812322 (2002).
- 20 Komatsu, T., Araki, Y., Namba, S. & Yashima, T. in *Stud. Surf. Sci. Catal.* Vol. Volume 84 (eds H. G. Karge H. Pfeifer J. Weitkamp & W. Hölderich) 1821-1828 (Elsevier, 1994).
- 21 Millini, R. *et al.* A priori selection of shape-selective zeolite catalysts for the synthesis of 2,6-dimethylnaphthalene. *J. Catal.* **217**, 298-309, doi:Doi: 10.1016/s0021-9517(03)00071-x (2003).
- 22 Knifton, J. F., Anantaneni, P. R., Dai, P. E. & Stockton, M. E. A New, Improved, Solid-Acid Catalyzed Process for Generating Linear Alkylbenzenes (LABs). *Catal. Lett.* **75**, 113-117, doi:10.1023/a:1016775820865 (2001).
- 23 Liang, W. *et al.* Alkylation of benzene with dodecene over HY zeolite: Deactivation, regeneration, and product distribution. *Zeolites* **17**, 297-303, doi:Doi: 10.1016/0144-2449(96)00034-6 (1996).
- 24 Bordoloi, A., Devassy, B. M., Niphadkar, P. S., Joshi, P. N. & Halligudi, S. B. Shape selective synthesis of long-chain linear alkyl benzene (LAB) with AlMCM-41/Beta zeolite composite catalyst. *J. Mol. Catal. A* **253**, 239-244, doi:DOI: 10.1016/j.molcata.2006.03.045 (2006).

- 25 Magnoux, P., Mourran, A., Bernard, S. & Guisnet, M. in *Stud. Surf. Sci. Catal.* Vol. Volume 108 (eds H.U. Blaser, A. Baiker, & R. Prins) 107-114 (Elsevier, 1997).
- 26 Zhao, Z.-K., Li, Z.-S., Qiao, W.-H., Wang, G.-R. & Cheng, L.-B. Alkylation of α -Methylnaphthalene with Long-Chain Olefins over Large-Pore Zeolites. *Catal. Lett.* **98**, 145-151, doi:10.1007/s10562-004-7930-8 (2004).
- 27 Zhao, Z. *et al.* HY zeolite catalyst for alkylation of [alpha]-methylnaphthalene with long-chain alkenes. *Micropor. Mesopor. Mater.* **93**, 164-170, doi:DOI: 10.1016/j.micromeso.2005.05.058 (2006).
- 28 Hu, X. C., Chuah, G. K. & Jaenicke, S. Liquid-phase regioselective benzylation of bromobenzene and other aromatics over microporous zeolites. *Micropor. Mesopor. Mater.* **53**, 153-161, doi:Doi: 10.1016/s1387-1811(02)00336-0 (2002).
- 29 Singh, A. P., Jacob, B. & Sugunan, S. Liquid-phase selective benzylation of o-xylene using zeolite catalysts. *Appl. Catal. A* **174**, 51-60, doi:Doi: 10.1016/s0926-860x(98)00194-x (1998).
- 30 Van der Beken, S. *et al.* Alkylation of deactivated aromatic compounds on zeolites. Adsorption, deactivation and selectivity effects in the alkylation of bromobenzene and toluene with bifunctional alkylating agents. *J. Catal.* **235**, 128-138, doi:DOI: 10.1016/j.jcat.2005.06.029 (2005).
- 31 Xiao, F.-S. *et al.* Catalytic Properties of Hierarchical Mesoporous Zeolites Templated with a Mixture of Small Organic Ammonium Salts and Mesoscale Cationic Polymers. *Angew. Chem. Int. Edit.* **45**, 3090-3093, doi:10.1002/anie.200600241 (2006).
- 32 Groen, J. C., Abelló, S., Villaescusa, L. A. & Pérez-Ramírez, J. Mesoporous beta zeolite obtained by desilication. *Micropor. Mesopor. Mater.* **114**, 93-102, doi:DOI: 10.1016/j.micromeso.2007.12.025 (2008).
- 33 Sun, Y. & Prins, R. Friedel-Crafts alkylations over hierarchical zeolite catalysts. *Appl. Catal. A* **336**, 11-16, doi:DOI: 10.1016/j.apcata.2007.08.015 (2008).
- 34 Abelló, S., Bonilla, A. & Pérez-Ramírez, J. Mesoporous ZSM-5 zeolite catalysts prepared by desilication with organic hydroxides and comparison with NaOH leaching. *App. Catal. A* **364**, 191-198, doi:DOI: 10.1016/j.apcata.2009.05.055 (2009).
- 35 Shih, P.-C., Wang, J.-H. & Mou, C.-Y. Strongly acidic mesoporous aluminosilicates prepared from zeolite seeds: acylation of anisole with octanoyl chloride. *Catal. Today* **93-95**, 365-370, doi:DOI: 10.1016/j.cattod.2004.06.025 (2004).
- 36 Chaube, V. D., Moreau, P., Finiels, A., Ramaswamy, A. V. & Singh, A. P. A novel single step selective synthesis of 4-hydroxybenzophenone (4-HBP) using zeolite H-beta. *Catal. Lett.* **79**, 89-94 (2002).

- 37 Andy, P. *et al.* Acylation of 2-Methoxynaphthalene and Isobutylbenzene over Zeolite Beta. *J. Catal.* **192**, 215-223, doi:DOI: 10.1006/jcat.2000.2855 (2000).
- 38 Heinichen, H. K. & Hölderich, W. F. Acylation of 2-Methoxynaphthalene in the Presence of Modified Zeolite HBEA. *J. Catal.* **185**, 408-414, doi:DOI: 10.1006/jcat.1999.2526 (1999).
- 39 Vogt, A. & Pfenninger, A. EP 701987 (1994).
- 40 Botella, P., Corma, A. & Sastre, G. Al-ITQ-7, a Shape-Selective Zeolite for Acylation of 2-Methoxynaphthalene. *J. Catal.* **197**, 81-90, doi:DOI: 10.1006/jcat.2000.3057 (2001).
- 41 Botella, P., Corma, A., Navarro, M. T., Rey, F. & Sastre, G. On the shape selective acylation of 2-methoxynaphthalene over polymorph C of Beta (ITQ-17). *J. Catal.* **217**, 406-416, doi:Doi: 10.1016/s0021-9517(03)00053-8 (2003).
- 42 Cervený, L., Mikulcová, K. & Cejka, J. Shape-selective synthesis of 2-acetylnaphthalene via naphthalene acylation with acetic anhydride over large pore zeolites. *Appl. Catal. A* **223**, 65-72, doi:Doi: 10.1016/s0926-860x(01)00743-8 (2002).
- 43 Bhattacharya, D., Sharma, S. & Singh, A. P. Selective benzylation of naphthalene to 2-benzoylnaphthalene using zeolite H-beta catalysts. *Appl. Catal. A* **150**, 53-62, doi:Doi: 10.1016/s0926-860x(96)00300-6 (1997).
- 44 Hou, Q. *et al.* Liquid-phase cascade acylation/dehydration over various zeolite catalysts to synthesize 2-methylantraquinone through an efficient one-pot strategy. *J. Catal.* **268**, 376-383, doi:DOI: 10.1016/j.jcat.2009.10.010 (2009).
- 45 Yamashita, H., Mitsukura, Y. & Kobashi, H. Microwave-assisted acylation of aromatic compounds using carboxylic acids and zeolite catalysts. *J. Mol. Catal. A* **327**, 80-86, doi:DOI: 10.1016/j.molcata.2010.05.016 (2010).
- 46 Lecomte, J., Finiels, A., Geneste, P. & Moreau, C. Selective hydroxymethylation of furfuryl alcohol with aqueous formaldehyde in the presence of dealuminated mordenites. *Appl. Catal. A* **168**, 235-241, doi:Doi: 10.1016/s0926-860x(97)00349-9 (1998).
- 47 Finiels, A. *et al.* Role of hydrophobic effects in organic reactions catalysed by zeolites. *J. Mol. Catal. A* **148**, 165-172, doi:Doi: 10.1016/s1381-1169(99)00046-1 (1999).
- 48 Wu, X. & Anthony, R. G. Alkylation of Benzene with Formaldehyde over ZSM-5. *J. Catal.* **184**, 294-297, doi:DOI: 10.1006/jcat.1999.2426 (1999).
- 49 Marion, P., Jacquot, R., Ratton, S. & Guisnet, M. in *Zeolites for Cleaner Technologies* (eds M. Guisnet & J. P. Gilson) Ch. 14, 281-299 (Imperial College Press, 2002).
- 50 Moreau, C., Rzigade-Trousselier, S., Finiels, A., Fajula, F. & Gilbert, L. US 5811587 (1998).

- 51 Cavani, F., Corrado, M. & Mezzogori, R. A note on the role of methanol in the homogeneous and heterogeneous acid-catalyzed hydroxymethylation of guaiacol with aqueous solutions of formaldehyde. *J. Mol. Catal. A* **182-183**, 447-453, doi:Doi: 10.1016/s1381-1169(01)00473-3 (2002).
- 52 Bolognini, M. *et al.* Guaiacol hydroxyalkylation with aqueous formaldehyde: role of surface properties of H-mordenites on catalytic performance. *App. Catal. A* **272**, 115-124, doi:DOI: 10.1016/j.apcata.2004.05.021 (2004).
- 53 de Angelis, A., Ingallina, P. & Perego, C. Solid Acid Catalysts for Industrial Condensations of Ketones and Aldehydes with Aromatics. *Ind. Eng. Chem. Res.* **43**, 1169-1178, doi:10.1021/ie030429+ (2004).
- 54 Álvaro, M., Das, D., Cano, M. & Garcia, H. Friedel-Crafts hydroxyalkylation: reaction of anisole with paraformaldehyde catalyzed by zeolites in supercritical CO₂. *J. Catal.* **219**, 464-468, doi:Doi: 10.1016/s0021-9517(03)00274-4 (2003).
- 55 Corma, A., Botella, P. & Mitchell, C. Replacing HCl by solid acids in industrial processes: synthesis of diamino diphenyl methane (DADPM) for producing polyurethanes. *Chem. Commun.*, 2008-2010 (2004).
- 56 Perego, C. *et al.* Amorphous aluminosilicate catalysts for hydroxyalkylation of aniline and phenol. *Appl. Catal. A* **307**, 128-136, doi:DOI: 10.1016/j.apcata.2006.03.013 (2006).
- 57 Ichihashi, H. *et al.* The catalysis of vapor-phase Beckmann rearrangement for the production of epsilon-caprolactam. *Catalysis Surveys from Asia* **7**, 261-270 (2003).
- 58 Eickelberg, W. & Hoelderich, W. F. Beckmann-rearrangement of cyclododecanone oxime to omega-lauro lactam in the gas phase. *Journal of Catalysis* **263**, 42-55, doi:10.1016/j.jcat.2009.01.010 (2009).
- 59 Climent, M. J., Corma, A. & Iborra, S. Synthesis of nonsteroidal drugs with anti-inflammatory and analgesic activities with zeolites and mesoporous molecular sieve catalysts. *Journal of Catalysis* **233**, 308-316, doi:10.1016/j.jcat.2005.05.003 (2005).
- 60 Levecque, P., Gammon, D. W., Jacobs, P., De Vos, D. & Sels, B. The use of ultrastable Y zeolites in the Ferrier rearrangement of acetylated and benzylated glycals. *Green Chemistry* **12**, 828-835, doi:10.1039/b921051b (2010).
- 61 de la Torre, O., Renz, M. & Corma, A. Biomass to chemicals: Rearrangement of beta-pinene epoxide into myrtanal with well-defined single-site substituted molecular sieves as reusable solid Lewis-acid catalysts. *Applied Catalysis a-General* **380**, 165-171, doi:10.1016/j.apcata.2010.03.056 (2010).
- 62 Maxwell, I. E., Downing, R. S. & Vanlangen, S. A. J. Copper-exchanged zeolite catalysts for the cyclo-dimerization of butadiene. 1. Catalyst stability and regenerability. *Journal of Catalysis* **61**, 485-492 (1980).

- 63 Maxwell, I. E., Deboer, J. J. & Downing, R. S. Copper-exchanged zeolite catalysts for the cyclo-dimerization of butadiene. 2. Catalyst Structure. *Journal of Catalysis* **61**, 493-502 (1980).
- 64 Liu, H. F. *et al.* ZnCl₂ supported on NaY zeolite by solid-state interaction under microwave irradiation and used as heterogeneous catalysts for high regioselective Diels-Alder reaction of myrcene and acrolein. *Journal of Molecular Catalysis a-Chemical* **209**, 171-177, doi:10.1016/j.molcata.2003.08.011 (2004).
- 65 Eklund, L., Axelsson, A. K., Nordahl, A. & Carlson, R. Zeolite and Lewis acid catalysis in Diels-Alder reactions of isoprene. *Acta Chemica Scandinavica* **47**, 581-591 (1993).
- 66 Olmos, A., Sommer, J. & Pale, P. Scandium(III) zeolites as new heterogeneous catalysts: [4+2]cyclocondensation of in situ generated aryl imines with alkenes. *Chemistry-a European Journal* **17**, 1907-1914, doi:10.1002/chem.201002649 (2010).
- 67 Gomez, M. V., Cantin, A., Corma, A. & de la Hoz, A. Use of different microporous and mesoporous materials as catalyst in the Diels-Alder and retro-Diels-Alder reaction between cyclopentadiene and p-benzoquinone activity of Al-, Ti- and Sn-doped silica. *Journal of Molecular Catalysis a-Chemical* **240**, 16-21, doi:10.1016/j.molcata.2005.06.030 (2005).
- 68 Demuynek, A. L. W. *et al.* Retro-Diels-Alder reactions of masked cyclopentadienones catalyzed by heterogeneous Bronsted acids. *Advanced Synthesis & Catalysis* **352**, 3419-3430, doi:10.1002/adsc.201000571 (2010).
- 69 Wuyts, S., De Temmerman, K., De Vos, D. E. & Jacobs, P. A. Acid zeolites as alcohol racemization catalysts: Screening and application in biphasic dynamic kinetic resolution. *Chemistry-a European Journal* **11**, 386-397, doi:10.1002/chem.200400713 (2005).
- 70 Zhu, Y. Z., Fow, K. L., Chuah, G. K. & Jaenicke, S. Dynamic kinetic resolution of secondary alcohols combining enzyme-catalyzed transesterification and zeolite-catalyzed racemization. *Chemistry-a European Journal* **13**, 541-547, doi:10.1002/chem.200600723 (2007).
- 71 Grundling, C., EderMirth, G. & Lercher, J. A. Selectivity enhancement in methylamine synthesis via postsynthesis modification of Bronsted acidic mordenite - An infrared spectroscopic and kinetic study on the reaction mechanism. *Journal of Catalysis* **160**, 299-308 (1996).
- 72 Corbin, D. R., Schwarz, S. & Sonnichsen, G. C. Methylamines synthesis: A review. *Catalysis Today* **37**, 71-102 (1997).
- 73 Jeon, H. Y., Shin, C. H., Jung, H. J. & Hong, S. B. Catalytic evaluation of small-pore molecular sieves with different framework topologies for the synthesis of methylamines. *Applied Catalysis a-General* **305**, 70-78, doi:10.1016/j.apcata.2006.02.044 (2006).

- 74 Tijsebaert, B. *et al.* Shape-selective synthesis of methylamines over the RRO zeolite Al-RUB-41. *Journal of Catalysis* **278**, 246-252, doi:10.1016/j.jcat.2010.12.010 (2011).
- 75 Patil, N. M., Gupte, S. P. & Chaudhari, R. V. Heterogenized copper catalysts for the amination of arylhalide: Synthesis, characterization and catalytic applications. *Applied Catalysis a-General* **372**, 73-81, doi:10.1016/j.apcata.2009.10.013 (2010).
- 76 Jimenez, O., Muller, T. E., Schwieger, W. & Lercher, J. A. Hydroamination of 1,3-cyclohexadiene with aryl amines catalyzed with acidic form zeolites. *Journal of Catalysis* **239**, 42-50, doi:10.1016/j.jcat.2006.01.007 (2006).
- 77 Penzien, J., Muller, T. E. & Lercher, J. A. Hydroamination of 6-aminohex-1-yne over zinc based homogeneous and zeolite catalysts. *Micropor Mesopor Mat* **48**, 285-291 (2001).
- 78 Huang, W., McCormick, J. R., Lobo, R. F. & Chen, J. G. Selective hydrogenation of acetylene in the presence of ethylene on zeolite-supported bimetallic catalysts. *J Catal* **246**, 40-51, doi:DOI 10.1016/j.jcat.2006.11.013 (2007).
- 79 Dessau, R. M. Shape selective hydrogenation of aromatics over modified non-acidic platinum/ZSM-5 catalysts. US patent 5350504 (1994).
- 80 Weitkamp, J., Ernst, S., Bock, T., Kiss, A. & Kleinschmitt, P. Vol. 94 278 (Elsevier, 1995).
- 81 Altwasser, S., Glaser, R. & Weitkamp, J. Ruthenium-containing small-pore zeolites for shape-selective catalysis. *Microporous and Mesoporous Materials* **104**, 281-288, doi:DOI 10.1016/j.micromeso.2007.02.046 (2007).
- 82 Creighton, E. J., Grotenbreg, R. A. W., Downing, R. S. & vanBekum, H. Regioselective hydrogenation of alkenes over Pt-loaded zeolite BEA. *Journal of the Chemical Society-Faraday Transactions* **92**, 871-877 (1996).
- 83 Creighton, E. J. & Downing, R. S. Shape-selective hydrogenation and hydrogen transfer reactions over zeolite catalysts. *Journal of Molecular Catalysis a-Chemical* **134**, 47-61 (1998).
- 84 Zahmakiran, M., Tonbul, Y. & Ozkar, S. Ruthenium(0) Nanoclusters Stabilized by Nanozeolite Framework: Isolable, Reusable, and Green Catalyst for the Hydrogenation of Neat Aromatics under Mild Conditions with the Unprecedented Catalytic Activity and Lifetime (vol 132, pg 6541, 2010). *Journal of the American Chemical Society* **132**, 10205-10205, doi:Doi 10.1021/Ja103871s (2010).
- 85 Gallezot, P., Giroirfendler, A. & Richard, D. Chemoselectivity in Cinnamaldehyde Hydrogenation Induced by Shape Selectivity Effects in Pt-Y-Zeolite Catalysts. *Catalysis Letters* **5**, 169-174 (1990).
- 86 Gallezot, P., Blanc, B., Barthomeuf, D. & Pais da Silva, M. I. Vol. 84 1433 (Elsevier, 1994).

- 87 De Bruyn, M. *et al.* Chemoselective reduction of complex alpha,beta-unsaturated ketones to allylic alcohols over Ir-metal particles on beta zeolites. *Angewandte Chemie-International Edition* **42**, 5333-5336, doi:DOI 10.1002/anie.200352275 (2003).
- 88 Zhu, Y. Z., Chuah, G. K. & Jaenicke, S. Selective Meerwein-Ponndorf-Verley reduction of alpha, beta-unsaturated aldehydes over Zr-zeolite beta. *J Catal* **241**, 25-33, doi:DOI 10.1016/j.jcat.2006.04.008 (2006).
- 89 Neatu, F. *et al.* Heterogeneous Catalytic Transformation of Citronellal to Menthol in a Single Step on Ir-Beta Zeolite Catalysts. *Topics in Catalysis* **52**, 1292-1300, doi:DOI 10.1007/s11244-009-9270-9 (2009).
- 90 Nie, Y. T., Jaenicke, S. & Chuah, G. K. Zr-Zeolite Beta: A New Heterogeneous Catalyst System for the Highly Selective Cascade Transformation of Citral to (+/-)-Menthol. *Chemistry-a European Journal* **15**, 1991-1999, doi:DOI 10.1002/chem.200801776 (2009).
- 91 Komatsu, T. & Hirose, T. Gas phase synthesis of para-aminophenol from nitrobenzene on Pt/zeolite catalysts. *Appl Catal a-Gen* **276**, 95-102, doi:DOI 10.1016/j.apcata.2004.07.044 (2004).
- 92 Perego, C., Carati, A., Ingallina, P., Mantegazza, M. A. & Bellussi, G. Production of titanium containing molecular sieves, and their application in catalysis. *Appl Catal a-Gen* **221**, 63-72 (2001).
- 93 Clerici, M. G. & Ingallina, P. Epoxidation of Lower Olefins with Hydrogen-Peroxide and Titanium Silicalite. *J Catal* **140**, 71-83 (1993).
- 94 Tuel, A. & Bentaarit, Y. Comparison between Ts-1 and Ts-2 in the Hydroxylation of Phenol with Hydrogen-Peroxide. *Appl Catal a-Gen* **102**, 69-77 (1993).
- 95 Mantegazza, M. A., Petrini, G., Spano, G., Bagatin, R. & Rivetti, F. Selective oxidations with hydrogen peroxide and titanium silicalite catalyst. *Journal of Molecular Catalysis a-Chemical* **146**, 223-228 (1999).
- 96 Wu, P. & Tatsumi, T. Unique trans-selectivity of Ti-MWW in epoxidation of cis/trans-alkenes with hydrogen peroxide. *Journal of Physical Chemistry B* **106**, 748-753, doi:Doi 10.1021/Jp0120965 (2002).
- 97 Wu, P. & Tatsumi, T. A novel titanosilicate with MWW structure III. Highly efficient and selective production of glycidol through epoxidation of allyl alcohol with H₂O₂. *J Catal* **214**, 317-326, doi:Doi 10.1016/S0021-9517(02)00170-7 (2003).
- 98 Reichinger, M. *et al.* Alkene epoxidation with mesoporous materials assembled from TS-1 seeds - Is there a hierarchical pore system? *J Catal* **269**, 367-375, doi:DOI 10.1016/j.jcat.2009.11.023 (2010).
- 99 Xin, H. C. *et al.* Enhanced Catalytic Oxidation by Hierarchically Structured TS-1 Zeolite. *Journal of Physical Chemistry C* **114**, 6553-6559, doi:Doi 10.1021/Jp912112h (2010).

- 100 Renz, M. *et al.* Selective and shape-selective Baeyer-Villiger oxidations of aromatic aldehydes and cyclic ketones with Sn-Beta zeolites and H₂O₂. *Chemistry-a European Journal* **8**, 4708-4717 (2002).
- 101 Aubry, J. M., Cazin, B. & Duprat, F. Chemical Sources of Singlet Oxygen .3. Peroxidation of Water-Soluble Singlet Oxygen Carriers with the Hydrogen-Peroxide Molybdate System. *Journal of Organic Chemistry* **54**, 726-728 (1989).
- 102 Wahlen, J. *et al.* Lanthanum-exchanged zeolites as active and selective catalysts for the generation of singlet oxygen from hydrogen peroxide. *Chemical Communications*, 927-929, doi:DOI 10.1039/B414597f (2005).
- 103 Ren, N. *et al.* Novel, efficient hollow zeolitically microcapsulized noble metal catalysts. *J Catal* **251**, 182-188, doi:DOI 10.1016/j.jcat.2007.07.009 (2007).
- 104 Laursen, A. B. *et al.* Substrate Size-Selective Catalysis with Zeolite-Encapsulated Gold Nanoparticles. *Angewandte Chemie-International Edition* **49**, 3504-3507, doi:DOI 10.1002/anie.200906977 (2010).
- 105 Moreau, C., Durand, R., Roux A. & Tichit, D. Isomerization of glucose into fructose in the presence of cation-exchanged zeolites and hydrotalcites. *Applied Catalysis A: General* **193**, 257-264 (2000).
- 106 Moliner, M., Roman-Leshkov, Y. & Davis, M. E. Tin-containing zeolites are highly active catalysts for the isomerization of glucose in water. *Proceedings of the National Academy of Sciences* **107**(14), 6164-6168 (2010)
- 107 Roman-Leshkov, Y., Moliner, M., Labinger, J. A. & Davis, M. E. Mechanism of Glucose Isomerization Using a Solid Lewis Acid Catalyst in Water. *Angew. Chem. Int. Ed.* **49**, 8954-8957 (2010)
- 108 Janssen, K. P. F., Paul, J. S., Sels, B. F. & Jacobs, P. A. Glyoxylase biomimics: zeolite catalyzed conversion of trioses. *Stud. Surf. Sci. Catal.* **170B**, 1222-1227 (2007)
- 109 Pescarmona, P. P., Janssen, K. P. F., Delaet, C., Stroobants, C., Houthoofd, K., Philippaerts, A., De Jonghe, C., Paul, J. S., Jacobs, P. A. & Sels, B. F. Zeolite-catalysed conversion of C₃ sugars to alkyl lactates. *Green Chemistry* **12**, 1083-1089 (2010)
- 110 West, R. M., Holm M. S., Saravanamurugan S., Xiong, J., Beversdorf, Z., Taarning, E. & Christensen, C. H. Zeolite H-USY for the production of lactic acid and methyl lactate from C₃-sugars. *Journal of Catalysis* **269**, 122-130.(2010)
- 111 Taarning, E., Saravanamurugan S., Holm M. S., Xiong, J., West, R. M. & Christensen, C. H. Zeolite-Catalyzed isomerization of Triose Sugars. *ChemSusChem* **2**, 625-627 (2009)
- 112 Corma, A., Domine M.E., Nemeth, L. & Valencia S. Al-Free Sn-Beta Zeolite as a Catalyst for the Selective Reduction of Carbonyl Compounds

- (Meerwein-Ponndorf-Verley Reaction). *Journal of the American Chemical Society* **124**, 3194-3195 (2002)
- 113 Li L., Stroobants, C., Lin, K., Jacobs, P. A., Sels, B. F. & Pescarmona, P. P. Selective conversion of trioses to lactates over Lewis acid heterogeneous catalysts. *Green Chemistry* **13**, 1175-1181 (2011)
- 114 Holm, M. S., Saravanamurugan S. & Taarning, E. Conversion of sugars to lactic acid derivatives using heterogeneous zeotype catalysts. *Science* **328**, 602-605 (2010)
- 115 Lobo, R. F. Synthetic Glycolysis. *ChemSusChem* **3**, 1237-1240 (2010)
- 116 Herrera, S., *Nature Biotechnology* **24**, 755-760 (2006).
- 117 a) Van de Vyver, S., Geboers, J., Jacobs, P. and Sels, B., *ChemCatChem* **3**, 82-94 (2011); b) Corma, A., Iborra, S. and Velty, A., *Chemical Reviews* **107**, 2411-2502 (2007); c) Wyman, C., Decker, R., Himmel, M., Brady, W., Skopec, C. and Viikari, L. *Polysaccharides*, 994-1004 (2005); d) Alonso, D., Bon, J. and Dumesic, J. *Green Chemistry* **12**, 1493-1513 (2010); e) Rinaldi, R. and Schüth, F. *ChemSusChem* **2**, 1096-1110 (2009); f) Geboers, J., Van de Vyver, S., Ooms, R., Op de Beeck, B., Jacobs, P. and Sels, B., *Catalysis Science & Technology*, 2011, DOI: 10.1039/c1cy00093d; g) Clark, J. and Deswarte, F. *Introduction to Chemicals from Biomass*, Wiley VCH, Weinheim (2008).
- 118 Huber, G., Iborra, S. and Corma, A. *Chemical Reviews* **106**, 4044-4098 (2006); Rinaldi, R. and Schüth, F. *Energy & Environmental Science* **2**, 610-626 (2009).
- 119 a) Fukuoka, A. and Dhepe, P. *Angewandte Chemie International Edition* **45**, 5161-5163 (2006); b) Geboers, J., Van de Vyver, S., Carpentier, K., de Blochouse, K., Jacobs, P. and Sels, B., *Chemical Communications* **46**, 3577-3579 (2010); c) Van de Vyver, S., Geboers, J., Dusselier, M., Schepers, H., Vosch, T., Zhang, L., Van Tendeloo, G., Jacobs, P. and Sels, B., *ChemSusChem* **3**, 698-701 (2010); d) Palkovits, R., Tajvidi, K., Procelewska, J., Rinaldi, R. and Ruppert, A., *Green Chemistry* **12**, 972-978 (2010); e) Zheng, M., Wang, A., Ji, N., Pang, J., Wang, X. and Zhang, T., *ChemSusChem* **3**, 63-66 (2010); f) Palkovits, R., Tajvidi, K., Ruppert, A. and Procelewska, J., *Chemical Communications* **47**, 576-578 (2011).
- 120 a) Balandin, A., Vasyunina, N., Chepigo, S. and Barysheva, G., *Doklady Akademii Nauk SSSR* **128**, 941-944 (1959); b) Sharkow, I., *Angewandte Chemie International Edition* **2**, 405-409 (1963).
- 121 Sabadie, J., Barthomeuf, D., Charcosset, H. and Descotes, G., *Bulletin de la Société Chimique de France* **7-8**, 288-292 (1981).
- 122 Jacobs, P. and Hinnekens, H. (Synfina-Oleofina), **EP 0329923** (1989).
- 123 Geboers, J., Van de Vyver, S., Carpentier, K., Jacobs, P. and Sels, B., *Chemical Communications* **47**, 5590-5592 (2011).

- 124 Huber, G. and Corma, A., *Angewandte Chemie International Edition* **46**, 7184-7201 (2007).
- 125 Jae, J., Tompsett, G., Foster, A., Hammond, K., Auerbach, S., Lobo, R., and Huber, G., *Journal of Catalysis* **279**, 257-268 (2011).
- 126 Sels, B. F., D'Hondt, E. & Jacobs, P. A. in *Catalysis for Renewables* (eds Centi, G. & van Santen, R. A.) Ch. 11, 223-256 (2007).
- 127 Taarning, E., Osmundsen, C. M., Yang, X.; Voss, B., Andersen, S. I. & Christensen, C. H. Zeolite-catalyzed biomass conversion to fuels and chemicals. *Energy & Environmental Science* **4**, 793-804 (2011).
- 128 Pagliaro, M., Ciriminna, R., Kimura, H., Rossi, M. & Della Pina, C. From Glycerol to Value-Added Products. *Angewandte Chemie International Edition* **46**, 4434-4440 (2007).
- 129 Katryniok, B., Paul, S., Capron, M. & Dumeignil, F. Towards the Sustainable Production of Acrolein by Glycerol Dehydration. *ChemSusChem* **2**, 719-730 (2009).
- 130 Corma, A., Huber, G. W., Sauvanaud, L. & O'Connor, P. Biomass to chemicals: Catalytic conversion of glycerol/water mixtures into acrolein, reaction network. *Journal of Catalysis* **257**, 163-171 (2008).
- 131 Nakagawa, Y. & Tomishige, K. Heterogeneous catalysis of the glycerol hydrogenolysis. *Catalysis Science & Technology* **1**, 179-190 (2011).
- 132 D'Hondt, E., Van de Vyver, S., Sels, B. F. & Jacobs, P. A. Catalytic glycerol conversion into 1,2-propanediol in absence of added hydrogen. *Chemical Communications* 6011-6012 (2008).
- 133 Van de Vyver, S., D'Hondt, E., Sels, B. F. & Jacobs, P. A. Preparation of Pt on NaY Zeolite Catalysts for Conversion of Glycerol into 1,2-Propanediol. *Studies in Surface Science and Catalysis* **175**, 771-774 (2010).
- 134 a) Hastert, R.C. In *Introduction to Fats and Oils Technology* Ed Wan, P.J.; AOCS press: Illinois (1991). b) Hastert, R.C. In *Bailey's Industrial Oil & Fat Products 5th edition* Ed Hui, Y.H.; John Wiley & Sons, Inc.: New York (1996).
- 135 a) Clifton, P.M., Keogh, J.B., Noakes, M. Trans fatty acids in adipose tissue and the food supply are associated with myocardial infarction. *Journal of Nutrition* **134**, 874-879 (2004); b) Mozaffarian, D., Katan, M.B., Ascherio, A., Stampfer, M.J., Willett, W.C. Medical progress: Trans fatty acids and cardiovascular diseases. *New England Journal of Medicine* **354**, 1601-1613 (2006).
- 136 Philippaerts, A., Paulussen, S., Turner, S., Lebedev, O.I., Van Tendeloo, G., Poelman, H., Bulut, M., De Clippel, F., Smeets, P., Sels, B., Jacobs, P., Selectivity in sorption and hydrogenation of methyl oleate and elaidate on MFI zeolites. *Journal of Catalysis* **270**, 172-184 (2010).
- 137 Philippaerts, A., Paulussen, S., Breesch, A., Turner, S., Lebedev, O.I., Van Tendeloo, G., Sels, B., Jacobs, P., Unprecedented shape selectivity in

- hydrogenation of triacylglycerol molecules with Pt/ZSM-5 zeolite. *Angewandte Chemie International Edition* **50**, 3947-3949 (2011).
- 138 Philippaerts, A., Breesch, A., De Cremer, G., Kayaert, P., Hofkens, J., Van den Mooter, G., Jacobs, P., Sels, B., Physical properties of nutritive shortenings produced from regioselective hardening of soybean oil with Pt containing zeolite. *Journal of the American Oil Chemists' Society* (2011) (accepted).
- 139 a) Bradley, T.F., US 2 350 583 (1944); b) Sleeter, R.T., US 5719301 (1998).
- 140 Lu, Y., Larock, R.C., *ChemSusChem* **2**, 136-147 (2009).
- 141 a) Bhattacharya, A., Banu, J., Rahman, M., Causey, J., Fernandes, G., Biological effects of conjugated linoleic acids in health and disease. *Journal of Nutritional Biochemistry* **17**, 789-810 (2006); b) Pariza, M. W., Park, Y., Cook, M. E., The biological active isomers of conjugated linoleic acids. *Progress in Lipid Research* **40**, 283-298 (2001).
- 142 a) Coakley, M., Johnson, M.C., McGrath, E., Rahman, S., Ross, R.P., Fitzgerald, G.F., Devery, R., Stanton, C., Intestinal bifidobacteria that produce trans-9,trans-11 conjugated linoleic acid: a fatty acid with antiproliferative activity against human colon SW480 and HT-29 cancer cells. *Nutrition and Cancer* **56**, 95-102 (2006); b) Lee, Y., Vanden Heuvel, J.P., J. *Journal of Nutritional Biochemistry* **21**, 490-497 (2010); c) J. Ecker, G. Liebisch, W. Patsch, G. Schmitz, *Biochemical and Biophysical Research Communications* **388**, 660-666 (2009).
- 143 a) Saebo, A., Skarie, C., Jerome, D., Haroldsson, G., US 6 410 761 B1 (2002); b) Westfechtel, A., Albiez, W., Zander, L., Horlacher, P., US 2006/0106238 A1 (2006).
- 144 a) Radlove, S.B., DeJong, W., Falkenburg, L., A continuous process for the dehydration of castor oil. *Journal of the American Oil Chemists' Society* **25**, 268-271 (1948); b) Terrill, R.L., Dehydration of castor oil. *Journal of the American Oil Chemists' Society* **27**, 477-481 (1950).
- 145 Philippaerts, A., Goossens, S., Jacobs, P., Sels, B. Catalytic production of conjugated fatty acids and oils, *ChemSusChem* (2011) (accepted).
- 146 Philippaerts, A., Goossens, S., Vermandel W., Tromp, M., Turner, S., Geboers, J., Van Tendeloo, G., Jacobs, P., Sels, B., Design of Ru zeolites for hydrogen-free production of conjugated linoleic acids, *ChemSusChem*, DOI 10.1002/cssc.201100015 (2011).
- 147 a) Verdonck, J.J., Jacobs, P.A., Redox behaviour of transition metal ions in zeolites. *J.C.S. Faraday I* **76**, 403-416 (1980); b) Chen, Y.W., Wang, H.T., Goodwin, J.G., Effects of preparation methods on the catalytic properties of zeolite supported ruthenium in the Fischer-Tropsch synthesis. *Journal of Catalysis* **83**, 415-427 (1983).
- 148 Kinsman, D.V., Branched-chain fatty acids. In *Fatty acids in industry*, eds. Johnson, R.W., Fritz, E., Dekker, M., New York (USA), pp. 233-276 (1989).

- 149 Biermann, U., Metzger, J. O., Synthesis of alkyl-branched fatty acids. *European Journal of Lipid Science and Technology* **110**, 805-811 (2008).
- 150 Ngo, H.L., Nunez, A., Lin, W., Foglia, T.A., Zeolite-catalyzed isomerisation of oleic acid to branched-chain isomers, *European Journal of Lipid Science and Technology* **108**, 214-224 (2007).

Perspectives for zeolite chemistry and catalysis

Takashi TATSUMI*

Tokyo Institute of Technology, Yokohama 226-8503, Japan

Abstract

Over the past three decades, versatile approaches to the synthesis of zeolites have been taken, leading to discoveries of a great many new synthetic zeolites. Some of them have unique pore structures that make them promising for serving as catalysts. To bring these zeolites into practical use as catalysts, facile methods for synthesizing the zeolites need to be devised. Metals other than aluminum can be inserted into the zeolite framework, giving a group of materials named metallosilicates. Striking developments have been attained in the oxidation catalysis exhibited by isolated titanium atoms incorporated into the zeolite framework.

1. Designing Pore Structures

1.1 Diversity of zeolite pore structures

Zeolites and related microporous materials offers the abundant chemical diversity to the porous solids. Over the past four decades, a great many new synthetic zeolites have been discovered. The Structure Commission of International Zeolite Association has approved 197 framework types as of March 2011. In addition, there are numerous other zeolites whose structure is not yet known or only hypothetical. The availability of a great number of these synthetic zeolites has greatly expanded the realm of shape selectivity in catalytic transformation and sorption accumulation since the diameter of the channels and cavities are different depending on the structure. Furthermore, it is possible to make alterations in the pore size of zeolites by their modification. Pore size engineering can be achieved by a number of modification techniques such as (1) modification by a preadsorption of molecules, (2) modification by a cation exchange, (3) internal pore modification, and (4) pore opening size modification; however, these researches are rather conventional, and hence will not be discussed here.

The use of organic structure-directing agents (SDAs) has been the primary strategy for discovering new zeolites. Since the first report on the use of methylammonium cations by Barrer and Denny¹, an enormous variety of organic SDAs has been utilized for synthesizing zeolites, which led to the discovery of a large number of

new zeolite structures. Because restrictions as to the molecular size are imposed by conventional zeolites, there has been a continued interest in the synthesis of extra-large pore zeolites that can be used for the manufacturing of fine chemicals such as pharmaceutical intermediates, fragrance, and organic electronic materials and as well as for conversions of heavy oil fractions. The size, geometry, rigidity, hydrophobicity, and stability of SDAs are very important factors that dominate the crystallization of zeolite structures. SDAs that are spherical in shape and relatively small tend towards small cages and nonporous clathrasils. SDAs of diquaternary ammonium cations connected by a linear chain often form monodimensional (1-D) channel zeolites, because these molecules are quite flexible. SDAs provided with rigidity have been found to be suitable for giving large-pore multidimensional frameworks. This type of complex molecule is not simply obtained from easily available amines. By using a polycyclic rigid SDA, *N,N,N',N'*-tetraethylbicyclo[2.2.2]oct-7-ene-2,3:5,6-dipyrrolidinium cation (Figure 1) synthesized through a multistep procedure including a Diels-Alder reaction, MCM-68 (MSE) was prepared; it is the first zeolite that has an intersecting 12 x 10 x 10 membered-ring (MR) channel system².

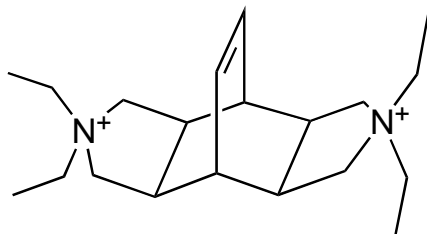


Figure 1. *N,N,N',N'*-tetraethylbicyclo[2.2.2]oct-7-ene-2,3:5,6-dipyrrolidinium cation.

Zones *et al.* used SDAs derived from nitriles. For instance, the use of [1-(4-fluorophenyl)cyclopentylmethyl]trimethyl ammonium cation led to a new high silica zeolite SSZ-53 (SFH)³, which possesses extra-large 14-MR pores in spite of a 1-D channel system.

Other organic reactions such as reductive amination of ketones, amination of acyl halids, and the Beckmann rearrangement as well as the simple alkylation of amines have been utilized for producing new zeolites. Although these complex organic molecules are highly effective in making novel and interesting zeolite frameworks, their cost may hamper them from being used as commercial catalyst. The challenge is to synthesize these zeolites with inexpensive and easily available SDAs.

Other primary approaches for discovering new zeolite materials include extension to phosphate materials, the use of fluoride as a mineralizer instead of hydroxide,

dry gel conversion⁴ (*vide infra*), isomorphous substitution of other heteroatoms for trivalent aluminium, *etc.* Recently, Corma adopted a strategy of using germanium that stabilizes the double 4-ring (D4R)⁵, to synthesize a large number of new frameworks with multidimensional large and extra-large pores. Because the presence of Ge in a framework reduces the stability of zeolite structures, it is highly desirable to solve the challenge to synthesize these new structures without germanium.

1.2 Delamination and interlayer expansion

Zeolites are three-dimensional (3-D) crystalline materials containing tetrahedral framework atoms, while clays are two-dimensional (2-D) materials containing both tetrahedral and octahedral atoms. The 2-D building units can be regarded as layers that are aligned along the third dimension by ionic or hydrogen bonds. About four decades ago, researchers found that the interlayer inorganic cations of smectite clays were replaceable with oligomeric polycations^{6,7}. Upon calcination, the cations are converted to oxide pillars such as alumina, titania and zirconia, which keep the layers separated from each other to build 3-D interlayer microporous network structures.

There are a family of zeolites whose structures can be regarded as being built from layers of tetrahedral silicates. These layers are fully connected with Si-O or Al-O bonds in the third dimension. However, just after a hydrothermal synthesis a zeolite precursor is sometimes found, which consists of the stacking of the zeolite layers without being connected by covalent bonds. This type of precursor can be transformed into a zeolite by the topotactic dehydration-condensation of silanols on both sides of the interlayers. Early reports were given on the structural transformation of layered precursors PREFER⁸ and MCM-22(P)⁹ into ferrierite (**FER**) and MCM-22 (**MWW**), respectively.

The layered precursor of **MWW** zeolite MCM-22(P) can be swollen, exfoliated and pillared under suitable conditions. In 1993, Kresge and Roth successfully synthesized MCM-36, a catalytically active material with a high surface area, by swelling the MCM-22(P) with tetrapropylammonium hydroxide (TPAOH) and cetyltrimethylammonium chloride (CTMACl) in base conditions followed by pillaring with silica species, *e.g.*, TEOS¹⁰. Subsequently, Corma *et al.* successfully synthesized delaminated zeolite material, ITQ-2, by swelling MCM-22(P) with cetyltrimethylammonium bromide (CTMABr) and delaminating the **MWW** precursor by a simple ultrasonic treatment¹¹⁻¹³. *Figure 2* shows a scheme for the preparation of the different materials obtained from the MCM-22(P)¹². In this way, the solid thin sheets (approximately 2.5 nm high) with an extremely high external surface area (> 700 m²/g) were produced. These sheets consist of a hexagonal array of cups that penetrate into the sheet from both sides. These cups have an aperture

of approximately 0.7 nm, formed by a 12-member ring (12 MR). ITQ-2 showed greatly enhanced activities in acid-catalyzed reactions of large molecules¹²⁻¹⁴, e.g., alkylation of biphenyl with propylene as well as cracking of *n*-decane and gas oil in comparison with MCM-36 and MCM-22. This is due to the much higher well defined external surface area, *i.e.* a larger number of cups present in the ITQ-2 structure, which in turn gives a larger amount of structurally accessible acid sites.

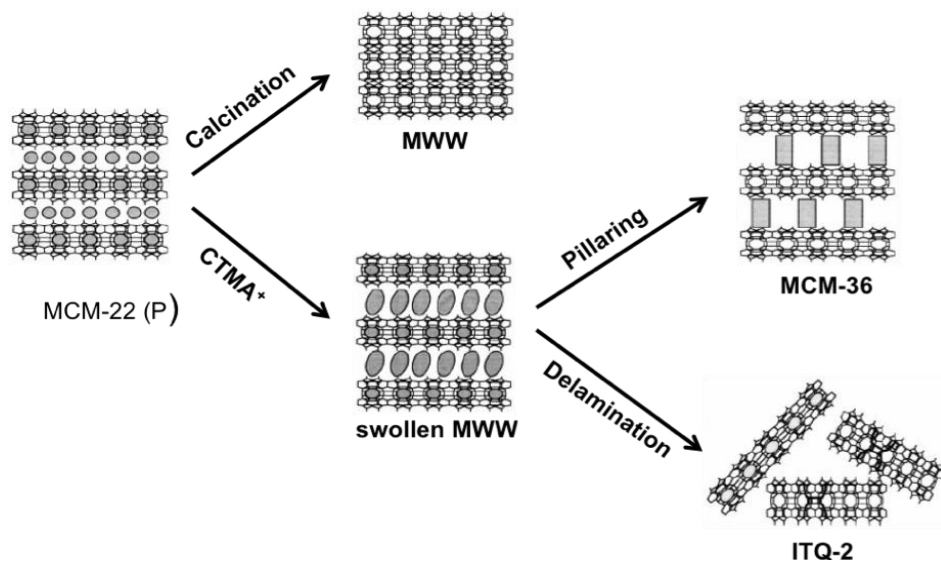


Figure 2. Scheme for the preparation of various materials from the MWW-type zeolite precursor MCM-22 (P) (Ref. 12).

On the other hand, when used for alkylation of toluene, ITQ-2 showed a poor *p*-xylene selectivity in contrast to MCM-22, which showed a moderate selectivity to *p*-xylene¹⁵. By selectively poisoning the acid sites on the external surface of ITQ-2 and MCM-22 with 2,4,6-trimethylpyridine, the *p*-xylene selectivity was remarkably increased. Thus it is implied that the external surface of MWW-type zeolites showed nonselective alkylation of toluene with methanol. It is noteworthy that Ryoo *et al.* recently prepared zeolite nanosheets through a completely different approach¹⁶; MFI zeolite nanosheets were directly hydrothermally synthesized using an organic surfactant functionalized with a diquaternary ammonium group in the head that acts as SDA.

Mochizuki *et al.*¹⁷ developed a novel methodology for constructing ordered silica nanostructures with 2-D and 3-D networks. The method involves silylation of a

layered silicate octosilicates with alkoxytrichlorosilanes and subsequent reaction within the interlayer spaces.

We have applied a similar strategies to layered zeolite precursors to obtain crystalline microporous materials, which were named interlayer expanded zeolites (IEZ)¹⁸. Treatment of the zeolitic layered precursor of Al-MWW (MCM-22(P)) with diethoxydimethylsilane (DEDMS) in acid media gave an aluminosilicate-type interlayer-expanded zeolite MWW (Al-IEZ-MWW) with expanded 12-MR micropores (Figure 3). By the interlayer-silylation of Al-MWW(P), the micropore diameter of interlayers with 12-MR supercages enlarged from ca. 7.0 to 8.0 Å, verifying the formation of the interlayer-expanded structure. Thus prepared Al-IEZ-MWW serves as a useful acid catalyst for large molecules, *e.g.*, the Friedel-Crafts acylation of anisole with acetic anhydride¹⁹, and the Beckmann rearrangement of cyclohexanone oxime¹⁸, being superior to Al-MWW with only 10-MR micropores. Vapor-phase silylation and two-step silylation techniques have been found to be effective in carrying out the interlayer-expansion with the framework Al content well retained^{19,20}. Since catalytic reactions of cyclic or substituted-aromatic compounds are considered to require ample reaction space, the activity improvement of IEZ catalysts should be contributed by the enlarged micropores between the layers via the interlayer-silylation. Moreover, Ti and Ga-containing IEZ-MWW oxidation catalysts showed much higher conversion and turnover number in the cyclohexane oxidation with H₂O₂ and Baeyer-Villiger oxidation of cyclohexanone with H₂O₂, respectively¹⁸.

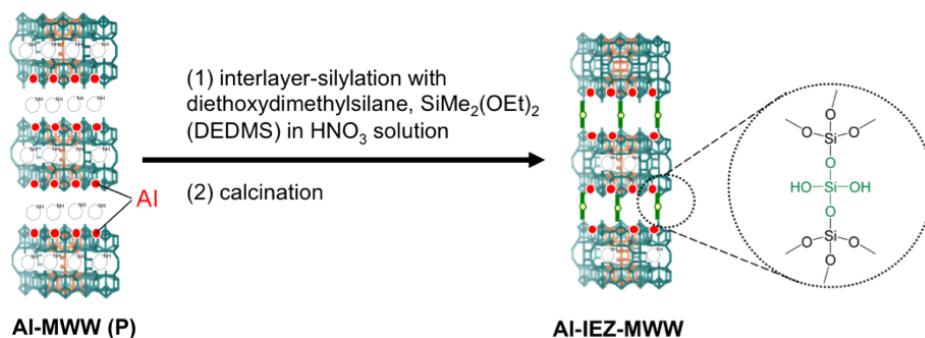


Figure 3. Formation of interlayer-expanded zeolite (IEZ) of Al-MWW as an example.

This novel methodology for preparing IEZ materials can be widely applied to various layered zeolitic precursors such as MWW(P), PREFER, PLS-1 and MCM-47 in addition to MWW(P)¹⁸. The interlayer-expanded zeolite materials are

constructed as a result of insertion of monomeric silica sources forming Si-O-Si linkage between the layers, proven by detailed characterization by using a variety of analytical techniques. HR-TEM observation of interlayer-expanded zeolite FER (IEZ-FER)²¹ indicated the formation of two adjacent 5-MRs between the FER layers, probably due to the insertion of monomeric silica species between the layers to give Si(OH)₂(OSi)₂ moieties and the following condensation of two nearest Si(OH)₂(OSi)₂ moieties each other to give (SiO)₃(HO)Si-O-Si(OH)(SiO)₃ linkages.

Recently, using dichlorodimethylsilane (DCDMS) as a silylating agent, the hydrous layered silicate RUB-39 (**RRO**) was converted to interlayer expanded zeolites COE-1 and COE-2, in methyl-group carrying as-made and oxidized calcined forms, respectively²². An intersecting 2-D channel system of 10- and 12-MR dimension is formed. The interlayer-expanded silicate framework does not exhibit a simple IEZ-**RRO** structure, but suffers from stacking disorder. The COE-1 and COE-2 materials are composed of two framework realizations, one of which is pure IEZ-**RRO** and the other of which is intergrown IEZ-1**RRO**/9**HEU** (IEZ-**HEU** 10% intergrown with IEZ-**RRO**) in the mass ratio of 2:1.

The as-made materials with the organic groups retained are considered to be novel microporous organic-inorganic nanocomposites that enable us to control the porosity and surface properties. We reported the interlayer silylation of pure silica PLS-1 with DCDMS under the acidic conditions to give a novel organic-inorganic hybrid zeolite IEZ (interlayer-expanded zeolite)-1²³. Benzene molecules were adsorbed into the hydrophobic micropores of IEZ-1, in the interlayer 10-MR apertures of which the methyl groups derived from DCDMS were retained. In contrast, purely inorganic analogue IEZ-2 having geminal silanol groups, obtained by the calcination of IEZ-1, hardly adsorbed benzene. Here, selectivity in adsorption seems to be not due to size exclusion but to the hydrophobicity/hydrophilicity of the aperture admitting the molecules to the channel. Corma *et al.* have successfully synthesized novel layered zeolitic organic-inorganic materials (**MWW**-BTEB) by intercalation and stabilization of aryl silsesquioxane molecules between inorganic zeolitic **MWW** layers²⁴. The resultant **MWW**-BTEB materials can act as bifunctional catalysts for performing a two-step cascade reaction that involves the catalytic conversion of benzaldehyde dimethylacetal into benzylidene malononitrile.

1.3 Hierarchical zeolites

Much research has been carried out to prepare zeolites with hierarchical structures. Pore openings of zeolites as microporous materials limit their applications to large molecules. Since the discovery by Mobil researchers²⁵ and Kuroda and his co-workers²⁶, mesoporous molecular sieves with size-tunable mesopores have been well developed and have attracted a great deal of attention because of their

controllable structures and compositions, which make them suitable for a wide range of applications in catalysis, adsorption, separation, chromatography, etc. Note that mesoporous materials can be targeted for bulky molecules that cannot enter micropores of zeolites. However, unlike zeolites, the wall of mesopores is amorphous, not crystalline. Consequently, acidity of mesoporous aluminosilicates is weaker than that of acidic zeolites. Therefore, mesoporous aluminosilicates cannot exhibit the spectacular catalytic properties unlike acidic zeolites. Moreover, their hydrothermal stability is low and their industrial use as catalysts is rather limited to date.

To overcome the diffusion problems that badly affect the performance of zeolite catalysts, various strategies, including a decrease in the particle size and the creation of additional meso/macro-porosities, have been successfully pursued, and the outcomes are summarized in excellent review papers²⁷⁻²⁹. Here developments of hierarchical micro- and mesoporous aluminosilicates as acid catalysts are featured.

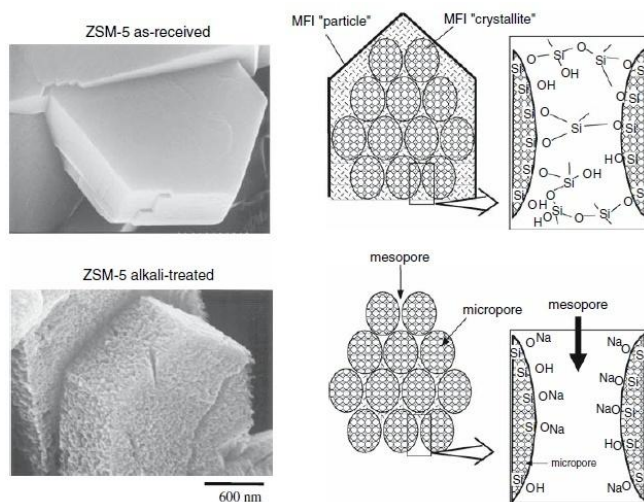


Figure 4. Schematic diagram of dissolution of ZSM-5 by NaOH aqueous solution. (Ref. 29)

Zeolites dissolve in a highly concentrated aqueous NaOH solution. The controlled alkaline treatment of zeolite leads to the formation of mesopores inside the crystal as well as desilication³⁰. The amount of adsorbed nitrogen at a relatively low pressure was not significantly changed, indicating that the microporous structure remains through the process of alkali treatment. Figure 4 illustrates a schematic diagram of dissolution of ZSM-5 by an aqueous solution of NaOH²⁹. Catalytic activities of the parent ZSM-5 and the ZSM-5 samples alkali-treated with the

treatment time varied were examined for cumene cracking investigated²⁹. The alkali-treated ZSM-5 sample treated for 300 min exhibited a conversion 1.5 times as high as the parent ZSM-5. Ogura *et al.* claimed that alkali post-treatment does not lead to stronger acidity but leads to a greater degree of diffusivity inside the zeolite crystal, providing easier access to the microporous entrance via the mesopores created by the treatment^{29,31}.

Jansen *et al.* first reported the preparation of a composite consisting of a mesoporous molecular sieve with interporous tectosilicate, designated as porous nanocrystalline aluminosilicate (PNA)³². PNA-1 and PNA-2 were synthesized through partial recrystallization of the interporous aluminosilicate surface of MCM-41 and HMS by ion-exchanged tetrapropylammonium (TPA) template, respectively.

Catalytic activities of PNAs and parent mesoporous materials in cumene cracking were investigated. Considering that cumene conversions over the four mesoporous aluminosilicates are not diffusion-limited, the enhanced cumene conversion over the PNAs is ascribed to enhanced Brønsted acidity, which is also reflected by the initial *n*-hexane cracking activity of the PNAs that is about four times as high as that of the MCM-41 and HMS materials. The PNAs showed no significant deactivation during 3 h on stream in the cumene reaction. This type of approach based on the nucleation of a zeolite building unit on the wall of mesoporous materials was extensively investigated because this enabled us to obtain the composite materials that possess the characteristics of both zeolite and mesoporous materials. Pinnavaia *et al.* reported the preparation of the mesoporous composites of the **FAU**-, **MFI** and **BEA**-type zeolites by assembling zeolite seeds, and their enhanced activities for acid-catalyzed reactions³³⁻³⁵.

Creation of intracrystalline mesoporosity during the synthesis of zeolites is an effective way to obtain hierarchical zeolites; the crystallization is performed in the presence of a removable nanostructured template such as carbon particles and polymer beads^{36,37}. These templating methods exert much better control of the pore size than conventional steaming and chemical leaching approaches to the formation of mesopores in zeolites. In general, however, such particle templates typically afford average pore sizes that are too large (> 10 nm) and pore size distributions that are too broad (>10 nm widths at half maximum) to attain high product selectivity in catalytic cracking reactions.

Wang and Pinnavaia reported the preparation of the **MFI** zeolite with small and uniform intracrystal mesopores³⁸; the nucleation of ZSM-5 in the presence of silylated polyethylenimine polymers produced the composite crystals that contain phase-segregated polymer. Calcination of the crystals resulted in zeolites with uniform intracrystal mesopores smaller than 10 nm, which were ideally suited for size-selective catalytic conversions of large molecules.

Sakthivel *et al.* showed a novel route to the synthesis of mesoporous molecular sieves with microporous characteristics, namely replicated mesoporous aluminosilicate molecular sieves RMM-1 and RMM-3, which are respectively replicated from carbon mesoporous molecular sieves CMK-1 and CMK-3, by using precursors of ZSM-5 zeolite³⁹. They proved to exhibit mesoporous structures analogous to Al-MCM-48 and Al-SBA-15, respectively, but possess unique microporous characteristics attributed to the presence of zeolite secondary building units in the framework.

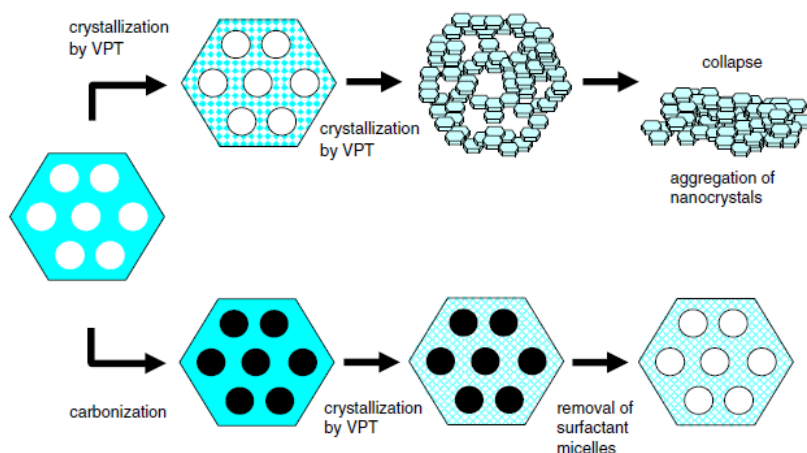


Figure 5. Formation of composite material using VPT method with the help of carbon filling inside mesopores (Ref. 29).

Ogura *et al.* have opened a unique route to the synthesis of mesoporous materials with zeolitic characteristics⁴⁰. The synthesis was based on the solid rearrangement process inside the framework of mesoporous aluminosilicate, Al-SBA-15, using a vapor phase transport (VPT) method⁴. The synthesis of this material consists of the following steps (Figure 5)²⁹: 1. Preparation of mesoporous material, SBA-15; 2. Introduction of Al on the mesopore surface; 3. Filling of carbon inside the mesopores; and 4. VPT for zeolitization. The Al-SBA-15/carbon composite was crystallized in the presence of the vapor of the structure directing agent (SDA) consisting of ethylenediamine and triethylamine. In this process, the nucleation is limited to the walls of the mesopores. Consequently, the formation of a physical mixture of zeolite and Al-SBA-15 was suppressed. Furthermore, the carbon component introduced into the mesopores acts as a “filler” to restrain the collapse of the mesostructure. If the carbon filler was absent, a typical aggregation of the zeolite was formed. The calcined products are designated as zeolitic mesoporous

material (ZMM-1). Although the XRD pattern of the calcined ZMM-1 showed no diffraction peaks in the 2θ range of $5 - 40^\circ$ ascribed to zeolite crystal, the FT-IR spectrum of ZMM-1 displayed an intense peak at 560 cm^{-1} , which is attributed to the absorption band of the five-membered rings in ZSM-5 framework. These results suggest that ZMM-1 has a zeolitic primary or secondary building unit.

The activation energy of cumene cracking on ZMM-1 was half of that on amorphous Al-SBA-15 and the value was apparently close to that on crystalline ZSM-5. These results implied that the active site, acidity in this case, was generated on ZMM-1, whose character was close to that on ZSM-5. Triisopropylbenzenes (TIPB) is more bulky than cumene, and too large to enter into 10MR channels of ZSM-5, resulting in the low conversion and full selectivity to diisopropylbenzenes (DIPBs). The conversion on ZMM-1 was much higher and cumene, the secondary cracked product of TIPB, was observed in the products.

A cationic polymer has been used as template for preparing hierarchical zeolites⁴¹. A hierarchical mesoporous beta zeolite was crystallized in the presence of tetraethylammonium hydroxide (TEAOH) and a mesoscale cationic polymer, polydiallyldimethylammonium chloride (PDADMAC) with a molecular weight of $1 \times 10^5 - 1 \times 10^6$. The SEM images of the calcined sample revealed the presence of almost uniform particles about 600 nm in size. Furthermore, the SEM and TEM images under high magnification clearly exhibited a hierarchical mesoporosity in the range of $5 - 40\text{ nm}$. The formation of the hierarchical mesoporosity is attributed to the aggregation of the cationic polymer PDADMAC. The cationic polymers could effectively interact with negatively charged inorganic silica species in alkaline media, resulting in the hierarchical mesoporosity. Various beta zeolites thus obtained were used for the alkylation of benzene with propan-2-ol as a model catalytic reaction. The hierarchical mesoporous beta zeolite showed a high activity and selectivity as well as a long catalyst life compared with conventional beta zeolites. The synthesis of hierarchical mesoporous zeolites is not limited to the beta variety; hierarchical mesoporous ZSM-5 zeolites were obtained using a mixture of tetrapropylammonium hydroxide and dimethyldiallyl ammonium chloride acrylamide copolymer.

The combination of zeolite-structure directing agents and meso-structure directing agents can be useful for preparing hierarchical zeolite. Ryoo *et al.* newly designed amphiphilic surfactant molecules with different chain lengths, $[(\text{CH}_3\text{O})_3\text{SiC}_3\text{H}_6\text{N}(\text{CH}_3)_2\text{C}_n\text{H}_{2n+1}]\text{Cl}$, $n = 12-18$, which contain a surfactant-like long-chain alkylammonium moiety and a hydrolysable methoxysilyl group, linked together by a Si-C bond, which is chemically stable under various zeolite synthesis conditions⁴². Consequently, mesoporous ZSM-5 and LTA with tunable mesopores have been successfully synthesized. The size of mesopore can be finely tuned in the range of $2 - 20\text{ nm}$, depending on the molecular structure of the mesopore-directing

silanes and the hydrothermal synthesis conditions. The NH₃-TPD profiles indicated that the mesoporous ZSM-5 (H⁺ form, Si/Al = 20) possessed strong acid sites, similar to a typical ZSM-5. The seed-assembled mesoporous (SAM) ZSM-5 material³⁴ showed a slightly high acidity compared with Al-MCM-41, but its acidity was still much weaker than this mesoporous ZSM-5 zeolite and a typical ZSM-5. This acidity difference was confirmed by the transformation of methanol to olefin/gasoline; the mesoporous ZSM-5 and typical ZSM-5 were similarly active (86 versus 90% conversion), while Al-MCM-41 and SAM exhibited no measurable catalytic conversion. From these results, Ryoo *et al.* claimed that the SAM possessing only a short-range atomic order ('pseudozeolitic' or 'protozeolite') cannot exhibit the true zeolite-like strong acidity. The catalytic properties for the reactions involving large organic molecules were also investigated. As expected, the mesoporous ZSM-5 also exhibited an outstanding catalytic activity in the synthesis of jasminaldehyde (α -*n*-amylcinnamaldehyde) and vesidryl (2',4,4'-trimethoxychalcone) compared to typical ZSM-5, Al-MCM-41 and SAM.

2. Development of facile methods of synthesizing zeolites

2.1 Cutback in organic SDA usage and SDA-free synthesis

While organic SDAs are highly competent in affording new and interesting zeolite structures, their cost may be too high for them to be used as commercial catalysts. The challenge is to find ways to prepare these zeolites with cheaper SDAs or less amount of SDAs. The organic SDAs ultimately fill the pore space in zeolite, and removal of these enclathrated species normally requires high temperature combustion that destroys this expensive component. Furthermore, the associated heat generation in combination with the formed water can be detrimental to the zeolite structure. Takewaki *et al.* reported that tertaethylammonium (TEA) cation can be easily extracted with acetic acid from zincosilicate CIT-6 that has the *BEA-type structure because the interaction between TEA⁺ and CIT-6 framework is weak⁴³. In contrast, most TEA cations in the Al-containing CIT-6 strongly interact with the Si-O-Al linkage. Lee *et al.* established a new methodology for completely recycling the organic SDAs in the synthesis of ZSM-5⁴⁴. The organic SDAs they developed can be disassembled within the zeolite space to allow removal of their fragments for possible use again by reassembly.

Organic-SDA-saving or -free synthesis of zeolites has attracted much attention because such approach can not only decrease the production steps and costs but also contribute to economical and environmentally benign synthesis of advanced materials⁴⁵. There are numerous examples of organic SDA-free syntheses of zeolites such as A, X, Y, L, mordenite, ferrierite, ZSM-5, and ECR-1⁴⁶. Recently, Xiao and his co-workers succeeded in the synthesis of beta zeolite by the addition of calcined beta seeds to the starting aluminosilicate gel in the absence of any

organic-SDAs⁴⁷. It is well-known that the introduction of seeds crystals into a mother gel enhances the crystallization of zeolites. Subsequently, Majano *et al.*⁴⁸ and Kamimura *et al.*⁴⁹ also reported successful synthesis of beta zeolites by seeding routes. Beta zeolite could be synthesized by using organic SDA-free beta as seeds, named “green beta”⁴⁹, providing a basis for the establishment of a completely organic SDA-free, more environmentally benign synthesis of zeolite beta.

We have focused our attention on the improvement in the synthesis of the **RTH**-type zeolite. Discovered in 1995, The **RTH** structure consists of the **RTH** cages with the openings of 8MR and has two-dimensional channels with aperture size of 0.41 x 0.38 nm and 0.56 x 0.25 nm, which run parallel to the a-axis and the c-axis, respectively. Since its discovery, this zeolite has been expected to show unique properties in fields of catalysis and adsorption because of its unique structure. Unfortunately, only two examples on the **RTH**-type zeolites have been reported to date. One is a borosilicate zeolite, “RUB-13”, which is the first example of the **RTH**-type zeolite. This borosilicate (designated as [B]-RUB-13) can be synthesized by using the mixture of organic SDA of 1,2,2,6,6-pentamethylpiperidine [PMP] and ethylenediamine [EDA]⁵⁰. The other is “SSZ-50”, which is an aluminosilicate zeolite and will be useful as a solid-acid catalyst. Unfortunately, the synthesis of SSZ-50⁵¹ requires the special organic SDA, *N*-ethyl-*N*-methyl-5,7,7-trimethylazoniumbicyclo[4.1.1]octane cation (Figure 6), which is a commercially unavailable reagent and obtained through multiple and elaborate organic synthesis processes. The synthesis of SSZ-50 has not been remarkably advanced so far.

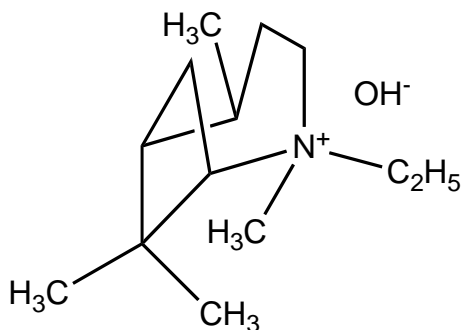


Figure 6. *N*-ethyl-*N*-methyl-5,7,7-trimethylazoniumbicyclo[4.1.1]octane cation.

As mentioned above, the original procedure for the synthesis of [B]-RUB-13 and [Al]-SSZ-50 requires the organic SDAs. From a practical viewpoint, the use of such organic-SDAs could significantly limit the industrial applications of **RTH**-type zeolites in catalytic reactions, and the drastic reduction in their amounts has

been desired. At the first trial calcined [B]-RUB-13 crystals were added as seeds into the mother gel of [B]-RUB-13 in the presence of ammonia in place of PMP and EDA. Unfortunately, this approach was unsuccessful. After intensive investigations, we succeeded in preparing the **RTH**-type zeolites without using any organic-SDAs⁵². The key points are the addition of sodium hydroxide and the molar composition of water as well as calcined [B]-RUB-13 crystals as seeds. Thus prepared **RTH**-type zeolites synthesized without any organic-templates are named “TTZ-1” (Tokyo Tech. Zeolite) series. Organic-template-free borosilicate products was crystallized with the molar ratio of Na varying in the range of 0 to 1.0 at the H₂O/Si molar ratio of 200 (seed 2 wt%). The product synthesized without adding NaOH was a mixture of amorphous silica and **RTH**-type zeolite. At the Na/Si ratio of 0.2, diffraction peaks derived from the RTH structure were observed. Hereafter, thus obtained organic-SDAs-free borosilicate with the **RTH** topology is named [B]-TTZ-1. When the ratio was increased up to 0.5, the peaks derived from both α -quartz and **RTH**-type zeolite were observed. Further increase in the ratio to 1.0 resulted in the formation of pure α -quartz. At the Na/Si molar ratio of 0.2, the effect of the molar ratio of H₂O/Si was investigated. When the ratio was increased from 200 to 300 or decreased to 100, either product was a mixture of amorphous silica and **RTH**-type zeolite. It has been clearly indicated that a pure phase of the **RTH**-type borosilicate was hydrothermally synthesized in the absence of any organic-SDAs, the optimum molar composition of the reactants being 1 SiO₂ : 0.25 H₃BO₃ : 0.2 NaOH : 200 H₂O.

For the purpose of applying **RTH**-type zeolites in catalytic reactions, a direct introduction of Al into the **RTH** framework during the crystallization of [B]-TTZ-1 in the absence of organic-SDAs was studied. The aluminosilicate ([Al,B]-TTZ-1) and gallosilicate ([Ga,B]-TTZ-1) products showed a highly crystalline **RTH** phase. Furthermore, we have developed a novel synthesis route to preparing pure aluminosilicate with an **RTH**-topology (*i.e.* SSZ-50) without using any organic-SDAs. Note that according to the original recipe for SSZ-50⁵¹, the ratio of Si/Al in the gel ranged from 15 to 65, while that in the product was not described. The synthesis procedures were similar to those for organic-SDAs-free [Al,B]-TTZ-1 except that deboronated RUB-13 crystals were used as seeds (2 wt%) in place of [B]-RUB-13 and that boric acid was not added. Thus pure aluminosilicates with an **RTH**-topology ([Al]-TTZ-1) were successfully synthesized in the absence of any organic-SDAs, although the Si/Al ratio was limited to the range of 37 to 57. The ²⁷Al MAS NMR spectrum of [Al,B]-TTZ-1 and [Al]-TTZ-1 exhibited only a sharp peak assigned to tetrahedrally coordinated aluminum in the framework. No remarkable peak assigned to octahedrally coordinated aluminum was observed.

We have found that the **RTH**-type zeolites show remarkable catalytic performance in the methanol-to-olefins (MTO) reaction. The selectivity to propene over the **RTH**-type zeolite samples was higher than those over either ZSM-5 or SAPO-34,

both of which are known to superior to other catalysts in the MTO reaction. In particular, the selectivity to propene over [Al,B]-RUB-13 reached about 47%. It is noteworthy that high conversion and selectivity over [Al,B]-RUB-13 were unchanged during the reaction time of 180 min. The selectivity to propene over SAPO-34 was found to be 41% for the reaction time of 90 min, while it was slightly decreased along with reaction time. In the case of ZSM-5, the selectivity to C4 – C6 parafines was the highest among all products at the reaction time > 60 min due to the medium pore of the **MFI**-type zeolite. These results indicate that the **RTH**-type zeolites would be a promising catalyst for the MTO reaction to selectively produce propene.

Very recently, Xial et al. have reported the seed-assisted synthesis of levine and heulandite zeolites in the absence of organic SDA⁵³. The core-shell growth mechanism in the organic SDA-free synthesis of beta has been also proposed.

2.2 Variations from the conventional hydrothermal synthesis of zeolites

In general, zeolites are synthesized under hydrothermal conditions using an amorphous aluminosilicate gel as a starting material. Sometimes the formation of a zeolite phase may be preceded with a different phase during the course of crystallization. This phenomenon could be an alternative synthesis strategy for synthesizing zeolites. Thus zeolite-zeolite transformation can be an expeditious route to obtain zeolites that cannot be easily crystallized by a conventional method. For example, Zones studied the hydrothermal conversion of P zeolite to SSZ-13⁵⁴. Zones and Nakagawa demonstrated the use of boron beta as a precursor for the synthesis of a borosilicate version of SSZ-24 and SSZ-33⁵⁵; the boron concentration of the precursor greatly affected the topology of the obtained zeolites with the same organic SDA employed. [Al]-SSZ-24 was synthesized from Al-beta⁵⁶.

Recently Sano *et al.* systematically investigated the potential of this interzeolite conversion method. Highly crystalline and pure ***BEA**⁵⁷, **RUT**⁵⁸, and **LEV**⁵⁹ zeolites were obtained from the **FAU** zeolite in the presence of various organic SDAs, which directed the crystallization of a particular phase. It was found that when the zeolite was used as the starting material, the crystallization rate was remarkably fast.

Usually, zeolites are synthesized in a reaction medium containing an aqueous phase of dissolved reagents and solid species, which could exist as gel percolates and be suspended in solution. In contrast, new methods of synthesizing zeolite starting with the solids species that are separated from the aqueous phase so as to never come in direct contact with water. These methods are generally referred to as Dry gel conversion (DGC) methods, which are classified into the vapor phase transport (VPT) and steam-assisted crystallization (SAC)⁴. The SAC method was successfully used to prepare pure-silica MCM-68 (**MSE**)⁶⁰. A dry gel containing the SDA for

MCM-68 (Figure 1) was converted to a siliceous product designated as YNU-2P, which was, however, decomposed upon calcination. In contrast, postsynthesis silylation with $\text{Si}(\text{OMe})_4$ in the presence of acid afforded YNU-2, which was thermally stable because most of the defects were eliminated by the treatment with the silylating agent.

3. Metal-Incorporated Zeolites for Oxidation Catalysis

3.1 Metal-incorporated zeolites

Although zeolites have long been used as solid acid catalysts, zeolites are also endowed with the redox property by the incorporation of a variety of metals. Incorporation of metals and the resultant oxidation catalysis are attracting growing interest.

The ways to introduce heteroatoms into zeolites are classified into two categories; heteroatoms can be introduced into framework as well as into voids as extraframework species. Most zeolites have an intrinsic ability to exchange cations. This exchange ability is a result of isomorphous substitution of a cation of trivalent (mostly Al) or lower charges for Si as a tetravalent framework cation. As a consequence of this substitution, a net negative charge develops on the framework of the zeolite, which is to be neutralized by cations present within the channels or cages that constitute the microporous part of the crystalline zeolite. These cations may be any of the metals, metal complexes or alkylammonium cations. If these cations are transition metals with redox properties, they can act as active sites for oxidation reactions. A metal complex of the appropriate dimensions can be encapsulated in a zeolite, being viewed as a bridge between homogeneous and heterogeneous systems.

The other way to introduce heterometals is their isomorphous substitution for Si in the framework, in a similar manner to the isomorphous substitution of Al. The heteroatoms should be tetrahedral (T) atoms. In hydrothermal synthesis, the type and amount of T atom, other than Si, that may be incorporated into the zeolite framework are restricted due to solubility and specific chemical behavior of the T-atom precursors in the synthesis mixture. Until the late seventies, exchangeable cations and other extraframework species had been the primary focus of the researchers.

The isomorphous substitution of Ti for Si was claimed by Taramasso et al. in 1983⁶¹. The resulting material has the structure of silicalite-1 (pure silica **MFI**) with Ti in the framework positions and named TS-1 or titanium silicalite-1. The new findings including the claim that other metals can be inserted into the zeolite lattice met with skepticism. Ione et al. predicted the probability of isomorphous substitution of metal ion (M^{n+}) and the stability of the M^{n+} position in the

tetrahedrally surrounding oxygen atoms by using the Pauling criterion⁶². Based on the ratio of ionic radii ρ of the cation and anion, the value for Ti and O ($\rho = 0.515$) falls out of the range ($\rho = 0.225 - 0.414$) for which tetrahedral coordination is expected. The allowed cation would include only Al^{3+} , Mn^{4+} , Ge^{4+} , V^{5+} , Cr^{6+} , Si^{4+} , P^{5+} , Se^{6+} , and Be^{2+} . Presumably this type of estimate is surely effective, which can explain the preference of B^{3+} for trigonal coordination and the resultant instability of B^{3+} in the zeolite matrix, although it is a very rough approximation; the completely ionic character of T-O bond is not the case and the model assumes the atoms have a perfect round shape. It has been discovered that Sn-beta catalyzes the Baeyer-Villiger oxidation of cyclic ketones to lactones without using peracids but using H_2O_2 ⁶³. Notably, this Sn-beta catalyst selectively promotes the Baeyer-Villiger oxidation when the substrate contains a carbon-carbon double bond besides the carbonyl bond. A pathway involving the activation of the carbonyl group by Sn is considered to be taken in this reaction.

The stability of metals isomorphously substituted is of great concern when metal-incorporated zeolites are used for catalytic reactions. Chromium-containing silicalite-2, CrS-2, has been synthesized and shown to catalyze oxidation reactions using TBHP as an oxidant⁶⁴. Lempers and Sheldon have reported that small amounts of chromium that are leached from CrAPO-5, CrAPO-11, and CrS-1 catalyze the liquid phase oxidation of bulky alkenes with TBHP⁶⁵. The leaching seems to be caused by TBHP that extracts chromium from the micropores. They emphasize that experiments demonstrating that heterogeneous catalysts can be recovered and recycled without apparent loss of activity is not a definite proof of heterogeneity.

3.2 Titanium-containing zeolites as catalysts for liquid phase oxidation

Here the oxidation catalysis exhibited by isolated Ti atoms incorporated into the framework of zeolites is dealt with. TS-1 proved to be a very good catalyst for liquid phase oxidation of various organic compounds using H_2O_2 as oxidant, and several industrial processes utilizing TS-1 are being operated. The success of TS-1 has encouraged the researchers to synthesize other titanosilicates with different zeolite structures, especially those with larger pores, since TS-1 encountered with a limitation of inapplicability to bulky molecules owing to the medium 10-MR pores.

A very comprehensive review was made on TS-1 and other titanium-containing molecular sieves⁶⁶. TS-1 was synthesized by the hydrothermal crystallization of a gel obtained from $\text{Si}(\text{OC}_2\text{H}_5)_4$ and $\text{Ti}(\text{OC}_2\text{H}_5)_4$ ^{61,67} (Enichem method, hereafter named **method A**). The incorporation of Ti into the framework of **MFI** structure was demonstrated by the increase in unit cell size in XRD pattern, and the appearance of tetrahedral Ti species in UV-Vis spectra. The maximum amount of

Ti that can be accommodated in the framework positions is claimed to be limited to $x = \text{Ti}/(\text{Ti} + \text{Si})$ of 0.025.

TS-1 is capable of serving as highly efficient catalysts for the oxidation of various organic substrates, *e.g.* alkanes, alkenes, alcohols and aromatics, with H_2O_2 as an oxidant under mild conditions^{68,69}. The epoxidation reaction catalyzed by TS-1 may be performed under mild conditions in dilute aqueous or methanolic solution. The active oxygen content H_2O_2 , 47 wt % (16/34), is much higher than that of organic peracids and hydroperoxides; water is an only co-product. Besides epoxidation, TS-1 catalyzes a broad range of oxidation reactions with hydrogen peroxide as oxidant shown in Table 1.

Table 1. Catalytic chemistry with TS-1

Substrate	Product
olefins	epoxides
olefins and methanol	glycol monomethyl ethers
diolefins	monoepoxides
phenol	hydroquinone and catechol
benzene	phenol
paraffins	alcohols and ketones
primary alcohols	aldehydes
secondary alcohols	ketones
ketones (plus ammonia)	oximes
N,N-dialkylamines	N,N-dialkylhydroxylamines
thioethers	sulfoxides

The catalytic property of TS-1 depends on the lattice Ti content, which is usually less than 2 wt%⁷⁰. The effective way to increase the Ti content in the framework of TS-1 is still a huge challenge. Thangaraj and Sivasanker reported that 8 Ti ions could be incorporated in the lattice sites per unit cell ($\text{Si}/\text{Ti} = \text{ca. } 10$) by an improved method (**method B**) in which titanium tetra-*n*-butoxide was first dissolved in isopropyl alcohol before addition to the hydrolyzed tetraethyl orthosilicate aqueous solution for the purpose of avoiding formation of TiO_2 precipitate by reducing the hydrolysis rate of the alkoxide⁷¹.

To synthesize Ti-rich TS-1, it is necessary and helpful to make its crystallization mechanism clear. However, very few reports have devoted to the study of this subject⁷². The crystallization process of titanosilicates is much more complex than that of aluminosilicates because Ti^{4+} has a weak structure-directing role and is much more difficult to be incorporated into the framework than Al^{3+} . Isomorphous

substitution of metal atoms for Si in zeolites is not only related to zeolite structures/framework composition flexibility and the chemical nature of metals but also strongly influenced by the crystallization mechanism. The framework composition flexibility of zeolites is chemically important. Ti K-edge EXAFS studies have shown that Ti-O bond length of tetrahedral Ti(OSi)₄ species is about 1.80 Å in contrast to 1.61 Å of Si-O bond length⁷³. The Ti-O bond is much longer than the Si-O bond, probably making the local structure around Ti seriously distorted. This results in the slow inclusion of Ti into the framework, compared to Si ions. If crystallization proceeded too fast, Ti ions would not have enough time to be incorporated into the lattice. However, too slow crystallization would possibly cause the formation of transition metal oxides, preventing metal cations from being incorporated into the framework. In addition, the difficult crystallization may also result from the strong competition between the interaction of soluble silicate ions and mother liquor and the condensation of silicate ions. Thirdly, a mismatch among hydrolysis of Ti and Si alkoxides, polymerization of Ti⁴⁺ and/or Si⁴⁺ ions, nucleation and crystal growth would lead to much difficulty in the inclusion of Ti in the framework. Since the chemical nature of Ti and the rigidity of the framework of TS-1 cannot be altered, to find an effective crystallization-mediating agent would be the sole way to increase the lattice Ti content in TS-1 by harmonizing the hydrolysis rate of Ti alkoxide with that of silicate species as well as the nucleation and crystal growth rates.

In this respect, a new route to the synthesis of TS-1 has been developed by using (NH₄)₂CO₃ as a crystallization-mediating agent (the YNU method)⁷⁴. By this method, the framework Ti content can be significantly increased without forming extraframework Ti species. The prepared catalyst has a Si/Ti ratio as low as 34, although under the same synthesis conditions the ratio of 58 was only achieved by the methods **A** and **B** established by the Enichem group⁶⁷ and Thangaraj and Sivasanker⁷¹, respectively. The YNU samples are well crystalline, containing less defect sites than the samples synthesized by the other two methods. The ²⁹Si NMR spectra indicates that the YNU-50 sample has a higher Q⁴/Q³ ratio of 23.1 than the Enichem Method A-50 sample (4.9), which indicates that more defective sites are present in the **A** samples. These defective sites reduce the hydrophobicity of the sample because they could adsorb water molecules. Higher hydrophilicity of the **A** samples than of the YNU samples is further corroborated by the fact that the weight loss below 150 °C due to the desorption of water was about 1.0 wt% for as-synthesized **A**-50 in contrast to 0.3 wt% for as-synthesized YNU-50.

Although the catalytic properties of titanosilicates are related to their crystalline structures and/or characters, the hydrophilicity caused by the presence of more defect sites in titanosilicates would be unfavorable for the oxidation of hydrocarbon reactants, as suggested by the following facts: (i) compared with TS-1, Ti-MWW and Ti-Beta with more defect sites showed very low activity for the oxidation of

hexane, styrene and benzene; (ii) Ti-MCM-41, with a low Q^4/Q^3 ratio, showed very low activity in the oxidation of hexane and 1-hexene; however, silylation resulted in a remarkable improvement in the oxidation activity⁷⁵. The YNU sample showed much higher activity for the oxidation of various organic substrates, such as linear alkanes/alkenes and alcohols, styrene and benzene than the sample A, because of their high hydrophobicity.

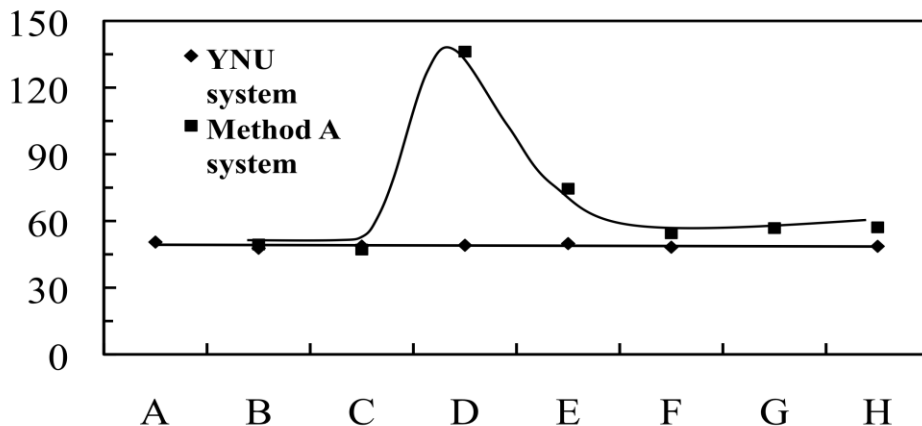
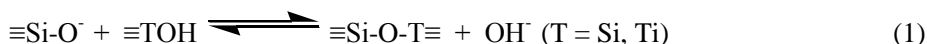


Figure 7. Dependence of the Si/Ti molar ratio of the solid fraction on the crystallization conditions in the YNU and method A systems. (A) 30 °C, 1 day; (B) 60 °C, 1 day; (C) 80 °C, 1 day; (D) 100 °C, 1 day; (E) 140 °C, 1 day; (F) 170 °C, 1 day; (G) 170 °C, 2 days; (H) 170 °C, 3 days.

Figure 7 shows the Si/Ti ratio of the solid samples collected in the whole crystallization process. The Si/Ti ratio in the solid samples synthesized in the YNU system was kept almost constant, being in the range of 48 and 50.5. This constant Si/Ti ratio is similar to that found in the synthesis of TS-1 from amorphous wetness impregnated $\text{SiO}_2\text{-TiO}_2$ xerogels and the nonaqueous synthesis of zeolites with solid reaction mixtures where solid phase transformation mechanism predominated⁷². On the other hand, the Si/Ti ratio of the samples synthesized by the method A drastically increased during the period of crystal growth; the solid samples in the induction period were directly obtained by drying the liquid at 100 °C since no solid was formed during this period. This suggests that during the period of rapid crystal growth in the method A system, silicic and/or silicate species ($\equiv\text{Si-OH}$, $\equiv\text{Si-O}^-$) were polymerized with each other at a much higher rate than the condensation of silicic or silicate species and titanate or titanate ($\equiv\text{Ti-OH}$, $\equiv\text{Ti-O}^-$) species to form TS-1 crystals. The Ti content in the solid remarkably increased after the sample reached the highest crystallinity. The crystallization in the method A

system occurred via a homogeneous nucleation mechanism although precursor aggregates might be formed before nucleation..

A very high alkaline condition would make the synthesis gel unreacted, but dissolve the silicate/titanosilicate species (eq. (1), from right to left), resulting in a lower crystallinity of the products crystallized in the method **A** system and the presence of more defect sites. In contrast, for the YNU system, the synthesis gel was quickly solidified after the addition of $(\text{NH}_4)_2\text{CO}_3$. Thus, most of TPA^+ species were embedded in the solid with the amount of free OH^- species drastically decreasing and with the pH value of the liquid lowering down. The lower the pH value, the higher the yield of crystalline material, or the more well-crystallized the product because the condensation reaction (eq. (1), from left to right) proceeds to a greater extent. This accounts for the higher crystallinity of the TS-1 samples achieved by the YNU method than by the method **A**.



The higher OH^- concentration in the method **A** system also accelerates the crystal growth. Such a high crystallization rate is not beneficial for the incorporation of Ti into the framework since this process would make the local structure around Ti distorted. In addition, the high alkalinity of the liquid is unfavorable to the condensation of Ti-OH and silicate species. In contrast, the presence of $(\text{NH}_4)_2\text{CO}_3$ appropriately slows down the crystallization rate by significantly decreasing the pH value, buffering the synthesis gel and introducing NH_4^+ , which is a structure-breaking cation in water⁷⁶, and consequently reducing the polymerization rate of silicic/silicate/titanic/titanate species. This would provide enough time for Ti species to be inserted into the lattice during the crystallization process, as indicated by the much lower Si/Ti ratio in the solid samples obtained during the crystal growth period in the YNU system than in the method **A** system.

MWW aluminosilicate (generally known as MCM-22) is hydrothermally synthesized without difficulty; however, the synthesis of **MWW** titanosilicate (Ti-MWW) has been a challenge until it was shown for the first time that Ti is effectively incorporated into the **MWW** framework when boric acid coexists in the synthesis media⁷⁷.

Since titanosilicates generally require specific synthesis conditions in comparison to silicalites and aluminosilicates, many efforts made to synthesize those of numerous zeolite structures have led to a very limited success. This has been also the case with the **MWW** zeolite. Although it is possible to hydrothermally synthesize **MWW** silicalite in alkali-free media using a specific organic SDA of trimethyladamantylammonium hydroxide, the addition of other metal cations such as Al and Ti into the synthesis gel results in failure⁷⁸. When boric acid, with its

amount even more than that of silicon, and a Ti source were co-existent in the synthesis gel composed of fumed silica and cyclic amine SDA such as hexamethylenimine (HM) or piperidine (PI), Ti-MWW was crystallized readily by autoclaving the gel at 403-443 K^{77,79}. These are designated as Ti-MWW-HM or Ti-MWW-PI.

All the as-synthesized samples of Ti-MWW-PI and Ti-MWW-HM showed the XRD patterns totally consistent with those of the lamellar precursor of **MWW** topology, generally designated as MCM-22(P)^{80,81}. Upon calcination at 803 K, all the samples were converted to the porous three-dimensional (3D) **MWW** structure with good quality. The amount of B incorporated into the products was in the Si/B range of 11 to 13, far lower than that in the gel of the Si/B ratio of 0.75. In contrast, there was little difference in the Si/Ti ratios between the gel and the solid product except for the gel of Si/Ti=100, indicating that the synthesis system is very effective for Ti incorporation.

The UV-visible spectra of Ti-MWW-PI without calcination are quite different from those reported for TS-1 and Ti-Beta that generally show only a narrow band around 210 nm. Irrespective of the Si/Ti ratio and the SDA used, all as-synthesized Ti-MWW samples exhibited a main band at 260 nm together with a weak shoulder around 220 nm. The 220 nm band, resulting from the charge transfer from O²⁻ to Ti⁴⁺, has been widely observed for Ti-substituted zeolites and is characteristic of tetrahedrally coordinated Ti highly dispersed in the framework⁶⁹. The 260 nm band has been attributed to octahedral Ti species, related to a kind of extraframework Ti species probably with Ti-O-Ti bonds in the case of Ti-Beta⁸².

The calcination process also led to a change in the nature of the Ti species; a new band around 330 nm in the UV-visible spectra is ascribed to the anatase. The anatase-type Ti species are not active and may cause unproductive decomposition of the oxidant H₂O₂ when employed as an oxidation catalyst. Once octahedral Ti species are converted to anatase, which could not be removed by washing with a HNO₃ or H₂SO₄ solution under refluxing conditions. However, when as-synthesized Ti-MWW was first refluxed with an acid solution and then calcined, the octahedral Ti species were eliminated selectively; only the narrow band at 220 nm due to tetrahedral Ti species was observed for the samples prepared by acid-treating the precursors with the Si/Ti ratio of 100-30. Thus it should be emphasized that the pretreatment sequences are essential for obtaining Ti-MWW with tetrahedrally substituted Ti species. Together with extraframework Ti, a part of framework boron was also extracted to a level corresponding to the Si/B ratio of about 30.

Large pore titanosilicates developed after TS-1, e.g., Ti-beta, Ti-ITQ-7, Ti-MCM-41, and Ti-MCM-48, have been considered to have advantages for the oxidation of bulky alkenes because of their pore size. However, none of them is intrinsically more active than TS-1 in the reactions of small substrates that have no obvious

diffusion problem for the medium pores. Therefore, in parallel with developing large pore titanosilicates, the search for more intrinsically active ones than TS-1 is also an important research subject. The catalytic performance of Ti-MWW is compared in the oxidation of linear alkenes with H_2O_2 with that of TS-1 and Ti-beta. Consistent with the results reported elsewhere⁸²⁻⁸⁴, TS-1 showed higher conversion than Ti-beta with a similar Ti content. However, Ti-MWW exhibited activity about three times as high as TS-1 based on the specific conversion per Ti site.

3.3 Postsynthesis Ti-incorporation into zeolite framework

As described above, despite a relatively high content of boron (generally corresponding to a Si/B ratio of 30) contained in the framework, hydrothermally synthesized Ti-MWW proved to be an extremely active catalyst for alkene epoxidation. Then, B-free Ti-MWW is expected to exhibit much higher activity than B-containing Ti-MWW. Since the direct synthesis of Ti-MWW without using boric acid is still a matter of challenge, the postsynthesis is an alternative choice for the preparation of B-free catalysts. The treatment with TiCl_4 vapor at elevated temperatures has been employed for modifying zeolites of 12-MR channels^{85,86}. Actually, the preparation of Ti-MCM-22 by the reaction of dealuminated MCM-22 with TiCl_4 vapor has been patented⁸⁷. However, it is suspected that the TiCl_4 treatment method is actually ineffective for the MWW zeolite because TiCl_4 $6.7 \times 6.7 \text{ \AA}$ in molecular size is expected to suffer serious steric restriction when penetrating the 10-MR pores ($4.0 \times 5.9 \text{ \AA}$, $4.0 \times 5.4 \text{ \AA}$) of MWW and thus might give rise to uneven Ti distribution.

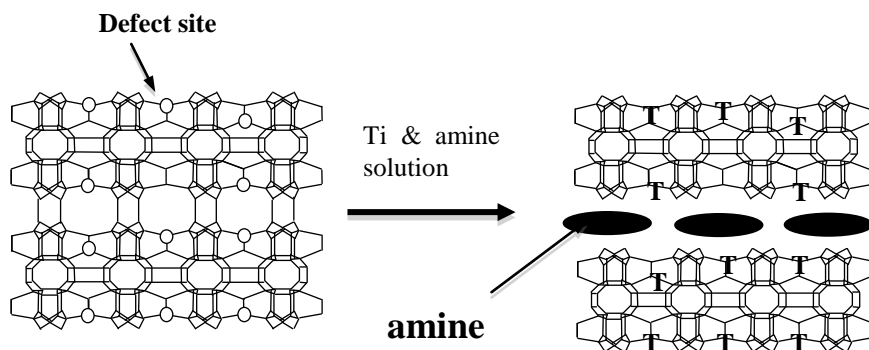


Figure 8. Reversible structural conversion from MWW to MWW(P) lamellar precursor as the method of postsynthesizing Ti-MWW.

As a totally different postsynthesis method that is firmly based on the structural characteristics of **MWW**, reversible structural conversion between 3D **MWW** silicate and its corresponding 2D lamellar precursor **MWW(P)** has been developed to construct more active Ti species within the framework⁸⁸. *Figure 8* illustrates the strategy of this postsynthesis method, “reversible structural conversion.” First, highly siliceous **MWW** is prepared from hydrothermally synthesized **MWW** borosilicate by the combination of calcination and acid treatment. Secondly, the **MWW** silicalite is treated with an aqueous solution of HM or PI and a Ti source. A Reversible structure conversion from **MWW** to the corresponding lamellar precursor occurred as a result of Si-O-Si bond hydrolysis catalyzed by OH⁻, which is supplied by basic amine molecules. This is accompanied by the intercalation of the amine molecules.

Calcination and acid treatment of the as-synthesized borosilicate **MWW(P)** removed the framework boron and simultaneously converted the lamellar precursor into a **MWW** silicate (Si/B > 500). When this deboronated **MWW** was treated with Ti(OBu)₄ (TBOT) in the presence of HM or PI, the incorporation of Ti was achieved and more interestingly, the lamellar structure was simultaneously restored. Namely, Ti species entered the interlayer space freely through the pore entrance of expanded layers to fill up the defect sites such as hydroxyl nests. Extraction of the extraframework Ti species by acid treatment followed by calcination caused the layers to dehydroxylate, resulting in B-free Ti-**MWW**. It should be noted that this structural conversion occurred only in the presence of HM or PI, the two typical SDAs for the crystallization of **MWW** zeolites, but was never caused by pyridine or piperazine although these cyclic amines have similar molecular shapes. This means that there is a “molecular recognition” of amine molecules given by the layered **MWW** sheets and that HM or PI molecules stabilize the lamellar **MWW** (P) structure (*Figure 8*).

The catalytic properties of postsynthesized PS-Ti-**MWW** were compared with directly hydrothermally synthesized HTS-Ti-**MWW** and TS-1 in the epoxidation of 1-hexene with H₂O₂ (*Figure 9*). HTS-Ti-**MWW** showed an intrinsic activity several times as high as TS-1 for 1-hexene. PS-Ti-**MWW** further proved to be about 2 times as active as HTS-Ti-**MWW**. The efficiency of H₂O₂ utilization was also very high on PS-Ti-**MWW**. Thus in terms of the activity, epoxide selectivity and H₂O₂ efficiency, PS-Ti-**MWW** has so far been a most efficient heterogeneous catalyst for liquid-phase epoxidation of linear alkenes.

At first, the main difference between PS-Ti-**MWW** and HTS-Ti-**MWW** seemed to be the boron content. A further treatment with refluxing 2 M HNO₃ was able to deboronate HTS-Ti-**MWW** to produce a sample nearly free of boron (Si/B > 500), while removing the Ti species only slightly. However, this did not result in any substantial increase in TON. The reason other than the boron content thus may

account for the above results. Since HTS-Ti-MWW is prepared by using boric acid as a structure-supporting agent, the coexisting boron would preferentially occupy the specific framework position (T site), which would hinder the uniform incorporation of titanium. On the other hand, PS-Ti-MWW was prepared through inserting the Ti species mainly into defect sites formed by elimination of boron atoms. Thus the Ti species occupying crystallographically different T sites may account for the different catalytic behaviour between PS-Ti-MWW and HTS-Ti-MWW.

Ti-MWW catalysts have also been found to exhibit catalytic performance superior to conventional titanasilicates such as TS-1 and Ti-beta in other oxidation reactions.

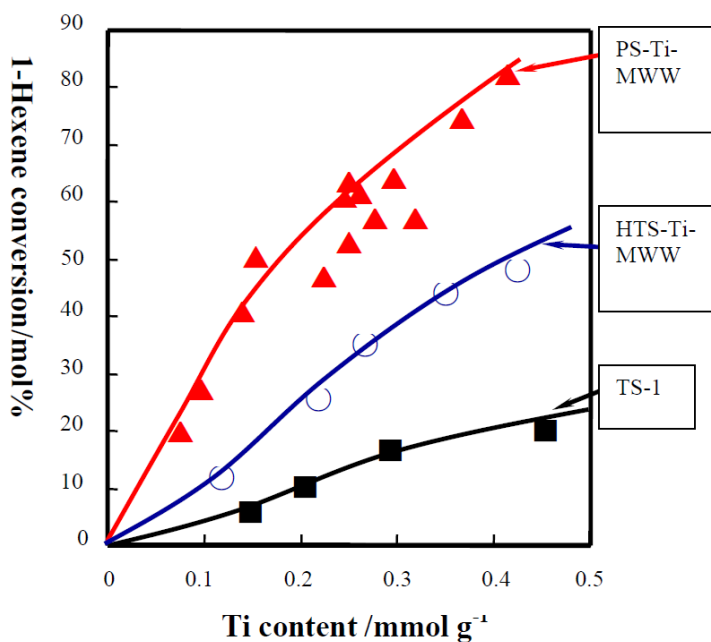


Fig. 9. The catalytic properties of postsynthesized PS-Ti-MWW, directly hydrothermally synthesized HTS-Ti-MWW and TS-1 in the epoxidation of 1-hexene with H_2O_2 .

For example, epoxidation of allyl alcohol to glycidol, epoxidation of diallyl ether to allyl glycidyl ether, epoxidation of allyl chloride to epichlorohydrin, epoxidation of

2,5-dihydrofuran to 3,4-epoxytetrahydrofuran, hydroxylation of 1,4-dioxane to 1,4-dioxane-2-ol, and ammoximation of cyclohexanone to cyclohexanone oxime.

Reversible structural conversion did not occur when as synthesized Ti-MWW (P) with the Si/Ti ratio of > 100 was calcined subsequent to washing with 2 M HNO_3 . Thus obtained novel titanosilicate with the structure analogues to the **MWW** precursor, designated as Ti-YNU-1, shows much higher oxidation ability, epoxide selectivity and stability than Ti-Beta in the oxidation of bulky cycloalkenes^{89,90}. Ti-YNU-1 has proved to have a large interlayer pore space corresponding to 12-MR zeolites⁹¹. Whereas direct condensation of the layers results in the formation of the **MWW** structure having a 10-MR interlayer pore, apparently monomeric Si species have been inserted into the interlayer spaces followed by condensation to provide a 12MR pore. Since no Si source has been added, it is assumed that silica “debris” formed by decomposition of a part of the **MWW** layer acted as Si source. This assumption has been tested by deliberately adding a Si source to the as-synthesized **MWW**(P); by using silylating agents such as $\text{SiMe}_2(\text{OR})_2$ and SiMe_2Cl_2 silylene units can be inserted between the layers, which was followed by removal of the organic moieties to give the material that essentially the same as Ti-YNU-1. Furthermore, it has been revealed that this method of inserting monomeric Si sources into the interlayer spaces can be widely applied to the conversion of a variety of 2D lamellar precursors into novel 3D crystalline zeolites with expanded pore apertures between the layers, as has been described in Section 1.2.

The treatment with TiCl_4 vapor at elevated temperatures is a usual method well employed for modifying **MOR** and **BEA** zeolites of 12-MR channels^{85,86}. Recently, Kubota *et al.* reported the synthesis of Ti-MCM-68 (**MSE**) by post-synthetic modification, namely dealumination by acid treatment followed by gas-phase Ti insertion using vapor phase TiCl_4 as a Ti source⁹². Ti-MSE was highly active in olefin epoxidation on a level of Ti-MWW. Particularly noteworthy is that Ti-MSE showed superior performance to TS-1, Ti-beta, and Ti-MWW for phenol oxidation.

References

- [1] Barrer, R. M. & Denny, D. J. Hydrothermal Chemistry of the Silicates. Part IX. Nitrogenous Aluminosilicates. *J. Chem. Soc.* 971-982 (1961).
- [2] Dorset, D. L., Weston, S. C. & Dhingra, S. S. Crystal Structure Zeolite MCM-68: a New Three-Dimensional Framework with Large Pores. *J. Phys. Chem. B* **110**, 2045-2050 (2006).

- [3] Burton, A., Elomari, S., Chen, C. Y., Medrud, R. C., Chan, I. Y., Bull, L. M., Kibby, C., Harris, T. V., Zones, S. I. & Vittoratos E. S. SSZ-53 and SSZ-59: Two Novel Extra-Large Pore Zeolites. *Chem. Eur. J.* **9**, 5737-5748 (2003).
- [4] Matsukata, M., Ogura, M., Osakim T., Prasad Rao, P. R., Nomura, M. & Kikuchi, E. Conversion of Dry Gel to Microporous Crystals in Gas Phase, *Top. Catal.*, **9**, 77-92 (1999).
- [5] Blasco, T., Corma, A., Diaz-Cabanas, M. J., Rey, F., Vidal-Moya, J. M. & Zicovich-Wilson, C. M. Preferential Location of Ge in the Double Four-Membered Ring Units of ITQ-7 Zeolite. *J. Phys. Chem. B*, **106**. 2634-2642 (2002).
- [6] Vaughan, D. E. W., Lussier, J. & Magee, J. S. *U.S. Patent*, 4 176 090 (1993).
- [7] Pinnavaia, T. J., Intercalated Clay Minerals, *Science*, **220**, 365-371 (1983).
- [8] Schreyeck, L., Caullet, P., J.C. Mougénel, J. C., Guth, J.-L. & Marler, B., PREFER: a New Layered (Alumini)silicate Precursor of FER-type Zeolite. *Microporous Mater.*, **6** 259-271 (1996).
- [9] Leonowicz, M., Lawton, J., Lawton, S. & Rubin, M. MCM-22: A Molecular Sieve with Two Independent Multidimensional Channel Systems. *Science*, **264**, 1910-1913 (1994).
- [10] Kresge, C. T. & W. J., Roth *U.S. Patent*, 5 266 541 and 5 278 115 (1993).
- [11] Corma, V., Fornés, S. B., Pergher, S., Maesen, Th L. M. & Buglass, J. G. Delaminated zeolite precursors as selective acidic catalysts. *Nature (London)*, **396**, 353-356 (1998).
- [12] Corma, V., Fornés, J., Martínez-Triguero, J., Pergher, S. B., Delaminated Zeolites: Combining the Benefits of Zeolites and Mesoporous Materials for Catalytic Uses. *J. Catal.* **186**, 57 (1999).
- [13] Corma, A., Fornés, V., Guil, J. M., Pergher, S., Maesen, Th. L. M. & Buglass, J. G. Preparation, characterisation and catalytic activity of ITQ-2, a delaminated zeolite. *Microporous Mesoporous Mater.*, **38**, 301-309. (2000).
- [14] Aguilar, J., Pergher, S. B. C., Detoni, C., Corma, A., Melo, F. V. & Sastre, E. Alkylation of biphenyl with propylene using MCM-22 and ITQ-2 zeolites. *Catal. Today*, **133-135**, 667-672 (2008).
- [15] Inagaki, S., Kamino, K., Kikuchi, E. & Matsukata, M. Shape selectivity of MWW-type aluminosilicate zeolites in the alkylation of toluene with methanol. *Appl. Catal. A*. **318**, 22-27 (2007).

- [16] Choi, M., Na, K., Kim, J., Sakamoto, Y., Terasaki, O. & Ryoo, R. Stable single-unit-cell nanosheets of zeolite MFI as active and long-lived catalysts. *Nature (London)*, **461**, 246-250 (2009).
- [17] Mochizuki, D., Shimojima, A., Imagawa & Kuroda, K. Molecular Manipulation of Two- and Three-Dimensional Silica Nanostructures by Alkoxysilylation of a Layered Silicate Octosilicate and Subsequent Hydrolysis of Alkoxy Groups. *J. Am. Chem. Soc.* **127**, 7183 (2005).
- [18] Wu, P., Ruan, J., Wang, L., Wu, L., Wang, Y., Liu, Y., Fan, W., He, M., Terasaki, O. & Tatsumi, T. A Methodology for Synthesizing Crystalline Metallosilicates with Expanded Pore Windows Through Molecular Alkoxysilylation of Zeolitic Lamellar Precursors. *J. Am. Chem. Soc.* **130**, 8178-8187 (2008).
- [19] Inagaki, S., Imai, H., Tsujiuchi, S., Yakushiji, H., Yokoi, T. & Tatsumi, T. Enhancement of catalytic properties of interlayer-expanded zeolite Al-MWW via the control of interlayer silylation conditions. *Microporous Mesoporous Mater.* **142**, 354-362 (2011).
- [20] Inagaki, S. & Tatsumi, T. Vapor-phase silylation for the construction of monomeric silica puncheons in the interlayer micropores of Al-MWW layered *Chem. Commun.* 2583-2585 (2009).
- [21] Ruan, J., Wu, P., Slater, B., Zhao, Z., Wu, L. & Terasaki, O. Structural Characterization of Interlayer-Expanded Zeolite Prepared from Ferrierte Lamellar Precursor. *Chem. Mater.* **21**, 2904-2911 (2009).
- [22] Gies, H., Müller, U., Yilmaz, B., Tatsumi, T., Xie, B., Xiao, F. -S., Bao, X., Zhang, W., De Vos, D., Interlayer Expansion of the Layered Zeolite Precursor RUB-39: A Universal Method to Sythesize Functionaized Microporous Materials. *Chem. Mater.* **23**, 2545-2554 (2011).
- [23] Inagaki, S. & Tatsumi, T., Unique adsorption properties of organic-inorganic hybrid zeolites IEZ-1 with dimethylsilylene moieties. *Chem. Commun.* 2583 (2009).
- [24] Corma, A., Díaz, U., García, T., Sastre, G. & Velly, A. Multifunctional Hybrid Organic-Inorganic Catalytic Materials with a Hierarchical System of Well-Defined Micro- and Mesopores. *J. Am. Chem. Soc.* **132**, 15011-15021 (2010).
- [25] Kresge, C. T., Leonowicz, M. E., Roth, W. J., Vartuli, J. C. & Beck, J. S. Ordered mesoporous molecular sieves synthesized by a liquid-crystal template mechanism. *Nature* **359**, 710-712 (1992).
- [26] Inagaki, S., Fukushima, Y. & Kuroda, K. Synthesis of highly ordered mesoporous materials from a layered polysilicate. *J. Chem. Soc. Chem. Commun.* 680-682 (1993).

- [27] Tao, Y., Kanoh, H., Abrams, L. & Kaneko, K. Mesopore-Modified Zeolites: Preparation, Characterization, and Applications. *Mesopore-Modified Zeolites: Preparation, Characterization, and Applications. Chem. Rev.* **106**, 896-910 (2006).
- [28] Pérez-Ramírez, J., Christensen, C. H., Egeblad, K., Christensen, C. H. & Groen J. C. Hierarchical zeolites: enhanced utilisation of microporous crystals in catalysis by advances in materials design. *Chem. Soc. Rev.* **37**, 2530-2542 (2008).
- [29] Ogura, M. Towards Realization of a Micro- and Mesoporous Composite Silicate Catalyst(2008) *Catal. Surv. Asia* **12**, 16-27 (2008).
- [30] Dessau, R. M., Valyocsik, E. W. & Goetze, N. H. Aluminum zoning in ZSM-5 as revealed by selective silica removal. *Zeolites* **12**, 776-779 (1992).
- [31] Ogura, M., Shinomiya, S., Tateno, J., Nara, Y., Nomura, M., Kikuchi, E. & Matsukata, M. Alkali-treatment technique - new method for modification of structural and acid-catalytic properties of ZSM-5 zeolites. *Appl. Catal. A* **219**, 33-43 (2001).
- [32] Kloetstra, K. R., van Bekkum, H. & Jansen, J. C. Mesoporous material containing framework tectosilicate by pore-wall recrystallization. *Chem. Commun.* 2281-2282 (1997).
- [33] Liu, Y., Zhang, W. & Pinnavaia, T. J. Steam-Stable Aluminosilicate Mesostructures Assembled from Zeolite Type Y Seeds. *J. Am. Chem. Soc.* **122**, 8791-8792 (2000).
- [34] Liu, Y., Zhang, W. & Pinnavaia, T. J. Steam-Stable MSU-S Aluminosilicate Mesostructures Assembled from Zeolite ZSM-5 and Zeolite Beta Seeds. *Angew. Chem. Int. Ed.* **40**, 1255-1258 (2001).
- [35] Liu, Y. & Pinnavaia, T. J. Assembly of Hydrothermally Stable Aluminosilicate Foams and Large-Pore Hexagonal Mesostructures from Zeolite Seeds under Strongly Acidic Conditions. *Chem. Mater.* **14**, 3-5 (2002).
- [36] Jacobsen, C. J. H., Madsen, C., Houzvicka, J., Schmidt, I. & Carlsson, A. Mesoporous Zeolite Single Crystals. *J. Am. Chem. Soc.* **122**, 7116-7117 (2000).
- [37] Schmidt, I., Boisen, A., Gustavsson, E., Stahl, K., Pehrson, S., Dahl, S., Carlsson, A. & Jacobsen, C. J. H. Carbon Nanotube Templated Growth of Mesoporous Zeolite Single Crystals. *Chem. Mater.* **13**, 4416-4418 (2001).
- [38] Wang, H. & Pinnavaia, T. J. MFI Zeolite with Small and Uniform Intracrystal Mesopores. *Angew. Chem. Int. Ed.* **45**, 7603-7606 (2006).
- [39] Sakthivel, A., Huang, S.-J., Chen, W.-H., Lan, Z.-H., Chen, K.-H., Kim, T.-W., Ryoo, R., Chiang, A. S. T. & Liu, S.-B. Replication of Mesoporous Aluminosilicate

Molecular Sieves (RMMs) with Zeolite Framework from Mesoporous Carbons (CMKs). *Chem. Mater.* **16**, 3168-3175 (2004).

[40] Zhang, Y., Okubo, T. & Ogura, M. Synthesis of mesoporous aluminosilicate with zeolitic characteristics using vapor phase transport. *Chem. Commun.* 2719-2720 (2005).

[41] Xiao, F.-S., Wang, L., Yin, C., Lin, K., Di, Y., Li, J., Xu, R., Su, D. S., Schlögl, R., Yokoi, T. & Tatsumi, T. "Catalytic Properties of Hierarchical Mesoporous Zeolites Templated with a Mixture of Small Organic Ammonium Salts and Mesoscale Cationic Polymers. *Angew. Chem. Int. Ed.* **45**, 3090-3093 (2006).

[42] Choi, M., Cho, H. S., Srivastava, R., Venkatesan, C., Choi, D. H. & Ryoo, R. Amphiphilic organosilane-directed synthesis of crystalline zeolite with tunable mesoporosity. *Nature Mater.*, **5**, 718-723 (2006).

[43] Takewaki, T. Beck, L. W. & Davis, M. E. Zincosilicate CIT-6: A Precursor to a Family of *BEA-Type Molecular Sieves. *J. Phys. Chem. B* **103**, 2674-2679 (1999).

[44] Lee, H., Zones, S. I. & Davis, M. E. A combustion-free methodology for synthesizing zeolites and zeolite-like materials. *Nature (London)* **425**, 385-388 (2003).

[45] Cundy, C.S. & Cox, P.A. The Hydrothermal Synthesis of Zeolites: History and Development from the Earliest Days to the Present Time. *Chem. Rev.* **103**, 663-702 (2003).

[46] Song, J., Dai, L., Ji, Y. & Xiao, F. -S. Organic Template Synthesis of Aluminosilicate Zeolite ECR-1. *Chem. Mater.* **18**, 2775-2777 (2006).

[47] Xie, B., Song, J., Ren, L., Ji, Y., Li, J. & Xiao, F. -S. Organotemplate-Free and Fast Route for Synthesizing Beta Zeolite. *Chem. Mater.* **20**, 4533-4535 (2008).

[48] Majano, G., Delmotte, L., Valtchev, V. & Mintova, S. Al-Rich Zeolite Beta by Seeding in the Absence of Organic Template. *Chem. Mater.* **21**, 4184-4191 (2008).

[49] Kamimura, Y., Chaikittisilp, W., Itabasgi, K., Shimojima, A. & Okubo, T. Critical Factors in the Seed-Assisted Synthesis of Zeolite Beta and "Green Beta" from OSDA-Free Na⁺-Aluminosilicate Gels. *Chem. Asian J.*, **5**, 2182-2191 (2010).

[50] Vortmann, S., Marler, B., Gies, H. & Daniels, P. Synthesis and crystal structure of the new borosilicate zeolite RUB-13. *Microporous Mater.* **4**, 111-121 (1995).

[51] Lee, G. S. & Zones, S. I. Polymethylated[4.1.1]octanes Leading to Zeolite SSZ-50. *J. Solid State Chem.* **167**, 289-298 (2002).

- [52] Yokoi, T., Yoshioka, M., Imai, H. & Tatsumi, T. Diversification of RTH-type zeolite and its catalytic application. *Angew. Chem. Int. Ed.* **48**, 9884-9887 (2009).
- [53] Xie, B., Zhang, H., Yang, C., Liu, S., Ren, L., Zhang, L., Meng, X., Yilmaz, B., Müller, U. & Xiao, F. –S. Seed-directed synthesis of zeolites with enhanced performance in the absence of organic templates. *Chem. Commun.* **47**, 3945-3947 (2011).
- [54] Zones, S. I. Direct Hydrothermal Conversion of Cubic P Zeolites to Organozeolite SSZ-13. *J. Chem. Soc. Faraday Trans.* **86**, 3467-3472 (1990).
- [55] Zones, S. I. & Nakagawa, Y. Boron-beta zeolite hydrothermal conversions: the influence of template structure and of boron concentration and source. *Microporous Mater.* **2**, 543-555 (1994).
- [56] Kubota, Y., Maekawa, H., Miyata, S., Tatsumi, T. & Sugi, Y. Hydrothermal synthesis of metallosilicate SSZ-24 from metallosilicate beta as precursors. *Microporous Mesoporous Mater.* **101**, 115-126 (2007).
- [57] Jon, H., Ikawa, N., Oumi, Y. & Sano, T. An Insight into the Process Involved in Hydrothermal Conversion of FAU to *BEA Zeolite. *Chem. Mater.* **20**, 4135-4141 (2008).
- [58] Jon, H., Takahashi, S., Sasaki, H., Oumi, Y. & Sano, T. Hydrothermal conversion of FAU zeolite into RUT zeolite in TMAOH system. *Microporous Mesoporous Mater.* **113**, 56-63 (2008).
- [59] Inoue, T., Itakura, M., Jon, H., Oumi, Y., Takahashi, A., Fujitani, T. & Sano, T. Synthesis of LEV zeolite by interzeolite conversion method and its catalytic performance in ethanol to olefins reaction. *Microporous Mesoporous Mater.* **122**, 149-154 (2009).
- [60] Koyama, Y., Ikeda, T., Tatsumi, T. & Kubota, Y. Synthetic investigation on MCM-68 zeolite with MSE topology and its application for shape-selective alkylation of biphenyl, *Angew. Chem. Int. Ed.* **47**, 1042-1046 (2008).
- [61] Taramasso, M., Perego, G. & Notari, B. *U.S. Patent*, 4 401 051 (1983).
- [62] Ione, K.G., Vostrikova, L. A. & Mastikhin, V. M. Synthesis of crystalline metal silicates having zeolite structure and study of their catalytic properties. *J. Mol. Catal.* **31**, 355-370 (1985).
- [63] Corma, A., L. T. Nemeth, L. T., Renz, M., & Valencia, S. Sn-zeolite beta as a heterogeneous chemoselective catalyst for Baeyer-Villiger oxidations. *Nature* **412**, 423-425 (2001).

- [64] Jayachandran, B., Sasidhran, M., Sudalai, A., T. & Ravindranathan, T. Chromium silicalite-2 (CrS-2): an efficient catalyst for the chemoselective epoxidation of alkenes with TBHP. *J. Chem. Soc. Chem. Commun.* 1341-1342 (1995).
- [65] Lempers, H. E. B. & Sheldon, R. A. The stability of chromium in chromium molecular sieves under the conditions of liquid phase oxidation with *tert*-butyl hydroxide. *Stud. Surf. Sci. Catal.* **105**, 1061-1068 (1997).
- [66] Notari, B.. in *Advances in Catalysis* (eds D. D. Eley, Werner O. Haag, Bruce Gates) Academic Press, San Diego, Vol. 41, 253-334 (1996).
- [67] Clerici, M. G., Bellussi, G. & Romano, U. Synthesis of propylene oxide from propylene and hydrogen peroxide catalyzed by titanium silicalite. *J. Catal.* **129**, 159-167 (1991).
- [68] Reddy, J.S., Kumar, R. & Ratnasamy, P. Titanium silicalite-2: Synthesis, characterization and catalytic properties. *Appl. Catal.* **58**, L1-L4 (1990).
- [69] Bellussi, G. & Rigutto, M. S. Metal Ions Associated to Molecular Sieve Frameworks as Catalytic Sites for Selective Oxidation Reactions. *Stud. Surf. Sci. Catal.* **137**, 911-955 (1994).
- [70] Lamberti, C., Bordiga, S., Zecchina, A., Artioli, G., Marra, G. & Spano, G. Ti Location in the MFI Framework of Ti-Silicalite-1: A Neutron Powder Diffraction Study. *J. Am. Chem. Soc.* **123**, 2204-2212 (2001).
- [71] Thangaraj, A. & Sivasanker, S. An Improved Method for TS-1 Synthesis: ²⁹Si NMR Studies. *J. Chem. Soc., Chem. Commun.* 123-124 (1992).
- [72] Serrano, D. P., Uguina, M. A., Ovejero, G., van Grieken, R. & Camacho, M. Evidence of solid-solid transformations during the TS-1 crystallization from amorphous wetness impregnated SiO₂-TiO₂ xerogels. *Microporous Mater.* **7**, 309-321 (1996).
- [73] Thomas, J. M. & Sankar, G. The Role of Synchrotron-Based Studies in the Elucidation and Design of Active Sites in Titanium-Silica Epoxidation Catalysts. *Acc. Chem. Res.* **34**, 571-581 (2001).
- [74] Fan, W., Duan, R. -G., Yokoi, T., Wu, P., Kubota, Y. & Tatsumi, T. Synthesis, Crystallization Mechanism, and Catalytic Properties of Titanium-Rich TS-1 Free of Extraframework Titanium Species. *J. Am. Chem. Soc.*, **130**, 10150-10164 (2008).
- [75] Tatsumi, T., Koyano, K. A. & Igarashi, N. Remarkable activity enhancement by trimethylsilylation in oxidation of alkenes and alkanes with H₂O₂ catalyzed by titanium-containing mesoporous molecular sieves. *Chem. Commun.* 325-326 (1998)

- [76] Gabelica, Z., Blom, N. & Derouane, E. G. Synthesis and characterization of ZSM-5 type zeolites: III. A critical evaluation of the role of alkali and ammonium cations. *Appl. Catal.* **5**, 227-248 (1983).
- [77] Wu, P., Tatsumi, T., Komatsu, T. & Yashima, T. Hydrothermal Synthesis of a Novel Titanosilicate with MWW Topology. *Chem. Lett.* 774-775 (2000).
- [78] Cambor, M.A., Corma, A., Díaz-Cabanas, M. J. & Baerlocher, C. Synthesis and Structural Characterization of MWW Type Zeolite ITQ-1, the Pure Silica Analog of MCM-22 and SSZ-25. *J. Phys. Chem. B* **102**, 44-51 (1998).
- [79] Wu, P., Tatsumi, T., Komatsu, T. & Yashima, T. A Novel Titanosilicate with MWW Structure. I. Hydrothermal Synthesis, Elimination of Extraframework Titanium, and Characterization. *J. Phys. Chem. B* **105**, 2897-2905 (2001).
- [80] Roth, W. J., Kresge, C. T., Vartuli, J. C., Leonowicz, M. E., Fung, A.S. & McCullen, S. B. MCM-36: The First Pillared Molecular Sieve with Zeolite Properties. *Stud. Surf. Sci. Catal.* **94**, 301-308 (1995).
- [81] Corma, A., Fornés, V., Pergher, S. B., Maesen, Th. L. M. & Buglass, G. Delaminated zeolite precursors as selective acidic catalysts. *Nature* **396**, 353-356 (1998).
- [82] Cambor, M.A., Constantini, M., Corma, A., Gilbert, L., Esteve, P., Martínez, A. & Valencia S. Synthesis and catalytic activity of aluminium-free zeolite Ti- β oxidation catalysts. *Chem. Commun.* 1339-1340 (1996).
- [83] Blasco, T., Cambor, M. A., Corma, A., Esteve, P., Guil, J. M. Martínez, A., Perdigon-Melon, J.A. & Valencia, S. Direct Synthesis and Characterization of Hydrophobic Aluminum-Free Ti-Beta Zeolite. *J. Phys. Chem. B* **102**, 75-88 (1998).
- [84] Tatsumi, T. & Jappar, N. Properties of Ti-Beta Zeolites Synthesized by Dry-Gel Conversion and Hydrothermal Methods. *J. Phys. Chem. B* **102**, 7126-7131 (1998).
- [85] Wu, P., Komatsu, T. & Yashima, T. Characterization of Titanium Species Incorporated into Dealuminated Mordenites by Means of IR Spectroscopy and ^{18}O -Exchange Technique. *J. Phys. Chem. B* **100**, 10316-10322 (1996).
- [86] Goa, Y., P. Wu, P. & Tatsumi, T. Influence of Fluorine on the Catalytic Performance of Ti-Beta Zeolite. *J. Phys. Chem. B* **108**, 4242-4244 (2004).
- [87] Levin, D., Chang, A. D., Luo, S., Santiestebana G. & Vartuli, J. C. *U.S. Patent*, 6 114 551 (2000).
- [88] Wu, P. & Tatsumi T. A new generation of titanosilicate catalyst: preparation and application to liquid-phase epoxidation of alkenes. *Catal. Surveys Asia* **8**, 137-148 (2004).

- [89] Fan, W., Wu, P., Namba, S. & Tatsumi T. A Titanosilicate That Is Structurally Analogous to an MWW-Type Lamellar Precursor. *Angew. Chem. Int. Ed.* **43**, 236-240 (2004).
- [90] Fan, W., Wu, P., Namba, S. & Tatsumi T. Synthesis and catalytic properties of a new titanosilicate molecular sieve with the structure analogous to MWW-type lamellar precursors. *J. Catal.* **243**, 183-191 (2006).
- [91] Ruan, J., Wu, P., Slater, B. & Terasaki, O. Structure Elucidation of the Highly Active Titanosilicate Catalyst Ti-YNU-1. *Angew. Chem. Int. Ed.* **44**, 6719-6723 (2005).
- [92] Kubota, Y., Koyama, Y., Yamada, T., Inagaki, S. & Takashi, T. Synthesis and catalytic performance of Ti-MCM-68 for effective oxidatoin reactions. *Chem. Commun.* 6224-6226 (2008).